



SMALL MOLECULES BRIDGING TERRESTRIAL MICROBIAL INTERACTIONS IN MULTITROPHIC SYSTEMS

EDITED BY: Elisa Korenblum, Paolina Garbeva and Monica T. Pupo
PUBLISHED IN: *Frontiers in Microbiology*



frontiers

Frontiers eBook Copyright Statement

The copyright in the text of individual articles in this eBook is the property of their respective authors or their respective institutions or funders. The copyright in graphics and images within each article may be subject to copyright of other parties. In both cases this is subject to a license granted to Frontiers.

The compilation of articles constituting this eBook is the property of Frontiers.

Each article within this eBook, and the eBook itself, are published under the most recent version of the Creative Commons CC-BY licence.

The version current at the date of publication of this eBook is CC-BY 4.0. If the CC-BY licence is updated, the licence granted by Frontiers is automatically updated to the new version.

When exercising any right under the CC-BY licence, Frontiers must be attributed as the original publisher of the article or eBook, as applicable.

Authors have the responsibility of ensuring that any graphics or other materials which are the property of others may be included in the CC-BY licence, but this should be checked before relying on the CC-BY licence to reproduce those materials. Any copyright notices relating to those materials must be complied with.

Copyright and source acknowledgement notices may not be removed and must be displayed in any copy, derivative work or partial copy which includes the elements in question.

All copyright, and all rights therein, are protected by national and international copyright laws. The above represents a summary only. For further information please read Frontiers' Conditions for Website Use and Copyright Statement, and the applicable CC-BY licence.

ISSN 1664-8714

ISBN 978-2-88976-295-8

DOI 10.3389/978-2-88976-295-8

About Frontiers

Frontiers is more than just an open-access publisher of scholarly articles: it is a pioneering approach to the world of academia, radically improving the way scholarly research is managed. The grand vision of Frontiers is a world where all people have an equal opportunity to seek, share and generate knowledge. Frontiers provides immediate and permanent online open access to all its publications, but this alone is not enough to realize our grand goals.

Frontiers Journal Series

The Frontiers Journal Series is a multi-tier and interdisciplinary set of open-access, online journals, promising a paradigm shift from the current review, selection and dissemination processes in academic publishing. All Frontiers journals are driven by researchers for researchers; therefore, they constitute a service to the scholarly community. At the same time, the Frontiers Journal Series operates on a revolutionary invention, the tiered publishing system, initially addressing specific communities of scholars, and gradually climbing up to broader public understanding, thus serving the interests of the lay society, too.

Dedication to Quality

Each Frontiers article is a landmark of the highest quality, thanks to genuinely collaborative interactions between authors and review editors, who include some of the world's best academicians. Research must be certified by peers before entering a stream of knowledge that may eventually reach the public - and shape society; therefore, Frontiers only applies the most rigorous and unbiased reviews.

Frontiers revolutionizes research publishing by freely delivering the most outstanding research, evaluated with no bias from both the academic and social point of view. By applying the most advanced information technologies, Frontiers is catapulting scholarly publishing into a new generation.

What are Frontiers Research Topics?

Frontiers Research Topics are very popular trademarks of the Frontiers Journals Series: they are collections of at least ten articles, all centered on a particular subject. With their unique mix of varied contributions from Original Research to Review Articles, Frontiers Research Topics unify the most influential researchers, the latest key findings and historical advances in a hot research area! Find out more on how to host your own Frontiers Research Topic or contribute to one as an author by contacting the Frontiers Editorial Office: frontiersin.org/about/contact

SMALL MOLECULES BRIDGING TERRESTRIAL MICROBIAL INTERACTIONS IN MULTITROPHIC SYSTEMS

Topic Editors:

Elisa Korenblum, Institute of Plant Sciences, Agricultural Research Organization, Volcani Center, Israel

Paolina Garbeva, Netherlands Institute of Ecology (NIOO-KNAW), Netherlands

Monica T. Pupo, University of São Paulo, Brazil

Citation: Korenblum, E., Garbeva, P., Pupo, M. T., eds. (2022). Small Molecules Bridging Terrestrial Microbial Interactions in Multitrophic Systems. Lausanne: Frontiers Media SA. doi: 10.3389/978-2-88976-295-8

Table of Contents

- 05** *Lenzimycons A and B, Metabolites With Antibacterial Properties From Brevibacillus sp. Associated With the Dung Beetle Onthophagus lenzii*
Joon Soo An, Seong-Heon Hong, Elisabeth Somers, Jayho Lee, Byung-Yong Kim, Donghee Woo, Suk Won Kim, Hee-Jeon Hong, Shin-Il Jo, Jongheon Shin, Ki-Bong Oh and Dong-Chan Oh
- 15** *Penicillium italicum: An Underexplored Postharvest Pathogen*
Aline Midori Kanashiro, Daniel Yuri Akiyama, Katia Cristina Kupper and Taícia Pacheco Fill
- 32** *Pseudonocardia Symbionts of Fungus-Growing Ants and the Evolution of Defensive Secondary Metabolism*
Sarah L. Goldstein and Jonathan L. Klassen
- 40** *Insights Into the Ecological Role of Pseudomonas spp. in an Ant-plant Symbiosis*
Taise T. H. Fukuda, Camila F. Pereira, Weilan G. P. Melo, Carla Menegatti, Paulo H. M. Andrade, Milton Groppo, Paulo T. Lacava, Cameron R. Currie and Mônica T. Pupo
- 51** *Pollen Streptomyces Produce Antibiotic That Inhibits the Honey Bee Pathogen Paenibacillus larvae*
Kirk J. Grubbs, Daniel S. May, Joseph A. Sardina, Renee K. Dermenjian, Thomas P. Wyche, Adrián A. Pinto-Tomás, Jon Clardy and Cameron R. Currie
- 60** *Biphenyl 2,3-Dioxygenase in Pseudomonas alcaliphila JAB1 Is Both Induced by Phenolics and Monoterpenes and Involved in Their Transformation*
Andrea Zubrova, Klara Michalikova, Jaroslav Semerad, Michal Strejcek, Tomas Cajthaml, Jachym Suman and Ondrej Uhlik
- 72** *Metabolic Profiling of Rhizobacteria Serratia plymuthica and Bacillus subtilis Revealed Intra- and Interspecific Differences and Elicitation of Plipastatins and Short Peptides Due to Co-cultivation*
Riya C. Menezes, Birgit Piechulla, Dörte Warber, Aleš Svatoš and Marco Kai
- 93** *Volatile Compounds From Bacillus, Serratia, and Pseudomonas Promote Growth and Alter the Transcriptional Landscape of Solanum tuberosum in a Passively Ventilated Growth System*
Darren Heenan-Daly, Simone Coughlan, Eileen Dillane and Barbara Doyle Prestwich
- 114** *Multi-Omic Analysis of Symbiotic Bacteria Associated With Aedes aegypti Breeding Sites*
Katherine D. Mosquera, Luis E. Martinez Villegas, Sacha J. Pidot, Chindhda Sharif, Sven Klimpel, Timothy P. Stinear, Luciano A. Moreira, Nicholas J. Tobias and Marcelo G. Lorenzo
- 124** *Antimicrobial Compounds in the Volatilome of Social Spider Communities*
Alexander Lammers, Hans Zweers, Tobias Sandfeld, Trine Bilde, Paolina Garbeva, Andreas Schramm and Michael Lalk

- 135** *A Bacterial Quorum Sensing Molecule Elicits a General Stress Response in *Saccharomyces cerevisiae**
Antonia Delago, Rachel Gregor, Luba Dubinsky, Rambabu Dandela, Adi Hendler, Pnina Krief, Josep Rayo, Amir Aharoni and Michael M. Meijler
- 147** *L-Canavanine, a Root Exudate From Hairy Vetch (*Vicia villosa*) Drastically Affecting the Soil Microbial Community and Metabolite Pathways*
Hossein Mardani-Korrani, Masaru Nakayasu, Shinichi Yamazaki, Yuichi Aoki, Rumi Kaida, Takashi Motobayashi, Masaru Kobayashi, Naoko Ohkama-Ohtsu, Yosei Oikawa, Akifumi Sugiyama and Yoshiharu Fujii
- 158** *Genetic Elucidation of Quorum Sensing and Cobamide Biosynthesis in Divergent Bacterial-Fungal Associations Across the Soil-Mangrove Root Interface*
Zhengyuan Zhou, Ruiwen Hu, Yanmei Ni, Wei Zhuang, Zhiwen Luo, Weiming Huang, Qingyun Yan, Zhili He, Qiuping Zhong and Cheng Wang
- 173** *Predominant Biphenyl Dioxygenase From Legacy Polychlorinated Biphenyl (PCB)-Contaminated Soil Is a Part of Unusual Gene Cluster and Transforms Flavone and Flavanone*
Jachym Suman, Michal Strejcek, Andrea Zubrova, Jan Capek, Jiri Wald, Klara Michalikova, Miluse Hradilova, Kamila Sredlova, Jaroslav Semerad, Tomas Cajthaml and Ondrej Uhlik
- 190** *Soil Microbial Resource Limitations and Community Assembly Along a *Camellia oleifera* Plantation Chronosequence*
Hang Qiao, Longsheng Chen, Yajun Hu, Chenghua Deng, Qi Sun, Shaohong Deng, Xiangbi Chen, Li Mei, Jinshui Wu and Yirong Su



Lenzimycins A and B, Metabolites With Antibacterial Properties From *Brevibacillus* sp. Associated With the Dung Beetle *Onthophagus lenzii*

Joon Soo An¹, Seong-Heon Hong¹, Elisabeth Somers², Jayho Lee³, Byung-Yong Kim⁴, Donghee Woo¹, Suk Won Kim¹, Hee-Jeon Hong², Shin-Il Jo⁵, Jongheon Shin¹, Ki-Bong Oh³ and Dong-Chan Oh^{1*}

¹ Natural Products Research Institute, College of Pharmacy, Seoul National University, Seoul, South Korea, ² Department of Biological and Medical Sciences, Faculty of Health and Life Sciences, Oxford Brookes University, Oxford, United Kingdom, ³ Department of Agricultural Biotechnology, College of Agriculture and Life Sciences, Seoul National University, Seoul, South Korea, ⁴ ChunLab, Inc., Seoul, South Korea, ⁵ Animal Welfare Division, Seoul Zoo, Seoul Grand Park, Seoul, South Korea

OPEN ACCESS

Edited by:

Monica T. Pupo,
University of São Paulo, Brazil

Reviewed by:

Humberto Ortega,
University of Panama, Panama
Emily Mevers,
Virginia Tech, United States

*Correspondence:

Dong-Chan Oh
dongchanoh@snu.ac.kr

Specialty section:

This article was submitted to
Microbial Symbioses,
a section of the journal
Frontiers in Microbiology

Received: 28 August 2020

Accepted: 07 October 2020

Published: 30 October 2020

Citation:

An JS, Hong S-H, Somers E,
Lee J, Kim B-Y, Woo D, Kim SW,
Hong H-J, Jo S-I, Shin J, Oh K-B and
Oh D-C (2020) Lenzimycins A and B,
Metabolites With Antibacterial
Properties From *Brevibacillus* sp.
Associated With the Dung Beetle
Onthophagus lenzii.
Front. Microbiol. 11:599911.
doi: 10.3389/fmicb.2020.599911

Symbiotic microorganisms associated with insects can produce a wide array of metabolic products, which provide an opportunity for the discovery of useful natural products. Selective isolation of bacterial strains associated with the dung beetle, *Onthophagus lenzii*, identified two strains, of which the antibiotic-producing *Brevibacillus* sp. PTH23 inhibited the growth of *Bacillus* sp. CCARM 9248, which is most closely related to the well-known entomopathogen, *Bacillus thuringiensis*. A comprehensive chemical investigation based on antibiotic activity discovered two new antibiotics, named lenzimycins A and B (**1-2**), which inhibited growth of *Bacillus* sp. CCARM 9248. The ¹H and ¹³C NMR, MS, MS/MS, and IR analyses elucidated the structures of **1** and **2**, which comprised a novel combination of fatty acid (12-methyltetradecanoic acid), glycerol, sulfate, and *N*-methyl ethanolamine. Furthermore, the acid hydrolysis of **1** revealed the absolute configuration of 12-methyltetradecanoic acid as 12S by comparing its optical rotation value with authentic (*R*)- and (*S*)-12-methyltetradecanoic acid. In addition to inhibition of *Bacillus* sp. CCARM 9248, lenzimycins A and B were found to inhibit the growth of some human pathogenic bacteria, including *Enterococcus faecium* and certain strains of *Enterococcus faecalis*. Furthermore, the present study elucidated that lenzimycins A and B activated a reporter system designed to detect the bacterial cell envelope stress, thereby indicating an activity against the integrity of the bacterial cell wall.

Keywords: antibiotic, *Brevibacillus*, *Bacillus*, dung beetle, lenzimycin, natural product

INTRODUCTION

Insects harbor symbiotic or pathogenic microorganisms; therefore, they have gained increasing interest as a reservoir for biotechnologically and pharmaceutically important microbes (Bode, 2010). In the past 20 years, several studies on insect-microbe interactions have reported on the role of bacterial natural products as molecular mediators in symbiotic insect systems

(Cantley and Clardy, 2015; Pishchany and Kolter, 2020). There is an accumulating body of research which reports the insect symbiosis as biotechnological resources. For instance, Oh et al. (2009) analyzed the mutualistic associations in fungus-growing ant, *Apterostigma dentigerum* at the molecular level and found that the symbiotic bacterium, *Pseudonocardia*, produces dentigerumycin, a cyclic depsipeptide with highly modified amino acids, to selectively inhibit the associated parasitic fungus (*Escovopsis* sp.). Similarly, chemical ecological investigation of attine ants, *Acromyrmex rugosus* and their symbionts revealed a combination of antifungal compounds that inhibited the specialized fungal pathogen, *Escovopsis*. These small bacterial molecules were also evaluated as inhibitors against the human protozoan parasite *Leishmania donovani* (Ortega et al., 2019). It has also been reported that the symbiotic *Streptomyces* bacteria, located in specialized antennal glands, excrete antibiotics to protect wasp larvae from pathogenic fungal infestation (Kaltenpoth et al., 2005; Kroiss et al., 2010). Furthermore, studies have shown that the stingless bees, *Melipona scutellaris*, engage in defensive symbiosis with actinobacteria that produce antibacterial small molecules including the lobophorin, anthracycline, and cyclic hexadepsipeptide families, helping to protect their colonies against the entomopathogenic *Paenibacillus* larvae (Rodríguez-Hernández et al., 2019; Menegatti et al., 2020).

Dung beetles (Coleoptera: Scarabaeidae) are interesting Coleopteran insects, which feed on herbivores' feces and make brood balls with feces for larval development. Although the ecology has not been studied much in most of the dung beetle species, their life cycle is closely linked with feces. Therefore, they may possess symbiotic relationships with chemically prolific bacteria, some of which may aid in control of the microbes in their ecosystems. In our previous studies, we have isolated a new tricyclic macrocyclic lactam, tripartilactam from the *Streptomyces* sp. found in the brood ball of a dung beetle species, *Copris tripartitus* (Park et al., 2012; Hwang et al., 2020). Furthermore, Kim et al. (2013) have isolated a *Streptomyces* strain producing tripartin, a novel dichlorinated indanone from the larva of *C. tripartitus*. Additionally, new alkenyl cinnamic acid-bearing cyclic peptides, coprisamides A and B (Um et al., 2015), and naphthoquinone-oxindole alkaloids, coprisidins A and B (Um et al., 2016), have also been discovered as natural products of bacterial isolates obtained from the gut of dung beetles.

Given the abundant species diversity of dung beetles and their ecological functions, it is expected to serve as a promising source in discovery of chemical compounds with potential pharmaceutical applications. In this study, we focused on a dung beetle species, *Onthophagus lenzii* (Yasuda, 1986), which is phylogenetically distant from *C. tripartitus*. The dung beetle *O. lenzii* (specimen shown in **Figure 1**) was collected from the city of Osan-si located on the outskirts of Seoul in South Korea. During the selective cultivation of bacteria using the excretion of the dung beetles, a *Brevibacillus* sp. PTH23 with an ability to inhibit a co-isolate, *Bacillus* sp. CCARM9247, which is a close relative of the well-known entomopathogen *Bacillus thuringiensis*, was isolated and further investigated to identify its antibiotic metabolites. Subsequent large-scale cultivation



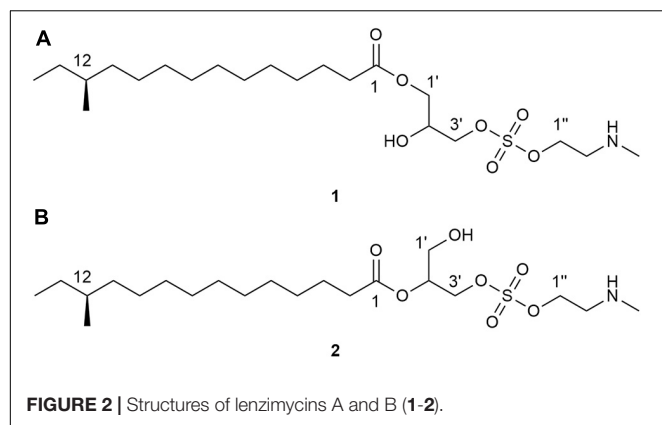
FIGURE 1 | A specimen *Onthophagus lenzii*.

of PTH23 strain and chromatographic purification combined with a series of bioassay tests discovered two novel sulfated amino lipid antibiotics, lenzimycins A and B (**Figure 2**), which were also effective against some nosocomial human pathogenic bacteria such as *Staphylococcus aureus*, *Enterococcus faecium*, and *Enterococcus faecalis*. Furthermore, we also elucidated the structures and evaluated the biological functions of lenzimycins A and B (1-2).

MATERIALS AND METHODS

General Experimental Procedures

Optical rotations were measured using a JASCO P-2000 polarimeter with a 1-cm cell. The ^1H NMR spectra were measured with the Bruker Avance III HD 850 MHz spectrometer at the National Center for Inter-University Research Facilities (NCIRF) at Seoul National University; the ^{13}C and 2D NMR spectra were recorded on the Bruker-800 MHz and JEOL JNM-ECA-600 MHz NMR spectrometers, respectively, at the College of Pharmacy, Seoul National University. Chemical shifts of all NMR spectra were referenced to the residual protonated solvent peaks for CDCl_3 ($\delta_{\text{H}}/\delta_{\text{C}}$, 7.26/77.0). Low-resolution electrospray ionization (ESI) LC/MS data were acquired on an Agilent Technologies 6130 quadrupole mass spectrometer coupled with an Agilent Technologies 1200-series HPLC. High-resolution fast atom bombardment (HR-FAB) mass spectra were obtained using a JEOL JMS-600W high-resolution mass spectrometer at NCIRF. High-resolution electrospray ionization (ESI) LC/MS and ESI MS/MS data were obtained using an AB SCIEX Q-TOF 5600 high-resolution mass spectrometer



at the National Instrumentation Center for Environmental Management (NICEM, Seoul, South Korea).

Collection of *Onthophagus lenzii* (Harold)

A specimen of *O. lenzii* used in this study was collected from the entrance of the Doksanseong Fortress, Osan-si, Gyeonggi-do Province, South Korea, in March 2016. The adult dung beetle was secured inside a container using a tweezer and immediately transferred to the laboratory at Seoul National University. The collected specimen had a body length 6–12 mm and a glossy black body color, based on which it was identified as the dung beetle, *Onthophagus (Strandius) lenzii* Harold, 1874 (Coleoptera: Scarabaeidae). *O. lenzii*, widely distributed throughout Asia including Korea, Japan, and China, is the most dominant species among the genus *Onthophagus* (Coleoptera: Scarabaeidae: Scarabaeinae) in Korea (Kim, 2012). The prevailing appearance period of adults occurs annually from April to October, as they emerge from underground after an overwintering adult stage. These are the environmental cleanup insects, which eat and decompose the feces of cows, horses, and other large mammals (Yasuda, 1986). Moreover, the females of *O. lenzii* (Harold) make brood rooms and lay eggs under cow dung pats.

Isolation of Bacterial Strains From the Dung Beetle

The regurgitated dark red excretion from the mouth of the dung beetle was scrapped by using a sterilized loop and a needle and diluted in 40 mL distilled water. The suspension was heated in a water bath at 55°C for 5 min. For bacterial isolation, 1 mL of the bacterial suspension was spread on each isolation agar medium (ISP1, ISP2, ISP4, CD, K, Chitin, and actinomycete isolation medium with cycloheximide) (Supplementary Table S1) and incubated at 30°C for 2 weeks. Based on their initial phenotypic observations, two types of colonies were selected and isolated from actinomycete isolation medium, and they were designated as PTH23 and CCARM924 (Supplementary Figure S15).

Identification and Phylogenetic Analysis of Bacterial Isolates

The genomic DNAs of the isolated strains, PTH23 and CCARM924, were extracted from the cell suspension cultures.

The 16S rRNA gene was amplified by PCR with the bacterial universal forward primer 27F and reverse primer 1525R (Xu et al., 2003), and sequenced. Subsequently, similarity searches for the 16S rRNA gene sequences of the isolates were performed by the EzBioCloud server¹ (Yoon et al., 2017) (GenBank accession number for PTH23: MT947196, and GenBank accession number for CCARM924: MT947187), and the phylogenetic analysis was performed by the neighbor-joining method (Saitou and Nei, 1987) in the MEGA 7.0 program package (Kumar et al., 2016). Kimura's two-parameter model was used to calculate the evolutionary distances (Kimura, 1980), and the bootstrap values were determined based on 1000 replications (Felsenstein, 1985).

Cultivation and Extraction of PTH23

Based on the inhibitory zones, the strain PTH23 was presumed to have inhibitory effects on the growth of CCARM924. Therefore, the PTH23 strain was further cultured on a large scale. First, the PTH23 strain was cultivated in 50 mL of ISP2 medium (4 g yeast extract, 10 g malt extract, and 4 g glucose in 1 L distilled water) in a 125-mL flask, and incubated for 2 days on a rotary shaker at 180 rpm at 30°C. Five milliliters of the broth culture was transferred to 200 mL of ISP2 medium in a 500-mL flask for initial scale up and incubated for 2 days on a rotary shaker at 160 rpm at 25°C. Then for the large-scale culture, 25 mL of the broth culture (obtained through initial scale up) was inoculated to 1 L of ISP2 medium in 2.8-L flasks (60 ea × 1 L, total volume 60 L) and incubated for 3 days on a rotator shaker at 160 rpm at 25°C. Further, the 60-L culture broth of the PTH23 strain was extracted with 90 L of ethyl acetate using a separation funnel. The residual water in the collected ethyl acetate layer was removed by adding anhydrous sodium sulfate. The extract was concentrated to dryness in a rotary evaporator *in vacuo* to obtain the final concentrated extract of 15 g.

Purification of the PTH23 Extract

The extract of PTH23 was absorbed onto Celite, then loaded on a 2 g Sep-Pak C₁₈ cartridge and fractionated with a step gradient solvent system (five fractions eluted with 100 mL each of MeOH-H₂O from 20 to 100%). This process was repeated ten times to fractionate all the extract. After fractionation, lenzimycins A and B (1-2) were detected in the 80% MeOH-H₂O fraction. The fraction eluted with 80% MeOH-H₂O was filtered with a syringe filter (Advantec, 25HP045AN) and purified by semi-preparative reversed-phase HPLC column (YMC triart C₁₈: 250 mm × 10 mm, 5 μm) with an isocratic solvent system [90% MeOH-H₂O, refractive index (RI) detection, flow rate: 2 mL/min]. The antibiotics lenzimycins A (1) (3 mg) and B (6 mg) (2) were eluted at 18 min and 16 min, respectively.

Lenzimycin A (1)

Colorless powder; $[\alpha]_D^{25}$ −5.2 (c 0.50, MeOH) IR (neat) ν_{max} 3274, 2924, 2853, 1735, 1633, 1464 cm^{−1}; ¹H and ¹³C NMR data, see Table 1; HRFABMS [M+H]⁺ *m/z* 454.2832 (calcd. for C₂₁H₄₄NO₇S, 454.2838, error: −1.4 ppm).

¹www.ezbiocloud.net/identify

TABLE 1 | ^1H and ^{13}C NMR spectral data for lenzimycins A and B (**1-2**) in CDCl_3 .

Position	1^a				2^b			
	δ_{C}	Type	δ_{H}	mult (J in Hz)	δ_{C}	Type	δ_{H}	mult (J in Hz)
1	173.8	C			173.3	C		
2	34.1	CH_2	2.30	t (7.7)	34.3	CH_2	2.30	t (7.0)
3	24.9	CH_2	1.60	m	24.9	CH_2	1.60	m
4–10	30.0–27.1	CH_2	1.31–1.23	m	30.0–27.1	CH_2	1.31–1.23	m
11	36.6	CH_2	1.27, 1.07	m	36.6	CH_2	1.27, 1.07	m
12	34.4	CH	1.28	m	34.4	CH	1.28	m
12-Me	19.2	CH_3	0.83	t (6.5)	19.2	CH_3	0.84	t (6.5)
13	29.5	CH_2	1.25, 1.12	m	29.5	CH_2	1.25, 1.12	m
14	11.4	CH_3	0.84	t (7.2)	11.4	CH_3	0.85	t (7.2)
1'	64.5	CH_2	4.11	m	59.8	CH_2	3.73	d (5.3)
2'	69.1	CH	3.98	m	72.5	CH	4.97	m
3'	68.1	CH_2	4.00, 3.90	m	63.4	CH_2	4.08	m
1''	61.6	CH_2	4.19	m	61.2	CH_2	4.20	m
2''	49.7	CH_2	3.15	m	49.9	CH_2	3.14	m
2''-NH			9.64	br s			9.73	br s
2''-N-Me	33.6	CH_3	2.70	s	33.7	CH_3	2.71	s

^a ^1H and ^{13}C NMR were recorded at 800 MHz and 200 MHz, respectively.
^b ^1H and ^{13}C NMR were recorded at 850 MHz and 212.5 MHz, respectively.

Lenzimycin B (2)

Colorless powder; $[\alpha]_{\text{D}}^{25} -1.0$ (c 0.95, MeOH) IR (neat) ν_{max} 3398, 2925, 2853, 1733, 1643, 1466 cm^{-1} ; ^1H and ^{13}C NMR data, see **Table 1**; HRFABMS $[\text{M}+\text{H}]^+$ m/z 454.2833 (calcd. for $\text{C}_{21}\text{H}_{44}\text{NO}_7\text{S}$, 454.2838, error: -1.3 ppm).

Acid Hydrolysis of Lenzimycin A (1)

To elucidate the absolute configurations of the fatty acid component, **1** (2.5 mg) was hydrolyzed in 0.5 mL of 6 N HCl and stirred at 120°C for 1 h. Then the reaction vial was cooled in an ice bath for 3 min. After the evaporation of the solvent *in vacuo*, the obtained dry material was dissolved in 0.5 mL of water and evaporated *in vacuo* for three times to remove residual HCl. The hydrolysate was purified by semi-preparative reversed-phase HPLC column (YMC triart C₁₈: 250 mm \times 10 mm, 5 μm) with an isocratic solvent system (90% MeOH- H_2O , RI detection, flow rate: 2 mL/min). The desired product eluted at 31 min and confirmed as (S)-12-methyltetradecanoic acid (**3**, 0.5 mg) using ^1H NMR and ESI-HRMS analyses.

(S)-12-Methyltetradecanoic Acid (3)

Colorless oil; $[\alpha]_{\text{D}}^{25} +5.6$ (c 0.33, CHCl_3) ESI-HRMS $[\text{M}-\text{H}]^-$ at m/z 241.2167 (calcd for $\text{C}_{15}\text{H}_{29}\text{O}_2$, 241.2162, error: 2.1 ppm) ^1H NMR (600 MHz, CDCl_3), δ_{H} 2.35 (2H, t, $J = 7.4$), 1.64 (2H, q, $J = 7.4$), 1.26 (17H, m), 1.12 (1H, m), 1.07 (1H, m), 0.86 (3H, t, $J = 7.4$), 0.84 (3H, d, $J = 6.4$).

Minimum Inhibitory Concentration Assays Using Lenzimycins and Other Antibiotics

To investigate the antimicrobial activity of **1** and **2**, a series of minimal inhibitory concentration (MIC) tests was performed against various microbial strains, mostly the well-known nosocomial pathogens (**Table 2**). The MIC evaluation

for the strains listed in **Table 2A** was carried out using a plate media dilution method (dilution range from 0.25 to 128 $\mu\text{g/mL}$) following the guidelines of Clinical Laboratory Standard Institute (Clinical and Laboratory Standards Institute [CLSI], 2018) and by using Mueller-Hinton I medium (BBL, Sparks, MD, United States). The MIC testing of the panel of four *E. faecalis* strains shown in **Table 2B** was performed in liquid culture using Brain Heart Infusion Broth (FLUKA). Several clinically important antibiotics, such as ampicillin, norfloxacin, vancomycin, teicoplanin, and bacitracin (Sigma-Aldrich) were used for comparative analysis of the antimicrobial activities of **1** and **2**.

Bioassays for Activity Against the Bacterial Cell Wall

To elucidate the mechanism of action of **1** and **2**, the cell wall stress bioassay was performed. For the assay, approximately 10^7 spores of the *Streptomyces coelicolor* reporter strain harboring plasmid pIJ6880 (Hong et al., 2002) were spread onto MMCGT agar medium supplemented with 80 $\mu\text{g/mL}$ kanamycin; then, lenzimycins A and B dissolved in DMSO were applied to paper disks, and incubated for 2–4 days at 30°C. The antibiotics vancomycin (10 μg) and bacitracin (50 μg) were used as positive controls, whereas novobiocin (50 μg), that acts by targeting the DNA gyrase enzyme, was used as a negative control. DMSO (5 μL) was included as a solvent blank.

Additionally, we also performed the vancomycin synergy assay. The vancomycin-resistant strain *S. coelicolor* wild type M600 was spread onto MMCGT agar containing either 0 $\mu\text{g/mL}$ or 10 $\mu\text{g/mL}$ vancomycin, and the antibiotics were applied to paper disks. The results were scored after 2–4 days of incubation at 30°C. Any change in diameter of the dark zone of inhibition around the white paper disks was assessed by comparing the results on the plates containing and lacking vancomycin.

TABLE 2A | Antibacterial activity of lenzimycins A and B (1-2) against a panel of bacterial species.

Number	Strain	Accession number	Remarks	MIC (μg/mL)			
				1 ^a	2 ^b	AMP ^c	NOR ^d
1	<i>Bacillus</i> sp.	CCARM 9248		64	8	16	0.12
2	<i>Bacillus cereus</i>	CCARM 0002		128	128	8	1
3	<i>Enterococcus faecalis</i>	CCARM 5171	susceptible ^e	> 128	> 128	2	1
4	<i>Enterococcus faecalis</i>	CCARM 5025	VRE ^e (<i>vanB</i>)	> 128	> 128	2	2
5	<i>Enterococcus faecium</i>	CCARM 5024	VRE ^e (<i>vanA</i>)	0.5	1	32	4
6	<i>Staphylococcus aureus</i>	CCARM 0205	susceptible	32	64	2	1
7	<i>Staphylococcus aureus</i>	CCARM 3855	susceptible	> 128	> 128	0.25	1
8	<i>Staphylococcus aureus</i>	CCARM 3089	MDR ^f	> 128	> 128	64	128
9	<i>Escherichia coli</i>	CCARM 0230		> 128	> 128	2	0.03
10	<i>Escherichia coli</i>	CCARM 0237		> 128	> 128	8	0.5
11	<i>Escherichia coli</i>	CCARM 0235		> 128	> 128	4	0.06
12	<i>Pseudomonas aeruginosa</i>	CCARM 0219		> 128	> 128	> 128	1
13	<i>Pseudomonas aeruginosa</i>	CCARM 0223		> 128	> 128	> 128	0.5
14	<i>Pseudomonas aeruginosa</i>	CCARM 0225		> 128	> 128	0.5	0.25
15	<i>Salmonella Typhimurium</i>	CCARM 0240		> 128	> 128	1	0.06
16	<i>Enterobacter cloacae</i>	CCARM 0252		> 128	> 128	> 128	0.06
17	<i>Enterobacter cloacae</i>	CCARM 0253		> 128	> 128	1	0.03
18	<i>Klebsiella oxytoca</i>	CCARM 0248		> 128	> 128	> 128	0.03
19	<i>Klebsiella aerogenes</i>	CCARM 0249		> 128	> 128	2	0.06
20	<i>Escherichia coli</i>	ATCC 25922	QC ^g strain	> 128	> 128	4	0.06
21	<i>Enterococcus faecalis</i>	ATCC 29212	QC ^g strain	> 128	> 128	0.5	2 ~ 8
22	<i>Enterococcus faecium</i>	ATCC 19434	QC ^g strain	16	8	0.5	–
23	<i>Pseudomonas aeruginosa</i>	ATCC 27853	QC ^g strain	> 128	> 128	> 128	1 ~ 4 ^h
24	<i>Staphylococcus aureus</i>	ATCC 29213	QC ^g strain	> 128	> 128	0.13	0.5 ~ 2 ^h
25	<i>Salmonella enteric</i>	ATCC 14028	QC ^g strain	128	128	0.13	–
26	<i>Klebsiella pneumoniae</i>	ATCC 10031	QC ^g strain	> 128	> 128	32	–

^a lenzimycin A, ^blenzimycin B, ^cAmpicillin, ^dNorfloxacin, ^eVancomycin-resistant Enterococci, ^fMultiple drug resistance, ^gQuality control, and ^hAcceptable range.

TABLE 2B | Antibacterial activity of lenzimycins A and B (1-2) against additional clinical isolates of Enterococci.

Strain	Remarks	MIC (μg/mL)				
		1 ^a	2 ^b	V ^c	T ^d	B ^e
<i>Enterococcus faecalis</i> JH2-2	Parent strain, vancomycin sensitive	3.1	1.6	25	3.1	25
<i>Enterococcus faecalis</i> BM4316	JH2-2::Tn1546, inducible resistance, VanA-type VRE ^f	4.2	10.4	> 100	> 100	83
<i>Enterococcus faecalis</i> JH2-2::I	JH2-2::Tn1549, inducible resistance, VanB-type VRE ^f	6.3	6.3	> 100	50	83
<i>Enterococcus faecalis</i> JH2-2::I C1	point mutation in <i>vanS</i> , constitutive resistance	4.2	6.3	100	83	83

^a lenzimycin A, ^blenzimycin B, ^cVancomycin, ^dTeicoplanin, ^eBacitracin, and ^fVancomycin-resistant Enterococci.

Bacitracin (B, 50 μg) was used as a positive control, whereas teicoplanin (T, 5 μg) was used as a control for antagonism. Kanamycin (K, 5 μg), which acts through inhibition of protein synthesis by targeting the 30S subunit of rRNA, was used as a negative control.

RESULTS AND DISCUSSION

Isolation of *Brevibacillus* sp. PTH23 From the Dung Beetle, *Onthophagus lenzii*

Two different types of isolates, PTH23, and CCARM9248, were identified from the excretion of the *O. lenzii*. As

shown in **Supplementary Figure S15**, the colonies pertaining to PTH23 (middle of the clear circular zone of growth inhibition on the agar) inhibited the growth of CCARM9248, (growing around the zone of inhibition) on the isolation plate. Sequencing of the 16S rRNA genes and phylogenetic analysis revealed that the strains PTH23 and CCARM9248 shared high similarity with *Brevibacillus brevis* NBRC 15304^T (100%) and *B. thuringiensis* ATCC 10792^T (99.8%), respectively (**Supplementary Figures S16, S17**). We therefore designated them as *Brevibacillus* sp. PTH23 and *Bacillus* sp. CCARM9248. The zone of inhibition on the agar could be due to the production of antibiotic metabolites from *Brevibacillus* sp. PTH23 which inhibited the growth of the co-isolate, *Bacillus* sp. CCARM9248.

Identification and Structure Elucidation of Key Metabolic Inhibitors of *Bacillus* sp. CCARM9248, Lenzimycins, From the *Brevibacillus* sp. PTH23 Extract

The *Brevibacillus* sp. PTH23 extract was fractionated by C₁₈ reversed-phase column chromatography, and the fraction (80% MeOH-H₂O), which displayed antibacterial activity, was analyzed by LC/MS. The chemical profile of the fraction revealed the presence of two metabolites, which had the molecular ions [M+H]⁺ commonly at *m/z* 454 in low-resolution ESI-MS analysis. Then, these compounds were further purified and designated as lenzimycins A and B (**1-2**) (Figure 2). Lenzimycin A (**1**) was obtained as a colorless oil. Its molecular formula C₂₁H₄₃NO₇S, corresponding to one degree of unsaturation number, was deduced by the high resolution fast-atom bombardment mass spectroscopy (HR-FAB-MS) and NMR data (Table 1). The ¹H NMR spectra of **1** (in CDCl₃ at 800 MHz) identified one exchangeable proton (δ_H 9.64), seven protons attached to oxygenated carbons [δ_H 4.19 (2H overlapped), 4.11 (2H overlapped), 4.00, 3.98, and 3.90], five protons attached to a nitrogenous carbon [δ_H 3.15 (2H overlapped), 2.70 (3H)], twenty-three aliphatic protons (δ_H 2.30-1.12), and two aliphatic methyl groups (δ_H 0.84 and 0.83). The ¹³C and HSQC NMR data of **1** revealed the presence of one carbonyl carbon (δ_C 173.8), one oxymethine carbon (δ_C/δ_H 69.1/3.98), three oxymethylene carbons (δ_C/δ_H 68.1/4.00 and 3.90, 64.5/4.11, and 61.6/4.19), one methylene carbon bearing a nitrogen (δ_C/δ_H 49.7/3.15), twelve *sp*³ methylene carbons (δ_C/δ_H 36.6-24.9/2.30-1.23), one *N*-methyl group (δ_C/δ_H 33.6/2.70), and two methyl carbons (δ_C/δ_H 19.2/0.83 and 11.4/0.84) (Table 1).

Based on the COSY correlation analyses, three partial structures were elucidated. An array of COSY correlations from H₂-2 (δ_H 2.30) to the terminal methyl protons H₃-14 (δ_H 0.84) assembled a long lipophilic chain. The branch methyl group 12-Me (δ_C 19.2) was connected to C-12 (δ_C 34.4) by COSY correlation between H₃-12-Me (δ_H 0.83) and H-12 (δ_H 1.28). This connectivity was further confirmed by HMBC correlations from H₃-12-Me to C-11 (δ_C 36.6), C-12, and C-13 (δ_C 29.5). The HMBC correlation between H₂-2/C-1 (δ_C 173.8) finally identified this substructure as 12-methyltetradecanoic acid. Consecutive COSY correlations from H₂-1' (δ_H 4.11) to H₂-3' (δ_H 4.00 and 3.90) through H-2' (δ_H 3.98) established the three-carbon spin system from C-1' (δ_C 64.5) to C-3' (δ_C 68.1). Based on the ¹³C chemical shifts of C-1', C-2' (δ_C 69.1), and C-3', these carbons were deduced to bear oxygen, thus confirming the second partial structure as glycerol. COSY correlation between H₂-1'' (δ_H 4.19) and H₂-2'' (δ_H 3.15) established the connectivity between C-1'' (δ_C 61.6) and C-2'' (δ_C 49.7). A broad singlet NH proton (δ_H 9.64) showed COSY correlations with H₂-2'' and *N*-methyl protons (δ_H 2.70), thereby elucidating *N*-methyl ethanolamine which was supported by HMBC correlation from *N*-methyl protons to C-2'' (Figure 3A).

HMBC correlations further assembled these partial structures. The H₂-1'/C-1 HMBC correlation secured the connectivity between 12-methyltetradecanoic acid and glycerol through an ester linkage at the C-1' position, and explained the molecular

structure with C₁₈H₃₅O₄, which in combination with *N*-methyl ethanolamine (C₃H₈NO) accounted for C₂₁H₄₃NO₅ of **1**. Furthermore, the IR data showed a strong absorption at 1464 cm⁻¹ (Pretsch et al., 2008), thereby indicating the presence of a sulfate group, which was speculated to fit between the oxygenated terminal at C-3' and C-2'' by placing the sulfur and two oxygen atoms. This addition connected glycerol and *N*-methyl ethanolamine thus completed the planar structure of **1** (Figure 3A).

The NMR-based structure of lenzimycin A (**1**) was confirmed by HR-ESI-MS/MS analysis. C-O at C-3' and S-O bond connected at C-1'' were fragmented to yield the ion at *m/z* 397 by losing *N*-methyl ethanolamine; subsequently, it identified an ion at *m/z* 317 which represented the loss of the sulfate group along with *N*-methyl ethanolamine. Moreover, the mass difference between *m/z* 397 and 317 also confirmed the identity and location of a sulfate group, whereas, 12-methyltetradecanoic acid was represented by the ion at *m/z* 243 (Figure 3B).

Lenzimycin B (**2**) was obtained as a colorless oil, and its molecular formula was deduced to be C₂₁H₄₃NO₇S, [identical to lenzimycin A (**1**)] through HR-FAB-MS data. The ¹H and ¹³C NMR spectra of **2** displayed high similarity with those of **1** but the chemical shifts of the glycerol substructure (C-1'-C-3') were noticeably different between these. Lenzimycin B (**2**) showed ¹H signals at δ_H 4.97 (1H), 4.08 (2H), and 3.73 (2H) and ¹³C resonances at δ_C 72.5, 63.4, and 59.8 whereas lenzimycin A (**1**) displayed the corresponding protons at δ_H 4.11 (2H), 4.00 (1H), 3.98 (1H), and 3.90 (1H) and the carbons at δ_C 69.1, 68.1, and 64.5. Analysis of the HSQC NMR spectrum assigned all the C-H one bond correlations. Subsequent analysis of COSY and HMBC correlations assigned the three partial structures, 12-methyltetradecanoic acid, glycerol, and *N*-methyl ethanolamine, identical to **1**. The IR absorption at 1466 cm⁻¹ (Pretsch et al., 2008) also indicated the same sulfate group as lenzimycin A (**1**). Although mostly similar HMBC correlations were observed for the entire molecule of **2**, 12-methyltetradecanoic acid was connected to C-2' through an ester bond based on the crucial H-2' (δ_H 4.97)/C-1 (δ_C 173.3) HMBC correlation, which finally determined its structure as a regioisomer of **1** with a different substitution pattern in the glycerol moiety (Figure 3A).

Lenzimycins A and B (**1-2**) have two stereogenic centers in their structures. The absolute configuration of C-12 in 12-methyltetradecanoic acid was determined by acid hydrolysis of lenzimycin A (**1**) followed by measurement of the optical rotation. After acid hydrolysis, 12-methyltetradecanoic acid (**3**) was obtained and structurally confirmed by ¹H NMR and ESI-HR-MS analysis. The optical rotation value ([α]_D²⁵ +5.6) was consistent with that of (*S*)-12-methyltetradecanoic acid ([α]_D²⁵ +5.4) but opposite to the value of (*R*)-12-methyltetradecanoic acid ([α]_D²⁵ -5.8) (Hansen et al., 1953), clearly assigning a 12*S* configuration, whereas the other chiral center at C-2' remained unassigned. During purification and structure elucidation of the lenzimycins, it was observed that lenzimycin B (**2**) was converted to lenzimycin A (**1**) (Figure 3C). This could be due to the rearrangement of the fatty acid chain from the C-2' to the C-1' position as reported in other fatty acid glycerides (Biswas and Ganguly, 1960).

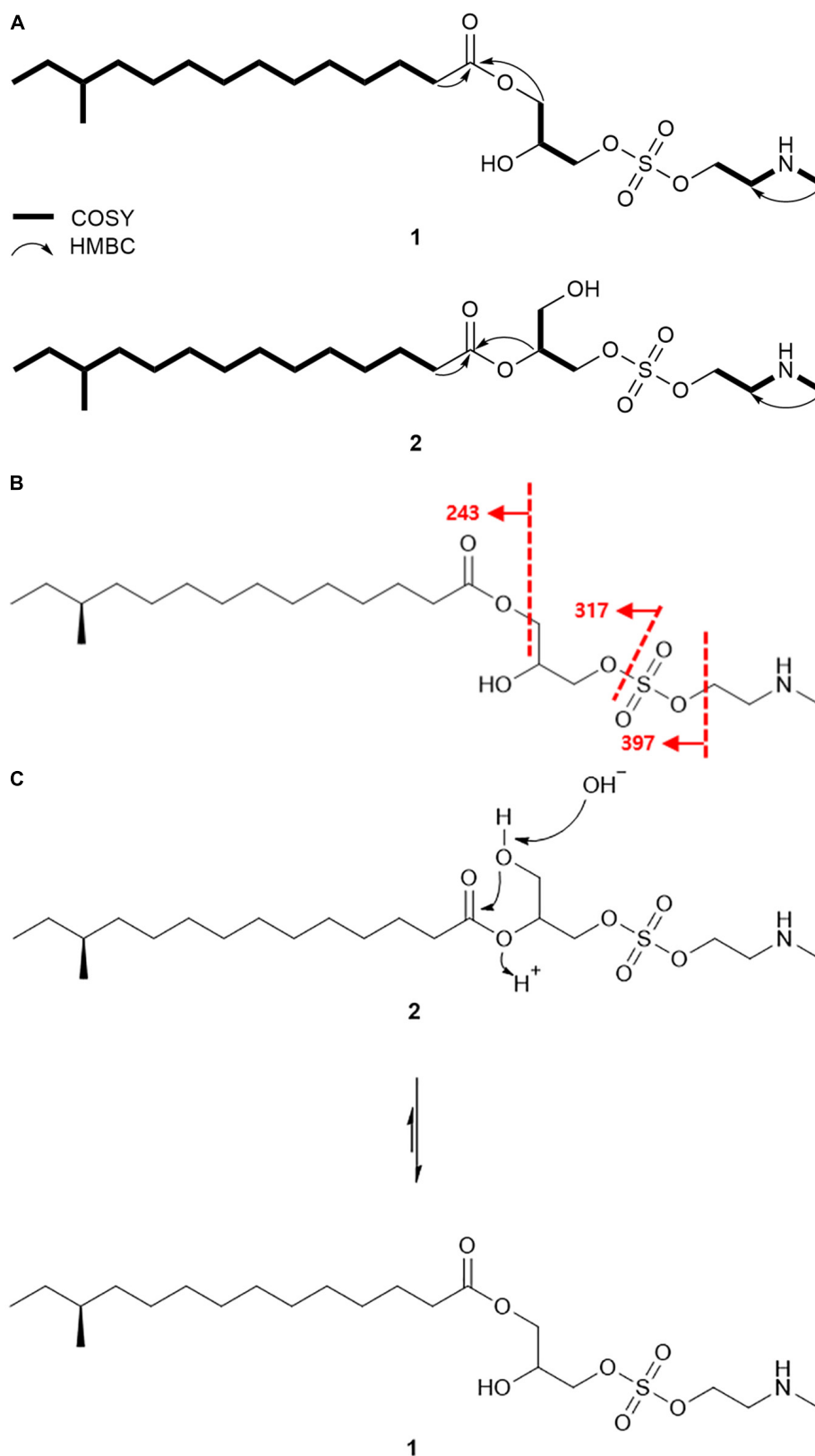


FIGURE 3 | Detailed analysis of planar structures of lenzimycins. **(A)** Key ^1H - ^1H COSY and HMBC correlations of lenzimycins A and B (**1-2**). **(B)** ESI-HR-MS/MS fragmentation of lenzimycin A (**1**). **(C)** Rearrangement between lenzimycins A and B (**1-2**).

Lenzimycins A and B (1-2) were structurally novel as evidenced by the unprecedented combination of fatty acid, glycerol, sulfate, and *N*-methyl ethanolamine, which has not been reported either as natural products or synthetic compounds. The partial combination of 12-methyltetradecanoic acid and glycerol in 1 reported as aggregeride A (Supplementary Figure S19), showing inhibitory activity against platelet aggregation, has been identified from a *Streptomyces* strain (Ōmura et al., 1986). However, to the best of our knowledge, fatty acid monoglycerides coupled with a sulfate group have not been reported as natural products, thereby indicating the novelty of the lenzimycins.

Antibiotic Activity of Lenzimycins

Even though the ecology of the oriental dung beetle *Onthophagus* species, including *O. lenzii*, is not well understood, it is clear that this dung beetle species is exposed to various entomopathogens in their habitat as they utilize microbe-rich feces of herbivores. *B. thuringiensis* is a representative entomopathogenic bacterium that is ubiquitously found in insect ecosystems. From the excretion of *O. lenzii* dung beetle, we isolated a potential symbiont of *Brevibacillus* sp. PTH23 and this bacterial strain seem to produce metabolites that inhibit the growth of entomopathogenic *Bacillus* species. Some metabolic agents isolated from *Brevibacillus* sp. are useful as a broad-spectrum treatment for Gram-positive bacteria, while some are even effective against Gram-negative bacterial infections (Hassi et al., 2012). We investigated the potential antibiotic activity of lenzimycins A and B against the *Bacillus* sp. CCARM9248. The estimated MIC values were 64 µg/mL and 8 µg/mL, respectively. Further, a panel of Gram-positive and Gram-negative bacteria that are mostly well-known nosocomial pathogens, including *E. faecalis*, *E. faecium*, *S. aureus*, *Escherichia coli*, *Pseudomonas aeruginosa*, *Klebsiella oxytoca*, *Klebsiella aerogenes*, *Klebsiella pneumoniae*, *Enterobacter cloacae*, *Salmonella enterica*, and *Bacillus cereus* were also tested to elucidate the broad range applicability of 1 and 2. The analyses showed markedly narrow-spectrum antibiotic effects as they were effective against only a few *Enterococcus* strains such as vancomycin-resistant *E. faecium* (VREF: *vanA*) with MIC values of 0.5 ~ 1.0 µg/mL, *E. faecium* ATCC 19434 with MIC values of 8.0 ~ 16 µg/mL, and an *S. aureus* strain CCARM 0205 with MIC values of 32 ~ 64 µg/mL (Table 2A).

To further define the anti-enterococcal activity of the lenzimycins, additional MIC tests were performed using a different set of four well-studied clinical isolates of *E. faecalis* that respond differently to the glycopeptide antibiotic vancomycin (Foucault et al., 2010). *E. faecalis* JH2-2 is a clinical isolate which possesses no vancomycin resistance system and is sensitive to glycopeptide antibiotics. *E. faecalis* JH2-2::I is a derivative of JH2-2 containing a transposon, Tn1549, which confers an inducible, VanB-type resistance to glycopeptide antibiotics. The related strain, *E. faecalis* JH2-2::I C1, exhibits a constitutive resistance to glycopeptide antibiotics due to a point mutation in the *vanS* gene of the parent JH2-2::I strain. *E. faecalis* BM4316 is another clinical isolate containing transposon Tn1546 that confers an inducible, VanA-type glycopeptide resistance. VanA- or -B type VRE are distinguished by their susceptibility toward the two glycopeptide antibiotics, vancomycin and teicoplanin. Both VanA- and B-type

VREs show high level, inducible resistance to vancomycin, but only the VanA-type is also highly resistant to teicoplanin, while the VanB-type shows teicoplanin sensitivity. This is believed to be due to the differences in how VanS senses the two different glycopeptide structures. VanS in VanA-type strains is activated in the presence of vancomycin, teicoplanin and other structurally unrelated cell wall-targeting antibiotics like moenomycin or bacitracin, while VanS in VanB-type strains is activated only by vancomycin and closely structurally related glycopeptides. The lenzimycins were found to be most active against the vancomycin-sensitive strain JH2-2 but also showed activity against both the inducible VanA- and VanB-type resistant strains, and the constitutively resistant JH2-2::I C1 strain (Table 2B). The growth of the other bacterial strains tested was not significantly affected except those of *B. cereus* CCARM 0002 and *S. enterica* ATCC 14028 which showed a weak inhibition (MIC = 128 µg/mL) (Table 2A).

Lenzimycins Induce Bacterial Cell Wall Stress

To investigate the activity of lenzimycins against the bacterial cell wall, a disk diffusion assay using a *S. coelicolor* reporter strain was performed. The reporter strain harbors a plasmid pIJ6880 that contains a *sigEp-neo* gene fusion construct designed to express the *neo* kanamycin resistance gene from a *sigE* promoter, which is inducible by cell wall stress (Hong et al., 2002). Growth in the presence of kanamycin, therefore, indicates cell wall stress, and this system has previously been used to provide a simple but effective bioassay screening tool to identify compounds which compromise the integrity of the bacterial cell envelope (Truman et al., 2014). In the disk diffusion assay, both lenzimycins A and B (1-2) stimulated the growth of the reporter strains, thereby indicating the bioactivity via weakening of the bacterial cell envelope (Supplementary Figure S18A). Interestingly, this activity was synergistic with the activity of the peptidoglycan biosynthesis inhibitor vancomycin in *S. coelicolor* which possesses an inducible VanB-type vancomycin resistance gene, *vanJ*, which is natively under the control of a vancomycin inducible promoter (Novotna et al., 2012; Supplementary Figure S18B). The findings suggested a different mode of action for the lenzimycins than that for vancomycin.

CONCLUSION

Chemical investigation of a *Brevibacillus* strain associated with the dung beetle, *O. lenzii*, revealed new antibiotic compounds, lenzimycins A and B (1-2). As the symbiotic interactions in the *O. lenzii* ecosystem have not been studied, it remains unclear whether the lenzimycins are the small molecules bridging microbial interactions in the dung beetle ecosystem. However, based on the antibiotic activity of the lenzimycins against *Bacillus* sp. CCARM 9248, most closely related to the entomopathogen *B. thuringiensis*, these compounds were shown to potentially have a protective role against general entomopathogenic bacteria that threaten the beetle's health. Structural elucidation of the lenzimycins A and B (1-2) revealed that these unique antibiotics

comprised unprecedented combination of a fatty acid, a glycerol, a sulfate, and an *N*-methyl ethanolamine moiety, which has not been reported in any natural and/or synthetic chemical compounds. Additionally, these new natural products exhibit antibiotic activity against some nosocomial human pathogenic bacteria including certain strains of *Enterococcus* that are resistant to the front-line glycopeptide antibiotic, vancomycin. Collectively, these results suggested the pharmaceutical potential of the lenzimycins. Furthermore, this study implicated that the chemical studies of insect-associated bacteria could be an effective research direction in the search for sources of novel natural antibiotics.

DATA AVAILABILITY STATEMENT

The original contributions presented in the study are included in the article/Supplementary Material, further inquiries can be directed to the corresponding author.

AUTHOR CONTRIBUTIONS

D-CO conceptualized the study. JA, S-HH, and SK cultured and isolated the compound. B-YK analyzed the phylogeny of the bacterial strains. DW collected the dung beetle specimen. S-HH,

DW, JA, JS, and D-CO performed spectroscopic analysis. H-JH, ES, K-BO, and JL designed and performed the microbial activity assays. S-IJ identified the beetle specimen. JA, S-IJ, JS, H-JH, and D-CO wrote and edited the text. All authors contributed to the article and approved the submitted version.

FUNDING

This work was supported by the National Research Foundation of Korea (NRF) grant fund by the Korean Government (Ministry of Science and ICT) (2018R1A4A1021703).

ACKNOWLEDGMENTS

The authors appreciate the significant help of the Culture Collection of Antimicrobial Resistant Microbes for antimicrobial assays against antibiotic resistant pathogens.

SUPPLEMENTARY MATERIAL

The Supplementary Material for this article can be found online at: <https://www.frontiersin.org/articles/10.3389/fmicb.2020.599911/full#supplementary-material>

REFERENCES

- Biswas, A. K., and Ganguly, D. (1960). Esterification of fatty acids with glycerol. *Nature* 188, 56–57. doi: 10.1038/188056b0
- Bode, H. B. (2010). “Insect-associated microorganisms as a source for novel secondary metabolites with therapeutic potential,” in *Insect Biotechnology*, ed. A. Vilcinskis (Dordrecht: Springer), 77–93. doi: 10.1007/978-90-481-9641-8_5
- Cantley, A. M., and Clardy, J. (2015). Animals in a bacterial world: opportunities for chemical ecology. *Nat. Prod. Rep.* 32, 888–892. doi: 10.1039/c4np00141a
- Clinical and Laboratory Standards Institute [CLSI] (2018). *Methods for Dilution Antimicrobial Susceptibility Tests for Bacteria that Grow Aerobically*, 7th Edn. Wayne, PA: Clinical and Laboratory Standards Institute.
- Felsenstein, J. (1985). Confidence limits on phylogenies: an approach using the bootstrap. *Evolution* 39, 783–791. doi: 10.2307/2408678
- Foucault, M. L., Depardieu, F., Courvalin, P., and Grillot-Courvalin, C. (2010). Inducible expression eliminates the fitness cost of vancomycin resistance in enterococci. *Proc. Natl. Acad. Sci. U.S.A.* 107, 16964–16969. doi: 10.1073/pnas.1006855107
- Hansen, R. P., Shorland, F. B., and Cooke, N. J. (1953). The branched-chain fatty acids of Mutton Fat. II. The isolation of (+)-12-methyltetradecanoic acid and of 13-methyltetradecanoic acid. *Biochem. J.* 53, 373–375.
- Hassi, M., Guendouzi, S. E., Haggoud, A., David, S., Ibsouda, S., Houari, A., et al. (2012). Antimycobacterial activity of a *Brevibacillus laterosporus* strain isolated from a moroccan soil. *Braz. J. Microbiol.* 43, 1516–1522. doi: 10.1590/s1517-83822012000400036
- Hong, H., Paget, M., and Buttner, M. (2002). A signal transduction system in *Streptomyces coelicolor* that activates expression of a putative cell wall glycan operon in response to vancomycin and other cell wall-specific antibiotics. *Mol. Microbiol.* 44, 1199–1211. doi: 10.1046/j.1365-2958.2002.02960.x
- Hwang, S., Kim, E., Lee, J., Shin, J., Yoon, Y. J., and Oh, D.-C. (2020). Structure revision and the biosynthetic pathway of tripartilactam. *J. Nat. Prod.* 83, 578–583. doi: 10.1021/acs.jnatprod.9b00819
- Kaltenpoth, M., Göttler, W., Herzner, G., and Strohm, E. (2005). Symbiotic bacteria protect wasp larvae from fungal infestation. *Curr. Biol.* 15, 475–479. doi: 10.1016/j.cub.2004.12.084
- DW, JA, JS, and D-CO performed spectroscopic analysis. H-JH, ES, K-BO, and JL designed and performed the microbial activity assays. S-IJ identified the beetle specimen. JA, S-IJ, JS, H-JH, and D-CO wrote and edited the text. All authors contributed to the article and approved the submitted version.
- Kim, J. I. (ed.) (2012). “Laparosticti (Arthropoda: Insecta: Coleoptera: Scarabaeoidea),” in *Insect Fauna of Korea*, (Incheon: National Institute of Biological Resources), 78–79.
- Kim, S.-H., Kwon, S. H., Park, S.-H., Lee, J. K., Bang, H.-S., Nam, S.-J., et al. (2013). Tripartin, a histone demethylase inhibitor from a bacterium associated with a dung beetle larva. *Org. Lett.* 15, 1834–1837. doi: 10.1021/ol4004417
- Kimura, M. (1980). A simple method for estimating evolutionary rates of base substitutions through comparative studies of nucleotide sequences. *J. Mol. Evol.* 16, 111–120. doi: 10.1007/bf01731581
- Kroiss, J., Kaltenpoth, M., Schneider, B., Schwinger, M.-G., Hertweck, C., Maddula, R. K., et al. (2010). Symbiotic streptomycetes provide antibiotic combination prophylaxis for wasp offspring. *Nat. Chem. Biol.* 6, 261–263. doi: 10.1038/nchembio.331
- Kumar, S., Stecher, G., and Tamura, K. (2016). MEGA7: molecular evolutionary genetics analysis version 7.0 for bigger datasets. *Mol. Biol. Evol.* 33, 1870–1874. doi: 10.1093/molbev/msw054
- Menegatti, C., Lourenzon, V. B., Rodríguez-Hernández, D., da Paixao Melo, W. G., Ferreira, L. L. G., Andricopulo, A. D., et al. (2020). Meliponamycins: antimicrobials from stingless bee-associated *Streptomyces* sp. *J. Nat. Prod.* 83, 610–616. doi: 10.1021/acs.jnatprod.9b01011
- Novotna, G., Hill, C., Vincent, K., Liu, C., and Hong, H.-J. (2012). A novel membrane protein, VanJ, conferring resistance to teicoplanin. *Antimicrob. Agents Chemother.* 56, 1784–1796. doi: 10.1128/aac.05869-11
- Oh, D.-C., Poulsen, M., Currie, C. R., and Clardy, J. (2009). Dentigerumycin: a bacterial mediator of an ant-fungus symbiosis. *Nat. Chem. Biol.* 5, 391–393. doi: 10.1038/nchembio.159
- Ōmura, S., Nakagawa, A., Fukamachi, N., Otaguro, K., and Kobayashi, B. (1986). Aggregeride, a new platelet aggregation inhibitor from *Streptomyces*. *J. Antibiot.* 39, 1180–1181. doi: 10.7164/antibiotics.39.1180
- Ortega, H. E., Ferreira, L. L., Melo, W. G., Olivera, A. L. L., Alvarenga, R. F. R., Lopes, N. P., et al. (2019). Antifungal compounds from *Streptomyces* associated with attine ants also inhibit *Leishmania donovani*. *PLoS Negl. Trop. Dis.* 13:e0007643. doi: 10.1371/journal.pntd.0007643
- Park, S.-H., Moon, K., Bang, H.-S., Kim, S.-H., Kim, D.-G., Oh, K.-B., et al. (2012). Tripartilactam, a cyclobutane-bearing tricyclic lactam from a *Streptomyces* sp.

- in a dung beetle's brood ball. *Org. Lett.* 14, 1258–1261. doi: 10.1021/ol300108z
- Pishchany, G., and Kolter, R. (2020). On the possible ecological roles of antimicrobials. *Mol. Microbial.* 113, 580–587. doi: 10.1111/mmi.14471
- Pretsch, E., Buhlmann, P., and Affolter, C. (2008). "IR spectroscopy," in *Structure Determination of Organic Compounds: Tables of Spectral Data*, 4th Edn, ed. E. Pretsch (Berlin: Springer), 304–307.
- Rodríguez-Hernández, D., Melo, W. G. P., Menegatti, C., Lourenzon, V. B., Nascimento, F. S., and Pupo, M. T. (2019). Actinobacteria associated with stingless bees biosynthesize bioactive polyketides against bacterial pathogens. *New J. Chem.* 43, 10109–10117. doi: 10.1039/c9nj01619h
- Saitou, N., and Nei, M. (1987). The neighbor-joining method: a new method for reconstructing phylogenetic trees. *Mol. Biol. Evol.* 4, 406–425.
- Truman, A. W., Kwun, M. J., Cheng, J., Yang, S. H., Suh, J.-W., and Hong, H.-J. (2014). Antibiotic resistance mechanisms inform discovery: identification and characterization of a novel amycolatopsis strain producing ristocetin. *Antimicrob. Agents Chemother.* 58, 5687–5695. doi: 10.1128/aac.03349-14
- Um, S., Bach, D.-H., Shin, B., Ahn, C.-H., Kim, S.-H., Bang, H.-S., et al. (2016). Naphthoquinone–oxindole alkaloids, coprisidins A and B, from a gut-associated bacterium in the dung beetle, *Copris tripartitus*. *Org. Lett.* 18, 5792–5795. doi: 10.1021/acs.orglett.6b02555
- Um, S., Park, S. H., Kim, J., Park, H. J., Ko, K., Bang, H.-S., et al. (2015). Coprisamides A and B, new branched cyclic peptides from a gut bacterium of the dung beetle *Copris tripartitus*. *Org. Lett.* 17, 1272–1275. doi: 10.1021/acs.orglett.5b00249
- Xu, P., Li, W. J., Xu, L. H., and Jiang, C. L. (2003). A microwave-based method for genomic DNA extraction from actinomycetes. *Microbiology* 30, 82–84.
- Yasuda, H. (1986). Fecundity of two dung beetle species, *Onthophagus lenzii* Harold and *Liatongus phanaeoides* Westwood (Coleoptera: Scarabacidae). *Appl. Ent. Zool.* 21, 177–179. doi: 10.1303/aez.21.177
- Yoon, S.-H., Ha, S.-M., Kwon, S., Lim, J., Kim, Y., Seo, H., et al. (2017). Introducing EzBioCloud: a taxonomically united database of 16S rRNA gene sequences and whole-genome assemblies. *Int. J. Syst. Evol. Microbiol.* 67, 1613–1617. doi: 10.1099/ijsem.0.001755

Conflict of Interest: The authors submitted a patent application for this work. B-YK was employed by the company ChunLab, Inc.

The remaining authors declare that the research was conducted in the absence of any commercial or financial relationships that could be construed as a potential conflict of interest.

Copyright © 2020 An, Hong, Somers, Lee, Kim, Woo, Kim, Hong, Jo, Shin, Oh and Oh. This is an open-access article distributed under the terms of the Creative Commons Attribution License (CC BY). The use, distribution or reproduction in other forums is permitted, provided the original author(s) and the copyright owner(s) are credited and that the original publication in this journal is cited, in accordance with accepted academic practice. No use, distribution or reproduction is permitted which does not comply with these terms.



Penicillium italicum: An Underexplored Postharvest Pathogen

Aline Midori Kanashiro¹, Daniel Yuri Akiyama¹, Katia Cristina Kupper² and Taícia Pacheco Fill^{1*}

¹ Institute of Chemistry, Universidade Estadual de Campinas, Campinas, Brazil, ² Advanced Citrus Research Center, Sylvio Moreira/Campinas Agronomic Institute, São Paulo, Brazil

OPEN ACCESS

Edited by:

Monica T. Pupo,
University of São Paulo, Brazil

Reviewed by:

Vito Valiante,
Leibniz Institute for Natural Product
Research and Infection
Biology, Germany
Samuel J. Martins,
University of Florida, United States

*Correspondence:

Taícia Pacheco Fill
taicia@unicamp.br

Specialty section:

This article was submitted to
Terrestrial Microbiology,
a section of the journal
Frontiers in Microbiology

Received: 15 September 2020

Accepted: 06 November 2020

Published: 04 December 2020

Citation:

Kanashiro AM, Akiyama DY,
Kupper KC and Fill TP (2020)
Penicillium italicum: An Underexplored
Postharvest Pathogen.
Front. Microbiol. 11:606852.
doi: 10.3389/fmicb.2020.606852

In the agricultural sector, citrus is one of the most important fruit genus in the world. In this scenario, Brazil is the largest producer of oranges; 34% of the global production, and exporter of concentrated orange juice; 76% of the juice consumed in the planet, summing up US\$ 6.5 billion to Brazilian GDP. However, the orange production has been considerable decreasing due to unfavorable weather conditions in recent years and the increasing number of pathogen infections. One of the main citrus post-harvest phytopathogen is *Penicillium italicum*, responsible for the blue mold disease, which is currently controlled by pesticides, such as Imazalil, Pyrimethanil, Fludioxonil, and Tiabendazole, which are toxic chemicals harmful to the environment and also to human health. In addition, *P. italicum* has developed considerable resistance to these chemicals as a result of widespread applications. To address this growing problem, the search for new control methods of citrus post-harvest phytopathogens is being extensively explored, resulting in promising new approaches such as biocontrol methods as “killer” yeasts, application of essential oils, and antimicrobial volatile substances. The alternative methodologies to control *P. italicum* are reviewed here, as well as the fungal virulence factors and infection strategies. Therefore, this review will focus on a general overview of recent research carried out regarding the phytopathological interaction of *P. italicum* and its citrus host.

Keywords: *Penicillium italicum*, virulence factors, natural products, pathogen host interaction, blue mold disease, blue mold

INTRODUCTION

Citrus is one of the most produced and exported fruit genus in the world (Liu et al., 2012; Papoutsis et al., 2019) being consumed *in natura* or as derived products. Many substances that constitute citrus fruits are essential for humans, being used in medicine and other sectors (Talibi et al., 2014; Al-snafi, 2016), such as flavonoids that have anti-cancer and anti-inflammatory properties (Benavente-García and Castillo, 2008). Brazil is the largest citrus producer and exporter in the world (Lopes et al., 2011; de Vilhena Araújo et al., 2019), mainly of oranges. The country produces 34% of the global orange production and 76% of the juice consumed in the world, generating about 200 thousand direct and indirect jobs, and a contribution to the Brazilian GDP of US\$ 6.5 billion (Neves and Trombim, 2017; Bazioli et al., 2019).

However, unfavorable climatic conditions in recent years (USDA, 2020), such as warm temperatures and below-average rainfall after the first two blooms and fruit set, and the increasing number of pathogen infections have triggered a considerable decrease in the orange production (**Figure 1**) (Palou et al., 2002; Tayel et al., 2015; Cunha et al., 2018; Yang et al., 2020). The resulting economic losses are estimated to account for up to 30 to 50% of all production (Singh et al., 2012; Vitoratos et al., 2013; Yun et al., 2013; Aloui et al., 2015; Wan et al., 2017; Youssef and Hussien, 2020).

Due to oranges acidic pH, around 4–5 in healthy fruits (Costa et al., 2019a), most of the orange rot is caused by fungi and not bacteria (Talibi et al., 2014). Phytopathogenic fungi can produce and proliferate mycotoxins, secondary metabolites of low molecular mass produced by filamentous fungi (Amadi and Adeniyi, 2009; Zain, 2011), which are often toxic to the host and other organisms that cohabit the same microenvironment (Zain, 2011; Dukare et al., 2019). Currently, more than 500 different mycotoxins have already been reported, including economically, and toxicologically relevant compounds that threat human and animal life such as: aflatoxins, trichothecenes, fumonisins, zearalenone, ochratoxin, and patulin (Bennett and Klich, 2003; CAST, 2003; Köppen et al., 2010; Medeiros et al., 2012). The FDA has estimated that more than half billion dollars have been invested in mitigating costs due to only three mycotoxins: aflatoxins, fumonisins, and trichothecenes (Bhatnagar et al., 2006).

The most harmful phytopathogenic fungi of oranges are *Penicillium digitatum*, which causes the green mold disease, responsible for about 90% of post-harvest losses (Costa et al., 2019b; Papoutsis et al., 2019), and *Penicillium italicum* Wehmer, the causing agent of the blue mold disease. The latter disease develops more slowly, however, it presents higher resistance to cold (Whiteside et al., 1993; Palou et al., 2002; Iqbal et al., 2012, 2017) and to low water availability (Plaza et al., 2003), easily spreading and contaminating a greater number of healthy oranges. The presence of wounds in the fruit surface is essential for infection by these fungi (Caccioni et al., 1998; Talibi et al., 2014).

Louw and Korsten (2015) noted that *P. italicum* caused significantly large lesions on ambient storage lemon fruit (33.9 ± 11 mm) being also able to cause smaller lesions (19.9 ± 11.0 mm) under cold-storage conditions ($86.4 \pm 4.5\%$ relative humidity). The lesions growth rates are 4.8 and 1.4 mm/day at ambient and cold conditions storage, respectively. Additionally, infections caused by *P. italicum* showed the first signs of lesion development under cold conditions after 12–13 days, while under ambient conditions, the first signs were observed after 2–3 days (Louw and Korsten, 2015). The symptoms of blue mold disease consist of a watery soaked fruit appearance, soft and discolored (due to the production of pathogenic hydrolytic enzymes such as polygalacturonase and glucosidase (Papoutsis et al., 2019), causing losses of smoothness in infected rind tissue and increasing susceptibility to mechanical damage (Louw and Korsten, 2015). As the white mycelium grows and extend deeper into the infected tissue, it later sporulates into blue conidia (Louw and Korsten, 2015). The infection's proliferation occurs

through the spread of fungal spores in the air, being only able to contaminate by direct contact with wounded healthy fruits before or after harvest (Kellerman et al., 2016; Papoutsis et al., 2019). The disease severity increases with fruit maturity. Temperature at the range of 20–25°C and high spore concentration in skin wounds also increases the severity of disease development (Papoutsis et al., 2019).

CONTROL METHODS

Concerning food waste and financial losses, some measures were taken to decrease post-harvest decay due to fungal infections, such as the one caused by *P. italicum*, in which chemical methods are the most used today. Currently, the main pesticides used to control *P. italicum* are sterol demethylase inhibitor (DMI) Zhang et al. (2019) fungicides, like Imazalil (IMZ), Pyrimethanil, Fludioxonil, and Tiabendazole, which are toxic chemicals that are harmful to the fruit and also to human health (Ragsdale and Sisler, 1994; Singh et al., 2012; Papoutsis et al., 2019). Studies demonstrated that *P. italicum* has developed higher resistance to these chemicals as a result of its continued use (Iwao, 1999; Arrebola et al., 2010; Tayel et al., 2015).

Fungal Resistance

Ghosoph et al. (2007), Hamamoto et al. (2000), and Kiralj and Ferreira (2008) elucidated the mechanism of IMZ resistance in *P. digitatum* as a unique sequence insertion in the PdCYP51 gene promoter region, resulting in an increased production of P450-dependant sterol 14- α -demethylase, affecting IMZ sterol demethylase inhibition capabilities (Erasmus et al., 2015; de Ramón-Carbonell and Sánchez-Torres, 2020).

To further understand the molecular basis of IMZ resistance, Zhang et al. (2020) analyzed the comparative transcriptome profile of two strains of *P. italicum* (Pi-R, highly resistant vs. Pi-S, highly sensitive to DMI fungicides) treated with prochloraz. Several differentially expressed genes were identified in Pi-R, which are probably associated with *P. italicum*'s DMI-resistance. Among them, ergosterol biosynthesis-related genes, such as ERG2, ERG11 (CYP51 isoform), and ERG6, which encodes a sterol isomerase, sterol 14- α -demethylase (Martel et al., 2010), and sterol methyltransferase, respectively. Besides those, ATP-binding cassette (ABC) transporter family proteins, multi-drug and toxic compound extrusion (MATE) family proteins and major facilitator superfamily (MFS) proteins have also been up-regulated in fungal resistance. Ergosterol biosynthesis related enzymes have been described as important factors to cycloheximide resistance in *Saccharomyces cerevisiae* (Abe and Hiraki, 2009). Similarly, the ABC transporter family and the MFS proteins were already reported as up-regulated in *P. digitatum* fungal resistance (Nakaune et al., 2002; Sánchez-torres and Tuset, 2011; Wang et al., 2012; Wu et al., 2016b). The similarities between transcriptomic analysis of resistant *P. italicum* and *P. digitatum* strains indicate common resistance factors in both citrus pathogens.

Other metabolism regulating enzymes are thought to play an important role in fungicide resistance. The cascade signaling regulator effect of the mitogen-activated protein kinase (MAPK)

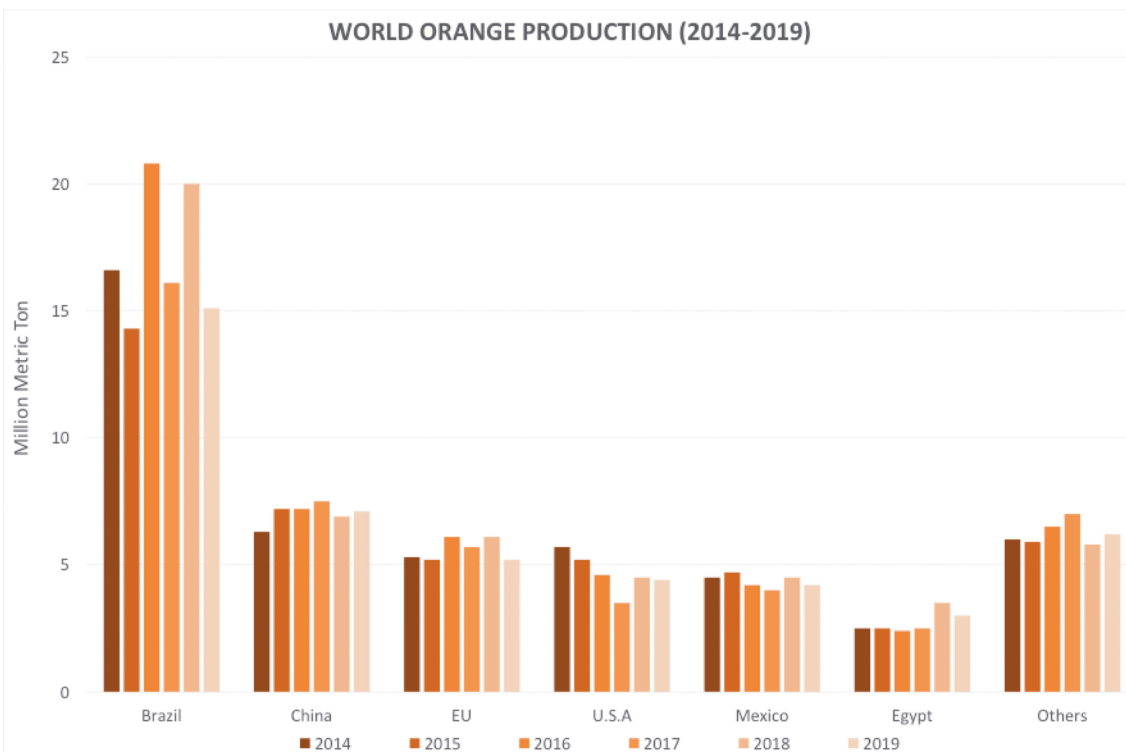


FIGURE 1 | Global orange production in the last 6 years. Source: (USDA, 2020). Accessed on: Jan. 27, 2020.

regulates a series of other important protein kinases, resulting in stress-induced cell wall remodeling regulation. To further support the importance of MAPK activity in fungicide resistance, Wang et al. (2014) reported that the Hog1-MAPK (PdOs2)-mediated cell wall integrity (CWI) signaling system is involved in *P. digitatum*'s resistance to fludioxonil and iprodione. Since Ca^{2+} and Ca^{2+} /calmodulin-dependent kinase (CaMK) are usually linked with MAPK pathway regulation, the overexpression of the CaMK2 gene was evaluated in *S. cerevisiae*, indicating facilitated resistance to azole-fungicides as well as fungal cell wall protective activity against oxidative and heat stresses (Dudgeon et al., 2008; Kumar and Tamuli, 2014). The MAPK/calcium signaling-related genes were once again up-regulated in prochloraz-treated Pi-R strains of *P. italicum*, indicating another important resistance factor in this species. Furthermore, Nicolopoulou-Stamati et al. (2016) confirmed the toxicity to human health of these fungicides, thus being necessary to develop other methods to control post-harvest fungi diseases.

To address this growing problem, the search for new methods of post-harvest phytopathogen control is being explored. Alternative methods for controlling the blue mold disease include the application of natural products (NPs) found in microbial or plant extracts and essential oils from plants (Table 1) (Solgi and Ghorbanpour, 2014; Trabelsi et al., 2016), the use of organic and inorganic salts (Youssef and Hussien, 2020), biocontrol methods, such as yeasts (Parafati et al., 2016; Cunha et al., 2018; Bazioli et al., 2019), and physical methods (Figure 2).

Natural Product and Plant Extract Applications

Several studies indicate that secondary phenolic metabolites, flavonoids, anthraquinones, acetaldehyde, alkaloids, allicin, benzaldehyde, benzyl alcohol, (E)-2-hexanal, ethanol, ethyl benzoate, ethyl formate, glucosinolates, hexanal, isothiocyanates, isoverbascocide, lipoxigenases, methyl salicylate, phenylpropanoids, quinones, saponins, sterols, tannis, terpenes, verbacocide play a considerable role in *P. italicum* fungal control (Palou et al., 2002; Askarne et al., 2012; Papoutsis et al., 2019). The isoprenoid citral, naturally produced by citrus fruits with two isomers, has been reported for its antifungal activity against *P. digitatum*, *P. italicum*, and *G. citri-aurantii*. Citral solutions and vapors in different concentrations have the ability to inhibit fungal growth, spore germination, and germ tube growth of these pathogens (Klieber et al., 2002; Droby et al., 2008).

Chen et al. (2019b) explored the antifungal capacity of the flavonoid pinocembroside, which is the main antifungal component present in the Chinese propolis, through optical and scanning electron microscopy (SEM) analysis to evaluate changes in hyphal morphology. Due to the low toxicity described, in addition to the higher antioxidant potential, and strong antibacterial properties, the compound could be applied as a promising method for the control of the blue mold disease. Studies have shown that the complete inhibition of

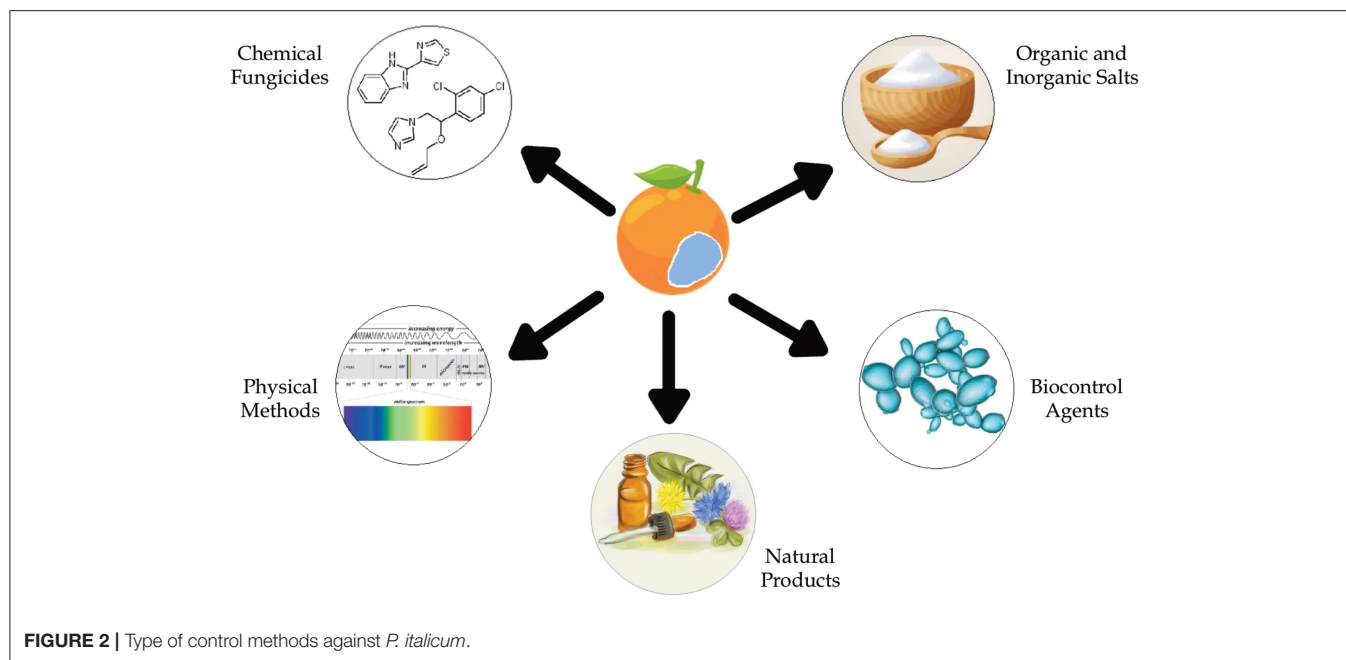
TABLE 1 | Alternative methods based in natural products (NPs) found in microbial or plant extracts and essential oils from plants.

Organism	Natural products	Minimum inhibitory concentration (MIC)	References
<i>Aspergillus</i> , <i>Penicillium</i> , or <i>Acetobacter</i> species	Kojic Acid (KA) combined with H ₂ O ₂	12.8 and 1.5 mm (KA and H ₂ O ₂ , respectively)	Kim and Chan, 2014
<i>Aspergillus terreus</i> SCSIO 41202	Sinulolide I, (9Z, 12Z)-N-(2-hydroxyethyl)-octadeca-9,12-dienamide, dodecanoic acid and decanoic acid	0.031-0.125 mg mL ⁻¹	Yang et al., 2020
<i>Bacillus pumilus</i> (<i>B. pumilus</i>)	Volatile Organic Compounds (VOCs): methyl isobutyl ketone, ethanol, 5-methyl-2-heptanone, and S-(-)-2-methylbutylamine	-	Morita et al., 2019
Chinese propolis	Pinocembrin	400 mg L ⁻¹	Peng et al., 2012
Chinese propolis	Pinocembroside	200 mg L ⁻¹	Chen et al., 2019c
<i>Citrus aurantium</i>	α -terpineol, terpinen-4-ol, linalool, and limonene	2.5 μ L mL ⁻¹	Trabelsi et al., 2016
Cinnamon bark (<i>Cinnamomum cassia</i> L.)	Cinnamaldehyde and eugenol	130–398.11 μ L mL ⁻¹	Kanan and Al-Najar, 2009
Citrus fruits	Citral	0.5 μ L mL ⁻¹	Droby et al., 2008; Tao et al., 2014b
Citrus fruits	Octanal	1.0 μ L mL ⁻¹	Klieber et al., 2002; Droby et al., 2008; Tao et al., 2014a
Garlic oil nanoemulsion (GO NE)	Dimethyl trisulfide, diallyl disulfide, diallyl sulfide, diallyl tetrasulfide, 3-vinyl-4H-1,2-dithiin, diallyl trisulfide, 1,4-dimethyl tetrasulfide, methyl allyl disulfide and methyl allyl trisulfide	0.01265%	Ding et al., 2014; Li et al., 2014; Li W.-R. et al., 2015; Long et al., 2020
<i>Laminaceae</i> spp.	Carvacrol and thymol	-	Pérez-Afonso et al., 2012
<i>Peganum harmala</i> L. (<i>harmal</i> seeds)	Harmine, harmaline, and tetrahydroharmine (THH) alkaloids	263.03–514.81 μ L mL ⁻¹	Kanan and Al-Najar, 2009
Pomegranate (<i>Punica granatum</i>) peel extract (PGE)	Phenolic compounds	-	Nicosia et al., 2016; Pangallo et al., 2017
<i>Populus euramericana</i> cv. "Neva" (poplar buds)	Flavonoids of pinocembrin, chrysin, and galangin	-	Yang et al., 2016
<i>Ramulus cinnamomi</i>	Cinnamic acid and cinnamaldehyde	-	Wan et al., 2017
<i>Sedum aizoon</i> L. (FSAL)	Gallic acid, quercetin and kaempferol	1.75 mg mL ⁻¹	Luo et al., 2020
<i>Streptomyces globisporus</i> JK-1	Dimethyldisulfide, dimethyltrisulfide and acetophenone	-	Li et al., 2010
<i>Thymus</i> species (<i>T. leptobotris</i> , <i>T. riatarum</i> , <i>T. broussonnetii</i> subsp. <i>hannonis</i> , and <i>T. satureioides</i> subsp. <i>pseudomastichina</i>)	Thymol, carvacrol, geraniol, eugenol, octanal, and citral	<500 μ L L ⁻¹	Boubaker et al., 2016
<i>Thymus leptobotris</i>	Thymol and carvacrol	-	Ameziane et al., 2007
<i>Thymus vulgaris</i> L.	Thymol	0.13 e 0.50 μ L mL ⁻¹ (mycelium growth and spore germination, respectively)	Vitoratos et al., 2013

P. italicum's mycelial growth by pinocembroside occurred at a minimum inhibitory concentration (MIC) of 200 mg/L, half the concentration required for the effect of both pinocembrin (Peng et al., 2012), and sodium dehydroacetate. Higher concentrations of the compounds 7-demethoxytylophorine (1.56 μ g/mL) (Chen et al., 2019b), citral (0.5 μ L/mL) (Tao et al., 2014b), and octanal (1.0 μ L/mL) (Tao et al., 2014a) were required for activity. Despite the known mechanism of action of flavonoids, which inhibit the mycelial growth mainly by causing cell membrane damage accompanied by the outflowing of certain intracellular components interrupting metabolic respiration and disturbing enzymes related to fungus energy production, the antifungal mechanisms of pinocembroside have not been fully elucidated. However, the authors suggest that the mechanism is related to changes in the cell membrane structure,

increasing permeability, accelerating lipid peroxidation and reducing the activity of antioxidant enzymes (Chen et al., 2019b,c).

Some bioactive compounds derived from fatty acids can also be effective in fungal growth control as they move easily into fungal cells to exert their toxic effects. In the study of the ethyl acetate extract from the marine-derived fungus *Aspergillus terreus* SCSIO 41202, Yang et al. (2020) found four bioactive compounds derived from fatty acids that had antifungal activity: sinulolide I, (9Z, 12Z)-N-(2-hydroxyethyl)-octadeca-9,12-dienamide, dodecanoic acid, and decanoic acid. The antifungal activity was related to the long aliphatic chain and the acidic group of these compounds, presenting MIC values between 0.031 and 0.125 mg/mL, indicating that these compounds may be an effective



alternative method for the control of *P. italicum* (Yang et al., 2020).

In addition, there are some volatile NPs produced by the fruit that collaborates with the fungus growth. According to Droby et al. (2008), the meroterpenes limonene, α -pinene, β -pinene and myrcene were stimulatory for *P. digitatum* and *P. italicum*, probably serving as host recognition signaling, since they also presented small inhibitory effect to non-citrus pathogens. Although these are promising results, it is necessary more studies concerning the basic biochemistry and molecular understanding of how these chemicals trigger germination or inhibition activities in *P. italicum* and *P. digitatum*. New studies on this phytopathological relationship are increasingly needed, since understanding the fungus-host interaction is an essential step in the development of new, safe, and efficient control methods.

In the general review of non-chemical methods used for prevention of postharvest fungal rotting caused by *P. digitatum* and *P. italicum*, Papoutsis et al. (2019) discovered that, in general, extracts from isolated or combined plants are promising fungicides with well-documented antifungal activity, low phytotoxicity, systemic mechanism of action, decomposability, and low environmental toxicity. Methanolic extracts from cinnamon bark (*Cinnamomum cassia* L.) and sticky fleabane leaves (*Inula viscosa* L.) have been associated with a high amount of phenols, flavonoids, and anthraquinones, while the antifungal activity of harmal seeds (*Peganum harmala* L.) has been attributed to its high concentration of phenolic compounds and alkaloids (Kanan and Al-Najar, 2009). Phenolic extracts from pomegranate (*Punica granatum*) peels didn't cause any phytotoxic syndrome in citrus, being an excellent candidate for fungal control (Nicosia et al., 2016; Pangallo et al., 2017).

In general, the molecular mechanisms involved in growth inhibition by plant extracts are: the inhibition of DNA gyrase, responsible for DNA biosynthesis, energy production metabolism and cellular respiration; inactivation of essential enzymes and the function of genetic material; and interference with membrane permeability, modification of the fungal cell structure. (Telezhemetskaya and D'yakonov, 1991; Cushnie and Lamb, 2005; Xu et al., 2011; Wu et al., 2013; Silva et al., 2014; Yang et al., 2016; Pangallo et al., 2017). In addition, plant extracts can stimulate the host's defensive responses, initiate oxidative stress and react with the pathogen's cell membrane proteins (Yang et al., 2016; Papoutsis et al., 2019).

The flavonoids from *Sedum aizoon* L. (FSAL), which are mainly composed of gallic acid, also contain significant amounts of quercetin and kaempferol, presenting antifungal activity against plant pathogens. Transcriptomic analyses performed by Luo et al. (2020) on *P. italicum* grown in the presence of FSAL indicated the flavonoids inhibitory activity against *P. italicum*. Eighty-three genes encoding plasma membrane and 23 genes related to the hyphal cell wall were differentially expressed in this study, resulting in cell wall disintegration and hyphal collapse. Furthermore, many critical oxidative stress resistance-encoding genes were up-regulated in the presence of FSAL, indicating an increase in reactive oxygen species (ROS) levels.

Another promising category of antifungal agents is antimicrobial peptides (AMPs), which are polypeptides synthesized by ribosomes and encoded by genes that are present in a range of organisms. Most AMPs are cationic, amphipathic and have low phytotoxicity (Wang et al., 2018). Wang et al. (2018) found that AMPs could reduce the growth of *P. italicum* *in vitro* by 70% or more and inhibit the progression of the disease *in vivo*, by changing the permeability of the cell membrane and the structure of the cell wall. Inhibition assays were performed

utilizing 64 μM of PAF56 (amino acid sequence: GHRKKFWF), and the molecular inhibition mechanism was confirmed. The peptide acts on fungal membranes and cell wall, resulting in fungal death. Essential Oils (EOs) are also showing excellent results against phytopathogens, as they are natural products safe to human health and to the ecosystem, in addition to producing low levels of traceable residues and having a smaller chance of inducing pathogen resistance since they contain several volatile substances, each with a different mechanism of action (Ameziane et al., 2007; de Moraes, 2009; Wu et al., 2016a; Papoutsis et al., 2019). Research using essential oils such as those obtained from *Cinnamomum zeylanicum*, *Citrus aurantium*, *Thymus vulgaris*, *Thymus leptobotris*, *Thymus riatarum*, *Thymus broussonnetii*, *Eugenia caryophyllata* Thunb, Bergamot, Thyme, Tea tree, and *Thymus capitatus* may be promising to inhibit *P. italicum* (Palou, 2014; Boubaker et al., 2016; Chen et al., 2019a; Dukare et al., 2019; Papoutsis et al., 2019). Also, thymol, carvacrol and the mixture of both (Pérez-Afonso et al., 2012) proved to be effective in controlling this fungus. In their experiments with oranges, Li et al. (2010) found that the volatile organic compounds (VOCs) produced by *Streptomyces globisporus* JK-1 dimethyl trisulfide and acetophenone showed effective inhibitory activity *in vitro* and *in vivo*, being the first study to confirm such antifungal action. VOCs produced by bacterial strains have been reported to inhibit fungal mycelial growth and, in some cases, to be responsible for the induction of plant resistance in stressed hosts (Girón-Calva et al., 2012; Martins et al., 2019).

Other studies confirmed the antifungal effects of Garlic Oil (GO) (Li et al., 2014; Long et al., 2020), which is rich in organosulfur compounds, mono to hexa diallyl sulfides and vinyl dithiin isomers, such as dimethyl trisulfide, diallyl disulfide, diallyl sulfide, diallyl tetrasulfide, 3-vinyl-4H-1,2-dithiin, diallyl trisulfide, 1,4-dimethyl tetrasulfide, methyl allyl disulfide, and methyl allyl trisulfide. However, the low stability, high volatility, and hydrophobic properties limit GO applications for antifungal studies, in addition to having antioxidant activity, which aids the development of fungal infection. To work around these problems, Long et al. (2020) formulated a GO nanoemulsion (NE) through ultrasonic technique. This method allows increased bioavailability of GO as well as reducing the cost of sterilization. The NE was composed of the surfactants Span 80 and Tween 80 (Smix), which do not show antifungal activity in the absence of GO. Research involving GO NE as an antifungal controller managed to reveal its antifungal mechanism on *P. italicum* based on structural and molecular analyses, using micro-confocal and surface-enhanced Raman spectroscopy that showed the inhibition of mycelia in the medium and the destruction of membranes and the cell wall of the fungus. On the other hand, the authors are still looking for alternatives to remove the strong odor of garlic to make it applicable on a commercial scale.

Another possibility for controlling the blue mold disease is the use of chemosensitizing antifungal agents combined with oxidative stressors. In the studies conducted by Kim and Chan (2014), the antifungal efficacy of Kojic Acid (KA) produced by certain filamentous fungi of the *Aspergillus* and *Penicillium* genera (Liu et al., 2014) was analyzed considering different treatment temperatures in the presence or absence of H_2O_2 .

In treatments at relatively high temperatures (35–45°C) H_2O_2 was more efficient, however, at higher temperatures (55°C) this efficiency decreases. KA, on the other hand, does not change its effectiveness with increasing temperature. As KA induces the generation of reactive oxygen species in cells, such as in macrophages, stimulating phagocytosis, the combined chemosensitization (KA + H_2O_2) generated high oxidative stress, possibly being the mechanism of increased activity resulting from this combination. Studies have shown that H_2O_2 damages the cellular integrity of *P. italicum* strains, inhibiting the cell division cycle, in the antioxidant defense and metabolism of the fungus. In short, the combined treatment of KA and H_2O_2 can be promising in the control of fungal pathogens, since KA is a safe natural compound, as demonstrated by Fickova et al. (2008) through cytotoxic assays, being used in cosmetic products and medicines (Niwa and Akamatsu, 1991; Fickova et al., 2008; Rodrigues et al., 2011; Kim and Chan, 2014; Liu et al., 2014; Saedi et al., 2019). Moreover, the treatment can be done in considerably low temperatures, which reduces damage to crops, the environment and health. However, it should be considered the lack of sensitivity of several strains of *P. italicum* to this treatment, explained by the fact that KA is produced by different strains of *Penicillium*.

The study of Morita et al. (2019) explored bacteria that produce volatile organic compounds as biocontrol agents. The TM-R strain of the gram-positive bacterium *Bacillus pumilus* (*B. pumilus*) showed the greatest antifungal activity among 136 bacterial isolates. Small and large-scale tests were performed on four types of agar (Nutrient Agar—NA, Tripto-Soya Agar—TSA, Luria-Bertani Agar—LBA, and TM Enterprise Agar—TMEA). Despite the limitations to identify VOCs due to their low concentrations, complexity of their compositions and differences of the culture medium, four predominant VOCs were detected and correlated to the antifungal activity, namely: methyl isobutyl ketone, ethanol, 5-methyl-2-heptanone, and S-(–)-2-methylbutylamine. Regarding the antifungal effect, *B. pumilus* TM-R was able to inhibit from 95 to 100% (depending on the medium) of the growth of *P. italicum* in the plaque test and 93% in the large-scale test in TMEA. Since it does not produce hemolysin or DNase, *B. pumilus* TM-R has a high chance of not being pathogenic to humans, which makes it very promising in commercial applications. In addition, this study proved that the bacteria promoted the growth of one of the tested fungus species (*Aspergillus niger*), which obtained growth values of 36% in the 12 L TMEA test and 9% in the plaque test, which can be a potential problem in antifungal treatment if it stimulates the growth of another citrus pathogen not studied.

Organic and Inorganic Salts

In the United States, the use of sodium carbonates and bicarbonates is allowed to control mold, however, the disposal of the used substances proved to be a problem due to their high pH, sodium content and conductivity of sodium carbonate (Smilanick et al., 2008; Li et al., 2010). Potassium sorbate, ammonium bicarbonate, calcium polysulfide, sodium ethyl paraben and sodium hydrosulfide also had their antifungal activities tested (Papoutsis et al., 2019). In fact, the mechanism

TABLE 2 | Biocontrol methods against *P. italicum*.

Antagonist agent	Mechanism of action	References
<i>Candida oleophila</i>	Increase phenylalanine ammonia lyase activity and accumulation of the phytoalexins such as umbelliferone, scoparone, and scopoletin, which led to resistance induction.	Droby et al., 2002; Liu et al., 2019
<i>Candida stellimalicola</i>	"Killer" activity, inhibition of conidial germination, and stimulates production of chitinase.	Cunha et al., 2018
<i>Cryptococcus laurentii</i> associated with cinnamic acid	Loss of membrane integrity which led to leakage of cytoplasmic materials and death of the fungal pathogen	Li J. et al., 2019
<i>Debaryomyces hansenii</i>	Competition for space and nutrients	Droby et al., 1989; Chalutz and Wilson, 1990; Hernández-Montiel et al., 2010
<i>Kazachstania exigua</i> and <i>Pichia fermentans</i>	"Killer" activity	Comitini et al., 2009
<i>Metschnikowia citriensis</i>	Iron depletion, biofilm formation, and adhesion to mycelia.	Liu et al., 2019
<i>Metschnikowia pulcherrima</i> , and <i>Aureobasidium pullulans</i>	Competition for nutrients and influence in superoxide dismutase and peroxidase activities, which led to fruit resistance induction.	Parafati et al., 2016
<i>Pseudozyma antarctica</i>	Direct parasitism, which causes fungal cell wall degradation.	Liu et al., 2019
<i>Saccharomyces cerevisiae</i>	"Killer" activity and competition for space and nutrients	Comitini et al., 2009; Platania et al., 2012; Kupper et al., 2013; Cunha et al., 2018
<i>Saccharomycopsis schoenii</i>	Predation, competition for nutrients and other antagonistic interactions	Pimenta et al., 2008
<i>Wickerhamomyces anomalus</i> (or <i>Pichia anomala</i>)	"Killer" activity based on β -glucanase production, competition for nutrients, fruit resistance induction, and antibiosis.	Comitini et al., 2009; Platania et al., 2012; Aloui et al., 2015; Parafati et al., 2016

of action of these salts has not been determined yet, which have greater efficacy when associated with other methods. However, the osmotic stress generated by high concentrations of salts applied to the fruit can decrease fungal population, in addition to influencing the growth of the pathogen as fungi thrive best at acidic and neutral pH. These salts combined with waxes or other antifungal methods can induce an increase in SOD (superoxide dismutases) (Parafati et al., 2016), PAL (phenylalanine ammonia lyase) (Chen et al., 2019a), CHI (chitinase) (Pangallo et al., 2017; Chen et al., 2019a), ROS (reactive oxygen species) (Pangallo et al., 2017), and β -1,3-glucanases levels (Santos et al., 1978, 1979).

Biocontrol Agents

Recent studies increasingly indicate that the products generated by biocontrollers are promising agents in the antifungal activity, being safe for the environment and to human health (Table 2). Killer yeasts can secrete lethal protein toxins or low molecular weight glycoproteins to other susceptible yeasts (Aloui et al., 2015), fungi and filamentous bacteria (Pimenta et al., 2008). The advantages of using killer yeasts as biocontrol agents are based on their adaptive characteristics, the low cost to quickly produce large amounts of yeast, the absence of the production of toxic compounds and the ability to colonize and survive on the fruit surface for a long period of time and in various environmental conditions. These advantages make killer yeasts possibly better antagonists than other sources, acting by adhering to the specific site, such as other yeasts or pathogenic cells, and forming colonies in the wound that compete with the fungus for nutrients. They secrete specific enzymes and antimicrobial substances, which can be soluble or volatile, and so they help to inhibit the pathogen, by forming a biofilm on the inner surface of the wounds, which act as a protective layer so that

the fungus cannot progress the infection process (Liu et al., 2019). The efficiency of the yeast *Saccharomycopsis schoenii* (*S. schoenii*) against three phytopathogenic species of *Penicillium* was evaluated, with a 35.7% reduction in the severity of the disease in oranges. Despite some desirable effects of *S. schoenii* as a fungal controller, a high concentration of this yeast was necessary for its effectiveness, as also demonstrated in other yeast species (Pimenta et al., 2008). According to Ferraz et al. (2016), the yeast *Candida azyma* presented potential as a biological control agent against *G. citri-aurantii* and ability to produce killer toxin, as a mechanism of action. To Cunha et al. (2018), the killer activity from *C. stellimalicola* strains might be the main action mechanism involved in *P. italicum* biocontrol, when these yeasts were preventively applied on citrus fruits for the blue mold control.

In another analysis with biocontrol agents, Perez et al. (2016) isolated 437 strains of native yeasts from leaves and fruits of citrus plants as well as water from washing lemon peels, in order to investigate the Killer potential against citrus pathogens. The study identified, through the analysis of the D1/D2 sequence of the 26S rDNA gene, six different genera: *Pichia* (8.1%), *Saccharomyces* (13.5%), *Kazakhstan* (40.5%), *Wickerhamomyces* (2.7%), *Clavispora* (8.1%), and *Candida* (21, 7%). Three types of analysis were performed for determining how many strains had the killer phenotype: eclipse assay (22 strains—5%), diffusion plate technique (30 strains—6.9%), and diffusion plate with addition of NaCl 2% (37 strains—8.5%). As the pH proved to be of vital importance for the killer activity, these analyses were carried out at a pH equal to 4.5, which showed to be another advantage, since the pH of the infected fruit becomes more acidic (around 5). Regarding the antifungal effect, 11 strains of *P. italicum* had growth inhibition of $\geq 40\%$; 18 strains were

inhibited between 16 and 39%; and the remaining 8 strains showed $\leq 15\%$ inhibition. *S. cerevisiae* (137) and *Kazachstania exigua* (120) strains showed protective properties against the attack of *P. italicum*. The authors also managed to define that the killer and resistance genes were located on the same plasmid (~ 4 kb in size) and concluded that despite the positive results, more studies should be performed since species such as *Candida catenulata*, *Candida Pararugosa*, and *Clavispora lusitaniae* are related to infections in immunocompromised patients.

Physical Applications

In addition to these methods involving plant extracts, salts and biocontrol agents, new alternatives involving physical methods are being analyzed and tested for the control of post-harvest pathogens. One involves ionizing irradiation, such as gamma and x-ray, and non-ionizing irradiation, such as UV and Blue Light irradiation (Papoutsis et al., 2019). The fruit is exposed to a certain distance from a lamp that radiates UV for a certain period, with varying intensity of treatment. Many studies have focused on the treatment with UV-B and UV-C, however, at high intensities, the latter can alter the fruit's flavor and affect its quality. UV-B presents less harmful effects compared to UV-C, which reduces the incidence of blue mold. The mechanisms of action of UV irradiation are divided between direct, due to the absorption of radiation by the surface of the fungus that inactivates its conidia, and indirect, by the induction of metabolic and anatomical alterations in the citrus flavedo, increasing the resistance of the fruit against the pathogen, making their cell walls thicker (Yamaga et al., 2016; Ruiz et al., 2017; Papoutsis et al., 2019). In addition, after treatment, there is an accumulation of polyphenols and phytoalexins in the flavedo, which are secondary metabolites with antifungal activities. Although the mechanisms of action of Blue Light (which radiates between 400 and 500 nm) have not been clarified yet, some authors suggest that there are direct and indirect actions such as UV irradiation, which damages the morphology and sporulation of the fungus and regulates the metabolic pathways of plant tissues via up-regulated expression of the phospholipase A2 (PLA2) gene. Concerning ionizing irradiations, gamma irradiation is a promising treatment because it is able to delay the ripening of the fruit, since it inhibits ethylene production, as well as the respiration rate, which regulates the enzymatic activity related to the elimination of free radicals. Thus, the gamma irradiation penetrates the fungus, damaging its physiology. However, this treatment impairs the quality of the fruit and there are not many studies on its action concerning *P. italicum*. In addition, it is a strategy with high public resistance and fear of application, due to the popular negative view on this type of irradiation. In this sense, further analysis is still needed to reduce the treatment's impact in the fruit, in addition to promoting greater acceptance by the population about the potential benefits of gamma irradiation. The ionizing x-ray irradiation promotes water photolysis, generating free hydroxyl and hydrogen radicals, stimulating physiological functions in living organisms (Vaseghi et al., 2018; Papoutsis et al., 2019). Furthermore, x-rays can induce the synthesis of antifungal NP such as phytoalexins, scoparone, and scopoletin, but their effectiveness is dependent

on the combination with carbonic acid salts (Palou et al., 2007; Rojas-argudo et al., 2012; Papoutsis et al., 2019). Like gamma irradiation, the x-ray is not a well-regarded method and will possibly work better in association with other methods, which still need to be explored (Papoutsis et al., 2019). Finally, the last physical method discussed by Papoutsis et al. (2019) is the treatment with hot water, which is already used to reduce the deterioration caused by pathogens and to increase the useful life of the fruit. The fruits can be dipped or sprayed with hot water (52–53°C and 62°C, respectively), which can instigate the accumulation of CHI and β -1,3-glucanases and disinfect the fruit from the spores of *P. italicum*.

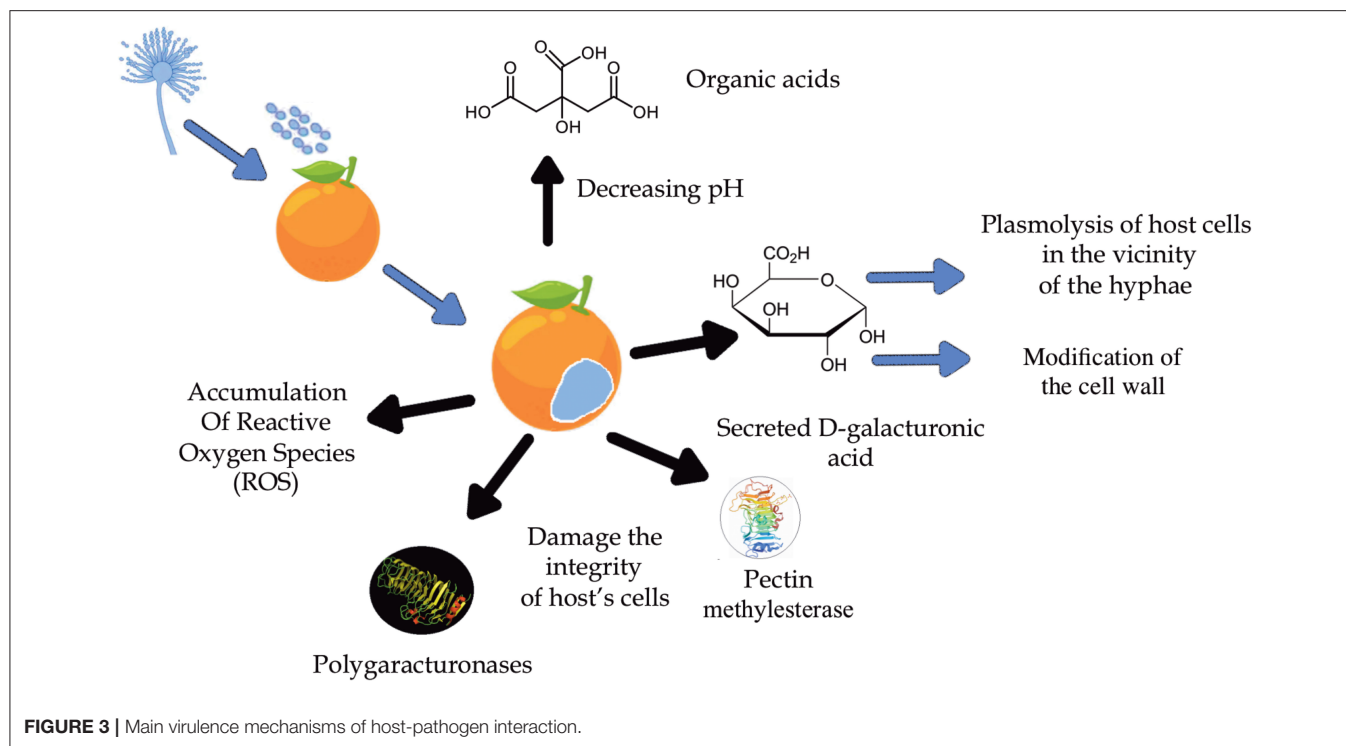
In general, these studies established the basis for better understanding some mechanisms of antifungal treatment, as well as several promising possibilities for the control of the blue mold disease (Luo et al., 2020). However, although there are many promising alternatives, there are none that have the same efficiency as the current commercialized chemicals (Palou et al., 2002; Talibi et al., 2014) and there are not enough studies to prove that the exchange of chemical compounds currently used by physical and biological alternatives have satisfactory efficacy, well-documented antifungal activity, low phytotoxicity, and environmental toxicity, economic and process viability (Papoutsis et al., 2019).

Papoutsis et al. (2019) proposes some parameters to be considered in order to develop new antifungals: (a) being effective even after a short treatment period, (b) the quality of the fruit should not be negatively affected, (c) the minimum effective dose must be considerably low, (d) the efficacy of the product cannot be affected by external conditions, (e) low residual activity, in addition to being non-toxic to human health, and (f) not having ample fungal activity against multiple phytopathogens. In addition, the authors also point out that there should be acceptance of the new control methods by consumers so that there are no significant drops in consumption (Talibi et al., 2014).

Furthermore, *P. italicum* is more resistant to the described antifungal compounds, such as essential oils from citrus fruits (Caccioni et al., 1998) and from some plant extracts (Vitoratos et al., 2013), which instigates the need to focus attention on this mold, once that there are few studies aimed at trying to understand the mechanisms of infection of this phytopathogen, the NPs produced *in vivo* during infection and their possible toxicities against the host and human health.

VIRULENCE FACTORS

In order to develop new and safer strategies for effective fungal control against the blue mold disease, it is important to understand the molecular mechanisms of the fungi-host interactions (Figure 3), as well as the pathogenicity and disruption of the fruit's defensive systems (Cheng et al., 2020). Regarding infection in orange, the main virulence and colonization factor known in this phytopathological interaction are promoted by the hydrolytic enzymes polygalacturonases (PG) produced by *P. italicum* and by other fungi that cause tissue maceration or fruit rot (Prusky et al., 2004; Papoutsis et al., 2019).



These enzymes work better at lower pH and, since *P. italicum* is able to acidify the environment with the accumulation of organic acids, especially citric acid, the activity of these enzymes is favored during infection (Prusky et al., 2004). This knowledge suggests that pH is a regulator of gene expression, as it ensures that genes encoding extracellular enzymes are expressed, such as the PEPG1 of the polygalacturonase (PG) enzyme (Prusky et al., 2004). In addition to PG, the enzymes pectate lyase (PL) and pectin lyase (PNL) are also responsible for fruit tissue maceration. However, instead of catalyzing hydrolytic cleavage as PG does, PL and PNL act by splitting the α -glycosidic bond between galacturonic acid residues by trans elimination (Alana et al., 1990). Although *P. italicum* produces only one type of PNL, this strategy seems to be more effective since PNL has a greater stability compared to the others, being active in different culture media and a wide temperature and pH range, proving to be important in the process pathology of *P. italicum* (Alana et al., 1990).

Li T. et al. (2019) suggested in their studies that the modification/degradation of the cell wall caused by enzymatic and non-enzymatic factors is a crucial strategy for the infection of the fruit promoted by *P. italicum*. Increased bioactivities of both PG and pectin methylesterase (PME) and the increased expression levels of xyloglucan endotransglucosylases/hydrolases (XTH) help disassemble the cell wall and damage the integrity of the host's cells. The modification of the cell wall polysaccharides was indicated by the decrease in acid-soluble pectin (ASP) and hemicellulose as well as the increase in water-soluble pectin (WSP), all symptoms caused by the infection of *P. italicum*. The accumulation of reactive oxygen species (ROS) is also observed,

promoted by the reduction of antioxidant metabolites as well as the activity of antioxidant enzymes such as superoxide dismutase (SOD), catalase (CAT), peroxidase (POD) (Chen et al., 2019a), and ascorbate peroxidase (APX).

Furthermore, histopathological studies in the tissues of citrus peels infected by both *P. italicum* and *P. digitatum* showed extensive demethylation of pectin, edema of the cell wall and plasmolysis of cells in the vicinity of the hyphae. The dissolution of the cell wall did not occur until hyphae penetration. The reported symptoms of the early stages of their development are linked to a high accumulation of D-galacturonic acid secreted by these fungi (Hershenhorn et al., 1990).

Another mechanism of *P. italicum* infection is the downregulation of hydroxyproline-rich glycoprotein (HRGP) and germin-like protein (GLP) gene expressions, which are related to fruit cell wall. At the transcriptional level, *P. italicum* induced the modification of the cell wall by increasing the expression of the XTH21, XTH29, XTH33, and Expansin-A16 genes, which contribute to cell wall degradation. Although the study revealed an increase in lignin production, which is related to a citrus defense mechanism, infection of the fruit by *P. italicum* was still successful (Li T. et al., 2019).

Li T. et al. (2019) and Yin et al. (2020) observed that Dicer-type genes, which encodes an RNase III-like endonuclease, an important component of RNAi metabolism, play an important role in the condition and pathogenicity of *P. italicum*. One of the proposed virulence mechanisms is the cross-kingdom RNA interference (ck-RNAi), which is a natural phenomenon where small interference RNAs (siRNAs) are transferred between host and pathogen. In this case, only a few siRNAs from

TABLE 3 | Main virulence factors of *P. italicum*'s infection.

Action	Agents responsible	References
Accumulation of reactive oxygen species (ROS)	Reduction of antioxidant metabolites and activity of antioxidant enzymes such as SOD, CAT, POD, and APX	Chen et al., 2019a
Damage the integrity of the host's cells	Increase PME, PG, and XTH	Li T. et al., 2019
Decreasing pH	Organic acids, especially citric acid	Prusky et al., 2004
Demethylation of pectin	Accumulation of D-galacturonic and CAZymes such as PL1, PL3, PL4, GH28, GH78, GH95, GH105, CE8 e CE12	Hershenhorn et al., 1990; Li T. et al., 2019; Yin et al., 2020
Fruit tissue maceration	PG, PL and PNL	Alana et al., 1990; Prusky et al., 2004; Papoutsis et al., 2019
Modification of the cell wall	Decreasing ASP and hemicellulose. Increasing PME, PG, XTH, WSP, D-galacturonic acid and expression of the XTH21, XTH29, XTH33, and Expansin-A16 genes	Hershenhorn et al., 1990; Li B. et al., 2015; Li T. et al., 2019
Neutralization or silencing of defense of host	ck-RNAi and proteases contained in secretomes	Li B. et al., 2015; Li T. et al., 2019; Yin et al., 2020
Plasmolysis of cells in the vicinity of the hyphae	Accumulation of D-galacturonic acid	Hershenhorn et al., 1990

ASP, Acid-soluble pectin; APX, Ascorbate peroxidase; CAT, Catalase; CAZyme, Carbohydrate active enzymes; ck-RNAi, Cross-kingdom RNA interference; PG, Polygalacturonases; PL, Pectate lyase; PNL, Pectin lyase; PME, Pectin methyltransferase; POD, Peroxidase; WSP, Water-soluble pectin; XTH, Xyloglucan endotransglucosylases/hydrolases.

P. italicum manage to cross the borders of the plant and silence its defensive genes, facilitating virulence, while most remaining siRNAs act endogenously.

Genome analyses indicated that nine carbohydrate active enzymes (CAZyme) families related to pectin, namely: PL1, PL3, PL4, GH28, GH78, GH95, GH105, CE8, and CE12 are encoded by *P. italicum* genes. Since cell wall of fruit cells present an abundant amount of pectin, most of the virulence mechanisms are related to the modification/degradation of polysaccharides (Li B. et al., 2015). *P. italicum* also has a secretome of 662 predicted secreted proteins (7.1% of the proteome) and, considering that secretomes contain abundant proteases, they also help the fungus in virulence, since the proteases allow the fungus to exploit various environmental nutrients and neutralize defense responses based on host proteins. **Table 3** shows the main virulence factors:

Interactions between pathogen and fruit remain relatively unexplored (Cheng et al., 2020), mainly regarding the lack of clarity of the virulence mechanisms of the phytopathogen *P. italicum*. Furthermore, the development of these analyses is hampered by the difficulty in individually identifying *Penicillium* species, especially those whose genetics are remarkably similar. However, this distinction is essential for estimating fungal resistance and adapting effective strategies to control decomposition and mycotoxin accumulation.

SECONDARY METABOLITES PRODUCED BY *P. italicum*

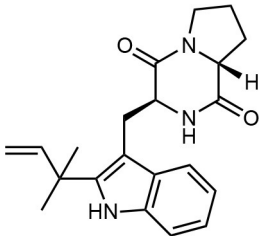
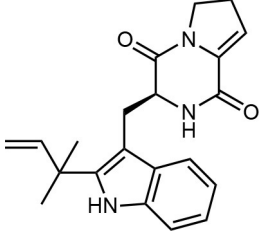
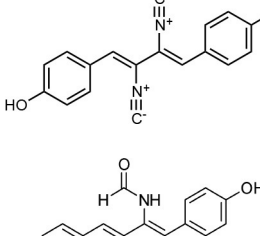
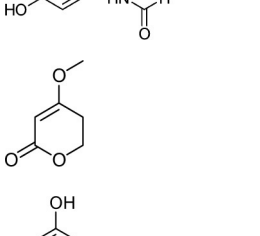
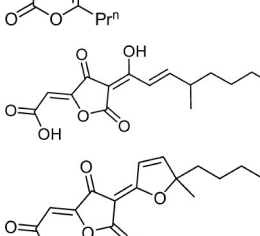
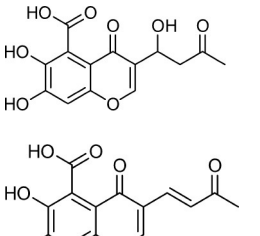
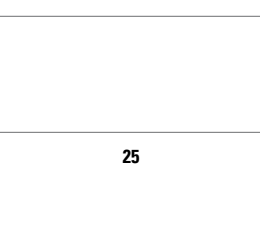
Only few studies are dedicated to understand the infection mechanisms of *P. italicum* and so far, no secondary metabolites produced by this fungus are described as virulence factors. It is well documented that these molecules enhance disease development, as well as inhibit or hinder fruit's defensive system in different pathogen-host interactions. Thus, comprehending

the secondary metabolites produced by the fungus during infection including their role in virulence is crucial when searching for new strategies to inhibit disease spread.

Frisvad and Filtenborg (1983) performed tests with species of *Penicillium* to analyze mycotoxins and other secondary metabolites (**Table 4**) and detected two NPs produced by *P. italicum*. However, structure elucidation was not possible in this study. Thus, it became unfeasible to characterize them as mycotoxins or not. Nevertheless, further analysis by Frisvad and Samson (2004) did not add *P. italicum* among mycotoxigenic producers but reported secondary metabolites such as deoxybrevianamide E (**1**), xanthocyllin (**3**), and PI-3 (**9**) (Arai et al., 1989). Other studies developed by Faid and Tantaoui-Elaraki (1989), Scott et al. (1974), and Arai et al. (1989) and collaborators have also managed to identify some NPs produced by *P. italicum* (**Table 4**), such as 5,6-dihydroxy-4-methoxy-2H-pyran-2-one (**5**), which is classified as a mycotoxin according to the Human Metabolome Database¹ (HMDB) (Faid and Tantaoui-Elaraki, 1989), low amounts of deoxybrevianamide E (**1**) and dehydrodeoxybrevianamide E (**2**), common metabolites from *Aspergillus ustus* (Scott et al., 1974), and 4-methoxy-6-n-propenyl-2-pyrone (**6**) as well as new compounds such as PI-1 (**7**) PI-2 (**8**), PI-3 (**9**), and PI-4 (**10**) (Arai et al., 1989). Whilst searching for NPs produced by species of *Penicillium*, Frisvad and Samson (2004) listed the NPs already mentioned as well as other NPs, such as arabenoic acid (**12**), dehydrofulvic acid (**11**), formylxanthocyllin X (**4**), 5-hydroxymethylfurfic acid (**13**), and other metabolites, which could not be identified. In this study, Frisvad et al. (2004) pointed out NPs that could be characterized as mycotoxins (**5**, **6**, and **7**), herbicides (**1**, **12**, and **11**) and those with potential antibiotic activity (**2**, **6**, and **13**). Although these metabolites have been detected *in vitro* in artificial culture

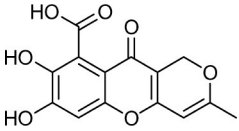
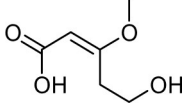
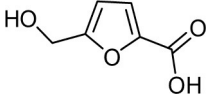
¹Available online at: <https://hmdb.ca/metabolites/HMDB0033517#ontology> (accessed February 20, 2020).

TABLE 4 | Structure of the secondary metabolites produced by *P. italicum* already identified.

N°	Secondary metabolite	Chemical structure	References
1	Deoxybrevianamide E		Scott et al., 1974; Arai et al., 1989; Frisvad et al., 2004; Smedsgaard et al., 2004
2	Dehydrodeoxybrevianamide E		Scott et al., 1974
3	Xanthocyllin X		Frisvad et al., 2004
4	Formylxanthocyllin X		Frisvad et al., 2004
5	5,6-dihydroxy-4- methoxy-2H-pyran-2-one		Faid and Tantaoui-Elaraki, 1989
6	4-methoxy-6-n-propenyl-2-pyrone		Arai et al., 1989
7	PI-1		Arai et al., 1989
8	PI-2		Arai et al., 1989
9	PI-3		Arai et al., 1989; Frisvad et al., 2004
10	PI-4		Arai et al., 1989

(Continued)

TABLE 4 | Continued

N°	Secondary metabolite	Chemical structure	References
11	Dehydrofulvic acid		Frisvad et al., 2004
12	Arabenoic acid		Frisvad et al., 2004
13	5-hydroxymethylfuroic acid		Frisvad et al., 2004

media, these metabolites have not been linked to infection yet and many other metabolites remain to be identified (Frisvad et al., 2004). In addition, there are no studies concerning the toxicity of these NPs against humans, plants, animals and bacteria (Faid and Tantaoui-Elaraki, 1989).

The *P. italicum* genome has already been sequenced, however, the biosynthetic potential encoded is still untapped. It is considered a necrotrophic plant pathogen and, due to the relationship between host variety and genome size for fruit pathogens, as proposed by studies such as Ballester et al. (2015) and Marcet-Houben et al. (2012), *P. italicum* has an intermediate host range (genome of about 29 Mb), meaning it can infect other fruits, despite having a larger pathogenicity in citrus fruits. *P. digitatum*, for example, has a smaller genome size (genome of about 25.7 Mb) being only capable of infecting citrus fruits (Ropars et al., 2016).

Li B. et al. (2015) sequenced the genome of three phytopathogenic fungal species of the genus *Penicillium* and functional analyses revealed interesting aspects about the biosynthesis of secondary metabolites and pathogenicity in the fungi *P. expansum* (apple pathogen), *P. digitatum*, and *P. italicum*. Comparative genomic analysis of the three phytopathogens evaluated the natural products biosynthetic gene clusters (BGCs), using the antiSMASH bioinformatics program, revealing 55 BGCs in the genome of *P. expansum*, compared with 30 in *P. italicum*, and 24 clusters in *P. digitatum*. According to Li B. et al. (2015), some biosynthetic gene clusters, interestingly, are shared by all three or two of the studied *Penicillium* species, indicating that the species have chemically similar secondary metabolite production potential. Comparative analysis of the genome also indicated 10 clusters of biosynthetic genes shared by *P. digitatum* and *P. italicum*, pathogens that have great specificity with the citrus host. Such metabolites could be important for their virulence/pathogenicity and the biosynthetic studies of these compounds, as well as functional analyses, would be important, contributing to the understanding of the relationship between host-pathogen. The understanding of the active secondary metabolites involved in the pathogen-host interaction could increase the knowledge of

the disease and, in the future, be used to research safe ways of control.

Studies in this field could contribute to a higher understanding of the fungal metabolomic profile. Comparative analyses of the DNA isolated from *P. italicum* were performed by Akhtar et al. (2013), managing to characterize the fungus from different locations and observe the mutations suffered through the RAPD (Random Amplified Polymorphic DNA) technique. The isolation of the CYP51 gene, which encodes eburicol 14- α demethylase (P450_{14DM}) in *P. italicum* was studied by Nistelrooy et al. (1996) in order to understand better the selective activity of demethylation inhibitors (DMIs), which were a promising antifungal not only for its selectivity but also because it is highly economical and meets the registration standards, as well as presenting already known fungal resistance mechanisms. DMIs were effective inhibitors of P450_{14DM} activity in *P. italicum* (Nistelrooy et al., 1996). However, it is now known that these fungicides are outdated, as previously discussed, being toxic to humans and the environment, in addition to the fact that *P. italicum* and other pathogens have already developed resistance to them.

CONCLUSION

The fungus *P. italicum* is one of the main responsible pathogen for post-harvest diseases in oranges. It is responsible for significant drops in fruit production, and directly affects the economy of many countries, especially Brazil, as it is the largest producer and exporter of this product in the world. Since common control methods used today are quite toxic to human health, their application has been increasingly controlled, also considering that the fungus is developing a higher resistance to them. Alternative methods are being explored to replace them. The most promising ones are “killer” yeasts, such as *S. schoenii*; physical methods, such as UV and hot water treatment; essential oils, such as thymol and carvacrol; and volatile substances, such as dimethyl trisulfide. However, to this date, there are not enough studies on the effectiveness of these methods on a large-scale production or on their

mechanisms of action against the fungus, containing possible undesirable effects, or even significant risks to human and plant health. For this reason, some studies have already been focused on understanding how *P. italicum* infects the fruit; its virulence factors (in which the PG enzyme seems to be the main responsible factor); the secondary metabolites produced, such as Italian acids, PI-1-4 and others mentioned in this article, which represent few NPs identified in comparison to the fungus cryptic biosynthetic potential, in addition to the lack of studies to prove which of them are directly linked to the infection; and the genomic aspect of the fungus, which has already clarified the selective activity of the DMIs and also *P. italicum*'s potential for producing chemically similar NPs to other species of the *Penicillium* genus. Although the studies presented in this article have helped to understand better this phytopathological interaction, further investigations are still essential, since there are many aspects to be explored, especially concerning the fungus genome and their relationship with cryptic secondary

metabolites. Understanding the biological role of these molecules in the pathogen-host interaction is essential for the development of new, more effective, nontoxic, and economically viable on large-scale control methods.

AUTHOR CONTRIBUTIONS

All authors listed have made a substantial, direct and intellectual contribution to the work, and approved it for publication.

FUNDING

This study was financed in part by the Coordenação de Aperfeiçoamento de Pessoal de Nível Superior—Brasil (CAPES)—Finance Code 001, Fundação de Amparo à Pesquisa no Estado de São Paulo [grant number FAPESP 2017/24462-4, 2018/13027-8 and 2019/06359-7], together with ABC and UNESCO in Brazil.

REFERENCES

- Abe, F., and Hiraki, T. (2009). Mechanistic role of ergosterol in membrane rigidity and cycloheximide resistance in *Saccharomyces cerevisiae*. *BBA Biomembr.* 1788, 743–752. doi: 10.1016/j.bbmem.2008.12.002
- Akhtar, N., Anjum, T., and Jabeen, R. (2013). Isolation and identification of storage fungi from citrus sampled from major growing areas of Punjab, Pakistan. *Int. J. Agric. Biol.* 15, 1283–1288.
- Alana, A., Alkorta, I., Dominguez, J. B., Llama, M. J., and Serra, J. L. (1990). Pectin lyase activity in a *Penicillium italicum* strain. *Appl. Environ. Microbiol.* 56, 3755–3759. doi: 10.1128/AEM.56.12.3755-3759.1990
- Aloui, H., Licciardello, F., Khwaldia, K., Hamdi, M., and Restuccia, C. (2015). *Physical properties and antifungal activity of bioactive films containing wickerhamomyces anomalus* killer yeast and their application for preservation of oranges and control of postharvest green mould caused by *Penicillium digitatum*. *Int. J. Food Microbiol.* 200, 22–30. doi: 10.1016/j.ijfoodmicro.2015.01.015
- Al-snafi, A. E. (2016). Nutritional value and pharmacological importance of citrus species grown in Iraq. *IOSR J. Pharm.* 6, 76–108. doi: 10.9790/3013-0680176108
- Amadi, J. E., and Adeniyi, D. O. (2009). Mycotoxin production by fungi isolated from stored grains. *African J. Biotechnol.* 8, 1219–1221.
- Ameziane, N., Boubaker, H., Boudyach, H., Msanda, F., Jilal, A., and Benaoumar, A. A. (2007). Antifungal activity of moroccan plants against citrus fruit pathogens. *Agronomy* 27, 273–277. doi: 10.1051/agro:2007022
- Arai, K., Miyajima, H., Mushiroda, T., and Yamamoto, Y. (1989). Metabolites of *Penicillium italicum* WEHMER: isolation and structures of new metabolites including naturally occurring 4-ylidene-acyltetronic acids, italicinic acid and italicic acid. *Chem. Pharm. Bull.* 37, 3229–3235. doi: 10.1248/cpb.37.3229
- Arrebola, E., Sivakumar, D., and Korsten, L. (2010). Effect of volatile compounds produced by bacillus strains on postharvest decay in citrus. *Biol. Control* 53, 122–128. doi: 10.1016/j.biocontrol.2009.11.010
- Askarne, L., Talibi, I., Boubaker, H., Boudyach, E. H., Msanda, F., Saad, B., et al. (2012). *In vitro* and *in vivo* antifungal activity of several moroccan plants against *penicillium italicum*, the causal agent of citrus blue mold. *Crop Prot.* 40, 53–58. doi: 10.1016/j.cropro.2012.04.023
- Ballester, A.-R., Marcet-Houben, M., Levin, E., Sela, N., Selma-Lázaro, C., Carmona, L., et al. (2015). Genome, transcriptome, and functional analyses of *Penicillium expansum* provide new insights into secondary metabolism and pathogenicity. *Mol. Plant-Microbe Interact.* 28, 232–248. doi: 10.1094/MPMI-09-14-0261-FI
- Bazioli, J. M., Costa, J. H., Akiyama, D. Y., Pontes, D. M., Kupper, K. C., and Augusto, F. (2019). Biological control of citrus postharvest phytopathogens. *Toxins* 11:460. doi: 10.3390/toxins11080460
- Benavente-García, O., and Castillo, J. (2008). Update on uses and properties of Citrus flavonoids: new findings in anticancer, cardiovascular, and anti-inflammatory activity. *J. Agric. Food Chem.* 56, 6185–6205. doi: 10.1021/jf8006568
- Bennett, J. W., and Klich, M. (2003). *Mycotoxins*. 5th Edn. Washington: Clinical Microbiology Reviews. doi: 10.1128/CMR.16.3.497-516.2003
- Bhatnagar, D., Cary, J. W., Ehrlich, K., Yu, J., and Cleveland, T. E. (2006). Understanding the genetics of regulation of aflatoxin production and *Aspergillus flavus* development. *Mycopathologia* 162, 155–166. doi: 10.1007/s11046-006-0050-9
- Boubaker, H., Karim, H., Hamdaoui, A., El Msanda, F., Leach, D., Bombarda, I., et al. (2016). Chemical characterization and antifungal activities of four thymus species essential oils against postharvest fungal pathogens of citrus. *Ind. Crop. Prod.* 86, 95–101. doi: 10.1016/j.indcrop.2016.03.036
- Caccioni, D. R. L., Guizzardi, M., Biondi, D. M., Renda, A., and Ruberto, G. (1998). Relationship between volatile components of citrus fruit essential oils and antimicrobial action on *Penicillium digitatum* and *Penicillium italicum*. *Int. J. Food Microbiol.* 43, 73–79. doi: 10.1016/S0168-1605(98)00099-3
- CAST. Council for Agricultural Science and Technology (2003). *Mycotoxins: Risk in Plant, Animal and Human Systems*. Task Force Report no 139, Ames, IA.
- Chalutz, E., and Wilson, C. L. (1990). Postharvest biocontrol of green and blue mold and sour rot of citrus fruit by *Debaryomyces hansenii*. *Plant Dis.* 74, 134–137. doi: 10.1094/PD-74-0134
- Chen, C., Cai, N., and Chen, J. (2019a). Clove essential oil as an alternative approach to control postharvest blue mold caused by *Penicillium italicum* in citrus fruit. *Biomolecules* 9:197. doi: 10.3390/biom9050197
- Chen, C., Qi, W., Peng, X., Chen, J., and Wan, C. (2019b). Inhibitory effect of 7-demethoxytylophorine on *Penicillium italicum* and its possible mechanism. *Microorganisms* 7:36. doi: 10.3390/microorganisms7020036
- Chen, C., Wan, C., Peng, X., and Chen, J. (2019c). A flavonone pinocembrin inhibits *penicillium italicum* growth and blue mold development in 'Newhall' navel oranges by targeting membrane damage mechanism. *Pestic. Biochem. Physiol.* 165:104505. doi: 10.1016/j.pestbp.2019.11.025
- Cheng, Y., Lin, Y., Cao, H., and Li, Z. (2020). Citrus postharvest green mold: recent advances in fungal pathogenicity and fruit resistance. *Microorganisms* 8:449. doi: 10.3390/microorganisms8030449
- Comitini, F., Mannazzu, I., and Ciani, M. (2009). Tetrapisispora Phaffii killer toxin is a highly specific beta -glucanase that disrupts the integrity of the yeast cell wall. *Microb. Cell Fact.* 11, 1–11. doi: 10.1186/1475-2859-8-55

- Costa, J. H., Bazioli, J. M., de Moraes Pontes, J. G., and Fill, T. P. (2019a). *Penicillium digitatum* infection mechanisms in citrus: what do we know so far? *Fungal Biol.* 123, 584–593. doi: 10.1016/j.funbio.2019.05.004
- Costa, J. H., Wassano, C. I., Angolini, C. F. F., Scherlach, K., Hertweck, C., and Fill, T. P. (2019b). Antifungal potential of secondary metabolites involved in the interaction between citrus pathogens. *Sci. Rep.* 9:18647. doi: 10.1038/s41598-019-55204-9
- Cunha, T., da, Ferraz, L. P., Wehr, P. P., and Kupper, K. C. (2018). Antifungal activity and action mechanisms of yeasts isolates from citrus against *Penicillium italicum*. *Int. J. Food Microbiol.* 276, 20–27. doi: 10.1016/j.jfoodmicro.2018.03.019
- Cushnie, T. P. T., and Lamb, A. J. (2005). Antimicrobial activity of flavonoids. *Int. J. Antimicrob. Agents* 26, 343–356. doi: 10.1016/j.ijantimicag.2005.09.002
- de Moraes, L. A. S. (2009). “Óleos essenciais no controle Fitossanitário,” in *Biocontrole de Doenças de Plantas: Uso e Perspectivas* (Jaguariúna), 139–152. Available online at: <https://www.alice.cnptia.embrapa.br/bitstream/doc/580600/1/2009CL08.pdf>
- de Ramón-Carbonell, M., and Sánchez-Torres, P. (2020). Significance of 195 bp-enhancer of PdCYP51B in the acquisition of *Penicillium digitatum* DMI resistance and increase of fungal virulence. *Pestic. Biochem. Physiol.* 165, 1–12. doi: 10.1016/j.pestbp.2020.01.003
- de Vilhena Araújo, Ê., Vendramini, P. H., Costa, J. H., Eberlin, M. N., Montagner, C. C., and Fill, T. P. (2019). Determination of Tryptoquialanines A and C produced by *Penicillium digitatum* in oranges: are we safe? *Food Chem.* 301:125285. doi: 10.1016/j.foodchem.2019.125285
- Ding, X., Yu, Q., Zhang, B., Xu, N., Jia, C., Dong, Y., et al. (2014). The type II Ca^{2+} /calmodulin-dependent protein kinases are involved in the regulation of cell wall integrity and oxidative stress response in *Candida albicans*. *Biochem. Biophys. Res. Commun.* 446, 1073–1078. doi: 10.1016/j.bbrc.2014.03.059
- Droby, S., Chalutz, E., Wilson, C. L., and Wisniewski, M. (1989). Characterization of the biocontrol activity of *Debaryomyces hansenii* in the control of *Penicillium digitatum* on grapefruit. *Can. J. Microbiol.* 35, 794–800. doi: 10.1139/m89-132
- Droby, S., Eick, A., Macarasin, D., Cohen, L., Rafael, G., Stange, R., et al. (2008). Role of citrus volatiles in host recognition, germination and growth of *Penicillium digitatum* and *Penicillium italicum*. *Postharvest Biol. Technol.* 49, 386–396. doi: 10.1016/j.postharvbio.2008.01.016
- Droby, S., Vinokur, V., Weiss, B., Cohen, L., Daus, A., Goldschmidt, E. E., et al. (2002). Induction of resistance to *penicillium digitatum* in grapefruit by the yeast biocontrol agent *Candida oleophila*. *Phytopathology*. 92:393–399. doi: 10.1094/PHYTO.2002.92.4.393
- Dudgeon, D. D., Zhang, N., Ositelu, O. O., Kim, H., and Cunningham, K. W. (2008). Nonapoptotic death of *Saccharomyces cerevisiae* cells that is stimulated by Hsp90 and inhibited by calcineurin and Cmk2 in response to endoplasmic reticulum stresses. *Eukaryot. Cell* 7, 2037–2051. doi: 10.1128/EC.00291-08
- Dukare, A. S., Paul, S., Nambi, V. E., Gupta, R. K., Singh, R., Sharma, K., et al. (2019). Exploitation of microbial antagonists for the control of postharvest diseases of fruits: a review. *Crit. Rev. Food Sci. Nutr.* 59, 1498–1513. doi: 10.1080/10408398.2017.1417235
- Erasmus, A., Lennox, C. L., Korsten, L., Lesar, K., and Fourie, P. H. (2015). Imazalil resistance in *Penicillium digitatum* and *P. italicum* causing citrus postharvest green and blue mould: impact and options. *Postharvest Biol. Technol.* 107, 66–76. doi: 10.1016/j.postharvbio.2015.05.008
- Faid, M., and Tantaoui-Elaraki, A. (1989). Production of toxic metabolites by *Penicillium italicum* and *P. digitatum* isolated from citrus fruits. *J. Food Prot.* 52, 194–197. doi: 10.4315/0362-028X-52.3.194
- Ferraz, L. P., Cunha, T., da, da Silva, A. C., and Kupper, K. C. (2016). Biocontrol ability and putative mode of action of yeasts against *Geotrichum citri-aurantii* in citrus fruit. *Microbiol. Res.* 188–189, 72–79. doi: 10.1016/j.micres.2016.04.012
- Fickova, M., Pravdova, E., Rondhal, L., Uher, M., and Brtko, J. (2008). *In vitro* antiproliferative and cytotoxic activities of novel kojic acid derivatives: 5-benzoyloxy-2-selenocyanatomethyl- and 5-methoxy-2-selenocyanatomethyl-4-pyranone. *J. Appl. Toxicol.* 28, 554–559. doi: 10.1002/jat.1300
- Frisvad, J. C., and Filtenborg, O. (1983). Classification of terverticillate penicillia based on profiles of micotoxins and other secondary metabolites. *Appl. Environ. Microbiol.* 46, 1301–1310. doi: 10.1128/AEM.46.6.1301-1310.1983
- Frisvad, J. C., Smedsgaard, J., Larsen, T. O., and Samson, R. A. (2004). Mycotoxins, drugs and other extrolites produced by species in *Penicillium* subgenus *Penicillium*. *Stud. Mycol.* 49, 201–241.
- Frisvad, J. C., and Samson, R. A. (2004). Polyphasic taxonomy of *Penicillium* subgenus *Penicillium*. A guide to identification of food and air-borne terverticillate *Penicillia* and their mycotoxins. *Stud. Mycol.* 49, 1–174.
- Ghosoph, J. M., Schmidt, L. S., Margosan, D. A., and Smilanick, J. L. (2007). Imazalil resistance linked to a unique insertion sequence in the PdCYP51 promoter region of *Penicillium digitatum*. *Postharvest Biol. Technol.* 44, 9–18. doi: 10.1016/j.postharvbio.2006.11.008
- Girón-Calva, P. S., Molina-Torres, J., and Heil, M. (2012). Volatile dose and exposure time impact perception in neighboring plants. *J. Chem. Ecol.* 38, 226–228. doi: 10.1007/s10886-012-0072-3
- Hamamoto, H., Hasegawa, K., Nakaune, R., Lee, Y. J., Makizumi, Y., Akutsu, K., et al. (2000). Tandem repeat of a transcriptional enhancer upstream of the sterol 14 α -demethylase gene (CYP51) in *Penicillium digitatum*. *Appl. Environ. Microbiol.* 66, 3421–3426. doi: 10.1128/AEM.66.8.3421-3426.2000
- Hernández-Montiel, L. G., Ochoa, J. L., Troyo-Díéguez, E., and Larralde-Corona, C. P. (2010). Biocontrol of postharvest blue mold (*Penicillium italicum* Wehmer) on Mexican lime by marine and citrus *Debaryomyces hansenii* isolates. *Postharvest Biol. Technol.* 56, 181–187. doi: 10.1016/j.postharvbio.2009.12.010
- Hershenhorn, J., Manulis, S., and Barash, I. (1990). Polygalacturonases associated with infection of valencia orange by *penicillium italicum*. *Physiol. Biochem.* 80, 1374–1376. doi: 10.1094/Phyto-80-1374
- Iqbal, Z., Singh, Z., Khangura, R., and Ahmad, S. (2012). Management of citrus blue and green moulds through application of organic elicitors. *Australas. Plant Pathol.* 41, 69–77. doi: 10.1007/s13313-011-0091-5
- Iqbal, Z., Iqbal, J., Abbas, I., and Kamran, M. (2017). Innovative strategies for eco-friendly management of citrus blue mold disease caused by *Penicillium italicum* WHEMER. *J. Int. Sci. Publ.* 5, 361–365.
- Iwao, T. (1999). Benzimidazole-tolerant *Penicillium crustosum* isolated from the edible mushroom factories in Hokkaido. *Nippon Kin Gakkai Kaiho* 40, 11–13.
- Kanan, G. J. M., and Al-Najar, R. A. K. (2009). *In vitro* and *in vivo* activity of selected plant crude extracts and fractions against *Penicillium italicum*. *J. Plant Prot. Res.* 49, 341–352. doi: 10.2478/v10045-009-0054-9
- Kellerman, M., Joubert, J., Erasmus, A., and Fourie, P. H. (2016). Postharvest Biology and Technology The effect of temperature, exposure time and pH on imazalil residue loading and green mould control on citrus through dip application. *Postharvest Biol. Technol.* 121, 1–6. doi: 10.1016/j.postharvbio.2016.06.014
- Kim, J. H., and Chan, K. L. (2014). Augmenting the antifungal activity of an oxidizing agent with kojic acid: control of *Penicillium* strains infecting crops. *Molecules* 19, 18448–18464. doi: 10.3390/molecules191118448
- Kiralj, R., and Ferreira, M. M. C. (2008). Chemometric analysis of the multidrug resistance in strains of *Penicillium digitatum*. *SAR QSAR Environ. Res.* 19, 55–70. doi: 10.1080/10629360701844118
- Klieber, A. A., Scott, E. B., and Wuryatmo, E. A. (2002). Effect of method of application on antifungal efficacy of citral against postharvest spoilage fungi of citrus in culture. *Australas. Plant Pathol.* 31, 329–332. doi: 10.1071/AP02034
- Köppen, R., Koch, M., Siegel, D., Merkel, S., Maul, R., and Nehls, I. (2010). Determination of mycotoxins in foods: Current state of analytical methods and limitations. *Appl. Microbiol. Biotechnol.* 86, 1595–1612. doi: 10.1007/s00253-010-2535-1
- Kumar, R., and Tamuli, R. (2014). Calcium/calmodulin-dependent kinases are involved in growth, thermotolerance, oxidative stress survival, and fertility in *Neurospora crassa*. *Arch. Microbiol.* 196, 295–305. doi: 10.1007/s00203-014-0966-2
- Kupper, K. C., Cervantes, A. L. L., Klein, M. N., and Silva, A. C. (2013). Avaliação de microrganismos Antagônicos, *saccharomyces cerevisiae* e *Bacillus subtilis* para o Controle de *Penicillium digitatum*. *Rev. Bras. Frutic.* 35, 425–436. doi: 10.1590/S0100-29452013000200011
- Li, B., Zong, Y., Du, Z., Chen, Y., Zhang, Z., Qin, G., et al. (2015). Genomic characterization reveals insights into patulin biosynthesis and pathogenicity in *Penicillium* Species. *Mol. Plant Microbe Interact.* 28, 635–647. doi: 10.1094/MPMI-12-14-0398-FI

- Li, J., Li, H., Ji, S., Chen, T., Tian, S., and Qin, G. (2019). Enhancement of biocontrol efficacy of *Cryptococcus laurentii* by cinnamic acid against *Penicillium italicum* in citrus fruit. *Postharvest Biol. Technol.* 149, 42–49. doi: 10.1016/j.postharvbio.2018.11.018
- Li, Q., Ning, P., Zheng, L., Huang, J., Li, G., and Hsiang, T. (2010). Fumigant activity of volatiles of *Streptomyces globisporus* JK-1 against *Penicillium italicum* on citrus microcarpa. *Postharvest Biol. Technol.* 58, 157–165. doi: 10.1016/j.postharvbio.2010.06.003
- Li, T., Shi, D., Wu, Q., Yin, C. X., Li, F., Shan, Y., et al. (2019). Mechanism of cellwall polysaccharides modification in harvested 'Shatangju' Mandarin (Citrus Reticulate Blanco) fruit caused by *Penicillium italicum*. *Biomolecules* 9:160. doi: 10.3390/biom9040160
- Li, W.-R., Shi, Q.-S., Dai, H.-Q., Liang, Q., Xie, X.-B., Huang, X.-M., et al. (2015). Antifungal activity, kinetics and molecular mechanism of action of garlic oil against *Candida albicans*. *Sci. Rep.* 6:22805. doi: 10.1038/srep22805
- Li, W.-R., Shi, Q.-S., Liang, Q., Huang, X.-M., and Chen, Y.-B. (2014). Antifungal effect and mechanism of garlic oil on *Penicillium funiculosum*. *Appl. Microbiol. Biotechnol.* 98, 8337–8346. doi: 10.1007/s00253-014-5919-9
- Liu, X., Xia, W., Jiang, Q., Xu, Y., and Yu, P. (2014). Synthesis, characterization, and antimicrobial activity of kojic acid grafted chitosan oligosaccharide. *J. Agric. Food Chem.* 62, 297–303. doi: 10.1021/jf404026f
- Liu, Y., Heying, E., and Tanumihardjo, S. A. (2012). History, global distribution, and nutritional importance of citrus fruits. *Compr. Rev. Food Sci. Food Saf.* 11, 530–545. doi: 10.1111/j.1541-4337.2012.00201.x
- Liu, Y., Yao, S., Deng, L., Ming, J., and Zeng, K. (2019). Different mechanisms of action of isolated epiphytic yeasts against *Penicillium digitatum* and *Penicillium italicum* on citrus fruit. *Postharvest Biol. Technol.* 152, 100–110. doi: 10.1016/j.postharvbio.2019.03.002
- Long, Y., Huang, W., Wang, Q., and Yang, G. (2020). Green synthesis of garlic oil nanoemulsion using ultrasonication technique and its mechanism of antifungal action against *Penicillium italicum*. *Ultrason. Sonochem.* 64, 1–58. doi: 10.1016/j.ultrasonch.2020.104970
- Lopes, J. M. S., Déo, T. F. G., Andrade, B. J. M., Glroto, M., Felipe, A. L. S., Junior, C. E. L., et al. (2011). Importância Econômica do Citrus no Brasil. *Rev. Científica Eletrônica Agron.* 10, 1–3. Available online at: www.fae.revista.inf.br
- Louw, J. P., and Korsten, L. (2015). Pathogenicity and Host Susceptibility of *Penicillium* spp. on Citrus. *Plant Dis.* 99, 21–30. doi: 10.1094/PDIS-02-14-0122-RE
- Luo, J., Xu, F., Zhang, X., Shao, X., Wei, Y., and Wang, H. (2020). Transcriptome analysis of *Penicillium italicum* in response to the flavonoids from *Sedum aizoon* L. *World J. Microbiol. Biotechnol.* 36:62. doi: 10.1007/s11274-020-02836-z
- Marcet-Houben, M., Ballester, A.-R., de la Fuente, B., Harries, E., Marcos, J. F., González-Candelas, L., et al. (2012). Genome sequence of the necrotrophic fungus *Penicillium digitatum*, the main postharvest pathogen of citrus. *BMC Genomics* 13:646. doi: 10.1186/1471-2164-13-646
- Martel, C. M., Parker, J. E., Warrilow, A. G. S., Rolley, N. J., Kelly, S. L., and Kelly, D. E. (2010). Complementation of a *Saccharomyces cerevisiae* ERG11 / CYP51 and screening of the azole sensitivity of *Aspergillus fumigatus* Isoenzymes CYP51A and CYP51B. *Antimicrob. Agents Chemother.* 54, 4920–4923. doi: 10.1128/AAC.00349-10
- Martins, S. J., Faria, A. F., Pedroso, M. P., Cunha, M. G., Rocha, M. R., and Medeiros, F. H. V. (2019). Microbial volatiles organic compounds control anthracnose (*Colletotrichum lindemuthianum*) in common bean (*Phaseolus vulgaris* L.). *Biol. Control* 131, 36–42. doi: 10.1016/j.biocontrol.2019.01.003
- Medeiros, F. H. V., de Martins, S. J., Zucchi, T. D., de Melo, I. S., Batista, L. R., Machado, J., et al. (2012). Controle biológico de fungos de armazenamento produtores de micotoxinas. *Cienc. e Agrotecnologia* 36, 483–497. doi: 10.1590/S1413-70542012000500001
- Morita, T., Tanaka, I., Ryuda, N., Ikari, M., Ueno, D., and Someya, T. (2019). Antifungal spectrum characterization and identification of strong volatile organic compounds produced by *Bacillus pumilus* TM-R. *Heliyon* 5:e01817. doi: 10.1016/j.heliyon.2019.e01817
- Nakaune, R., Hamamoto, H., Imada, J., Akutsu, K., and Hibi, T. (2002). A novel ABC transporter gene, PMR5, is involved in multidrug resistance in the phytopathogenic fungus *Penicillium digitatum*. *Mol. Genet. Genomics* 267, 179–185. doi: 10.1007/s00438-002-0649-6
- Neves, M. F., and Trombim, V. G. (2017). Anuário da Citricultura 2017. *CitrusBR*, 57. Available online at: http://www.citrusbr.com/revista/dezembro2017/revista_citrus_1217.pdf
- Nicolopoulou-Stamati, P., Maipas, S., Kotampasi, C., Stamatis, P., and Hens, L. (2016). Chemical pesticides and human health: the urgent need for a new concept in agriculture. *Front. Public Heal.* 4:148. doi: 10.3389/fpubh.2016.00148
- Nicosia, M. L. D., Pangallo, S., Raphael, G., Romeo, F. V., Strano, M. C., Rapisarda, P., et al. (2016). Control of postharvest fungal rots on citrus fruit and sweet cherries using a pomegranate peel extract. *Postharvest Biol. Technol.* 114, 54–61. doi: 10.1016/j.postharvbio.2015.11.012
- Nistelrooy, J. G. M., van Den Brink, J. M., van Kan, J. A. L., van Gorcom, R. F. M., and de Waard, M. A. (1996). Isolation and molecular characterisation of the gene encoding eburicol 14 α -demethylase (CYP51) from *Penicillium italicum*. *Mol. Gen. Genet.* 250, 725–733. doi: 10.1007/BF02172984
- Niwa, Y., and Akamatsu, H. (1991). Kojic acid scavenges free radicals while potentiating leukocyte function's including free radical generation. *Inflammation* 15, 303–315. doi: 10.1007/BF00917315
- Palou, L., Marcilla, A., Rojas-argudo, C., Alonso, M., Jacas, J., Angel, M., et al. (2007). Effects of X-ray irradiation and sodium carbonate treatments on postharvest *Penicillium* decay and quality attributes of clementine mandarins. *Postharvest Biol. Technol.* 46, 252–261. doi: 10.1016/j.postharvbio.2007.05.006
- Palou, L., Usall, J., Smilanick, J. L., Aguilar, M. J., and Viñas, I. (2002). Evaluation of food additives and low-toxicity compounds as alternative chemicals for the control of *Penicillium digitatum* and *Penicillium italicum* on citrus fruit. *Pest Manag. Sci.* 58, 459–466. doi: 10.1002/ps.477
- Palou, L. (2014). "Penicillium digitatum, Penicillium italicum (Green Mold, Blue Mold)," in *Postharvest Decay* (Montcada), 45–102. doi: 10.1016/B978-0-12-411552-1.00002-8
- Pangallo, S., Nicosia, M. L. D., Raphael, G., Levin, E., Ballistreri, G., Cacciola, S. O., et al. (2017). Elicitation of resistance responses in grapefruit and lemon fruits treated with a pomegranate peel extract. *Plant Pathol.* 66, 633–640. doi: 10.1111/ppa.12594
- Papoutsis, K., Mathioudakis, M. M., Hasperué, J. H., and Ziogas, V. (2019). Non-chemical treatments for preventing the postharvest fungal rotting of citrus caused by *Penicillium digitatum* (Green Mold) and *Penicillium italicum* (Blue Mold). *Trends Food Sci. Technol.* 86, 479–491. doi: 10.1016/j.tifs.2019.02.053
- Parafati, L., Vitale, A., Restuccia, C., and Cirvilleri, G. (2016). The effect of locust bean gum (LBG)-based edible coatings carrying biocontrol yeasts against *Penicillium digitatum* and *Penicillium italicum* causal agents of postharvest decay of mandarin fruit. *Food Microbiol.* 58, 87–94. doi: 10.1016/j.fm.2016.03.014
- Peng, L., Yang, S., Cheng, Y. J., Chen, F., Pan, S., and Fan, G. (2012). Antifungal activity and action mode of pinocembrin from propolis against *Penicillium italicum*. *Food Sci. Biotechnol.* 21, 1533–1539. doi: 10.1007/s10068-012-0204-0
- Perez, M. F., Contreras, L., Garnica, N. M., Fernández-Zenoff, M. V., Farias, M. E., Sepulveda, M., et al. (2016). Native killer yeasts as biocontrol agents of postharvest fungal diseases in lemons. *PLoS One* 11:e0165590. doi: 10.1371/journal.pone.0165590
- Pérez-Afonso, C. O., Martínez-Romero, D., Zapata, P. J., Serrano, M., Valero, D., and Castillo, S. (2012). The effects of essential oils carvacrol and thymol on growth of penicillium digitatum and *P. italicum* involved in lemon decay. *Int. J. Food Microbiol.* 158, 101–106. doi: 10.1016/j.ijfoodmicro.2012.07.002
- Pimenta, R. S., Silva, F. L., Silva, J. F. M., Morais, P. B., Braga, D. T., Rosa, C. A., et al. (2008). Biological control of *Penicillium italicum*, *P. digitatum* and *P. expansum* by the predacious yeast *Saccharomycopsis schoenii* on oranges. *Brazilian J. Microbiol.* 39, 85–90. doi: 10.1590/S1517-83822008000100020
- Platanía, C., Restuccia, C., Muccilli, S., and Cirvilleri, G. (2012). Efficacy of killer yeasts in the biological control of *Penicillium digitatum* on Tarocco orange fruits (*Citrus sinensis*). *Food Microbiol.* 30, 219–225. doi: 10.1016/j.fm.2011.12.010
- Plaza, P., Usall, J., Teixidó, N., and Viñas, I. (2003). Effect of water activity and temperature on germination and growth of *Penicillium digitatum*, *P. italicum* and *Geotrichum candidum*. *J. Appl. Microbiol.* 94, 549–554. doi: 10.1046/j.1365-2672.2003.01909.x
- Prusky, D., McEvoy, J. L., Saftner, R., Conway, W. S., and Jones, R. (2004). Relationship Between Host Acidification and Virulence of *Penicillium* spp. on Apple and Citrus Fruit. *Phytopathology* 94, 44–51. doi: 10.1094/PHYTO.2004.94.1.44

- Ragsdale, N. N., and Sisler, H. D. (1994). Social and political implications of managing plant diseases with decreased availability of fungicides in the United States. *Fungic. Decreased Availab.* 32, 545–557. doi: 10.1146/annurev.py.32.090194.002553
- Rodrigues, A. P. D., Carvalho, S. C., Santos, A. S., Alves, C. N., and Luiz, M. (2011). Kojic acid, a secondary metabolite from *Aspergillus* sp. acts as an inducer of macrophage activation. *Cell Biol. Int.* 35, 335–343. doi: 10.1042/CBI.20100083
- Rojas-argudo, C., Palou, L., Bermejo, A., Cano, A., Angel, M., and González-mas, M. C. (2012). Effect of X-ray irradiation on nutritional and antifungal bioactive compounds of 'Clemenules' clementine mandarins. *Postharvest Biol. Technol.* 68, 47–53. doi: 10.1016/j.postharvbio.2012.02.004
- Ropars, J., Rodríguez De La Vega, R. C., Gouzy, J., Dupont, J., Swennen, D., Dumas, É., et al. (2016). *Diversity and Mechanisms of Genomic Adaptation in Penicillium*. *Aspergillus Penicillium post-genomic era*. doi: 10.21775/9781910190395.03
- Ruiz, V. E., Cerioni, L., Zampini, I. C., Cuello, S., Isla, I., Hilal, M., et al. (2017). UV-B radiation on lemons enhances antifungal activity of flavoed extracts against *Penicillium digitatum*. *LWT Food Sci. Technol.* 85, 96–103. doi: 10.1016/j.lwt.2017.07.002
- Saeedi, M., Eslamifard, M., and Khezri, K. (2019). Kojic acid applications in cosmetic and pharmaceutical preparations. *Biomed. Pharmacother.* 110, 582–593. doi: 10.1016/j.biopha.2018.12.006
- Sánchez-torres, P., and Tuset, J. J. (2011). Molecular insights into fungicide resistance in sensitive and resistant *Penicillium digitatum* strains infecting citrus. *Postharvest Biol. Technol.* 59, 159–165. doi: 10.1016/j.postharvbio.2010.08.017
- Santos, T., Sanchez, M., Villanueva, J. R., and Nombela, C. (1978). Regulation of the f3-1,3-glucanase system in *Penicillium italicum*: glucose repression of the various enzymes. *J. Bacteriol.* 133, 465–471. doi: 10.1128/JB.133.2.465-471.1978
- Santos, T., Sánchez, M., Villanueva, J. R., and Nombela, C. (1979). Derepression of fl-1,3-glucanases in *Penicillium italicum*: localization of the various enzymes and correlation with cell wall glucan mobilization and autolysis. *J. Bacteriol.* 137, 6–12. doi: 10.1128/JB.137.1.6-12.1979
- Scott, P. M., Kennedy, B. P. C., Harwig, J., and Chen, Y.-K. (1974). Formation of diketopiperazines by *Penicillium italicum* isolated from oranges. *Appl. Microbiol.* 28, 892–894. doi: 10.1128/AEM.28.5.892-894.1974
- Silva, É. O., da Martins, S. J., and Alves, E. (2014). Essential oils for the control of bacterial speck in tomato crop. *African J. Agric. Res.* 9, 2624–2629. doi: 10.5897/AJAR2014.8918
- Singh, H., Al-samarai, G., and Mohd Syarbil (2012). Exploitation of natural products as an alternative strategy to control postharvest fungal rotting of fruit and vegetables. *Int. J. Sci. Res. Publ.* 2, 108–111.
- Smedsgaard, J., Hansen, M. E., and Frisvad, J. C. (2004). Classification of tetraverticillate penicillia by electrospray mass spectrometric profiling. *Stud. Mycol.* 49, 243–251.
- Smilanick, J. L., Mansour, M. F., Mlikota, F., and Sorenson, D. (2008). Control of citrus postharvest green mold and sour rot by potassium sorbate combined with heat and fungicides. *Postharvest Biol. Technol.* 47, 226–238. doi: 10.1016/j.postharvbio.2007.06.020
- Solgi, M., and Ghorbanpour, M. (2014). Application of essential oils and their biological effects on extending the shelf-life and quality of horticultural crops. *Trakia J. Sci.* 12, 198–210.
- Talibi, I., Boubaker, H., Boudyach, E. H., and Aoumar, A. A., Ben (2014). Alternative methods for the control of postharvest citrus diseases. *J. Appl. Microbiol.* 117, 1–17. doi: 10.1111/jam.12495
- Tao, N., Jia, L., Zhou, H., and He, X. (2014a). Effect of octanal on the mycelial growth of *Penicillium italicum*. *World J. Microbiol. Biotechnol.* 30, 1169–1175. doi: 10.1007/s11274-013-1539-2
- Tao, N., Ouyang, Q., and Jia, L. (2014b). Citral inhibits mycelial growth of *penicillium italicum* by a membrane damage mechanism. *Food Control* 41, 116–121. doi: 10.1016/j.foodcont.2014.01.010
- Tayel, A. A., Moussa, S. H., Salem, M. F., Mazrou, K. E., and El-Tras, W. F. (2015). Control of citrus molds using bioactive coatings incorporated with fungal chitosan/plant extracts composite. *J. Sci. Food Agric.* 96, 1306–1312. doi: 10.1002/jsfa.7223
- Telezhemetskaya, M. V., and D'yakonov, A. L. (1991). Alkaloids of *Peganum harmala*. Unusual reaction of peganine and vasicinone. *Chem. Nat. Compd.* 27, 471–474. doi: 10.1007/BF00636573
- Trabelsi, D., Hamdane, A. M., and Said, M., Ben (2016). Chemical composition and antifungal activity of essential oils from flowers, leaves and peels of tunisian citrus aurantium against *Penicillium digitatum* and *Penicillium italicum*. *J. Essent. Oil Bear. Plants* 19, 1660–1674. doi: 10.1080/0972060X.2016.1141069
- USDA. (2020). *Citrus: World Markets and Trade Brazil's Orange Production*. USDA. Available online at: <https://apps.fas.usda.gov/psdonline/circulars/citrus.pdf> 33E
- Vaseghi, N., Bayat, M., Nosrati, A. C., Ghorannevis, M., and Hashemi, S. (2018). Evaluation of the plasma jet effects on the Citrinin and Ochratoxin A producing species of the genus *Penicillium*. *Bulg. Chem. Commun.* 50, 383–392.
- Vitoratos, A., Bilalis, D., Karkanis, A., and Efthimiadou, A. (2013). Antifungal activity of plant essential oils against *Botrytis cinerea*, *Penicillium italicum* and *Penicillium digitatum*. *Not. Botanicae Horti Agrobot. Cluj-Napoca* 41, 86–92. doi: 10.15835/nbha4118931
- Wan, C., Li, P., Chen, C., Peng, X., Li, M., Chen, M., et al. (2017). Antifungal activity of *Ramulus cinnamomi* explored by 1 H-NMR based metabolomics approach. *Molecules* 22, 1–11. doi: 10.3390/molecules22122237
- Wang, J., Sun, X., Lin, L., Zhang, T., Ma, Z., and Li, H. (2012). PdMfs1, a major facilitator superfamily transporter from *Penicillium digitatum*, is partially involved in the imazalil-resistance and pathogenicity. *African J. Microbiol. Res.* 6, 95–105. doi: 10.5897/AJMR11.1045
- Wang, M., Chen, C., Zhu, C., Sun, X., Ruan, R., and Li, H. (2014). Os2 MAP kinase-mediated osmotic stress tolerance in *Penicillium digitatum* is associated with its positive regulation on glycerol synthesis and negative regulation on ergosterol synthesis. *Microbiol. Res.* 169, 511–521. doi: 10.1016/j.micres.2013.12.004
- Wang, W., Deng, L., Yao, S., and Zeng, K. (2018). Control of green and blue mold and sour rot in citrus fruits by the cationic antimicrobial peptide PAF56. *Postharvest Biol. Technol.* 136, 132–138. doi: 10.1016/j.postharvbio.2017.10.0155
- Whiteside, J. O., Garnsey, S. M., and Timmer, L. W. (1993). *Compendium of Citrus Disease*. 2nd Edn. Saint Paul: APS Press.
- Wu, T., Zang, X., He, M., Pan, S., and Xu, X. (2013). Structure-activity relationship of flavonoids on their anti-*Escherichia coli* activity and inhibition of DNA gyrase. *J. Agric. Food Chem.* 61, 8185–8190. doi: 10.1021/jf402222v
- Wu, Y., Ouyang, Q., and Tao, N. (2016a). Plasma membrane damage contributes to antifungal activity of citronellal against *Penicillium digitatum*. *J. Food Sci. Technol.* 53, 3853–3858. doi: 10.1007/s13197-016-2358-x
- Wu, Z., Wang, S., Yuan, Y., Zhang, T., Liu, J., and Liu, D. (2016b). A novel major facilitator superfamily transporter in *Penicillium digitatum* (PdMFS2) is required for prochloraz resistance, conidiation and full virulence. *Biotechnol. Lett.* 38, 1349–1357. doi: 10.1007/s10529-016-2113-4
- Xu, X., Zhou, X. D., and Wu, C. D. (2011). The tea catechin epigallocatechin gallate suppresses cariogenic virulence factors of *Streptococcus mutans*. *Antimicrob. Agents Chemother.* 55, 1229–1236. doi: 10.1128/AAC.01016-10
- Yamaga, I., Kuniga, T., Aoki, S., Kato, M., and Kobayashi, Y. (2016). Effect of ultraviolet-B irradiation on disease development caused by *Penicillium italicum* in satsuma mandarin fruit. *Hortic. J.* 85, 86–91. doi: 10.2503/hortj.MI-074
- Yang, S., Liu, L., Li, D., Xia, H., Su, X., Peng, L., et al. (2016). Use of active extracts of poplar buds against *Penicillium italicum* and possible modes of action. *Food Chem.* 196, 610–618. doi: 10.1016/j.foodchem.2015.09.101
- Yang, Z., Kaliaperumal, K., Zhang, J., Liang, Y., Guo, C., Zhang, J., et al. (2020). Antifungal fatty acid derivatives against *Penicillium italicum* from the deep-sea fungus *Aspergillus terreus* SCSIO 41202. *Nat. Prod. Res.* 1–8. doi: 10.1080/14786419.2020.1716350
- Yin, C., Zhu, H., Jiang, Y., Shan, Y., and Gong, L. (2020). Silencing dicer-like genes reduces virulence and sRNA generation in *Penicillium italicum*, the cause of citrus blue mold. *Cells* 9, 363. doi: 10.3390/cells9020363
- Youssef, K., and Hussien, A. (2020). Electrolysed water and salt solutions can reduce green and blue molds while maintain the quality properties of 'Valencia' late oranges. *Postharvest Biol. Technol.* 159, 1–11. doi: 10.1016/j.postharvbio.2019.111025
- Yun, Z., Gao, H., Liu, P., Liu, S., Luo, T., Jin, S., et al. (2013). Comparative proteomic and metabolomic profiling of citrus fruit with enhancement of disease resistance by postharvest heat treatment. *BMC Plant Biol.* 13:44. doi: 10.1186/1471-2229-13-44

- Zain, M. E. (2011). Impact of mycotoxins on humans and animals. *J. Saudi Chem. Soc.* 15, 129–144. doi: 10.1016/j.jscs.2010.06.006
- Zhang, T., Cao, Q., Li, N., Liu, D., and Yuan, Y. (2020). Transcriptome analysis of fungicide-responsive gene expression profiles in two *Penicillium italicum* strains with different response to the sterol demethylation inhibitor (DMI) fungicide prochloraz. *BMC Genomics* 21:156. doi: 10.1186/s12864-020-6564-6
- Zhang, T., Li, N., Yuan, Y., Cao, Q., Chen, Y., Tan, B., et al. (2019). Blue-white colony selection of virus-infected isogenic recipients based on a chrysovirus isolated from *Penicillium italicum*. *Virol. Sin.* 34, 688–700. doi: 10.1007/s12250-019-00150-z

Conflict of Interest: The authors declare that the research was conducted in the absence of any commercial or financial relationships that could be construed as a potential conflict of interest.

Copyright © 2020 Kanashiro, Akiyama, Kupper and Fill. This is an open-access article distributed under the terms of the Creative Commons Attribution License (CC BY). The use, distribution or reproduction in other forums is permitted, provided the original author(s) and the copyright owner(s) are credited and that the original publication in this journal is cited, in accordance with accepted academic practice. No use, distribution or reproduction is permitted which does not comply with these terms.



Pseudonocardia Symbionts of Fungus-Growing Ants and the Evolution of Defensive Secondary Metabolism

Sarah L. Goldstein and Jonathan L. Klassen*

Department of Molecular and Cell Biology, University of Connecticut, Mansfield, CT, United States

OPEN ACCESS

Edited by:

Monica T. Pupo,
University of São Paulo, Brazil

Reviewed by:

Pepijn Wilhelmus Kooij,
São Paulo State University, Brazil
Laura V. Flórez,
Johannes Gutenberg University
Mainz, Germany

*Correspondence:

Jonathan L. Klassen
jonathan.klassen@uconn.edu

Specialty section:

This article was submitted to
Microbial Symbioses,
a section of the journal
Frontiers in Microbiology

Received: 24 October 2020

Accepted: 03 December 2020

Published: 22 December 2020

Citation:

Goldstein SL and Klassen JL
(2020) *Pseudonocardia* Symbionts
of Fungus-Growing Ants
and the Evolution of Defensive
Secondary Metabolism.
Front. Microbiol. 11:621041.
doi: 10.3389/fmicb.2020.621041

Actinobacteria belonging to the genus *Pseudonocardia* have evolved a close relationship with multiple species of fungus-growing ants, where these bacteria produce diverse secondary metabolites that protect the ants and their fungal mutualists from disease. Recent research has charted the phylogenetic diversity of this symbiosis, revealing multiple instances where the ants and *Pseudonocardia* have formed stable relationships in which these bacteria are housed on specific regions of the ant's cuticle. Parallel chemical and genomic analyses have also revealed that symbiotic *Pseudonocardia* produce diverse secondary metabolites with antifungal and antibacterial bioactivities, and highlighted the importance of plasmid recombination and horizontal gene transfer for maintaining these symbiotic traits. Here, we propose a multi-level model for the evolution of *Pseudonocardia* and their secondary metabolites that includes symbiont transmission within and between ant colonies, and the potentially independent movement and diversification of their secondary metabolite biosynthetic genes. Because of their well-studied ecology and experimental tractability, *Pseudonocardia* symbionts of fungus-growing ants are an especially useful model system to understand the evolution of secondary metabolites, and also comprise a significant source of novel antibiotic and antifungal agents.

Keywords: *Pseudonocardia*, attine ant mutualism, evolution, symbiosis, specialized (secondary) metabolite

INTRODUCTION

Actinomycete bacteria form many beneficial symbioses with eukaryotes, where the host typically provides nutritional support and the actinomycetes provide chemical defense (Van Arnam et al., 2018). The best-studied of these are insect-actinomycete mutualisms, which are widespread and the source of many novel secondary metabolites with antibacterial and antifungal activity (Chevrette and Currie, 2019). Insect-associated *Streptomyces* inhibited clinically relevant microbes more effectively than soil-isolated *Streptomyces* (Chevrette et al., 2019), perhaps due to co-evolution between insects and microbes that has selected for defensive metabolites inhibiting pathogens but not their hosts (Clardy et al., 2009). The potential rise of antimicrobial resistance in these symbioses must have also been overcome by selection consistently replenishing and diversifying their defensive metabolites. However, few systems exist where such ecological and evolutionary dynamics have been dissected in detail.

FUNGUS-GROWING ANTS: A MULTIPARTITE MUTUALISM

Fungus-growing (Attine) ants are one of the best-studied insect-microbe symbioses, encompassing > 250 described species from 17 genera (Schultz and Brady, 2008; Sosa-Calvo et al., 2018) that inhabit a geographic range stretching from the tip of Argentina to Long Island, New York, United States (Weber, 1972). Approximately 50–60 million years ago, these ants established a symbiotic relationship with a “cultivar” fungal symbiont that they farm in underground fungus gardens (Mueller et al., 1998). Fungus-growing ants provide fresh leaves (especially in the most-specialized leaf-cutting ants), grass clippings, fruits, berries, flowers, and insect frass to their fungal cultivar (De Fine Licht and Boomsma, 2010), which is the ants’ obligate food source. The cultivar relies on the ants for vertical propagation, and has lost its ability to reproduce sexually via spores (Weber, 1972). Virgin ant queens take a small piece of cultivar fungus from their native nests with them during their nuptial mating flights and use it to establish their new colonies, propagating the fungal cultivar in a largely clonal fashion (Mueller et al., 1998). It was originally believed that no other fungi were present in ant fungus gardens due to the effects of antimicrobials that the ants secrete (Hölldobler and Wilson, 1990) and their extensive grooming behaviors (Currie and Stuart, 2001). However, Currie et al. (1999a) demonstrated the persistent presence of a specialized fungal parasite *Escovopsis* within ant fungus gardens that is highly pathogenic toward the cultivar fungus, and suggested that the fungus-growing symbiosis be expanded to include the ants, their cultivar, and the *Escovopsis* fungal pathogen as a coevolving tripartite symbiosis (Currie et al., 2003c). Future research will likely clarify the conditions under which *Escovopsis* acts as such a pathogen, and the impact of other pathogens in this symbiosis.

Concurrent with the discovery of the fungal pathogen *Escovopsis*, Currie et al. (1999b) also established that an actinomycete bacterium comprises a fourth partner in the fungus-growing ant symbiosis. Many fungus-growing ant species have a region of their cuticle that is covered by a white or gray crust (Figure 1), which was initially described as a “waxy bloom” and dismissed as a cellular exudate (Weber, 1972). Upon closer inspection using scanning electron microscopy and targeted microbial isolations, this crust was subsequently determined to be a biofilm formed by the actinomycete *Pseudonocardia* (albeit initially misidentified as *Streptomyces*; Currie et al., 1999b, 2003b; Cafaro and Currie, 2005). These *Pseudonocardia* are housed in specialized structures on the ant cuticle that are connected to ant exocrine glands (Poulsen et al., 2003; Currie et al., 2006; Li et al., 2018), and their growth may be upregulated when an ant colony is under attack by *Escovopsis* (Currie et al., 2003a). *Pseudonocardia* symbionts can be parasitized by black yeast that compete with them for nutrients on the ant-cuticle, suppressing the growth of *Pseudonocardia* (Little and Currie, 2007). Such parasitism makes the fungus garden more susceptible to fungal infection, highlighting *Pseudonocardia*’s contribution to maintaining ant colony health (Little and Currie, 2008).

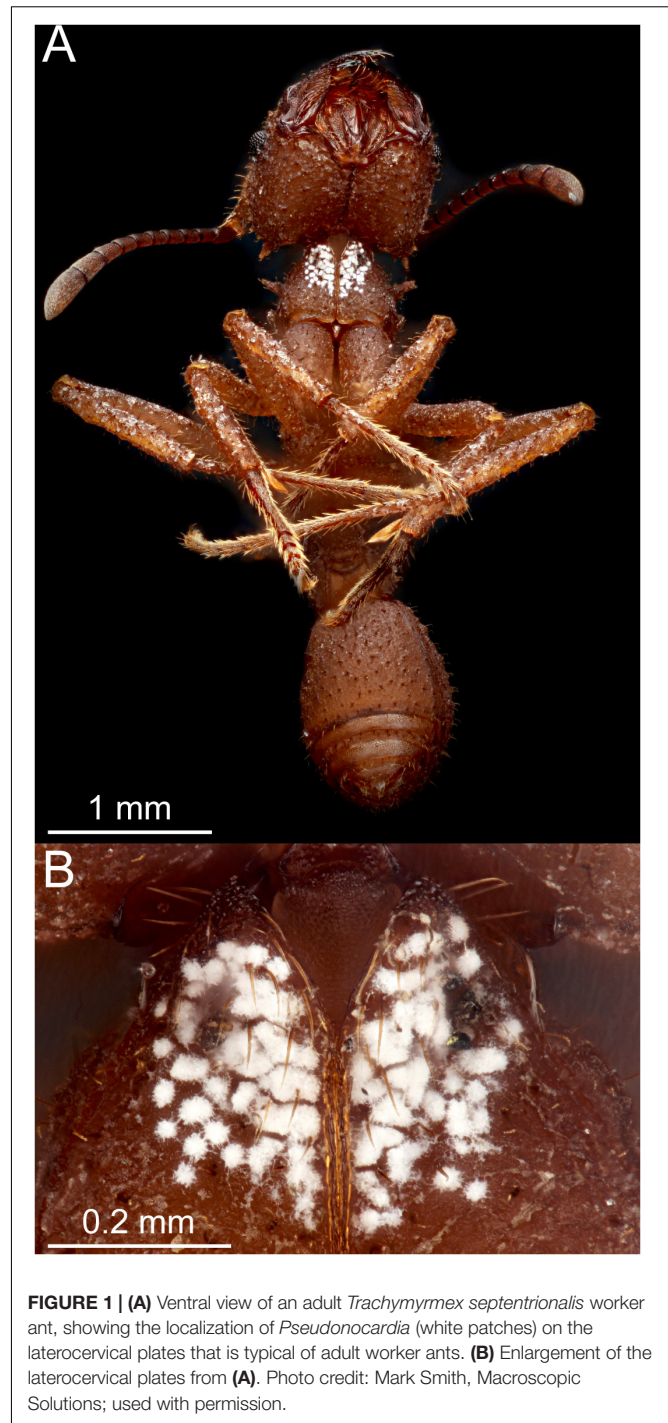


FIGURE 1 | (A) Ventral view of an adult *Trachymyrmex septentrionalis* worker ant, showing the localization of *Pseudonocardia* (white patches) on the laterocervical plates that is typical of adult worker ants. **(B)** Enlargement of the laterocervical plates from **(A)**. Photo credit: Mark Smith, Macroscopic Solutions; used with permission.

PSEUDONOCARDIA AS A DEFENSIVE SYMBIONT

Increased abundance of *Pseudonocardia* on ants in response to parasite infection underscores the predicted function of this bacterium in the system: to protect the fungal cultivar against *Escovopsis* (Currie et al., 1999b, 2003a). *Pseudonocardia* prevent *Escovopsis* infections of ant fungus gardens *in vivo*

(Currie et al., 2003a; Little and Currie, 2008; Poulsen et al., 2010), and *Pseudonocardia* isolates consistently inhibit *Escovopsis* cultures *in vitro* (Currie et al., 1999b, 2003a; Schoenian et al., 2011; Meirelles et al., 2013; Sit et al., 2015; Dângelo et al., 2016). Some researchers have therefore suggested that these symbionts co-evolve with one another, locked in an arms race where *Pseudonocardia* and *Escovopsis* constantly evolve new mechanisms to gain an advantage over each other (Woolhouse et al., 2002). However, *Pseudonocardia* defenses against *Escovopsis* can vary (Poulsen et al., 2010), and some fungus-growing ants are not pathogenized by *Escovopsis* (Rodrigues et al., 2008), despite hosting *Pseudonocardia*. Further studies have shown that *Pseudonocardia* isolates have broad-spectrum activities against fungi other than just *Escovopsis* (Sen et al., 2009; Meirelles et al., 2013; Dângelo et al., 2016), suggesting that *Pseudonocardia*'s antimicrobials inhibit diverse pathogens in the fungus-growing ant symbiosis.

Pseudonocardia strains can also inhibit entomopathogens that infect the ants (Sen et al., 2009; Mattoso et al., 2012), to which ants are inevitably exposed to as they excavate tunnels, tend to brood, or forage for plant matter (Hughes et al., 2004, 2009). Although the ants themselves possess an innate immune system that can defend against pathogens (Gillespie et al., 1997), and engage in allogrooming to reduce the potential for infection (Walker and Hughes, 2009), *Pseudonocardia* may add further protection against ant pathogens (de Souza et al., 2013). *Pseudonocardia* abundance peaks at 10–15 days post-eclosion before declining (Poulsen et al., 2003), and so *Pseudonocardia* may therefore particularly confer protection to young workers by giving their immune systems time to develop and recognize entomopathogens, in addition to protecting the fungal cultivar against *Escovopsis* (de Souza et al., 2013).

PSEUDONOCARDIA SYMBIONT TRANSMISSION AND SPECIFICITY

Pseudonocardia are thought to typically be transmitted vertically, similar to the fungal cultivar. *Pseudonocardia* symbionts were detected on foundress ant queens, but not on male alates, during their nuptial flights (Currie et al., 1999b). *Pseudonocardia* were also identified on virgin queens within their native nests, but not on males (Currie et al., 1999b), suggesting that founding queens need to maintain *Pseudonocardia* to successfully establish new colonies. Once a colony is established, *Pseudonocardia* are transmitted vertically to new workers within 2 h of eclosing via contact with an older worker ant that has an established *Pseudonocardia* biofilm, after which time vertical transmission is drastically reduced (Marsh et al., 2014). Vertical transmission of *Pseudonocardia*, therefore occurs both within and between ant colonies.

Phylogenetic studies have also revealed an evolutionary history of ant-associated *Pseudonocardia* that is largely, but not exclusively, consistent with vertical transmission. Most fungus-growing ant colonies maintain a single strain of *Pseudonocardia* (Poulsen et al., 2005; Andersen et al., 2013), and this specificity can be maintained in the lab for at least 10 years (Andersen et al.,

2013). Consistent with the dominance of vertical transmission, Cafaro et al. (2011) observed significant, but not absolute, patterns of specificity between lineages of *Pseudonocardia* and their ant host genera using a multi-locus gene phylogeny. Subsequent studies indicated that the *Pseudonocardia*-ant symbiosis has been gained and lost multiple times during ant evolution (Li et al., 2018), the most notable of these being the loss of *Pseudonocardia* in the highly derived *Atta* leaf-cutting ants (but see Marsh et al., 2013). *Pseudonocardia* symbionts of *Apterostigma dentigerum* ants have population structures that are consistent with vertical transmission between their dispersal-limited hosts (Caldera and Currie, 2012; McDonald et al., 2019), but similar population structures were not detected for *Pseudonocardia* symbionts of *Trachymyrmex septentrionalis* ants using methods with lower phylogenetic resolution (Mikheyev et al., 2008). Ants can recognize their native *Pseudonocardia* symbiont (Zhang et al., 2007; Poulsen et al., 2011), and experimental symbiont swaps decrease symbiont abundance and ant grooming behavior, thereby allowing increased pathogen infection (Armitage et al., 2011; Andersen et al., 2015). These results show that *Pseudonocardia* can be adapted to their specific ant hosts and vice versa, as expected from a predominantly vertical mode of transmission, although symbiont replacement remains possible.

Like many microbial symbionts (Garcia and Gerardo, 2014), the fitness benefits that *Pseudonocardia* gain from their relationship with fungus-growing ants remains unclear. Although exocrine gland secretions have been speculated to feed *Pseudonocardia* symbionts (Currie et al., 2006), this has not been demonstrated unequivocally. The vertical transfer of *Pseudonocardia* between ant generations implies fitness benefits that are received by these bacteria (otherwise the relationship would be expected to break down). However, *Pseudonocardia* presence varies between related ant species (Fernández-Marín et al., 2013) and genera (Li et al., 2018), indicating that the benefits of this relationship change over time. Further research is warranted to determine the conditions under which selection favors *Pseudonocardia* and/or their ant hosts, and how potential conflicts between these partners are resolved, which will define when and if *Pseudonocardia* functions as an ant mutualist, commensal, or parasite.

The predicted function of *Pseudonocardia* as a defensive symbiont provides an evolutionary incentive for ant colonies to maintain effective *Pseudonocardia* strains. There is a fitness cost for an ant to swap symbionts if a less effective strain replaces a more effective one (Sachs et al., 2011). However, strict maintenance and vertical transmission of clonal symbionts can lead to other potential problems, such as Muller's ratchet, which predicts that a symbiont is ultimately doomed to extinction due to the accumulation of deleterious mutations in the absence of recombination or symbiont replacement (Bennett and Moran, 2015). Considering that *Pseudonocardia* symbionts of fungus-growing ants were observed in a piece of 15 million year old amber (Li et al., 2018), it is likely the ant-*Pseudonocardia* symbiosis has been conserved over long evolutionary timescales, despite the predominantly vertical transmission of clonal symbiont populations.

CHALLENGING *PSEUDONOCARDIA* SPECIFICITY AND CLONALITY

How then does this ant-actinomycete symbiosis maintain enough diversity to avoid extinction or the loss of their defensive function? One hypothesis is that actinomycetes other than *Pseudonocardia* are also maintained as defensive symbionts of ants. Several studies have isolated such actinomycetes from fungus-growing ants and showed that they inhibit fungal pathogens *in vitro* (Kost et al., 2007; Mueller et al., 2008; Haeder et al., 2009; Sen et al., 2009; Barke et al., 2010; Dângelo et al., 2016). Schoenian et al. (2011) also found compounds known to be produced by *Streptomyces* strains on the cuticle of *Acromyrmex* ants, concluding that those actinomycetes were therefore ant symbionts. However, these studies have limitations that constrain their ability to unambiguously assign a symbiotic relationship or defensive function to these actinomycetes (Klassen, 2014, 2018, 2020). First, they typically sample few ant colonies, in contrast to the systematic sampling of *Pseudonocardia* that shows its widespread relationship with fungus-growing ants (Cafaro et al., 2011; Li et al., 2018). Such limited sampling cannot differentiate persistent symbionts from more transient microbial contaminants. Second, the widely used culture-based techniques are largely qualitative and can misrepresent the dominant taxa in samples (Andersen et al., 2013), instead leading to a focus on low-abundance microbes due to enrichment biases. Third, samples taken from whole ants instead of the specific locations where *Pseudonocardia* are known to localize (Figure 1) can introduce contaminants that mask the dominance of *Pseudonocardia* and its products in their more specific niche (Andersen et al., 2013; Gemperline et al., 2017). Thus, although it may be true that other actinomycetes occur in the fungus-growing ant symbiosis and produce secondary metabolites, additional evidence is required to confirm their functional role as fungus-growing ant symbionts and to rule out alternative interpretations such as transient contamination of ant colonies (Klassen, 2014, 2018, 2020).

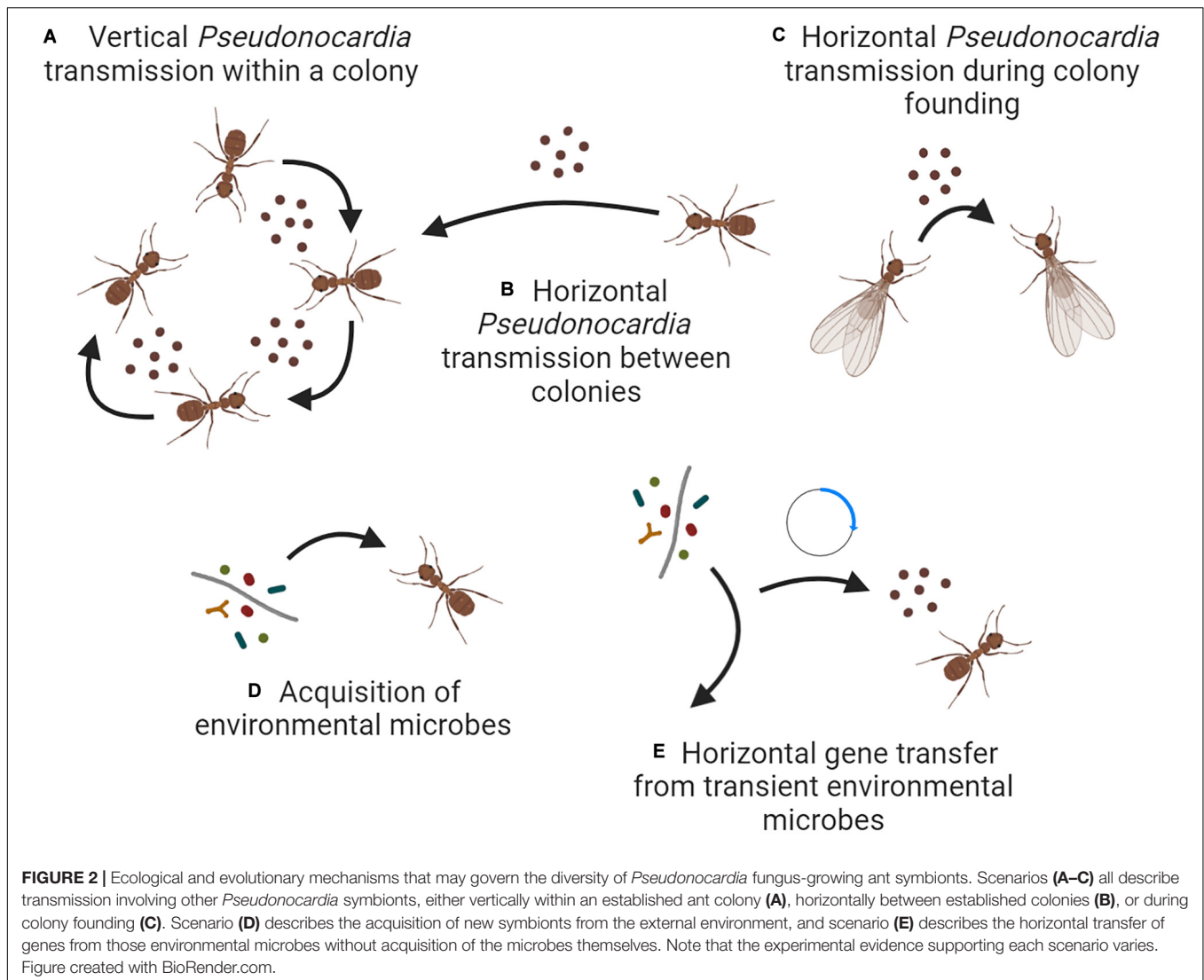
The clonality of *Pseudonocardia* symbionts within individual ant colonies has also been challenged. Culture-dependent and -independent 16S rRNA gene amplicon sequencing of *T. septentrionalis*-associated *Pseudonocardia* found an average of 2.9 strains of *Pseudonocardia* per ant (Ishak et al., 2011). However, this study sampled whole ants and ant sections instead of specifically targeting the propleural plates where *Pseudonocardia* is localized, perhaps including transient bacteria from within the ant and elsewhere on the cuticle. These criticisms also apply to similar studies (e.g., Sen et al., 2009), including those that sampled *Pseudonocardia* from ant fungus gardens instead of from on the ants themselves (e.g., Mueller et al., 2008). In contrast, laterocervical plates dissected from *Acromyrmex echinator* ants with the remaining internal soft tissue removed prior to 454 16S rRNA gene pyrosequencing hosted single *Pseudonocardia* strains in 25 of 26 ants sampled (Andersen et al., 2013), consistent with the prevalence of clonal *Pseudonocardia* populations in most, but not all, fungus-growing ant colonies. Finally, it is important to note that these and related studies investigating the clonality and transmission of *Pseudonocardia* strains (e.g., Mueller et al., 2010) have relied on

the partial sequencing of housekeeping genes that contain limited phylogenetic information and that are often superseded by the higher resolution provided by whole genome sequencing, which is able to more precisely resolve species and population-level differences (e.g., McDonald et al., 2019).

COMPETITION MAY DRIVE HORIZONTAL GENE TRANSFER

Despite the issues described above, the presence of other actinomycetes in association with fungus-growing ants should not be discounted. *Pseudonocardia* isolates may be maintained and vertically propagated in this symbiosis while also acquiring genetic diversity, particularly secondary metabolite biosynthetic gene clusters (BGCs), via genetic exchange with other environmental actinomycetes. This strategy would allow *Pseudonocardia* to avoid the consequences of strict vertical transmission, such as Muller's ratchet, and to increase their fitness by acquiring BGCs from other actinomycetes to overcome pathogen resistance. The ability to acquire BGCs may represent a preadaptation that makes *Pseudonocardia* an especially successful symbiotic partner (Toft and Andersson, 2010). Horizontal acquisition of defensive genes may also provide *Pseudonocardia* with the ability to compete against other strains that seek to colonize the ant host (Sachs et al., 2011). This ability to inhibit other actinomycetes may even have given rise to the vertical propagation of specific *Pseudonocardia* lineages, allowing what may have initially began as a parasitic relationship to transition to a mutualism (Sachs et al., 2011). Other theoretical models have suggested that such competition between actinomycetes may actively select for *Pseudonocardia* that produce high levels of bioactive compounds on the ants (Scheuring and Yu, 2012), although it should be noted that the antibacterial compounds deployed for competition between bacteria are likely to differ from those that mediate antifungal defense.

Native *Pseudonocardia* strains inhibit the growth of other *Pseudonocardia* that may seek to take over the ant cuticle. Resident *Pseudonocardia* strains inhibited ~60% of tested intruder strains, and most strongly inhibited intruders that were genetically distant from the resident strain, including strains from other fungus-growing ant species and non-ant environments (Poulsen et al., 2007). This pattern may result from genetically related *Pseudonocardia* possessing similar BGCs, and therefore similar resistance genes that are often genetically linked to these BGCs. Two *Pseudonocardia* isolates, BCI1 and BCI2, were isolated from *A. dentigerum* ants collected on Barro Colorado Island (BCI), located in the middle of the Panama Canal. These strains shared 100% identical 16S rRNA genes and >98% average nucleotide identity between their chromosomes (Van Arnam et al., 2015). However, only strain BCI2 inhibited all other tested actinomycete strains due its unique acquisition of a BGC that encoded for an analog of the antimicrobial metabolite rebeccamycin on a plasmid that was otherwise >96% conserved in strain BCI1. The presence of this novel plasmid-encoded BGC suggests that strain BCI2 acquired these genes horizontally



from environmental actinomycetes. Similarly, Chang et al. (2020) recently isolated thiopeptide GE37468 from *Trachymyrmex septentrionalis* ants, whose BGC was closely related to that of the non-symbiotic *Streptomyces* strain ATCC 55365. It is therefore, likely that *Pseudonocardia* symbionts acquire BGCs from environmental actinomycetes.

PSSEUDONOCARDIA AS A RESOURCE FOR NOVEL METABOLITE DISCOVERY

Both known and unknown antimicrobials have been identified from *Pseudonocardia* symbionts of fungus-growing ants and the antibiotics GE37468 (Chang et al., 2020), X-14881 E, and 6-deoxy-9-O-methylrebelomycin (Carr et al., 2012). Novel metabolites discovered from *Pseudonocardia* symbionts include the antibiotics pseudonocardone A, B, and C (Carr et al., 2012), and 9-methoxyrebeccamycin (Van Arnam et al., 2015), the depsipeptide natural products dentigerumycin (Oh et al.,

2009) and gerumycin A, B, and C (Sit et al., 2015), nystatin-like antifungals (Barke et al., 2010; Seipke et al., 2012; Holmes et al., 2016), and the atypical antifungal polyene selvamicin (Van Arnam et al., 2016). The variable genetic contexts in which the BGCs encoding for these metabolites occur is striking. The gerumycin BGC is encoded chromosomally in one *Pseudonocardia* strain but on the plasmid of another (Sit et al., 2015); the same is true for selvamicin (Van Arnam et al., 2016). This suggests that *Pseudonocardia* strains may horizontally acquire BGCs first on their plasmids, and then later move them to their chromosome. Alternatively, BGCs could move from the chromosome to plasmid(s), with either mechanism generating high levels of BGC diversity on plasmids that might be a fruitful target for the discovery of novel metabolites (Sit et al., 2015; Ruzzini and Clardy, 2016).

Pseudonocardia symbionts also vary in their BGC composition over local geographic scales. BGC composition varied between strains sampled across a 20 km transect in Panama (McDonald et al., 2019). Of the 27 BGC families identified

from these *Pseudonocardia* symbionts, 7 occurred only on BCI. *Pseudonocardia* symbiont strains obtained from BCI also displayed local adaptation to the *Escovopsis* strains that were endemic to that location (Caldera et al., 2019), suggesting that this may be a hotspot for evolving antifungal bioactivities. Other such hotspots likely exist throughout fungus-growing ant biodiversity and could also be targeted for the discovery of novel metabolites.

CONCLUSION

Having been initially established multiple times (Li et al., 2018), the fungus-growing ant-*Pseudonocardia* symbiosis now evolves simultaneously on multiple organizational levels. First, *Pseudonocardia* strains are occasionally transferred horizontally between colonies, despite the predominance of vertical transmission between ants and ant colonies (Figures 2A,B). Although data is lacking, such transfer may most likely occur during colony founding when the source populations of *Pseudonocardia* are small and therefore, more prone to stochastic variation (Figure 2C; cf. Poulsen et al., 2009). Transfer between colonies may also be facilitated by antibiotics that

allow invasion that overcomes native *Pseudonocardia* strains (Poulsen et al., 2007; Van Arnam et al., 2015). Second, niche-defining genes such as secondary metabolite BGCs may be horizontally transferred to *Pseudonocardia* from other microbes that pass through its ant-associated niche, and such transfer likely involves plasmids as a prominent mechanism of genome plasticity (Figures 2D,E; Van Arnam et al., 2015). Together, these mechanisms allow *Pseudonocardia* symbionts to avoid Mueller's ratchet and maintain their effectiveness as defensive mutualists of fungus-growing ants.

AUTHOR CONTRIBUTIONS

SG and JK conceived, wrote, and revised this manuscript. Both authors contributed to the article and approved the submitted version.

FUNDING

Funding for this work was provided by NSF IOS-1656475.

REFERENCES

- Andersen, S. B., Hansen, L. H., Sapountzis, P., Sørensen, S. J., and Boomsma, J. J. (2013). Specificity and stability of the *Acromyrmex*-*Pseudonocardia* symbiosis. *Mol. Ecol.* 22, 4307–4321. doi: 10.1111/mec.12380
- Andersen, S. B., Yek, S. H., Nash, D. R., and Boomsma, J. J. (2015). Interaction specificity between leaf-cutting ants and vertically transmitted *Pseudonocardia* bacteria. *BMC Evol. Biol.* 15:27. doi: 10.1186/s12862-015-0308-2
- Armitage, S. A. O., Broch, J. F., Marín, H. F., Nash, D. R., and Boomsma, J. J. (2011). Immune defense in leaf-cutting ants: a cross-fostering approach. *Evolution* 65, 1791–1799. doi: 10.1111/j.1558-5646.2011.01241.x
- Barke, J., Seipke, R. F., Gruschow, S., Heavens, D., Drou, N., Bibb, M. J., et al. (2010). A mixed community of actinomycetes produce multiple antibiotics for the fungus farming ant *Acromyrmex octospinosus*. *BMC Biol.* 8:109. doi: 10.1186/1741-7007-8-109
- Bennett, G. M., and Moran, N. A. (2015). Heritable symbiosis: the advantages and perils of an evolutionary rabbit hole. *Proc. Natl. Acad. Sci. U.S.A.* 112, 10169–10176. doi: 10.1073/pnas.1421388112
- Cafaro, M. J., and Currie, C. R. (2005). Phylogenetic analysis of mutualistic filamentous bacteria associated with fungus-growing ants. *Can. J. Microbiol.* 44, 441–446. doi: 10.1139/W05-023
- Cafaro, M. J., Poulsen, M., Little, A. E. F., Price, S. L., Gerardo, N. M., Wong, B., et al. (2011). Specificity in the symbiotic association between fungus-growing ants and protective *Pseudonocardia* bacteria. *Proc. R. Soc. B Biol. Sci.* 278, 1814–1822. doi: 10.1098/rspb.2010.2118
- Caldera, E. J., Chevrette, M. G., McDonald, B. R., and Currie, C. R. (2019). Local adaptation of bacterial symbionts within a geographic mosaic of antibiotic coevolution. *Appl. Environ. Microbiol.* 85:e01580-19. doi: 10.1128/AEM.01580-19
- Caldera, E. J., and Currie, C. R. (2012). The population structure of antibiotic-producing bacterial symbionts of *Apterostigma dentigerum* ants: impacts of coevolution and multipartite symbiosis. *Am. Nat.* 180, 604–617. doi: 10.1086/667886
- Carr, G., Derbyshire, E. R., Caldera, E., Currie, C. R., and Clardy, J. (2012). Antibiotic and antimalarial quinones from fungus-growing ant-associated *Pseudonocardia* sp. *J. Nat. Prod.* 75, 1806–1809. doi: 10.1021/np300380t
- Chang, P. T., Rao, K., Longo, L. O., Lawton, E. S., Scherer, G., and Van Arnam, E. B. (2020). Thiopetide defense by an ant's bacterial symbiont. *J. Nat. Prod.* 83, 725–729. doi: 10.1021/acs.jnatprod.9b00897
- Chevrette, M. G., Carlson, C. M., Ortega, H. E., Thomas, C., Ananiev, G. E., Barns, K. J., et al. (2019). The antimicrobial potential of *Streptomyces* from insect microbiomes. *Nat. Commun.* 10:516. doi: 10.1038/s41467-019-08438-0
- Chevrette, M. G., and Currie, C. R. (2019). Emerging evolutionary paradigms in antibiotic discovery. *J. Ind. Microbiol. Biotechnol.* 46, 257–271. doi: 10.1007/s10295-018-2085-6
- Clardy, J., Fischbach, M. A., and Currie, C. R. (2009). The natural history of antibiotics. *Curr. Biol.* 19, 437–441. doi: 10.1016/j.cub.2009.04.001
- Currie, C. R., Bot, A. N. M., and Boomsma, J. J. (2003a). Experimental evidence of a tripartite mutualism: bacteria protect ant fungus gardens from specialized parasites. *Oikos* 101, 91–102. doi: 10.1034/j.1600-0706.2003.12036.x
- Currie, C. R., Mueller, U. G., and Malloch, D. (1999a). The agricultural pathology of ant fungus gardens. *Proc. Natl. Acad. Sci. U.S.A.* 96, 7998–8002. doi: 10.1073/pnas.96.14.7998
- Currie, C. R., Scott, J. A., Summerbell, R. C., and Malloch, D. (2003b). Corrigenda: fungus-growing ants use antibiotic-producing bacteria to control garden parasites. *Nature* 423:461. doi: 10.1038/nature01563
- Currie, C. R., Scott, J. A., Summerbell, R. C., and Malloch, D. (1999b). Fungus-growing ants use antibiotic-producing bacteria to control garden parasites. *Nature* 398, 701–705. doi: 10.1038/19519
- Currie, C. R., Wong, B., Stuart, A. E., Schultz, T. R., Rehner, S. A., Mueller, U. G., et al. (2003c). Ancient tripartite coevolution in the attine ant-microbe symbiosis. *Science* 299, 386–388. doi: 10.1126/science.1078155
- Currie, C. R., Poulsen, M., Mendenhall, J., Boomsma, J. J., and Billen, J. (2006). Coevolved crypts and exocrine glands support mutualistic bacteria in fungus-growing ants. *Science* 311, 81–83. doi: 10.1126/science.1119744
- Currie, C. R., and Stuart, A. E. (2001). Weeding and grooming of pathogens in agriculture by ants. *Proc. R. Soc. B Biol. Sci.* 268, 1033–1039. doi: 10.1098/rspb.2001.1605
- Dângelo, R. A. C., de Souza, D. J., Mendes, T. D., Couceiro, J. D. C., and Lucia, T. M. C. D. (2016). Actinomycetes inhibit filamentous fungi from the cuticle of *Acromyrmex* leafcutter ants. *J. Basic Microbiol.* 56, 229–237. doi: 10.1002/jobm.201500593
- De Fine Licht, H. H., and Boomsma, J. J. (2010). Forage collection, substrate preparation, and diet composition in fungus-growing ants. *Ecol. Entomol.* 35, 259–269. doi: 10.1111/j.1365-2311.2010.01193.x
- de Souza, D. J., Lenoir, A., Kasuya, M. C. M., Ribeiro, M. M. R., Devers, S., Couceiro, J. D. C., et al. (2013). Ectosymbionts and immunity in the leaf-cutting ant *Acromyrmex subterraneus subterraneus*. *Brain. Behav. Immun.* 28, 182–187. doi: 10.1016/j.bbi.2012.11.014

- Fernández-Marín, H., Bruner, G., Gomez, E. B., Nash, D. R., Boomsma, J. J., and Wcislo, W. T. (2013). Dynamic disease management in *Trachymyrmex* fungus-growing ants (Attini: Formicidae). *Am. Nat.* 181, 571–582. doi: 10.1086/669664
- García, J. R., and Gerardo, N. M. (2014). The symbiont side of symbiosis: Do microbes really benefit? *Front. Microbiol.* 5:510. doi: 10.3389/fmicb.2014.00510
- Gemperline, E., Horn, H. A., Delaney, K., Currie, C. R., and Li, L. (2017). Imaging with mass spectrometry of bacteria on the exoskeleton of fungus-growing ants. *ACS Chem. Biol.* 12, 1980–1985. doi: 10.1021/acscchembio.7b00038
- Gillespie, J. P., Kanost, M. R., and Trenczek, T. (1997). Biological mediators of insect immunity. *Annu. Rev. Entomol.* 42, 611–643. doi: 10.1146/annurev.ento.42.1.611
- Haeder, S., Wirth, R., Herz, H., and Spiteller, D. (2009). Candidicin-producing *Streptomyces* support leaf-cutting ants to protect their fungus garden against the pathogenic fungus *Escovopsis*. *Proc. Natl. Acad. Sci. U.S.A.* 106, 4742–4746. doi: 10.1073/pnas.0812082106
- Hölldobler, B., and Wilson, E. O. (1990). *The Ants*. Cambridge, MA: Belknap Press.
- Holmes, N., Innocent, T., Heine, D., Al Bassam, M., Worsley, S., Trottmann, F., et al. (2016). Genome analysis of two *Pseudonocardia* phylotypes associated with *Acromyrmex* leafcutter ants reveals their biosynthetic potential. *Front. Microbiol.* 7:2073. doi: 10.3389/fmicb.2016.02073
- Hughes, D. P., Evans, H. C., Hywel-Jones, N., Boomsma, J. J., and Armitage, S. A. O. (2009). Novel fungal disease in complex leaf-cutting ant societies. *Ecol. Entomol.* 34, 214–220. doi: 10.1111/j.1365-2311.2008.01066.x
- Hughes, W. O. H., Thomsen, L., Eilenberg, J., and Boomsma, J. J. (2004). Diversity of entomopathogenic fungi near leaf-cutting ant nests in a neotropical forest, with particular reference to *Metarhizium anisopliae* var. *anisopliae*. *J. Invertebr. Pathol.* 85, 46–53. doi: 10.1016/j.jip.2003.12.005
- Ishak, H. D., Miller, J. L., Sen, R., Dowd, S. E., Meyer, E., and Mueller, U. G. (2011). Microbiomes of ant castes implicate new microbial roles in the fungus-growing ant *Trachymyrmex septentrionalis*. *Sci. Rep.* 1:204. doi: 10.1038/srep00204
- Klassen, J. L. (2014). Microbial secondary metabolites and their impacts on insect symbioses. *Curr. Opin. Insect Sci.* 4, 15–22. doi: 10.1016/j.cois.2014.08.004
- Klassen, J. L. (2018). Defining microbiome function. *Nat. Microbiol.* 3, 864–869. doi: 10.1038/s41564-018-0189-4
- Klassen, J. L. (2020). Ecology helps bound causal explanations in microbiology. *Biol. Philos.* 35:3. doi: 10.1007/s10539-019-9728-5
- Kost, C., Lakatos, T., Böttcher, I., Arendholz, W.-R., Redenbach, M., and Wirth, R. (2007). Non-specific association between filamentous bacteria and fungus-growing ants. *Naturwissenschaften* 94, 821–828. doi: 10.1007/s00114-007-0262-y
- Li, H., Sosa-Calvo, J., Horn, H. A., Pupo, M. T., Clardy, J., Rabeling, C., et al. (2018). Convergent evolution of complex structures for ant–bacterial defensive symbiosis in fungus-farming ants. *Proc. Natl. Acad. Sci. U.S.A.* 115, 10720–10725. doi: 10.1073/pnas.1809332115
- Little, A. E. F., and Currie, C. R. (2007). Symbiotic complexity: discovery of a fifth symbiont in the attine ant-microbe symbiosis. *Biol. Lett.* 3, 501–504. doi: 10.1098/rsbl.2007.0253
- Little, A. E. F., and Currie, C. R. (2008). Black yeast symbionts compromise the efficiency of antibiotic defenses in fungus-growing ants. *Ecology* 89, 1216–1222. doi: 10.1890/07-0815.1
- Marsh, S. E., Poulsen, M., Gorosito, N. B., Pinto-Tomás, A., Masiulionis, V. E., and Currie, C. R. (2013). Association between *Pseudonocardia* symbionts and *Atta* leaf-cutting ants suggested by improved isolation methods. *Int. Microbiol.* 16, 17–25. doi: 10.2436/20.1501.01.176
- Marsh, S. E., Poulsen, M., Pinto-Tomás, A., and Currie, C. R. (2014). Interaction between workers during a short time window is required for bacterial symbiont transmission in *Acromyrmex* leaf-cutting ants. *PLoS One* 9:e103269. doi: 10.1371/journal.pone.0103269
- Mattoso, T. C., Moreira, D. D. O., and Samuels, R. I. (2012). Symbiotic bacteria on the cuticle of leaf-cutting ant *Acromyrmex subterraneus subterraneus* protect workers from attack by entomopathogenic fungi. *Biol. Lett.* 8, 461–464. doi: 10.1098/rsbl.2011.0963
- Mcdonald, B. R., Chevrette, M. G., Klassen, J. L., Horn, H. A., Caldera, E. J., Wendt-Pienkowski, E., et al. (2019). Biogeography and microscale diversity shape the biosynthetic potential of fungus-growing ant-associated *Pseudonocardia*. *bioRxiv* [Preprint]. doi: 10.1101/545640
- Meirelles, L. A., Mendes, T. D., Solomon, S. E., Bueno, O. C., Pagnocca, F. C., and Rodrigues, A. (2013). Broad *Escovopsis*-inhibition activity of *Pseudonocardia* associated with *Trachymyrmex* ants. *Environ. Microbiol. Rep.* 6, 339–345. doi: 10.1111/1758-2229.12132
- Mikheyev, A. S., Vo, T., and Mueller, U. G. (2008). Phylogeography of post-Pleistocene population expansion in a fungus-gardening ant and its microbial mutualists. *Mol. Ecol.* 17, 4480–4488. doi: 10.1111/j.1365-294X.2008.03940.x
- Mueller, U. G., Dash, D., Rabeling, C., and Rodrigues, A. (2008). Coevolution between attine ants and actinomycete bacteria: a reevaluation. *Evolution* 62, 2894–2912. doi: 10.1111/j.1558-5646.2008.00501.x
- Mueller, U. G., Ishak, H., Lee, J. C., Sen, R., and Gutell, R. R. (2010). Placement of attine ant-associated *Pseudonocardia* in a global *Pseudonocardia* phylogeny (Pseudonocardiaceae, Actinomycetales): a test of two symbiont-association models. *Antonie Van Leeuwenhoek* 98, 195–212. doi: 10.1007/s10482-010-9427-3
- Mueller, U. G., Rehner, S. A., and Schultz, T. R. (1998). The evolution of agriculture in ants. *Science* 281, 2034–2038. doi: 10.1126/science.281.5385.2034
- Oh, D.-C., Poulsen, M., Currie, C. R., and Clardy, J. (2009). Dentigerumycin: a bacterial mediator of an ant-fungus symbiosis. *Nat. Chem. Biol.* 5, 391–393. doi: 10.1038/nchembio.159
- Poulsen, M., Bot, A. N. M., Currie, C. R., Nielsen, M. G., and Boomsma, J. J. (2003). Within-colony transmission and the cost of transmission in the leaf-cutting bacterium a mutualistic ant *Acromyrmex octospinosus*. *Funct. Ecol.* 17, 260–269. doi: 10.1046/j.1365-2435.2003.00726.x
- Poulsen, M., Cafaro, M., Boomsma, J. J., and Currie, C. R. (2005). Specificity of the mutualistic association between actinomycete bacteria and two sympatric species of *Acromyrmex* leaf-cutting ants. *Mol. Ecol.* 14, 3597–3604. doi: 10.1111/j.1365-294X.2005.02695.x
- Poulsen, M., Cafaro, M. J., Erhardt, D. P., Little, A. E. F., Gerardo, N. M., Tebbets, B., et al. (2010). Variation in *Pseudonocardia* antibiotic defence helps govern parasite-induced morbidity in *Acromyrmex* leaf-cutting ants. *Environ. Microbiol. Rep.* 2, 534–540. doi: 10.1111/j.1758-2229.2009.00098.x
- Poulsen, M., Erhardt, D. P., Molinaro, D. J., Lin, T.-L., and Currie, C. R. (2007). Antagonistic bacterial interactions help shape host-symbiont dynamics within the fungus-growing ant-microbe mutualism. *PLoS One* 2:e960. doi: 10.1371/journal.pone.0000960
- Poulsen, M., Fernández-Marín, H., Currie, C. R., and Boomsma, J. J. (2009). Ephemeral windows of opportunity for horizontal transmission of fungal symbionts in leaf-cutting ants. *Evolution* 63, 2235–2247. doi: 10.1111/j.1558-5646.2009.00704.x
- Poulsen, M., Maynard, J., Roland, D. L., and Currie, C. R. (2011). The role of symbiont genetic distance and potential adaptability in host preference towards *Pseudonocardia* symbionts in *Acromyrmex* leaf-cutting ants. *J. Insect Sci.* 11:120. doi: 10.1673/031.011.12001
- Rodrigues, A., Bacci, M. Jr., Mueller, U. G., Ortiz, A., and Pagnocca, F. C. (2008). Microfungal “weeds” in the leafcutter ant symbiosis. *Microb. Ecol.* 56, 604–614. doi: 10.1007/s00248-008-9380-0
- Ruzzini, A. C., and Clardy, J. (2016). Gene flow and molecular innovation in bacteria. *Curr. Biol.* 26, R859–R864. doi: 10.1016/j.cub.2016.08.004
- Sachs, J. L., Skophammer, R. G., and Regus, J. U. (2011). Evolutionary transitions in bacterial symbiosis. *Proc. Natl. Acad. Sci. U.S.A.* 108, 10800–10807. doi: 10.1073/pnas.1100304108
- Scheuring, I., and Yu, D. W. (2012). How to assemble a beneficial microbiome in three easy steps. *Ecol. Lett.* 15, 1300–1307. doi: 10.1111/j.1461-0248.2012.01853.x
- Schoenian, I., Spiteller, M., Ghaste, M., Wirth, R., Herz, H., and Spiteller, D. (2011). Chemical basis of the synergism and antagonism in microbial communities in the nests of leaf-cutting ants. *Proc. Natl. Acad. Sci. U.S.A.* 108, 1955–1960. doi: 10.1073/pnas.1008441108
- Schultz, T. R., and Brady, S. G. (2008). Major evolutionary transitions in ant agriculture. *Proc. Natl. Acad. Sci. U.S.A.* 105, 5435–5440. doi: 10.1073/pnas.0711024105
- Seipke, R. F., Gruschow, S., Goss, R. J. M., and Hutchings, M. I. (2012). Isolating antifungals from fungus-growing ant symbionts using a genome-guided chemistry approach. *Methods Enzymol.* 517, 47–70. doi: 10.1016/B978-0-12-404634-4.00003-6
- Sen, R., Ishak, H. D., Estrada, D., Dowd, S. E., Hong, E., and Mueller, U. G. (2009). Generalized antifungal activity and 454-screening of *Pseudonocardia*

- and *Amycolatopsis* bacteria in nests of fungus-growing ants. *Proc. Natl. Acad. Sci. U.S.A.* 106, 17805–17810. doi: 10.1073/pnas.0904827106
- Sit, C. S., Ruzzini, A. C., Van Arnam, E. B., Ramadhar, T. R., Currie, C. R., and Clardy, J. (2015). Variable genetic architectures produce virtually identical molecules in bacterial symbionts of fungus-growing ants. *Proc. Natl. Acad. Sci. U.S.A.* 112, 13150–13154. doi: 10.1073/pnas.1515348112
- Sosa-Calvo, J., Schultz, T. R., Ješovnik, A., Dahan, R. A., and Rabeling, C. (2018). Evolution, systematics, and natural history of a new genus of cryptobiotic fungus-growing ants. *Syst. Entomol.* 43, 549–567. doi: 10.1111/syen.12289
- Toft, C., and Andersson, S. G. E. (2010). Evolutionary microbial genomics: insights into bacterial host adaptation. *Nat. Rev. Genet.* 11, 465–475. doi: 10.1038/nrg2798
- Van Arnam, E. B., Currie, C. R., and Clardy, J. (2018). Defense contracts: molecular protection in insect-microbe symbioses. *Chem. Soc. Rev.* 47, 1638–1651. doi: 10.1039/c7cs00340d
- Van Arnam, E. B., Ruzzini, A. C., Sit, C. S., Currie, C. R., and Clardy, J. (2015). A rebeccamycin analog provides plasmid-encoded niche defense. *J. Am. Chem. Soc.* 137, 14272–14274. doi: 10.1021/jacs.5b09794
- Van Arnam, E. B., Ruzzini, A. C., Sit, C. S., Horn, H., Pinto-Tomás, A. A., Currie, C. R., et al. (2016). Selvamycin, an atypical antifungal polyene from two alternative genomic contexts. *Proc. Natl. Acad. Sci. U.S.A.* 113, 12940–12945. doi: 10.1073/pnas.1613285113
- Walker, T. N., and Hughes, W. O. H. (2009). Adaptive social immunity in leaf-cutting ants. *Biol. Lett.* 5, 446–448. doi: 10.1098/rsbl.2009.0107
- Weber, N. A. (1972). *Gardening Ants - The Attines*. Philadelphia, PA: The American Philosophical Society.
- Woolhouse, M. E. J., Webster, J. P., Domingo, E., Charlesworth, B., and Levin, B. R. (2002). Biological and biomedical implications of the co-evolution of pathogens and their hosts. *Nat. Genet.* 32, 569–577. doi: 10.1038/ng1202-569
- Zhang, M. M., Poulsen, M., and Currie, C. R. (2007). Symbiont recognition of mutualistic bacteria by *Acromyrmex* leaf-cutting ants. *ISME J.* 1, 313–320. doi: 10.1038/ismej.2007.41

Conflict of Interest: The authors declare that the research was conducted in the absence of any commercial or financial relationships that could be construed as a potential conflict of interest.

Copyright © 2020 Goldstein and Klassen. This is an open-access article distributed under the terms of the Creative Commons Attribution License (CC BY). The use, distribution or reproduction in other forums is permitted, provided the original author(s) and the copyright owner(s) are credited and that the original publication in this journal is cited, in accordance with accepted academic practice. No use, distribution or reproduction is permitted which does not comply with these terms.



Insights Into the Ecological Role of *Pseudomonas* spp. in an Ant-plant Symbiosis

Taise T. H. Fukuda^{1†}, Camila F. Pereira^{1†}, Weilan G. P. Melo¹, Carla Menegatti¹, Paulo H. M. Andrade², Milton Groppo³, Paulo T. Lacava², Cameron R. Currie⁴ and Mônica T. Pupo^{1*}

¹ School of Pharmaceutical Sciences of Ribeirão Preto, University of São Paulo, Ribeirão Preto, Brazil, ² Laboratory of Microbiology and Biomolecules, Department of Morphology and Pathology, Center for Biological and Health Sciences, Federal University of São Carlos, São Carlos, Brazil, ³ Laboratory of Plant Systematics, Department of Biology, Faculty of Philosophy, Sciences and Letters at Ribeirão Preto, University of São Paulo, Ribeirão Preto, Brazil, ⁴ Department of Bacteriology, University of Wisconsin-Madison, Madison, WI, United States

OPEN ACCESS

Edited by:

Aymé Spor,
UMR1347 Agroécologie INRA, France

Reviewed by:

Ryan Seipke,
University of Leeds, United Kingdom
Victor González,
Center for Genomic Sciences,
National Autonomous University
of Mexico, Mexico

*Correspondence:

Mônica T. Pupo
mtpupo@fcfrp.usp.br

[†] These authors have contributed
equally to this work

Specialty section:

This article was submitted to
Terrestrial Microbiology,
a section of the journal
Frontiers in Microbiology

Received: 25 October 2020

Accepted: 08 January 2021

Published: 01 February 2021

Citation:

Fukuda TTH, Pereira CF,
Melo WGP, Menegatti C,
Andrade PHM, Groppo M, Lacava PT,
Currie CR and Pupo MT (2021)
Insights Into the Ecological Role
of *Pseudomonas* spp. in an Ant-plant
Symbiosis.
Front. Microbiol. 12:621274.
doi: 10.3389/fmicb.2021.621274

In the myrmecophytic mutualistic relationship between *Azteca* ants and *Cecropia* plants both species receive protection and exchange nutrients. The presence of microorganisms in this symbiotic system has been reported, and the symbiotic role of some fungi involved in the myrmecophytic interactions has been described. In this work we focus on bacteria within this mutualism, conducting isolations and screening for antimicrobial activities, genome sequencing, and biochemical characterization. We show that *Pantoea*, *Rhizobium*, *Methylobacterium*, *Streptomyces* and *Pseudomonas* are the most common cultivable genera of bacteria. Interestingly, *Pseudomonas* spp. isolates showed potent activity against 83% of the pathogens tested in our antimicrobial activity assays, including a phytopathogenic fungus isolated from *Cecropia* samples. Given the predicted nitrogen limitations associated with the fungal patches within this myrmecophyte, we performed nitrogen fixation analyses on the bacterial isolates within the Proteobacteria and show the potential for nitrogen fixation in *Pseudomonas* strains. The genome of one *Pseudomonas* strain was sequenced and analyzed. The gene cluster involved in the biosynthesis of cyclic lipodepsipeptides (CLPs) was identified, and we found mutations that may be related to the loss of function in the dual epimerization/condensation domains. The compound was isolated, and its structure was determined, corresponding to the antifungal viscosinamide. Our findings of diazotrophy and production of viscosinamide in multiple *Pseudomonas* isolates suggests that this bacterial genus may play an important role in the *Cecropia*-*Azteca* symbiosis.

Keywords: myrmecophytes, bacteria, antimicrobial activities, nitrogen fixation, genome mining, *Pseudomonas*, *Cecropia*, *Azteca* ants

INTRODUCTION

Myrmecophytic interactions are mutualistic relationships between ants and plants, in which nutrient exchanges and protection of both species are involved (Fonseca, 1999; Webber et al., 2007; Dejean et al., 2012). Some of these interactions are well studied, such as *Acacia*-*Pseudomyrmex*, *Tachigali*-*Pseudomyrmex*, *Leonardoxa*-*Petalomyrmex*, *Piper*-*Pheidole*, *Macaranga*-*Crematogaster*,

Cordia-Allomerus, and *Cecropia-Azteca* (Heil and McKey, 2003; Voglmayr et al., 2011; González-Teuber et al., 2014; Mayer et al., 2014; Hernández et al., 2017). Myrmecophytes offer shelters (hollow stems that provide nesting space) and food to associated ants through the production of structures such as glycogen-rich Müllerian corpuscles, pearl bodies, and extrafloral nectaries (Davidson and Fisher, 1991; Oliveira et al., 2015). In return, ants assist the host plant in defense against different kinds of enemies as parasitic plants, sap-sucking insects, competitors, pathogens, and a broad range of herbivores (Heil and McKey, 2003; Dejean et al., 2012).

The neotropical trees of the genus *Cecropia* (Cecropiaceae) are abundant and iconic examples of ant-plant mutualism (Heil and McKey, 2003; Oliveira et al., 2015; Treiber et al., 2016). Most myrmecophytic *Cecropia* species are associated with ants from the *Azteca* genus (Formicidae: Dolichoderinae). These ants comprise about 150 different described species found only in tropical regions (Ayala et al., 1996; Berg et al., 2005), and have evolved to be obligately associated with their mutualistic plants (Longino, 1991; Oliveira et al., 2015).

The symbiosis involving *Cecropia* plants and *Azteca* ants encompasses other species. Fungal mycelia are found inside the domatia, in contact with the plant; however, they do not invade the plant tissue. These fungi are classified as black yeasts belonging to the order Chaetothyriales (Mayer and Voglmayr, 2009; Voglmayr et al., 2011; Nepel et al., 2016; Pringle and Moreau, 2017). The larvae of the symbiotic ant ingest the fungus, indicating a nutritive function (Blatrix et al., 2012).

Proteobacteria and Actinobacteria associated with ant-plant systems have been reported and may be involved in different myrmecophyte interactions (Hanshew et al., 2015; Lucas et al., 2019; Ruiz-González et al., 2019). The microbial communities present inside the domatia of ant-plant symbioses appear to be influenced by ant species and, to a lower extent, by the local environment (Ruiz-González et al., 2019). The presence of these microbes and the potential that ants actively select for at least part of the associated microorganisms suggests that bacteria could play beneficial roles in the survival of the colonies and their host plants.

The bacterium *Pseudomonas citronellolis* (Gamma proteobacteria: Pseudomonadales) was recently proposed to be specifically associated with *Azteca* ants that engage in myrmecophyte interaction (Ruiz-González et al., 2019). Other bacteria including *Burkholderia*, *Enterobacter*, *Pantoea*, and *Rhizobium* were also found in *Cecropia-Azteca*, and it is believed that they may perform different roles, such as defense against parasites, plant substrate degradation, and nitrogen-fixing as described for fungus-growing ants (Pinto-Tomás et al., 2009; Zucchi et al., 2011; Lucas et al., 2019; Ruiz-González et al., 2019).

Although the *Cecropia-Azteca* mutualism has been described for more than a hundred years, there are few studies on the microbiome of this environment and the chemical compounds that mediate the interaction of present organisms. Here, we investigated the presence of bacteria involved in the *Cecropia-Azteca* interaction, seeking to understand the ecological role of these microorganisms within this symbiosis

as well as exploring such strains as promising sources of antimicrobial compounds.

MATERIALS AND METHODS

Strains Isolation and Identification

The research and collection of biological samples was authorized by the Brazilian government (SISBIO authorization 46555-6, CNPq process 010936/2014-9). Collections were performed in October 2015 and December 2018 in the Atlantic Forest at Itatiaia National Park, RJ, Brazil. GPS coordinates, information of isolated bacteria and *Cecropia* trees are in **Supplementary Table 1**. *Cecropia* species were identified using Gaglioti and Romaniuc-Neto (2012), and Brazil Flora Group (BFG) (2015). Vouchers were deposited at the Herbarium of the Department of Biology, FFCLRP-USP (Herbarium SPFR).

Samples of *Cecropia* were collected from the internodal space that was associated with *Azteca* ants. Fungal patches samples, worker ants, pupae, and larvae were also collected. For the isolation of bacteria, parts of the collected samples were placed in Petri dishes containing ISP-2 medium (4 g of yeast extract, 4 g of dextrose, 10 g of malt extract and 20 g of agar, and 1 L of distilled water), supplemented with the antifungals nystatin (40 mg/L) and cycloheximide (50 mg/L). Plates were incubated at 30°C and the appearance of colonies was monitored for four weeks. For the isolation of actinobacteria, fragments of the collected samples were placed on chitin plates (in one liter: 5.33 g of chitin, 0.767 g K₂HPO₄, 0.367 g KH₂PO₄, 0.244 g MgSO₄, 0.01 g FeSO₄·7H₂O, 0.001 g ZnSO₄·7H₂O, 0.001 g MnCl₂ · 4H₂O, 20 g of agar) supplemented with the antifungals nystatin (40 mg/L) and cycloheximide (50 mg/L) (Hsu and Lockwood, 1975). After four weeks of growth at 30°C, bacterial colonies were subcultured onto ISP-2-agar plates, and serial culturing was done until the obtention of pure cultures.

DNA Extraction From Microorganisms

The bacterial strains were grown in ISP-2 medium and incubated at a controlled temperature of 30°C for 2–3 days. After this the DNA extraction of the bacteria was carried out using the microLYSIS®-Plus solution according to the manufacturer's instructions.

Genomic DNA from actinobacteria was extracted using an adapted protocol (Kumar et al., 2010). Strains were grown in Tryptone Soy Broth (BD, United States) at 30°C and 300 rpm for 3–5 days. After this period, the culture was transferred to Eppendorf microtubes and centrifuged at 10,000 × g for 10 min. The supernatant was removed, and the pellet frozen at -20°C. The pellet was washed in 500 µL of sucrose 10.3%, centrifuged for 1 min at 10,000 × g, and the supernatant was discarded. Then 450 µL of TSE (50% Sucrose; 0.5 M EDTA pH 8 and 1 M Tris Buffer pH 8) were added with lysozyme and incubated for 20 min at 37°C. After that period, 13 µL of proteinase K were added and incubated for another 15 min at 55°C. At the end of the incubation time, 250 µL of 2% SDS was added, and then gently stirred until the formation of a clear

solution was observed. Then, 300 μ L of phenol: chloroform pH 8.0 were added, mixed, and then centrifuged for 10 min at 4°C. The supernatant was transferred to another tube, and 60 μ L of 3M NaOAc, pH 6.0, and 700 μ L of isopropanol were added. The contents were mixed until the appearance of "white strings". The tube was centrifuged down briefly and poured off the supernatant. The DNA was resuspended in 100–200 μ L of autoclaved deionized H₂O and quantified using NanoDrop®.

16S rRNA Sequencing

PCR amplification of the 16S rRNA gene of bacteria were performed using two primers: 27F (5'-AGAGTTTGATCMT GGCT-3') and 1492R (5'-TACGGYTACCTTGTTACGACTT-3'). The final reaction volume of 15 μ L contained: 8 μ L EconoTac® DNA Polymerase (Lucigen, United States), 0.5 μ L of each primer 27F and 1492R, 0.5 μ L DMSO, 4.5 μ L deionized H₂O, and 1 μ L DNA (10 ng/ μ L). An initial denaturation step at 94°C for 3 min was followed by 32 cycles of amplification of 94°C for 30 s, 60°C for 30 s, and 72°C for 2 min, and a final extension step of 72°C for 5 min. Amplicons were detected by agarose gel electrophoresis and visualized by ultraviolet (UV) fluorescence after staining with ethidium bromide. The Big Dye sequencing was done using 1.5 μ L 5X buffer, 1 μ L primer (10 μ M), 1 μ L BigDye 3.1 (Applied Biosystems), 0.5 μ L DMSO, 1 μ L PCR product DNA, and deionized water to make up the total volume of 10 μ L. The reaction started with 95°C for 3 min, followed by 35 cycles of 96°C for 10 s, 58°C for 3 min and a final extent of 72°C for 7 min. The sequencing reaction was purified with the Axyprep Mag Dyclean purification kit (Axygen). The DNA was resuspended in 25 μ L of deionized H₂O before submission to the Center for Genetics and Biotechnology at the University of Wisconsin (Biotech Center). The 16S rRNA sequences were searched for homologous sequences with BLASTn in the NCBI database. The sequences are deposited at NCBI GenBank under Accession numbers: MW139977 - MW140014.

ITS Sequencing

For a strain of the fungus *Pestalotiopsis clavispora* FB1 isolated from *Cecropia* leaves (Supplementary Figure 1) the ITS region (internal transcribed spacer) was amplified using the primers TS1 (5'-TCCGTAGGTGAACCTGCGG-3') and ITS4 (5'-TCCTCCGCTTATTGATATGC-3') (White et al., 1990). The PCR consisted of 4.0 μ L of dNTPs (1.25 mM each), 2.5 μ L of buffer 10X, 1.0 μ L of MgCl₂ (50 mM), 0.2 μ L de Taq-polymerase (5.0 U/ μ L), 2.0 μ L of each primer (10 μ M), 10.3 μ L of ultrapure water and 2.0 μ L DNA (10 ng/ μ L). An initial denaturation step at 94°C for 3 min was followed by 35 cycles of amplification of 94°C for 1 min, 55°C for 1 min and 72°C for 2 min, and a final extension step of 72°C for 5 min. Sequencing was performed as described above for bacteria.

Genome Sequencing

Genomic DNA from strain *Pseudomonas* sp. ICBG1301 was obtained as described previously in the 16S rRNA extraction from actinobacteria with additional steps. After the appearance of "white strings" it was centrifuged down briefly, poured

off the supernatant, and redissolved in 500 μ L TE. 10 μ L of RNase A (20 mg/mL) were added and rocked at room temperature until dissolved. 300 μ L phenol were added and mixed. 150 μ L of chloroform were also added and mixed. After that, the sample was spun at 4000 \times g for 10 min and the top layer was transferred to a new tube. 300 μ L chloroform were added and the solution was spun for 3 min at 4000 \times g. The top layer was transferred to a tube holding 50 μ L 3M NaOAc pH 6 and 350 μ L isopropanol, and the tube was inverted until the DNA appeared as a stringy clump. The supernatant was poured off and the DNA was dissolved in deionized H₂O. The genomic DNA was sequenced by Illumina MiSeq™ System 2 \times 300 bp at the Center for Genetics and Biotechnology at the University of Wisconsin (Biotech Center). The assembly method used was SPAdes V3.11.0, the genome coverage was 284.5 X and 29 contigs were obtained. The genome was deposited into Genbank, and its accession number is JAEKGB000000000.

Phylogenetic Analyses

We used the 16S rRNA gene of the four *Pseudomonas* strains isolated and others present in the NCBI database, that are known to be viscosin-producers, to construct a phylogenetic tree. The sequences were aligned using the MUSCLE alignment algorithm, trimmed manually and the alignments were refined using Geneious Prime 2020.0.4 (<https://www.geneious.com>). The construction of Maximum-likelihood phylogenetic trees was performed in the IQ-tree 1.6 software using ModelFinder to figure out the best nucleotide replacement model. The TPM3 + F + R2 model was used and branch support was assessed by ultrafast bootstrap UFBoot (1000 bootstrap replicates) (Minh et al., 2020). Phylogenetic tree was visualized with iTol v5 (Letunic and Bork, 2019). The analysis involved 33 nucleotide sequences and the phylogenetic tree was rooted by *Pseudomonas aeruginosa* PAO1.

Four conserved "housekeeping" genes were used for the multilocus sequence analysis (MLSA): 16S rRNA, *gyrB*, *rpoB*, and *rpoD*. All these genes were extracted from the genome of ICBG1301 and 30 other *Pseudomonas* spp. deposited in the NCBI database and the phylogenetic tree was rooted by *Pseudomonas aeruginosa* PAO1.

The sequences belonging to each gene were aligned using MUSCLE, trimmed manually and the alignments were refined using the same algorithm on Geneious Prime 2020.0.4 (<https://www.geneious.com>). Then the sequences were concatenated. The construction of Maximum-likelihood phylogenetic trees were performed in the IQ-tree 1.6 software using ModelFinder to figure out the best nucleotide replacement model. The TIM + F + I + G4 model was used and branch support was assessed by ultrafast bootstrap UFBoot (1000 bootstrap replicates) (Minh et al., 2020). Phylogenetic tree was visualized with iTol v5 (Letunic and Bork, 2019).

The same method was used for the construction of phylogenetic trees of adenylation and condensation domains. Amino acid sequences of these domains were obtained from the antiSMASH database (Blin et al., 2020). ModelFinder was used in this case to choose the best model for protein evolution.

Growth of Microorganisms in Nitrogen-free Culture Medium (NFb)

The ability to fix atmospheric nitrogen by the bacteria isolated from *Cecropia-Azteca* symbiosis was evaluated by growing the strains on the semisolid nitrogen-free medium (NFb), composed of malic acid 5 g/L, K₂HPO₄ 0.5 g/L, MgSO₄·7H₂O 0.2 g/L, NaCl 0.1 g/L, CaCl₂·2H₂O 0.01 g/L, 2 mL micronutrient solution (CuSO₄·5H₂O 0.04 g/L, ZnSO₄·7H₂O 1.2 g/L, H₃BO₃ 1.4 g/L, Na₂MoO₄·2H₂O 1 g/L and MnSO₄·H₂O 1.175 g/L completing the volume to 1 L with distilled H₂O); 2 mL bromothymol blue (solution 0.5% in 0.2N KOH); 4 mL Fe-EDTA (solution 1.64%); 2 mL vitamin solution (0.1 g/L biotin and 0.02 g/L pyridoxine completing the volume to 1 L with distilled H₂O); 4.5 g/L KOH; 2.3 g/L agar; make up to 1 L with distilled H₂O and adjust the pH to 6.8. Glass tubes were filled with 3 mL of the NFb medium, and after solidification, the microorganisms were inoculated in the tube and incubated at 28°C in the dark for 96 hours. Reading was carried out by observing the formation of a growth film close to the surface (Döbereiner et al., 1995; Cattelan et al., 1999; Batista et al., 2018). The strains that showed positive results in this stage were re-inoculated in triplicate to confirm the result.

Bioactivity Screening

Pairwise interactions against human pathogens (*Staphylococcus aureus* and *Candida albicans*), a phytopathogen (*Rhizopus oryzae*), an entomopathogen (*Metarhizium anisopliae*), and *Bacillus subtilis* were carried out using previously described methods (Getha and Vikineswary, 2002; Visser et al., 2012). A phytopathogen fungus (Lazarotto et al., 2012; Borrero et al., 2018) identified as *Pestalotiopsis clavispora* FB1, isolated from *Cecropia* sp. leaves causing damage to the plant, was also tested. After strains inoculation, plates were maintained at 30°C and monitored for 14 days. Then, we recorded the qualitative result, in which we classified it as “inhibition” or “no inhibition” according to the presence or absence of an inhibition zone.

Isolation and Structure Determination of Viscosinamide

HPLC purifications were carried out using an HPLC system (Shimadzu, Kyoto, Japan), comprising an LC-6AD solvent pump, a CBM-20A system controller, a CTO-20A column oven, a SIL-20AF injector, a SPD-M20A diode array detector (DAD), a FCR-10A collector, and LabSolutions software for data acquisition. Purification of viscosinamide (**1**) was performed at 3 mL/min with a reversed phase C18 semi-preparative column (Phenomenex Gemini, 10 mm, 250 mm, 5 µm) using a gradient solvent system with aqueous acetonitrile (50% to 100% acetonitrile) for 12 min. The absolute configuration of the amino acids present in the structure was determined using advanced Marfey's method (Harada et al., 1996). Viscosinamide (**1**) (1 mg) was hydrolyzed at 110°C in 500 µL of 6 N HCl for 24 h. HCl was removed under reduced pressure and the dry material was resuspended in 500 µL of H₂O and dried three times to remove residual acid. The hydrolyzate was dissolved

in 100 µL of 1 N NaHCO₃ and incubated with 50 µL of 1 mg/mL L-FDLA and L,D-FDLA (FDLA - 2,4-dinitro-5-fluorophenyl leucineamide), in acetone, at 80°C for 3 min. The reaction was quenched by adding 50 µL of 2 N HCl. Aqueous acetonitrile (1:1) was added to dissolve the mixture. A 10 µL aliquot of the hydrolyzate derivative was analyzed by HPLC-HR-ESI-MS using an analytical C18 column (Phenomenex Gemini, 4.6 mm, 250 mm, 5 µm), with a gradient solvent system (5% to 100% ACN with 0.1% formic acid over 30 min) and flow rate of 0.7 mL/min. The oven temperature was 35°C. The ionization source parameters were: End Plate Offset voltage, 500V; capillary voltage, 3500 V; nebulizer at 5.5 bar; drying gas flow rate of 10.0 L/min; drying gas temperature, 220°C; for positive mode ionization. The spectra rate of 2.0 Hz and mass range of 300 to 1000 m/z were maintained throughout the analysis. The Data Analysis® Software of Bruker Daltonics instrument was used to analyze the metabolic profile and UV spectrum data.

NMR spectra were recorded using a BRUKER® - DRX500 - Ultra Shield® (¹H: 500.13 MHz, ¹³C: 125.77 MHz). Spectra were processed using MestReNova 6.0.2. High-resolution MS spectra were obtained using a microTOF II-ESI-TOF (Bruker Daltonics®), positive ion mode using capillary voltage 3900 V, dry gas flow 4 L h⁻¹, and nitrogen as nebulizer gas. Na-TFA 10 mg/mL was used for internal calibration. Samples were prepared at 20 µg/mL, in EtOAc:MeOH:H₂O (1:2:2). The LC-MS was carried out on a Bruker Daltonics High Pressure Liquid Chromatographer coupled to a diode array UV detector, and a Mass Spectrometer with electrospray ionization source (ESI) and microTOF (Time of Flight) detector. MS/MS analysis was performed using the MALDI-TOF/TOF (Bruker Daltonics, UltrafleXtreme, Bremen, Germany). The matrix CHCA (α-cyano-4-hydroxycinnamic acid) was prepared using a saturated solution in aqueous acetonitrile 3:7 (0.1% TFA). The settings of the instrument were: positive ion reflector mode (RV1 e RV2 of 26.60 kV e 13.35 kV, respectively); 500 laser shots per spectrum; PIE (Pulsed ion extraction) of 110 ns, laser frequency of 1000 Hz; IS1 (ion source 1) and IS2 voltages were 25.00 kV e 23.00 kV, respectively; external calibration was carried out using a peptide mixture provided by Bruker. Samples were diluted in methanol and 1 µL of the sample was added to 1 µL of matrix and 1 µL of this mixture was applied to the MALDI plate.

RESULTS

Strain Isolation and Identification

Bacterial strains were isolated from *Cecropia* samples inhabited by *Azteca* ants collected at Itatiaia National Park (RJ, Brazil) in 2015 and 2018. Microbial isolations were performed from various parts of the samples gathered, ranging from ants, eggs, plant parenchyma, and fungal patches found in the hollows of *Cecropia*'s stalks. This process resulted in the isolation of 39 bacterial strains which had their 16S rRNA gene sequenced,

allowing their identification at the genus level (**Supplementary Table S1**). Among the isolates, 25 (64.1%) strains belong to the phylum Proteobacteria, 12 (30.8%) to Actinobacteria, and two (5.1%) to Firmicutes. Six bacterial orders were represented including: Actinomycetales (12), Rhizobiales (10), Pseudomonadales (7), Enterobacterales (5), Xanthomonadales (3), and Bacillales (2) (**Figure 1**). The isolates belonged to ten different genera namely *Acinetobacter*, *Actinomadura*, *Bacillus*, *Methylobacterium*, *Pantoea*, *Pseudomonas*, *Rhizobium*, *Raoultella*, *Stenotrophomonas*, and *Streptomyces*.

Isolates were obtained mainly from *Azteca* ants and fungal patches. *Pseudomonas* spp. and *Rhizobium* spp. were found in three of the four sampled sites (*Cecropia* parenchyma, *Azteca* sp. ant and fungal patches); *Methylobacterium* spp. also in three (*Azteca* sp. ant, *Azteca* sp. egg and *Cecropia* parenchyma); *Pantoea* spp. was found in two (*Azteca* sp. ant and *Azteca* sp. egg); *Bacillus* spp. in two (*Cecropia* parenchyma, fungal patches); *Stenotrophomonas* spp., *Streptomyces* spp. and *Actinomadura* spp. were sampled also in two (*Azteca* sp. ant and fungal patches); *Acinetobacter* spp. and *Raoultella* sp. in just one site (*Azteca* sp. ant and fungal patches, respectively).

Isolates Growth in Nitrogen-free Medium

Proteobacteria genera *Pantoea*, *Rhizobium*, *Methylobacterium*, and *Pseudomonas* have known diazotrophic potential (Borm et al., 2008; Pinto-Tomás et al., 2009; Ruiz-González et al., 2019; Bar-Shmuel et al., 2020). Due to the significant number of strains isolated from *Cecropia-Azteca* that could potentially fix nitrogen (22; 56.4%), the nitrogenase activity of these strains was tested. All bacteria grew in the nitrogen-free semi-solid NFb media under the tested culture conditions. However, only those belonging to the genus *Pseudomonas* (strains ICBG1870, ICBG1871, ICBG1301, and ICBG1881) showed potential for nitrogen fixation as they formed a white disk near the surface after two re-inoculation rounds. Although some other strains did exhibit growth on nitrogen-free medium they did not show potential to perform biological nitrogen fixation (BNF) as indicated by the re-inoculation step, which is important for confirmation of the result (Cattelan et al., 1999), indicating that their growth may have occurred at the expense of energetic reserves of bacterial cells.

Biological Activity

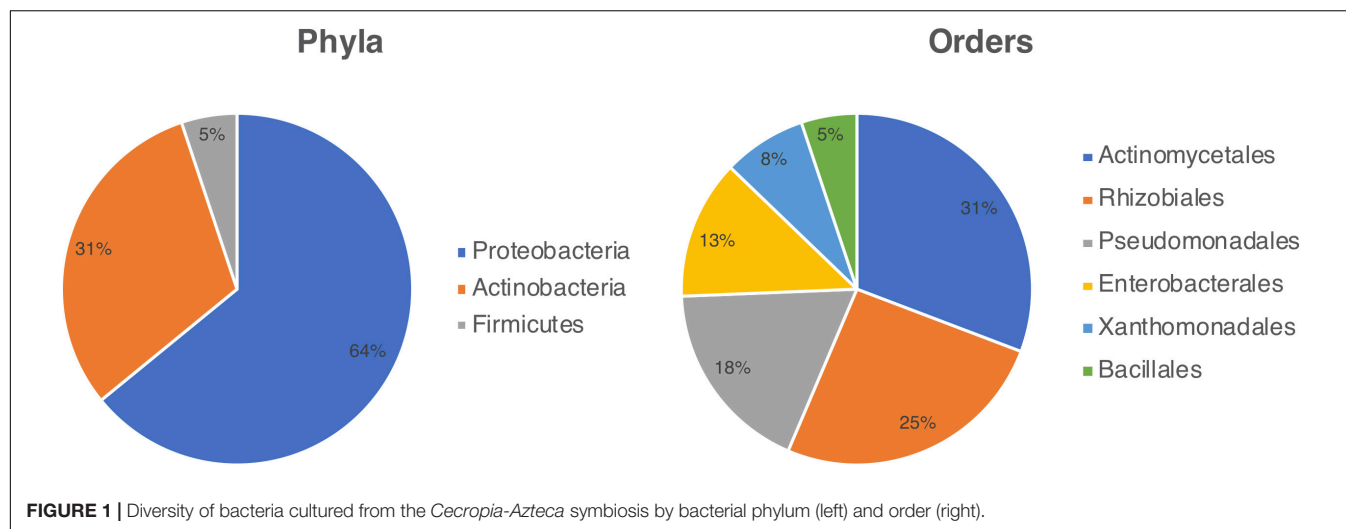
Bioassays of the 39 isolated strains were performed against human pathogens, phytopathogens and entomopathogen (**Supplementary Figure 2**). Sixteen isolates (41%) inhibited at least one of the microorganisms tested, and eight strains (20.5%) inhibited at least two. *Bacillus* spp. strains inhibited the growth of at least three pathogens, including the human pathogen *C. albicans*. The isolates with biological activity against phytopathogens and the entomopathogen were of particular interest since this inhibition could denote ecological relevance. Five out of the 16 strains referred above were active against *P. clavispora*, ten against *R. oryzae*, and seven against *M. anisopliae*. Interestingly, four strains identified as *Pseudomonas* spp. inhibited the growth of almost

all microorganisms tested, including the phytopathogen *P. clavispora* FB1 (**Supplementary Figure 3**).

Pseudomonas sp. ICBG1301 Genome Sequencing and Analysis

According to the biological screening, *Pseudomonas* spp. were the most bioactive bacterial isolates. We selected one strain (ICBG1301) to sequence its genome and analyze the respective biosynthetic gene clusters. Genome analysis of *Pseudomonas* sp. ICBG1301 with antiSMASH 5.0 (Blin et al., 2019) revealed 14 biosynthetic gene clusters (BGCs), encoding the production of siderophore, non-ribosomal peptides, N-acetylglutaminylglutamine amide, beta-lactone, thiopeptide, arylpolyene, and bacteriocins. We therefore decided to investigate BGCs encoding for the production of antifungal compounds. Cluster 9.1 showed 43% similarity to the antifungal non-ribosomal peptide (NRP) viscosin according to the antiSMASH output. NRPs are biosynthesized by specialized enzymes called Non-Ribosomal Peptide Synthetases (NRPS). These NRPS are megaenzymes, which have several catalytic domains, each of which is responsible for a stage of the biosynthesis of the final product. Essential domains are involved in the formation of the mature peptide, called PCP (peptide carrier protein), A (adenylation), C (condensation) and TE (thioesterase termination, usually found only once in a gene cluster) (Finking and Marahiel, 2004). Bioinformatic analyses on these domains can give us insights into the specificities of the monomers recruited and their stereochemistry. In order to evaluate whether the BGC could be responsible for the production of viscosin or not, analyses were performed with its condensation and adenylation domains.

Phylogenetic analyses of the adenylation domains of cluster 9.1 and other 20 viscosin-producing strains were done and the final prediction of the peptide was obtained based on the substrate specificity of nine modules, being: Leu1-Gln2/Glu2-Thr3-Val4-Leu5-Ser6-Leu-7-Ser8-Ile9. These analyses showed that the adenylation domains responsible for recruiting the same monomer, in the case of modules 6/8 (Ser) and 1/7 (Leu), are subdivided according to the groups observed in **Figure 2** (**Supplementary Figure 8**). The compound encoded by cluster 9.1 belongs to a group – the viscosin group – of cyclic lipodepsipeptides. Members of this group comprise viscosin, viscosinamide, WLIP (White Line-Inducing Principle), pseudodesmin and massetolide (**Supplementary Figure 16**). These compounds differ from each other in the absolute configuration of one amino acid (Leu5) or in the amino acid composition of the third and/or fourth positions. Adenylation domains were grouped according to the amino acid incorporated, and each one formed two clades. The domains of *Pseudomonas* strains that produce pseudodesmin or WLIP were grouped together, and the domains involved in the biosynthesis of viscosin and massetolide formed another. A specific analysis of *Pseudomonas* sp. ICBG1301 showed that the A domains are grouped with those of *P. fluorescens* SBW25, *P. antarctica* PAMC 27494 and *Pseudomonas* sp. LBUM990. *P. fluorescens*



SBW25 produces viscosin, as confirmed by NMR, raising the hypothesis that the ICBG1301 strain also produces viscosin. It could be possible to bioinformatically differentiate viscosin, viscosinamide, WLIP, pseudodesmin and massetolide producers by analyzing the specificity of the adenylation domain of the second module. Strains that show such specificity for glutamic acid could be classified as producers of viscosin, WLIP and massetolide, whereas those that show specificity for glutamine could be producers of viscosinamide and pseudodesmin. However, the structural difference between these two amino acids is not so significant and the adenylation domains are grouped together.

Furthermore, phylogenetic analysis of the condensation domains revealed that, except for modules 1 and 8 (C_{starter} and L_{CL} , respectively), all modules contain a C_{dual} domain (Supplementary Figures 5–7). C_{dual} domains are responsible for catalyzing the condensation reaction and epimerization of the upstream amino acid. Intriguingly, domains belonging to the sixth module were split into two different groups (Supplementary Figure 7). Except for one strain (*Pseudomonas* sp. LBUM920), strains that belong to group 2 have a Histidine → Tyrosine mutation in the N-terminal catalytic triad (Figure 2). According to the literature, all viscosin group members show an L-amino acid in the first position. Thus, during the evolution of this pathway, a mutation in the C-domain of the second module has possibly occurred, and this domain has lost its function. Similarly, another mutation might have occurred in the region coding for the sixth module C-domain. This mutation could be responsible for the loss of function of their respective C_{dual} domains. Consequently, it is possible to infer that group 1 strains have the functional domain; thus, they may produce pseudodesmin, showing a D-Leu5, while group 2 strains produce viscosin, showing a L-Leu5. In general, the gene clusters related to viscosin, viscosinamide and massetolide biosynthesis are split into two loci, while the pseudodesmin and WLIP clusters are in contiguous clusters. This observation is consistent with our analyses, since group 1 strains show a contiguous gene cluster and group 2 strains show clusters split

into two loci. BGC 9.1 of *Pseudomonas* sp. ICBG1301 is split into two loci, therefore, potentially related to the production of viscosin or viscosinamide.

Pseudomonas spp. Phylogenetic Analysis

After analyzing the gene clusters involved with viscosin biosynthesis, we decided to investigate the evolutionary relationship between *Pseudomonas* strains. We built a Maximum likelihood tree using the 16S rRNA (Supplementary Figure 4) and a multilocus phylogeny based on the 16S rRNA, *gyrB*, *rpoB*, and *rpoD* gene sequences (Figure 3).

It is noteworthy that the strains that showed the mutation in the C6-domain also have the cluster split into two loci and share a common ancestor, forming a monophyletic group. Viscosinamide (*P. synxantha* 2-79, *Pseudomonas* sp. J380, *Pseudomonas* sp. MYb193, *Pseudomonas* sp. A2W4.9 and *Pseudomonas* sp. U2W1.5) and massetolide (*P. synxantha* 30B and *P. lactis* SS101) producers formed a group, apart from the viscosin clade. Viscosinamide production appears either as an ancestor in the group or appearing three times in the evolution of the group. Massetolide appears twice in the evolution of the group and viscosin only once. The most reasonable hypothesis in this clade is the ancestral production of viscosinamide, with later change to massetolide (two evolutionary events) and viscosin (one evolutionary event). Strain ICBG1301 is related to viscosin-producing strains (*P. fluorescens* SBW25, *P. antarctica* PAMC 27494 and *Pseudomonas* sp. LBUM990). This raises the hypothesis that ICBG1301 could either produce viscosin or viscosinamide.

Viscosinamide

Cultures of *Pseudomonas* spp. ICBG1870 and ICBG1881, isolated from different ant colonies, were scaled up and extracted with ethyl acetate. Rounds of bioguided fractionation led to the isolation of the active compound, with an m/z 1147.6976 $[M + Na]^+$ (error 2.4 ppm) (Supplementary Figure 9). Both

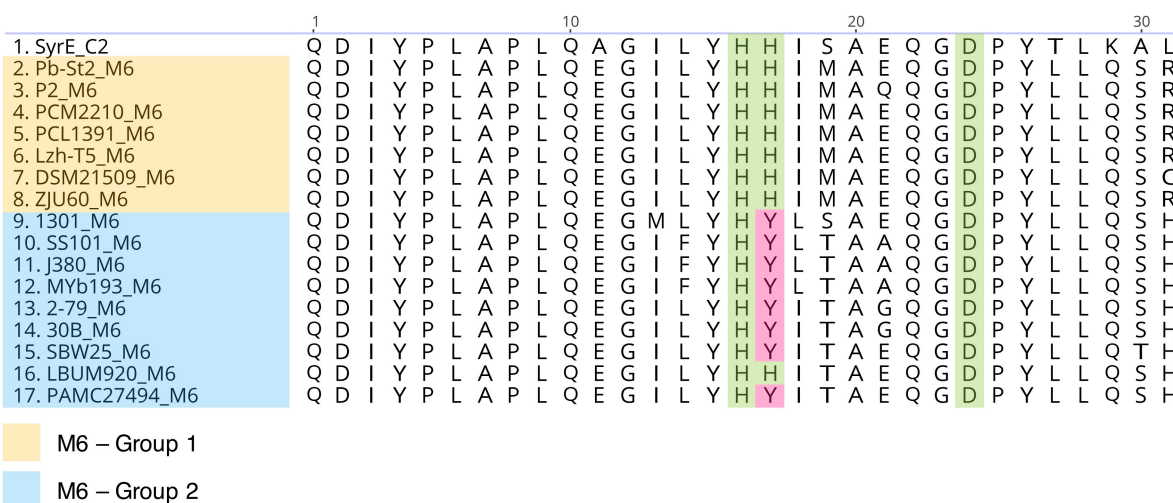


FIGURE 2 | Alignment of the condensation domains (C_{dual}) of the sixth module involved in the biosynthesis of viscosin CLPs. The first 30 amino acids of the N-terminal portion are shown. Highlighted amino acids are those described as belonging to the catalytic triad (Balibar et al., 2005).

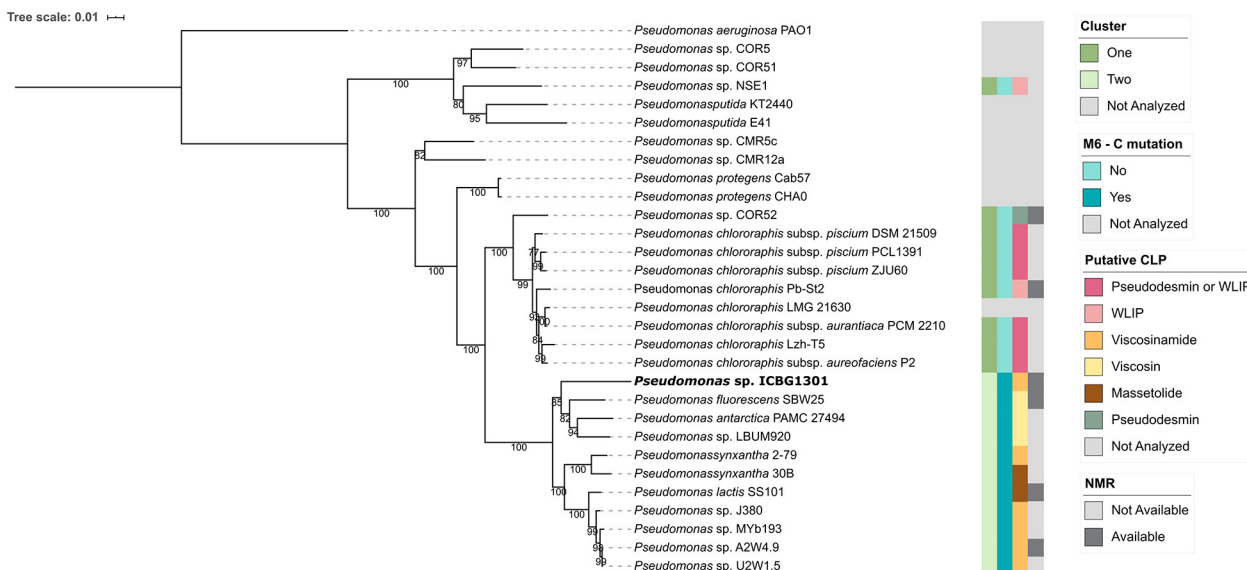


FIGURE 3 | Phylogenetic representation of *Pseudomonas* strains. The phylogeny is based on the concatenated sequence of 16S rRNA, *gyrB*, *rpoB*, and *rpoD* genes. The bootstrap support values are based on 1000 bootstrap replicates. The phylogeny was reconstructed using IQ-TREE, using the TIM + F + I + G4 model of nucleotide substitution and including *P. aeruginosa* PAO1 as outgroup. Strains whose BGCs were not analyzed were either due to the absence of a publicly available sequence or they produce CLPs that do not belong to the viscosin class.

samples showed identical ¹H NMR profiles, corresponding to the same compound. NMR and MALDI-MS/MS data confirmed the structure of the CLP (Supplementary Table S2, Supplementary Figures 10–14). Signals in the region of δ_H 3.44–4.57 were observed in the ¹H NMR spectrum, which correspond to the α-protons of the amino acids. These α-protons are bonded to carbons at δ_C 53.4–65.8, as deduced from gHSQC spectrum. The gCOSY spectrum showed α-protons are coupled with the side chain hydrogens (δ_H 1.87, 2.02, 5.36, 2.19, 1.77, 3.79, 1.60, 3.65, and 1.98). The α-protons also correlate with the carbonyl

carbons of the adjacent amino acid (δ_C 170.1–176.6), as seen in the gHMBC spectrum. Hydrogens at δ_H 4.04 and 5.11 have no correlations with carbons in gHSQC and are directly linked to oxygens in the side chains of Ser6 and Ser8. Other hydrogen signals that do not show correlations in the gHSQC spectrum are those linked to the nitrogens of the peptide bonds (δ_H 9.23, 8.74, 8.47, 8.25, 8.02, 7.95, 7.47, 7.08, and 6.61). Resonances of CH₂ hydrogens are observed in the most shielded region of the spectrum signals (δ_H 0.7–2.6) and correspond to the alkyl chain of the fatty acid.

Hydrolysis and advanced Marfey's derivatization, followed by LC-MS, confirmed the bioinformatic predictions of the stereocenters. The chromatogram shows the presence of D-Glu instead of D-Gln, causing a divergence of one mass unit with the HRESI-MS analysis, due to the conversion of Gln to Glu during the hydrolysis process (Shih, 1985; Li et al., 2010). In addition, the chromatogram showed the presence of only L-Leu in the structure (**Supplementary Figure 15**), corresponding to the antifungal viscosinamide (**1**) (**Figure 4**; Nielsen et al., 1999). This compound was also detected by LC-MS in the extract of *Pseudomonas* sp. ICBG1301. This result agrees with the antifungal activity of the producer strains against *M. anisopliae*, *P. clavispora*, and *R. oryzae*.

DISCUSSION

The occurrence of bacterial strains in the myrmecophytic interactions has been reported (Heil et al., 2010; Lucas et al., 2019; Ruiz-González et al., 2019). Here, we observed that the ant-plant system *Cecropia-Azteca* harbors a rich bacterial community belonging to three phyla: Proteobacteria, Actinobacteria, and Firmicutes. Proteobacteria and Actinobacteria strains correspond to 94.9% of the isolated bacteria. Our results agree with previous studies that analyzed the abundance of the microbial community in the interaction between *Cecropia peltata* and *Azteca alfari*. Although Lucas et al. (2019) identified microorganisms belonging to a higher number of phyla ($n = 22$), they also found the largest proportion (90%) corresponding to Proteobacteria and Actinobacteria. This difference in the number of phyla isolated in our work could be explained by two factors: (i) isolation and cultivation conditions can restrict the growth of strains; (ii) Lucas et al. (2019) analyzed the diversity of internal and external regions of *Cecropia-Azteca* whereas, in our work, we analyzed only samples of internal regions of *Cecropia-Azteca* such as ants,

fungal spots, parenchyma, and eggs. Also, external areas, such as nest entrances and the branches, hosted microbiomes distinct from the workers' chambers and the brood. In comparison, the carton colonized by ants, composed of macerated plant tissue and Chaetothyrialean fungi, also showed a smaller diversity than the external environment (Lucas et al., 2019). Interestingly, most of the genera we obtained were mainly from worker ants and fungal patches. These data obtained by culture-dependent methods are also in line with data obtained by culture-independent methods that showed a similarity in the structure of the *Azteca* ant community and the carton (fungal patches) (Lucas et al., 2019).

Pseudomonas, *Rhizobium*, *Methylobacterium*, *Pantoea* and *Streptomyces* were found in different parts of the sampled *Cecropia* and *Azteca* ants. The presence of these genera in ant-plant systems has been reported and could contribute to preparing vegetal substrate, acting in reinforcing the active transfer of nitrogen and playing a role in the defense of the domatia against diseases by limiting pathogen proliferation (Ruiz-González et al., 2019).

Potential diazotrophic microorganisms have already been recovered from different insect orders, such as Coleoptera, Blattodea, Diptera, Hemiptera and Hymenoptera (Behar et al., 2005; Morales-Jiménez et al., 2009; Pinto-Tomás et al., 2009; Bar-Shmuel et al., 2020). Bacteria belonging to the genus *Pantoea*, for example, have repeatedly been isolated from the leaf-cutting ants symbiosis sampled in different countries, such as Brazil, Argentina and Panama, and have been able to fix nitrogen in the fungus garden. The ants may have established symbiotic relationships with nitrogen-fixing microorganisms in order to provide the necessary demand for this element in the fungus garden (Pinto-Tomás et al., 2009).

Here, we found *Pseudomonas* isolates from the *Cecropia-Azteca* symbiosis carry out BNF *in vitro* and, thus, may be potentially involved in nitrogen fixation in the ant-plant interaction. This genus was suggested to be specifically associated

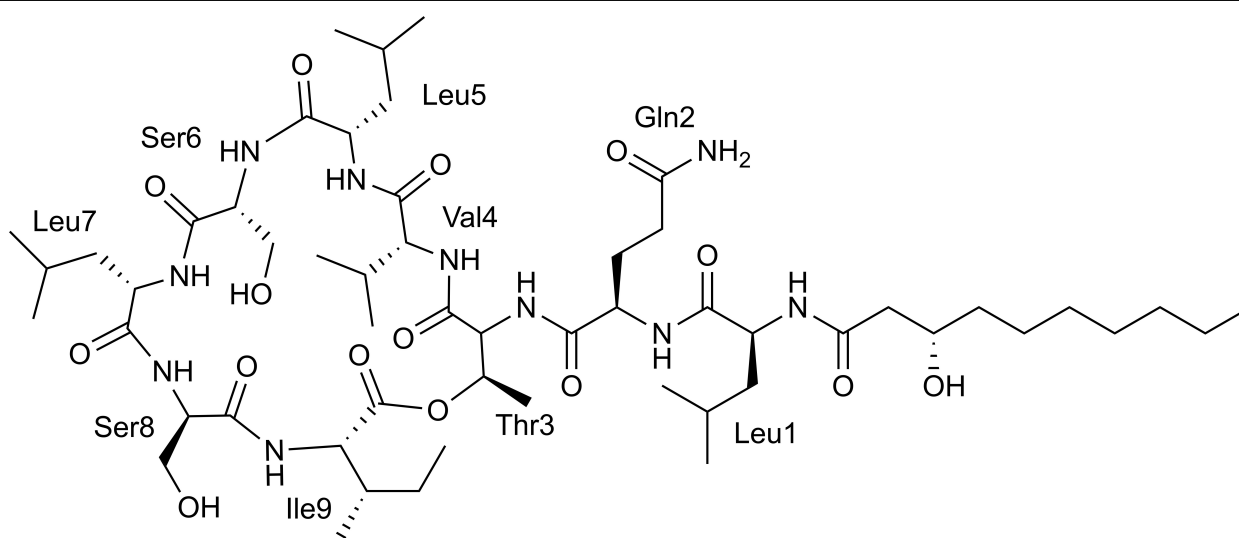


FIGURE 4 | Chemical structure of viscosinamide.

with *Azteca* ants in recent work investigating microorganisms from *Cecropia-Azteca* in Panama (Lucas et al., 2019; Ruiz-González et al., 2019).

In addition to the possible nitrogen fixation function, we observed that *Pseudomonas* spp. strains may also play a role in protecting the colony, since they inhibited the growth of fungal entomopathogens and phytopathogens, including *P. clavispora* FB1 isolated from *Cecropia* sp. tree. Analysis of the microbial composition in different nests samples of *Azteca alfari* in *Cecropia* trees revealed that the absence of ants in the abandoned chambers showed significant growth of fungal pathogens. The presence of these fungi in the chambers and their absence in occupied ones, suggests that ants are important in regulating the development of such pathogens in their nests. Yet, this change is also related to the decrease of bacteria from phylum Proteobacteria, indicating that the microbiome can also play an important role in the control of pathogens (Lucas et al., 2019). This result supports our findings since proteobacteria, such as *Pseudomonas*, inhibited different pathogens.

Bioinformatic analysis revealed that *Pseudomonas* sp. ICBG1301 showed a BGC with 43% similarity to viscosin, thus this BGC could potentially be a member of the viscosin group of CLPs. Analysis on the adenylation and condensation domains showed that *Pseudomonas* sp. ICBG1301 is capable of producing viscosinamide. In addition, the second-module C_{dual}-domain showed a mutation that potentially inactivated its epimerizing function, and a similar mutation might have occurred in the sixth module. Furthermore, the viscosinamide biosynthetic gene cluster is split into two loci, whereas the pseudodesmin BGC, its isomer, shows a contiguous gene cluster.

In order to confirm the structure of this product, we isolated and determined the structure of the CLP produced by *Cecropia-Azteca*-associated *Pseudomonas*. The CLP was unequivocally identified as viscosinamide, which is in accordance with our bioinformatic analyses. Furthermore, this result is also in agreement with the biological activity of its producer. All *Pseudomonas* strains showed antifungal activity in our binary screening and viscosinamide is a well-known antifungal agent. Its isomer, pseudodesmin A, does not show the same inhibitory properties, being selectively active against Gram-positive bacteria (Nielsen et al., 1999).

Our results have demonstrated that *Pseudomonas* spp. strains isolated from *Cecropia-Azteca* samples are active against ecological pathogens and show diazotroph activity. In addition, it was possible to gain insights on the biosynthesis of CLPs of the viscosin group. The cyclic lipodepsipeptide associated with the *Cecropia-Azteca* symbiosis was isolated and identified as viscosinamide. This compound has antifungal activity and can play an important ecological role in this symbiosis, since it was isolated from more than one strain and bacteria of the genus *Pseudomonas* are recurrently isolated from these samples. The fact that these strains seem to be relevant in different levels, providing nitrogen for the system and producing secondary metabolites that can inhibit the growth of potential pathogens,

reinforces the importance of these bacteria for the *Cecropia-Azteca* symbiosis.

DATA AVAILABILITY STATEMENT

The datasets presented in this study can be found in online repositories. The names of the repository/repositories and accession number can be found below: <https://www.ncbi.nlm.nih.gov/bioproject/> (Accession ID: PRJNA684609).

AUTHOR CONTRIBUTIONS

TF, CP, CC, and MP performed conceptualization. TF, CP, WM, and MP performed data curation and wrote the original draft. TF, CP, WM, CM, PA, PL, and MP performed formal analysis. TF, CP, WM, PA, MG, PL, CC, and MP performed investigation. TF, CP, WM, CM, PA, PL, and MP performed methodology. MP performed supervision. TF, CP, WM, CM, PA, MG, PL, CC, and MP performed visualization and wrote, review and editing the manuscript. All authors contributed to the article and approved the submitted version.

FUNDING

The project was supported by funding of the São Paulo Research Foundation (FAPESP), grants N°. 2015/26349-5 (TF), N°. 2017/17305-0 (T.T.H.F.), N°. 2016/26230-0 (CP), N°. 2015/01001-6 (W.G.P.M), N°. 2019/19099-3 (WM), N°. 2016/15576-3 (C.M), N°. 2013/50954-0 (MP), N°. 2016/06260-2 (MG), and Fogarty International Center, National Institutes of Health (FIC-NIH), grant N°. U19TW009872. This study was financed in part by the Brazilian federal funding agencies Conselho Nacional de Desenvolvimento Científico e Tecnológico (CNPq) and Coordenação de Aperfeiçoamento de Pessoal de Nível Superior (CAPES), Finance Code 001.

ACKNOWLEDGMENTS

Research developed with HPC resources provided by the Information Technology Superintendence of the University of São Paulo. We also would like to thank Dr. Camila Carlos-Shanley, Dr. Marc G. Chevette, Dr. Heidi Horn, Caitlin M. Carlson, Julian Cagnazzo, and Evelyn Wendt-Pienkowski for technical support in the Currie Lab, and Claudia C. Macedo in the Pupo Lab.

SUPPLEMENTARY MATERIAL

The Supplementary Material for this article can be found online at: <https://www.frontiersin.org/articles/10.3389/fmicb.2021.621274/full#supplementary-material>

REFERENCES

- Ayala, F. J., Wetterer, J. K., Longino, J. T., and Hartl, D. L. (1996). Molecular phylogeny of *Azteca* ants (Hymenoptera: Formicidae) and the colonization of *Cecropia* trees. *Mol. Phylogenet. Evol.* 5, 423–428. doi: 10.1006/mpev.1996.0037
- Balibar, C. J., Vaillancourt, F. H., and Walsh, C. T. (2005). Generation of D amino acid residues in assembly of arthrofactin by dual condensation/epimerization domains. *Chem. Biol.* 12, 1189–1200. doi: 10.1016/j.chembiol.2005.08.010
- Bar-Shmuel, N., Behar, A., and Segoli, M. (2020). What do we know about biological nitrogen fixation in insects? Evidence and implications for the insect and the ecosystem. *Insect Sci.* 27, 392–403. doi: 10.1111/1744-7917.12697
- Batista, B. D., Lacava, P. T., Ferrari, A., Teixeira-Silva, N. S., Bonatelli, M. L., Tsui, S., et al. (2018). Screening of tropically derived, multi-trait plant growth-promoting rhizobacteria and evaluation of corn and soybean colonization ability. *Microbiol. Res.* 206, 33–42. doi: 10.1016/j.micres.2017.09.007
- Behar, A., Yuval, B., and Jurkevitch, E. (2005). Enterobacteria-mediated nitrogen fixation in natural populations of the fruit fly *Ceratitis capitata*. *Mol. Ecol.* 14, 2637–2643. doi: 10.1111/j.1365-294X.2005.02615.x
- Berg, C. C., Rosselli, P. F., and Davidson, D. W. (2005). *Cecropia*. *Fl. Neotrop.* 94, 1–230. doi: 10.2307/4393938
- Blatrix, R., Djieto-Lordon, C., Mondolot, L., La Fisca, P., Voglmayr, H., and McKey, D. (2012). Plant-ants use symbiotic fungi as a food source: new insight into the nutritional ecology of ant-plant interactions. *Proc. R. Soc. B* 279, 3940–3947. doi: 10.1098/rspb.2012.1403
- Blin, K., Shaw, S., Kautsar, S. A., Medema, M. H., and Weber, T. (2020). The antiSMASH database version 3: increased taxonomic coverage and new query features for modular enzymes. *Nucleic Acids Res.* 49:gkaa978. doi: 10.1093/nar/gkaa978
- Blin, K., Shaw, S., Steinke, K., Villebro, R., Ziemert, N., Lee, Y., et al. (2019). AntiSMASH 5.0: updates to the secondary metabolite genome mining pipeline. *Nucleic Acids Res.* 47, 81–87. doi: 10.1093/nar/gkz310
- Borm, S. V., Buschinger, A., Boomsma, J. J., and Billen, J. (2008). *Tetraponera* ants have gut symbionts related to nitrogen-fixing root-nodule bacteria. *Proc. R. Soc. Lond. B* 269, 2023–2027. doi: 10.1098/rspb.2002.2101
- Borrero, C., Castaño, R., and Avilés, M. (2018). First report of *Pestalotiopsis clavispora* (*Neopestalotiopsis clavispora*) causing canker and twig dieback on blueberry bushes in Spain. *Plant Dis.* 102, 1178–1178. doi: 10.1094/PDIS-10-17-1529-PDN
- Brazil Flora Group (BFG) (2015). Growing knowledge: an overview of seed plant diversity in Brazil. *Rodriguésia* 66, 1085–1113. doi: 10.1590/2175-7860201566411
- Cattelan, A. J., Nepomuceno, A. L., Moscardi, F., Liberatti, I. A., Kaster, M., Neumaier, N., et al. (1999). Métodos qualitativos para determinação de características bioquímicas e fisiológicas associadas com bactérias promotoras do crescimento vegetal. *Embrapa Soja* 139:36.
- Davidson, D. W., and Fisher, B. L. (1991). “Symbiosis of ants with *Cecropia* as a function of light regime,” in *Ant-Plant Interactions*, eds C. R. Huxley, and D. F. Cutler (Oxford: Oxford University Press), 289–309.
- Dejean, A., Petitclerc, F., Roux, O., Orivel, J., and Leroy, C. (2012). Does exogenic food benefit both partners in an ant-plant mutualism? The case of *Cecropia obtusa* and its guest *Azteca* plant-ants. *C. R. Biol.* 335, 214–219. doi: 10.1016/j.crvi.2012.01.002
- Döbereiner, J., Baldini, V. L. D., and Baldini, J. I. (1995). *Como Isolar e Identificar Bactérias Diazotróficas de Plantas Não-Leguminosas*. Itaguaí: Embrapa SPI, 60.
- Finking, R., and Marahiel, M. A. (2004). Biosynthesis of nonribosomal peptides. *Annu. Rev. Microbiol.* 58, 453–488. doi: 10.1146/annurev.micro.58.030603.123615
- Fonseca, C. R. (1999). Amazonian ant-plant interactions and the nesting space limitation hypothesis. *J. Trop. Ecol.* 15, 807–825. doi: 10.1017/S0266467499001194
- Gaglioti, A. L., and Romaniuc-Neto, S. (2012). “Urticaceae,” in *Flora Fanerogâmica do Estado de São Paulo*, eds M. G. L. Wanderley, G. J. Shepherd, T. S. Melhem, A. M. Giullietti, and S. E. Martins (São Paulo: Instituto de Botânica), 331–361.
- Getha, K., and Vikineswary, S. (2002). Antagonistic effects of *Streptomyces violaceusniger* strain G10 on *fusarium oxysporum* f.sp. *cubense* race 4: indirect evidence for the role of antibiosis in the antagonistic process. *J. Ind. Microbiol. Biotechnol.* 28, 303–310. doi: 10.1038/sj/jim/7000247
- González-Teuber, M., Jiménez-Alemán, G. H., and Boland, W. (2014). Foliar endophytic fungi as potential protectors from pathogens in myrmecophytic *Acacia* plants. *Commun. Integr. Biol.* 7:e970500. doi: 10.4161/19420889.2014.970500
- Hanshew, A. S., McDonald, B. R., Díaz, C. D., Djieto-Lordon, C., Blatrix, R., and Currie, C. R. (2015). Characterization of actinobacteria associated with three ant-plant mutualisms. *Microb. Ecol.* 69, 192–203. doi: 10.1007/s00248-014-0469-3
- Harada, K. I., Fujii, K., Hayashi, K., Suzuki, M., Ikai, Y., and Oka, H. (1996). Application of D,L-FDLA derivatization to determination of absolute configuration of constituent amino acids in peptide by advanced Marfey's method. *Tetrahedron Lett.* 37, 3001–3004. doi: 10.1016/0040-4039(96)00484-4
- Heil, M., and McKey, D. (2003). Protective ant-plant interactions as model systems in ecological and evolutionary research. *Annu. Rev. Ecol. Syst.* 34, 425–453. doi: 10.1146/132410
- Heil, M., Orona-Tamayo, D., Eilmus, S., Kautz, S., and González-Teuber, M. (2010). Chemical communication and coevolution in an ant-plant mutualism. *Chemoecology* 20, 63–74. doi: 10.1007/s00049-009-0036-4
- Hernández, A., Lina, M., Sanders, J. G., Miller, G. A., Ravenscraft, A., and Frederickson, M. E. (2017). Ant-plant mutualism: a dietary by-product of a tropical ant's macronutrient requirements. *Ecology* 98, 3141–3151. doi: 10.1002/ecy.2036
- Hsu, S. C., and Lockwood, J. L. (1975). Powdered chitin agar as a selective medium for enumeration of Actinomycetes in water and soil. *Appl. Microbiol.* 29, 422–426. doi: 10.1128/aem.29.3.422-426.1975
- Kumar, V., Bharti, A., Gusain, O., and Bisht, G. S. (2010). An improved method for isolation of genomic DNA from filamentous Actinomycetes. *J. Eng. Technol. Manag.* 2, 10–13.
- Lazarotto, M., Muniz, M. F. B., Poletto, T., Dutra, C. B., Blume, E., Harakawa, R., et al. (2012). First report of *Pestalotiopsis clavispora* causing leaf spot of *Carya illinoensis* in Brazil. *Plant Dis.* 96, 1826–1826. doi: 10.1094/PDIS-07-12-0615-PDN
- Letunic, I., and Bork, P. (2019). Interactive tree of life (ITOL) v4: recent updates and new developments. *Nucleic Acids Res.* 47, 256–259. doi: 10.1093/nar/gkz239
- Li, X., Lin, C., and O'connor, P. B. (2010). Glutamine deamidation: differentiation of glutamic acid and γ -glutamic acid in peptides by electron capture dissociation. *Anal. Chem.* 82, 3606–3615. doi: 10.1021/ac9028467
- Longino, J. T. (1991). “*Azteca* ants in *Cecropia* trees: taxonomy, colony structure, and behaviour,” in *Ant-Plant Interactions*, eds C. R. Huxley, and D. F. Cutler (Oxford: Oxford University Press), 271–288.
- Lucas, J. M., Madden, A. A., Penick, C. A., Epps, M. J., Marting, P. R., Stevens, J. L., et al. (2019). *Azteca* ants maintain unique microbiomes across functionally distinct nest chambers. *Proc. Royal Soc. B* 286:20191026. doi: 10.1098/rspb.2019.1026
- Mayer, V. E., Frederickson, M. E., McKey, D., and Blatrix, R. (2014). Current issues in the evolutionary ecology of ant-plant symbioses. *New Phytol.* 202, 749–764. doi: 10.1111/nph.12690
- Mayer, V. E., and Voglmayr, H. (2009). Mycelial carton galleries of *Azteca brevis* (Formicidae) as a multi-species network. *Proc. Royal Soc. B* 276, 3265–3273. doi: 10.1098/rspb.2009.0768
- Minh, B. Q., Schmidt, H. A., Chernomor, O., Schrempf, D., Woodhams, M. D., von Haeseler, A., et al. (2020). IQ-TREE 2?: new models and efficient methods for phylogenetic inference in the genomic era. *Mol. Bio. Evol.* 37, 1530–1534. doi: 10.1093/molbev/msaa015
- Morales-Jiménez, J., Zúñiga, G., Villa-Tanaca, L., and Hernández-Rodríguez, C. (2009). Bacterial community and nitrogen fixation in the red *Turpentine* beetle, *Dendroctonus valens* LeConte (Coleoptera: Curculionidae: Scolytinae). *Microb. Ecol.* 58, 879–891. doi: 10.1007/s00248-009-9548-2
- Nepel, M., Voglmayr, H., Blatrix, R., Longino, J. T., Fiedler, K., Schönenberger, J., et al. (2016). Ant-cultivated Chaetothyriales in hollow stems of myrmecophytic *Cecropia* sp. trees – diversity and Patterns. *Fungal Ecol.* 23, 131–140. doi: 10.1016/j.funeco.2016.07.007
- Nielsen, T. H., Christophersen, C., Anthoni, U., and Sørensen, J. (1999). Viscosinamide, a new cyclic depsipeptide with surfactant and antifungal properties produced by *Pseudomonas fluorescens* DR54. *J. Appl. Microbiol.* 87, 80–90. doi: 10.1046/j.1365-2672.1999.00798.x

- Oliveira, K. N., Coley, P. D., Kursar, T. A., Kaminski, L. A., Moreira, M. Z., and Campos, R. I. (2015). The effect of symbiotic ant colonies on plant growth: a test using an *Azteca-Cecropia* system. *PLoS One* 10:e0120351. doi: 10.1371/journal.pone.0120351
- Pinto-Tomás, A. A., Anderson, M. A., Suen, G., Stevenson, D. M., Chu, F. S. T., Cleland, W. W., et al. (2009). Symbiotic nitrogen fixation in the fungus gardens of leaf-cutter ants. *Science* 326, 1120–1123. doi: 10.1126/science.1173036
- Pringle, E. G., and Moreau, C. S. (2017). Community analysis of microbial sharing and specialization in a Costa Rican ant – plant – Hemipteran symbiosis. *brevis* (Formicidae) as a multi-species network. *Proc. Royal Soc. B* 284:20162770. doi: 10.1098/rspb.2016.2770
- Ruiz-González, M. X., Leroy, C., Dejean, A., Gryta, H., Jargeat, P., Armijos Carrión, A. D., et al. (2019). Do host plant and associated ant species affect microbial communities in myrmecophytes? *Insects* 10:391. doi: 10.3390/insects10110391
- Shih, F. F. (1985). Analysis of glutamine, glutamic acid and pyroglutamic acid in protein hydrolysates by high-performance liquid chromatography. *J. Chromatogr. A* 322, 248–256. doi: 10.1016/S0021-9673(01)97681-2
- Treiber, E. L., Gaglioti, A. L., Romaniuc-Neto, S., Madriñan, S., and Weiblen, G. D. (2016). Phylogeny of the Cecropieae (Urticaceae) and the evolution of an ant-plant mutualism. *Syst. Bot.* 41, 56–66. doi: 10.1600/036364416X690633
- Visser, A. A., Nobre, T., Currie, C. R., Aanen, D. K., and Poulsen, M. (2012). Exploring the potential for Actinobacteria as defensive symbionts in fungus-growing termites. *Microb. Ecol.* 63, 975–985. doi: 10.1007/s00248-011-9987-4
- Voglmayr, H., Mayer, V., Maschwitz, U., Moog, J., Djieto-Lordon, C., and Blatrix, R. (2011). The diversity of ant-associated black yeasts: insights into a newly discovered world of symbiotic interactions. *Fungal Biol.* 115, 1077–1091. doi: 10.1016/j.funbio.2010.11.006
- Webber, B. L., Moog, J., Curtis, A. S. O., and Woodrow, I. E. (2007). The diversity of ant-plant interactions in the rainforest understorey tree, *Ryparosa* (Achariaceae): food bodies, domatia, prostomata, and hemipteran trophobionts. *Bot. J. Linn. Soc.* 154, 353–371. doi: 10.1111/j.1095-8339.2007.00651.x
- White, T. J., Bruns, T., Lee, S., and Taylor, J. (1990). “Amplification and direct sequencing of fungal ribosomal RNA genes for phylogenetics,” in *PCR Protocols: A Guide to Methods and Applications*, eds M. A. Innis, D. H. Gelfand, J. J. Sninsky, and T. J. White (San Diego, CA: Academic Press, Inc.), 315–322. doi: 10.1016/b978-0-12-372180-8.50042-1
- Zucchi, T. D., Guidolin, A. S., and Consoli, F. L. (2011). Isolation and characterization of actinobacteria ectosymbionts from *Acromyrmex Subterraneus Brunneus* (Hymenoptera, Formicidae). *Microbiol. Res.* 166, 68–76. doi: 10.1016/j.micres.2010.01.009

Conflict of Interest: The authors declare that the research was conducted in the absence of any commercial or financial relationships that could be construed as a potential conflict of interest.

Copyright © 2021 Fukuda, Pereira, Melo, Menegatti, Andrade, Groppo, Lacava, Currie and Pupo. This is an open-access article distributed under the terms of the Creative Commons Attribution License (CC BY). The use, distribution or reproduction in other forums is permitted, provided the original author(s) and the copyright owner(s) are credited and that the original publication in this journal is cited, in accordance with accepted academic practice. No use, distribution or reproduction is permitted which does not comply with these terms.



Pollen *Streptomyces* Produce Antibiotic That Inhibits the Honey Bee Pathogen *Paenibacillus larvae*

Kirk J. Grubbs^{1,2†}, Daniel S. May^{1†}, Joseph A. Sardina³, Renee K. Dermenjian⁴, Thomas P. Wyche⁴, Adrián A. Pinto-Tomás¹, Jon Clardy⁴ and Cameron R. Currie^{1*}

¹Department of Bacteriology, University of Wisconsin-Madison, Madison, WI, United States, ²Department of Cellular and Molecular Pathology, University of Wisconsin-Madison, Madison, WI, United States, ³Laboratory of Genetics, University of Wisconsin-Madison, Madison, WI, United States, ⁴Department of Biological Chemistry and Molecular Pharmacology, Harvard Medical School, Boston, MA, United States

OPEN ACCESS

Edited by:

Monica T. Pupo,
University of São Paulo, Brazil

Reviewed by:

Dong-Chan Oh,
Seoul National University,
South Korea
Juan F. Martin,
Universidad de León, Spain
Rita De Cassia Pessotti,
University of California, Berkeley,
United States

*Correspondence:

Cameron R. Currie
currie@bact.wisc.edu

[†]These authors have contributed
equally to this work

Specialty section:

This article was submitted to
Microbial Symbioses,
a section of the journal
Frontiers in Microbiology

Received: 23 November 2020

Accepted: 13 January 2021

Published: 04 February 2021

Citation:

Grubbs KJ, May DS, Sardina JA,
Dermenjian RK, Wyche TP,
Pinto-Tomás AA, Clardy J and
Currie CR (2021) Pollen
Streptomyces Produce Antibiotic
That Inhibits the Honey Bee
Pathogen *Paenibacillus larvae*.
Front. Microbiol. 12:632637.
doi: 10.3389/fmicb.2021.632637

Humans use natural products to treat disease; similarly, some insects use natural products produced by Actinobacteria to combat infectious pathogens. Honey bees, *Apis mellifera*, are ecologically and economically important for their critical role as plant pollinators and are host to diverse and potentially virulent pathogens that threaten hive health. Here, we provide evidence that Actinobacteria that can suppress pathogenic microbes are associated with *A. mellifera*. We show through culture-dependent approaches that Actinobacteria in the genus *Streptomyces* are commonly isolated from foraging bees, and especially common in pollen stores. One strain, isolated from pollen stores, exhibited pronounced inhibitory activity against *Paenibacillus larvae*, the causative agent of American foulbrood. Bioassay-guided HPLC fractionation, followed by NMR and mass spectrometry, identified the known macrocyclic polyene lactam, piceamycin that was responsible for this activity. Further, we show that in its purified form, piceamycin has potent inhibitory activity toward *P. larvae*. Our results suggest that honey bees may use pollen-derived Actinobacteria and their associated small molecules to mediate colony health. Given the importance of honey bees to modern agriculture and their heightened susceptibility to disease, the discovery and development of antibiotic compounds from hives could serve as an important strategy in supporting disease management within apiaries.

Keywords: pollen, *Apis mellifera*, piceamycin, *Streptomyces*, American foulbrood, *Paenibacillus larvae*, natural product

INTRODUCTION

Natural products play a critical role in human health, serving as drugs or drug leads that are used to treat diverse human afflictions, including cancer and hypertension (Newman and Cragg, 2020). Their role as antibiotics to treat infectious disease has had the largest impact on human health (Demain, 2009; Lewis, 2012). Most of the antibiotics used pharmaceutically are derived from Actinobacteria, especially soil dwelling members of the genus *Streptomyces*. Thousands of natural products have been discovered from Actinobacteria, and bioinformatic

analysis of sequenced genomes has revealed that past efforts have overlooked many potentially useful compounds (Bachmann et al., 2014; Baltz, 2017). Despite their critical importance to human health, our understanding of the function of these secondary metabolites in their natural context is limited.

In addition to their use by humans, Actinobacteria and their natural products are known to be used by some insects to combat pathogens. One of the most well-studied systems is the complex and ancient symbiosis associated with fungus-growing ants. Many of these ants engage in an obligate mutualism with Actinobacteria in the genus *Pseudonocardia*, which produce antibiotics that help defend against parasitic infections of the mutualist fungus that the ants cultivate for food (Currie and Scott, 1999; Currie et al., 2002; Cafaro et al., 2011; Li et al., 2018). Similar to the symbiosis between fungus-growing ants and *Pseudonocardia*, digger wasps (*Philanthus* spp.; Kaltenpoth et al., 2005, 2006; Kroiss et al., 2010; Kai et al., 2018) and southern pine beetles (*Dendroctonus frontalis*; Scott et al., 2008) associate with antibiotic-producing *Streptomyces* in defensive mutualisms. Targeted isolations, culture-independent studies, and biochemical characterization of *Streptomyces* associated with solitary mud dauber wasps, termites, dung beetles, and other insects have suggested that such associations occur frequently (Poulsen et al., 2011; Visser et al., 2012; Kim et al., 2014; Um et al., 2016; Klassen et al., 2019; Song et al., 2019; Hwang et al., 2020). Indeed, a recent study of 2,561 insects spanning 15 orders and more than 10,000 *Streptomyces* isolates suggests that these types of defensive mutualisms are likely more widespread than currently recognized and may serve as a source for discovering novel natural products that could serve as antibiotic drug leads (Chevrette et al., 2019).

Honey bees (*Apis mellifera*) are social organisms that live in very dense colonies of closely related individuals, which makes honey bees more vulnerable to pathogens through increased pathogen transmission and host susceptibility (Schmidt-Hempel, 1998; Evans and Schwarz, 2011; **Figure 1A**). A number of pathogens and parasites affect honey bees including viruses, bacteria, fungi, and mites (Bailey and Ball, 1991; Chen and Siede, 2007). *Paenibacillus larvae* (Firmicutes: Bacillales), the causative agent of American foulbrood, is one of the most widespread and destructive pathogens of honey bees. This honey bee specific pathogen is a spore forming Gram-positive bacteria that infects the larvae of honey bees through its highly infectious spores. The spores are consumed by larvae and germinate and grow vegetatively in the larval midgut leading to bacteremia and the formation of new spores. These spores are then spread throughout the hive and to other hives by contaminated worker bees, infecting new larvae as they are deposited in the hive environment (Genersch, 2010; Grady et al., 2016). To defend themselves and their hives from microbes, honey bees have developed a number of alternative immune and resistance strategies, including hygienic behavior (Rothenbuhler, 1964; Spivak and Reuter, 2001), use of antimicrobial materials in nest construction (Przybyłek and Karpiński, 2019), social fever (Starks et al., 2000), immune trait transference (Traniello et al., 2002; Sadd et al., 2005), and increased risk-taking behaviors by diseased individuals

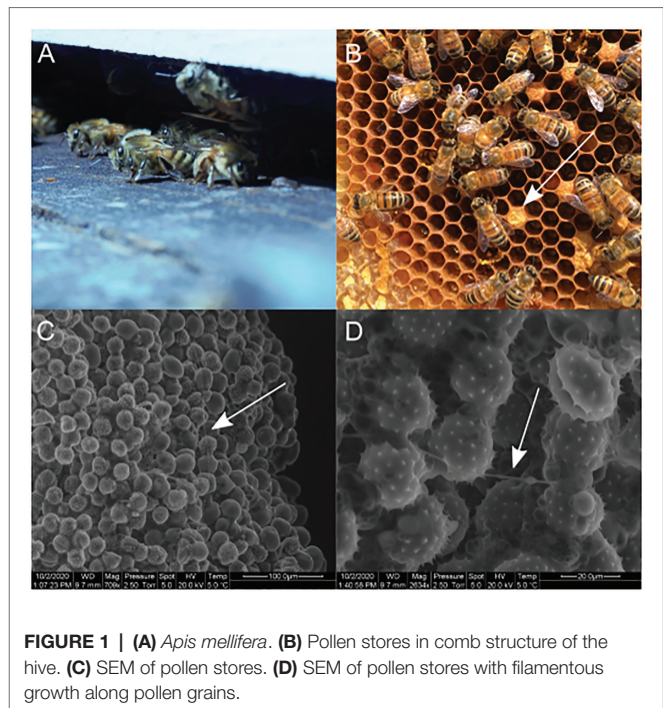


FIGURE 1 | (A) *Apis mellifera*. **(B)** Pollen stores in comb structure of the hive. **(C)** SEM of pollen stores. **(D)** SEM of pollen stores with filamentous growth along pollen grains.

(Schmid-Hempel, 2005). Nevertheless, the presence of defensive symbionts might be expected within honey bee colonies. Indeed, recent interest in the honey bee gut and hive microbiota has identified the symbiotic gut bacteria *Snodgrassella alvi* and hive bacteria *Bombella apis* which are both capable of defending against parasites and opportunistic pathogens. In addition, other bee species have been shown to have associations with antibiotic-producing Actinobacteria including stingless bees in South and Central America and Asian honey bees in Thailand (Promnuan et al., 2009; Cambroner-Heinrichs et al., 2019; Menegatti et al., 2020).

In this study, we use Actinobacteria-specific culture methods and multi-gene phylogenetics to identify a diverse set of *Streptomyces* strains associated with honey bees and their hives. Growth inhibition assays were used to identify *Streptomyces* strains capable of inhibiting *P. larvae*, the causative agent of American foulbrood, and other insect and plant pathogens. Additionally, analytical chemistry and genome mining techniques were used to identify antibiotics capable of inhibiting pathogens of honey bees and their hives.

MATERIALS AND METHODS

Isolation of Actinobacteria

We focused our sampling of honey bees and their different hive components from eight different hives. One hive in Wild Rose, WI, United States, two hives in Verona, WI, United States, three hives in Waukesha, WI, United States, and two hives in Mt. Horeb, WI, United States were sampled in 2007, 2008, 2008, and 2010, respectively. Honey, pollen stores, propolis, empty combs, bees in the hive, pupae, and newly eclosed bees

emerging from brood cells were sampled from each hive. Additionally, four starter packages of bees, including workers and a queen, were obtained and sampled from Bee Charmer, Brooklyn, WI, United States and CA, United States (commercial bees). A swarm formed from a honey bee colony maintained in the Currie laboratory at the University of Wisconsin-Madison in 2008 was located and the swarming bees were sampled. Finally, foraging bees were found at flowers and fruit around Madison, WI, United States and sampled.

Enrichment isolation for Actinobacteria was conducted on single individuals for worker bees and pupae, and on a single cell for comb and pollen stores. For honey and propolis, we used 10 μ l and 100 mg, respectively. Samples were homogenized in 500 μ l of sterile diH₂O by shaking in a beadbeater for 3 min without beads. For each sample type, 10 biological replicates were completed. Once homogenized, 100 μ l of sample was plated in duplicate on chitin solid media (agar 20 g/L, unbleached chitin 4 g/L, K₂HPO₄ 0.77 g/L, MgSO₄ \times 7H₂O 0.5 g/L, KH₂PO₄ 0.37 g/L, FeSO₄ \times 7H₂O 0.01 g/L, MnCl₂ \times 4H₂O 0.001 g/L, and ZnSO₄ \times 7H₂O 0.001 g/L) with cyclohexamide (0.05 g/L) and nystatin (0.032 g/L) added to suppress the growth of fungus. Plates were allowed to dry, wrapped with parafilm, and then incubated at 30°C for a minimum of 4 weeks or until microbial growth covered the plate. Colonies exhibiting spores and/or a concentric ring growth pattern were enumerated, then subcultured onto chitin plates to obtain pure cultures, and subsequently grown on yeast malt extract agar medium (YMEA: yeast extract 4 g/L, malt extract 10 g/L, dextrose 4 g/L, and agar 15 g/L).

Scanning Electron Microscopy

Environmental scanning electron microscopy (SEM) was used to visualize filamentous bacteria in pollen stores. Pollen samples were stored for 2 weeks at 4°C before imaging. Samples were mounted on SEM stubs with carbon bi-adhesive tabs, and images were taken at 2.5 torr, 5.0 spot size, and 5°C using a FEI QUANTA 200 eSEM.

DNA Extraction

DNA was extracted from isolates *via* a CTAB Phenol/Chloroform protocol. Briefly, approximately 15 μ l of bacterial tissue was scraped from cultures and homogenized *via* mortar and pestle in a 1.7 ml centrifuge tube containing 500 μ l of a 2x CTAB solution. To the resulting slurry, 500 μ l of a phenol:chloroform:isoamyl alcohol solution (25:24:1) was added. After vigorous mixing, the solution was centrifuged at max speed for 15 min and the resulting upper aqueous phase was removed and mixed with 500 μ l of a chloroform:isoamyl alcohol (24:1) solution. The resulting solution was mixed and centrifuged at max speed for 15 min. The aqueous phase was then removed and combined with an equal volume of ice-cold isopropanol. Samples were incubated at -20°C overnight to allow DNA precipitation. Samples were then centrifuged at max speed for 30 min at 4°C. Resulting DNA was rinsed three times with 70% ethanol, air dried, resuspended in TE buffer, and stored at -20°C for future use.

16S Sequencing and Core-Genomic Phylogeny

Primers 27f and 1392r were used to obtain 16S sequences in PCR reactions with cycle parameters of 95°C for 2 min, 35 cycles of 95°C for 45 s, 55°C for 45 s, 72°C for 90 s, and 72°C for 5 min and hold at 4°C. Products were cleaned using ExoSapIT (USB) according to the manufacturer's protocol. Sequencing reactions consisted of 2 μ l of BigDye Terminator v. 3.1 mix (Applied Biosystems), 3 μ l of dilution buffer (Applied Biosystems), 5–20 pmol of primer, and 0.2 μ g of template DNA in a final reaction volume of 20 μ l. Cycle conditions were 95°C for 3 min, then 35 cycles of 95°C for 20 s, 45°C for 30 s, and 60°C for 4 min, followed by 7 min at 72°C. Excess dye terminators were removed using CleanSeq magnetic beads (Agencourt Biosciences). Samples were then resuspended in 40 μ l of ddH₂O and sequenced at the University of Wisconsin-Madison Biotechnology Center using an Applied Biosystems 3730xl automated DNA sequencing instrument, using 50 cm capillary arrays and POP-7 polymer.

16S sequences were assembled using Bionumerics v6.5 (Applied Maths). Sequences were aligned in MEGAX (Kumar et al., 2018) using the MUSCLE algorithm. The alignment was inspected in MEGAX to ensure consistent reading frame, accurate gap placement, and reduction of sequence overhang at the ends. The model test module of MEGAX was used to ensure accurate choice of substitution model, and maximum likelihood phylogenies were inferred using 200 bootstrap replicates.

A multilocus phylogeny was created from the sequenced genomes of eight diverse bee-associated *Streptomyces* strains using methods described in (Chevrette et al., 2019). In brief, prodigal v2.6.0 (Hyatt et al., 2010) was used to call genes for each genome and HMMER v3.1b2 (Eddy, 2011) was used to search the genomes for 93 TIGRFAM amino acid sequences in the “core bacterial protein” set (GenProp0799). Protein families were aligned using MAFFT v7.245 (Katoh and Standley, 2013) and converted to codon alignments. RAXML v8.1.24 (Stamatakis, 2014) was used to generate phylogenetic trees for each codon alignment using the GTR gamma substitution model with 100 bootstraps. Finally, ASTRAL-II (Mirarab and Warnow, 2015) was used to generate the species phylogenetic tree from the individual codon aligned trees with 100 bootstraps. FigTree v1.4.3 was used to root the tree and display branch lengths proportional to the root. 16S sequences can be found on GenBank with accession numbers MW444694-MW444787.

Growth Inhibition Bioassays

All isolates were assessed for growth inhibition against the honey bee specific pathogen American foulbrood (*P. larvae*), as well as an insect generalist pathogen *Beauveria bassiana* and a plant generalist pathogen *Fusarium oxysporum*. Actinobacteria isolates were inoculated in the center of 85 mm diameter YMEA plates and incubated at 30°C for 4 weeks. Fungi were then inoculated on the edge of the plate and incubated at 30°C until controls without bacterial isolates occupied half or more of the plate. Bacterial pathogens were grown in fresh liquid cultures and spread in the areas where

the isolates had not grown. The area of fungal pathogens was measured using ImageJ (Schindelin et al., 2015) and compared to control fungal areas using an unpaired two-sample *t*-test. The minimum distance between isolate and pathogen was measured in bacterial pathogen assays and compared to zero using a single sample *t*-test.

Analytical Chemistry Methods and Instrumentation

NMR experiments were performed in DMSO- d_6 with a symmetrical NMR microtube (Shigemi, Inc.) on a Varian INOVA 600 MHz NMR. HPLC fractionation was performed on an Agilent 1100 Series HPLC system. LC/MS analysis was performed on an Agilent 1200 Series HPLC/6130 Series mass spectrometer. High resolution mass spectra were obtained on a Waters Micromass Q-ToF Ultima ESI-TOF mass spectrometer. Circular dichroism spectrum was obtained on an Aviv Biomedical Inc. (Lakewood, NJ, United States) Circular Dichroism Spectrometer, Model 410. Optical rotation measurements were obtained using a Jasco R-2000 digital polarimeter with a sodium lamp.

Isolation and Identification of Piceamycin

Streptomyces sp. AmelAP-1 was isolated from pollen stores and maintained on YMEA at room temperature. Single colonies were used to inoculate 10 ml YME broth (4 g yeast extract, 10 g malt extract, and 4 g dextrose per L) seed cultures, which were incubated at 25°C with shaking at 250 rpm for 48 h. This seed was then used to inoculate 500 ml cultures of YME broth, also incubated at 25°C, 250 rpm for 48 h. Extraction and fractionation procedures were performed in the dark due to photosensitivity of piceamycin. Bacterial cultures were centrifuged and the supernatant extracted twice with an equal volume of ethyl acetate. The organic extract was dried over sodium sulfate, and then concentrated *in vacuo*. The extract was then resuspended in a minimum volume of methanol, and adsorbed onto celite. This mixture was dried, loaded onto a 2 g C₁₈ Sep-Pak SPE cartridge, and fractionated by eluting with a step gradient of methanol/water. The 80% methanol fraction was most active, as deduced by spotting fractions onto lawns of *Bacillus subtilis* on LB agar and assessing zones of inhibition. This fraction was subsequently purified by reverse-phase HPLC with UV detection using a semi-preparative Discovery HS-C₁₈ column (Supelco, 25 cm × 10 mm, 10 μm particle size) with an acetonitrile:water gradient at 3 ml/min: 0–15 min, 55% MeCN; 15–17 min, 55–100% MeCN. Piceamycin eluted at ~15 min. The overall yield of piceamycin is approximately 0.6 mg/L. For acetylation, piceamycin was dissolved in pyridine, and a stoichiometric amount of acetic anhydride was added. The reaction was stirred at room temperature for 1 h, evaporated to dryness, and redissolved in methanol for LC/MS analysis.

Genome Sequencing and Biosynthetic Gene Cluster Identification

DNA was isolated as described above and prepared for Illumina MiSeq 2 × 300 bp paired-end sequencing by the University of Wisconsin-Madison Biotechnology Center. The resulting

reads were corrected with MUSKET v1.1, and paired-ends were merged with FLASH v1.2.7 and finally assembled with SPAdes v3.11.0. The assembly (GenBank assembly accession: GCA_009865135.1) was submitted to AntiSMASH v5.0 for the identification of biosynthetic gene clusters. A putative piceamycin polyketide synthase was identified based on high similarity to the published bombyxamycin/piceamycin polyketide synthase. The two biosynthetic gene clusters were directly compared by BLAST and MultiGeneBlast v1.1.14 (Medema et al., 2013).

Antibacterial Assays of Piceamycin

All bioassays were performed in triplicate. Overnight cultures of all strains assayed were diluted to ~10⁶ cells/ml in LB and transferred to sterile 96-well plates (200 μl per well). A serial dilution of piceamycin dissolved in DMSO or only DMSO, as a negative control, was added to the cultures, and the plates were incubated without shaking at 30°C (for *Paenibacillus* and *Bacillus* strains) or 37°C (for *Escherichia coli*). OD₆₀₀ measurements were performed on a Molecular Devices SpectraMax® M5 plate reader after 15 h.

RESULTS

Apis mellifera pupae, newly eclosed bees, adult bees found in hives, adult bees found foraging (found at flowers or fruit), swarming bees, commercial bees, empty combs, propolis, honey, and pollen stores were all sampled for the presence of Actinobacteria. Enrichment isolation for Actinobacteria resulted in at least one isolate from all sampled material (Table 1; Supplemental Table 2). Fewer actinobacterial colony forming units (CFUs) were isolated from the bee brood or hive environment such as pupae, newly eclosed workers, honey, empty combs, or propolis. Actinobacterial CFUs were more common from older adult bees such as hive bees, foraging bees, swarming bees, and commercial bees. Pollen stores, however, consistently showed the greatest number of actinobacterial CFUs (Figure 1B; Table 1). Scanning electron microscopic (SEM) examination of honey bee adults did not identify Actinobacteria; however, SEM of pollen stores in hives revealed growth consistent with Actinobacteria morphology (Figures 1C,D).

TABLE 1 | Average colony forming units (CFU) count from bee and bee environment sources.

Source	Average CFU (SEM)
Pupae	1.1 (0.97)
Newly eclosed workers	0.33 (0.2)
Adult hive bees	5.6 (1.3)
Adult foraging bees	9.4 (1.4)
Swarming bees	13.8 (7.3)
Commercial bees	14 (3.4)
Honey	0.05 (0.04)
Empty comb	0.91 (0.56)
Propolis	0.95 (0.68)
Pollen stores	25.4 (3.0)

Ten biological replicates were collected from each source and SEM is shown in parentheses.

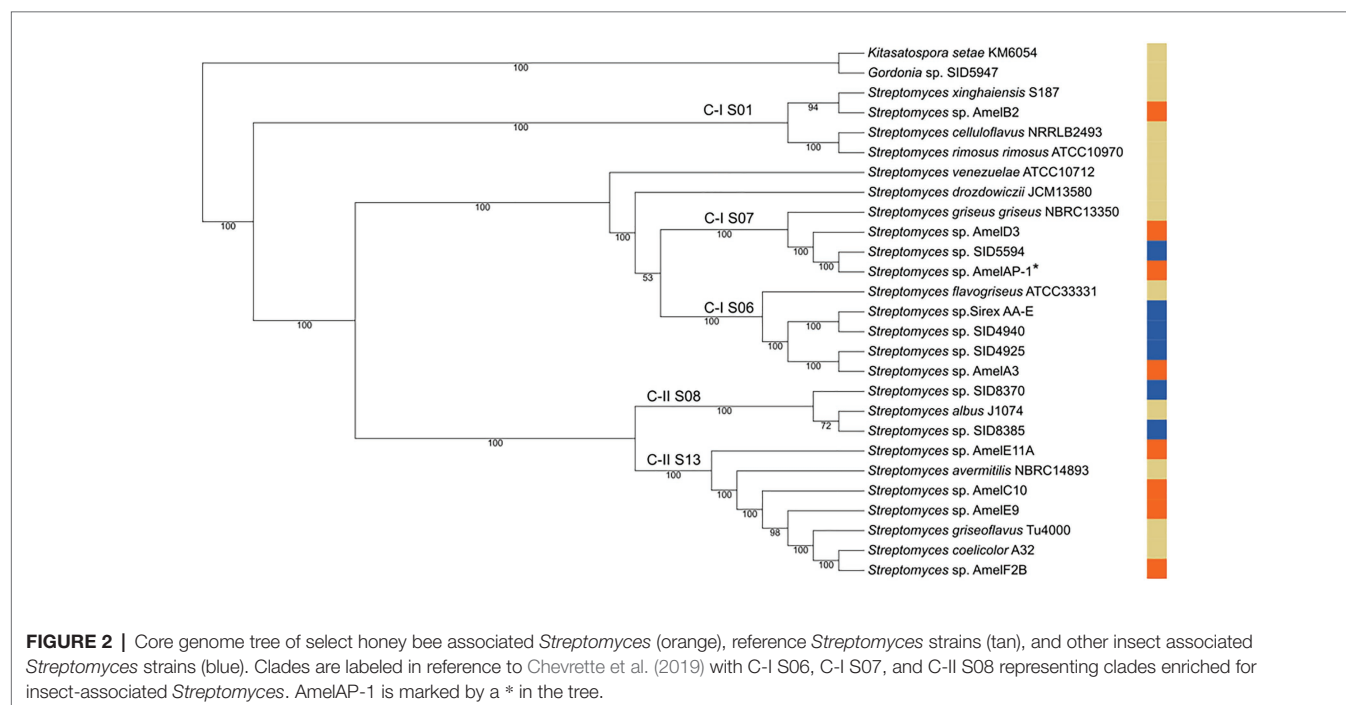
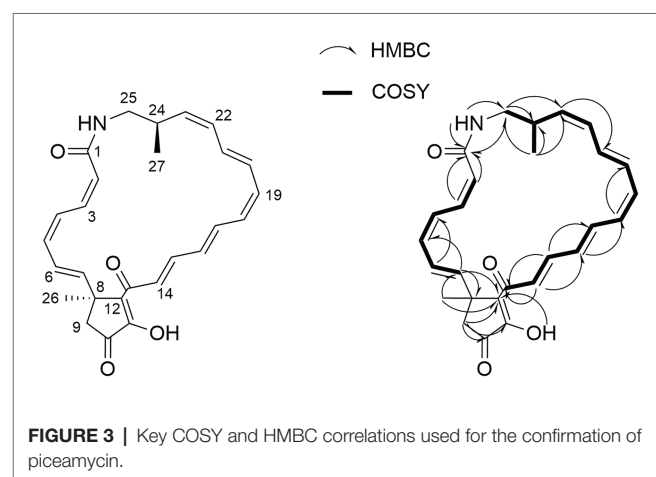
Streptomyces isolates from bees and hive material were selected for genome sequencing based on a preliminary 16S rDNA analysis. Eight strains were selected to represent the diversity of *Streptomyces* strains observed in the 16S rDNA analysis. The strains were sequenced and assembled, and a phylogenomic tree of the strains was created based on 93 core genes. Both the 16S analysis and the core genome tree demonstrate a diversity of *Streptomyces* can be isolated from honey bees and their hives (Figure 2; Supplementary Figure 1). Three of the strains in the core genome tree are in clades that are enriched with insect-associated symbiotic *Streptomyces* spp., AmelAP-1, AmelD3, and AmelA3. Based on the phylogeny in Chevrette et al. (2019), *Streptomyces* spp. AmelAP-1 and AmelD3 are in Clade I S07 and are closely related to several *Streptomyces* strains isolated from solitary mud dauber wasps. *Streptomyces* sp. AmelA3 is in Clade I S06 and is closely related to *Streptomyces* strains isolated from mountain pine beetles and fungus-growing termites. Other strains are located widely throughout the genus *Streptomyces*.

All isolated *Streptomyces* were screened in pairwise assays against *P. larvae* the causative agent of American foulbrood, *Beauveria bassiana* an entomopathogenic fungus, and *Fusarium oxysporum* a common plant pathogen. Each isolate demonstrated inhibition against at least one pathogen with several inhibiting only the bacterial pathogens or inhibiting only the fungal pathogen (Supplemental Table 2). *Streptomyces* sp. AmelAP-1, isolated from pollen stores, was found to inhibit all three pathogens and was particularly active against *P. larvae*. Additionally, *Streptomyces* AmelAP-1 was shown to be closely related to other insect associated *Streptomyces* strains; therefore, it was chosen for further analysis.

AmelAP-1 was grown in Yeast Malt-extract media in liquid culture and the supernatant was extracted with ethyl

acetate and dried *in vacuo* to yield a crude extract. The extract was confirmed to be active against *P. larvae* and bioactivity guided HPLC fractionation revealed a pure compound (1) with strong inhibition against *P. larvae* ($[\alpha]_D^{28}$ 74.4 ($c = 0.34$, CH₃OH)). HRESIMS analysis of this compound (m/z 432.2163) indicated a molecular formula of C₂₇H₂₉NO₄ (calcd. m/z for [M + H]⁺, 432.2169). The fourteen degrees of unsaturation indicated by this formula, coupled with the absorption spectrum ($\lambda_{max} = 410$ nm) and extreme photosensitivity of the compound suggested a polyene moiety. This was confirmed by NMR analysis using one- and two-dimensional NMR techniques including ¹H, gCOSY, gHSQC, gHMBC, and ROESY.

Two distinct polyene-containing spin systems were detected by ¹H and gCOSY experiments (Figure 3). Configurations of



all double bonds in these units were determined by analysis of proton coupling constants and ROESY correlations. HSQC and long-range HMBC correlations established the presence of a cyclopentenone moiety linking these two polyene units at one end, and an amide bond closing the 23-membered lactam ring at the other (Figure 3). To confirm assignment of the hydroxy group, the compound was acetylated with acetic anhydride in pyridine. Subsequent mass spectral analysis revealed a mass of m/z 473.2 $[M + H]^+$, corresponding to acetylation at the only hydroxy group.

The planar structure of 1 was identical to the previously reported piceamycin (Schulz et al., 2009); however, there were significant differences in the ^{13}C chemical shifts of the cyclopentenone moiety, suggesting that 1 could be an isomer of piceamycin (Table 2). A ROESY correlation observed between the two methyl groups combined with minimum energy modeling of the possible stereoisomers indicated that the methyl groups are likely to be within range for coherence transfer in the 24R, 8S configuration. This is the same configuration as reported by Shin et al. (2020), suggesting that 1 is piceamycin; however, this does not explain the deviation of the cyclopentenone ^{13}C chemical shifts. Further NMR experiments were hindered by the photosensitivity of the compound, but four peaks with identical m/z values were detected by HR-LCMS in the extract of

AmelAP-1, suggesting that several conformational isomers may be present in the extract with one at much higher abundance than the others.

To provide further evidence that 1 is piceamycin, we examined the biosynthetic gene clusters present in the genome of *Streptomyces* sp. AmelAP-1 using AntiSMASH 5.0 (Blin et al., 2019). A polyketide synthase (PKS) biosynthetic gene cluster (BGC) with homology and synteny to that of the reported bombyxamycin and piceamycin biosynthetic gene cluster was identified (Shin et al., 2020). A comparison of the two BGCs was performed using BLASTP and MultiGeneBlast. Each gene in the bombyxamycin and piceamycin biosynthetic gene cluster contained a homologous gene in the PKS identified in the genome of AmelAP-1 (Figure 4; Supplemental Table 1). The PKS in AmelAP-1 contains six PKS genes composed of 12 modules. This deviates from the published piceamycin BGC that has six PKS genes composed of 11 modules. The biosynthetic gene cluster in AmelAP-1 also contains a duplicated type II thioesterase gene, which may be responsible for skipping or off-loading the growing polyketide chain from one of the extra modules containing a putatively inactive domain (Heathcote et al., 2001; Wu et al., 2018). The homology and synteny to the published bombyxamycin and piceamycin biosynthetic gene cluster suggests that the identified PKS is putatively responsible for the production of piceamycin in AmelAP-1.

A growth inhibition bioassay using purified piceamycin at decreasing concentrations was used to determine the activity and specificity of the compound toward *P. larvae* (Figure 5). Piceamycin was found to have high inhibition of *P. larvae*, with a minimum inhibitory concentration (MIC) of 48 nM. *Bacillus subtilis* and *E. coli* BAS849 were less sensitive with MICs of 213 nM and 6 μM , respectively. Growth of the wild-type *E. coli* K12 was not inhibited at the concentrations tested.

DISCUSSION

Here, we identified a known antibiotic produced by a *Streptomyces* isolated from the pollen stores of honey bees. The compound was confirmed based on NMR and LC-MS data as well as the identification of a PKS gene cluster with homology and synteny to the reported piceamycin biosynthetic gene cluster. Piceamycin is a macrocyclic polyene lactam, which has been recently reported in association with other insects (Shin et al., 2020). We reveal that piceamycin has high inhibitory activity, with a MIC of 48 nM, against *P. larvae*, a common and destructive Gram-positive bacterial pathogen of honey bees. Interestingly, this compound had significantly less inhibitory activity toward another closely related Gram-positive bacteria, *B. subtilis*, with a MIC of 213 nM. Additionally, a mutant *E. coli* that is sensitive to antibiotics due to a compromised outer membrane was only slightly inhibited by piceamycin, while wildtype *E. coli* was not inhibited at all. The apparent specificity of piceamycin toward *P. larvae* suggests that this small molecule could help mediate pathogen dynamics within honey bee colonies.

TABLE 2 | ^1H and ^{13}C assignments of piceamycin (1) in d_6 -DMSO.

#	δ_{C}	Type	δ_{H}	mult (J, Hz)
1	163.9	C		
2	121.2	CH	5.06	d (12.9)
3	132.5	CH	6.26	dd (12.7)
4	122.5	CH	7.07	dd (11.4)
5	134.4	CH	6.13	dd (11.4)
6	119.9	CH	5.99	dd (11.4, 14.7)
7	147.1	CH	5.92	d (14.7)
8	40.8	C		
9	49.4	CH_2	2.04	d (18.9)
			2.06	d (18.9)
10	213.3	C		
11	171.0	C		
11-OH			6.74	br s
12	127.6	C		
13	188.8	C		
14	133.4	CH	8.01	d (15.4)
15	136.1	CH	6.81	dd (15.4, 11.4)
16	130.8	CH	6.43	dd (14.2, 11.4)
17	133.2	CH	6.89	dd (14.2, 10.4)
18	128.0	CH	6.20	m (<11) ^a
19	130.7	CH	6.22	m (<11) ^a
20	127.3	CH	6.64	dd (15.2, 8.7)
21	130.4	CH	6.53	dd (15.0, 10.4)
22	129.1	CH	6.06	dd (10.4)
23	135.2	CH	5.07	m^a
24	33.2	CH	2.67	m^a
25	43.6	CH_2	2.64	m^a
			3.35	m^a
26	29.2	CH_3	1.53	s
27	17.6	CH_3	0.95	d (6.3)
NH			7.40	d (9.9)

^aOverlapped peaks; coupling constant unknown.

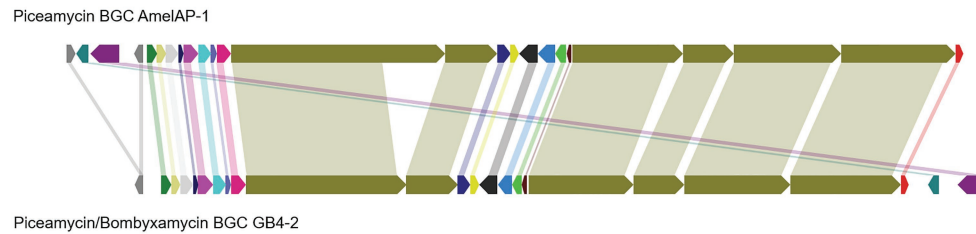


FIGURE 4 | Comparison of the identified polyketide synthase (PKS) biosynthetic gene cluster (BGC) in AmelAP-1 to the published BGC for bombyxamycin and piceamycin. Shaded bars between BGCs identify homologous genes between the two BGCs.

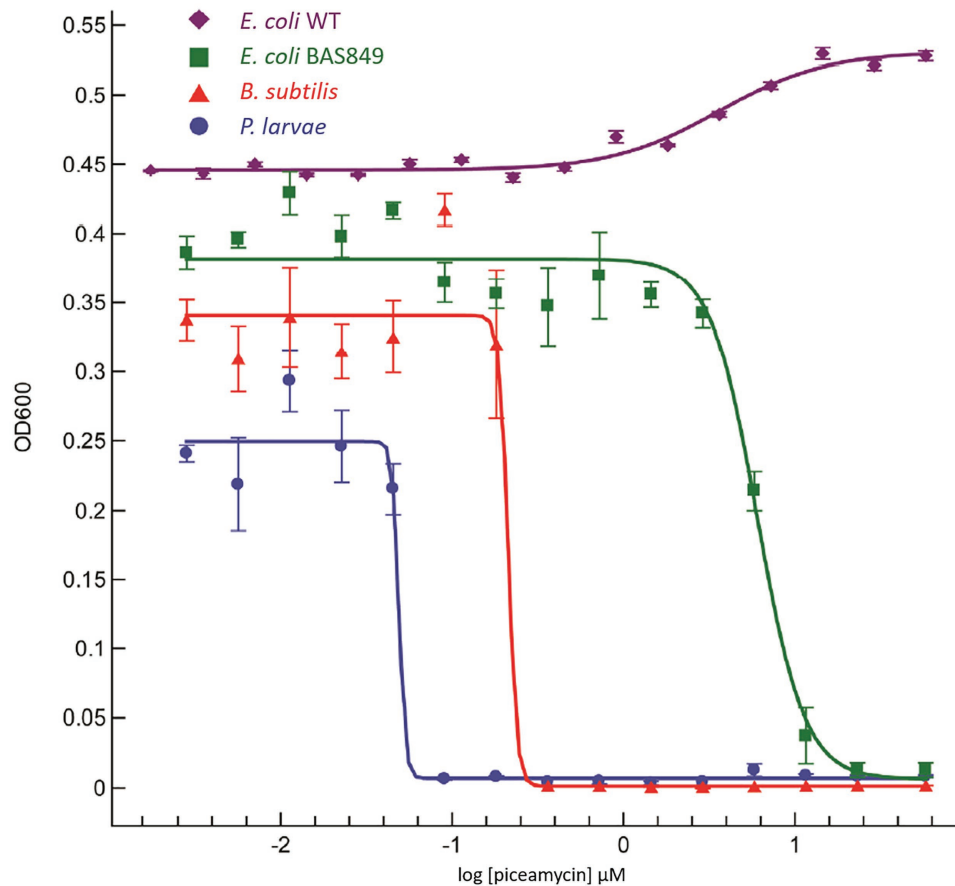


FIGURE 5 | Dose response curve using piceamycin against *Paenibacillus larvae*, *Bacillus subtilis*, and two strains of *Escherichia coli*.

Diverse *Streptomyces* strains were isolated from adult bees in managed hives, purchased adult bees, swarming bees, and various parts of bee hives. Interestingly, the most numerous isolations consistently came from pollen stores, and filamentous, Actinobacteria-like, bacteria were observed on pollen stores using scanning electron microscopy. Similar findings were described in a recent publication describing the tripartite symbiosis of *Streptomyces*, honey bees (*Apis mellifera*), and strawberry plants (Kim et al., 2019). Other publications have

also recently reported *Streptomyces* associated with various bee species and it is possible that many of these bee species are gathering beneficial *Streptomyces* strains through the pollen collected from plants. Many of these *Streptomyces* strains have the ability to inhibit both bee pathogens and plant pathogens, as was demonstrated by Kim et al. (2019), as well as by the inhibition of both *P. larvae* and *Fusarium oxysporum* by AmelAP-1 in this study. Additionally, several other strains isolated in our study were capable of inhibiting either *P. larvae*

or other potential bee or bee hive pathogens; however, the small molecules responsible for the inhibition have not yet been identified. While there is no consistent phylogenetic signal of a single vertically transferred symbiont, it is possible that pollinators and their plants are using a diverse suite of protective bacteria that produce compounds capable of inhibiting both plant and pollinator pathogens.

The eusocial nature of honey bees leads to increased susceptibility to disease. The living together of closely related individuals in high density increases pathogen transmission and virulence within hives. Interestingly, despite this prediction, the genome of *A. mellifera* contains only a third the number of immune related genes than does the *Drosophila* genome (Evans et al., 2006). In response, honey bees have developed a number of alternative immune strategies, which may include the use of antibiotic-producing bacteria. The apparent use of natural products derived from bacteria by honey bees parallels the importance of natural products for treating pathogens by humans. Given the dramatic decrease in the discovery of novel antibiotics, this work and others suggest that *A. mellifera* and other bees may represent a valuable source for discovering novel antibiotics. Indeed, in the last several years studies have identified both Actinobacteria and Proteobacteria associated with the hive environment that can inhibit both bacterial and fungal pathogens of bees (Cambroner-Heinrichs et al., 2019; Menegatti et al., 2020; Miller et al., 2020; Smith and Newton, 2020). Additionally, the specificity of piceamycin makes it a prime candidate for development into a biological hive treatment to protect against American foulbrood. Given the apparent increase in pathogen pressure currently experienced by managed hives and our reliance on honey bees as important pollinators for a number of agriculture crops, piceamycin, and other compounds identified using similar approaches could have important implications for human agriculture and the apiculture industry.

REFERENCES

- Bachmann, B. O., Van Lanen, S. G., and Baltz, R. H. (2014). Microbial genome mining for accelerated natural products discovery: is a renaissance in the making? *J. Ind. Microbiol. Biotechnol.* 41, 175–184. doi: 10.1007/s10295-013-1389-9
- Bailey, L., and Ball, B. (1991). *Honey bee pathology. 2nd Edn.* London: Academic Press, Elsevier Ltd.
- Baltz, R. H. (2017). Gifted microbes for genome mining and natural product discovery. *J. Ind. Microbiol. Biotechnol.* 44, 573–588. doi: 10.1007/s10295-016-1815-x
- Blin, K., Shaw, S., Steinke, K., Villebro, R., Ziemert, N., Lee, Y., et al. (2019). antiSMASH 5.0: updates to the secondary metabolite genome mining pipeline. *Nucleic Acids Res.* 47, 81–87. doi: 10.1093/nar/gkz310
- Cafaro, M. J., Poulsen, M., Little, A. E. F., Price, S. L., Gerardo, N. M., and Wong, B., et al. (2011). Specificity in the symbiotic association between fungus-growing ants and protective *Pseudonocardia* bacteria. *Proc. R. Soc. B Biol. Sci.* 278, 1814–1822. doi: 10.1098/rspb.2010.2118
- Cambroner-Heinrichs, J. C., Matarrita-Carranza, B., Murillo-Cruz, C., Araya-Valverde, E., Chavarría, M., and Pinto-Tomás, A. A. (2019). Phylogenetic analyses of antibiotic-producing *Streptomyces* sp. isolates obtained from the stingless-bee *Tetragonisca angustula* (Apidae: Meliponini). *Microbiology* 165, 292–301. doi: 10.1099/mic.0.000754
- Chen, Y. P., and Siede, R. (2007). Honey bee viruses. *Adv. Virus Res.* 70, 33–80. doi: 10.1016/S0065-3527(07)70002-7

DATA AVAILABILITY STATEMENT

The datasets presented in this study can be found in online repositories. The names of the repository/repositories and accession number(s) can be found in the article/**Supplementary Material**.

AUTHOR CONTRIBUTIONS

The collection, isolation, and screening of bee associated *Streptomyces* were performed by KG and AP-T. Scanning electron microscopy was performed by JS. 16S phylogenetic analysis was performed by KG and DM and the core-genome phylogenetic analysis was performed by DM. Isolation and analytical analysis of piceamycin were performed by TW and RD. Identification and analysis of the biosynthetic gene cluster that encodes the production of piceamycin in AmelAP-1 were performed by DM. The manuscript was written by DM and KG. Funding was acquired by KG, JC, and CC. All authors contributed to the article and approved the submitted version.

FUNDING

This work was supported by a grant from the National Institute for Health U19 AI142720 (to JC and CC) and a National Institute of Food and Agriculture, U.S. Department of Agriculture grant, under identification number WISO1321 (KG and CC).

SUPPLEMENTARY MATERIAL

The Supplementary Material for this article can be found online at: <https://www.frontiersin.org/articles/10.3389/fmicb.2021.632637/full#supplementary-material>

- Chevrette, M. G., Carlson, C. M., Ortega, H. E., Thomas, C., Ananiev, G. E., Barns, K. J., et al. (2019). The antimicrobial potential of *Streptomyces* from insect microbiomes. *Nat. Commun.* 10, 1–11. doi: 10.1038/s41467-019-08438-0
- Currie, C. R., Mueller, U. G., and Malloch, D. (2002). The agricultural pathology of ant fungus gardens. *Proc. Natl. Acad. Sci. U. S. A.* 96, 7998–8002. doi: 10.1073/pnas.96.14.7998
- Currie, C. R., and Scott, J. A. (1999). Fungus-growing ants use antibiotic-producing bacteria to control garden parasites. *Nature* 398, 701–705. doi: 10.1038/19519
- Demain, A. L. (2009). Antibiotics: natural products essential to human health. *Med. Res. Rev.* 29, 821–842. doi: 10.1002/med.20154
- Eddy, S. R. (2011). Accelerated profile HMM searches. *PLoS Comput. Biol.* 7:e1002195. doi: 10.1371/journal.pcbi.1002195
- Evans, J., Aronstein, K., Chen, Y., Hetru, C., Imler, J., Jiang, H., et al. (2006). Immune pathways and defence mechanisms in honey bees *Apis mellifera*. *Insect Mol. Biol.* 15, 645–656. doi: 10.1111/j.1365-2583.2006.00682.x
- Evans, J. D., and Schwarz, R. S. (2011). Bees brought to their knees: microbes affecting honey bee health. *Trends Microbiol.* 19, 614–620. doi: 10.1016/j.tim.2011.09.003
- Genersch, E. (2010). American Foulbrood in honeybees and its causative agent, *Paenibacillus larvae*. *J. Invertebr. Pathol.* 103, S10–S19. doi: 10.1016/j.jip.2009.06.015
- Grady, E. N., MacDonald, J., Liu, L., Richman, A., and Yuan, Z. C. (2016). Current knowledge and perspectives of *Paenibacillus*: a review. *Microb. Cell Fact.* 15, 1–18. doi: 10.1186/s12934-016-0603-7

- Heathcote, M. L., Staunton, J., and Leadlay, P. F. (2001). Role of type II thioesterases: evidence for removal of short acyl chains produced by aberrant decarboxylation of chain extender units. *Chem. Biol.* 8, 207–220. doi: 10.1016/S1074-5521(01)00002-3
- Hwang, S., Le, L. T., Jo, S. I., Shin, J., Lee, M. J., and Oh, D. C. (2020). Pentaminomycins C–E: cyclic pentapeptides as autophagy inducers from a mealworm beetle gut bacterium. *Microorganisms* 8, 1–16. doi: 10.3390/microorganisms8091390
- Hyatt, D., Chen, G. L., LoCascio, P. F., Land, M. L., Larimer, F. W., and Hauser, L. J. (2010). Prodigal: prokaryotic gene recognition and translation initiation site identification. *BMC Bioinformatics* 11:119. doi: 10.1186/1471-2105-11-119
- Kai, M., Engl, T., Nechitaylo, T. Y., Kroiss, J., Kaltenpoth, M., and Svatoš, A. (2018). Evolutionary stability of antibiotic protection in a defensive symbiosis. *Proc. Natl. Acad. Sci.* 115, E2020–E2029. doi: 10.1073/pnas.1719797115
- Kaltenpoth, M., Goettler, W., Dale, C., Stubblefield, J. W., Herzner, G., Roeser-mueller, K., et al. (2006). “Candidatus *Streptomyces philanthi*,” an endosymbiotic streptomycete in the antennae of *Philanthus* digger wasps printed in Great Britain. *Int. J. Syst. Evol. Microbiol.* 56, 1403–1411. doi: 10.1099/ijs.0.64117-0
- Kaltenpoth, M., Götter, W., Herzner, G., and Strohm, E. (2005). Symbiotic bacteria protect wasp larvae from fungal infestation. *Curr. Biol.* 15, 475–479. doi: 10.1016/j.cub.2004.12.084
- Katoh, K., and Standley, D. M. (2013). MAFFT multiple sequence alignment software version 7: improvements in performance and usability. *Mol. Biol. Evol.* 30, 772–780. doi: 10.1093/molbev/mst010
- Kim, D. R., Cho, G., Jeon, C. W., Weller, D. M., Thomashow, L. S., Paulitz, T. C., et al. (2019). A mutualistic interaction between *Streptomyces* bacteria, strawberry plants and pollinating bees. *Nat. Commun.* 10:4802. doi: 10.1038/s41467-019-12785-3
- Kim, K. H., Ramadhar, T. R., Beemelmans, C., Cao, S., Poulsen, M., Currie, C. R., et al. (2014). Natalamycin A, an ansamycin from a termite-associated *Streptomyces* sp. *Chem. Sci.* 5, 4333–4338. doi: 10.1039/C4SC01136H
- Klassen, J. L., Lee, S. R., Poulsen, M., Beemelmans, C., and Kim, K. H. (2019). Efomycins K and L from a termite-associated *Streptomyces* sp. M56 and their putative biosynthetic origin. *Front. Microbiol.* 10:1739. doi: 10.3389/fmicb.2019.01739
- Kroiss, J., Kaltenpoth, M., Schneider, B., Schwinger, M., Hertweck, C., and Maddula, R. K., et al. (2010). Symbiotic streptomycetes provide antibiotic combination prophylaxis for wasp offspring. *Nat. Chem. Biol.* 6, 261–263. doi: 10.1038/nchembio.331
- Kumar, S., Stecher, G., Li, M., Knyaz, C., and Tamura, K. (2018). MEGA X: molecular evolutionary genetics analysis across computing platforms. *Mol. Biol. Evol.* 35, 1547–1549. doi: 10.1093/molbev/msy096
- Lewis, K. (2012). Antibiotics: recover the lost art of drug discovery. *Nature* 485, 439–440. doi: 10.1038/485439a
- Li, H., Sosa-Calvo, J., Horn, H. A., Pupo, M. T., Clardy, J., Rabeling, C., et al. (2018). Convergent evolution of complex structures for ant-bacterial defensive symbiosis in fungus-farming ants. *Proc. Natl. Acad. Sci. U. S. A.* 115, 10720–10725. doi: 10.1073/pnas.1809332115
- Medema, M. H., Takano, E., and Breitling, R. (2013). Detecting sequence homology at the gene cluster level with multigeneblast. *Mol. Biol. Evol.* 30, 1218–1223. doi: 10.1093/molbev/mst025
- Menegatti, C., Lourenzon, V. B., Rodríguez-Hernández, D., Da Paixão Melo, W. G., Ferreira, L. L. G., Andricopulo, A. D., et al. (2020). Meliponamycins: antimicrobials from stingless bee-associated *Streptomyces* sp. *J. Nat. Prod.* 83, 610–616. doi: 10.1021/acs.jnatprod.9b01011
- Miller, D., Smith, E., and Newton, I. (2020). A bacterial symbiont protects honey bees from fungal disease. *bioRxiv* [Preprint]. doi: 10.1101/2020.01.21.914325
- Mirarab, S., and Warnow, T. (2015). ASTRAL-II: coalescent-based species tree estimation with many hundreds of taxa and thousands of genes. *Bioinformatics* 31, i44–i52. doi: 10.1093/bioinformatics/btv234
- Newman, D. J., and Cragg, G. M. (2020). Natural products as sources of new drugs over the nearly four decades from 01/1981 to 09/2019. *J. Nat. Prod.* 83, 770–803. doi: 10.1021/acs.jnatprod.9b01285
- Poulsen, M., Oh, D., Clardy, J., and Currie, C. R. (2011). Chemical analyses of wasp-associated *Streptomyces* bacteria reveal a prolific potential for natural products discovery. *PLoS One* 6:e16763. doi: 10.1371/journal.pone.0016763
- Promnuan, Y., Kudo, T., and Chantawannakul, P. (2009). Actinomycetes isolated from beehives in Thailand. *World J. Microbiol. Biotechnol.* 25, 1685–1689. doi: 10.1007/s11274-009-0051-1
- Przybyłek, I., and Karpiński, T. M. (2019). Antibacterial properties of Propolis. *Molecules* 24, 11–13. doi: 10.3390/molecules24112047
- Rothenbuhler, W. C. (1964). Behavior genetics of nest gleaning in honey bees. IV. Responses of F t and backcross generations to disease-killed brood. *Am. Zool.* 4, 111–123. doi: 10.1093/icb/4.2.111
- Sadd, B. M., Kleinlogel, Y., Schmid-Hempel, R., and Schmid-Hempel, P. (2005). Trans-generational immune priming in a social insect. *Biol. Lett.* 1, 386–388. doi: 10.1098/rsbl.2005.0369
- Schindelin, J., Rueden, C. T., Hiner, M. C., and Eliceiri, K. W. (2015). The ImageJ ecosystem: an open platform for biomedical image analysis. *Mol. Reprod. Dev.* 82, 518–529. doi: 10.1002/mrd.22489
- Schmid-Hempel, P. (1998). *Parasites in social insects*. New Jersey: Princeton University Press.
- Schmid-Hempel, P. (2005). Evolutionary ecology of insect immune defenses. *Annu. Rev. Entomol.* 50, 529–551. doi: 10.1146/annurev.ento.50.071803.130420
- Schulz, D., Nachtigall, J., Riedlinger, J., Schneider, K., Poralla, K., Imhoff, J. F., et al. (2009). Piceamycin and its N-acetylcysteine adduct is produced by *Streptomyces* sp. GB 4-2. *J. Antibiot.* 62, 513–518. doi: 10.1038/ja.2009.64
- Scott, J. J., Oh, D., Yuceer, M., Klepzig, K. D., Clardy, J., and Currie, C. R. (2008). Bacterial protection of beetle-fungus mutualism. *Science* 322:63. doi: 10.1126/science.1160423
- Shin, Y. H., Kang, S., Byun, W. S., Jeon, C. W., Chung, B., Beom, J. Y., et al. (2020). Absolute configuration and antibiotic activity of piceamycin. *J. Nat. Prod.* 83, 277–285. doi: 10.1021/acs.jnatprod.9b00678
- Smith, E. A., and Newton, I. L. G. (2020). Genomic signatures of honey bee association in an acetic acid symbiont. *Genome Biol. Evol.* 12, 1882–1894. doi: 10.1093/gbe/evaa183
- Song, Y. J., Zheng, H. B., Peng, A. H., Ma, J. H., Lu, D. D., Li, X., et al. (2019). Streptantibins A–C: hexokinase II inhibitors from a mud dauber wasp associated *Streptomyces* sp. *J. Nat. Prod.* 82, 1114–1119. doi: 10.1021/acs.jnatprod.8b00821
- Spivak, M., and Reuter, G. S. (2001). Resistance to American foulbrood disease by honey bee colonies *Apis mellifera* bred for hygienic behavior. *Apidologie* 32, 555–565. doi: 10.1051/apido:2001103
- Stamatakis, A. (2014). RAxML version 8: a tool for phylogenetic analysis and post-analysis of large phylogenies. *Bioinformatics* 30, 1312–1313. doi: 10.1093/bioinformatics/btu033
- Starks, P. T., Blackie, C. A., and Seeley, T. D. (2000). Fever in honeybee colonies. *Naturwissenschaften* 87, 229–231. doi: 10.1007/s001140050709
- Traniello, J. F. A., Rosengaus, R. B., and Savoie, K. (2002). The development of immunity in a social insect: evidence for the group facilitation of disease resistance. *Proc. Natl. Acad. Sci. U. S. A.* 99, 6838–6842. doi: 10.1073/pnas.102176599
- Um, S., Bach, D. H., Shin, B., Ahn, C. H., Kim, S. H., Bang, H. S., et al. (2016). Naphthoquinone-oxindole alkaloids, coprisidins A and B, from a gut-associated bacterium in the dung beetle, *Copris tripartitus*. *Org. Lett.* 18, 5792–5795. doi: 10.1021/acs.orglett.6b02555
- Visser, A. A., Nobre, T., Currie, C. R., Aanen, D. K., and Poulsen, M. (2012). Exploring the potential for Actinobacteria as defensive symbionts in fungus-growing termites. *Microb. Ecol.* 63, 975–985. doi: 10.1007/s00248-011-9987-4
- Wu, H., Liang, J., Gou, L., Wu, Q., Liang, W. J., Zhou, X., et al. (2018). Recycling of overactivated acyls by a type II thioesterase during calcimycin biosynthesis in *Streptomyces chartreusis* NRRL 3882. *Appl. Environ. Microbiol.* 84, 1–13. doi: 10.1128/AEM.00587-18

Conflict of Interest: The authors declare that the research was conducted in the absence of any commercial or financial relationships that could be construed as a potential conflict of interest.

Copyright © 2021 Grubbs, May, Sardina, Dermentjian, Wyche, Pinto-Tomás, Clardy and Currie. This is an open-access article distributed under the terms of the Creative Commons Attribution License (CC BY). The use, distribution or reproduction in other forums is permitted, provided the original author(s) and the copyright owner(s) are credited and that the original publication in this journal is cited, in accordance with accepted academic practice. No use, distribution or reproduction is permitted which does not comply with these terms.



Biphenyl 2,3-Dioxygenase in *Pseudomonas alcaliphila* JAB1 Is Both Induced by Phenolics and Monoterpenes and Involved in Their Transformation

OPEN ACCESS

Andrea Zubrova¹, Klara Michalikova², Jaroslav Semerad², Michal Strejcek¹, Tomas Cajthaml^{2,3}, Jachym Suman^{1*} and Ondrej Uhlik^{1*}

Edited by:

Elisa Korenblum,
Agricultural Research Organization,
Volcani Center, Israel

Reviewed by:

Stephen Seah,
University of Guelph, Canada
Ying Teng,
Institute of Soil Science, Chinese
Academy of Sciences (CAS), China

*Correspondence:

Ondrej Uhlik
ondrej.uhlik@vscht.cz
Jachym Suman
jachym.suman@vscht.cz

Specialty section:

This article was submitted to
Terrestrial Microbiology,
a section of the journal
Frontiers in Microbiology

Received: 22 January 2021

Accepted: 29 March 2021

Published: 30 April 2021

Citation:

Zubrova A, Michalikova K,
Semerad J, Strejcek M, Cajthaml T,
Suman J and Uhlik O (2021) Biphenyl
2,3-Dioxygenase in *Pseudomonas*
alcaliphila JAB1 Is Both Induced by
Phenolics and Monoterpenes and
Involved in Their Transformation.
Front. Microbiol. 12:657311.
doi: 10.3389/fmicb.2021.657311

¹Department of Biochemistry and Microbiology, Faculty of Food and Biochemical Technology, University of Chemistry and Technology, Prague, Czechia, ²Institute of Microbiology, Academy of Sciences of the Czech Republic, Prague, Czechia, ³Faculty of Science, Institute for Environmental Studies, Charles University, Prague, Czechia

The involvement of bacterial aromatic ring-hydroxylating dioxygenases (ARHDs) in the degradation of aromatic pollutants, such as polychlorinated biphenyls (PCBs), has been well studied. However, there is considerable speculation as to the origin of this ability. One hypothesis is centered on a connection between the ability to degrade aromatic pollutants and the necessity of soil bacteria to cope with and/or utilize secondary plant metabolites (SPMs). To investigate this connection, we researched the involvement of biphenyl 2,3-dioxygenase (BPDO), an ARHD essential for the degradation of PCBs, in the metabolism of SPMs in the soil bacterium *Pseudomonas alcaliphila* JAB1, a versatile degrader of PCBs. We demonstrated the ability of the strain JAB1 to transform a variety of SPMs, namely the flavonoids apigenin, flavone, flavanone, naringenin, fisetin, quercetin, morin, and catechin, caffeic acid, *trans*-cinnamic acid, and the monoterpenes (*S*)-limonene and (*R*)-carvone. Of those, the transformation of flavone, flavanone, and (*S*)-limonene was conditioned by the activity of JAB1-borne BPDO and thus was researched in more detail, and we found evidence for the limonene monooxygenase activity of the BPDO. Furthermore, the *bphA* gene in the strain JAB1 was demonstrated to be induced by a wide range of SPMs, with monoterpenes being the strongest inducers of the SPMs tested. Thus, our findings contribute to the growing body of evidence that ARHDs not only play a role in the catabolism of aromatic pollutants, but also of natural plant-derived aromatics, and this study supports the hypothesis that ARHDs participate in ecological processes mediated by SPMs.

Keywords: secondary plant metabolites, aromatic ring-hydroxylating dioxygenases, biphenyl dioxygenase, phenolics, monoterpenes

INTRODUCTION

Secondary plant metabolites (SPMs) are a highly diverse group of compounds of plant origin with numerous functions in ecological processes. Among other roles, SPMs act as allelopathic chemicals, agents that protect the plant from pathogens and herbivores, and are involved in the plant's protection against abiotic stress, in nutrient acquisition, attraction of pollinators, etc. (Rauscher, 2001; Cesco et al., 2012; Böttger et al., 2018). SPMs also represent a significant proportion of rhizodeposits, i.e., plant-derived organic matter released into soil (Dennis et al., 2010; Leewis et al., 2016). The SPMs released into soil include monoterpenes and a variety of phenylpropanoid pathway-synthesized phenolics, which can be further divided into acetophenones, phenolic acids, flavonoids, lignins and lignans, tannins, xanthenes, etc. (Vuolo et al., 2019).

SPMs have a wide range of both positive and negative effects on soil microbial communities (reviewed by Musilova et al., 2016). They can serve as growth substrates for many bacteria (Donnelly et al., 1994; Fraraccio et al., 2017) or are involved in plant-microbe crosstalk during the establishment of mutualistic symbiosis (Liu and Murray, 2016). On the other hand, they can exert antimicrobial activity (Singer et al., 2003) or disrupt bacterial quorum sensing (Koh et al., 2013). As a result, due to the presence of various SPMs, the rhizosphere becomes a highly selective environment (Kim et al., 1995; Dakora and Phillips, 1996; Xu and Lee, 2001). To deal with the selective pressure resulting from the detrimental effect of SPMs, soil microbiota responds with two mechanisms of resistance. The first is the exclusion of toxic compounds *via* transmembrane efflux pumps (Parniske et al., 1991; Palumbo et al., 1998; González-Pasayo and Martínez-Romero, 2000; Papadopoulos et al., 2008; Martínez et al., 2009); the other is the enzymatic transformation of a SPM to a non-toxic form or its mineralization, which provides the further benefit of a carbon and/or energy yield (Shaw et al., 2006; Marmulla and Harder, 2014). One group of enzymes involved in the bacterial transformation of aromatic compounds is aromatic ring-hydroxylating dioxygenases (ARHDs), multicomponent non-heme oxidoreductases that usually exhibit broad substrate specificity (Baldwin et al., 2000). ARHDs have been mostly described in connection with the degradation of aromatic pollutants, including polychlorinated biphenyls (PCBs), under aerobic conditions (Eltis and Bolin, 1996; Vezina et al., 2008); they attack aromatic compounds, which are usually inert and stable, and activate the substrate for subsequent reactions leading to the cleavage of the aromatic ring (Parales and Resnick, 2006).

The chemical structures of a variety of SPMs, such as phenolics, are remarkably similar to those of aromatic pollutants (Singer et al., 2003). This resemblance led to the hypothesis that broad-substrate-specificity biodegradative enzymes, such as ARHDs, that were identified to degrade aromatic pollutants originally evolved in bacteria to provide them with the ability to degrade

SPMs (Donnelly et al., 1994; Focht, 1995; Hernandez et al., 1997; Singer et al., 2003; Furukawa et al., 2004). An example supporting this hypothesis is the enzymes of the biphenyl/PCB degradation pathway (*bph*); although the presence of biphenyl is not common in soils, biphenyl-degrading bacteria are ubiquitous, even in pristine soils and sediments (Focht, 1995). Additionally, bacteria efficiently degrading PCBs have been isolated from termite guts, where a lignin-rich diet is decomposed (Chung et al., 1994). More recently, Sylvestre and colleagues concluded that the biphenyl degradation pathway in soil bacteria may have evolved to serve different ecological functions, including the metabolism of SPMs (Toussaint et al., 2012; Pham et al., 2015). These studies, however, only provide a partial understanding of how SPMs are linked with biodegradative enzymes with broad substrate specificities, including ARHDs.

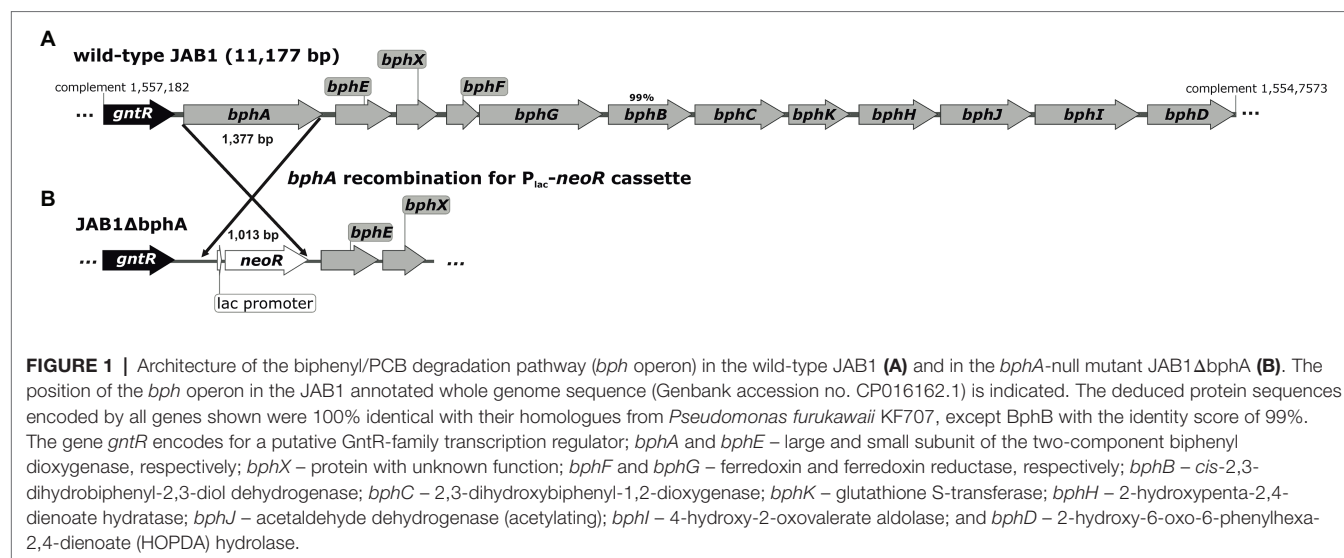
In this study, we worked under the hypothesis that ARHDs might have originally evolved for the degradation/detoxification of SPMs, and that they were, due to their broad substrate specificity, exapted for the degradation of aromatic pollutants. Thereby, the SPMs may act as (i) substrates for ARHDs and (ii) efficient inducers of the ARHD genes. With the example of biphenyl 2,3-dioxygenase (BPDO) from the soil PCB-degrader *Pseudomonas alcaliphila* JAB1 (Ryslava et al., 2003; Ridl et al., 2018), we provide a complex investigation of how a wide variety of SPMs, including flavonoids, phenolic acids, coumarins, and monoterpenes, induce the expression of this BPDO, and that this BPDO is involved in the degradation of some of these SPMs. BPDO is an exemplary ARHD, which catalyzes the first step of biphenyl degradation pathway and has a key role in substrate specificity of the whole pathway (Mondello et al., 1997). It is a multicomponent enzyme that consists of a terminal dioxygenase and an electron transfer chain. The terminal dioxygenase comprises large subunits (α) with a substrate-binding domain and small subunits (β), encoded by *bphAE* genes (also known as *bphA1A2* in the literature). The electron transfer chain contains ferredoxin genes (encoded by *bphF* or *bphA3*), and ferredoxin reductase genes (encoded by *bphG* or *bphA4*; Furukawa and Fujihara, 2008; Kumar et al., 2011; Pham et al., 2012). In the strain JAB1, these genes are encoded within the chromosome-borne cluster *bphAEXFGBCKHJID*, the organization of which is identical to that from *Pseudomonas furukawaii* KF707 (**Figure 1**). Moreover, the deduced protein sequences encoded by the JAB1-borne *bph* genes are >99% identical with their KF707 orthologs (Watanabe et al., 2000; Furukawa and Fujihara, 2008; Ridl et al., 2018). Our results contribute to the knowledge on the role of ARHDs in the SPM-mediated plant-microbe interactions occurring in soil and broaden our understanding of soil ecology.

MATERIALS AND METHODS

Bacterial Strains, Culture Media, and Growth Conditions

The bacterial strain *P. alcaliphila* JAB1 was isolated from legacy PCB-contaminated soil (Ryslava et al., 2003) and has been shown to be a versatile degrader of PCBs (Ridl et al., 2018).

Abbreviations: aa, Amino acid; ARHD, Aromatic ring-hydroxylating dioxygenases; BPDO, Biphenyl 2,3-dioxygenase; HOPDA, 2-Hydroxy-6-oxo-6-phenyl-2,4-hexadienoic acid; RCA, Resting cell assay; PCBs, Polychlorinated biphenyls; SPMs, Secondary plant metabolites.



A JAB1 *bphA*-null mutant with non-functional BPDO, designated JAB1Δ*bphA* (Figure 1), was constructed in this study as described further. *Escherichia coli* DH11S was used for the purposes of plasmid cloning and manipulation (Lin et al., 1992).

Lysogeny broth (LB) medium (Sigma-Aldrich, United States) and mineral salt solution (MSS; Uhlik et al., 2012) were used for the cultivation of the JAB1 strain, the latter amended with a carbon source: pyruvate (Sigma-Aldrich, United States), biphenyl (Sigma-Aldrich, United States), or individual SPMs. Solid MSS-based medium was solidified with 2% agar (w/v), and biphenyl as a sole carbon source was provided as vapors from biphenyl crystals deposited in the lid of the Petri dish. Media for the cultivation of the strains JAB1Δ*bphA* and JAB1/pUCP18-RedS-catR were amended with the antibiotics kanamycin (10 mg.L⁻¹) and chloramphenicol (300 mg.L⁻¹), respectively. Liquid cultures were grown at 28°C on a rotary shaker at 130 RPM. Bacterial strains were maintained in glycerol stock (25% v/v) at -80°C and revived on LB plates. *Escherichia coli* transformants were selected and cultivated on LB plates amended with ampicillin (150 mg.L⁻¹) or chloramphenicol (25 mg.L⁻¹).

Chemicals

Biphenyl and SPMs (Figure 2) were purchased from Sigma-Aldrich. Stock solutions of biphenyl and SPMs were prepared in molecular biology-grade ethanol (VWR Chemicals, United States), except for quercetin and morin that were prepared immediately prior to use by dissolving in ethanol and alkalization by KOH, and fisetin and chrysin that were dissolved in ethanol:dimethyl sulphoxide (DMSO; 1:1, v/v). Stock solutions were sterilized by filtration with a pore size of 0.2 μm (GD/X PES Filter Media, Whatman™) and stored at 5°C in the dark.

Utilization of SPMs by the Strain JAB1

The ability of the strain JAB1 to utilize the SPMs listed in Figure 2 as a sole carbon source was monitored by measuring OD₆₀₀ in liquid MSS. See Supplementary Material for details.

Construction of the JAB1 *bphA*-Null Mutant

To determine the contribution of the JAB1-borne BPDO activity to the transformation of SPMs, the JAB1-derivative JAB1Δ*bphA* with a deleted *bphA* gene was prepared (Figure 1). For this purpose, the L-arabinose-inducible lambda Red recombinase system was employed, borne on the plasmid pUCP18-RedS, which enables site-specific homologous recombination in *Pseudomonas*. The methodology was adopted from Lesic and Rahme (2008) with modifications as described in Supplementary Material.

Transformation of SPMs by the Strain JAB1

To test the ability of the JAB1 strain to transform the SPMs listed in Figure 2 and determine the contribution of the BPDO, a resting cell assay (RCA) was employed as described in Vergani et al. (2019) and Garrido-Sanz et al. (2020). The strains JAB1 and JAB1Δ*bphA* were cultivated O/N in LB, the latter amended with kanamycin (10 mg.L⁻¹). Cells were harvested by centrifugation, washed twice in 0.85% NaCl, and adjusted to an OD₆₀₀ = 1 with MSS. For the low-volatile compounds (flavonoids, phenolic acids, and coumarins, Figure 2), 5 ml aliquots of washed cell suspensions were distributed into 50 ml polypropylene tubes amended with a substrate from which ethanol was evaporated, to yield a final concentration of 0.25 mM. For the terpenoids (Figure 2), the RCA was performed in 50 ml glass vials without previous evaporation of the solvent to avoid substrate loss. Each combination of a SPM and a bacterial strain was prepared in triplicate; the abiotic control was MSS with the added substrate without cells. Samples were incubated for 24 h at 28°C/130 rpm and then stored at -80°C until further analysis (see Supplementary Material for details). The depletions rates of SPMs were expressed as $R = (\text{SPM content in the presence of a respective strain})/(\text{SPM content in the abiotic control sample})$. The calculation of standard deviations (SD) of resulting *R* values was based on the error propagation according to Tellinghuisen

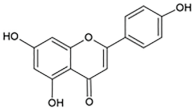
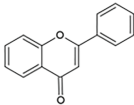
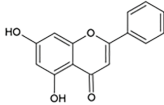
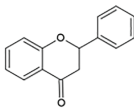
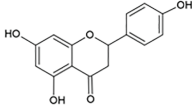
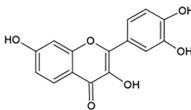
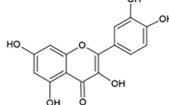
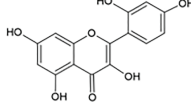
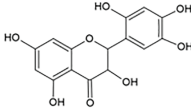
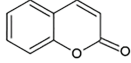
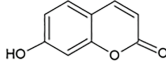
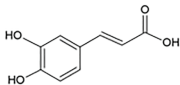
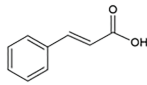
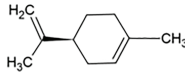
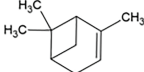
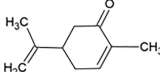
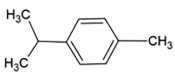
FLAVONOIDS	Flavones	Flavanones	Flavonols	Flavan-3-ols
	<p>Apigenin</p>  <p>Flavone</p>  <p>Chrysin</p> 	<p>Flavanone</p>  <p>Naringenin</p> 	<p>Fisetin</p>  <p>Quercetin</p>  <p>Morin</p> 	<p>Catechin</p> 
COUMARINS	<p>Coumarin</p> 	<p>Umbelliferone</p> 		
PHENOLIC ACIDS	<p>Caffeic acid</p> 	<p><i>trans</i>-Cinnamic acid</p> 		
MONOTERPENES	<p>(S)-Limonene</p> 	<p>α-Pinene</p> 	<p>Carvone</p> 	<p><i>p</i>-Cymene</p> 

FIGURE 2 | Secondary plant metabolites used in this study.

(2001). The depletion of SPMs and the degradation products of flavone, flavanone, and (S)-limonene were analyzed by liquid and gas chromatography coupled with mass spectrometry, for details of the analyses see **Supplementary Material**. The obtained depletion rates of each SPM were analyzed by the single factor ANOVA ($p < 0.05$) and Tukey-Kramer *post-hoc* test.

Induction of the *bphA* Gene in the Strain JAB1 by SPMs

The ability of SPMs (**Figure 2**) to induce the *bphA* gene in JAB1 was determined as the level of *bphA* transcripts in JAB1 cells upon incubation with individual SPMs, using quantitative reverse transcription-PCR (RT-qPCR) and cDNA obtained from JAB1's total RNA as the template and the 16S RNA gene as the reference gene.

Briefly, JAB1 cells from the starting culture in LB medium were harvested, washed, and resuspended to $OD_{600} = 0.025$ in MSS amended with 30 mM of sodium pyruvate. This suspension (0.5 l) in a 2 l Erlenmeyer flask was grown for ca 9 h at 28°C/130 RPM until the mid-log phase was reached (OD_{600} 0.1–0.2). Cells were harvested by centrifugation, washed in 0.85% NaCl, and concentrated to $OD_{600} = 1$ in MSS. Aliquots of cell suspension (10 ml) were distributed into 100 ml Erlenmeyer

flasks amended with 0.25 mM of an individual SPM or biphenyl with the ethanol evaporated prior to the addition of the cell suspension. Bacterial culture with no addition was used as a control. Cells were incubated for 1 and 3 h at 28°C/130 RPM. All the samples were prepared in four replicates. After co-incubation, the cells from 2 ml of each culture were pelleted by centrifugation (10 min, 7,000 RCF at 4°C), the resultant cell pellets were stored at –80°C.

The total RNA was isolated using a Qiagen RNeasy Mini Kit according to the manufacturer's protocol, slightly modified as follows. The enzymatic lysis of pelleted cells was performed in 300 μ l of TE buffer amended with 1 mg/ml of lysozyme incubated for 10 min at room temperature on a benchtop shaker. RLT buffer (400 μ l) amended with 10 μ l/ml β -mercaptoethanol was added to the reaction mix. After the addition of 500 μ l of molecular biology-grade ethanol, the precipitate formed was removed from microtubes with the end of a pipette tip. The whole reaction volume was then transferred into an RNeasy Mini spin column, followed by RNA cleanup according to the manufacturer's instructions. The obtained RNA was eluted into 40 μ l of molecular biology-grade water and stored at –80°C. The quality and quantity of obtained RNA were assessed with an Agilent RNA 6000 Nano Kit (Agilent

Technologies, DE), in combination with a P330 NanoPhotometer (Implen, DE). Only RNA samples with an RNA Integrity Number (RIN) >7 were used for further analysis. Residual DNA was digested with 2.4 U of TURBO DNase (Thermo Fisher Scientific, United States) in a 50 µl reaction containing a total of 2 µg of nucleic acid. The completeness of DNA digestion was verified by qPCR using a set of primers targeting the 16S rRNA gene, only samples with c_p values corresponding to the non-template control were included in further analyses. Reverse transcription was performed with 200 U of M-MuLV Reverse Transcriptase (New England Biolabs, United States), in a 20 µl reaction containing 150 ng of total RNA and 8 U of Murine RNase inhibitor (New England Biolabs, United States), according to the manufacturer's protocol.

Quantitative PCR was performed in a CFX Connect Real-Time PCR Detection System (Bio Rad, United States) employing a KAPA SYBR FAST qPCR Master Mix (2x) Kit (KAPA Biosystems, United States), in a total volume of 12 µl containing 0.25 µM primers targeting the gene *bphA* (forward primer 5'-GAGATCCAGAAGGGGCTAC, reverse primer 5'-GCGCATCCAGTGGTGATAC) or the reference 16S rRNA gene (forward primer 5'-GGATTAGATACCCTGGTA, reverse primer 5'-CCGTCATTTCATTTGAGTTT), with the addition of 0.5 µl of cDNA obtained in the previous step. The reaction conditions were as follows: (1) 95°C for 7 min; (2) 95°C for 20 s; (3) 60°C for 30 s; and (4) 72°C for 20 s, and 35 and 31 cycles were used for the *bphA* and 16S rRNA gene amplification, respectively. Each sample was run in triplicate. Non-template control was represented by the use of molecular biological water instead of the template. Specificity of amplification by all primer sets used in this study was determined by melting curve analysis of qPCR products and Sanger sequencing (data not shown).

The obtained c_p values were processed by the Common Base Method according to Ganger et al. (2017), thus the level of *bphA* transcripts in a sample was normalized by the level of 16S rRNA copies. The induction of the *bphA* gene by the SPMs was expressed relative to the non-induced control, i.e., bacterial culture incubated without any amendment. Thus, the basal background transcription of the *bphA* gene corresponds to an induction rate of 1 in the presented data. The induction rates were tested with respect to the difference from the control (no inducer added) by multiple *t* tests with *p* values adjusted by the BH procedure to control the false discovery rate (Benjamini and Hochberg, 1995) at the level of 5%.

RESULTS

Utilization of SPMs and Their Transformation by JAB1 and JAB1Δ*bphA*

In order to be able to distinguish the involvement of the JAB1-borne BPDO in the transformation of SPMs, the strain JAB1Δ*bphA* was employed alongside the wild-type strain. None of the SPMs tested (Figure 2) supported the growth of the JAB1 strain under the conditions applied (data not shown). Nevertheless, both JAB1 and JAB1Δ*bphA* were found to degrade apigenin (to 60 and 50% of the abiotic control, respectively), naringenin (84

and 73%), fisetin (11 and 14%), quercetin (58 and 85%), morin (10 and 2%), catechin (2% for both strains), caffeic acid (27% for both strains), *trans*-cinnamic acid (2 and 1%), and (*R*)-carvone (52 and 60%; Figure 3). In contrast, flavone, flavanone, and (*S*)-limonene were depleted solely by the strain JAB1 to 32, 7, and 42% of the control, respectively, and their levels were unaffected by the JAB1Δ*bphA* strain (Figure 3). This indicates that their transformation is mediated by the JAB1-borne BPDO. Chrysin, coumarin, umbelliferone, and α-pinene were neither degraded by JAB1 nor JAB1Δ*bphA* (Figure 3).

Degradation Products of Flavone, Flavanone, and (*S*)-Limonene

To shed light on the mechanism of the degradation of flavone, flavanone, and (*S*)-limonene by JAB1, an analysis of their degradation products was performed. Three degradation products of flavone were found in the chromatogram of the extracts from the JAB1's RCA reactions that were not present in the corresponding JAB1Δ*bphA* extracts (Supplementary Table S2; Supplementary Figure S2). The three compounds were identified as 4-oxo-4H-chromene-2-carboxylic acid (compound III in Figure 4A; Supplementary Table S2; Supplementary Figure S2), methyl 4-oxo-4H-chromene-2-carboxylate (compound II in Figure 4A; Supplementary Table S2), and 2-(*m,n*-dihydroxyphenyl)chromane-4-one (compound I in Figure 4A; Supplementary Table S2; Supplementary Figure S2). Analogously, two products of flavanone degradation by JAB1 were detected, which were identified as flavone 4-oxo-4H-chromene-2-carboxylic acid and 2-(*m,n*-dihydroxyphenyl)chromane-4-one (compounds III and IV, respectively, in Figure 4B; Supplementary Table S3; Supplementary Figure S2). Finally, six different products of JAB1-mediated (*S*)-limonene degradation were found and identified as perillyl alcohol (compound V in Figure 4C; Supplementary Table S4; Supplementary Figure S2), perillyl aldehyde (VI), perillic acid (VII), carveol (VIII), carvone (IX), and limonene 1,2-epoxide (X). Perillyl aldehyde and perillic acid were the major compounds in terms of quantity, whereas the levels of limonene-1,2-epoxide were the lowest, close to the limit of detection of the method (Supplementary Table S4).

Induction of the *bphA* Gene in the JAB1 Strain by SPMs

The ability of SPMs to induce the *bphA* gene in the JAB1 strain was tested by RT-qPCR; relative induction rates after 1 and 3 h of incubation with individual SPMs are shown in Figure 5. Seven out of the nine tested flavonoids, namely apigenin, catechin, fisetin, flavanone, morin, naringenin, and quercetin, increased the levels of *bphA*-transcripts after 1 h of co-incubation, ranging from a 1.8 (quercetin) to 3.6-fold (flavanone) induction of the non-induced control (no SPM added; Figure 5). Upon 3 h of incubation, these induction rates generally decreased (Figure 5). With flavone, a significant decrease in *bphA* transcripts compared to the control was observed at both time points, reaching up to 0.5-fold of the control after 3 h (Figure 5).

Upon the incubation of JAB1 cells with coumarin, *bphA*-transcript levels were significantly lowered compared to the

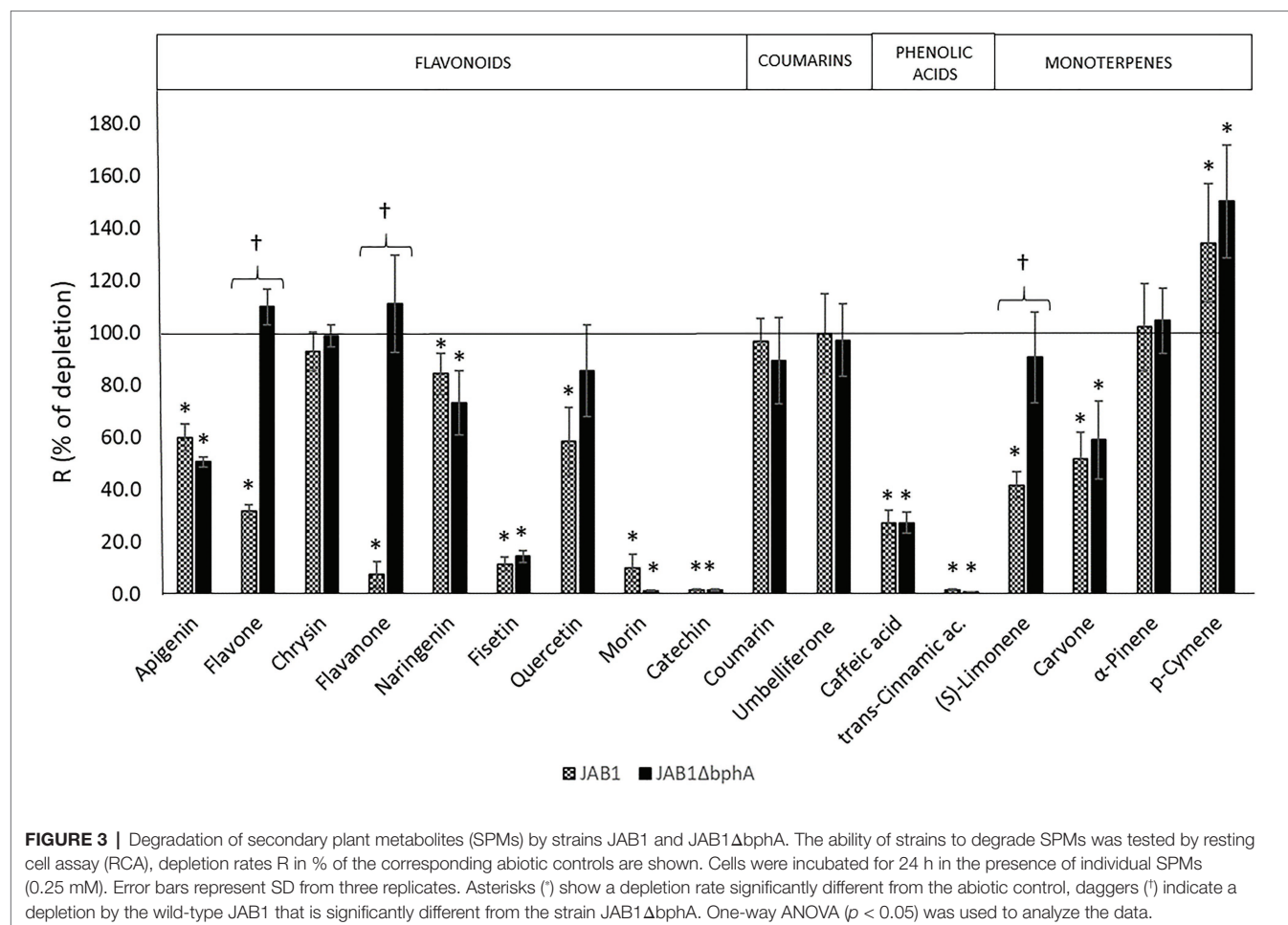


FIGURE 3 | Degradation of secondary plant metabolites (SPMs) by strains JAB1 and JAB1ΔbphA. The ability of strains to degrade SPMs was tested by resting cell assay (RCA), depletion rates R in % of the corresponding abiotic controls are shown. Cells were incubated for 24 h in the presence of individual SPMs (0.25 mM). Error bars represent SD from three replicates. Asterisks (*) show a depletion rate significantly different from the abiotic control, daggers (†) indicate a depletion by the wild-type JAB1 that is significantly different from the strain JAB1ΔbphA. One-way ANOVA ($p < 0.05$) was used to analyze the data.

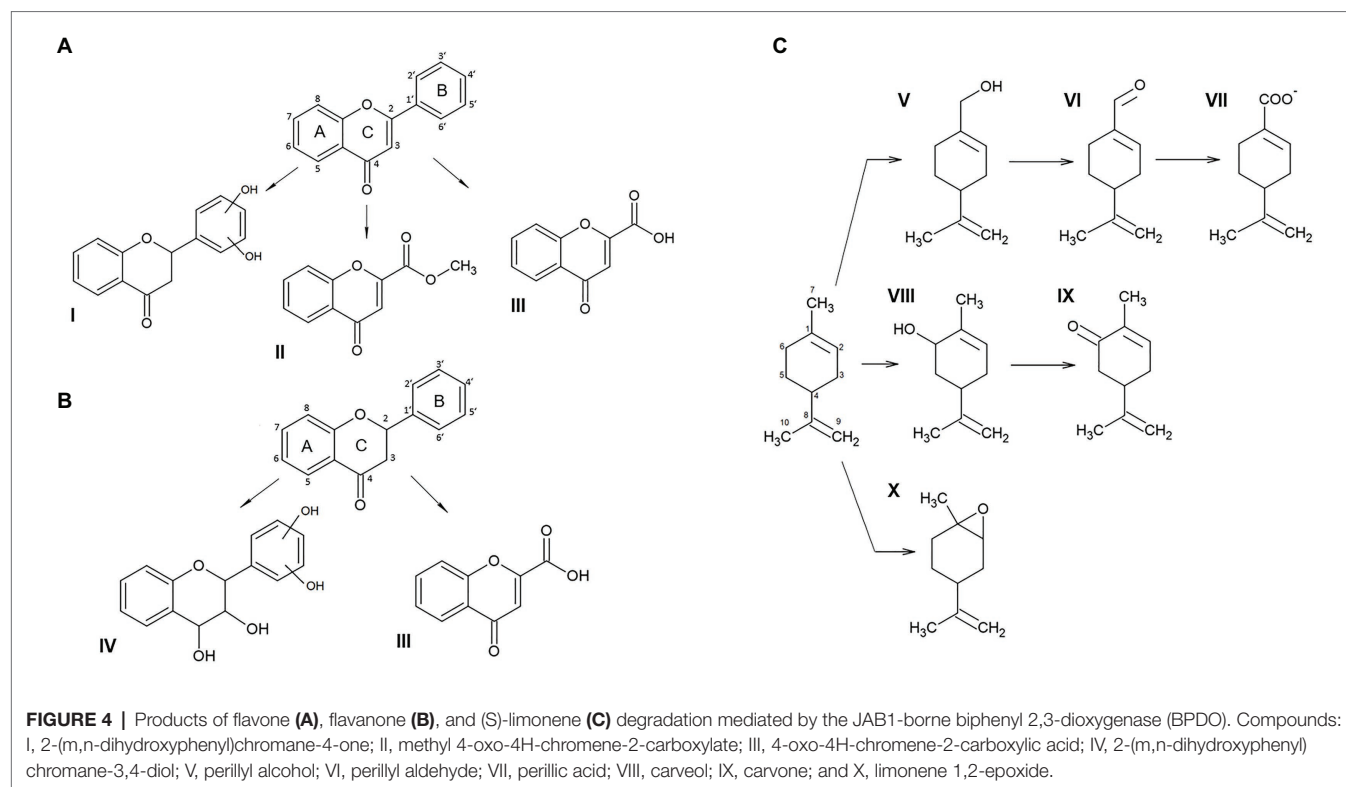
non-induced control (by 0.4–0.8-fold of the control); in contrast, exposure to umbelliferone (7-hydroxycoumarin) resulted in *bphA* induction (2.8-fold, **Figure 5**). Two tested phenolics, *trans*-cinnamic acid and caffeic acid, increased the level of *bphA* transcripts after both 1 h (3.1 and 1.3-fold, respectively) and 3 h (3.8 and 1.7-fold respectively) of incubation (**Figure 5**).

Among the SPMs tested, monoterpenes were the strongest inducers of *bphA* in JAB1. Upon 1 h of exposure to all the monoterpenes tested, namely (S)-limonene, α-pinene, *p*-cymene, and (R)-carvone, the levels of *bphA* transcripts were approximately 4-fold of the non-induced control (**Figure 5**). After 3 h, the levels decreased to approximately 3-fold of the control for (S)-limonene, α-pinene, *p*-cymene, and (R)-carvone. The levels of *bphA* transcripts upon exposure to biphenyl, a common laboratory model inducer of the biphenyl pathway, culminated after 1 h incubation (9.6-fold of the control), and followed by a decrease to 2.1-fold at 3 h.

DISCUSSION

Pseudomonads have been reported to degrade a wide spectrum of aromatic pollutants, such as halogenated biphenyls, benzene, toluene, ethylbenzene, xylene, polyaromatics, dioxins, or DDT

(Kimura et al., 1996; Baldwin et al., 2000; Ishiguro et al., 2000; Kamanavalli and Ninnekar, 2004; Uhlik et al., 2012; Wald et al., 2015). Generally, the aerobic degradation of such compounds is initiated by ARHDs. These enzymes incorporate two hydroxyl groups on the vicinal C-atoms of the aromatic ring, resulting in its activation for subsequent fission (Kweon et al., 2008). ARHDs have been reported to have broad substrate specificity, thus they are generally able to attack multiple structurally similar pollutants at the same time (Baldwin et al., 2000; Kweon et al., 2008). Apart from their involvement in the degradation of aromatic pollutants, ARHDs have been proposed to mediate the transformation of various compounds of natural origin, including SPMs (Focht, 1995; Pham et al., 2012). Indeed, in several studies, various bacterial ARHDs have been reported to catalyze the transformation of certain SPMs, including multiple flavonoids and mono- and diterpenes (Aoki et al., 1996; Eaton, 1996; Martin and Mohn, 1999; Kim et al., 2003; Seo et al., 2011a; Pham et al., 2012; Groeneveld et al., 2016; Agullo et al., 2017). Moreover, SPMs have been reported to induce ARHD activity (Park et al., 1999; Master and Mohn, 2001; Pham et al., 2015; Agullo et al., 2017). Based on all these studies, ARHDs have been hypothesized to also sustain environmental processes other than the degradation of aromatic pollutants (Pham et al., 2012; Pham and Sylvestre, 2013). In the soil environment, these processes



could include the utilization of plant-derived compounds and the quenching of antimicrobial or signal compounds (Shaw et al., 2006; Cesco et al., 2010).

In our study, we aimed to provide a more complex insight into the involvement of the BPDO in the metabolism of plant-derived compounds in the soil bacterium *P. alcaliphila* JAB1. In its genome (Ridl et al., 2018), the strain JAB1 bears a single chromosome-encoded copy of the *bph* operon with architecture analogous to that of the model PCB-degrader *P. furukawaii* KF707 (Taira et al., 1992; Triscari-Barberi et al., 2012). Moreover, the predicted amino acid (aa) sequence of BphA from the strain JAB1 is identical to that from KF707, which was reported to mediate the transformation of flavone, flavanone, isoflavone, and isoflavanol (Harborne and Williams, 2000; Kim et al., 2003; Han et al., 2005; Seo et al., 2011b). The presence of a single copy of the *bphA* gene in the strain JAB1 enabled us to “switch off” the BPDO activity *via* a single site-specific recombination step (Figure 1). For that purpose, a lambda Red recombination system, originally designed for *P. aeruginosa*, was employed (Lesic and Rahme, 2008). The resulting strain JAB1Δ*bphA* and the wild-type strain were then used to assess the BPDO-mediated degradation of a range of SPMs including flavonoids, phenolic acids, coumarins, and monoterpenes (Figure 2). Although none of the SPMs supported the growth of JAB1, we demonstrated that the JAB1 strain is capable of degrading a wide range of aromatic SPMs, including flavonoids, monoterpenes, and phenolic acids (Figure 3). Importantly, the degradation of flavone, flavanone, and (S)-limonene by the JAB1 strain was found to be dependent on the presence of a functional BPDO (Figure 3). We therefore

investigated the fate of these three compounds in JAB1 through the analysis of their degradation products.

Based on the analysis of flavone and flavanone degradation products mediated by the JAB1-borne BPDO (Figures 4A,B), we suggest that the enzyme attacked the B-ring of both flavone and flavanone, yielding 2-(m,n-dihydroxyphenyl)chromane-4-one. However, we were not able to determine the precise position of the hydroxylated carbons. The assumption that the dihydroxylation takes place on the B-ring is strongly supported by another structure identified among the degradation products of both flavone and flavanone, 4-oxo-4H-chromene-2-carboxylic acid, and, additionally, the by-product of flavone transformation, methyl-4-oxo-4H-chromene-2-carboxylate (Figures 4A,B). These structures support the scenario that the BPDO mediates initial dihydroxylation of the B-ring of flavone and flavanone, which is followed by subsequent reactions leading to its degradation. Attack on the unsubstituted B-ring of flavonoids (flavone, isoflavone, flavanone, and isoflavanol) was also reported for the BPDO of *P. furukawaii* KF707, producing 2',3'-dihydrodiols or 2',3'-epoxides (Kim et al., 2003; Han et al., 2005). In another study, the hybrid BPDO that had arisen from the DNA shuffling between *bphA* genes from *P. furukawaii* KF707 and *Paraburkholderia xenovorans* LB400 was shown to mediate the 2',3'-dihydroxylation and 3'-monohydroxylation of both flavone and flavanone, along with the 2'-monohydroxylation of flavanone (Chun et al., 2003). Further degradation of the hydroxylated flavonoid structures, resulting in the products identical or analogous to 4-oxo-4H-chromene-2-carboxylic acid found here, was proposed to be mediated by the rest of the biphenyl degradation pathway in *Par. xenovorans* LB400, *Pandora* *pnomenusa* B-356

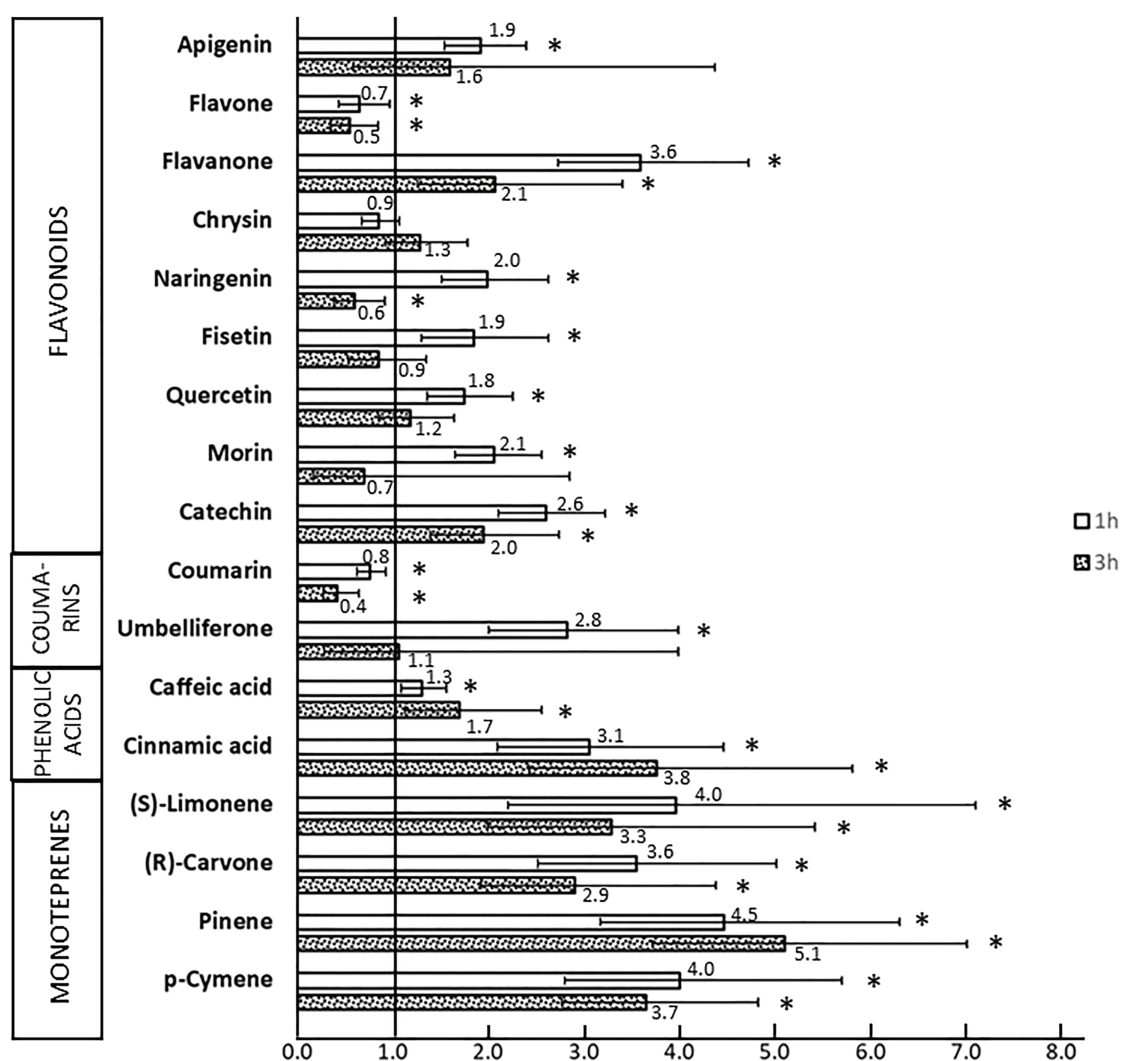


FIGURE 5 | Relative levels of *bphA* transcripts in JAB1 strain exposed to SPMS. JAB1 cells were exposed to individual 0.25 mM SPMS for 1 and 3 h; the level of *bphA* transcripts was quantified by quantitative reverse transcription-PCR (RT-qPCR). The 16S rRNA transcript was used as a reference. The levels of *bphA* transcripts are shown as the average fold change in the non-induced control (cells without SPMS added, induction rate equals 1) with 95%-confidence intervals. The obtained c_p values were processed by the common base method according to Ganger et al. (2017). Asterisks (*) denote a significant difference from the control as tested by *t* test ($\alpha = 0.05$).

(Pham et al., 2012), and *Rhodococcus erythropolis* U23A (Toussaint et al., 2012; Pham et al., 2015). Apart from flavone and flavanone, the transformation of which was shown to be BPDO-dependent, other flavonoids were found to be depleted by both the JAB1 wild-type and *bphA*-null strains, and therefore presumably transformed by enzymes other than BPDO (Figure 3).

The JAB1 strain was also found to be able to transform monoterpenes. Besides (*R*)-carvone that was depleted by both wild-type JAB1 and the *bphA*-null mutant, the degradation of (*S*)-limonene was demonstrated to depend on the presence of BPDO (Figure 3). The analysis of (*S*)-limonene degradation products in JAB1 suggests that the transformation is initiated by the monooxygenase activity of the BPDO targeting the C7 or C6 of the substrate, yielding perillyl alcohol and carveol, respectively.

These products are further dehydrogenated into perillyl aldehyde (and eventually perillic acid) and carvone, respectively (Figure 4C). We therefore conclude that, apart from the dioxygenase activity, JAB1-borne BPDO is capable of mediating monooxygenation reactions, as was reported for, for instance, the naphthalene dioxygenase from *Pseudomonas* sp. strain NCIB 9816 (Resnick et al., 1996) or toluene dioxygenase from *P. putida* F1 (Robertson et al., 1992). Analogously, the transformation of monoterpenes, including (*S*)-limonene, by monooxygenation was also reported for the putative ARHD from *Pseudomonas* sp. PWD32 (Groeneveld et al., 2016). The hydroxylation of the C7 was also reported for the limonene dehydrogenase (CtmAB) from the betaproteobacterium *Castellaniella defragrans* 65Phen (Puentes-Cala et al., 2018). To rule out the possibility that a homologous enzyme would

be responsible for the reaction in JAB1, the CmtA and CmtB protein sequences (Genbank accession no. CDM25290 and CDM25289, respectively) were blasted against the JAB1 complete genome but their orthologs were not identified. The hydroxylation of limonene at the C6 yielding carveol, which was further dehydrogenated into carvone, was also reported in *Rhodococcus opacus* PWD4 (Duetz et al., 2001). The degradation of (S)-limonene via perillyl alcohol and perillyl aldehyde, yielding perillic acid, was also demonstrated in the (S)-limonene-utilizing bacteria *Geobacillus stearothermophilus* BR388 (Cheong and Oriel, 1994), *P. gladioli* (Cadwallader et al., 1989), or in multiple fungi (Prema and Bhattacharyya, 1962; Noma et al., 1992; van Rensburg et al., 1997). Perillic acid as the product of (R)-limonene degradation was also found in *P. putida* GS1 (Speelmans et al., 1998). Another limonene-utilizing bacterium *Rhodococcus erythropolis* DCL14 was shown to employ the flavoprotein limonene 1,2-monooxygenase, which catalyzes the formation of 1,2-epoxy limonene (van der Werf et al., 1999). It is worth noting that a minute amount of 1,2-epoxy limonene was also detected in both the JAB1 wild-type and *bphA*-null strains (**Supplementary Table S4**), nevertheless, no homologue of the *R. erythropolis* DCL14 limonene 1,2-monooxygenase was found in the JAB1 genome (Ridl et al., 2018).

Additionally, we aimed to elucidate the role of SPMs in the regulation of the BPDO in the strain JAB1 as a representative of the KF707-type of the *bph* operon widely found in pseudomonads (Taira et al., 1992; Furukawa et al., 2004). In JAB1, a putative GntR-type transcription regulator encoded by the gene *gntR* found upstream of the *bphA* gene in JAB1 (**Figure 1**) shares 100% identity with the BphR1 from KF707 (formerly Orf0; Watanabe et al., 2000; Ridl et al., 2018). BphR1 was reported to act as the transcriptional activator involved in the upregulation of the *bph* operon promoted by 2-hydroxy-6-oxo-6-phenylhexa-2,4-dienoate (HOPDA), the product of BphC enzyme activity (Watanabe et al., 2000). Although the involvement of GntR-type regulators in the degradation of aromatic compounds is considered to be rather rare, members of this family were also found in several *bph* operons (Furukawa and Fujihara, 2008; Durante-Rodríguez et al., 2018); these include negative regulators BphS on the transposon Tn4371 from *Ralstonia eutropha* A5 (Mouz et al., 1999) and *Pseudomonas* sp. KKS102 (Ohtsubo et al., 2000). Moreover, the regulation of transcription of the *bph* operon in KF707 was found to be two-tiered. The transcription of both *bphR1* and structural *bph* genes in KF707 is promoted by another regulator LysR-type BphR2 encoded outside of the *bph* region that binds to the operators of *bphR1* and *bphAEFGBC* in response to the presence of biphenyl (Watanabe et al., 2003). When BphR2 homologue was searched for in the JAB1 genome, an ORF was found (positions 1,539,377–1,540,279 in the annotated genome sequence) outside of the *bph* cluster, the deduced protein sequence of which (300 aa, GenBank accession no. APU29489.1) shares 98.67% identity with BphR2. Therefore, based on the sequence and structural homology of their *bph* clusters and the presence of homologues of both regulator genes *bphR1* and *bphR2*, we assume that the transcription of the *bph* operon in JAB1 is analogous to that reported for KF707. Despite the *bphA* induction rates by biphenyl, a model

laboratory substrate of BPDOs and inducer of *bph* operons, being the highest, we found that a wide range of SPM structures induced the *bphA* gene in JAB1 (**Figure 5**). Flavonoids that induce the *bphA* gene in JAB1 include the non-substituted flavone and flavanone, the flavone hydroxyderivative apigenin, flavonols fisetin, quercetin, morin, and the flavanol catechin (**Figure 5**). The decrease in *bphA*-transcript levels after 3 h of co-incubation observed for all the inducing flavonoids can be explained by their depletion through the activity of JAB1 cells. Indeed, all the flavonoids inducing the *bphA* gene in JAB1 were also degraded by this strain (**Figures 3, 5**). An analogous trend was also observed here for biphenyl (data not shown).

Since the chromone moiety was identified among flavone and flavanone degradation products, namely in the 4-oxo-4H-chromene-2-carboxylic acid (**Figures 4A,B**), we also tested the effect of coumarin and umbelliferone, i.e., structural analogues of chromone, on *bphA* transcription. Coumarin and umbelliferone differ only in the presence of the C7-hydroxyl group, and neither of them was degraded by the strain JAB1 (**Figure 3**). Despite this, umbelliferone acted as the inducer of *bphA* transcription, whereas exposure to coumarin even led to a decrease in *bphA*-transcript levels (**Figure 5**). Apparently, the presence of C7-hydroxyl in the umbelliferone structure seems to play a key role in the induction of *bphA* in JAB1.

The *bphA*-gene induction by the tested phenolic acids, specifically caffeic and cinnamic acid, was observed at both time points without a decreasing trend, even though they were both degraded by JAB1. Hence hypothetically, the induction effect of caffeic and cinnamic acid could be also attributed to the accumulated dead-end products of their degradation in JAB1. Nevertheless, the products of the JAB1-mediated degradation of caffeic and cinnamic acid were not analyzed within this study.

Furthermore, we demonstrated here that α -pinene, *p*-cymene, (R)-carvone, and (S)-limonene induced the *bphA* gene in the JAB1 strain. The levels of *bphA* transcripts in the presence of (S)-limonene, α -pinene, (R)-carvone, and *p*-cymene after 3 h of incubation were even higher than those of the model inducer biphenyl. Presumably, with (S)-limonene, such an observation could be attributed to the emergence and accumulation of carvone as the (S)-limonene degradation product (**Figure 4C**). Analogously, the upregulation of the *bph* degradation pathway is mediated by the biphenyl-degradation intermediate HOPDA (Ohtsubo et al., 2001; Watanabe et al., 2003). We therefore expect that in the JAB1 strain, the upregulation of the *bphA* gene observed for multiple flavonoids and terpenes is mediated either by the inducer *per se* or by intermediates of their degradation. Nevertheless, experiments that would provide evidence to support this hypothesis were beyond the scope of this study.

SPMs, either in the form of root exudates or artificial mixtures, were already reported to promote the degradation of PCBs (Donnelly et al., 1994; Focht, 1995; Gilbert and Crowley, 1997, 1998; Hernandez et al., 1997; Singer et al., 2000; Tandlich et al., 2001; Toussaint et al., 2012). Nevertheless, studies that would elucidate a molecular basis of this

phenomenon have been relatively scarce. A few pieces of evidence showed, for instance, that the monoterpene carvon acts as the inducer of the *bphC* gene in *Cupriavidus necator* H850 (Park et al., 1999). On the other hand, the study of Master and Mohn (2001) showed a negative effect of SPMs on the *bphA* expression in *Pseudomonas* sp. Cam-10, including monoterpenes (carvone, cumene, limonene, and cymene) and the flavonoid myricetin. More recently, Pham et al. (2015) reported multiple flavonoids to induce the activity of the biphenyl pathway in *R. erythropolis* U23A. The induction of *bphA* genes by various SPMs observed in that study as well as in this report suggests that such an upregulation is an adaptive trait, and not an experimental artifact or only a consequence of a leakiness of regulatory mechanisms caused by their low signal specificity. Our research, which is the first more complex report which takes into account multiple classes of SPMs and investigates their ability to induce and act as substrates of BPDO, supports the hypothesis that the ability of BPDO to degrade aromatic pollutants might have evolved from its ability to degrade SPMs. While this ability may have been weakened in bacterial isolates evolving in a contaminated environment, the inductive effects of SPMs have remained. This prediction, however, requires further investigations.

In summary, our results are in line with the previous findings of Pham et al. (2012), who suggested that bacterial BPDOs serve ecological roles other than the degradation of anthropogenic aromatic pollutants. These roles should specifically include the transformation of SPMs, a process with multiple implications for the fate of soil plant-derived carbon fluxes and signaling. Our study demonstrates the capacity of the JAB1 strain to transform a wide range of SPMs and indicates the possible involvement of JAB1's BPDO in soil processes mediated by SPMs, namely flavonoids and terpenoids. Presumably, besides its potential role in the attenuation of PCB contamination in the soil of origin, the BPDO in JAB1 could participate in the

protection of the bacterium against the selective pressure caused by these specific SPMs through their degradation (Falcone Ferreyra et al., 2012; Górniak et al., 2019; Huang and Osbourn, 2019). With this in mind, more research needs to be conducted to disclose the role of the *bph* pathway in the response to plant-derived compounds in the background of the real soil environment.

DATA AVAILABILITY STATEMENT

The raw data supporting the conclusions of this article will be made available by the authors, without undue reservation.

AUTHOR CONTRIBUTIONS

AZ, JSum, and OU planned and designed the research and wrote the manuscript. AZ, KM, JSem, MS, TC, and JSum performed experiments and/or analyzed data. All authors contributed to the article and approved the submitted version.

FUNDING

The research reported herein was supported by the Czech Science Foundation under grant no. 17-00227S and consecutive grant no. 20-00291S.

SUPPLEMENTARY MATERIAL

The Supplementary Material for this article can be found online at: <https://www.frontiersin.org/articles/10.3389/fmicb.2021.657311/full#supplementary-material>

REFERENCES

- Agullo, L., Romero-Silva, M. J., Domenech, M., and Seeger, M. (2017). *p*-cymene promotes its catabolism through the *p*-cymene and the *p*-cumate pathways, activates a stress response and reduces the biofilm formation in *Burkholderia xenovorans* LB400. *PLoS One* 12:e0169544. doi: 10.1371/journal.pone.0169544
- Aoki, H., Kimura, T., Habe, H., Yamane, H., Kodama, T., and Omori, T. (1996). Cloning, nucleotide sequence, and characterization of the genes encoding enzymes involved in the degradation of cumene to 2-hydroxy-6-oxo-7-methylocta-2,4-dienoic acid in *Pseudomonas fluorescens* IP01. *J. Ferment. Bioeng.* 81, 187–196. doi: 10.1016/0922-338X(96)82207-0
- Baldwin, B. R., Mesarch, M. B., and Nies, L. (2000). Broad substrate specificity of naphthalene- and biphenyl-utilizing bacteria. *Appl. Microbiol. Biotechnol.* 53, 748–753. doi: 10.1007/s002539900300
- Benjamini, Y., and Hochberg, Y. (1995). Controlling the false discovery rate: A practical and powerful approach to multiple testing. *J. R. Stat. Soc. Ser. B Methodol.* 57, 289–300. doi: 10.1111/j.2517-6161.1995.tb02031.x
- Böttger, A., Vothknecht, U., Bolle, C., and Wolf, A. (eds.) (2018). "Plant Secondary Metabolites and Their General Function in Plants," in *Lessons on Caffeine, Cannabis & Co: Plant-derived Drugs and Their Interaction With Human Receptors*. (Cham: Springer International Publishing), 3–17.
- Cadwallader, K. R., Braddock, R. J., Parish, M. E., and Higgins, D. P. (1989). Bioconversion of (+)-limonene by *Pseudomonas gladioli*. *J. Food Sci.* 54, 1241–1245. doi: 10.1111/j.1365-2621.1989.tb05964.x
- Cesco, S., Mimmo, T., Tonon, G., Tomasi, N., Pinton, R., Terzano, R., et al. (2012). Plant-borne flavonoids released into the rhizosphere: impact on soil bio-activities related to plant nutrition. A review. *Biol. Fertil. Soils* 48, 123–149. doi: 10.1007/s00374-011-0653-2
- Cesco, S., Neumann, G., Tomasi, N., Pinton, R., and Weisskopf, L. (2010). Release of plant-borne flavonoids into the rhizosphere and their role in plant nutrition. *Plant Soil* 329, 1–25. doi: 10.1007/s11104-009-0266-9
- Cheong, T. K., and Oriel, P. J. (2000). Cloning and expression of the limonene hydroxylase of *Bacillus stearothermophilus* BR388 and utilization in two-phase limonene conversions. *Appl. Biochem. Biotechnol.* 84, 903–915. doi: 10.1385/abab:84-86:1-9:903
- Chun, H.-K., Ohnishi, Y., Shindo, K., Misawa, N., Furukawa, K., and Horinouchi, S. (2003). Biotransformation of flavone and flavanone by *Streptomyces lividans* cells carrying shuffled biphenyl dioxygenase genes. *J. Mol. Catal. B Enzym.* 21, 113–121. doi: 10.1016/S1381-1177(02)00085-1
- Chung, S.-Y., Maeda, M., Song, E., Horikoshij, K., and Kudo, T. (1994). A gram-positive polychlorinated biphenyl-degrading bacterium, *Rhodococcus erythropolis* strain TA421, isolated from a termite ecosystem. *Biosci. Biotechnol. Biochem.* 58, 2111–2113. doi: 10.1271/bbb.58.2111
- Dakora, F. D., and Phillips, D. A. (1996). Diverse functions of isoflavonoids in legumes transcend anti-microbial definitions of phytoalexins. *Physiol. Mol. Plant Pathol.* 49, 1–20. doi: 10.1006/pmpp.1996.0035
- Dennis, P. G., Miller, A. J., and Hirsch, P. R. (2010). Are root exudates more important than other sources of rhizodeposits in structuring rhizosphere bacterial communities? *FEMS Microbiol. Ecol.* 72, 313–327. doi: 10.1111/j.1574-6941.2010.00860.x

- Donnelly, P. K., Hegde, R. S., and Fletcher, J. S. (1994). Growth of PCB-degrading bacteria on compounds from photosynthetic plants. *Chemosphere* 28, 981–988. doi: 10.1016/0045-6535(94)90014-0
- Duetz, W. A., Fjallman, A. H., Ren, S., Jourdat, C., and Witholt, B. (2001). Biotransformation of D-limonene to (+) *trans*-carveol by toluene-grown *Rhodococcus opacus* PWD4 cells. *Appl. Environ. Microbiol.* 67, 2829–2832. doi: 10.1128/AEM.67.6.2829-2832.2001
- Durante-Rodríguez, G., Gómez-Álvarez, H., Nogales, J., Carmona, M., and Díaz, E. (2018). “One-Component Systems That Regulate the Expression of Degradation Pathways for Aromatic Compounds,” in *Cellular Ecophysiology of Microbe: Hydrocarbon and Lipid Interactions*. ed. T. Krell (Cham: Springer International Publishing), 137–175.
- Eaton, R. W. (1996). *p*-Cumate catabolic pathway in *Pseudomonas putida* Fl: cloning and characterization of DNA carrying the *cmt* operon. *J. Bacteriol.* 178, 1351–1362. doi: 10.1128/JB.178.5.1351-1362.1996
- Eltis, L. D., and Bolin, J. T. (1996). Evolutionary relationships among extradiol dioxygenases. *J. Bacteriol.* 178, 5930–5937. doi: 10.1128/JB.178.20.5930-5937.1996
- Falcone Ferreyra, M. L., Rius, S. P., and Casati, P. (2012). Flavonoids: biosynthesis, biological functions, and biotechnological applications. *Front. Plant Sci.* 3:222. doi: 10.3389/fpls.2012.00222
- Focht, D. D. (1995). Strategies for the improvement of aerobic metabolism of polychlorinated biphenyls. *Curr. Opin. Biotechnol.* 6, 341–346. doi: 10.1016/0958-1669(95)80057-3
- Fraraccio, S., Strejcek, M., Dolinova, I., Macek, T., and Uhlik, O. (2017). Secondary compound hypothesis revisited: selected plant secondary metabolites promote bacterial degradation of *cis*-1,2-dichloroethylene (cDCE). *Sci. Rep.* 7:11. doi: 10.1038/s41598-017-07760-1
- Furukawa, K., and Fujihara, H. (2008). Microbial degradation of polychlorinated biphenyls: biochemical and molecular features. *J. Biosci. Bioeng.* 105, 433–449. doi: 10.1263/jbb.105.433
- Furukawa, K., Suenaga, H., and Goto, M. (2004). Biphenyl dioxygenases: functional versatility and directed evolution. *J. Bacteriol.* 186, 5189–5196. doi: 10.1128/JB.186.16.5189-5196.2004
- Ganger, M. T., Dietz, G. D., and Ewing, S. J. (2017). A common base method for analysis of qPCR data and the application of simple blocking in qPCR experiments. *BMC Bioinform.* 18:534. doi: 10.1186/s12859-017-1949-5
- Garrido-Sanz, D., Sansegundo-Lobato, P., Redondo-Nieto, M., Suman, J., Cajthaml, T., Blanco-Romero, E., et al. (2020). Analysis of the biodegradative and adaptive potential of the novel polychlorinated biphenyl degrader *Rhodococcus* sp. WAY2 revealed by its complete genome sequence. *Microb. Genom.* 6:e000363. doi: 10.1099/mgen.0.000363
- Gilbert, E. S., and Crowley, D. E. (1997). Plant compounds that induce polychlorinated biphenyl biodegradation by *Arthrobacter* sp. strain B1B. *Appl. Environ. Microbiol.* 63, 1933–1938. doi: 10.1128/AEM.63.5.1933-1938.1997
- Gilbert, E. S., and Crowley, D. E. (1998). Repeated application of carvone-induced bacteria to enhance biodegradation of polychlorinated biphenyls in soil. *Appl. Microbiol. Biotechnol.* 50, 489–494. doi: 10.1007/s002530051325
- González-Pasayo, R., and Martínez-Romero, E. (2000). Multiresistance genes of *Rhizobium etli* CFN42. *Mol. Plant-Microbe Interact.* 13, 572–577. doi: 10.1094/MPMI.2000.13.5.572
- Górniak, I., Bartoszewski, R., and Króliczewski, J. (2019). Comprehensive review of antimicrobial activities of plant flavonoids. *Phytochem. Rev.* 18, 241–272. doi: 10.1007/s11101-018-9591-z
- Groeneveld, M., van Beek, H. L., Duetz, W. A., and Fraaije, M. W. (2016). Identification of a novel oxygenase capable of regiospecific hydroxylation of D-limonene into (+)-*trans*-carveol. *Tetrahedron* 72, 7263–7267. doi: 10.1016/j.tet.2015.12.061
- Han, J., Kim, S.-Y., Jung, J., Lim, Y., Ahn, J.-H., Kim, S.-I., et al. (2005). Epoxide formation on the aromatic B-ring of flavanone by biphenyl dioxygenase of *Pseudomonas pseudoalcaligenes* KF707. *J. Appl. Environ. Microbiol.* 71, 5354–5361. doi: 10.1128/AEM.71.9.5354-5361.2005
- Harborne, J. B., and Williams, C. A. (2000). Advances in flavonoid research since 1992. *Phytochemistry* 55, 481–504. doi: 10.1016/S0031-9422(00)00235-1
- Hernandez, B. S., Koh, S.-C., Chial, M., and Focht, D. D. (1997). Terpene-utilizing isolates and their relevance to enhanced biotransformation of polychlorinated biphenyls in soil. *Biodegradation* 8, 153–158. doi: 10.1023/A:1008255218432
- Huang, A. C., and Osbourn, A. (2019). Plant terpenes that mediate below-ground interactions: prospects for bioengineering terpenoids for plant protection. *Pest Manag. Sci.* 75, 2368–2377. doi: 10.1002/ps.5410
- Ishiguro, T., Ohtake, Y., Nakayama, S., Inamori, Y., Amagai, T., Soma, M., et al. (2000). Biodegradation of dibenzofuran and dioxins by *Pseudomonas aeruginosa* and *Xanthomonas maltophilia*. *Environ. Technol.* 21, 1309–1316. doi: 10.1080/09593330.2000.9619020
- Kamanavalli, C. M., and Ninnekar, H. Z. (2004). Biodegradation of DDT by a *Pseudomonas* species. *Curr. Microbiol.* 48, 10–13. doi: 10.1007/s00284-003-4053-1
- Kim, S. Y., Jung, J., Lim, Y., Ahn, J. H., Kim, S. I., and Hur, H. G. (2003). *Cis*-2', 3'-dihydrodiol production on flavone B-ring by biphenyl dioxygenase from *Pseudomonas pseudoalcaligenes* KF707 expressed in *Escherichia coli*. *Anton. Leeuw. Int. J. Gen. Mol. Microbiol.* 84, 261–268. doi: 10.1023/A:1026081824334
- Kim, J., Marshall, M. R., and Wei, C.-I. (1995). Antibacterial activity of some essential oil components against five foodborne pathogens. *J. Agric. Food Chem.* 43, 2839–2845. doi: 10.1021/jf00059a013
- Kimura, N., Kato, H., Nishi, A., and Furukawa, K. (1996). Analysis of substrate range of biphenyl-catabolic enzymes. *Biosci. Biotechnol. Biochem.* 60, 220–223. doi: 10.1271/bbb.60.220
- Koh, C.-L., Sam, C.-K., Yin, W.-F., Tan, L. Y., Krishnan, T., Chong, Y. M., et al. (2013). Plant-derived natural products as sources of anti-quorum sensing compounds. *Sensors* 13, 6217–6228. doi: 10.3390/s130506217
- Kumar, P., Mohammadi, M., Viger, J. F., Barriault, D., Gomez-Gil, L., Eltis, L. D., et al. (2011). Structural insight into the expanded PCB-degrading abilities of a biphenyl dioxygenase obtained by directed evolution. *J. Mol. Biol.* 405, 531–547. doi: 10.1016/j.jmb.2010.11.009
- Kweon, O., Kim, S.-J., Baek, S., Chae, J.-C., Adjei, M. D., Baek, D.-H., et al. (2008). A new classification system for bacterial Rieske non-heme iron aromatic ring-hydroxylating oxygenases. *BMC Biochem.* 9:11. doi: 10.1186/1471-2091-9-11
- Leewis, M.-C., Uhlik, O., Fraraccio, S., Mcfarlin, K., Kottara, A., Glover, C., et al. (2016). Differential impacts of willow and mineral fertilizer on bacterial communities and biodegradation in diesel fuel oil-contaminated soil. *Front. Microbiol.* 7:837. doi: 10.3389/fmicb.2016.00837
- Lesic, B., and Rahme, L. G. (2008). Use of the lambda red recombinase system to rapidly generate mutants in *Pseudomonas aeruginosa*. *BMC Mol. Biol.* 9:20. doi: 10.1186/1471-2199-9-20
- Lin, J. J., Smith, M., Jessee, J., and Bloom, F. (1992). DH11S: an *Escherichia coli* strain for preparation of single-stranded DNA from phagemid vectors. *BioTechniques* 12, 718–721.
- Liu, C.-W., and Murray, J. D. (2016). The role of flavonoids in nodulation host-range specificity: an update. *Plants* 5:33. doi: 10.3390/plants5030033
- Marmulla, R., and Harder, J. (2014). Microbial monoterpene transformations—a review. *Front. Microbiol.* 5:346. doi: 10.3389/fmicb.2014.00346
- Martin, V. J., and Mohn, W. W. (1999). A novel aromatic-ring-hydroxylating dioxygenase from the diterpenoid-degrading bacterium *Pseudomonas abietaniphila* BKME-9. *J. Bacteriol.* 181, 2675–2682. doi: 10.1128/JB.181.9.2675-2682.1999
- Martínez, J. L., Sánchez, M. B., Martínez-Solano, L., Hernández, A., Garmendia, L., Fajardo, A., et al. (2009). Functional role of bacterial multidrug efflux pumps in microbial natural ecosystems. *FEMS Microbiol. Rev.* 33, 430–449. doi: 10.1111/j.1574-6976.2008.00157.x
- Master, E. R., and Mohn, W. W. (2001). Induction of *bphA*, encoding biphenyl dioxygenase, in two polychlorinated biphenyl-degrading bacteria, psychrotolerant *Pseudomonas* strain Cam-1 and mesophilic *Burkholderia* strain LB400. *Appl. Environ. Microbiol.* 67, 2669–2676. doi: 10.1128/AEM.67.6.2669-2676.2001
- Mondello, F. J., Turcich, M. P., Lobos, J. H., and Erickson, B. D. (1997). Identification and modification of biphenyl dioxygenase sequences that determine the specificity of polychlorinated biphenyl degradation. *Appl. Environ. Microbiol.* 63, 3096–3103. doi: 10.1128/AEM.63.8.3096-3103.1997
- Mouz, S., Merlin, C., Springael, D., and Toussaint, A. (1999). A GntR-like negative regulator of the biphenyl degradation genes of the transposon Tn4371. *Mol. Gen. Genet.* 262, 790–799. doi: 10.1007/s004380051142
- Musilova, L., Ridl, J., Polivkova, M., Macek, T., and Uhlik, O. (2016). Effects of secondary plant metabolites on microbial populations: changes in community structure and metabolic activity in contaminated environments. *Int. J. Mol. Sci.* 17:1205. doi: 10.3390/ijms17081205
- Noma, Y., Yamasaki, S., and Asakawa, Y. (1992). Biotransformation of limonene and related compounds by *Aspergillus cellulosa*. *Phytochemistry* 31, 2725–2727. doi: 10.1016/0031-9422(92)83619-A
- Ohtsubo, Y., Delawary, M., Takagi, M., Ohta, A., Kimbara, K., and Nagata, Y. (2001). BphS, a key transcriptional regulator of *bph* genes involved in polychlorinated biphenyl/biphenyl degradation in *Pseudomonas* sp. KKS102. *J. Biol. Chem.* 276, 36146–36154. doi: 10.1074/jbc.M100302200

- Ohtsubo, Y., Nagata, Y., Kimbara, K., Takagi, M., and Ohta, A. (2000). Expression of the *bph* genes involved in biphenyl/PCB degradation in *Pseudomonas* sp. KKS102 induced by the biphenyl degradation intermediate, 2-hydroxy-6-oxo-6-phenylhexa-2,4-dienoic acid. *Gene* 256, 223–228. doi: 10.1016/S0378-1119(00)00349-8
- Palumbo, J. D., Kado, C. I., and Phillips, D. A. (1998). An isoflavonoid-inducible efflux pump in *Agrobacterium tumefaciens* is involved in competitive colonization of roots. *J. Bacteriol.* 180, 3107–3113. doi: 10.1128/JB.180.12.3107-3113.1998
- Papadopoulos, C. J., Carson, C. F., Chang, B. J., and Riley, T. V. (2008). Role of the MexAB-OprM efflux pump of *Pseudomonas aeruginosa* in tolerance to tea tree (*Melaleuca alternifolia*) oil and its monoterpene components terpinen-4-ol, 1,8-cineole, and alpha-terpineol. *Appl. Environ. Microbiol.* 74, 1932–1935. doi: 10.1128/AEM.02334-07
- Parales, R. E., and Resnick, S. M. (2006). “Aromatic Ring Hydroxylating Dioxygenases,” in *Pseudomonas: Volume 4 Molecular Biology of Emerging Issues*. eds. J.-L. Ramos and R. C. Levesque (Boston, MA: Springer, US), 287–340.
- Park, Y.-I., So, J., and Koh, S.-C. (1999). Induction by carvone of the polychlorinated biphenyl (PCB)-degradative pathway in *Alcaligenes eutrophus* H850 and its molecular monitoring. *J. Microbiol. Biotechnol.* 9, 804–810.
- Parniske, M., Ahlborn, B., and Werner, D. (1991). Isoflavonoid-inducible resistance to the phytoalexin glyceollin in soybean rhizobia. *J. Bacteriol.* 173, 3432–3439. doi: 10.1128/JB.173.11.3432-3439.1991
- Pham, T. T. M., Pino Rodriguez, N. J., Hijri, M., and Sylvestre, M. (2015). Optimizing polychlorinated biphenyl degradation by flavonoid-induced cells of the rhizobacterium *Rhodococcus erythropolis* U23A. *PLoS One* 10:e0126033. doi: 10.1371/journal.pone.0126033
- Pham, T. T. M., and Sylvestre, M. (2013). Has the bacterial biphenyl catabolic pathway evolved primarily to degrade biphenyl? The diphenylmethane case. *J. Bacteriol.* 195:3563. doi: 10.1128/JB.00161-13
- Pham, T. T., Tu, Y., and Sylvestre, M. (2012). Remarkable ability of *Pandoraea pnomenus* B356 biphenyl dioxygenase to metabolize simple flavonoids. *Appl. Environ. Microbiol.* 78, 3560–3570. doi: 10.1128/AEM.00225-12
- Prema, B. R., and Bhattacharyya, P. K. (1962). Microbiological transformation of terpenes: II. transformation of alpha-pinene. *Appl. Microbiol.* 10, 524–528.
- Puentes-Cala, E., Liebeke, M., Markert, S., and Harder, J. (2018). Limonene dehydrogenase hydroxylates the allylic methyl group of cyclic monoterpenes in the anaerobic terpene degradation by *Castellaniella defragrans*. *J. Biol. Chem.* 293, 9520–9529. doi: 10.1074/jbc.RA117.001557
- Rauscher, M. D. (2001). Co-evolution and plant resistance to natural enemies. *Nature* 411, 857–864. doi: 10.1038/35081193
- Resnick, S. M., Lee, K., and Gibson, D. T. (1996). Diverse reactions catalyzed by naphthalene dioxygenase from *Pseudomonas* sp. strain NCIB 9816. *J. Ind. Microbiol. Biotechnol.* 17, 438–457. doi: 10.1007/BF01574775
- Ridl, J., Suman, J., Fraraccio, S., Hradilova, M., Strejcek, M., Cajthaml, T., et al. (2018). Complete genome sequence of *Pseudomonas alcaliphila* JAB1 (=DSM 26533), a versatile degrader of organic pollutants. *Stand. Genomic Sci.* 13:3. doi: 10.1186/s40793-017-0306-7
- Robertson, J. B., Spain, J. C., Haddock, J. D., and Gibson, D. T. C. (1992). Oxidation of nitrotoluenes by toluene dioxygenase: evidence for a monooxygenase reaction. *Appl. Environ. Microbiol.* 58, 2643–2648. doi: 10.1128/AEM.58.8.2643-2648.1992
- Ryslava, E., Krejčík, Z., Macek, T., Sykorova, H., Denmerova, K., and Mackova, M. (2003). Study of PCB degradation in real contaminated soil. *Fresenius Environ. Bull.* 12, 296–301.
- Seo, J., Kang, S. I., Kim, M., Han, J., and Hur, H. G. (2011a). Flavonoids biotransformation by bacterial non-heme dioxygenases, biphenyl and naphthalene dioxygenase. *Appl. Microbiol. Biotechnol.* 91, 219–228. doi: 10.1007/s00253-011-3334-z
- Seo, J., Kang, S. I., Won, D., Kim, M., Ryu, J. Y., Kang, S. W., et al. (2011b). Absolute configuration-dependent epoxide formation from isoflavan-4-ol stereoisomers by biphenyl dioxygenase of *Pseudomonas pseudoalcaligenes* strain KF707. *Appl. Microbiol. Biotechnol.* 89, 1773–1782. doi: 10.1007/s00253-010-2989-1
- Shaw, L. J., Morris, P., and Hooker, J. E. (2006). Perception and modification of plant flavonoid signals by rhizosphere microorganisms. *Environ. Microbiol.* 8, 1867–1880. doi: 10.1111/j.1462-2920.2006.01141.x
- Singer, A. C., Crowley, D. E., and Thompson, I. P. (2003). Secondary plant metabolites in phytoremediation and biotransformation. *Trends Biotechnol.* 21, 123–130. doi: 10.1016/S0167-7799(02)00041-0
- Singer, A. C., Gilbert, E. S., Luepromchai, E., and Crowley, D. E. (2000). Bioremediation of polychlorinated biphenyl-contaminated soil using carvone and surfactant-grown bacteria. *Appl. Microbiol. Biotechnol.* 54, 838–843. doi: 10.1007/s002530000472
- Speelmans, G., Bijlsma, A., and Eggink, G. (1998). Limonene bioconversion to high concentrations of a single and stable product, perillaldehyde, by a solvent-resistant *Pseudomonas putida* strain. *Appl. Microbiol. Biotechnol.* 50, 538–544. doi: 10.1007/s002530051331
- Taira, K., Hirose, J., Hayashida, S., and Furukawa, K. (1992). Analysis of *bph* operon from the polychlorinated biphenyl-degrading strain of *Pseudomonas pseudoalcaligenes* KF707. *J. Biol. Chem.* 267, 4844–4853. doi: 10.1016/S0021-9258(18)42908-0
- Tandlich, R., Brezná, B., and Dercová, K. (2001). The effect of terpenes on the biodegradation of polychlorinated biphenyls by *Pseudomonas stutzeri*. *Chemosphere* 44, 1547–1555. doi: 10.1016/S0045-6535(00)00523-3
- Tellinghuisen, J. (2001). Statistical error propagation. *Chem. Eur. J.* 105, 3917–3921. doi: 10.1021/jp003484u
- Toussaint, J. P., Pham, T. T., Barriault, D., and Sylvestre, M. (2012). Plant exudates promote PCB degradation by a rhodococcal rhizobacteria. *Appl. Microbiol. Biotechnol.* 95, 1589–1603. doi: 10.1007/s00253-011-3824-z
- Triscari-Barberi, T., Simone, D., Calabrese, F. M., Attimonelli, M., Hahn, K. R., Amoako, K. K., et al. (2012). Genome sequence of the polychlorinated-biphenyl degrader *Pseudomonas pseudoalcaligenes* KF707. *J. Bacteriol.* 194, 4426–4427. doi: 10.1128/JB.00722-12
- Uhlík, O., Wald, J., Strejcek, M., Musilova, L., Ridl, J., Hroudova, M., et al. (2012). Identification of bacteria utilizing biphenyl, benzoate, and naphthalene in long-term contaminated soil. *PLoS One* 7:e40653. doi: 10.1371/journal.pone.0040653
- van Der Werf, M. J., Orru, R. V. A., Overkamp, K. M., Swarts, H. J., Ospran, I., Steinreiber, A., et al. (1999). Substrate specificity and stereospecificity of limonene-1,2-epoxide hydrolase from *Rhodococcus erythropolis* DCL14; an enzyme showing sequential and enantioconvergent substrate conversion. *Appl. Microbiol. Biotechnol.* 52, 380–385. doi: 10.1007/s002530051535
- van Rensburg, E., Moleleki, N., Van Der Walt, J. P., Botes, P. J., and Van Dyk, M. S. (1997). Biotransformation of (+)limonene and (-)piperitone by yeasts and yeast-like fungi. *Biotechnol. Lett.* 19, 779–782. doi: 10.1023/A:1018344411069
- Vergani, L., Mapelli, F., Suman, J., Cajthaml, T., Uhlík, O., and Borin, S. (2019). Novel PCB-degrading *Rhodococcus* strains able to promote plant growth for assisted rhizoremediation of historically polluted soils. *PLoS One* 14:e0221253. doi: 10.1371/journal.pone.0221253
- Vezina, J., Barriault, D., and Sylvestre, M. (2008). Diversity of the C-terminal portion of the biphenyl dioxygenase large subunit. *J. Mol. Microbiol. Biotechnol.* 15, 139–151. doi: 10.1159/000121326
- Vuolo, M. M., Lima, V. S., and Maróstica Junior, M. R. (2019). “Chapter 2 - Phenolic Compounds: Structure, Classification, and Antioxidant Power,” in *Bioactive Compounds*. ed. M. R. S. Campos (Cambridge: Woodhead Publishing), 33–50.
- Wald, J., Hroudova, M., Jansa, J., Vrchotova, B., Macek, T., and Uhlík, O. (2015). Pseudomonads rule degradation of polyaromatic hydrocarbons in aerated sediment. *Front. Microbiol.* 6:1268. doi: 10.3389/fmicb.2015.01268
- Watanabe, T., Fujihara, H., and Furukawa, K. (2003). Characterization of the second LysR-type regulator in the biphenyl-catabolic gene cluster of *Pseudomonas pseudoalcaligenes* KF707. *J. Bacteriol.* 185:7. doi: 10.1128/JB.185.12.3575-3582.2003
- Watanabe, T., Inoue, R., Kimura, N., and Furukawa, K. (2000). Versatile transcription of biphenyl catabolic *bph* operon in *Pseudomonas pseudoalcaligenes* KF707. *J. Biol. Chem.* 275, 31016–31023. doi: 10.1074/jbc.M003023200
- Xu, H. X., and Lee, S. F. (2001). Activity of plant flavonoids against antibiotic-resistant bacteria. *Phytother. Res.* 15, 39–43. doi: 10.1002/1099-1573(200102)15:1<39::AID-PTR684>3.0.CO;2-R

Conflict of Interest: The authors declare that the research was conducted in the absence of any commercial or financial relationships that could be construed as a potential conflict of interest.

Copyright © 2021 Zubrova, Michalikova, Semerad, Strejcek, Cajthaml, Suman and Uhlík. This is an open-access article distributed under the terms of the Creative Commons Attribution License (CC BY). The use, distribution or reproduction in other forums is permitted, provided the original author(s) and the copyright owner(s) are credited and that the original publication in this journal is cited, in accordance with accepted academic practice. No use, distribution or reproduction is permitted which does not comply with these terms.



Metabolic Profiling of Rhizobacteria *Serratia plymuthica* and *Bacillus subtilis* Revealed Intra- and Interspecific Differences and Elicitation of Plipastatins and Short Peptides Due to Co-cultivation

Riya C. Menezes¹, Birgit Piechulla², Dörte Warber², Aleš Svatoš¹ and Marco Kai^{1,2*}

¹ Research Group Mass Spectrometry/Proteomics, Max-Planck Institute for Chemical Ecology, Jena, Germany, ² Department of Biochemistry, University of Rostock, Institute for Biological Sciences, Rostock, Germany

OPEN ACCESS

Edited by:

Monica T. Pupo,
University of São Paulo, Brazil

Reviewed by:

Andres Mauricio Caraballo-Rodriguez,
California College San Diego,
United States
Camila Manoel Crnkovic,
University of São Paulo, Brazil

*Correspondence:

Marco Kai
marcokai@hotmail.de

Specialty section:

This article was submitted to
Terrestrial Microbiology,
a section of the journal
Frontiers in Microbiology

Received: 24 March 2021

Accepted: 22 April 2021

Published: 31 May 2021

Citation:

Menezes RC, Piechulla B, Warber D,
Svatoš A and Kai M (2021) Metabolic
Profiling of Rhizobacteria *Serratia*
plymuthica and *Bacillus subtilis*
Revealed Intra- and Interspecific
Differences and Elicitation of
Plipastatins and Short Peptides Due
to Co-cultivation.
Front. Microbiol. 12:685224.
doi: 10.3389/fmicb.2021.685224

Rhizobacteria live in diverse and dynamic communities having a high impact on plant growth and development. Due to the complexity of the microbial communities and the difficult accessibility of the rhizosphere, investigations of interactive processes within this bacterial network are challenging. In order to better understand causal relationships between individual members of the microbial community of plants, we started to investigate the inter- and intraspecific interaction potential of three rhizobacteria, the *S. plymuthica* isolates 4Rx13 and AS9 and *B. subtilis* B2g, using high resolution mass spectrometry based metabolic profiling of structured, low-diversity model communities. We found that by metabolic profiling we are able to detect metabolite changes during cultivation of all three isolates. The metabolic profile of *S. plymuthica* 4Rx13 differs interspecifically to *B. subtilis* B2g and surprisingly intraspecifically to *S. plymuthica* AS9. Thereby, the release of different secondary metabolites represents one contributing factor of inter- and intraspecific variations in metabolite profiles. Interspecific co-cultivation of *S. plymuthica* 4Rx13 and *B. subtilis* B2g showed consistently distinct metabolic profiles compared to mono-cultivated species. Thereby, putative known and new variants of the plipastatin family are increased in the co-cultivation of *S. plymuthica* 4Rx13 and *B. subtilis* B2g. Interestingly, intraspecific co-cultivation of *S. plymuthica* 4Rx13 and *S. plymuthica* AS9 revealed a distinct interaction zone and showed distinct metabolic profiles compared to mono-cultures. Thereby, several putative short proline-containing peptides are increased in co-cultivation of *S. plymuthica* 4Rx13 with *S. plymuthica* AS9 compared to mono-cultivated strains. Our results demonstrate that the release of metabolites by rhizobacteria alters due to growth and induced by social interactions between single members of the microbial community. These results form a basis to elucidate the functional role of such interaction-triggered compounds in establishment and maintenance of microbial communities and can be applied under natural and more realistic conditions, since rhizobacteria also interact with the plant itself and many other members of plant and soil microbiota.

Keywords: microbial interaction, metabolic profiling, *Serratia plymuthica*, *Bacillus subtilis*, sirius, global natural products social molecular networking, plipastatins

INTRODUCTION

In nature, bacteria live in diverse and dynamic communities (Fierer and Jackson, 2006; Little et al., 2008; Phelan et al., 2012). One hotspot of bacterial life is the rhizosphere, which represents the area of soil that surrounds plant roots (Hiltner, 1904; Reinhold-Hurek et al., 2015). Plants release their excess photosynthetic metabolites including organic acids, amino acids, sugars, peptides or proteins via the root into the rhizosphere (Vančura, 1964; Smith, 1969). As consequence of this accumulation of nutrients, bacteria flourish in the soil closely associated to the plant roots (Badri and Vivanco, 2009).

Bacteria living in the rhizosphere are termed as rhizobacteria. Together with surrounding neighboring bacterial cells they form diverse microbial communities (Shank, 2018). The microbial community itself has a high impact on plant growth and development (Lindow and Brandl, 2003; Buee et al., 2009; Berendsen et al., 2012; Vorholt, 2012). On one hand, community members beneficially influence plant growth by fixation of nitrogen, release of plant hormones, defending against plant pathogens or emission of volatiles (Ryu et al., 2003; Gray and Smith, 2005; Kai et al., 2007). On the other hand, some members of the microbial community can evoke plant diseases by secretion of cell wall degrading enzymes and toxins (Van der Wolf and De Boer, 2014). Thus, the composition of the microbiome is important as it influences plants in multiple ways. The structure of microbial communities has been ascertained for roots of several plant species, however, how interaction between members of the plant-associated microbiota influence the establishment of the microbial community is not fully understood (Hassani et al., 2018). Beside plant primary and secondary metabolites, the excreted metabolites released by different members of the microbial community are considered as primary drivers of microbial community interactions (Traxler and Kolter, 2015; Shank, 2018). Individual bacteria, for instance, outcompete bacterial rivals by toxin, antibiotic and siderophore production, sense their environment by secreting signaling compounds or develop cooperative partnerships by exchanging metabolites (Griffin et al., 2004; Waters and Bassler, 2005; Phelan et al., 2012; Pande et al., 2015; Lemfack et al., 2016).

Due to the complexity of the microbial communities and the difficulties in accessing the rhizosphere, investigations of interactive processes within this bacterial network are challenging (Bonkowski, 2019). Synthetic and reductionistic approaches can help to understand underlying principles of interactions in microbial communities (Ghoul and Mitri, 2016; Røder et al., 2016; Shank, 2018). Therefore, in order to better understand causal relationships between members of the microbial community of plants, we started to investigate the interaction potential of rhizobacteria using structured, low-diversity model communities. Limitation of such *in vitro* co-cultivation approaches is to capture the actual metabolic profile theoretically involved under natural and more realistic conditions, since rhizobacteria interact with the plant itself and many other members of plant and soil microbiota. However, the main benefit of low-diversity,

pair-wise bacterial colonies is the clear assignment of causative and responding strain, which can hardly be shown with the use of highly complex communities. Using this approach, we showed that co-cultivation of two rhizobacteria *Serratia plymuthica* 4Rx13 and *Bacillus subtilis* B2g revealed a distinct and wide interaction zone (Kai and Piechulla, 2018) indicating a high potential of interspecies interaction between both partners. In the present study, we questioned how metabolic features reflect this interaction. Since also closely related species inhabit same habitats, we were further interested in the intraspecific interaction potential of *S. plymuthica* 4Rx13 and chose the rhizobacterium *S. plymuthica* AS9 as model partner.

In order to get a comprehensive overview of the interplay, we extracted the metabolites released over 4 weeks of co-cultivation at specific time points and compared these metabolite profiles with the excreted metabolite profiles of mono-cultivated strains using multivariate data analyses. Furthermore, we started with the evaluation of most prominent co-cultivation correlating patterns using classical, manual identification of high resolution (HR) mass spectra (MS^1 and MS/MS) and computational HRMS/ MS identification using Global Natural Product Molecular Networking (GNPS, Wang et al., 2016) and Sirius (Dührkop et al., 2019). Our results demonstrate that the release of metabolites by rhizobacteria alters due to growth and induced by social interactions between single members of the microbial community.

MATERIALS AND METHODS

Bacterial Cultures

Bacillus subtilis B2g, *Serratia plymuthica* 4Rx13 (formally known as *S. odorifera* 4Rx13) (Weise et al., 2014) and *Serratia plymuthica* AS9 were originally isolated from *Brassica napus* (Marten et al., 2000; Alström, 2001; Berg et al., 2002; Neupane et al., 2012). All bacterial isolates were cultivated on nutrient agar II short-term cultures (NAII; peptone from casein 3.5 g l^{-1} , peptone from meat 2.5 g l^{-1} , peptone from gelatin 2.5 g l^{-1} , yeast extract 1.5 g l^{-1} , NaCl 5 g l^{-1} , agar-agar 15 g l^{-1} , pH 7.2, maximum 3 weeks old) or in liquid nutrient broth II (NBII: NAII without agar) at 30°C .

Bacterial Self-paired and Co-cultures

One colony was picked from a short-term culture and inoculated in 6 ml of NBII-medium. After 24 h of inoculation at 160 rpm (Bühler, Tübingen, Germany) and 30°C , the cultures were diluted with NBII to obtain a starting OD_{600} of 0.05. Twenty microliters of this diluted culture were dropped in overlaps on NBII containing agar (two droplets—one droplet per strain). Self-paired overlapping droplets were used as control mono-cultivations. Co-cultivation of strains were performed for 30 days at 20°C . Investigations were conducted in two independent setups with each three replicates from three different pre-cultures for *S. plymuthica* 4Rx13 and *B. subtilis* B2g interaction and one setup with each three replicates from three different pre-cultures for *S. plymuthica* 4Rx13 and *S. plymuthica* AS9 interaction.

Determination of Bacterial Growth During Co-cultivation

Cell growth was monitored by determination of colony forming units (cfu) within 30 days of growth (day 1, 3, 6, 7, 10, 14, 21, 28, 30). Both strains together were scraped from the agar with a pipette tip. The scraped cells were transferred into an Eppendorf tube filled with 3 ml NaCl solution (0.85%) and vortexed for 2 min. From this suspension a serial dilution was prepared with NaCl solution (0.85%) to obtain inocula of maximum 200 cells/10 μ l. Droplets (each of 10 μ l) of the last dilution (10^{-3} – 10^{-8} depending on the growth) were spotted onto a NAI agar containing Petri dish and spread to form thin lines. These Petri dishes were incubated at 30°C for 24 h to count the cells.

Metabolite Extraction

Metabolites were extracted from the agar medium according to Tyc et al. (2017) within 30 days of growth (day 1, 3, 6, 7, 10, 14, 21, 28, 30). After harvesting the cells from the agar, the agar was cut into slices of 13.6 cm² (4 × 3.4 cm). As control, the agar from non-inoculated agar was sliced into pieces of same size. These slices were transferred into Falcon tubes (50 ml, Carl Roth, Karlsruhe, Germany), which were immediately frozen in liquid nitrogen. The sample containing Falcon tubes were subsequently lyophilized for 72 h (Alpha 1-4 LSCbasic, Christ, Osterode am Harz, Germany). After lyophilization samples were crushed in a ceramic mortar containing 6 ml liquid nitrogen using a pestle. The powder was transferred into an Eppendorf tube (1.5 ml) using a paper funnel. Subsequently, one ml of 75% methanol including 10 μ M indole-3-propionic acid (internal standard) was added to 125 mg powder. This mixture was vortexed for 30 s and subsequently sonicated for 30 min in a chilled water-bath at 6°C (after 15 min tubes were shortly shaken). The tubes were afterwards vortexed for 10 s and centrifuged at 2,900 g for 10 min at 4°C. The supernatants were transferred into other 1.5 ml Eppendorf tubes, which were centrifuged at 2,900 g for 15 min at 4°C. The supernatants were again transferred into new Eppendorf tubes (1.5 ml), which were stored at –70°C. At the end of this approach a sample set of each independent setup was non-stop analyzed using UHPLC/ESI-Q Exactive HF-X-MS/MS.

UHPLC-ESI-Q Exactive MS/MS Analysis of Extracted Metabolites

Ultra-high performance liquid chromatography-tandem mass spectrometry (UHPLC/ESI-Q Exactive HF-X-MS/MS) analyses of the bacterial extracts were performed on a QE-HF-X equipped with an Ultimate 3000 series RSLC (Dionex, Sunnyvale, CA, USA) LC. Chromatographic separation was achieved on an Acclaim C18 column (150 × 2.1 mm, 2.2 μ m particles with 120 Å pore diameter, Dionex, Sunnyvale, CA, USA) with a flow rate of 300 μ l min^{–1} in a binary solvent system of water (solvent A) and acetonitrile (solvent B), both containing 0.1% (v/v) formic acid. Five μ l each of extract was loaded onto the column and eluted by using a gradient as follows: linear increase from 0% B to 100% B within 15 min—100% B constant for 5 min—equilibration time at 0% B for 5 min. The mass spectrometer was operated in positive ionization mode using Heated-Electrospray Ionization (H-ESI).

The source parameters were set to 4 kV for spray voltage, 35 V for transfer capillary voltage, capillary temperature 300°C and Funnel RF of 40 V. Fragmentation was performed using data-dependent acquisition mode with MS¹ full scan at m/z 150–1,500 at 60,000 $m/\Delta m$ resolving power and up to five MS/MS scans (TOP5) of the most abundant ions per duty cycle with 30,000 $m/\Delta m$ resolving power and stepped normalized collision energy of 20, 30 and 40. Data was evaluated and interpreted using Xcalibur v.3.0.63 software (Thermo Fisher Scientific, Waltham, MA, USA).

Data Processing

Conversion of raw data files to mzXML format files was performed using MSConvertGUI tool of the ProteoWizard 3.0.X software (Chambers et al., 2012). Further reprocessing was conducted either via uploading the mzXML files to XCMS Online (Tautenhahn et al., 2012) or manually via the XCMS package in RStudio version 1.0.153 (Smith et al., 2006; Tautenhahn et al., 2008; Benton et al., 2010).

For manual XCMS processing, feature detection was performed using *centWave* algorithm with following parameter: $\Delta m/z$ 5 ppm, peak width from 5 to 20 s [Command in RStudio CentWaveParam (ppm = 5, peakwidth = c(5, 20), integrate = 1, fitgauss = TRUE, snthresh = 30, mzdiff = –0.001)]. Retention time correction was performed using Obiwrap method (Prince and Marcotte, 2006). Chromatograms were aligned with minfrac = 0 and bw = 0.5.

For XCMS Online processing multigroup analysis in version 3.7.1 was applied. Feature detection was performed using *centWave* algorithm with following parameter: $\Delta m/z$ 5 ppm, peak width from 5 to 20 s, Signal/Noise threshold = 4, mzdiff = 0.01, integration method = 1, prefilter peaks 3, prefilter intensity = 100 and noise filter = 100. Retention time correction was performed using Obiwrap method (profStep = 1). Parameter for alignment were mzwid = 0.025, bw = 0.5, minfrac = 0.5, minsamp = 1, max = 100.

Data Analysis

Partitioning around medoids (PAM) clustering (Kaufman and Rousseeuw, 1990) was performed from the manually processed XCMS data in RStudio. Principal component analyses (PCAs) were performed using XCMS Online data. Further data processing, statistical analysis including correlation pattern analysis using Pearson r as distance measure was performed using Metaboanalyst 5.0 (ref. for preliminary versions, Xia et al., 2009; Chong et al., 2019; Pang et al., 2020). In MetaboAnalyst 5.0 the tool “Statistical analysis” was applied. After import, data were filtered using interquartile range and normalized using auto scaling. All analyses were performed two times (technical replicates) for every condition with three biological replicates each (except when indicated).

Identification

Classical, Manual Identification of High Resolution Mass Spectra

Classical identification was performed using accurate mass measurements of mass features (MS¹ and MS/MS). A mass

tolerance of ± 3 ppm was applied as threshold between accurate and exact mass. For plipastatin isomer identification, several diagnostic marker ions were used accordingly for the amino acids at position 6 and 10 of the plipastatin molecule (Pathak et al., 2012; Kaki et al., 2020). For plipastatin A1, we used m/z 966.45672 (corresponding to chemical formula $C_{46}H_{64}N_9O_{14}$) and m/z 1080.53603 (corresponding to chemical formula $C_{51}H_{74}N_{11}O_{15}$) representing alanine⁶/isoleucine¹⁰. For plipastatin A2 we used m/z 1066.52038 (corresponding to chemical formula $C_{50}H_{72}N_{11}O_{15}$) representing alanine⁶/valine¹⁰. For plipastatin B1 we used m/z 994.48802 (corresponding to chemical formula $C_{48}H_{68}N_9O_{14}$) and m/z 1108.56733 (corresponding to chemical formula $C_{53}H_{78}N_{11}O_{15}$) representing valine⁶/isoleucine¹⁰. For plipastatin B2 we used m/z 980.47375 (corresponding to chemical formula $C_{47}H_{66}N_9O_{14}$) and m/z 1094.55078 (corresponding to chemical formula $C_{52}H_{76}N_{11}O_{15}$) representing valine⁶/valine¹⁰.

Determination of Chemical Formulae Using Sirius 4

Conversion of raw data files to mzML format files was performed using MSConvertGUI tool of the ProteoWizard 3.0.X software (Chambers et al., 2012). The mzML files were imported into MZmine 2.53 (Pluskal et al., 2010) and processed as follows. MS¹ and MS/MS level detection with a noise level of 1.0E3. Chromatogram builder (MS¹ level) with a minimal time span of 0.01 min, a minimal height of 3.0E3 and a mass tolerance (m/z) of 5 ppm. Deisotoping was performed with a mass tolerance (m/z) of 5 ppm and a retention time tolerance of 0.2 min from ions with maximum charges of 2. Data were exported as mgf files and subsequently imported into Sirius 4.5.3 (Dührkop et al., 2019). For identification we considered the Sirius score, the fragmentation tree score (Rasche et al., 2012; Böcker and Dührkop, 2016) and isotopic pattern analysis (Böcker et al., 2009). For Oocydin A assignment, we further used CSI:FingerID (Dührkop et al., 2015).

Molecular Networking Workflow

A molecular network was created according to Wang et al. (2016) using the online workflow (<https://ccms-ucsd.github.io/GNPSDocumentation/>) on the GNPS website (<http://gnps.ucsd.edu>). The data was filtered by removing all MS/MS fragment ions within ± 17 Da of the precursor m/z . MS/MS spectra were window filtered by choosing only the top 6 fragment ions in the ± 50 Da window throughout the spectrum. The precursor ion mass tolerance was set to 2.0 Da and a MS/MS fragment ion tolerance of 0.5 Da. A network was then created where edges were filtered to have a cosine score above 0.7 and more than 6 matched peaks. Further, edges between two nodes were kept in the network if and only if each of the nodes appeared in each other's respective top 10 most similar nodes. Finally, the maximum size of a molecular family was set to 100, and the lowest scoring edges were removed from molecular families until the molecular family size was below this threshold. The spectra in the network were then searched against GNPS' spectral libraries. The library spectra were filtered in the same manner as the input data. All matches kept between network spectra and library spectra were required to have a score above 0.7 and at least 6 matched peaks. The IDs of the respective jobs that were used

for this study are ID = 6b27a2bb84ff491bb9ef8b7fb5cea822 for *S. plymuthica* 4Rx13 and AS9 interaction and ID = 0bb4c822bc4141f09a4ed723152db975 for *S. plymuthica* 4Rx13 and *B. subtilis* B2g interaction.

RESULTS

Metabolic Profiles From Mono-cultivated Isolates *S. plymuthica* 4Rx13 and AS9 and *B. subtilis* B2g Differ During Cultivation

Before the interaction of the rhizobacteria was investigated, we analyzed the metabolic features of the mono-cultivated isolates *S. plymuthica* 4Rx13, *S. plymuthica* AS9 and *B. subtilis* B2g during cultivation on solid medium. Since we were interested in metabolites excreted into the environment, we extracted agar slices using a recently established protocol (Tyc et al., 2017) at different time points (day 1, 3, 6, 7, 10, 14, 21, 28, and 30). The respective extracts were non-targeted analyzed using UHPLC/HRMS and processed with XCMS Online (Tautenhahn et al., 2012). To evaluate the dynamics of metabolite production during cultivation of the mono-cultivated isolates, unsupervised multivariate PCAs were conducted. These PCAs showed a clear separation of the released metabolites in relation to the time point of cultivation of all three tested bacterial isolates. Thereby, the biological replicates of each time point grouped together (Figure 1). For *S. plymuthica* 4Rx13, PC1 and PC2 explained 37% and 16% of the total variability, respectively (Figure 1A). For *B. subtilis* B2g, PC1 and PC2 explained 35 and 17% of the total variability, respectively (Figure 1B). For *S. plymuthica* AS9, PC1 and PC2 explained 41 and 16% of the total variability, respectively (Figure 1C). The metabolic profiles of all three bacteria were mainly separated along PC1, however, a cultivation dependent separation was also observed along PC2. Metabolite profiles from day 28 and day 30 did not separate neither along PC1 nor along PC2. These results clearly show a variation of metabolic profiles during the time of bacterial cultivation.

Metabolic Profiles of *S. plymuthica* 4Rx13 Differ Interspecifically to *B. subtilis* B2g and Intraspecifically to *S. plymuthica* AS9

To evaluate whether the metabolic profiles of the three mono-cultivated bacteria can differ in relation to each other, additional PCAs of the processed data from day 6 were exemplarily conducted. The metabolic profiles of *S. plymuthica* 4Rx13 and *B. subtilis* B2g and control (extracted non-inoculated agar) clearly separated from each other (Figure 2). The biological replicates of each cultivation also grouped together (Figure 2A). PC1 and PC2 explained 36 and 33% of the total variability, respectively. Thereby, 338 features (m/z /RT) and 414 features (m/z /RT) were exclusively present or significantly increased in *S. plymuthica* 4Rx13 (correlation > 0.9 , $p < 0.001$) and *B. subtilis* B2g, respectively (correlation > 0.9 , $p < 0.001$).

Surprisingly, the metabolites of *S. plymuthica* 4Rx13 and AS9 also showed distinct and separated pattern (Figure 2B). PC1 and PC2 explained 39% and 25% of the total variability, respectively. Thereby, 655 features (m/z /RT) and 72 features (m/z /RT) were

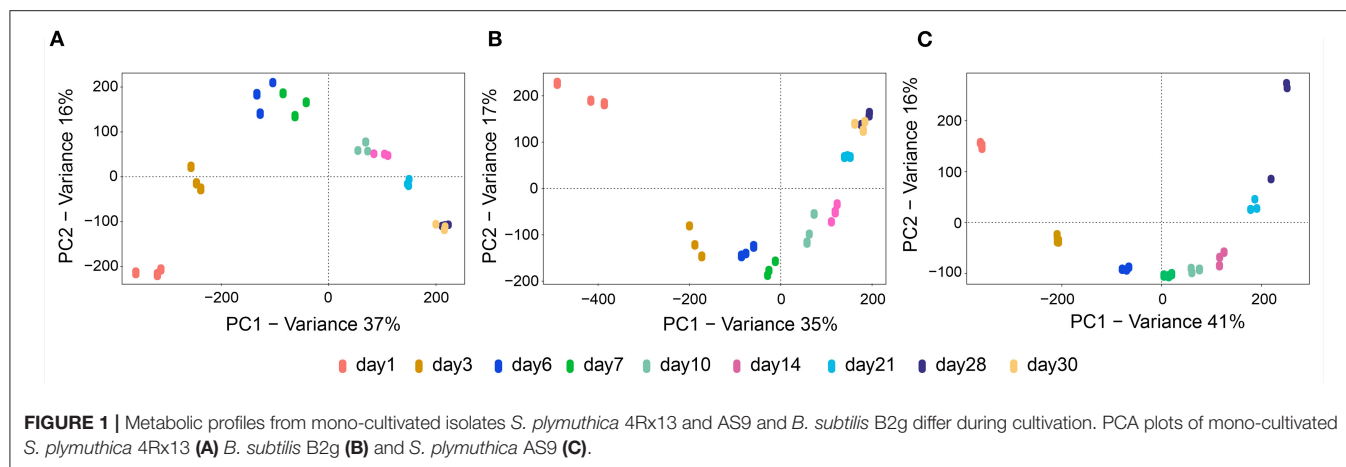


FIGURE 1 | Metabolic profiles from mono-cultivated isolates *S. plymuthica* 4Rx13 and AS9 and *B. subtilis* B2g differ during cultivation. PCA plots of mono-cultivated *S. plymuthica* 4Rx13 (A) *B. subtilis* B2g (B) and *S. plymuthica* AS9 (C).

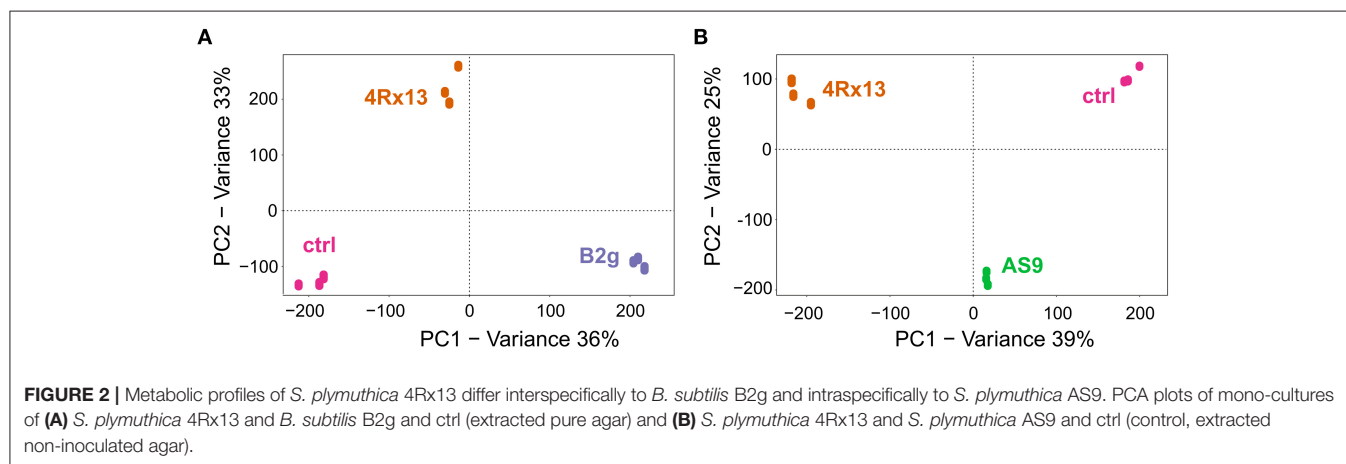


FIGURE 2 | Metabolic profiles of *S. plymuthica* 4Rx13 differ interspecifically to *B. subtilis* B2g and intraspecifically to *S. plymuthica* AS9. PCA plots of mono-cultures of (A) *S. plymuthica* 4Rx13 and *B. subtilis* B2g and ctrl (extracted pure agar) and (B) *S. plymuthica* 4Rx13 and *S. plymuthica* AS9 and ctrl (control, extracted non-inoculated agar).

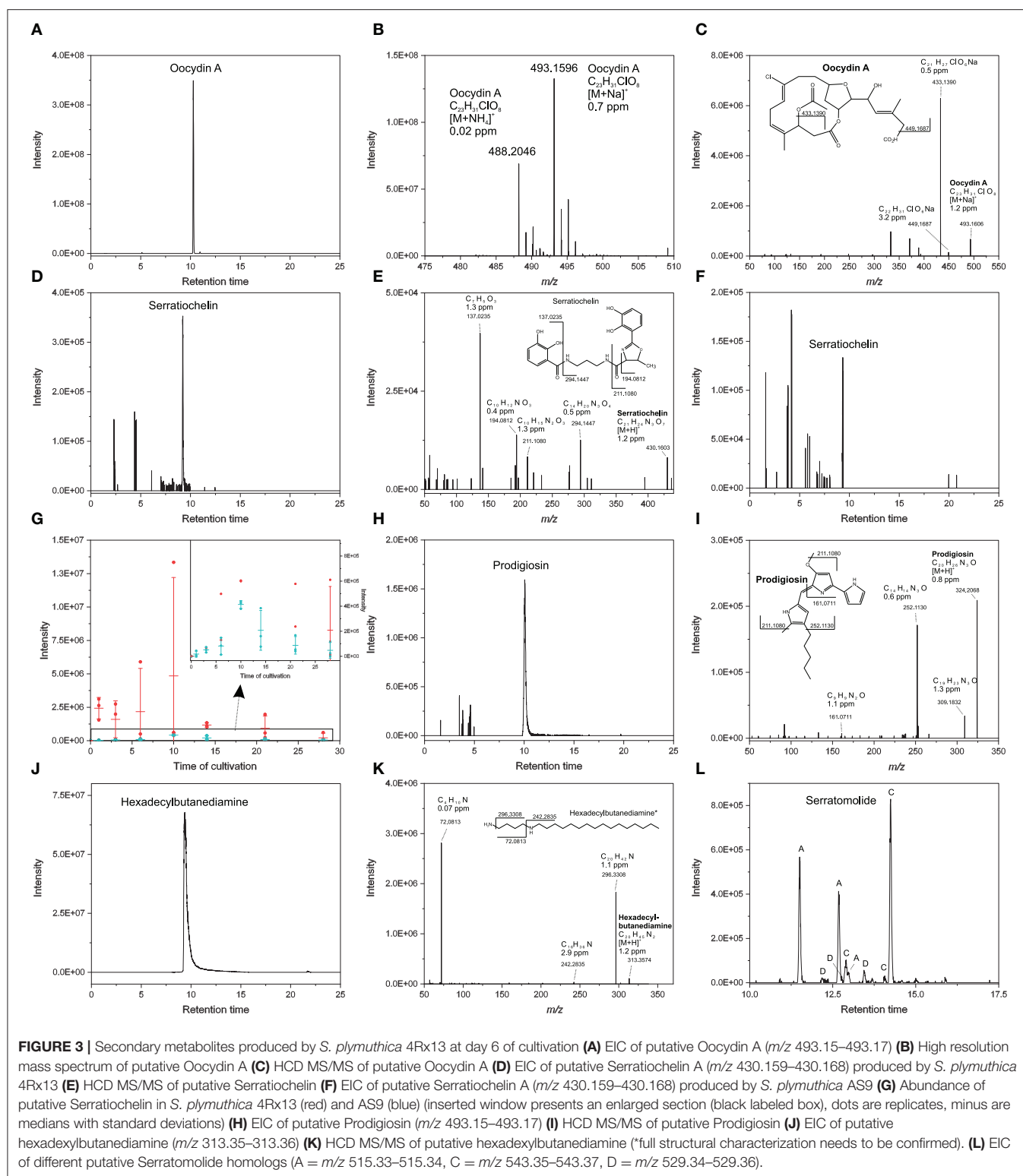
exclusively present or significantly increased in *S. plymuthica* 4Rx13 and *S. plymuthica* AS9, respectively (correlation > 0.9, $p < 0.001$).

These results demonstrated that the metabolic profiles of *S. plymuthica* 4Rx13 differ both interspecifically to *B. subtilis* B2g metabolites, but also intraspecifically to *S. plymuthica* AS9 metabolites.

Release of Different Secondary Metabolites Represents a Contributing Factor to Inter- and Intraspecific Variations in Metabolite Profiles

To explore whether secondary metabolites produced by *S. plymuthica* 4Rx13, *S. plymuthica* AS9 and *B. subtilis* B2g reflect inter- and intraspecific metabolic differences, we used a targeted approach by manually analyzing accurate masses, tandem mass spectra and computing Sirius and GNPS of exclusively present or significantly increased mass features at certain time points during growth of each strain. In *S. plymuthica* 4Rx13 we observed exclusive features with $[M+Na]^+$ m/z 493.1596 and $[M+NH_4]^+$ m/z 488.2046 corresponding to the molecular formula of $C_{23}H_{31}ClO_8$ ($\Delta ppm = 0.7$, calcd. m/z $[M+Na]^+$

493.15997, Δppm 0.02 calcd. m/z $[M+NH_4]^+$ 488.2045) (Figures 3A,B). This molecular formula was confirmed by Sirius (first hit with a Sirius score of 92.9%, isotope score: 10.2 tree score: 19.62; peak explained 3/15; total explained 34.251%) and isotopic patterns and corresponds to the haterumalide Oocycin A. The tandem mass spectrum, which showed fragments at m/z 449.1687 ($C_{22}H_{31}ClO_6Na$, Δppm 0.5) and m/z 433.1390 ($C_{21}H_{27}ClO_6Na$, Δppm 3.2), is in agreement with previously reported data of Oocycin A (Figure 3C, Matilla et al., 2012). With 42.295% similarity at rank 1, the computational tandem mass spectrum analysis using CSI:FingerID further supported the assignment of this feature as Oocycin A. Furthermore, we detected a mass feature of $[M+H]^+$ m/z 430.1603 corresponding to the molecular formula of $C_{21}H_{23}N_3O_7$ ($\Delta ppm = 1.2$, calcd. m/z $[M+H]^+$ 430.16088) (Figures 3D,E). Tandem mass spectral analysis showed fragments at m/z 294.1447 ($C_{14}H_{20}N_3O_4$, Δppm 0.5), m/z 211.1080 ($C_{10}H_{15}N_2O_3$, Δppm 1.3), m/z 194.0812 ($C_{10}H_{12}NO_3$, Δppm 0.4) and m/z 137.0235 ($C_7H_5O_3$, Δppm 0.02), which strongly indicated the production of the catecholate siderophore Serratichelin A by *S. plymuthica* 4Rx13 (Figure 3E). In contrast to Oocycin A, Serratichelin is also released by *S. plymuthica* AS9, however, in lower amounts compared to *S. plymuthica* 4Rx13 during cultivation period



(Figures 3E,G). *S. plymuthica* AS9 showed an exclusive mass feature at m/z 324.2068 corresponding to molecular formula of $C_{20}H_{25}N_3O$ ($\Delta\text{ppm} = 0.8$, calcd. $[M+H]^+$ m/z 324.2070) (Figures 3H,I). This molecular formula was confirmed by

Sirius as first hit with a Sirius score of 98.7%, tree score of 12.1%, 3 of 19 explained peaks and total explaining of 45.4%. The tandem mass spectral analysis showed fragments at m/z 309.1832 ($C_{19}H_{23}N_3O$, Δppm 1.3), m/z 252.1130

($C_{14}H_{14}N_3O$, Δ ppm 0.6), m/z 161.0711 ($C_9H_9N_2O$, Δ ppm 1.1) (**Figure 3I**), which is in agreement with entries in GNPS library for Prodigiosin (Spectrum ID CCMSLIB00005435440 and CCMSLIB00000072234). This collective information strongly indicates the presence of Prodigiosin. Prodigiosin was solely detected in *S. plymuthica* isolate AS9. Although *S. plymuthica* AS9 is genetically capable of producing broad-spectrum zeamine-related antibiotics (Masschelein et al., 2013), we did not detect mass features corresponding to these known zeamines (Zeamine I, II) in the extract of *S. plymuthica* AS9. During the search for the zeamines, we observed a *S. plymuthica* AS9 unique mass feature m/z 313.3576 corresponding to molecular formula of $C_{20}H_{44}N_2$ (Δ ppm = 0.7, calcd. m/z $[M+H]^+$ 313.3577; **Figures 3J,K**). This molecular formula corresponds to a hexadecylbutanediamine structure that shows similarities to the zeamine antibiotics (**Figure 3J**). Analysis using Sirius 4 revealed only one hit with a Sirius score of 100% corresponding to molecular formula of $C_{20}H_{44}N_2$ (tree score: 20.58; peak explained 3/22; total explained 47.16%) Tandem mass spectral fragments at m/z 296.3308 ($C_{20}H_{42}N$, Δ ppm 1.1), m/z 242.2835 ($C_{16}H_{36}N$, Δ ppm 2.9) and m/z 72.0813 ($C_4H_{10}N$, Δ ppm 0.07) strongly indicated the hexadecylbutanediamine structure (**Figure 3K**), however, full structural characterization via synthesis and NMR has to be performed in future. Further putatively identified exclusive secondary metabolites from *S. plymuthica* AS9 were found to belong to the Serratamolide family (**Figure 3I**), including three homologs of Serratamolide A ($[M+H]^+$ m/z 515.3343, Δ ppm 2, calcd. m/z $[M+H]^+$ 515.3327 for molecular formula $C_{26}H_{46}N_2O_8$, which was the first hit in Sirius with a Sirius score of 87.6%, isotope score of 6.25, tree score of 56.7 by 9 of 27 peaks explained and a total explaining of 51.7%), two homologs of Serratamolide C ($[M+H]^+$ m/z 543.3657, Δ ppm 2.2, calcd. m/z $[M+H]^+$ 543.36399 for $C_{28}H_{50}N_2O_8$, which was the first hit in Sirius with a Sirius score of 36.8%, isotope score of 5.57, tree score of 41.69 by 8 of 29 peaks explained leading to a total explaining of 37.8%) and three homologs of Serratamolide D ($[M+H]^+$ m/z 529.35034, Δ ppm 3, calcd. m/z $[M+H]^+$ 529.3483 for $C_{27}H_{48}N_2O_8$). Due to low abundances of Serratamolide D homologs, we have not been able to acquire sufficient mass spectra to confirm their identity via Sirius. Future investigations will have to focus on full characterization of the Serratamolide homologs produced by *S. plymuthica* AS9.

None of the *S. plymuthica* secondary metabolites were released by *B. subtilis* B2g. Accurate mass measurements revealed several putative lipopeptide isomers belonging to the families of surfactins, bacillomycin D and plipastatins in the extract of *B. subtilis* B2g (**Figure 4, Supplementary Table 1, Table 1**), which have been not observed in *S. plymuthica* isolates. Surfactins were detected at $[M+H]^+$ m/z 980.6283 ($C_{49}H_{85}N_7O_{13}$, Δ ppm 0.5), $[M+H]^+$ m/z 994.6440 ($C_{50}H_{87}N_7O_{13}$, Δ ppm 0.5), $[M+H]^+$ m/z 1008.659 ($C_{51}H_{89}N_7O_{13}$, Δ ppm 0.1), $[M+H]^+$ m/z 1022.6751 ($C_{52}H_{91}N_7O_{13}$, Δ ppm 0.4), $[M+H]^+$ m/z 1036.6907 ($C_{53}H_{93}N_7O_{13}$, Δ ppm 0.3), $[M+H]^+$ m/z 1050.7062 ($C_{54}H_{95}N_7O_{13}$, Δ ppm 0.2) and 1064.7222 ($C_{55}H_{97}N_7O_{13}$, Δ ppm 0.5) (**Figures 4A,B**). Members of

the bacillomycin D family were observed at $[M+H]^+$ m/z 1003.5094 ($C_{46}H_{70}O_{15}N_{10}$, Δ ppm 0.1), $[M+H]^+$ m/z 1017.5254 ($C_{47}H_{72}O_{15}N_{10}$, Δ ppm 0.3), $[M+H]^+$ m/z 1031.5423 ($C_{48}H_{74}N_{10}O_{15}$, Δ ppm 1.4), $[M+H]^+$ m/z 1045.5581 ($C_{49}H_{76}N_{10}O_{15}$, Δ ppm 1.7) (**Figures 4C,D**). Several plipastatins were detected at $[M+H]^+$ m/z 1449.7898 ($C_{71}H_{108}N_{12}O_{20}$, Δ ppm 1.5), $[M+H]^+$ m/z 1463.8047 ($C_{72}H_{110}N_{12}O_{20}$, Δ ppm 1), $[M+H]^+$ m/z 1477.8188 ($C_{73}H_{112}N_{12}O_{20}$, Δ ppm 1.4), $[M+H]^+$ m/z 1491.8362 ($C_{74}H_{114}N_{12}O_{20}$, Δ ppm 1.1), $[M+H]^+$ m/z 1505.84998 ($C_{75}H_{116}N_{12}O_{20}$, Δ ppm 0.1), $[M+H]^+$ m/z 1519.8639 ($C_{76}H_{118}N_{12}O_{20}$, Δ ppm 1.2) (**Figures 4E,F, Table 1**). For each lipopeptide different isomers could be detected, however, complete characterization of these isomers is beyond the scope of this study.

These results show that the release of different secondary metabolites is contributing to inter- and intraspecific variations in metabolite profiles between the *S. plymuthica* isolates 4Rx13 and AS9 and *B. subtilis* B2g. However, a high number of further varying, contributing factors still need to be elucidated.

Interspecific Co-cultivation of *S. plymuthica* 4Rx13 and *B. subtilis* B2g Showed Consistently Distinct Metabolic Profiles Compared to Mono-cultivated Species

In order to evaluate whether bacterial interaction-induced changes in released metabolites can be monitored by metabolic profiling, we used a structured low diversity co-culture model between *S. plymuthica* 4Rx13 and *B. subtilis* B2g, which previously indicated an enormous potential of interaction between both partners (Kai and Piechulla, 2018).

We reproduced the co-cultivation assays and observed that the interplay of *S. plymuthica* 4Rx13 with *B. subtilis* B2g caused a distinct and bright interaction zone [as already described in Kai and Piechulla (2018)], which was not observed in self-paired cultures (**Figure 5A**).

In order to evaluate how these different phenotypes are reflected by metabolic differences, we scraped off the cells of self-paired and co-cultivated bacteria from the agar and extracted the metabolites released into the agar at different time points (day 1, 3, 6, 7, 10, 14, 21, 28, and 30). These extracts were analyzed in a non-targeted approach using UHPLC/HRMS and processed with XCMS. To evaluate the metabolic profiles, PAM cluster analyses were conducted (Kaufman and Rousseeuw, 1990). PAM clustering plots from cultures at day 6 of cultivation showed four distinct clusters [**Figure 5B**, cluster 1–4Rx13 mono, cluster 2–4Rx13+B2g interaction, cluster 3 – B2g mono, cluster 4 – ctrl (agar)]. This clear separation was not observable at day 1 and 3 of cultivation (**Supplementary Figure 1**). From day 6, the clustering continued until the later stages of growth (**Supplementary Figure 1**, with the exemption of day 28). These results suggest that the metabolic profiles of the co-cultures of *S. plymuthica* 4Rx13 with *B. subtilis* B2g differ from the metabolic profiles of each mono-culture.

TABLE 1 | Members of the plipastatin family (known and putative variants) produced by *B. subtilis* B2g—plipastatin isomers and variants that are more pronounced in interaction are marked in red, n.d., not determined due to insufficient MS/MS.

Name	Chemical formula	Monoisotopic mass (M) <i>m/z</i>	Isomer	measured <i>m/z</i> [M+2H] ²⁺	calc. <i>m/z</i> [M+2H] ²⁺	Δppm	measured <i>m/z</i> [M+H] ⁺	calcd. <i>m/z</i> [M+H] ⁺	Δppm
Plipastatin	C ₇₁ H ₁₀₈ N ₁₂ O ₂₀	1448.7797	A1	725.39841	725.39742	1.4	1449.7898	1449.7875	1.5
			A1						
			A2						
Plipastatin	C ₇₂ H ₁₁₀ N ₁₂ O ₂₀	1462.7954	B1	732.40649	732.40524	0.8	1463.8047	1463.8032	1
			B2						
			A1 and B2						
			A1						
Plipastatin	C ₇₃ H ₁₁₂ N ₁₂ O ₂₀	1476.811	B1	739.41381	739.41307	1	1477.8208	1477.8188	1.4
			B1						
			B2						
			A1						
Plipastatin	C ₇₄ H ₁₁₄ N ₁₂ O ₂₀	1490.8266	B1	746.42243	746.42089	2.1	1491.8362	1491.8387	1.1
			B2						
			A1						
Plipastatin	C ₇₅ H ₁₁₆ N ₁₂ O ₂₀	1504.8423	n.d.	753.4287	753.4287	0.001	1505.84998	1505.8501	0.1
Plipastatin	C ₇₆ H ₁₁₈ N ₁₂ O ₂₀	1518.86799	n.d.	760.4363	760.4365	0.3	1519.8639	1519.86581	1.2
Plipastatin V1	C ₇₁ H ₁₁₀ N ₁₂ O ₂₁	1466.7902	n.d.	734.40378	734.40270	1.5	1467.7999	1467.79812	1.2
Plipastatin V2	C ₇₂ H ₁₁₂ N ₁₂ O ₂₁	1480.8059496	n.d.	741.41101	741.41053	0.7	1481.8151	1482.82160	0.9
Plipastatin V3	C ₇₃ H ₁₁₄ N ₁₂ O ₂₁	1494.8215996	n.d.	748.41870	748.41835	0.5	1495.83191	1495.8294246	1.7
Plipastatin V4	C ₇₄ H ₁₁₆ N ₁₂ O ₂₁	1508.8372497	n.d.	755.42680	755.42618	0.8	1509.8431	1509.8451	1.3
Plipastatin V5	C ₇₅ H ₁₁₈ N ₁₂ O ₂₁	1522.8523513	n.d.	762.43459	762.43400	0.7	1523.8575	1523.8607	2.1

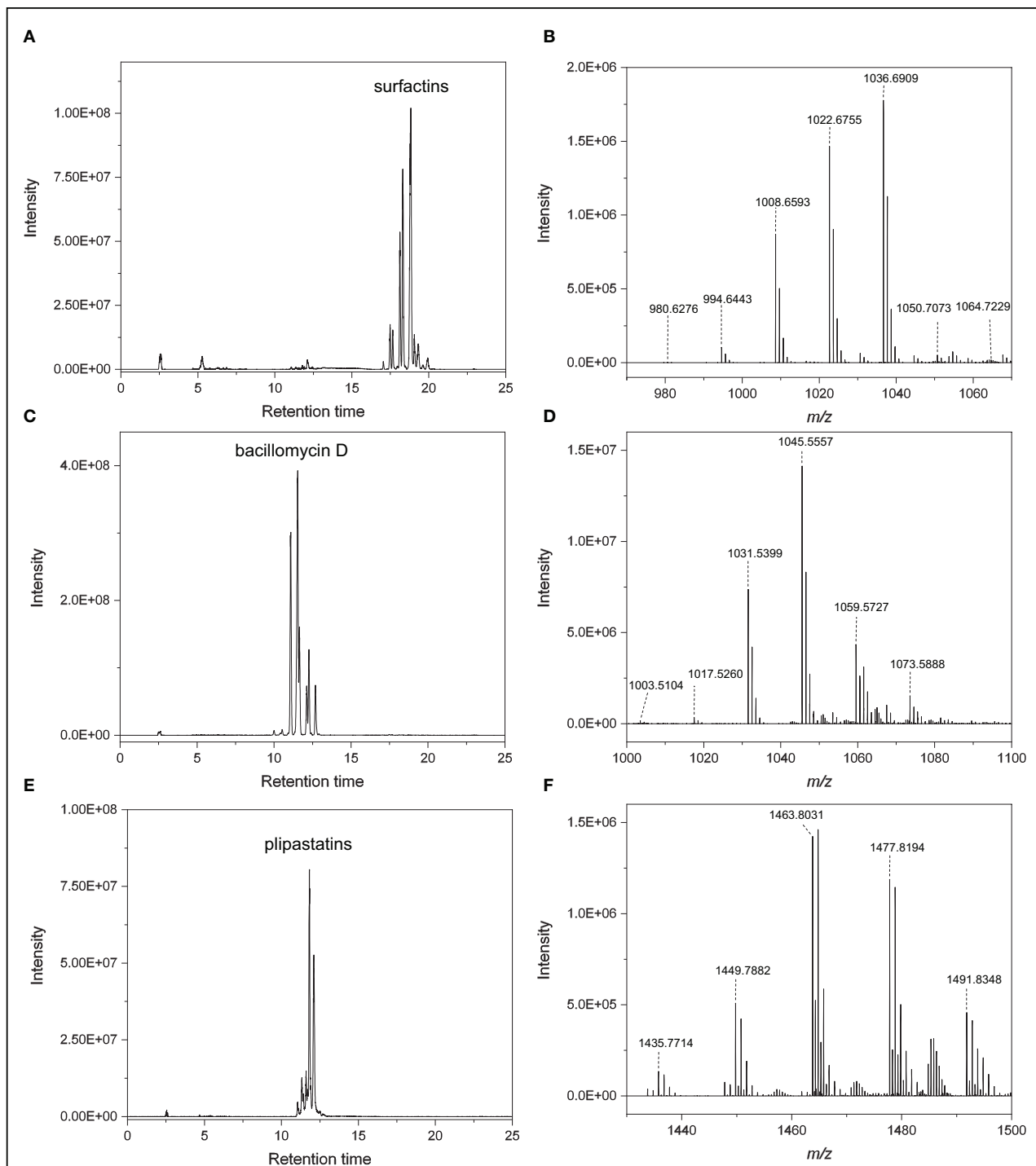
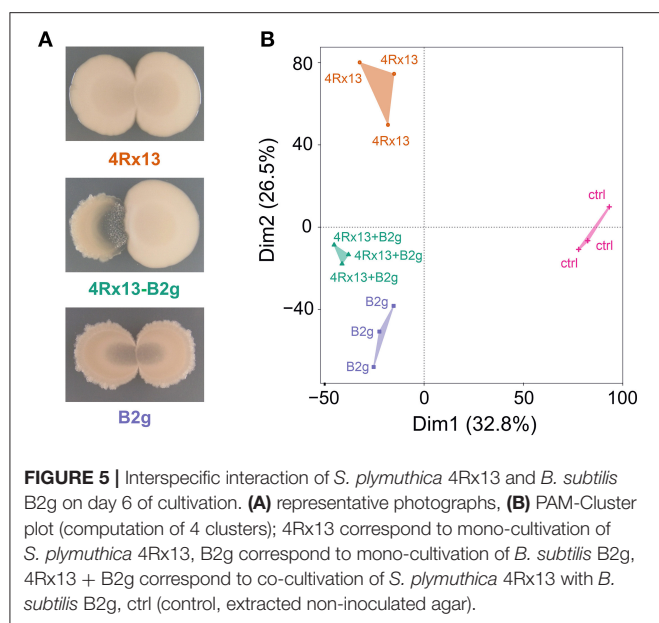


FIGURE 4 | Lipopeptides produced by *B. subtilis* B2g at day 21 of cultivation **(A)** EIC of compounds putatively belonging to the surfactin family (m/z 982, 986, 1,010, 1,023, 1,037, 1,050, 1,051, and 1,065). **(B)** High resolution mass spectrum (RT 16.78–21.46 min). **(C)** EIC of compounds putatively belonging to the bacillomycin D family (m/z 1,004, 1,018, 1,046, 1,060, 1,074). **(D)** High resolution mass spectrum (RT 9.45–12.75 min). **(E)** EIC of compounds putatively belonging to plipastatin family (m/z 1,436, 1,450, 1,464, 1,478, 1,492). **(F)** High resolution mass spectrum (RT 9.45–12.75 min).



Intraspecific Interaction of *S. plymuthica* 4Rx13 and *B. subtilis* B2g Showed Altered Mass Features Compared to Mono-cultivated Species

In order to ascertain the metabolic patterns connected to the distinct metabolic profiles, we performed correlation pattern analysis using MetaboAnalyst. Thereby, we searched for metabolic features that were altered in co-cultivation of interacting *S. plymuthica* 4Rx13 with *B. subtilis* B2g in comparison to both mono-cultivated strains and control. Setting a correlation threshold of 0.6, we found a total of 173 mass features (Supplementary Tables 2, 3). Using this approach, no mass feature was solely detected in co-cultivation. Mass features were instead differentially released by the co-cultivated strains in relation to the mono-cultivated ones (Figure 6, Supplementary Table 2). The longer both strains were co-cultivated, the more mass features were detected above the correlation threshold of 0.6 (Figure 6A). Next, we evaluated whether mass features were only altered at one single time point or over a certain time period. No mass feature was co-cultivation-induced over the whole time range. One hundred and three features (60 %) were differing at one single time point only, while 70 features (40%) were increased over a wider time range (44 features (25%) at two time points, 21 features (12%) at three time points, 6 features (3.5%) at four time points; Figure 6B, Supplementary Table 3).

Amount of Specific Compounds of the Plipastatin Family Is Increased in the Co-cultivation of *S. plymuthica* 4Rx13 With *B. subtilis* B2g

Next, we were interested in compounds corresponding to the mass features that are more pronounced in the co-cultivation

of *S. plymuthica* 4Rx13 and *B. subtilis* B2g. We focused on mass features, which showed most prominent correlation patterns over a wider cultivation range (Figure 7). Although we used the respective algorithm to demask isotopologues and adducts, admittedly not every single mass feature represents one individual compound. Especially, isotopologues of doubly protonated compounds were still observed, however, since these features correlated with the monoisotopic mass features, their presence supported the following results. Accurate masses of certain increased mass features corresponded to doubly protonated ions belonging to four compounds of the plipastatin family ($[M+2H]^{2+}$ m/z 725.39841, $[M+2H]^{2+}$ m/z 732.40524, $[M+2H]^{2+}$ m/z 739.41381, $[M+2H]^{2+}$ m/z 746.42243; Table 1). Verification of the statistical calculation was performed by extraction and plotting the respective m/z of every feature using XCMS package in RStudio (Figure 7). Interestingly, only specific homologs of the plipastatins were increased in co-cultivation. By determination of accurate masses of specific reporter ions in the acquired tandem mass spectra (Pathak et al., 2012, Kaki et al., 2020), we further characterized the isomers according to presence of specific amino acids in their peptide sequence and classified them into class A and B (Supplementary Figure 2, Table 1, Supplementary Table 4). Of those isomers, plipastatin A1 ($[M+H]^+$ m/z = 1448.7797), plipastatin B1 ($[M+H]^+$ m/z = 1476.811) and plipastatin B2 ($[M+H]^+$ m/z = 1490.8266) were increasingly produced by *B. subtilis* B2g due to co-cultivation with *S. plymuthica* 4Rx13. The peak corresponding to the co-cultivation triggered plipastatin with $[M+H]^+$ m/z = 1462.7954 showed class A and B reporter ions in its mass spectrum indicating two co-eluting plipastatin isomers. Therefore, we currently assume an increased production of either one or both of these isomers (Supplementary Figure 2). Future investigations including synthesis are needed to unambiguously verify these results, as well as to determine the exact fatty acid sequence for all four increased plipastatins.

In addition, we detected further co-cultivation increased doubly protonated features at $[M+2H]^{2+}$ m/z 734.40378 ($C_{71}H_{110}N_{12}O_{21}$, Δppm 1.5), $[M+2H]^{2+}$ m/z 741.41101 ($C_{72}H_{112}N_{12}O_{21}$, Δppm 0.7), $[M+2H]^{2+}$ m/z 748.41870 ($C_{73}H_{114}N_{12}O_{21}$, Δppm 0.5), $[M+2H]^{2+}$ m/z 755.42680 ($C_{74}H_{116}N_{12}O_{21}$, Δppm 0.8), $[M+H]^{2+}$ m/z 762.43459 ($C_{75}H_{118}N_{12}O_{21}$, Δppm 0.7) (Table 1). The accurate masses of these features showed a consecutive mass difference of m/z 18.01054 corresponding to H_2O (Δppm 1.4) to the known plipastatins indicating that these co-cultivation increased features correspond to plipastatin variants (labeled as V1-V5). For the proposed chemical formulas, we did not find literature references and no entries in PubChem (<https://pubchem.ncbi.nlm.nih.gov/>) suggesting putative novel plipastatin variants. Again, we verified the data by extraction and plotting of the respective m/z (Figure 8). As shown in Figure 8, the monoisotopic masses of each feature presented at least three to four isomers. Again, only certain isomers were increasingly produced in response to the interaction. Due to the low abundance of the putative plipastatin variants, the MS/MS spectra are so far insufficient for precise structure elucidation. However, molecular networking using these poor quality mass spectra already indicated a clear

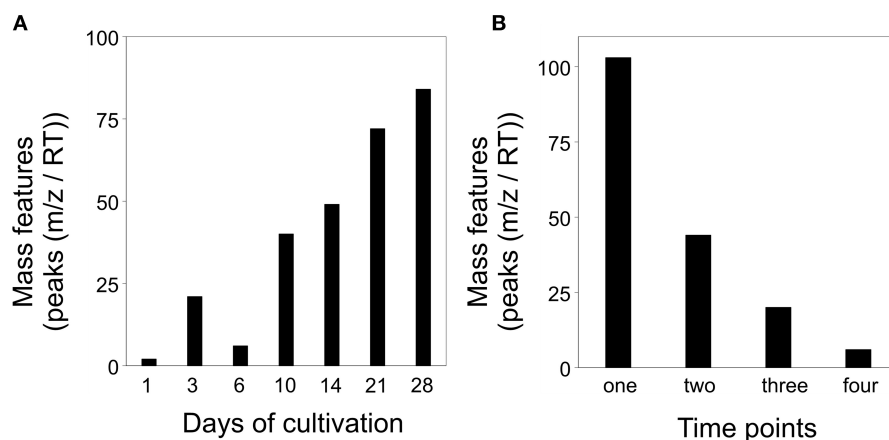


FIGURE 6 | Altered mass features [peaks (m/z /RT)] in co-cultivation of *S. plymuthica* 4Rx13 and *B. subtilis* B2g in comparison to mono-cultivated strains and medium control (correlation threshold > 0.6) **(A)** Number of co-cultivation correlating mass features in relation to each day of cultivation (extracts were sampled at day 1, 3, 6, 10, 14, 21, and 28 of mono and co-cultivation of *S. plymuthica* 4Rx13 and *B. subtilis* B2g). **(B)** Frequency of occurrence of each co-cultivation correlating mass feature.

connection for four of the searched features to members of the known plipastatins (Figure 9).

Intraspecific Co-cultivation of *S. plymuthica* 4Rx13 and *S. plymuthica* AS9 Revealed a Distinct Interaction Zone and Showed Distinct Metabolic Profiles Compared to Mono-cultures

Next, we were interested in the intraspecific interaction potential of *S. plymuthica* 4Rx13 and performed similar interaction assays with the rhizobacterial *S. plymuthica* isolate AS9.

Co-cultivation led to a clear and distinct interaction zone, which was not observed in self-paired cultures (Figure 10A). Images of the interaction zone indicate that both partners are suppressed by the interaction. Development of this zone starts at day 1 of interaction (Figure 10C). At day 6, small colony-like spots appeared in the interaction zone.

After metabolite extraction, XCMS analysis and data processing, the PAM clustering plots from cultures at day 6 of cultivation showed four distinct clusters [Figure 10B, Cluster 1—4Rx13 mono, 2—4Rx13+AS9 interaction, 3—AS9 mono, 4—ctrl (agar)]. Similar to the 4Rx13 – B2g interaction, this clear separation was not observed at day 1 and 3 of cultivation (Supplementary Figure 3). The clear separation was only present at day 6 and 7 of cultivation. At day 10, the PAM algorithm calculated one bigger cluster including mono-cultivated *S. plymuthica* 4Rx13 and co-cultivated *S. plymuthica* 4Rx13/AS9 metabolites, which was also observed in the further stages of cultivation. At day 28 the metabolic differences are completely abolished. These results suggest that the metabolic profiles of the co-cultures differ at specific culture stages from the metabolic profiles of the mono-cultures. During later growth, the metabolites released by *S. plymuthica* 4Rx13 seem to dominate the metabolic profiles of the co-culture.

Intraspecific Interaction of *S. plymuthica* 4Rx13 and *S. plymuthica* AS9 Showed Altered Mass Features Compared to Mono-cultivated Species

Next, we analyzed for patterns that were differentially featured in intraspecific co-cultivation of interacting *S. plymuthica* 4Rx13 with *S. plymuthica* AS9 in comparison to both mono-cultivated strains and control. We raised the threshold of the correlating patterns to 0.8 due to the lower number of replicates ($n = 3$). In total, we found in interaction 87 differentially-induced mass features (Supplementary Tables 5, 6). After a constant increase from day 1 until day 10, followed by a drop at day 14, the highest change was observed at day 21 of interaction (Figure 11A). At day 28 of interaction, the altered mass features decreased again. No single mass feature was increased over the whole time range of co-cultivation. Seventy-one features (81.6 %) differed at one single time point only, while 16 features (18.4%) were increased over a wider time range (14 features (16.1%) at two time points, 2 features (2.3%) at three time points; Figure 11B, Supplementary Table 6).

Several Short Peptides Are Increased in Co-cultivation of *S. plymuthica* 4Rx13 With *S. plymuthica* AS9

Across all co-cultivation correlating mass features, we focused on a group of single and doubly protonated features that showed similar tandem mass spectra, exemplarily shown for five prominent mass features in Figure 12. These features were mostly produced by *S. plymuthica* 4Rx13 mono-cultures, too, however in lower amounts (Figure 12, Supplementary Figure 4). Features that have been found to be increased in co-cultivation and which are also produced by both mono-cultivated strains were excluded in this studies (see Supplementary Figures 4D,E,G,Q,T,W). For

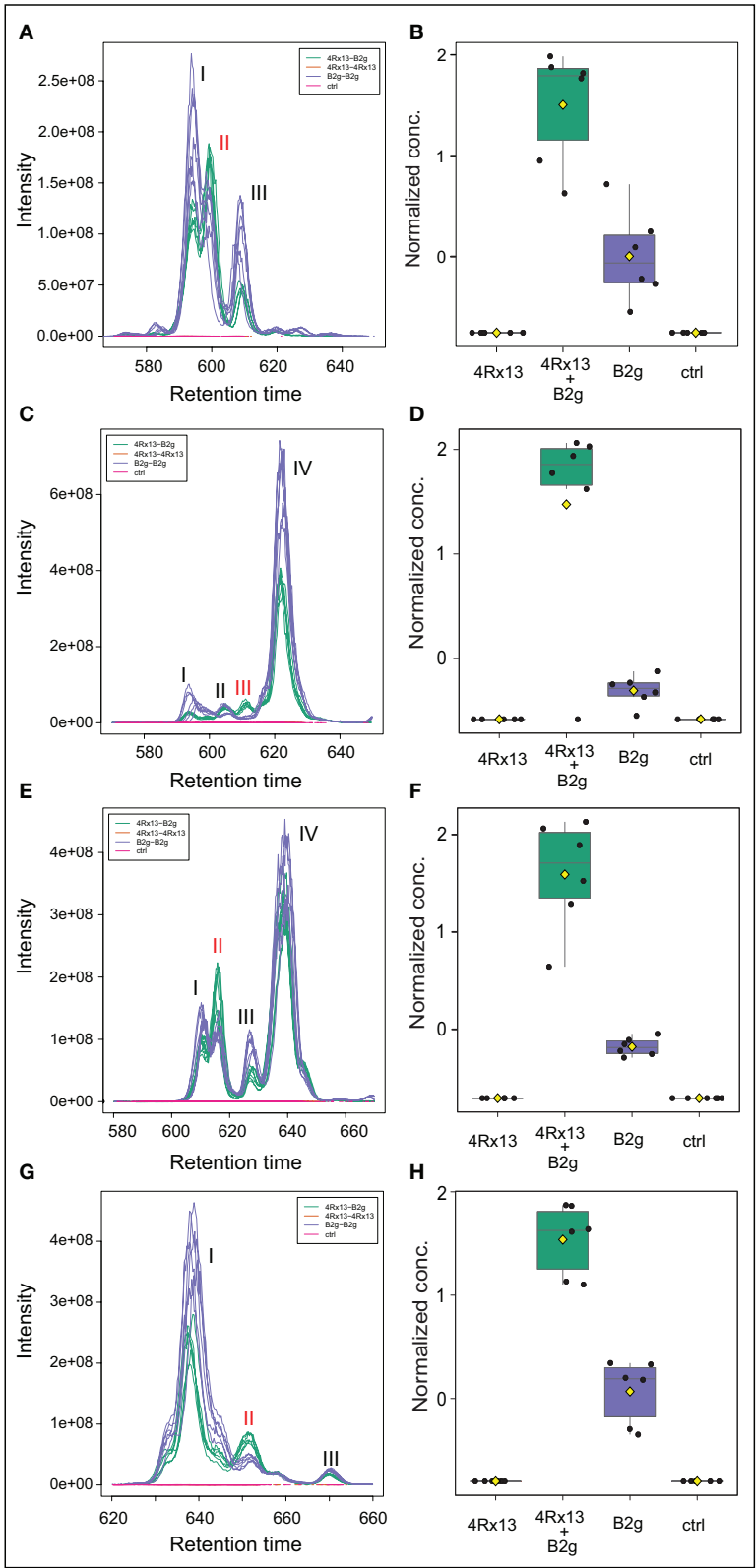


FIGURE 7 | Specific plipastatin isomers are increased in co-cultivation of *S. plymuthica* 4Rx13 with *B. subtilis* B2g. Computed extracted ion chromatograms (respective *m/z* of every plipastatin was extracted and plotted using XCMS, cEIC) and normalized concentration of plipastatins at day 21 of co-cultivation of (Continued)

FIGURE 7 | *S. plymuthica* 4Rx13 with *B. subtilis* B2g (4Rx13+B2g), mono-cultivation of respective species (4Rx13; B2g) and medium control (ctrl). **(A)** cEIC plipastatin [M+2H]²⁺ *m/z* 725.3984. **(B)** Normalized conc. of isomer II (A1). **(C)** cEIC plipastatin [M+2H]²⁺ *m/z* 732.4052. **(D)** Normalized conc. isomer III (A1 and B2). **(E)** cEIC plipastatin [M+2H]²⁺ *m/z* 739.4138. **(F)** Normalized conc. of isomer II (B1). **(G)** cEIC plipastatin [M+2H]²⁺ *m/z* 746.4209. **(H)** Normalized conc. of isomer II (B2).

some features, two isomers were detected (Figure 12M, Supplementary Figures 4B,D–F,H–L,O). Mass range of all other features along with occurring fragments at *m/z* 70.0657, 86.0605, 127.0867, and 155.0814 indicate related short proline-containing peptides. The high spectral similarities of tandem mass spectra and the peptide prediction was strengthened for several of these features by a molecular networking approach (Figure 13). Features with [M+H]⁺ *m/z* 414.2352, 430.2302, 471.2568, 511.2883, 529.2985, 584.3408, 651.3471, 792.4258, 865.4427 clustered in a network containing the previously annotated small peptides Lys-Ile, Ile-Val, Ile-Val-Lys, Lys-Val, PyroGlu-Pro-Lys and Pro-Val, while [M+H]⁺ *m/z* 346.2085 was networking with a Pro-Arg peptide. Fragmentation pattern analysis using Sirius was further used to putatively determine chemical formulae from single protonated ions only, since doubly protonated features are not supported by Sirius (Table 2). Thereby, nine out of eleven selected chemical formulae were computed at first rank with seven features showing a Sirius scores above 80 %. For two features, we selected the second ranked formula due to unlikely elemental composition of the first rank formula. PubChem search for these chemical formulae revealed several possibilities of short peptides with up to 8 amino acids. Future structural investigations are needed to confirm these assumptions, as well as to elucidate the relationship between these individual peptides.

DISCUSSION

Bacteria are not solitary organisms but rather, maintain complex interactions within microbial communities to ensure their survival (Nadell et al., 2016; Yanni et al., 2019). Bacterial metabolism differ in these communities due to competitive and cooperative actions compared to single existence (Little et al., 2008). As a result, some metabolites that are not produced by solitary living bacteria, or are produced only weakly, are assumed to be biosynthesized more abundantly by the same bacteria within communities, e.g., toxins, antibiotics or antifungal compounds. In contrast, when living in a community there is no need to synthesize metabolites equally to solitary life, since metabolites can be exchanged between members of the community (Phelan et al., 2012). To understand the basic principles of the relations between the individuals of bacterial species within these communities, we need to apply a wide range of experimental holistic and reductionistic approaches. Here, we evaluated metabolic profiling using multivariate analyses combined with classical mass spectrometry identification as well as emerging computational identification tools as approaches to study changes in metabolite excretion of the rhizobacteria *S. plymuthica* 4Rx13, *B. subtilis* B2g and *S. plymuthica* AS9 due to bacterial interaction.

Change of Metabolic Status During Cultivation

Our first results demonstrated that changes in metabolism during cultivation of all three tested bacteria, the *S. plymuthica* isolates 4Rx13 and AS9 as well as *B. subtilis* B2g, can be clearly distinguished using metabolic profiling of metabolites released into the agar. These changes are most likely due to the depletion of nutrients during the *in vitro* cultivation on agar (Meyer et al., 2014), but might also be related to biosynthesis of primary and specialized metabolites coordinated to different growth stages (Stein, 2005; Sanchez and Demain, 2008; Raaijmakers et al., 2010). The observed decrease of variations late in cultivation time (day 28 and day 30) might indicate a reached steady state of released metabolites, however, cultivation over a longer period of time is needed to clarify this hypothesis. Future investigations will tackle the exact background of the observed alterations. However, taking these results into consideration, we might already need to reconsider the currently applied co-cultivation assays, which are, for instance, performed by placing droplets of two liquid cultures at the same time point on solid media or in more recent approaches using microfluidic devices (Liu et al., 2010; Park et al., 2011; Watrous et al., 2012; Burmeister et al., 2019). Although these assays are very useful for evaluating molecular differences in interacting microbial communities (Watrous et al., 2012), we might miss a lot of interplay due to non-optimized time windows of co-cultivation. Inoculations of two bacterial strains each at a different time point might cause various effects always depending on the current metabolic status of each strain. More dynamic studies in which the bacteria are grown separately from each other over a certain time before allowing them to interact could verify this issue.

Inter- and Intraspecific Variations of Released Metabolites

Using metabolite profiling, we found an interspecific variation between metabolites of *S. plymuthica* 4Rx13 and *B. subtilis* B2g. This considerable interspecific contrast in which both strains showed almost similar numbers of different features was expectable, as the metabolism and physiology can be assumed to vary greatly due to the phylogenetic and morphological difference between *S. plymuthica* and *B. subtilis*. Chubukov and Sauer, for instance, found significant differences between metabolic phenotypes of model bacteria *E. coli*, which like *S. plymuthica* belong the family of *Enterobacteriaceae*, and *B. subtilis* when characterizing their stationary-phase metabolites (Chubukov and Sauer, 2014). Furthermore, *B. subtilis* is in general known for its production of different secondary metabolites including the lipopeptides surfactin, iturin, and plipastatin (Kakinuma et al., 1969; Peypoux et al., 1981; Nishikiori et al., 1986; Kluge et al., 1988; Stein, 2005), which are not described for *Serratia* species. Therefore, it was no surprise that exclusive lipopeptide

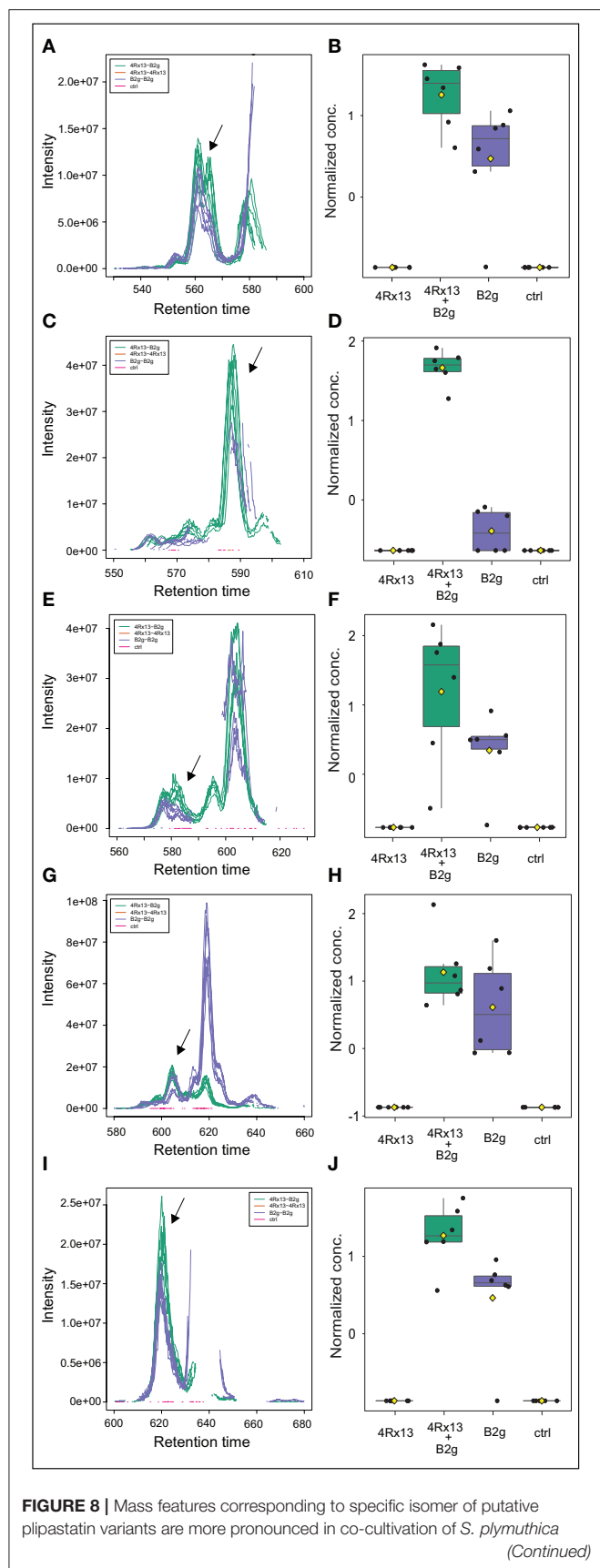
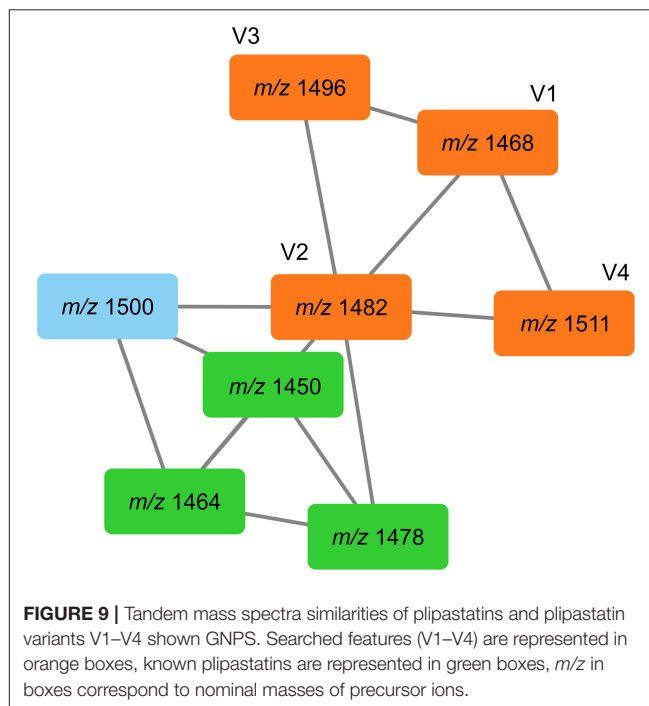
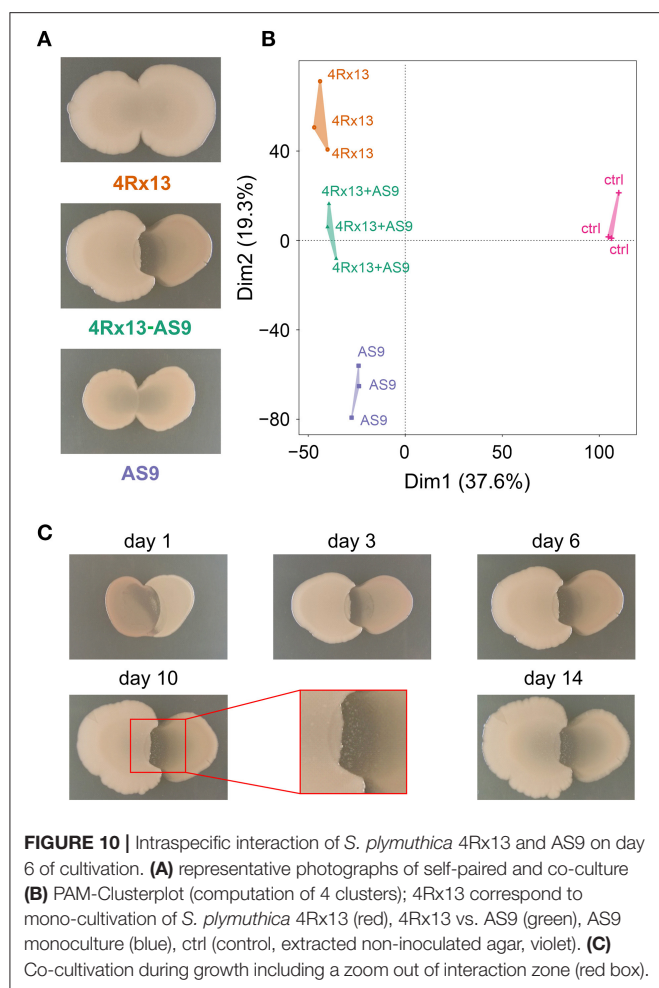


FIGURE 8 | 4Rx13 with *B. subtilis* B2g. Computed extracted ion chromatograms (respective m/z of every plipastatin variant was extracted and plotted using XCMS, cEIC) and normalized concentration of plipastatins at day 21 of co-cultivation of *S. plymuthica* 4Rx13 with *B. subtilis* B2g (4Rx13+B2g), mono-cultivation of respective species (4Rx13; B2g) and medium control (ctrl). (A) cEIC plipastatin variant 1 $[M+2H]^{2+}$ m/z 734.4037. (B) Normalized conc. of arrow labeled isomer. (C) cEIC plipastatin variant 2 $[M+2H]^{2+}$ m/z 741.411. (D) Normalized conc. of arrow labeled isomer. (E) cEIC plipastatin variant 3 $[M+2H]^{2+}$ m/z 748.4184. (F) Normalized conc. of arrow labeled isomer. (G) cEIC plipastatin variant 4 $[M+2H]^{2+}$ m/z 755.4268. (H) Normalized conc. of arrow labeled isomer. (I) cEIC plipastatin variant 5 $[M+2H]^{2+}$ m/z 762.4346. (J) Normalized conc. of arrow labeled isomer.



production (surfactin, bacillomycin D and plipastatin) by *B. subtilis* B2g were partly responsible for the interspecific differences, similarly to Oocycin A and Serratichelin that were exclusively produced by *S. plymuthica* 4Rx13. We have to admit that the extracts of both strains contained more promising secondary metabolites, which are currently under investigation.

More remarkable was the intraspecific variation we observed between excreted metabolites of the *S. plymuthica* isolates 4Rx13 and AS9. These high variations were unexpected since the main primary metabolism can be assumed to be similar, when related isolates from the same species that are isolated from similar rhizosphere habitats grow under identical *in vitro* conditions. With twice the number of exclusively—or increasingly produced features *S. plymuthica* 4Rx13 showed even higher intraspecific variation to *S. plymuthica* AS9 compared to interspecific variation to *B. subtilis* B2g. Of the differing features secondary metabolites produced by both isolates reflected the intraspecific metabolic differences.



While *S. plymuthica* 4Rx13 solely releases the haterumalide Oocydin A, *S. plymuthica* AS9 exclusively produces Prodigiosin, a putative hexadecylbutanediamine structure and several members of the Serratimolide family. The siderophore Serratiochelin was released by both strains, however, in higher amounts by *S. plymuthica* 4Rx13. The three secondary metabolites Serratiochelin A, Oocydin A and Prodigiosin have been previously described in *S. plymuthica* isolates (Grimont and Grimont, 2004; Matilla et al., 2012; Cleto et al., 2014). The production of the antimicrobial biosurfactant lipopeptide Serratimolide isomers has so far been found in the genus *Serratia*, however, only in two species *S. marcescens* and *S. surfactantifaciens* and not yet in *S. plymuthica* (Wassermann et al., 1961; Clements et al., 2019). Recent genome comparison via antiSMASH software revealed that *S. plymuthica* AS9 carries the Serratimolide *swrW* gene (Marques-Pereira et al., 2020). Our findings now demonstrate the ability of *S. plymuthica* AS9 to produce Serratimolide biosurfactants, although further profound structural characterization of individual isomers is needed to give an insight into the full lipopeptide profile. Since the found hexadecylbutanediamine structure shows similarities to the Zeamines, which are polyamine-polyketide-non-ribosomal

peptide antibiotics that are strongly active against various Gram-positive and Gram-negative bacteria by affecting the integrity of cell membranes; most probably due to interaction of the positively charged amino groups with the polyanionic LPS (Masschelein et al., 2015), their identity also needs structural confirmation in future. Furthermore, the remaining features that are exclusively released by *S. plymuthica* 4Rx13 and AS9 should be explored in more detail. These analyses in combination with continuing metabolite profiling of more *S. plymuthica* isolates will answer the question whether these high intraspecific variations represent a general phenomenon within the species *Serratia plymuthica*.

Interspecific Interaction Between *S. plymuthica* 4Rx13 and *B. subtilis* B2g

Preliminary phenotypic data of the interaction between the two rhizobacteria *S. plymuthica* 4Rx13 and *B. subtilis* B2g indicated an immense potential of inter-organismic crosstalk (Kai and Piechulla, 2018). Present PAM-clustering data show that the profiles of metabolites released during this interaction consistently vary from the profiles of both mono-cultivated bacteria. At the beginning of cultivation PAM-cluster analysis did not reveal clear separation. Since we found *B. subtilis* B2g mono-cultures clustering with non-inoculated agar extracts at day 1 and 3 of cultivation, we assume that is due to low concentration of released metabolites by *B. subtilis* B2g caused by their slower growth compared to *S. plymuthica* 4Rx13 (Kai and Piechulla, 2018). Similar results were observed by Zhou et al. (2011), who monitored the interaction of *Bacillus megaterium* and *Ketogulonicigenium vulgare* over 72 h using PCA. They found intracellular metabolites of co-cultures at a shorter distance to the mono-cultures at 48 h than at 72 h (Zhou et al., 2011). The fluctuation of PAM-clustering that we observed late in growth (day 28 and 30) indicates an decreasing variation of metabolite content between mono- and interacting cultures with increasing cultivation time. More precisely, the data suggest that metabolites, which are produced by *S. plymuthica* 4Rx13 might shape the metabolite content of an established structured co-culture between *S. plymuthica* 4Rx13 and *B. subtilis* B2g. Future investigations in which both strains interact with each other over a longer period of time can clarify this hypothesis.

In recent literature it is described that interspecies crosstalk can trigger “cryptic” genes to produce novel natural products (Scherlach and Hertweck, 2009; Ochi, 2017; Van Bergeijk et al., 2020). So far, we did not detect features that were solely present in co-cultivation indicating that the distinct multivariate cluster separation based most likely on altered production and consumption of metabolites by the co-cultured strains in comparison to the mono-cultivated ones rather than the release of “cryptic” encoded natural products. The number of metabolites varying between mono- and co-cultivation increased with the progressing of cultivation, indicating an enhanced interaction potential with establishment of the co-cultivation. Within this study we focused on exploring the most prominent metabolite differences occurring due to interaction. One class of

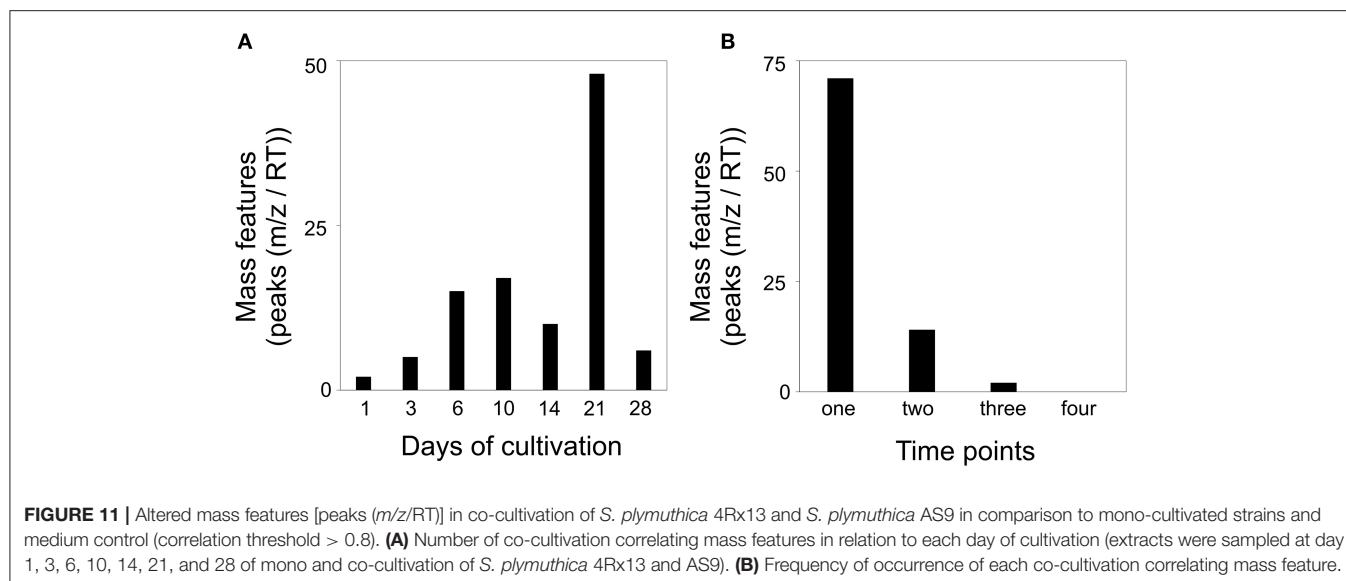


FIGURE 11 | Altered mass features [peaks (m/z /RT)] in co-cultivation of *S. plymuthica* 4Rx13 and *S. plymuthica* AS9 in comparison to mono-cultivated strains and medium control (correlation threshold > 0.8). **(A)** Number of co-cultivation correlating mass features in relation to each day of cultivation (extracts were sampled at day 1, 3, 6, 10, 14, 21, and 28 of mono and co-cultivation of *S. plymuthica* 4Rx13 and AS9). **(B)** Frequency of occurrence of each co-cultivation correlating mass feature.

metabolic features, which differed in later stages of interaction between *S. plymuthica* 4Rx13 and *B. subtilis* B2g belonged to compounds of the plipastatin family. Plipastatins are bioactive lipopeptides produced by isolates of *Bacillus subtilis* isolates (Nishikiori et al., 1986; Ongena et al., 2007; Hussein, 2019), mainly known for their striking antifungal activity (Kaspar et al., 2019; Kiesewalter et al., 2021). They occur as various isomers characterized by different structures (A1, A2, B1, and B2; Kaspar et al., 2019) of whom only specific isomers were increasingly produced by *B. subtilis* B2g in the co-cultivation with *S. plymuthica* 4Rx13. Interestingly, further increased features were putatively identified using accurate mass measurements and mass spectral molecular networking as specific isomers of not yet described plipastatin variants. These variants we would probably have overlooked, if they had not been triggered by co-cultivation. The response in production of only specific isomers both of plipastatins as well as plipastatin variants to the interplay with *S. plymuthica* 4Rx13 indicates either that specific precursors amino—or fatty acids are more abundant or a specific regulation by *B. subtilis* B2g due to the co-cultivation. Full characterization of the isomers in order to evaluate the exact structure is needed to initiate answering these questions. So far, an interaction-increased production of lipopeptides upon perception of bacterial competitors has not been shown (Andric et al., 2020). Recent data, however, has shown that fungal interaction triggered *B. subtilis* NCIB3610 to activate the regulator SigB leading to an enhanced surfactin production (Bartolini et al., 2019). Interestingly, the observed induced production does not generally apply for the lipopeptides produced by *B. subtilis* B2g since compounds of the surfactin and bacillomycin D family did not show an increase during interaction. That plipastatins are increasingly produced is thereby especially interesting, since plipastatins are so far described as antifungal metabolites, however, Raaijmakers and colleagues already stated that “lipopeptides might have different natural roles, some of

which may be unique to the producer” (Raaijmakers et al., 2010). The natural role of *B. subtilis* B2g plipastatin overproduction due to interplay with *S. plymuthica* 4Rx13 needs to be investigated in future.

Intraspecific Interaction Between *S. plymuthica* 4Rx13 and *S. plymuthica* AS9

The intraspecific co-cultivation of *S. plymuthica* 4Rx13 and AS9 was also characterized by a distinct interaction zone indicating high potential of intraspecific antagonism between both partners. Thereby, the intraspecific interplay between both isolates led to distinct metabolic profiles with a high number of differentially-featured masses compared to mono-cultivated species. Interestingly, several very short putatively proline-containing peptides were found to be more pronounced in co-cultivation compared to mono-cultivated strains. Short proline-rich antimicrobial peptides (PrAMPs), mostly isolated from insects, are promising antibiotics showing a broad range of antibacterial activities against several Gram-positive and Gram-negative bacteria (Otvos, 2002; Cardoso et al., 2019). However, the peptides observed in this study are shorter with presumably 2–8 amino acids compared to the PrAMPs mostly occurring with more than 18 amino acid residues (Otvos, 2002). In order to evaluate whether the observed peptides have antibacterial activity we firstly need their complete structural characterization. This characterization will also help to evaluate the identity of the producing partner, since, although our results indicate that the main source of these peptides seems to be *S. plymuthica* 4Rx13, we cannot exclude an induction of peptide production in *S. plymuthica* AS9 due to interplay with *S. plymuthica* 4Rx13. Currently, we also do not know whether these peptides are actively released or passively leak through membranes that have lost their integrity due to antagonism. It is also possible that higher proteins or peptides were increasingly degraded by proteases during interaction leading to shorter peptides since *S. plymuthica* AS9, for instance,

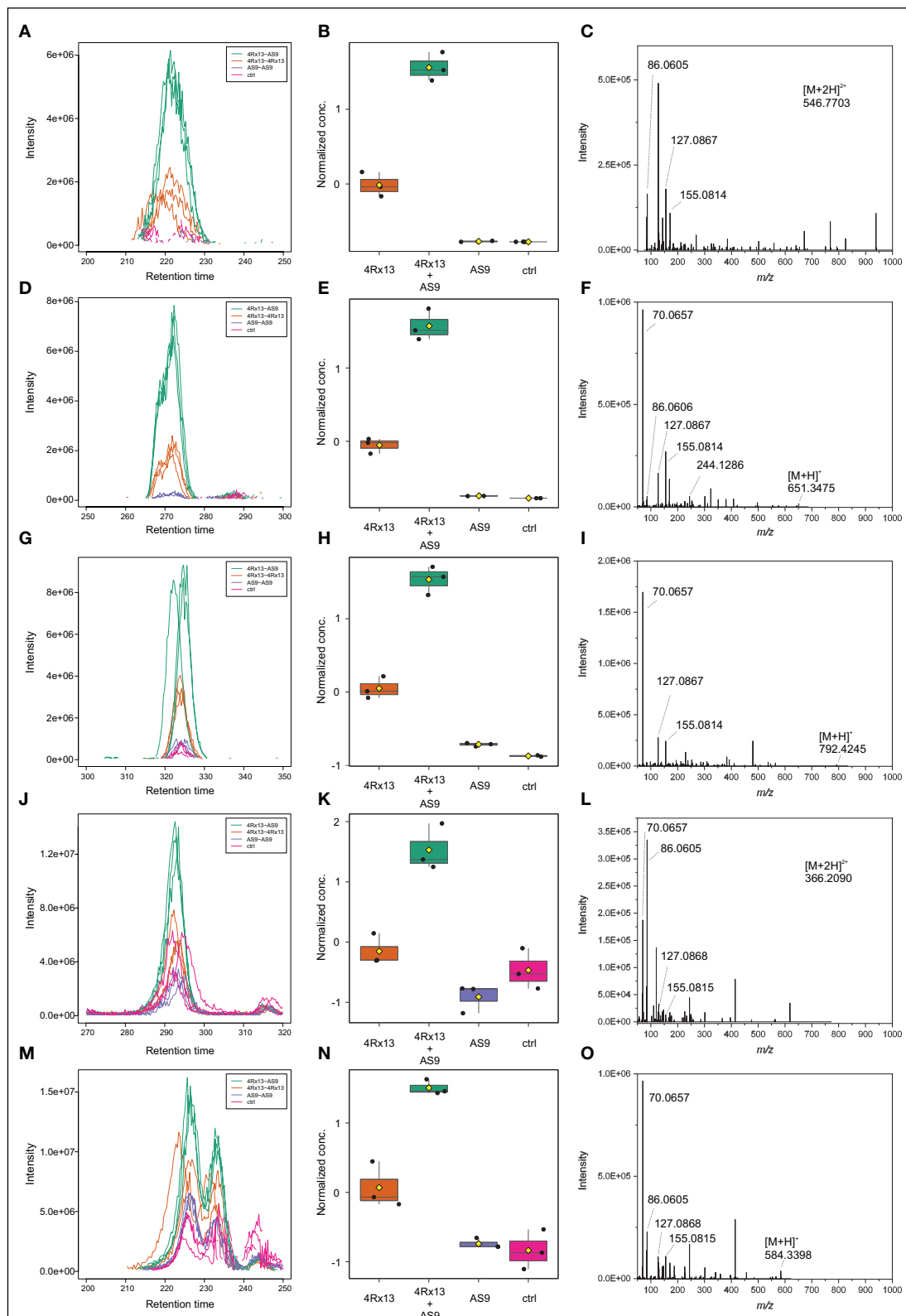


FIGURE 12 | Intraspecific co-cultivation triggered putative peptides. cEIC (A), Normalized conc. (B), MS/MS (C) of $[M+2H]^{2+}$ m/z 546.7703. cEIC (D), Normalized conc. (E), MS/MS (F) of $[M+H]^+$ m/z 651.3475. cEIC (G), Normalized conc. (H), MS/MS (I) of $[M+H]^+$ m/z 792.2445. cEIC (J), Normalized conc. (K), MS/MS (L) of $[M+H]^+$ m/z 366.2090. cEIC (M), Normalized conc. (N), MS/MS (O) of $[M+H]^+$ m/z 584.3398.

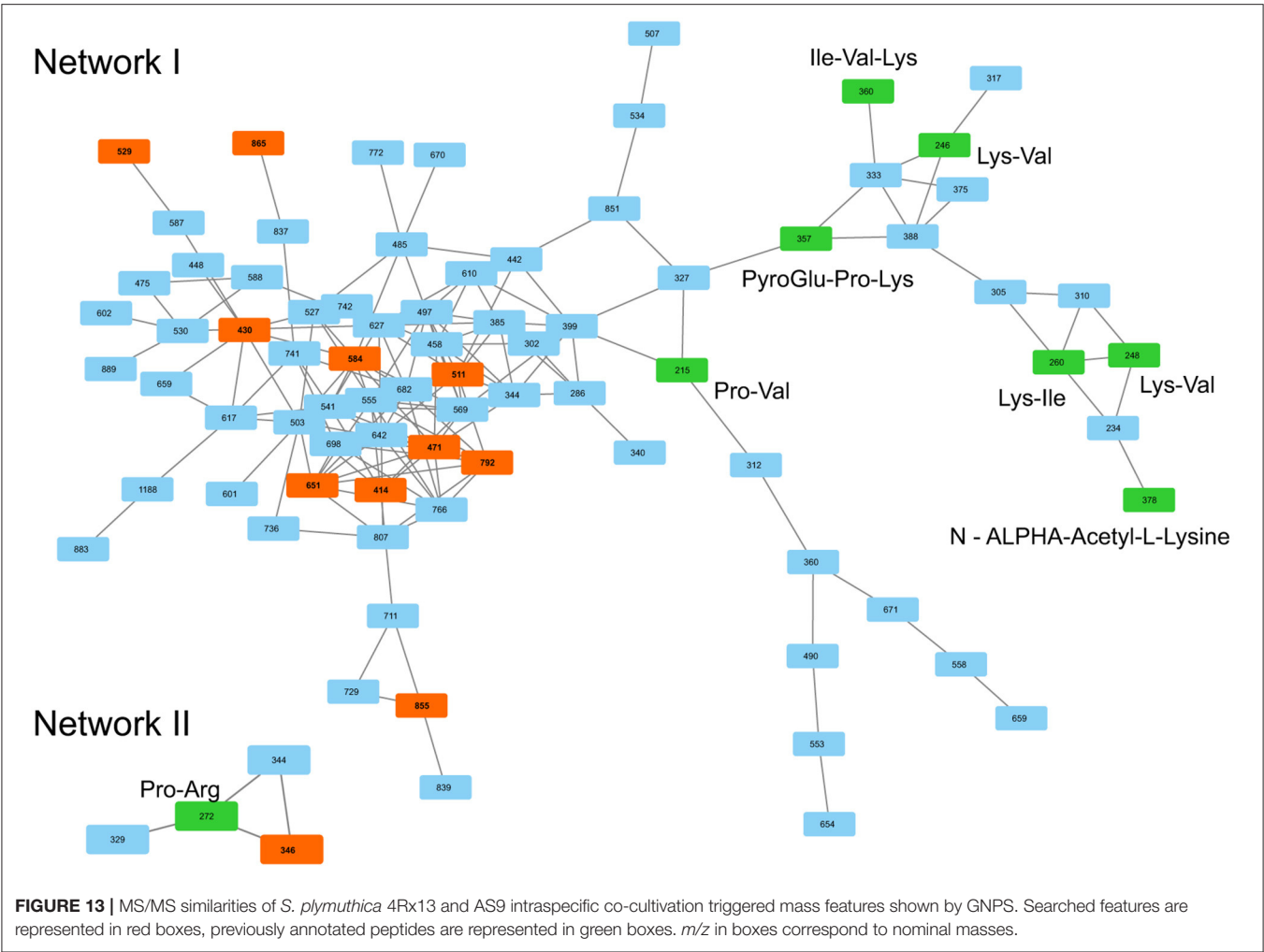


TABLE 2 | Putative chemical formulae of peptides increased in co-cultivation of *S. plymuthica* 4Rx13 and AS9 (* rank 2 in Sirius calculation).

<i>m/z</i> detected [M+H] ⁺	RT (sec)	Chemical formula	Sirius score (%)	Δppm
346.2085	250	C ₁₄ H ₂₇ N ₅ O ₅	99.982	0.05
404.2143	238	C ₁₆ H ₂₉ N ₅ O ₇	96.948	0.76
471.2568	243	C ₂₀ H ₃₄ N ₆ O ₇	91.21	1.41
529.2985	303	C ₂₃ H ₄₀ N ₆ O ₈	85.324	0.91
558.2884	253	C ₂₃ H ₃₉ N ₇ O ₉	80.875	0.61
565.263	277	C ₂₅ H ₃₆ N ₆ O ₉	87.165	2.4
584.3408	233	C ₂₆ H ₄₅ N ₇ O ₈	82.769	0.95
651.3471	272	C ₂₉ H ₄₆ N ₈ O ₉ ⁺	34.999	1.6
792.4258	324	C ₃₆ H ₅₇ N ₉ O ₁₁	49.544	1.0
865.4427	294	C ₃₈ H ₆₀ N ₁₀ O ₁₃	25.154	1.5
1033.533	303	C ₅₁ H ₇₂ N ₁₀ O ₁₃	18.477	2.1

showed proteolytic activity in earlier studies (Alström, 2001). Future studies should tackle these questions of increased amounts of peptides and clarify their putative function in intraspecific crosstalk.

CONCLUSION

Due to the complexity of rhizobacterial communities investigations of interactive processes within this bacterial

network are challenging. Using metabolic profiling, we showed interspecific and intraspecific variations of metabolic profiles and further that the excretion of certain metabolites, i.e., plipastatins and putative proline-containing peptides, can change induced by social interactions between single members of bacterial communities. These results form a basis for biological assays to further investigate the functional role of these interaction-triggered compounds in establishment and maintenance of microbial communities. Furthermore, they can be applied under natural and more realistic conditions, since rhizobacteria also interact with the plant itself and many other members of plant and soil microbiota.

DATA AVAILABILITY STATEMENT

The datasets presented in this study can be found in online repositories. The names of the repository/repositories and accession number(s) can be found in the article/**Supplementary Material**.

AUTHOR CONTRIBUTIONS

MK conceived, designed the experiments, interpreted the results, and wrote the manuscript. MK, DW, and RM performed the experiments. RM measured the metabolic profiles. MK, RM, and AS analyzed the data. BP discussed preliminary results and the manuscript and provided financial support (BP153/36-1). All authors critically revised and consented to the final version of the manuscript.

FUNDING

This study received funding from the DFG (to BP) and University of Rostock (to BP).

REFERENCES

- Alström, S. (2001). Characteristics of bacteria from oilseed rape in relation to their biocontrol activity against *Verticillium dahliae*. *J. Phytopathol.* 149, 57–64. doi: 10.1046/j.1439-0434.2001.00585.x
- Andric, S., Meyer, T., and Ongena, M. (2020). *Bacillus* responses to plant-associated fungal and bacterial communities. *Front. Microbiol.* 11:1350. doi: 10.3389/fmicb.2020.01350
- Badri, D. V., and Vivanco, J. M. (2009). Regulation and function of root exudates. *Plant Cell and Environ.* 32, 666–681. doi: 10.1111/j.1365-3040.2009.01926.x
- Bartolini, M., Cogliati, S., Vileta, D., Bauman, C., Ramirez, W., and Grau, R. (2019). Stress responsive alternative sigma factor SigB plays a positive role in the antifungal proficiency of *Bacillus subtilis*. *Appl. Environ. Microbiol.* 85:e00178–e00119. doi: 10.1128/AEM.00178-19
- Benton, H. P., Want, E. J., and Ebbels, T. M. D. (2010). Correction of mass calibration gaps in liquid chromatography-mass spectrometry metabolomics data. *Bioinformatics* 26:2488. doi: 10.1093/bioinformatics/btq441

ACKNOWLEDGMENTS

We thank both reviewers for their valuable input, which strongly improved the manuscript.

SUPPLEMENTARY MATERIAL

The Supplementary Material for this article can be found online at: <https://www.frontiersin.org/articles/10.3389/fmicb.2021.685224/full#supplementary-material>

Supplementary Figure 1 | Distinct metabolic profiles of interspecific co-cultivations of *S. plymuthica* 4Rx13 and *B. subtilis* B2g compared to their mono-cultures. PAM-Cluster plots.

Supplementary Figure 2 | Identification of plipastatin isomers using reporter fragment ions corresponding to amino acids at position 6 and 10 in the plipastatin peptide ring. *m/z* 966.45941 and 1080.53918 for Ala⁶/Ile¹⁰ corresponding to A1, *m/z* 1066.51892 for Ala⁶/Val¹⁰ corresponding to A2, *m/z* 994.49011 and 1108.56982 for Val⁶/Ile¹⁰ corresponding to B1, *m/z* 980.47394 and 1094.55005 for Val⁶/Val¹⁰ corresponding to B2.

Supplementary Figure 3 | Distinct metabolic profiles of intraspecific co-cultivations of *S. plymuthica* 4Rx13 and *S. plymuthica* B2g compared to their mono-cultures. PAM-Cluster plots.

Supplementary Figure 4 | Due to *S. plymuthica* 4Rx13 and AS9 co-cultivation increased features, respective *m/z* of every feature was extracted and plotted (cEIC).

Supplementary Table 1 | Lipopeptides produced by *B. subtilis* B2g.

Supplementary Table 2 | Differentially induced mass features in *Serratia plymuthica* 4Rx13 interaction with *Bacillus subtilis* B2g compared to mono-cultivated strains and medium control.

Supplementary Table 3 | Time points of detection of differentially induced mass features (*m/z*) in *Serratia plymuthica* 4Rx13 interaction with *Bacillus subtilis* B2g compared to mono-cultivated strains and medium control.

Supplementary Table 4 | Identification of plipastatin isomers (isomers that are more pronounced in interaction are labeled in red).

Supplementary Table 5 | Differentially induced mass features in *Serratia plymuthica* 4Rx13 interaction with *S. plymuthica* AS9 compared to mono-cultivated strains and medium control.

Supplementary Table 6 | Time points of detection of differentially induced mass features (*m/z*) in *Serratia plymuthica* 4Rx13 interaction with *S. plymuthica* AS9 compared to mono-cultivated strains and medium control.

- Berendsen, R. L., Pieterse, C. M. J., and Bakker, P. A. H. M. (2012). The rhizosphere microbiome and plant health. *Trends Plant Sci.* 17, 478–486. doi: 10.1016/j.tplants.2012.04.001
- Berg, G., Roskot, N., Steidle, A., Eberl, L., Zock, A., and Smalla, K. (2002). Plant-dependent genotypic and phenotypic diversity of antagonistic rhizobacteria isolated from different *Verticillium* host plants. *Appl. Environ. Microbiol.* 68, 3328–3338. doi: 10.1128/AEM.68.7.3328-3338.2002
- Böcker, S., and Dührkop, K. (2016). Fragmentation trees reloaded. *J. Cheminform.* 8:5. doi: 10.1186/s13321-016-0116-8
- Böcker, S., Letzel, M., Lipták, Z., and Pervukhin, A. (2009). SIRIUS: decomposing isotope patterns for metabolite identification. *Bioinformatics* 25, 218–224. doi: 10.1093/bioinformatics/btn603
- Bonkowski, M. (2019). “Microcosm approaches to investigate multitrophic interactions between microbial communities in the rhizosphere of plants,” in *Methods in Rhizosphere Biology Research*, eds D. Reinhardt and A. Sharma (Singapore: Springer), 255–270. doi: 10.1007/978-981-13-5767-1_14
- Buee, M., De Boer, W., Martin, F., van Overbeek, L., and Jurkevitch, E. (2009). The rhizosphere zoo: an overview of plant-associated communities

- of microorganisms, including phages, bacteria, archaea, and fungi, and of some of their structuring factors. *Plant Soil* 321, 189–212. doi: 10.1007/s11104-009-9991-3
- Burmeister, A., Hilgers, F., Langner, A., Westerwalbesloh, C., Kerkhoff, Y., Tenhaef, N., et al. (2019). A microfluidic co-cultivation platform to investigate microbial interactions at defined microenvironments. *Lab Chip* 19, 98–110. doi: 10.1039/C8LC00977E
- Cardoso, M. H., Meneguetti, B. T., Costa, B. O., Bucchini, D. F., Oshiro, K. G. N., Preza, S. L. E., et al. (2019). Non-lytic antibacterial peptides that translocate through bacterial membranes to act on intracellular targets. *Int. J. Mol. Sci.* 20:4877. doi: 10.3390/ijms20194877
- Chambers, M. C., Maclean, B., Burke, R., Amodei, D., Ruderman, D. L., Neumann, S., et al. (2012). A cross-platform toolkit for mass spectrometry and proteomics. *Nat. Biotechnol.* 30, 918–920. doi: 10.1038/nbt.2377
- Chong, J., Wishart, D. S., and Xia, J. (2019). Using MetaboAnalyst 4.0 for comprehensive and integrative metabolomics data analysis. *Curr. Protoc. Bioinformatics* 68:e86. doi: 10.1002/cpbi.86
- Chubukov, V., and Sauer, U. (2014). Environmental dependence of stationary-phase metabolism in *Bacillus subtilis* and *Escherichia coli*. *Appl. Environ. Microbiol.* 80, 2901–2909. doi: 10.1128/AEM.00061-14
- Clements, T., Ndlovu, T., and Khan, W. (2019). Broad-spectrum antimicrobial activity of secondary metabolites produced by *Serratia marcescens* strains. *Microbiol. Res.* 229:126329. doi: 10.1016/j.micres.2019.126329
- Cleto, S., Van der Auwera, G., Almeida, C., Vieira, M. J., Vlamakis, H., and Kolter, R. (2014). Genome sequence of *Serratia plymuthica* V4. *Genome Announc.* 2:e00340–e00314. doi: 10.1128/genomeA.00340-14
- Dührkop, K., Fleischauer, M., Ludwig, M., Aksenov, A. A., Melnik, A. V., Meusel, M., et al. (2019). SIRIUS4: a rapid tool for turning tandem mass spectra into metabolite structure information. *Nat. Methods* 16, 299–302. doi: 10.1038/s41592-019-0344-8
- Dührkop, K., Shen, S., Meusel, M., Rousu, J., and Böcker, S. (2015). Searching molecular structure databases with tandem mass spectra using CSI:FingerID. *Proc. Natl. Acad. Sci. U.S.A.* 112, 12580–12585. doi: 10.1073/pnas.1509788112
- Fierer, N., and Jackson, R. B. (2006). The diversity and biogeography of soil bacterial communities. *Proc. Natl. Acad. Sci. U.S.A.* 103, 626–631. doi: 10.1073/pnas.0507535103
- Ghoul, M., and Mitri, S. (2016). The Ecology and Evolution of microbial competition. *Trends Microbiol.* 24, 833–845. doi: 10.1016/j.tim.2016.06.011
- Gray, E. J., and Smith, D. L. (2005). Intracellular and extracellular PGPR: commonalities and distinctions in the plant-bacterium signaling processes. *Soil Biol. Biochem.* 37, 395–412. doi: 10.1016/j.soilbio.2004.08.030
- Griffin, A. S., West, S. A., and Buckling, A. (2004). Cooperation and competition in pathogenic bacteria. *Nature* 430, 1024–1027. doi: 10.1038/nature02744
- Grimont, P., and Grimont, F. (2004). “Genus *Serratia* bizio 1823, 288^{AL},” in *Bergey’s Manual of Systematic Bacteriology*, eds N. R. Krieg and J. G. Holt (Baltimore, MD: Williams and Wilkins, Baltimore).
- Hassani, M. A., Durán, P., and Hacquad, S. (2018). Microbial interactions within the plant holobiont. *Microbiome* 6:58. doi: 10.1186/s40168-018-0445-0
- Hiltner, L. (1904). Über neuere Erfahrungen und Probleme auf dem Gebiete der Bodenbakteriologie unter besonderer Berücksichtigung der Gründüngung und Brache. *Arb. DLG* 98, 59–78.
- Hussein, W. (2019). Fengycin or plipastatin? A confusing question in *Bacilli*. *BioTechnologia* 100, 47–55. doi: 10.5114/bta.2019.83211
- Kai, M., Effmert, U., Berg, G., and Piechulla, B. (2007). Volatiles of bacterial antagonists inhibit mycelial growth of the plant pathogen *Rhizoctonia solani*. *Arch. Microbiol.* 187, 351–360. doi: 10.1007/s00203-006-0199-0
- Kai, M., and Piechulla, B. (2018). Interspecies interaction of *Serratia plymuthica* 4Rx13 and *Bacillus subtilis* B2g alters the emission of odoriferous. *FEMS Microbiol. Lett.* 365:fny253. doi: 10.1093/femsle/fny253
- Kaki, A. A., Smargiasso, N., Ongena, M., Ali, M. K., Moula, N., De Pauw, E., et al. (2020). Characterization of new fengycin cyclic lipopeptide variants produced by *Bacillus amyloliquefaciens* (ET) originating from a Salt Lake of Eastern Algeria. *Curr. Microbiol.* 77, 443–451. doi: 10.1007/s00284-019-01855-w
- Kakinuma, A., Hori, M., Isono, M., Tamura, G., and Arima, K. (1969). Determination of amino acid sequence in surfactin, a crystalline peptidolipid surfactant produced by *Bacillus subtilis*. *Agric. Biol. Chem.* 33, 971–972. doi: 10.1080/00021369.1969.10859408
- Kaspar, F., Neubauer, P., and Gimpel, M. (2019). Bioactive secondary metabolites from *Bacillus subtilis*: a comprehensive review. *J. Nat. Prod.* 82, 2038–2053. doi: 10.1021/acs.jnatprod.9b00110
- Kaufman, L., and Rousseeuw, P. J. (1990). “Partitioning around medoids (Program PAM),” in *Finding Groups in Data: An Introduction to Cluster Analysis*, eds L. Kaufman and P. J. Rousseeuw (Hoboken, NJ: John Wiley and Sons Inc.), 68–125. doi: 10.1002/9780470316801.ch2
- Kiesewalter, H. T., Lozano-Andrade, C. N., Wibowo, M., Strube, M. L., Maróti, G., Snyder, D., et al. (2021). Genomic and chemical diversity of *Bacillus subtilis* secondary metabolites against plant pathogenic fungi. *mSystems* 6:e00770–e00720. doi: 10.1128/mSystems.00770-20
- Kluge, B., Vater, J., Salnikow, J., and Eckard, K. (1988). Studies on the biosynthesis of surfactin, a lipopeptide antibiotic from *Bacillus subtilis* ATCC 21332. *FEBS Lett.* 231, 107–110. doi: 10.1016/0014-5793(88)80712-9
- Lemfack, M. C., Ravello, S. R., Lorenz, N., Kai, M., Jung, K., Schulz, S., et al. (2016). Novel volatiles of skinborne bacteria inhibit the growth of gram-positive bacteria and affect quorum-sensing controlled phenotypes of Gram-negative bacteria. *Syst. Appl. Microbiol.* 39, 503–515. doi: 10.1016/j.syapm.2016.08.008
- Lindow, S. E., and Brandl, M. T. (2003). Microbiology of the phyllosphere. *Appl. Environ. Microbiol.* 69, 1875–1883. doi: 10.1128/AEM.69.4.1875-1883.2003
- Little, A. E. F., Robinson, C. J., Peterson, S. B., and Handelsman, J. (2008). Rules of engagement: interspecies interactions that regulate microbial communities. *Annu. Rev. Microbiol.* 62, 375–401. doi: 10.1146/annurev.micro.030608.101423
- Liu, W.-T., Yang, Y.-L., Xu, Y., Lamsa, A., Haste, N. M., Yang, J. Y., et al. (2010). Imaging mass spectrometry of intraspecies metabolic exchange revealed the cannibalistic factors of *Bacillus subtilis*. *Proc. Natl. Acad. Sci. U.S.A.* 107, 16286–16290. doi: 10.1073/pnas.1008368107
- Marques-Pereira, C., Proença, D. N., and Morais, P. V. (2020). Genome sequences of *Serratia* strains revealed common genes in both serratomolides gene clusters. *Biology* 9:482. doi: 10.3390/biology9120482
- Marten, P., Smalla, K., and Berg, G. (2000). Genotypic and phenotypic differentiation of antifungal biocontrol strains belonging to *Bacillus subtilis*. *J. Appl. Microbiol.* 89, 463–473. doi: 10.1046/j.1365-2672.2000.01136.x
- Masschelein, J., Clauwers, C., Stalmans, K., Nuyts, K., De Borggraeve, W., Briers, Y., et al. (2015). The zeamine antibiotics affect the integrity of bacterial membranes. *Appl. Environ. Microbiol.* 81, 1139–1146. doi: 10.1128/AEM.03146-14
- Masschelein, J., Mattheus, W., Gao, L. J., Moons, P., Van Houdt, R., Uytterhoeven, B., et al. (2013). A PKS/NRPS/FAS hybrid gene cluster from *Serratia plymuthica* RVH1 encoding the biosynthesis of three broad spectrum, zeamine-related antibiotics. *PLoS ONE* 8:e54143. doi: 10.1371/journal.pone.0054143
- Matilla, M., Stöckmann, H., Leeper, F., and Salmond, G. P. C. (2012). Bacterial biosynthetic gene clusters encoding the anti-cancer haterumalide class of molecules: biogenesis of the broad spectrum antifungal and anti-oomycete compound, oocydin A. *J. Biol. Chem.* 287, 39125–39138. doi: 10.1074/jbc.M112.401026
- Meyer, H., Weidmann, H., Mäder, U., Hecker, M., Völker, U., and Lalk, M. (2014). A time resolved metabolomics study: the influence of different carbon sources during growth and starvation of *Bacillus subtilis*. *Mol. Biosyst.* 10, 1812–1823. doi: 10.1039/c4mb00112e
- Nadell, C. D., Drescher, K., and Foster, K. R. (2016). Spatial structure cooperation and competition in biofilms. *Nat. Rev. Microbiol.* 14, 589–600. doi: 10.1038/nrmicro.2016.84
- Neupane, S., Högberg, N., Alström, S., Lucas, S., Han, J., Lapidus, A., et al. (2012). Complete genome sequence of the rapeseed plant-growth promoting *Serratia plymuthica* AS9. *Stand. Genomic. Sci.* 6, 54–62. doi: 10.4056/signs.2595762
- Nishikiori, T., Naganawa, H., Muraoka, A., Aoyagi, T., and Umezawa, H. (1986). Plipastatins: new inhibitors of phospholipase A2, produced by *Bacillus cereus* BMG302-ff67. III. Structural elucidation of plipastatins. *J. Antibiot.* 39, 755–761. doi: 10.7164/antibiotics.39.755
- Ochi, K. (2017). Insights into microbial cryptic gene activation and strain improvement: principle, application and technical aspects. *J. Antibiot.* 70, 25–40. doi: 10.1038/ja.2016.82
- Ongena, M., Jourdan, E., Adam, A., Paquot, M., Brans, A., Joris, B., et al. (2007). Surfactin and fengycin lipopeptides of *Bacillus subtilis* as elicitors of induced systemic resistance in plants. *Environ. Microbiol.* 9, 1084–1090. doi: 10.1111/j.1462-2920.2006.01202.x

- Otvos, L. Jr. (2002). The short proline-rich antibacterial peptide family. *Cell. Mol. Life Sci.* 59, 1138–1150. doi: 10.1007/s00018-002-8493-8
- Pande, S., Shitut, S., Freund, L., Westermann, M., Bertels, F., Colesie, C., et al. (2015). Metabolic cross-feeding via intercellular nanotubes among bacteria. *Nat. Commun.* 6:6237. doi: 10.1038/ncomms7238
- Pang, Z., Chong, J., Li, S., and Xia, J. (2020). MetaboAnalystR 3.0: toward an optimized workflow for global metabolomics. *Metabolites* 10:186. doi: 10.3390/metabo10050186
- Park, J., Kerner, A., Burns, M. A., and Lin, X. N. (2011). Microdroplet-enabled highly parallel co-cultivation of microbial communities. *PLoS ONE* 6:e17019. doi: 10.1371/journal.pone.0017019
- Pathak, K. V., Keharia, H., Gupta, K., Thakur, S. S., and Balam, P. (2012). Lipopeptides from the banyan endophyte, *Bacillus subtilis* K1: mass spectrometric characterization of a library of fengycins. *J. Am. Soc. Mass Spectrom.* 23, 1716–1728. doi: 10.1007/s13361-012-0437-4
- Peypoux, F., Besson, F., Michel, G., and Delcambe, L. (1981). Structure of bacillomycin D, a new antibiotic of the iturin group. *Eur. J. Biochem.* 118, 323–327. doi: 10.1111/j.1432-1033.1981.tb06405.x
- Phelan, V. V., Liu, W.-T., Pogliano, K., and Dorrestein, P. C. (2012). Microbial metabolic exchange – the chemotype-to-phenotype link. *Nat. Chem. Biol.* 8, 26–35. doi: 10.1038/nchembio.739
- Pluskal, T., Castillo, S., Villar-Briones, A., and Orešič, M. (2010). MZmine 2: Modular framework for processing, visualizing, and analyzing mass spectrometry-based molecular profile data. *BMC Bioinformatics* 11:395. doi: 10.1186/1471-2105-11-395
- Prince, J. T., and Marcotte, E. M. (2006). Chromatographic alignment of ESI-LC-MS proteomics data sets by ordered bijective interpolated warping. *Anal. Chem.* 78, 6140–6152. doi: 10.1021/ac0605344
- Raaijmakers, M. J., De Bruijn, I., Nybroe, O., and Ongena, M. (2010). Natural functions of lipopeptides from *Bacillus* and *Pseudomonas*: more than surfactants and antibiotics. *FEMS Microbiol. Rev.* 34, 1037–1062. doi: 10.1111/j.1574-6976.2010.00221.x
- Rasche, F., Scheubert, K., Hufsky, F., Zichner, T., Kai, M., Svatos, A., et al. (2012). Identifying the unknowns by aligning fragmentation Trees. *Anal. Chem.* 84, 3417–3426. doi: 10.1021/ac300304u
- Reinhold-Hurek, B., Büniger, W., Burbano, C. S., Sabale, M., and Hurek, T. (2015). Roots shaping their microbiome: global hotspots for microbial activity. *Annu. Rev. Phytopathol.* 53, 403–424. doi: 10.1146/annurev-phyto-082712-102342
- Røder, H. L., Sørensen, S. J., and Burmolle, M. (2016). Studying bacterial multispecies biofilms: where to start? *Trends Microbiol.* 24, 503–513. doi: 10.1016/j.tim.2016.02.019
- Ryu, C. M., Farag, M. A., Hu, C. H., Reddy, M. S., Wei, H.-X., Pare, P. W., et al. (2003). Bacterial volatiles promote growth in *Arabidopsis*. *Proc. Natl. Acad. Sci. U.S.A.* 100, 4927–4932. doi: 10.1073/pnas.0730845100
- Sanchez, S., and Demain, A. L. (2008). Metabolic regulation and overproduction of primary metabolites. *Microb. Biotechnol.* 1, 283–319. doi: 10.1111/j.1751-7915.2007.00015.x
- Scherlach, K., and Hertweck, C. (2009). Triggering cryptic natural product biosynthesis in microorganism. *Org. Biomol. Chem.* 7, 1753–1760. doi: 10.1039/b821578b
- Shank, E. (2018). Considering the lives of microbes in microbial communities. *mSystems* 3:e00155–e00117. doi: 10.1128/mSystems.00155-17
- Smith, C. A., Want, E. J., O'Maille, G., Abagyan, R., and Siuzdak, G. (2006). XCMS: processing mass spectrometry data for metabolite profiling using non-linear peak alignment, matching and identification. *Anal. Chem.* 78, 779–787. doi: 10.1021/ac051437y
- Smith, W. H. (1969). Release of organic materials from the roots of tree seedlings. *Forest Sci.* 15, 138–142. doi: 10.1093/forestscience/15.2.138
- Stein, T. (2005). *Bacillus subtilis* antibiotics: structures, syntheses and specific functions. *Mol. Microbiol.* 56, 845–857. doi: 10.1111/j.1365-2958.2005.04587.x
- Tautenhahn, R., Boettcher, C., and Neumann, S. (2008). Highly sensitive feature detection for high resolution LC/MS. *BMC Bioinform.* 9:504. doi: 10.1186/1471-2105-9-504
- Tautenhahn, R., Patti, G. J., Rinehard, D., and Siuzdak, G. (2012). XCMS online: a web-based platform to process untargeted metabolomic data. *Anal. Chem.* 84, 5035–5039. doi: 10.1021/ac300698c
- Traxler, M. F., and Kolter, R. (2015). Natural products in soil microbe interactions and evolution. *Nat. Prod. Rep.* 32, 956–970. doi: 10.1039/c5np00013k
- Tyc, O., De Jager, V. C. L., Van den Berg, M., Gerards, S., Janssens, T. K. S., Zaagman, N., et al. (2017). Exploring bacterial interspecific interactions for discovery of novel antimicrobial compounds. *Microb. Biotechnol.* 10, 910–925. doi: 10.1111/1751-7915.12735
- Van Bergeijk, D. A., Terlouw, B. R., Medema, M. H., and Wezel van, G. P. (2020). Ecology and genomics of actinobacteria: new concepts for natural product discovery. *Nat. Rev. Microbiol.* 18, 546–558. doi: 10.1038/s41579-020-0379-y
- Van der Wolf, J., and De Boer, S. H. (2014). “Phytopathogenic bacteria,” in *Principles of Plant-Microbe Interactions*, ed B. Lugtenberg (Cham: Springer), 65–77. doi: 10.1007/978-3-319-08575-3_9
- Vančura, V. (1964). Root exudates of plants. *Plant Soil* 21, 231–248. doi: 10.1007/BF01373607
- Vorholt, J. A. (2012). Microbial life in the phyllosphere. *Nat. Rev. Microbiol.* 10, 828–840. doi: 10.1038/nrmicro2910
- Wang, M., Carver, J. J., Phelan, V. V., Sanchez, L. M., Garg, N., Peng, Y., et al. (2016). Sharing and community curation of mass spectrometry data with global natural products social molecular networking. *Nat. Biotechnol.* 34, 828–837. doi: 10.1038/nbt.3597
- Wassermann, H. H., Keggi, J. J., and McKeon, J. E. (1961). Serratamolide, a metabolic product of *Serratia*. *J. Am. Chem. Soc.* 83, 4107–4108. doi: 10.1021/ja01480a046
- Waters, C. M., and Bassler, B. L. (2005). Quorum sensing: cell-to-cell communication in bacteria. *Annu. Rev. Cell Dev. Biol.* 21, 319–346. doi: 10.1146/annurev.cellbio.21.012704.131001
- Watrous, J., Roach, P., Alexandrov, T., Heath, B. S., Yang, J. Y., Kersten, R. D., et al. (2012). Mass spectral molecular networking of living microbial colonies. *Proc. Natl. Acad. Sci. U.S.A.* 109, E1743–E1752. doi: 10.1073/pnas.1203689109
- Weise, T., Thürmer, A., Brady, S., Kai, M., Gottschalk, G., and Piechulla, B. (2014). VOC emission of various *Serratia* species and isolates and genome analysis of *Serratia plymuthica* 4Rx13. *FEMS Microbiol. Lett.* 352, 45–53. doi: 10.1111/1574-6968.12359
- Xia, J., Psychogios, N., Young, N., and Wishart, D. S. (2009). MetaboAnalyst: a web server for metabolomic data analysis and interpretation. *Nucleic Acids Res.* 37, W652–W660. doi: 10.1093/nar/gkp356
- Yanni, D., Márquez-Zacarias, P., Yunker, P. J., and Ratcliff, W. C. (2019). Drivers of spatial structure in social microbial communities. *Curr. Biol.* 29, R545–R550. doi: 10.1016/j.cub.2019.03.068
- Zhou, J., Ma, Q., Yi, H., Wang, L., Song, H., and Yuan, Y.-J. (2011). Metabolome profiling reveals metabolic cooperation between *Bacillus megaterium* and *Ketogulonicigenium vulgare* during induced swarm motility. *Appl. Environ. Microbiol.* 77, 7023–7030. doi: 10.1128/AEM.05123-11

Conflict of Interest: The authors declare that the research was conducted in the absence of any commercial or financial relationships that could be construed as a potential conflict of interest.

Copyright © 2021 Menezes, Piechulla, Warber, Svatoš and Kai. This is an open-access article distributed under the terms of the Creative Commons Attribution License (CC BY). The use, distribution or reproduction in other forums is permitted, provided the original author(s) and the copyright owner(s) are credited and that the original publication in this journal is cited, in accordance with accepted academic practice. No use, distribution or reproduction is permitted which does not comply with these terms.



Volatile Compounds From *Bacillus*, *Serratia*, and *Pseudomonas* Promote Growth and Alter the Transcriptional Landscape of *Solanum tuberosum* in a Passively Ventilated Growth System

Darren Heenan-Daly^{1,2}, Simone Coughlan³, Eileen Dillane^{1,2} and Barbara Doyle Prestwich^{1,2*}

¹ School of Biological, Earth and Environmental Sciences, University College Cork, Cork, Ireland, ² Environmental Research Institute, University College Cork, Cork, Ireland, ³ School of Mathematics, Statistics and Applied Mathematics, National University of Ireland, Galway, Ireland

OPEN ACCESS

Edited by:

Elisa Korenblum,
Institute of Plant Sciences,
Agricultural Research Organization,
Volcani Center, Israel

Reviewed by:

Manoj Kumar Solanki,
University of Silesia in Katowice,
Poland
Marco Kai,
Max Planck Institute for Chemical
Ecology, Germany

*Correspondence:

Barbara Doyle Prestwich
b.doyle@ucc.ie

Specialty section:

This article was submitted to
Terrestrial Microbiology,
a section of the journal
Frontiers in Microbiology

Received: 11 November 2020

Accepted: 07 June 2021

Published: 21 July 2021

Citation:

Heenan-Daly D, Coughlan S,
Dillane E and Doyle Prestwich B
(2021) Volatile Compounds From
Bacillus, *Serratia*, and *Pseudomonas*
Promote Growth and Alter
the Transcriptional Landscape
of *Solanum tuberosum* in a Passively
Ventilated Growth System.
Front. Microbiol. 12:628437.
doi: 10.3389/fmicb.2021.628437

The interaction of an array of volatile organic compounds (VOCs) termed bacterial volatile compounds (BVCs) with plants is now a major area of study under the umbrella of plant-microbe interactions. Many growth systems have been developed to determine the nature of these interactions *in vitro*. However, each of these systems have their benefits and drawbacks with respect to one another and can greatly influence the end-point interpretation of the BVC effect on plant physiology. To address the need for novel growth systems in BVC-plant interactions, our study investigated the use of a passively ventilated growth system, made possible via Microbox[®] growth chambers, to determine the effect of BVCs emitted by six bacterial isolates from the genera *Bacillus*, *Serratia*, and *Pseudomonas*. Solid-phase microextraction GC/MS was utilized to determine the BVC profile of each bacterial isolate when cultured in three different growth media each with varying carbon content. 66 BVCs were identified in total, with alcohols and alkanes being the most abundant. When cultured in tryptic soy broth, all six isolates were capable of producing 2,5-dimethylpyrazine, however BVC emission associated with this media were deemed to have negative effects on plant growth. The two remaining media types, namely Methyl Red-Voges Proskeur (MR-VP) and Murashige and Skoog (M + S), were selected for bacterial growth in co-cultivation experiments with *Solanum tuberosum* L. cv. 'Golden Wonder.' The BVC emissions of *Bacillus* and *Serratia* isolates cultured on MR-VP induced alterations in the transcriptional landscape of potato across all treatments with 956 significantly differentially expressed genes. This study has yielded interesting results which indicate that BVCs may not always broadly upregulate expression of defense genes and this may be due to choice of plant-bacteria co-cultivation apparatus, bacterial growth media and/or strain, or likely, a complex interaction between these factors. The multifactorial complexities of observed effects of BVCs on target organisms, while intensely studied in recent years, need to be further elucidated before the translation of lab to open-field applications can be fully realized.

Keywords: volatile organic compounds, plant-bacteria interactions, plant growth-promotion, biocontrol, GC/MS, transcriptomics

INTRODUCTION

The relationship between plants and their consortia of microbial associates is recognized as one of the most ancient relationships on Earth. Today, we have the opportunity to exploit this relationship which can benefit the environment and thus, society as a whole. Numerous studies have demonstrated the ability of plant-associated bacteria, particularly rhizobacteria which are found in and around the root zone of the plant, to aid plant development and growth (Bloemberg and Lugtenberg, 2001; Adesemoye et al., 2009; Lugtenberg and Kamilova, 2009; Vejan et al., 2016; Méndez-Bravo et al., 2018; Basu et al., 2021). In the natural environment, rhizobacteria employ both direct and indirect plant growth-promoting (PGP) activities to optimize the health and growth of their plant hosts (Ghyselinck et al., 2013). Direct PGP activities include the sequestration of iron through the production of siderophores (Ghosh et al., 2020), the solubilization of phosphorus (Adnan et al., 2020), alteration of phytohormone levels such as IAA (Raut et al., 2017) and the modulation of ethylene levels within the host (Nascimento et al., 2018). Indirect mechanisms can include the secretion of lytic enzymes (Jadhav et al., 2017), competition for nutrients (Haggag and Timmusk, 2008), the induction of systemic resistance (Jacob et al., 2020) and the emission of volatile organic compounds (Fincheira et al., 2021). The latter two of these activities can often work synergistically where volatiles alone can induce systemic resistance as demonstrated in *Arabidopsis thaliana* (Ryu et al., 2004). Volatile compounds, particularly volatile organic compounds, often serve as chemical communication signals in both intra- and interspecific communication between kingdoms (Schulz-Bohm et al., 2017). Of the numerous activities that rhizobacteria employ to aid plant growth, BVCs have emerged as a key area of investigation over the last two decades (Ryu et al., 2003; Farag et al., 2006, 2017) and their future application to agricultural production systems are an attractive option, especially with regard to sustainable agriculture (Heenan-Daly et al., 2019; Garbeva and Weiskopf, 2020).

The fact that these chemical signals are naturally produced by many rhizobacterial species presents an opportunity for application in the field as part of a sustainable approach to agricultural production systems. Application of the rhizobacterial isolates themselves to release potentially beneficial BVCs or indeed the application of pure volatile compounds may help to reduce the application of environmentally harmful biocides and fertilizers, and numerous studies have addressed how this could be implemented in the field, with particular interest in overcoming problems with high volatility such as applying volatiles as part of oil-in-water multilayer emulsions (Choi et al., 2014; Fincheira et al., 2019, 2020). BVCs can act in two ways to promote plant growth; firstly, they can directly inhibit the growth of fungal and bacterial phytopathogens so as to prevent them from damaging or killing a potential host (Vespermann et al., 2007; Asari et al., 2016). Secondly, they can act to modulate gene expression within the sensor plant perceiving the volatile signal, often involving genes involved in growth, defense and nutrient acquisition (Gutiérrez-Luna et al., 2010; Farag et al., 2013; Zamioudis et al., 2015; Hernández-Calderón et al., 2018;

Romera et al., 2019). It is widely reported that during *in vitro* experimentation the substrate on which the bacterial isolate proliferates and its own particular capacity for volatile emission can affect the composition of its corresponding VOC profile, having both positive and negative effects on growth, for example different *Pseudomonas* strains were shown to emit varying amounts of hydrogen cyanide when grown on Luria Broth (LB) agar and this could lead to severely deleterious phytotoxic effects in *A. thaliana* when excessive emission occurred ($> 17 \mu\text{mol}$), in fact when compared to other media such as nutrient rich MR-VP or the less nutrient rich Angle and M + S, LB media was the only one to show plant lethality (Blom et al., 2011a,b). This can have implications for the effect of BVCs applied both in the lab and in the field with conditions such as temperature, humidity and nutrient availability affecting the emission and volatilization of these compounds and thus, potentially, their respective effect on growth (Chung et al., 2016). The effect of BVCs on modulation of gene expression related to defense, growth and nutrient acquisition has been demonstrated in numerous studies since the publications of Ryu et al. (2003) and Ryu et al. (2004) regarding the volatile-mediated regulation of gene expression in *A. thaliana*. Indeed, this activity, rather than the direct inhibition of phytopathogens, has become a more attractive option for improved agricultural practices as BVCs can “prime” the target plant by activation of an induced systemic resistance (ISR) (Choi et al., 2014).

In the lab, closed systems have been the popular choice for observing the experimental effects of VOCs on target organisms due to their relative ease-of-use and affordability. The most common approach is the use of split-plate Petri dishes, often referred to as ‘I plates,’ where VOCs can diffuse from one chamber of the plate to the other over a central dividing septum (Velivelli et al., 2015). Closed systems have a number of drawbacks, however, the first being that the build-up and subsequent increased concentration of VOCs within these systems is highly unlikely to occur in an open system or especially in the field. The second is that given the right conditions, the effect of VOCs can be detrimental, or even lethal, to the target organism (Blom et al., 2011b), as we observed in plants that were exposed to BVCs from TSB-cultured isolates. Open systems represent a more true-to-life effect of VOCs on target organisms (Kai and Piechulla, 2009) but have the drawback of laborious mechanical apparatus such as pumps and the added expense which these can bring. This study investigates the effect of BVCs on plant growth and defense in *S. tuberosum* L. cv. ‘Golden Wonder’ utilizing a novel co-cultivation method, and solid phase micro-extraction gas chromatography/mass spectrometry (SPME-GC/MS). Our approach was to find a “middle ground,” where the outer and inner atmosphere of the system could passively interact and exchange between one another to avoid an excessive accumulation of bacterial and indeed plant-derived volatiles, while still maintaining an axenic environment within the system thanks to the Microbox® growth chamber, along with providing relative ease-of-use and affordability. Volatiles affect all areas of plant morphology both above- and belowground (Wenke et al., 2010; Sharifi and Ryu, 2018) and therefore it is prudent to allow BVC blends to potentially access all areas of the plant during

experimental analyses to determine the systemic effect on plant growth and/or gene expression. To address this, polyurethane (PE) foam was selected in which to grow potato microplants for this study as it represented a more neutral substrate in which to cultivate the plant compared to sterilized soil, which has been used in some closed systems (Park et al., 2015; Tahir et al., 2017). The additional advantage of using PE foam is that, like soil, the foam is a porous matrix thus allowing potential diffusion of BVCs to the root system. Taken together, the use of the passively ventilated system investigated here may serve to negate any potential effects (positive and/or negative) of the over-accumulation of BVCs within closed *in vitro* growth systems, the use of PE foam may negate any potential nutritive effects of sterilized soil which could impact plant growth rates and also allows plant-wide exposure to BVCs from the shoots to the roots. Additionally, the size of this system allows for the investigation of larger and more mature plants than *A. thaliana* which is often studied in I-plates, the expanded range of plant subjects which can be investigated in this system may help to further elucidate species-specific effects of certain volatiles. Indeed, more than one microbe at a time may be investigated, and the potential inclusion of insects within the system could be employed as part of a wider biocontrol investigation using PGP microbes.

The aim of this study was to investigate the effect of BVCs on plant growth with five rhizobacterial isolates obtained from Irish potato soils growing on two different media types, MR-VP and M + S, in the presence of *S. tuberosum* L. cv. 'Golden Wonder' within a passively ventilated growth system. Studies concerning the effect of BVCs on plant growth employ either closed or open growth systems which can affect the experimental outcome and as a consequence, can potentially misrepresent the efficiency of these molecules in any potential agricultural field application. SPME-GC/MS was used in this study to qualitatively determine the volatile profiles of bacterial isolates in three different media types, each with varying levels of carbon content. Transcriptomic analysis using MACE (massive analysis of cDNA ends) RNA-seq allowed identification of differentially expressed genes in *S. tuberosum* in response to BVCs from *Bacillus amyloliquefaciens* FZB24® and *Serratia fonticola* LAC2.

MATERIALS AND METHODS

Solanum tuberosum Tissue Culture Maintenance

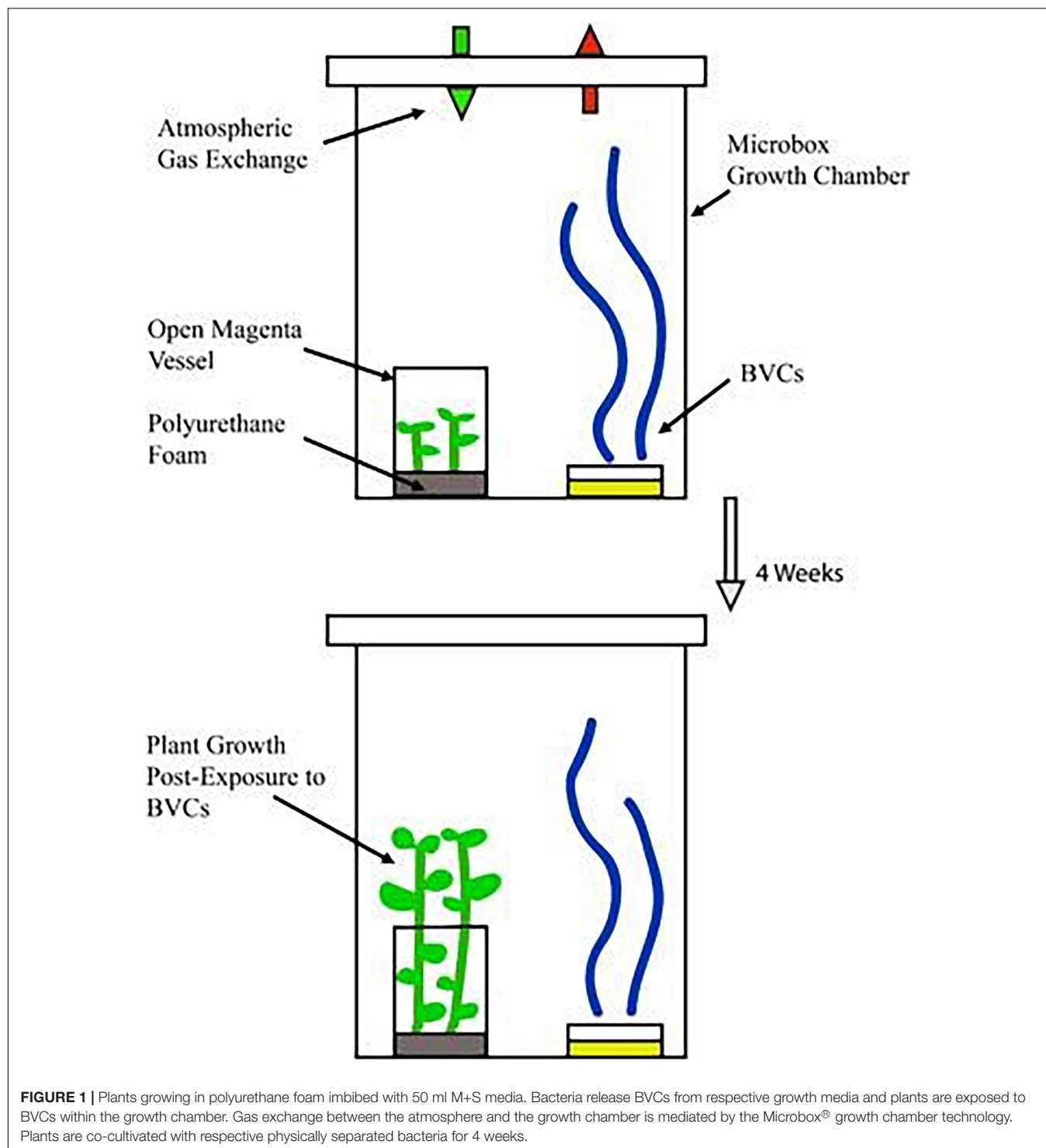
Microplants of *S. tuberosum* L. cv. 'Golden Wonder' were supplied by the TOPS potato centre (Department of Agriculture, Food and Marine, Raphoe, Donegal, Ireland). Stocks were maintained on 1/2 strength Murashige and Skoog (M + S) agar consisting of: 2.2 g basal M + S medium (Sigma Aldrich #5519), 15 g sucrose, 6 g agar (Sigma Aldrich) per liter with final pH adjusted to 5.80. Nodal sections of microplants were subcultured on fresh media under aseptic conditions every 4–5 weeks in Microbox® 'TP 3000' growth chambers equipped with 'XXL + ' filters (Combiness, Belgium). The microplants were kept in a growth room at 23°C under a 16 h d⁻¹ photoperiod and a photosynthetic photon flux (PPF) of 225 μmol m⁻² s⁻¹.

Bacterial Stock Maintenance

The commercial PGPR strain *Bacillus amyloliquefaciens* FZB24® and the following isolates from Irish potato soils *Serratia fonticola* LAC2, *Pseudomonas azotoformans* BRP14, *Bacillus toyonensis* BMC10, *Bacillus mycoides* LAM7 and *Serratia myotis* LAM10 were used in all experiments. Bacterial isolates were maintained on tryptic soy agar (TSA) (Sigma Aldrich). A single bacterial colony was streaked on TSA in a 90 mm Petri dish (Sarstedt, Germany) and allowed to grow overnight at 28°C ± 2°C or until visible colonies were observed. Cultures were Parafilm®ed and stored at 4°C for 4–5 weeks or maintained long term at -80°C in a 50% glycerol solution. The 16S rRNA sequences for potato soil isolates are deposited in GenBank under the accession numbers MT373405, MT373394, MT373410, MT373402, and MT373403.

GC/MS Analysis of Putative BVCs From Selected Rhizobacteria

Solid phase micro-extraction gas chromatography/mass spectrometry analysis was utilized to determine VOC profiles of rhizobacteria according to Velivelli et al. (2015) with slight modifications. SPME fibers were sourced from Supelco (Sigma Aldrich) and conditioned prior to use as per manufacturer's instructions. Rhizobacterial isolates were grown overnight on plates of TSA and incubated at 28 ± 2°C. A single colony from each isolate was used to inoculate 20 ml glass vials (Sigma Aldrich) containing 9 ml of TSB, MR-VP or M + S under aseptic conditions. The vials were sealed with metal crimp caps (Sigma Aldrich) fitted with rubber septa (Sigma Aldrich) ensuring that they were gastight. All components were autoclaved individually prior to inoculation. Vials were incubated at 28°C ± 2°C for 24–72 h at 170 rpm. Volatile analysis was carried out after 24, 48, and 72 h using a Shimadzu GC/MS-QP5000 equipped with a DB-5 column (30 m × 0.25 mm × 0.25 μm). Sample vials were placed in an incubator at 50°C. The SPME fiber (divinylbenzene/carboxen/polydimethylsiloxane (DCP, 50/30 μm)) was then inserted and exposed to each rhizobacterial BVC sample in the vial headspace for 40 min to allow adsorption of respective volatiles. The fiber containing the volatiles was then desorbed at 210°C for 1 min in the injection port of a gas chromatograph coupled to a mass spectrometer. The GC/MS run time was 22 min, and the injection port was operated in a split mode with a constant He flow of 1.0 ml min⁻¹. The initial oven temperature was set at 33°C for 3 min, increased to 180°C at a rate of 10°C min⁻¹, further increased to 220°C at a rate of 40°C min⁻¹, and with a final hold for 5 min at 220°C. Mass spectra were obtained in the electron ionization (EI) mode at 70 eV, with a continuous *m/z* scan from 40 to 250. The SPME fiber was conditioned after each run for 10 min at 210°C in the injection port and a cleaning run 'burn-off' was conducted before the next sample was analyzed. Identification of the resulting VOCs was done by comparison of volatile blend mass spectra with those of the NIST05/21, SZTERP mass spectra library (similarity index > 90%). The experiment was repeated twice per isolate/media combination and media controls were included during bacterial media inoculation.



Plant/Bacteria Co-cultivation for BVC Exposure

Four nodal sections of 4-week-old stock plants of *S. tuberosum* L. cv. 'Golden Wonder' were placed in polyurethane foams (supplied by the School of Biological, Earth and Environmental Sciences, UCC, Ireland) in magenta containers imbibed with

50 ml autotrophic medium (1/2 strength M + S basal medium (Sigma Aldrich #5519) 2.2 g per liter, pH adjusted to 5.80). These planted magentas were placed in 'TP5000 + TPD5000' Microbox® growth chambers equipped with 'XXL + ' filters (Combiness, Belgium). These growth chambers were placed in a growth room under a 16 h photoperiod at 23°C for

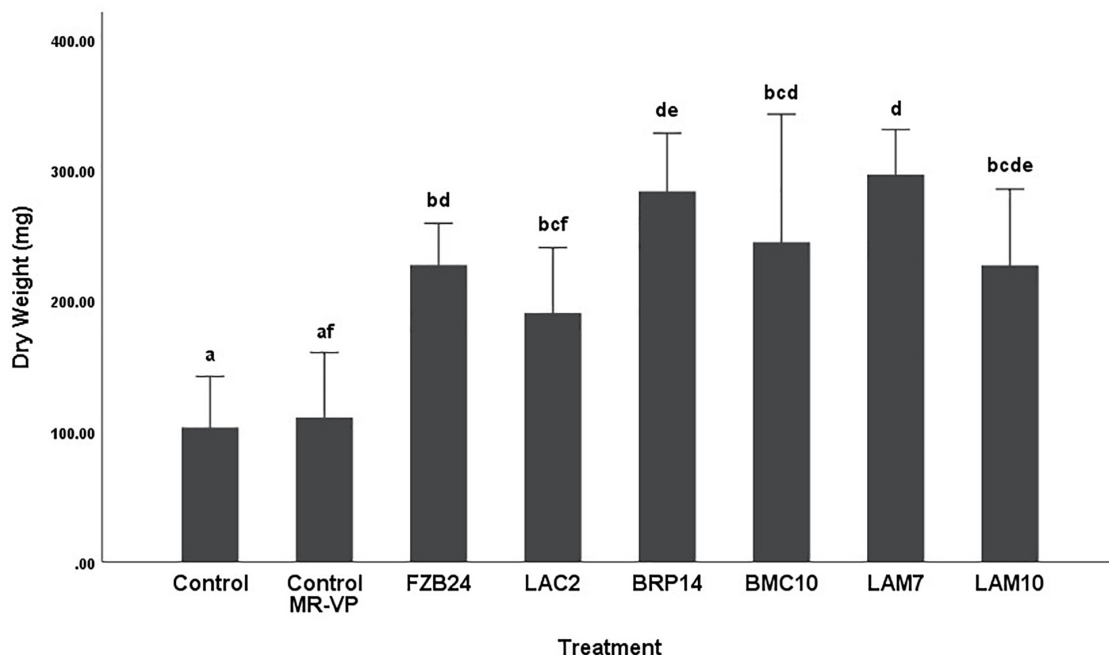


FIGURE 2 | Growth response of plants exposed to BVCs from isolates growing on solid MR-VP media. Dry weight of plants is measured in (mg), error bars represent confidence interval of the mean 99% ($n = 8$). Isolates which share a common letter are not significantly different to one another ($p > 0.01$) according to one-way between groups ANOVA with *post hoc* Tukey test.

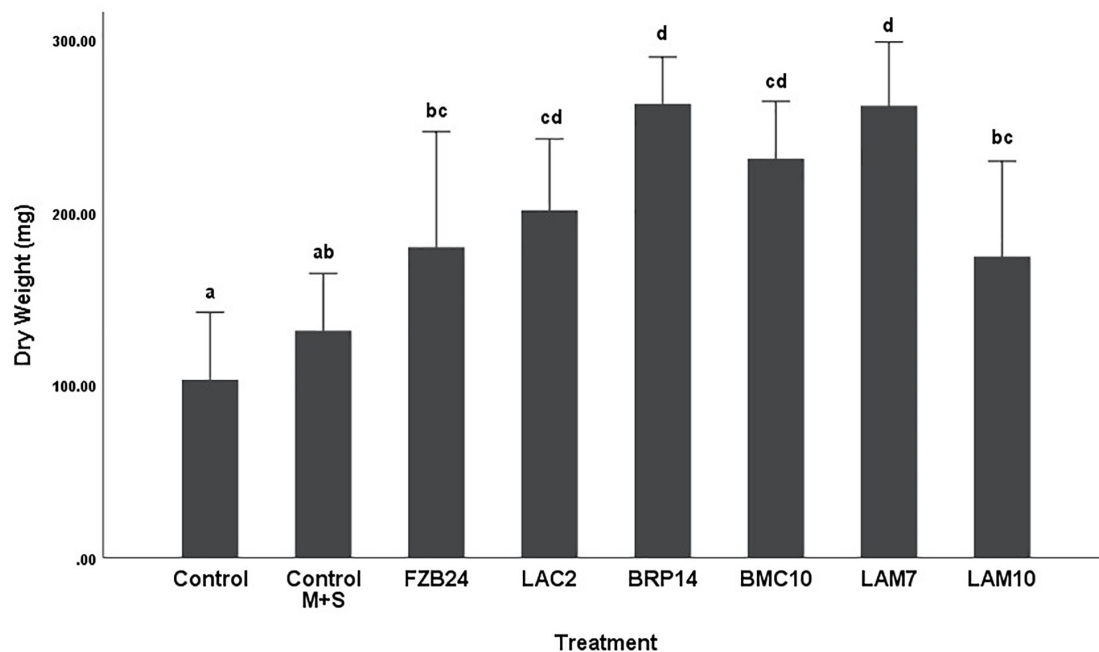


FIGURE 3 | Growth response of plants exposed to BVCs from isolates growing on solid M+S media. Dry weight of plants is measured in (mg), error bars represent confidence interval of the mean 99% ($n = 8$). Isolates which share a common letter are not significantly different to one another ($p > 0.01$) according to one-way between groups ANOVA with *post hoc* Tukey test.

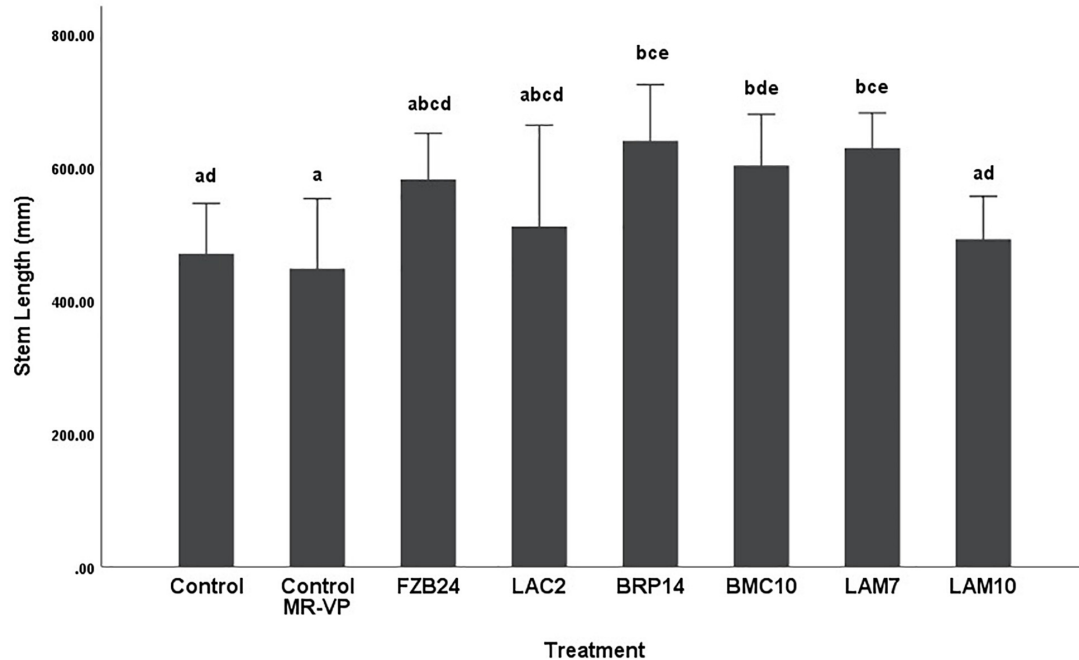


FIGURE 4 | The effect on plant stem length of BVCs from isolates growing on solid MR-VP media. Stem length of plants is measured in (mm), error bars represent confidence interval of the mean (99%) ($n = 8$). Isolates which share a common letter are not significantly different to one another ($p > 0.01$) according to one-way between groups ANOVA with *post hoc* Tukey test.

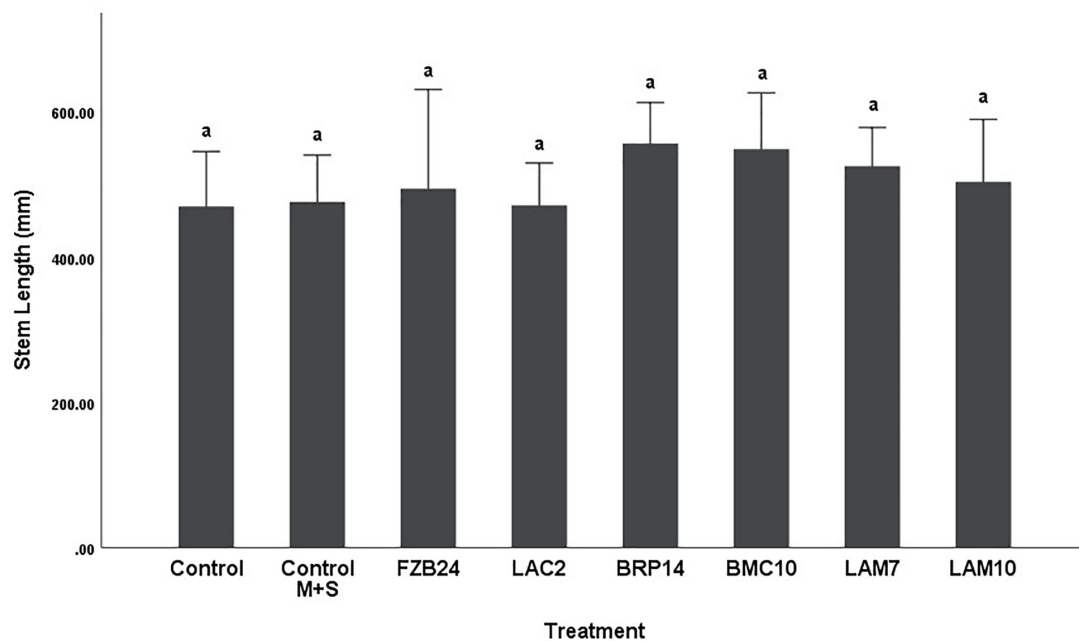


FIGURE 5 | The effect on plant stem length of BVCs from isolates growing on solid M+S media. Stem length of plants is measured in (mm), error bars represent confidence interval of the mean (99%) ($n = 8$). Isolates which share a common letter are not significantly different to one another ($p > 0.01$) according to one-way between groups ANOVA with *post hoc* Tukey test.

2 weeks to allow the microplants to acclimatize to surrounding environmental conditions. Following this the plantlets were exposed to BVCs by dropping 20 μ l of each bacterial culture at OD 600nm = 1.0 on the center of a 50 mm Petri dish containing either Methyl Red-Voges Proskeur (MR-VP) broth (Sigma Aldrich) supplemented with 14 g agar (Sigma Aldrich) per liter; or 1/2 strength M + S media containing 2.2 g M + S basal medium (Sigma Aldrich #5519), 15 g sucrose and 6 g agar per liter. The bacterial inoculum was allowed to air-dry under aseptic conditions for ~15 min and the Petri dish was then placed inside the Microbox® growth chamber containing the microplants under aseptic conditions. The microplants were exposed to the resulting rhizobacterial BVCs for a period of 4 weeks. Control microplants were set up with either un-inoculated axenic media or no media at all. Experiment was repeated twice with four technical replicates and each technical replicate consisted of four microplants.

RNA Extraction

Microplants exposed to BVCs from LAC2 (L), FZB24 (F), or absolute control (C) or control with axenic media (M) were cultivated as described above in an independent experiment. Plants were harvested under aseptic conditions and RNA extractions from stem tissue were carried out using the QIAGEN® RNeasy™ plant extraction kit according to the manufacturer's specifications. To eliminate genomic DNA contamination the Ambion® TURBO™ DNase kit was used according to manufacturer's specifications (Life Technologies, Carlsbad, CA, United States). RNA quantification was measured using a Nanodrop™ 2000c spectrophotometer (Thermo Fisher Scientific, Waltham, MA, United States). Samples were immediately snap frozen in liquid nitrogen and stored at -80°C to prevent degradation of RNA.

MACE Sequencing

Massive analysis of cDNA (MACE) is a 3'mRNA sequencing method based on the analysis of Illumina reads derived from fragments that originate from 3' mRNA ends (Müller et al., 2014). The samples were prepared by GenXPro GmbH (Frankfurt, Germany) using the MACE-Kit v1 according to the manual of the manufacturers (GenXPro GmbH). Briefly, RNA was fragmented and polyadenylated mRNA was enriched by poly-A specific reverse transcription. A specific adapter was ligated to the 5' ends and the 3' ends were amplified by competitive PCR. Duplicate reads as determined by the implemented unique molecular identifiers (TrueQuant IDs) were removed from the raw dataset. Low quality sequence-bases were removed by the software cutadapt¹ and poly(A)-tails were clipped by an in-house Python-Script. The RNA-seq data discussed in this publication have been deposited in NCBI's Gene Expression Omnibus (Edgar et al., 2002) and are accessible through GEO Series accession number GSE160297.

¹<https://github.com/marcelm/cutadapt/>

Statistical and Bioinformatic Analysis

Growth data was statistically analyzed using SPSS 25 (IBM). Two-way analysis of variance (ANOVA) was used to determine the interaction effect of bacterial isolate and media type on plant growth. Significant differences among BVC treatments were estimated using one-way between groups ANOVA with Tukey test for *post hoc* comparisons. For transcriptomic analysis, DeSeq2 version 1.24 was used on raw counts provided by GenXPro, removing genes with no counts or only a single count across all samples prior to analysis. Genes were considered to be differentially expressed if they had a Benjamini Hochberg adjusted *p*-Value of (<0.05) and absolute log2 fold change (≥ 2). Gene Ontology (GO) enrichment was performed using GoSeq version 1.36.0 with significant GO terms identified as those with adjusted *p*-Values (<0.05) for over-represented terms. Gene IDs, descriptions and GO terms were retrieved from Ensembl Biomart v2.40.5 using *Solanum tuberosum* (SolTub_3.0) as the reference. The pheatmap function from the pheatmap v1.0.12 package was used to plot the heat map with clustering distance for rows and columns set to correlation, scale set to row, and row and column clustering set to use complete linkage hierarchical clustering. R version 3.6.1 was used for all analysis. The UpSetR plots were created using UpSetR version 1.4.0 using the gene IDs of genes that were differentially expressed in each comparison.

RESULTS

Effect of BVCs on Plant Dry Weight and Stem Length

To test the effect of BVCs from isolates cultured on MR-VP and M + S on plant dry weight and stem length, a 50 mm Petri dish inoculated with each respective isolate, or none in the case of media control treatments, was placed in a TP5000 + TPD5000 Microbox® growth chamber to allow BVCs to diffuse within the chamber thus exposing the plants within the open Magenta vessel to each of the respective isolate BVCs, the inclusion of the XXL + grade allowed maximal passive-ventilation between the growth chamber and outer atmosphere (Figure 1).

Two-way ANOVA was carried out to examine the relationship between bacterial isolate, media type and their interaction effect on plant growth and the resulting dry weight and stem length respectively. The interaction effect of isolate*media on dry weight was not statistically significant ($p = 0.083$) ($p < 0.01$). The interaction effect of isolate*media on stem length was also not statistically significant ($p = 0.055$) ($p < 0.01$).

To further examine the main effects of isolate and media on dry weight and stem length, one-way between groups ANOVA was carried out for isolates cultured on both types of media and their effects were determined, respectively. All isolate BVCs increased plant dry weight and stem length compared to plants in both controls when isolates were cultured on MR-VP. When cultured on M + S, all isolate BVCs also increased dry weight compared to both controls and five of six isolates increased

TABLE 1 | Putative volatile organic compound production over 72 h from six bacterial isolates growing in tryptic soy broth (TSB), liquid MR-VP and liquid M + S.

Volatile organic compound	TSB	MR-VP	M + S
3-hydroxy-2-butanone	FZB24, BMC10, LAM7, LAM10	FZB24, BMC10, LAM7	BMC10
2,3-butanediol	FZB24, BMC10, LAM7, LAM10	FZB24, BMC10, LAM7	Not Detected
2,5-dimethylpyrazine	FZB24, LAC2, BRP14, BMC10, LAM7, LAM10	Not Detected	Not Detected
3-methyl-1-butanol	LAC2, BRP14, LAM7	LAC2, LAM7	LAC2, LAM7
Dimethylamine	LAC2	LAC2, LAM7	Not Detected
2-butanamine	LAM7	LAC2	Not Detected
1-decanol	LAC2, LAM7	LAC2, LAM7	Not Detected
1-dodecanol	LAC2, LAM7	LAC2, LAM7	Not Detected
2-undecanone	LAC2	LAC2	LAC2
2-tridecanone	LAC2, LAM7	LAC2	LAC2, LAM7
2-heptadecanone	LAC2	LAC2	LAC2
1-methyldecylamine	LAC2	Not Detected	Not Detected
Dodecane	BMC10	FZB24, LAM7	Not Detected
2-piperidinone	Not Detected	LAC2, BMC10, LAM7, FZB24	Not Detected
2-nonanone	LAC2	LAC2	LAC2
1-undecene	BRP14	BRP14	BRP14
Benzaldehyde	FZB24, BMC10, LAM10	BMC10	Not Detected
Dimethyl disulfide	LAM7	Not Detected	Not Detected
2-methyl-1-butanol	Not Detected	LAM7	LAC2
2-ethyl-1-pentanol	Not Detected	LAC2	Not Detected
Hexadecane	BMC10	FZB24, LAC2, LAM7, LAM10	BRP14
2-ethyl-1-hexanol	BMC10, BRP14, LAM10	BMC10, FZB24	Not Detected
2-nonanol	BRP14	Not Detected	Not Detected
1,4-undecadiene	BRP14	Not Detected	Not Detected
2,9-dimethyldecane	Not Detected	BRP14, LAM10	BRP14, LAM10
Decane	Not Detected	BRP14	BMC10
1-octanol	Not Detected	LAM7	Not Detected
1-heptadecanol	LAM7	LAM7, LAC2	Not Detected
Cyclopropyl carbinol	LAC2, BMC10, LAM10	LAC2	Not Detected
1-tetradecanol	Not Detected	LAM7	Not Detected
2-propanamine	LAC2, BMC10	Not Detected	Not Detected
2-octanamine	LAM10	Not Detected	Not Detected
1-tridecanol	Not Detected	LAM7	Not Detected
Undecane	Not Detected	Not Detected	BRP14
Pentanal	Not Detected	LAC2	Not Detected
Octanal	Not Detected	LAC2	Not Detected
Nonanal	Not Detected	BRP14	Not Detected
Decanal	Not Detected	BRP14	Not Detected
3-methylbutanal	Not Detected	Not Detected	LAC2
3-tridecanone	LAC2	Not Detected	Not Detected
4-methyl-2-heptanone	LAM10	Not Detected	BRP14, BMC10
Hexadecanal	Not Detected	LAC2	Not Detected
Di-tert-butyl-dicarbonate	LAM10	Not Detected	BRP14, BMC10, LAM7
5-methylundecane	Not Detected	LAM7, LAC2	BRP14
2-ethyl-4-methyl-1-pentanol	LAC2, LAM10	Not Detected	BMC10, LAM7
Pentanoic Acid	Not Detected	BRP14	BRP14
4-methyldecane, 2,6-dimethylundecane, Ethyne, Ethylene oxide, Cyclobutanol	BMC10	Not Detected	Not Detected
1-nonene, Fluoroethyne, 2-octenal	BRP14	Not Detected	Not Detected
Benzene ethanol, 2-ethynyloxy-ethanol, 1,3-bis(1,1-dimethyl-ethyl)benzene	Not Detected	LAM7	Not Detected
Formic acid	Not Detected	Not Detected	BRP14
4-methyldecane	Not Detected	LAM10	BRP14

(Continued)

TABLE 1 | Continued

Volatile organic compound	TSB	MR-VP	M + S
Trimethylpyrazine, 3-ethyl-2,5-dimethylpyrazine	LAC2	Not Detected	Not Detected
4-methyl-2-pentanone, 2-ethoxy-2-methylpropane	Not Detected	Not Detected	BMC10, LAM7
4,6-dimethyl-2-heptanone	Not Detected	Not Detected	LAM7
Acetaldehyde	Not Detected	LAM10	Not Detected
2-butyric acid	Not Detected	Not Detected	LAM10

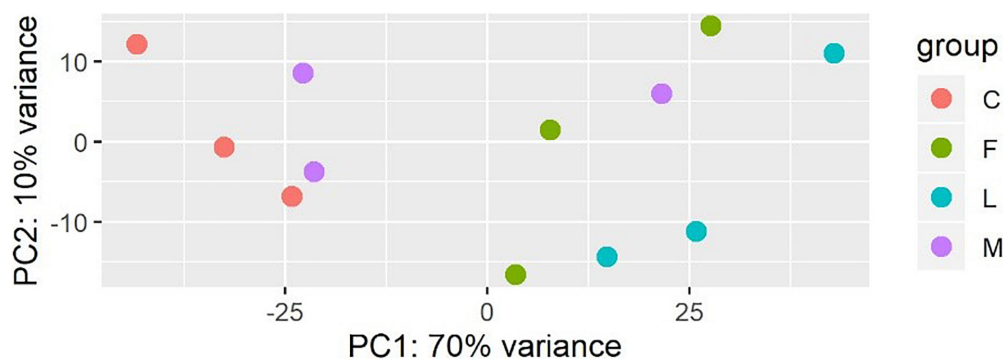


FIGURE 6 | Plot of the first two principal components of a PCA generated from the expression data (count data with variance stabilizing transformation from DeSeq2) colored by condition showing that samples in each condition group together.

stem length compared to both controls. Of the isolates cultured on MR-VP media, BRP14 and LAM7 had the greatest overall effect on biomass increase with a 2.57- and 2.69-fold increase in dry weight compared to that of the control with axenic media treatment respectively (**Figure 2**). No significant differences in dry weight were observed between respective *Bacillus* isolates (FZB24, BMC10, LAM7) cultured on MR-VP, additionally no significant differences were observed between the two respective *Serratia* isolates (LAC2, LAM10), however LAC2 was the only isolate significantly less effective at promoting plant growth when compared to LAM7 and BRP14 ($p > 0.01$). All isolates growing on M + S media significantly increased dry weight compared to the control treatment (**Figure 3**). The isolates FZB24 and LAM10 did not display a significant increase in growth compared to the control treatment with axenic M + S media ($p > 0.01$). The remaining isolates LAC2, BMC10, LAM7 and BRP14 significantly increased biomass compared to the axenic media control treatment ($p < 0.01$). The increase in biomass was again most pronounced in plants treated with BRP14 and LAM7 where dry weight was increased by ~2-fold compared to the control treatment.

Differences in stem length were not as pronounced as dry weight between both media types. In plants treated with MR-VP-derived BVCs, only BRP14 and LAM7 were significantly different from both control treatments ($p < 0.01$). The *Bacillus* isolate BMC10 was also found to significantly increase stem length compared to the axenic control treatment ($p < 0.01$) (**Figure 4**). No significant differences were observed between the control treatments and the FZB24, LAC2 and LAM10 isolates ($p > 0.01$). The effect of M + S-derived BVCs on stem length was not significantly different between the test isolates and the control

treatments ($p > 0.01$) (**Figure 5**), indicating that media type can affect the rate of growth with respect to stem length.

Detection of BVCs From Isolates Cultured in Three Different Media Types

Of the 66 BVCs detected across all isolates and media, alcohols were the most abundant (25.75%), followed by ketones (15.15%) and both alkanes and aldehydes (13.63%). Other chemical groups detected include the amines, alkenes, pyrazines and alkynes. All six isolates were capable of producing 2,5-dimethylpyrazine when cultured in TSB. In fact, all three pyrazines listed were only detected when isolates were cultured in TSB and LAC2 was the only isolate to emit each of these three pyrazines with trimethylpyrazine and 3-ethyl-2,5-dimethylpyrazine detected in addition to 2,5-dimethylpyrazine. The production of pyrazines from TSB-derived bacterial cultures has been reported previously (Rees et al., 2017).

Further analysis revealed media type influenced the number and scope of BVCs emitted by isolates. Of the three media types, M + S media was responsible for the least amount of BVCs detected, only 23 BVCs in total were detected in M + S-cultured isolates, with alkanes (30.43%) and ketones (34.78%) being the most prevalent. The best performing isolate in terms of BVC emission potential from M + S was BRP14 which emitted 10 (43.47%) of these 23 BVCs, in contrast, no volatiles of probable biogenic origin were detected when FZB24 was cultured in TSB.

The greatest number of BVC emissions was observed when isolates were cultured in MR-VP with 36 BVCs detected in total, alcohols (36.11%) and alkanes (16.66%) were the most prevalent. The greatest amount of BVCs detected from isolates cultured

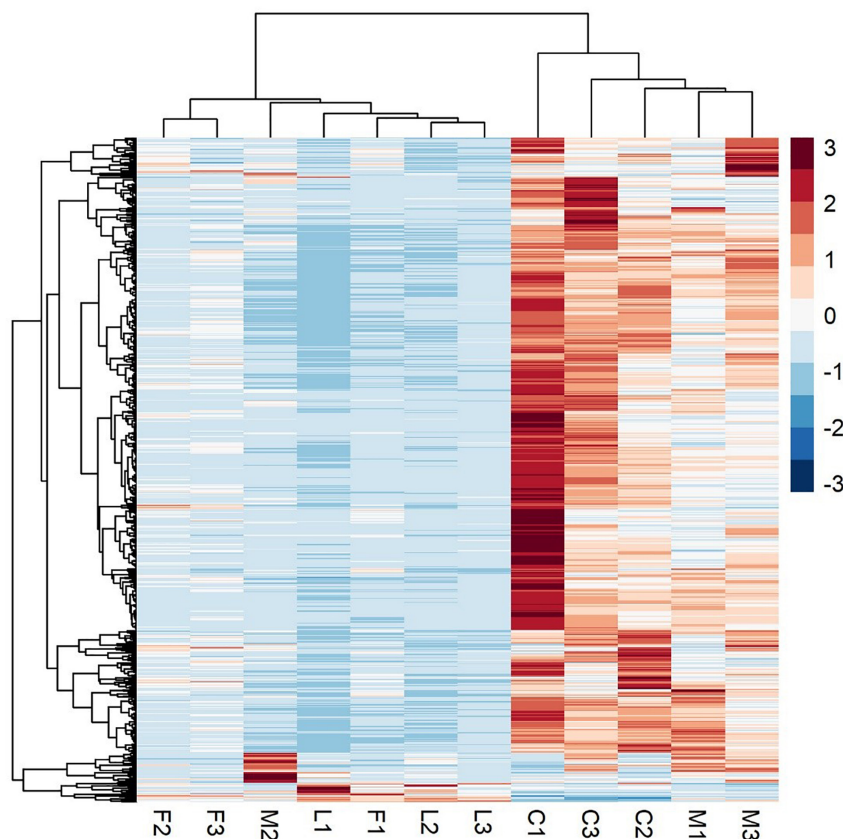


FIGURE 7 | A heatmap of RNA-Seq expression z-scores computed for genes that are significantly differentially expressed Benjamini-Hochberg adjusted p -Value ($p < 0.05$) in any comparison. The genes (rows) and samples (columns) are clustered using the Pearson Correlation distance and complete linkage hierarchical clustering. The color code shows the row z-score, with a red color indicating higher expression of a gene and blue color indicating lower expression of a gene. This heatmap demonstrates that C (control) and M (control with axenic MR-VP media) groups, and L (LAC2/MR-VP volatile blend) and F (FZB24/MR-VP volatile blend) groups cluster together and that the genes involved have higher expression in the C and M groups compared with the L and F groups.

in MR-VP was from LAC2 which emitted 18 (50%) of the 36 BVCs detected. Unlike the earlier observation in M + S, BRP14 emitted the least amount of BVCs when cultured in MR-VP with only six (16.66%) being detected from this isolate. A total of 32 BVCs were emitted from isolates cultured in TSB with alcohols (31.25%) and ketones (21.87%) being the most prevalent. Similar to the observation in MR-VP, LAC2 emitted the greatest number of BVCs, 15 (46.87%) in total, while BRP14 emitted the least with seven (21.87%) BVCs detected (**Table 1**).

Unique BVCs were identified in a number of isolate BVC emissions, for example, LAC2 emitted nine BVCs unique to this isolate in our study, among them 2-nonanone, 2-heptadecanone and 2-undecanone which were observed in the emission profiles associated with growth in all three media types. There were 10 unique BVCs emitted by BRP14 and one of these was common to all three media types namely 1-undecene, while other BVCs include 2-nonanol, 1,4-undecadiene, nonanal, decanal, 1-nonene, fluoroethyne, 2-octenal, formic acid and pentanoic acid. BMC10 emitted five unique BVCs; 4-methyldecane, 2,6-dimethylundecane, ethyne, ethylene oxide and cyclobutanol, but only when cultured in TSB. LAM10 was found to emit two unique

BVCs; acetaldehyde and 2-butyric acid, and LAM7 emitted seven unique BVCs; 1-octanol, 1-tetradecanol, tridecanol, benzene ethanol, 2-ethynoxy-ethanol, 1,3-bis(1,1-dimethyl-ethyl)benzene and dimethyl disulfide, the latter of which has been shown to both promote (Meldau et al., 2013) and slightly inhibit plant growth (Cordovez et al., 2018). A large amount of overlap was observed in the capability of LAC2 and LAM7 to emit the same BVCs as one another namely dimethylamine, 2-butanamine, 1-decanol, 1-dodecanol, 2-tridecanone, 2-methyl-1-butanol and 1-heptadecanol, representing 10.60% of all BVCs detected in our analysis.

Transcriptomic Response to BVC Exposure

A principal component analysis revealed that there were distinct differences in gene expression between BVC treatment and control groups, with treatment accounting for 80% of the variance in gene expression between groups in the first two principal components (**Figure 6**). A heatmap of differentially expressed genes (DEGs) between control and BVC treatments demonstrates that for the most part the respective treatments

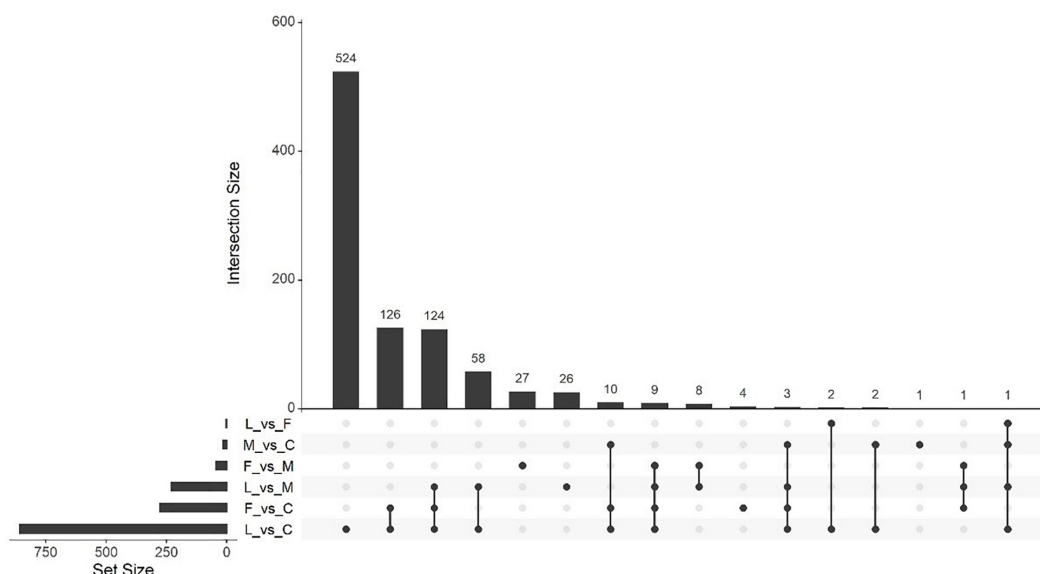


FIGURE 8 | UpSetR plot showing numbers of downregulated differentially expressed genes (DEGs), ($p < 0.05$) and Log2 fold change (≥ 2.0). Any DEGs common to plant treatments are shown by connected dots. Cumulative numbers of DEGs are calculated by adding numbers associated with dots in each respective treatment row.

co-cluster with one another except for one of the MR-VP axenic media control treatments (M2) (**Figure 7**). Overall, BVC treatment within our experimental set up, results in the relative downregulation of genes compared to the control treatments, regardless of whether the respective BVC-emitting isolate is from the *Bacillus* or *Serratia* genus. Enrichment of three gene ontologies was observed following plant exposure to BVCs emitted by LAC2, all of which were associated with photosynthesis. Two belong to the biological process, GO:0019684 (photosynthesis, light reaction) and GO:0009772 (photosynthetic electron transport in photosystem II) while the third belonged to molecular function GO:0045156 (electron transporter, transferring electrons within the cyclic electron transport pathway of photosynthesis activity).

Massive analysis of cDNA RNA-seq revealed that in all, 52 genes were upregulated between treatments and, the greatest number of DEGs, 17 altogether, was observed in the (C vs. M) comparison. The LAC2 BVC-treated plants had the next highest levels of upregulated genes with 14 and 13 DEGs observed in the (L vs. C) and (L vs. M) comparisons respectively. Very little upregulation of gene expression was observed in FZB24 BVC-treated plants with the (F vs. C), (F vs. M), and (F vs. L) yielding two, three and three DEGs respectively (**Figure 8**).

Of the upregulated genes observed in the (L vs. C) comparison a number of genes associated with photosynthetic processes and cell division were observed such as a chlorophyll a/b binding protein and the plastid division regulator MinE along with genes associated with a possible stress and/or defense responses such as Zinc finger (CCCH-type) protein and Hsp20/alpha crystallin family protein. The (L vs. M) comparison also resulted in the upregulation of genes associated with photosynthesis where four chlorophyll a/b binding proteins were identified. In the (F vs.

M) comparison the gene for protease inhibitor IIa was the only identifiable transcript from the PGSC genome (**Table 2**).

Massive analysis of cDNA RNA-seq revealed that 1,413 genes were downregulated across all comparisons, the greatest difference being observed in (L vs. C) with 859 DEGs identified (**Table 3**). As in the upregulation response, BVC treatment from the LAC2 isolate was responsible for the highest amount of DEG downregulation. The lowest amount of downregulated DEGs was in the (F vs. L) comparison with no DEGs observed (**Figure 9**). Generally, downregulation was far more pronounced than upregulation in BVC-treated plants with a large proportion of these DEGs being related to defense and stress responses (**Table 4**).

DISCUSSION

For almost two decades the interactions of BVCs with plants has been the focus of intense research. These interactions can be directly observed in the sensor plant, usually through the induction of a defense response via the upregulation of pathogenesis-related (PR) genes which are key for induced systemic resistance (ISR) or through an increased rate in plant growth and accumulation of biomass (Ryu et al., 2004; Kim et al., 2015). BVCs can also have indirect effects on plants via the inhibition of bacterial and especially fungal phytopathogens (Giorgio et al., 2015) and have also been observed to increase the rate of micronutrient-uptake in sensor plants, leading to a potentially biofortified harvest in crop plants (Orozco-Mosqueda et al., 2013).

We devised a novel growth system in which to study the effects of BVCs on potato plants in an enclosed, passively ventilated

TABLE 2 | Upregulated genes from PGSC genome annotations in response to BVC exposure.

Treatment	Gene ID	Gene name	Log2FC	References
LAC2 vs. Control	PGSC0003DMG400007123	Phytosulfokine peptide	2.075	Igarashi et al., 2012
	PGSC0003DMG400008309	Chlorophyll a/b binding protein	2.097	Zhu et al., 2020
	PGSC0003DMG400022062	Aspartic proteinase	2.413	Resjö et al., 2019
	PGSC0003DMG400028333	Plastid division regulator MinE	2.125	Chen et al., 2018
	PGSC0003DMG400026831	Conserved gene of unknown function	4.159	N/A
	PGSC0003DMG400020916	Fibrillarin homolog	4.499	Rajamäki et al., 2020
	PGSC0003DMG401031741	UPA16	2.274	Kay et al., 2009
	PGSC0003DMG400005792	Nucleoside diphosphate kinase	3.760	Lin et al., 2015
	PGSC0003DMG402025318	Zinc finger (CCCH-type) protein	2.075	Bogamuwa and Jang, 2014
	PGSC0003DMG400033693	UPA16	3.046	Kay et al., 2009
	PGSC0003DMG400008713	Hsp20/alpha crystallin family protein	3.918	Zhao et al., 2018
LAC2 vs. Axenic MR-VP	PGSC0003DMG400000493	Carbonic anhydrase	2.074	DiMario et al., 2018
	PGSC0003DMG400008309	Chlorophyll a/b binding protein	2.289	Zhu et al., 2020
	PGSC0003DMG400005884	Conserved gene of unknown function	3.288	Lekota et al., 2019
	PGSC0003DMG400013416	Chlorophyll a-b binding protein 3C, chloroplastic	2.074	Zhu et al., 2020
	PGSC0003DMG400004301	Chlorophyll a, b binding protein type I	2.185	Zhu et al., 2020
	PGSC0003DMG400007796	DNA-directed RNA polymerase II largest subunit	2.663	Zhou et al., 2017
	PGSC0003DMG400033046	Dof zinc finger protein	2.161	Venkatesh and Park, 2015
	PGSC0003DMG400013412	Chlorophyll a-b binding protein 3C	2.455	Gao and Bradeen, 2016
	PGSC0003DMG400012838	Non-specific lipid-transfer protein	4.402	N/A
	PGSC0003DMG400012839	Non-specific lipid-transfer protein	4.392	N/A
FZB24 vs. Axenic MR-VP	PGSC0003DMG400030593	Proteinase inhibitor IIa	2.088	Rehman et al., 2017

experimental setup. The model plant *Arabidopsis thaliana* is often the predominant target in lab-based *in vitro* studies of the BVC-mediated effects on plants (Bee Park et al., 2013; Sharifi and Ryu, 2016; Bhattacharyya et al., 2015). Here, we present the growth effects of BVCs on potato to study their effects on a major staple food crop plant. The type of growth system, either open or closed, in which to observe the effect of microbial VOCs on plants, phytopathogens and animals has been widely researched and discussed in recent years (Kai et al., 2007; Popova et al., 2014; Park et al., 2015; Kai et al., 2016; Sharifi and Ryu, 2018; Song et al., 2019). Extrapolating how these respective systems affect volatile concentrations, mixtures of volatiles, responses of test organisms and the combined spatiotemporal effects of these parameters has made the definitive translation of effects from the lab setting to the field more difficult. The physical nature of VOCs, such as a high vapor pressure, low boiling point and low molecular weight (<300 Da) lends to their short-term proximity to target organisms in the field, although a number of methodologies have been developed to mitigate this effect (Song and Ryu, 2013; Fincheira et al., 2019, 2020).

This study identified VOCs from six bacterial isolates from three genera; *Bacillus*, *Serratia*, and *Pseudomonas* cultured in three different types of liquid media via SPME-GC/MS. The growth medium of the bacteria is known to alter the blend of BVCs which are emitted (Blom et al., 2011a) and taking this into account we selected TSB, MR-VP and M + S liquid media from which to assess both the BVC-producing capability and variety from selected isolates. We identified 66 different putative BVCs in total, some of which are widely reported in the literature such as 2,3-butanediol, 3-hydroxy-2-butanone, 2,5-dimethylpyrazine,

2-nonanone, 2-tridecanone and 3-methyl-1-butanol (Ryu et al., 2003; Velivelli et al., 2015; Asari et al., 2016; Fincheira et al., 2017; Fincheira and Quiroz, 2018; Fincheira and Quiroz, 2019). Some BVCs were also observed to be isolate-specific such as 1-undecene, 2-nonanone and 1-tetradecanol produced by BRP14, LAC2 and LAM7 respectively. Interestingly, dimethyl disulfide, widely reported as a PGP volatile among many PGP bacterial isolates (Meldau et al., 2013; Tyc et al., 2017) was only detected once in our analysis by a single strain, LAM7, and only when cultured in TSB. Dimethyl disulfide has also been reported as a growth inhibitor with concentration-dependent effects (Kai et al., 2010; Cordovez et al., 2018).

When isolates cultured on MR-VP agar were co-cultivated with potato microplants there was a significant increase in growth between the control and all BVC treatments. This may be attributed to the carbon-rich composition of this media and the subsequent blend and/or concentration of BVCs present within the growth system. The most common BVCs observed between isolates utilizing MR-VP as a carbon source were hexadecane and 2-piperidinone, with four of six isolates emitting these particular BVCs, the latter was recently described as an insecticidal constituent from a biocontrol fertilizer (Qiu et al., 2019). The next most common were 3-hydroxy-2-butanone and 2,3-butanediol identified in the headspace of three isolates, FZB24, BMC10 and LAM7 all of which are members of *Bacillus*. The largest increases in dry biomass were observed after exposure to BVCs from LAM7 and BRP14, 2.69- and 2.57-fold greater than that of the axenic media control respectively, suggesting that the volatile blends from these isolates cultured in MR-VP are strong growth-promoters. Our analysis identified 2,3-butanediol

TABLE 3 | Numbers of upregulated and downregulated genes between BVC treatments from isolates cultured on MR-VP media according to MACE RNA-seq.

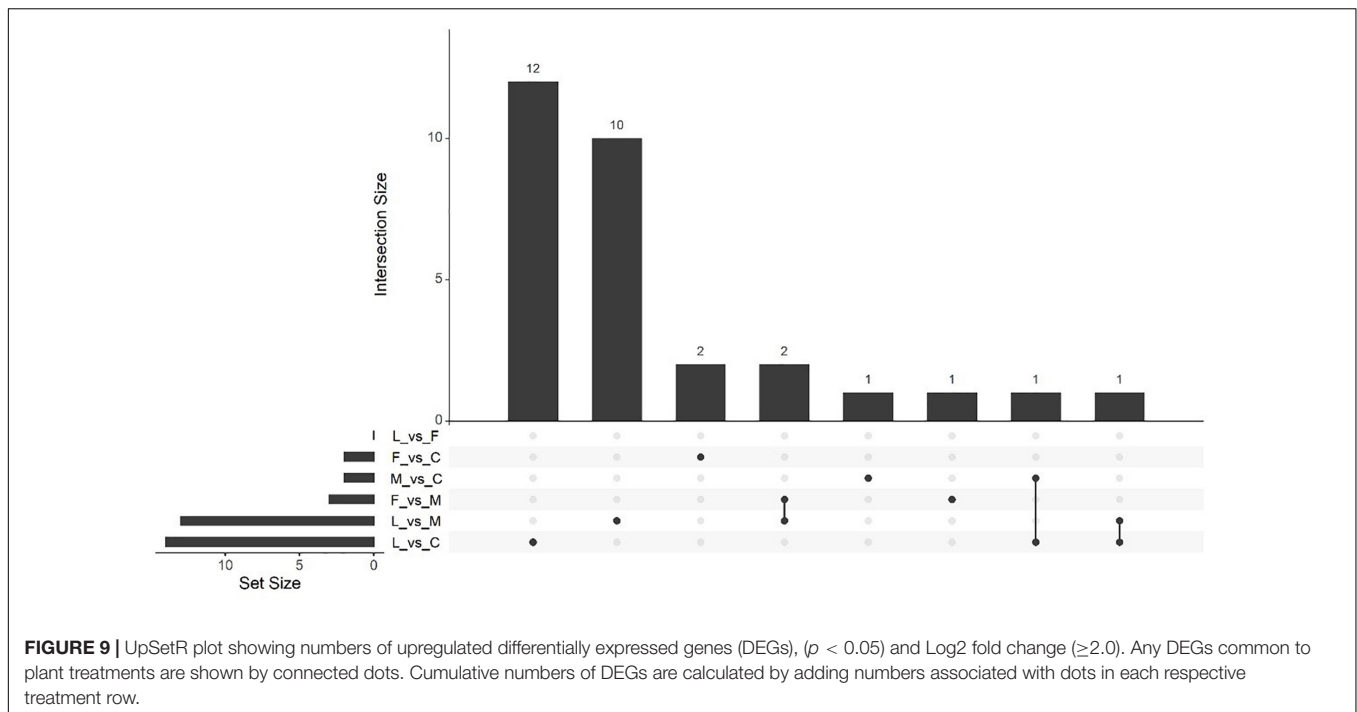
Treatment comparison	Upregulated genes	Downregulated genes
FZB24 vs. Control	2	277
LAC2 vs. Control	14	859
Control vs. Axenic MR-VP	17	2
FZB24 vs. LAC2	3	0
FZB24 vs. Axenic MR-VP	3	45
LAC2 vs. Axenic MR-VP	13	230
Total	52	1,413

and 3-hydroxy-2-butanone within the headspace of *B. mycoides* (LAM7), interestingly these were not detected in the headspace of *B. mycoides* strains (CHT2401) and (CHT2402) in a previous study (Huang et al., 2018). This may indicate that bacterial strains within a particular species may harbor the ability to employ strain-specific BVCs for exploitation of particular ecological niches under the correct environmental conditions as described for *Bacillus subtilis* (Kai, 2020), additionally, interlaboratory variation in volatile profiles cannot be discounted (Clark et al., 2021). Stem length was also significantly increased after exposure to BVCs from both LAM7 and BRP14 in comparison to both control treatments. There was a total of 18 volatiles identified in the LAM7/MR-VP BVC blend and consisted of, amongst others, 3-methyl-1-butanol, 1-decanol, 1-dodecanol, hexadecane, 1-octanol and 1-tridecanol which were also identified as growth promoters in previous studies (Velázquez-Becerra et al., 2011; Bee Park et al., 2013; Velivelli et al., 2015; Pérez-Flores et al., 2017; Camarena-Pozos et al., 2019). In BRP 14/MR-VP the predominant BVC, from a total blend of just five, was identified as 1-undecene, a particularly potent volatile in the biocontrol effect against some fungal phytopathogens mediated by many *Pseudomonas* strains (Kong et al., 2020). The greatest effect on stem length was observed with plants exposed to BVCs of BRP14/MR-VP.

A similar trend was seen in dry weight measurements from M + S-derived BVC treatments as was observed in MR-VP, however LAC2 BVCs marginally increased dry weight compared to those of FZB24 when cultured on M + S. No significant differences in stem length were observed post-exposure to M + S-cultured isolates to that of the respective control treatments. These differences in growth observed between both media types can be explained by the composition of the respective media, with MR-VP being a more carbon-rich media than M + S. Indeed, we observed that proliferation of isolates across the media surface was far more apparent in isolates which were cultured on MR-VP, while isolates cultured on M + S rarely expanded their radial growth beyond the point at which their starting culture was dropped on to the media. Members of the genus *Serratia* are reported as BVC-emitting biocontrol and PGP agents (Wenke et al., 2019) and while their BVC-mediated inhibition of phytopathogenic growth has been well reported, the effect of volatiles from two *Serratia* strains in this study, LAC2 and LAM10, were often not as effective as those of *Bacillus* and *Pseudomonas* at increasing plant growth.

LAC2 was the only isolate observed to produce 2-undecanone, 2-heptadecanone and 2-nonanone which have been the subject of particular research focus in recent years, particularly 2-nonanone both in the preservation of commercially important fruits such as strawberry from *Botrytis cinerea* (Abarca et al., 2017), as an inhibitor of bacterial quorum sensing, a disruptor of protein folding in bacteria and inducer of plant defense (Chernin et al., 2011; Melkina et al., 2017; Báez-Vallejo et al., 2020).

For transcriptomic analysis of potato plants exposed to BVCs in our system the isolates LAC2 and the commercially available isolate FZB24, members of *Serratia* and *Bacillus* respectively were chosen as the BVC source due to the fact they only share two common BVCs when grown on MR-VP, namely 2-piperidinone and hexadecane. Additionally, species of these genus have been well documented to emit antimicrobial and growth-promoting BVCs (Fincheira et al., 2016; Tahir et al., 2017). Therefore, we expected to see noticeable alterations in the plant transcriptomic landscape in response to these isolates. Interestingly, only 52 genes were upregulated across treatments, whereas 1,413 were downregulated. In BVC-treated plants, LAC2 was responsible for the upregulation of genes involved in photosynthetic activity, such as a number of genes coding for chlorophyll a/b binding proteins and the plastid division regulator MinE. Genes associated with defense and stress responses were also upregulated such as phytoalkaline peptide, aspartic proteinase and zinc finger (CCCH-type) protein. FZB24 was responsible for the upregulation of just one identifiable gene from the PGSC potato genome, proteinase inhibitor IIa, which is known to be involved in the defense response against phytopathogens and insect pests (Rehman et al., 2017; Table 2). The gene phytoalkaline peptide has been reported as an attenuator of pattern-triggered immunity in *Arabidopsis* and acts as a positive regulator of growth by balancing resource allocation between defense and growth (Igarashi et al., 2012). Unexpectedly, many of the downregulated genes were related to defense and stress responses. A similar response has been reported previously from the pure PGP volatile 1-decene emitted by the beneficial fungus *Trichoderma* which downregulated stress and defense genes such as WRKY transcription factors (Lee et al., 2019). Three WRKY transcriptions factors were also downregulated in our study. Five DEGs related to stress and/or defense were commonly downregulated in (L vs. C) and (F vs. C) namely enhanced disease susceptibility 1 protein (EDS1);



stress responsive gene 6 protein, Srg6; Rpi-vnt1; tospovirus resistance protein A and UPF0497 membrane protein 8. The protein (EDS1) has been shown, in association with salicylic acid (SA), to mediate redundant functions in R protein-mediated defense signaling confirmed by simultaneous mutations of EDS1 and a salicylic acid-synthesizing enzyme named SID2 resulting in a compromised defense and/or hypersensitive response mediated by R proteins which contain a coiled-coil domain residing in their N-terminal domains (Venugopal et al., 2009). A membrane protein involved in cell wall strengthening, UPF0497, was shown to be upregulated in the PTI response to *Phytophthora infestans* (Resjö et al., 2019), this class of membrane protein was also downregulated in our study. The fact that there are only three BVCs shared in common between LAC2 and FZB24 suggests that these BVCs may be responsible for the induction of the five commonly downregulated DEGs between these isolates and is worthy of future investigation.

Three DEGs downregulated in our analysis code for proteins named PEN1, EDS1 and SGT1 which are known to play crucial roles in plant defense, especially non-host resistance (NHR) to fungal pathogens. These three genes work in a hierarchical manner and sometimes directly co-operate to mediate the hosts innate defense response. PEN1 (PENETRATION 1) is involved in diminishing the successful entry of phytopathogens into the plant cell. *PEN1* encodes a syntaxin anchored in the plasma membrane which is part of the SNARE (soluble N-ethylmaleimide-sensitive factor attachment protein receptor) complex and is required for the timely arrival of papillae which contain callose and extracellular membrane material that aids penetration resistance (Collins et al., 2003; Nielsen et al., 2012). As part of the SNARE complex, the PEN1 protein forms part of the activation of

pre-invasion defense in the resistance to powdery mildews in *Arabidopsis* (Lipka et al., 2008). In the event that the frontline defense of the PEN1/SNARE complex fails, mechanisms to deal with post-invasion defense come into play, where EDS1 and SGT1 play a significant role. The post-invasion NHR response requires EDS1, phytoalexin-deficient 4 (PAD4) and senescence-associated gene 101 (SAG101) and has been confirmed through mutational analyses (Lipka et al., 2005; Stein et al., 2006). These proteins are homologous to lipases and comprise a regulatory node that is crucial for basal defense against the oomycete *Hyaloperonospora parasitica*, SA-mediated signaling and some resistance pathways mediated by R-genes (Kwon et al., 2008). As part of a crucial NHR response EDS1 is necessary for the resistance, including the hypersensitive response, mediated by TIR (Toll/interleukin 1 receptor)-containing proteins (Hu et al., 2005; Wiermer et al., 2005). SGT1 is also essential for the correct functioning of several R genes and the post-invasion NHR response in *Arabidopsis* and is a highly conserved constituent required for the function of certain Skp1/Cullin/F-Box protein (SCF)-type E3 ubiquitin ligase complexes (Austin et al., 2002; Liu et al., 2004a; Holt et al., 2005; Azevedo et al., 2006; Yu et al., 2019). While EDS1 and SGT1 have been shown to be essential components of the plant innate immune system, the never-ending arms race between pathogen and host can turn these genes into clandestine pathogenic weapons. El Oirdi and Bouarab (2007) demonstrated that *B. cinerea* can essentially flank the defenses of the Solanaeceous member *Nicotiana benthamiana* using a molecular distraction. EDS1 and SGT1 are part of the control mechanism for SA-dependent disease resistance toward biotrophic pathogens, while resistance against necrotrophic pathogens is mediated through the jasmonic acid (JA) pathway (McDowell and Dangel, 2000;

TABLE 4 | Downregulated genes from PGSC genome annotations directly involved in or related to plant defense and stress responses identified post-BVC exposure.

Treatment	Gene ID	Gene name	Log2FC	References
FZB24 vs. Control	PGSC0003DMG400033029	Enhanced disease susceptibility 1 protein	-2.412	El Oirdi and Bouarab, 2007; Venugopal et al., 2009
	PGSC0003DMG400007742	NBS-coding resistance gene protein	-2.190	N/A
	PGSC0003DMG400025437	Stress responsive gene 6 protein, Srg6	-2.043	Zhuang et al., 2012
	PGSC0003DMG400000241	Spotted leaf protein	-2.178	Zeng et al., 2004
	PGSC0003DMG400020587	Rpi-vnt1	-3.014	Roman et al., 2017
	PGSC0003DMG400029220	Tospovirus resistance protein A	-2.464	de Oliveira et al., 2018
	PGSC0003DMG400004413	Tm-2 protein	-2.414	Maayan et al., 2018
	PGSC0003DMG400012025	UPF0497 membrane protein 8	-2.714	Resjö et al., 2019
	PGSC0003DMG400002362	GYF domain-containing protein	-2.321	Wu et al., 2017
	PGSC0003DMG402030235	Disease resistance protein R3a	-2.570	Engelhardt et al., 2012
	PGSC0003DMG402029058	Disease resistance protein	-3.213	N/A
	PGSC0003DMG400012025	UPF0497 membrane protein 8	-4.407	Resjö et al., 2019
	PGSC0003DMG400021733	TNP2	-2.359	He et al., 2000
	PGSC0003DMG400030239	CC-NBS-LRR protein	-3.895	Goyer et al., 2015
LAC2 vs. Control	PGSC0003DMG400017065	Disease resistance protein RGA1	-2.679	Huang et al., 2005
	PGSC0003DMG400030462	Avr9/Cf-9 rapidly elicited protein 216	-3.260	Rowland et al., 2005
	PGSC0003DMG400033029	Enhanced disease susceptibility 1 protein	-3.932	El Oirdi and Bouarab, 2007; Venugopal et al., 2009
	PGSC0003DMG400020099	RPM1 interacting protein 4 transcript 2	-2.052	Lee et al., 2015
	PGSC0003DMG401031196	WRKY transcription factor 16	-2.213	Phukan et al., 2016
	PGSC0003DMG400001550	TSI-1 protein	-2.9046	Dahal et al., 2009
	PGSC0003DMG400028904	SGT1	-2.260	Yu et al., 2019
	PGSC0003DMG400007742	NBS-coding resistance gene protein	-3.812	N/A
	PGSC0003DMG400032555	NAC domain protein	-2.174	Kwenda et al., 2016
	PGSC0003DMG400004053	Protein CASP	-2.641	N/A
	PGSC0003DMG400021331	PEN1	-2.231	Collins et al., 2003; Nielsen et al., 2012
	PGSC0003DMG400016769	Double WRKY type transfactor (StWRKY8)	-2.163	Gao et al., 2020
	PGSC0003DMG400009238	Leucine-rich repeat family protein	-2.109	N/A
	PGSC0003DMG402029995	TMV resistance protein N	-3.358	Qian et al., 2018
	PGSC0003DMG400031839	RING-H2 finger protein ATL2	-2.898	Serrano and Guzmán, 2004
	PGSC0003DMG400009634	Bacterial spot disease resistance protein 4	-3.018	Schornack et al., 2004
	PGSC0003DMG400025437	Stress responsive gene 6 protein, Srg6	-2.531	Malatrasi et al., 2002
	PGSC0003DMG400024365	Rpi-vnt1	-4.841	Roman et al., 2017
	PGSC0003DMG400019104	Heat shock protein 70 (HSP70)-interacting protein	-2.261	Jiang et al., 2014
	PGSC0003DMG400000241	Spotted leaf protein	-2.903	Zeng et al., 2004
	PGSC0003DMG400044116	Beta-glucan-binding protein 4	-2.599	Fliegmann et al., 2004
	PGSC0003DMG400004327	Leucine-rich repeat resistance protein	-2.123	N/A
	PGSC0003DMG404026432	Tir-nbs-lrr resistance protein	-4.939	Li et al., 2017
	PGSC0003DMG401011899	Tospovirus resistance protein B	-2.391	de Oliveira et al., 2018
	PGSC0003DMG400029220	Tospovirus resistance protein A	-3.154	De Oliveira et al., 2016
	PGSC0003DMG400019667	Potato resistance I2GA-SH23-3	-2.709	Huang et al., 2005
	PGSC0003DMG401030700	Resistance gene	-3.319	Gu et al., 2020
	PGSC0003DMG400029371	DNA-binding protein NtWRKY3	-2.209	Liu et al., 2004b
	PGSC0003DMG400047046	Nematode resistance	-2.675	Goyer et al., 2015
	PGSC0003DMG400047346	BRASSINOSTEROID INSENSITIVE 1-associated receptor kinase 1	-2.153	Bentham et al., 2020
	PGSC0003DMG402026149	Mitogen-activated protein kinase kinase kinase	-2.646	Pitzschke et al., 2009
	PGSC0003DMG400030462	Avr9/Cf-9 rapidly elicited protein 216	-2.871	Rowland et al., 2005
	PGSC0003DMG400020099	RPM1 interacting protein 4 transcript 2	-2.547	Lee et al., 2015
	PGSC0003DMG400033029	Enhanced disease susceptibility 1 protein	-2.758	Venugopal et al., 2009
	PGSC0003DMG400019232	GRAS2	-2.851	Chang et al., 2015
LAC2 vs. Axenic MR-VP				

(Continued)

TABLE 4 | Continued

Treatment	Gene ID	Gene name	Log2FC	References
FZB24 vs. Axenic MR-VP	PGSC0003DMG400019824	JA-induced WRKY protein	-2.030	Wiesel et al., 2015
	PGSC0003DMG401031196	WRKY transcription factor 16	-2.644	Phukan et al., 2016
	PGSC0003DMG400028904	SGT1	-2.472	Yu et al., 2019
	PGSC0003DMG400007742	NBS-coding resistance gene protein	-2.564	N/A
	PGSC0003DMG400021331	PEN1	-2.248	Collins et al., 2003; Nielsen et al., 2012
	PGSC0003DMG401030700	Resistance gene	-2.550	Gu et al., 2020
	PGSC0003DMG400002562	F-box/kelch-repeat protein	-2.366	Wang et al., 2017
	PGSC0003DMG400002562	F-box/kelch-repeat protein	-2.417	Wang et al., 2017

da Cunha et al., 2006). The SA and JA pathways are known to be antagonistic (Mur et al., 2006). EDS1 acts as an activator of SA signaling but as a repressor of JA/Ethylene signaling (Brodersen et al., 2006), therefore the authors concluded that the activation of EDS1 and SGT1 signaling dampened the JA signaling response thus allowing *B. cinerea* pathogenesis to progress through exploitation of the plants own innate immune system (El Oirdi and Bouarab, 2007).

A number of research questions arising from the use of this growth system require further investigation. Most notably that of the effect of inorganic volatiles such as CO₂ and NH₃ emitted from bacterial cultures which can have both positive and negative effects on plant growth respectively (Kai and Piechulla, 2009; Weise et al., 2013; Piechulla et al., 2017). Gas exchange between the internal and external environment was not monitored in this study and likely plays an important role in the levels of growth and differential gene expression in the plants within this system due to different plant species, bacteria, culture media, filter types, temperature and photoperiod. A number of methodologies could be employed to further investigate this such as CO₂ trapping (Kai and Piechulla, 2009), alteration of Microbox[®] HEPA filter porosity with accompanying trace gas analysis of CO₂ for example and determination of the effect of differing concentrations of pure inorganic, and indeed organic, volatiles such as NH₃ and 2R, 3R-butanediol (Fincheira et al., 2021). Additionally, the effect of bacterial cell number to levels of volatile emissions within the system needs to be determined as this is known to ultimately effect plant growth (Kai, 2020). The use of liquid rather than solid media within the system may also affect BVC emission profiles as oxygen availability between both physical states of media can lead to shifts in volatile emissions (Farg et al., 2006; Somerville and Proctor, 2013; Kai et al., 2020). It is important to note that liquid media was agitated in our experimental procedure for putative VOC detection and this should be considered in any future comparative analyses. Additionally, opening and closing the lid of the system to exchange liquid media for example, may affect any internal equilibrium of volatiles and increase the risk of phytopathogenic contamination.

The use of this passively ventilated system has proved viable for observing the effect of BVCs on plant growth, and may mitigate the effects observed in closed growth systems which

often lack sufficient space for many plants other than *Arabidopsis thaliana* seedlings to grow freely. In many *in vitro* BVC-plant studies, fold changes in plant growth promotion can be quite striking (Blom et al., 2011a; Park et al., 2015). In our study the growth promotion is more modest, perhaps owing to the passive ventilation of the system, which may more closely mimic BVC kinetics found in open natural environments. The methodologies of Park et al. (2015); Cordovez et al. (2018) nicely demonstrate active exposure of volatiles from live bacterial cultures, however experimental conditions in these studies either result in the plant being exposed to the open air environment or enclosed in containers with no ventilation to the outer atmosphere, depending on whether BVC exposure was directed to the roots or shoots. Our system allows exposure of the shoots and roots to BVCs, while BVCs may first interact with the shoots, the co-cultivation time of 4 weeks allows ample opportunity for BVC diffusion through PE foam to the roots. Comparative transcriptomic analyses between the root systems of control vs. BVC-exposed plants should yield answers to this question. Furthermore, while sterilized soil may be lacking live microbes with potential PGP activity, it will still retain organic matter which can as a nutrient source thus masking or inadvertently misrepresenting, the absolute effect of BVCs on PGP potential, this is an implication which deserves further study. It should be noted that in our study root proliferation throughout the foam made it too difficult to obtain an adequate root length and root dry weight as it was not possible to simply wash away or melt the foam, as can be achieved using soil or agar, from the roots, while this may complicate accurate measurements of root parameters described above, it should not prohibit transcriptomic analyses of roots. The observed differences in gene expression between the stems of control vs. BVC-exposed plants within our system shows that foliar application of the PGPR tested in this system could possibly yield similar results in the greenhouse and/or field, this remains to be seen. The observation that genes involved in attenuating and mediating the plant immune response, both upregulated and downregulated respectively, demonstrates that BVC-mediated communication with the plant can involve more than just the upregulation of defense genes. Rather, the induction of a careful dance between up- and downregulation of a suite of genes, perhaps to optimize the pre-colonization internal environment of the host for an endophytic symbiont.

If the bacterial symbiont has an epiphytic life strategy in the rhizosphere of the host plant, and depends on host-derived root exudates as a carbon source, this dance may maintain the overall health status of the host by dampening the negative physiological effects of an over-reactive defense response. The use of this system is quite affordable and may allow for the study of more cumbersome or older plants that cannot be studied in relatively restrictive I-plates. Future analysis on the effect of plant type, plant substrate, microbe, microbial growth media, filter porosity and other parameters relevant to BVC-plant interactions in this system may help to elucidate specific genes or pathways activated in response to a particular single BVC or blend. The opportunity also presents itself to analyze the tripartite effect of fungal/bacterial/plant volatile organic compound interactions within this experimental setup. Systems such as this can help elucidate genes and/or their pathways modulated via BVC exposure for a better understanding of their effect on plant health and ultimately for better solutions to the looming concern of global food security in an ecologically uncertain future.

DATA AVAILABILITY STATEMENT

Datasets for plant growth are available from the corresponding author. Isolate 16S rRNA sequence data has been deposited in GenBank under accession numbers MT373405, MT373394, MT373410, MT373402, and MT373403. RNA-seq data has

been deposited in NCBI's GEO Series under accession number GSE160297.

AUTHOR CONTRIBUTIONS

DH-D and BD devised the experimental setup and layout. DH-D carried out the growth experiments, GC/MS analysis, and growth data analysis and compiled the main text. DH-D and ED extracted total RNA from plant tissue and carried out quality control of RNA and shipping to GenXPro. SC carried out all bioinformatic analyses of MACE RNA-seq data. All authors contributed to the proofreading and editing of the manuscript.

FUNDING

This project was funded by the Crawford Hayes fund at University College Cork.

ACKNOWLEDGMENTS

We thank GenXPro for their assistance with RNA-seq data generation. We also thank Gerry Doherty at TOPS potato centre, Donegal, Ireland for providing starting stock of *S. tuberosum* L. cv. Golden Wonder.

REFERENCES

- Abarca, R. L., Rodríguez, F. J., Guarda, A., Galotto, M. J., Bruna, J. E., Perez, M. A. F., et al. (2017). Application of β -cyclodextrin/2-nonanone inclusion complex as active agent to design of antimicrobial packaging films for control of *Botrytis cinerea*. *Food Bioproc. Technol.* 10, 1585–1594. doi: 10.1007/s11947-017-1926-z
- Adesemoye, A. O., Torbert, H. A., and Kloepper, J. W. (2009). Plant growth-promoting rhizobacteria allow reduced application rates of chemical fertilizers. *Microb. Ecol.* 58, 921–929. doi: 10.1007/s00248-009-9531-y
- Adnan, M., Fahad, S., Zamin, M., Shah, S., Mian, I. A., Danish, S., et al. (2020). Coupling phosphate-solubilizing bacteria with phosphorus supplements improve maize phosphorus acquisition and growth under lime induced salinity stress. *Plants* 9:900. doi: 10.3390/plants9070900
- Asari, S., Matzén, S., Petersen, M. A., Bejai, S., and Meijer, J. (2016). Multiple effects of *Bacillus amyloliquefaciens* volatile compounds: plant growth promotion and growth inhibition of phytopathogens. *FEMS Microbiol. Ecol.* 92:fiw070. doi: 10.1093/femsec/fiw070
- Austin, M. J., Muskett, P., Kahn, K., Feys, B. J., Jones, J. D., and Parker, J. E. (2002). Regulatory role of SGT1 in early R gene-mediated plant defenses. *Science* 295, 2077–2080. doi: 10.1126/science.1067747
- Azevedo, C., Betsuyaku, S., Peart, J., Takahashi, A., Noel, L., Sadanandom, A., et al. (2006). Role of SGT1 in resistance protein accumulation in plant immunity. *EMBO J.* 25, 2007–2016. doi: 10.1038/sj.emboj.7601084
- Báez-Vallejo, N., Camarena-Pozos, D. A., Monribo-Villanueva, J. L., Ramírez-Vázquez, M., Carrión-Villanova, G. L., Guerrero-Analco, J. A., et al. (2020). Forest tree associated bacteria for potential biological control of *Fusarium solani* and of *Fusarium kuroshium*, causal agent of *Fusarium dieback*. *Microbiol. Res.* 235:126440. doi: 10.1016/j.micres.2020.126440
- Basu, A., Prasad, P., Das, S. N., Kalam, S., Sayyed, R. Z., Reddy, M. S., et al. (2021). Plant Growth Promoting Rhizobacteria (PGPR) as Green Bioinoculants: Recent Developments, Constraints, and Prospects. *Sustainability* 13:1140. doi: 10.3390/su13031140
- Bee Park, H., Lee, B., Kloepper, J. W., and Ryu, C. M. (2013). One shot-two pathogens blocked: exposure of *Arabidopsis* to hexadecane, a long chain volatile organic compound, confers induced resistance against both *Pectobacterium carotovorum* and *Pseudomonas syringae*. *Plant Signal. Behav.* 8:e24619. doi: 10.4161/psb.24619
- Bentham, A. R., De la Concepcion, J. C., Mukhi, N., Zdrzalek, R., Draeger, M., Gorenkin, D., et al. (2020). A molecular roadmap to the plant immune system. *J. Biol. Chem.* 295, 14916–14935. doi: 10.1074/jbc.rev120.010852
- Bhattacharyya, D., Yu, S. M., and Lee, Y. H. (2015). Volatile compounds from *Alcaligenes faecalis* JBCS1294 confer salt tolerance in *Arabidopsis thaliana* through the auxin and gibberellin pathways and differential modulation of gene expression in root and shoot tissues. *Plant Growth Regul.* 75, 297–306. doi: 10.1007/s10725-014-9953-5
- Bloemberg, G. V., and Lugtenberg, B. J. (2001). Molecular basis of plant growth promotion and biocontrol by rhizobacteria. *Curr. Opin. Plant Biol.* 4, 343–350. doi: 10.1016/s1369-5266(00)00183-7
- Blom, D., Fabbri, C., Connor, E. C., Schiestl, F. P., Klausner, D. R., Boller, T., et al. (2011a). Production of plant growth modulating volatiles is widespread among rhizosphere bacteria and strongly depends on culture conditions. *Environ. Microbiol.* 13, 3047–3058. doi: 10.1111/j.1462-2920.2011.02582.x
- Blom, D., Fabbri, C., Eberl, L., and Weisskopf, L. (2011b). Volatile-mediated killing of *Arabidopsis thaliana* by bacteria is mainly due to hydrogen cyanide. *Appl. Environ. Microbiol.* 77, 1000–1008. doi: 10.1128/aem.01968-10
- Bogamuwa, S. P., and Jang, J. C. (2014). Tandem CCCH zinc finger proteins in plant growth, development and stress response. *Plant Cell Physiol.* 55, 1367–1375. doi: 10.1093/pcp/pcu074
- Brodersen, P., Petersen, M., Bjørn Nielsen, H., Zhu, S., Newman, M. A., Shokat, K. M., et al. (2006). *Arabidopsis* MAP kinase 4 regulates salicylic acid- and jasmonic acid/ethylene-dependent responses via EDS1 and PAD4. *Plant J.* 47, 532–546. doi: 10.1111/j.1365-3113.2006.02806.x
- Camarena-Pozos, D. A., Flores-Núñez, V. M., López, M. G., López-Bucio, J., and Partida-Martínez, L. P. (2019). Smells from the desert: Microbial volatiles that

- affect plant growth and development of native and non-native plant species. *Plant Cell Environ.* 42, 1368–1380. doi: 10.1111/pce.13476
- Chang, Y. H., Yan, H. Z., and Liou, R. F. (2015). A novel elicitor protein from *Phytophthora parasitica* induces plant basal immunity and systemic acquired resistance. *Mol. Plant Pathol.* 16, 123–136. doi: 10.1111/mpp.12166
- Chen, C., MacCready, J. S., Ducat, D. C., and Osteryoung, K. W. (2018). The molecular machinery of chloroplast division. *Plant Physiol.* 176, 138–151. doi: 10.1104/pp.17.01272
- Chernin, L., Toklikishvili, N., Ovadis, M., Kim, S., Ben-Ari, J., Khmel, I., et al. (2011). Quorum-sensing quenching by rhizobacterial volatiles. *Environ. Microbiol. Rep.* 3, 698–704. doi: 10.1111/j.1758-2229.2011.00284.x
- Choi, H. K., Song, G. C., Yi, H. S., and Ryu, C. M. (2014). Field evaluation of the bacterial volatile derivative 3-pentanol in priming for induced resistance in pepper. *J. Chem. Ecol.* 40, 882–892. doi: 10.1007/s10886-014-0488-z
- Chung, J. H., Song, G. C., and Ryu, C. M. (2016). Sweet scents from good bacteria: case studies on bacterial volatile compounds for plant growth and immunity. *Plant Mol. Biol.* 90, 677–687. doi: 10.1007/s11103-015-0344-8
- Clark, T. N., Houriet, J., Vidar, W. S., Kellogg, J. J., Todd, D. A., Cech, N. B., et al. (2021). Interlaboratory Comparison of Untargeted Mass Spectrometry Data Uncovers Underlying Causes for Variability. *J. Nat. Prod.* 84, 824–835. doi: 10.1021/acs.jnatprod.0c01376
- Collins, N. C., Thordal-Christensen, H., Lipka, V., Bau, S., Kombrink, E., Qiu, J. L., et al. (2003). SNARE-protein-mediated disease resistance at the plant cell wall. *Nature* 425, 973–977. doi: 10.1038/nature02076
- Cordovez, V., Schop, S., Hordijk, K., de Boulois, H. D., Coppens, F., Hanssen, I., et al. (2018). Priming of Plant Growth Promotion by Volatiles of Root-Associated *Microbacterium* spp. *Appl. Environ. Microbiol.* 84, e1865–e1818.
- da Cunha, L., McFall, A. J., and Mackey, D. (2006). Innate immunity in plants: a continuum of layered defenses. *Microbes Infect.* 8, 1372–1381. doi: 10.1016/j.micinf.2005.12.018
- Dahal, D., Heintz, D., Van Dorsselaer, A., Braun, H. P., and Wydra, K. (2009). Pathogenesis and stress related, as well as metabolic proteins are regulated in tomato stems infected with *Ralstonia solanacearum*. *Plant Physiol. Biochem.* 47, 838–846. doi: 10.1016/j.plaphy.2009.05.001
- de Oliveira, A. S., Boiteux, L. S., Kormelink, R., and Resende, R. O. (2018). The Sw-5 gene cluster: tomato breeding and research toward orthotospovirus disease control. *Front. Plant Sci.* 9:1055. doi: 10.3389/fpls.2018.01055
- De Oliveira, A. S., Koolhaas, I., Boiteux, L. S., Caldararu, O. F., Petrescu, A. J., Oliveira Resende, R., et al. (2016). Cell death triggering and effector recognition by Sw-5 SD–CNL proteins from resistant and susceptible tomato isolines to Tomato spotted wilt virus. *Mol. Plant Pathol.* 17, 1442–1454. doi: 10.1111/mpp.12439
- Orozco-Mosqueda, M., Macías-Rodríguez, L. I., Santoyo, G., Fariás-Rodríguez, R., and Valencia-Cantero, E. (2013). *Medicago truncatula* increases its iron-uptake mechanisms in response to volatile organic compounds produced by *Sinorhizobium meliloti*. *Folia Microbiol.* 58, 579–585. doi: 10.1007/s12223-013-0243-9
- DiMario, R. J., Machingura, M. C., Waldrop, G. L., and Moroney, J. V. (2018). The many types of carbonic anhydrases in photosynthetic organisms. *Plant Sci.* 268, 11–17. doi: 10.1016/j.plantsci.2017.12.002
- Edgar, R., Domrachev, M., and Lash, A. E. (2002). Gene Expression Omnibus: NCBI gene expression and hybridization array data repository. *Nucleic Acids Res.* 30, 207–210. doi: 10.1093/nar/30.1.207
- El Oirdi, M., and Bouarab, K. (2007). Plant signalling components EDS1 and SGT1 enhance disease caused by the necrotrophic pathogen *Botrytis cinerea*. *New Phytol.* 175, 131–139. doi: 10.1111/j.1469-8137.2007.02086.x
- Engelhardt, S., Boevink, P. C., Armstrong, M. R., Ramos, M. B., Hein, I., and Birch, P. R. (2012). Relocalization of late blight resistance protein R3a to endosomal compartments is associated with effector recognition and required for the immune response. *Plant Cell* 24, 5142–5158. doi: 10.1105/tpc.112.104992
- Farag, M. A., Ryu, C. M., Sumner, L. W., and Paré, P. W. (2006). GC–MS SPME profiling of rhizobacterial volatiles reveals prospective inducers of growth promotion and induced systemic resistance in plants. *Phytochemistry* 67, 2262–2268. doi: 10.1016/j.phytochem.2006.07.021
- Farag, M. A., Song, G. C., Park, Y. S., Audrain, B., Lee, S., Ghigo, J. M., et al. (2017). Biological and chemical strategies for exploring inter- and intrakingdom communication mediated via bacterial volatile signals. *Nat. Protoc.* 12:1359. doi: 10.1038/nprot.2017.023
- Farag, M. A., Zhang, H., and Ryu, C. M. (2013). Dynamic chemical communication between plants and bacteria through airborne signals: induced resistance by bacterial volatiles. *J. Chem. Ecol.* 39, 1007–1018. doi: 10.1007/s10886-013-0317-9
- Fincheira, P., and Quiroz, A. (2018). Microbial volatiles as plant growth inducers. *Microbiol. Res.* 208, 63–75. doi: 10.1016/j.micres.2018.01.002
- Fincheira, P., and Quiroz, A. (2019). Physiological response of *Lactuca sativa* exposed to 2-nonanone emitted by *Bacillus* sp. BCT9. *Microbiol. Res.* 219, 49–55. doi: 10.1016/j.micres.2018.11.002
- Fincheira, P., Parra, L., Mutis, A., Parada, M., and Quiroz, A. (2017). Volatiles emitted by *Bacillus* sp. BCT9 act as growth modulating agents on *Lactuca sativa* seedlings. *Microbiol. Res.* 203, 47–56. doi: 10.1016/j.micres.2017.06.007
- Fincheira, P., Quiroz, A., Medina, C., Tortella, G., Hermosilla, E., Diez, M. C., et al. (2020). Plant growth induction by volatile organic compound released from solid lipid nanoparticles and nanostructured lipid carriers. *Colloids Surf. A Physicochem. Engine. Aspects* 2020:124739. doi: 10.1016/j.colsurfa.2020.124739
- Fincheira, P., Quiroz, A., Tortella, G., Diez, M. C., and Rubilar, O. (2021). Current advances in plant-microbe communication via volatile organic compounds as an innovative strategy to improve plant growth. *Microbiol. Res.* 2021:126726. doi: 10.1016/j.micres.2021.126726
- Fincheira, P., Rubilar, O., Espinoza, J., Aníñir, W., Méndez, L., Seabra, A. B., et al. (2019). Formulation of a controlled-release delivery carrier for volatile organic compounds using multilayer O/W emulsions to plant growth. *Colloids Surf. A Physicochem. Engine. Aspects* 580:123738. doi: 10.1016/j.colsurfa.2019.123738
- Fincheira, P., Venthur, H., Mutis, A., Parada, M., and Quiroz, A. (2016). Growth promotion of *Lactuca sativa* in response to volatile organic compounds emitted from diverse bacterial species. *Microbiol. Res.* 193, 39–47. doi: 10.1016/j.micres.2016.09.008
- Fliegmann, J., Mithöfer, A., Wanner, G., and Ebel, J. (2004). An ancient enzyme domain hidden in the putative β -glucan elicitor receptor of soybean may play an active part in the perception of pathogen-associated molecular patterns during broad host resistance. *J. Biol. Chem.* 279, 1132–1140. doi: 10.1074/jbc.m308552200
- Gao, L., and Bradeen, J. M. (2016). Contrasting potato foliage and tuber defense mechanisms against the late blight pathogen *Phytophthora infestans*. *PLoS One* 11:e0159969. doi: 10.1371/journal.pone.0159969
- Gao, Y. F., Liu, J. K., Yang, F. M., Zhang, G. Y., Wang, D., Zhang, L., et al. (2020). The WRKY transcription factor WRKY8 promotes resistance to pathogen infection and mediates drought and salt stress tolerance in *Solanum lycopersicum*. *Physiol. Plant.* 168, 98–117. doi: 10.1111/pp.12978
- Garbeva, P., and Weiskopf, L. (2020). Airborne medicine: bacterial volatiles and their influence on plant health. *New Phytol.* 226, 32–43. doi: 10.1111/nph.16282
- Ghosh, S. K., Bera, T., and Chakrabarty, A. M. (2020). Microbial siderophore—A boon to agricultural sciences. *Biol. Control* 144:104214. doi: 10.1016/j.biocontrol.2020.104214
- Ghyselinck, J., Velivelli, S. L., Heylen, K., O’Herlihy, E., Franco, J., Rojas, M., et al. (2013). Bioprospecting in potato fields in the Central Andean Highlands: screening of rhizobacteria for plant growth-promoting properties. *Systemat. Appl. Microbiol.* 36, 116–127. doi: 10.1016/j.syapm.2012.11.007
- Giorgio, A., De Stradis, A., Lo Cantore, P., and Iacobellis, N. S. (2015). Biocide effects of volatile organic compounds produced by potential biocontrol rhizobacteria on *Sclerotinia sclerotiorum*. *Front. Microbiol.* 6:1056. doi: 10.3389/fmicb.2015.01056
- Goyer, A., Hamlin, L., Crosslin, J. M., Buchanan, A., and Chang, J. H. (2015). RNA-Seq analysis of resistant and susceptible potato varieties during the early stages of potato virus Y infection. *BMC Genomics* 16:472. doi: 10.1186/s12864-015-1666-2
- Gu, B., Cao, X., Zhou, X., Chen, Z., Wang, Q., Liu, W., et al. (2020). The histological, effectoromic, and transcriptomic analyses of *Solanum pinnatisectum* reveal an upregulation of multiple NBS-LRR genes suppressing *Phytophthora infestans* infection. *Int. J. Mol. Sci.* 21:3211. doi: 10.3390/ijms21093211
- Gutiérrez-Luna, F. M., López-Bucio, J., Altamirano-Hernández, J., Valencia-Cantero, E., de la Cruz, H. R., and Macías-Rodríguez, L. (2010). Plant growth-promoting rhizobacteria modulate root-system architecture in *Arabidopsis thaliana* through volatile organic compound emission. *Symbiosis* 51, 75–83. doi: 10.1007/s13199-010-0066-2

- Haggag, W. M., and Timmusk, S. (2008). Colonization of peanut roots by biofilm-forming *Paenibacillus polymyxa* initiates biocontrol against crown rot disease. *J. Appl. Microbiol.* 104, 961–969. doi: 10.1111/j.1365-2672.2007.03611.x
- He, Z. H., Dong, H. T., Dong, J. X., Li, D. B., and Ronald, P. C. (2000). The rice Rim2 transcript accumulates in response to *Magnaporthe grisea* and its predicted protein product shares similarity with TNP2-like proteins encoded by CACTA transposons. *Mol. General Genet. MGG* 264, 2–10. doi: 10.1007/s004380000278
- Heenan-Daly, D., Velivelli, S. L., and Prestwich, B. D. (2019). “The Role of Rhizobacterial Volatile Organic Compounds in a Second Green Revolution—The Story so Far,” in *Field Crops: Sustainable Management by PGPR*, eds D. K. Maheshwari and S. Dheeman (Cham: Springer), 191–220. doi: 10.1007/978-3-030-30926-8_8
- Hernández-Calderón, E., Aviles-García, M. E., Castulo-Rubio, D. Y., Macías-Rodríguez, L., Ramírez, V. M., Santoyo, G., et al. (2018). Volatile compounds from beneficial or pathogenic bacteria differentially regulate root exudation, transcription of iron transporters, and defense signaling pathways in *Sorghum bicolor*. *Plant Mol. Biol.* 96, 291–304. doi: 10.1007/s11103-017-0694-5
- Holt, B. F., Belkhadir, Y., and Dangel, J. L. (2005). Antagonistic control of disease resistance protein stability in the plant immune system. *Science* 309, 929–932. doi: 10.1126/science.1109977
- Hu, G., DeHart, A. K., Li, Y., Ustach, C., Handley, V., Navarre, R., et al. (2005). EDS1 in tomato is required for resistance mediated by TIR-class R genes and the receptor-like R gene Ve. *Plant J.* 42, 376–391. doi: 10.1111/j.1365-313x.2005.02380.x
- Huang, J. S., Peng, Y. H., Chung, K. R., and Huang, J. W. (2018). Suppressive efficacy of volatile compounds produced by *Bacillus mycoides* on damping-off pathogens of cabbage seedlings. *J. Agricult. Sci.* 156, 795–809. doi: 10.1017/s0021859618000746
- Huang, S., Van Der Vossen, E. A., Kuang, H., Vleeshouwers, V. G., Zhang, N., Borm, T. J., et al. (2005). Comparative genomics enabled the isolation of the R3a late blight resistance gene in potato. *Plant J.* 42, 251–261. doi: 10.1111/j.1365-313x.2005.02365.x
- Igarashi, D., Tsuda, K., and Katagiri, F. (2012). The peptide growth factor, phytosulfokine, attenuates pattern-triggered immunity. *Plant J.* 71, 194–204. doi: 10.1111/j.1365-313x.2012.04950.x
- Jacob, J., Krishnan, G. V., Thankappan, D., and Amma, D. K. B. N. S. (2020). “Endophytic bacterial strains induced systemic resistance in agriculturally important crop plants,” in *Microbial Endophytes*, eds A. Kumar and E. K. Radhakrishnan (Woodhead Publishing), 75–105. doi: 10.1016/b978-0-12-819654-0.00004-1
- Jadhav, H. P., Shaikh, S. S., and Sayyed, R. Z. (2017). Role of hydrolytic enzymes of rhizoflora in biocontrol of fungal phytopathogens: An overview. *Rhizotrophs Plant Growth Promot. Bioremed.* 2017, 183–203. doi: 10.1007/978-981-10-4862-3_9
- Jiang, S., Lu, Y., Li, K., Lin, L., Zheng, H., Yan, F., et al. (2014). Heat shock protein 70 is necessary for Rice stripe virus infection in plants. *Mol. Plant Pathol.* 15, 907–917. doi: 10.1111/mpp.12153
- Kai, M. (2020). Diversity and distribution of volatile secondary metabolites throughout *Bacillus subtilis* isolates. *Front. Microbiol.* 11:559. doi: 10.3389/fmicb.2020.00559
- Kai, M., and Piechulla, B. (2009). Plant growth promotion due to rhizobacterial volatiles—An effect of CO₂? *FEBS Lett.* 583, 3473–3477. doi: 10.1016/j.febslet.2009.09.053
- Kai, M., Crespo, E., Cristescu, S. M., Harren, F. J., Francke, W., and Piechulla, B. (2010). *Serratia odorifera*: analysis of volatile emission and biological impact of volatile compounds on *Arabidopsis thaliana*. *Appl. Microbiol. Biotechnol.* 88, 965–976. doi: 10.1007/s00253-010-2810-1
- Kai, M., Effmert, U., and Piechulla, B. (2016). Bacterial-plant-interactions: approaches to unravel the biological function of bacterial volatiles in the rhizosphere. *Front. Microbiol.* 7:108. doi: 10.3389/fmicb.2016.00108
- Kai, M., Effmert, U., Berg, G., and Piechulla, B. (2007). Volatiles of bacterial antagonists inhibit mycelial growth of the plant pathogen *Rhizoctonia solani*. *Arch. Microbiol.* 187, 351–360. doi: 10.1007/s00203-006-0199-0
- Kai, M., Elmassry, M., and Farag, M. A. (2020). “Sampling, Detection, Identification, and Analysis of Bacterial Volatile Organic Compounds (VOCs),” in *Bacterial Volatile Compounds as Mediators of Airborne Interactions*, eds C.-M. Ryu, L. Weisskopf, and B. Piechulla (Singapore: Springer), 281–304. doi: 10.1007/978-981-15-7293-7_12
- Kay, S., Hahn, S., Marois, E., Wieduwild, R., and Bonas, U. (2009). Detailed analysis of the DNA recognition motifs of the *Xanthomonas* type III effectors AvrBs3 and AvrBs3Δrep16. *Plant J.* 59, 859–871. doi: 10.1111/j.1365-313x.2009.03922.x
- Kim, J. S., Lee, J., Lee, C. H., Woo, S. Y., Kang, H., Seo, S. G., et al. (2015). Activation of pathogenesis-related genes by the rhizobacterium, *Bacillus* sp. JS, which induces systemic resistance in tobacco plants. *Plant Pathol. J.* 31:195. doi: 10.5423/ppj.nt.11.2014.0122
- Kong, W. L., Li, P. S., Wu, X. Q., Wu, T. Y., and Sun, X. R. (2020). Forest tree associated bacterial diffusible and volatile organic compounds against various phytopathogenic fungi. *Microorganisms* 8:590. doi: 10.3390/microorganisms8040590
- Kwenda, S., Motlolometsi, T. V., Birch, P. R., and Moleleki, L. N. (2016). RNA-seq profiling reveals defense responses in a tolerant potato cultivar to stem infection by *Pectobacterium carotovorum* ssp. *brasiliense*. *Front. Plant Sci.* 7:1905. doi: 10.3389/fpls.2016.01905
- Kwon, C., Neu, C., Pajonk, S., Yun, H. S., Lipka, U., Humphry, M., et al. (2008). Co-option of a default secretory pathway for plant immune responses. *Nature* 451, 835–840. doi: 10.1038/nature06545
- Lee, D., Bourdais, G., Yu, G., Robatzek, S., and Coaker, G. (2015). Phosphorylation of the plant immune regulator RPM1-INTERACTING PROTEIN4 enhances plant plasma membrane H⁺-ATPase activity and inhibits flagellin-triggered immune responses in Arabidopsis. *Plant Cell* 27, 2042–2056. doi: 10.1105/tpc.114.132308
- Lee, S., Behringer, G., Hung, R., and Bennett, J. (2019). Effects of fungal volatile organic compounds on *Arabidopsis thaliana* growth and gene expression. *Fungal Ecol.* 37, 1–9. doi: 10.1016/j.funeco.2018.08.004
- Lekota, M., Muzhinji, N., and Van der Waals, J. E. (2019). Identification of differentially expressed genes in tolerant and susceptible potato cultivars in response to *Spongospora subterranea* f. sp. *subterranea* tuber infection. *Plant Pathol.* 68, 1196–1206. doi: 10.1111/ppa.13029
- Li, Y., Hu, X., Chen, J., Wang, W., Xiong, X., and He, C. (2017). Integrated mRNA and microRNA transcriptome analysis reveals miRNA regulation in response to PVA in potato. *Sci. Rep.* 7, 1–16.
- Lin, T., Lashbrook, C. C., Cho, S. K., Butler, N. M., Sharma, P., Muppirala, U., et al. (2015). Transcriptional analysis of phloem-associated cells of potato. *BMC Genomics* 16:665. doi: 10.1186/s12864-015-1844-2
- Lipka, U., Fuchs, R., and Lipka, V. (2008). *Arabidopsis* non-host resistance to powdery mildews. *Curr. Opin. Plant Biol.* 11, 404–411. doi: 10.1016/j.pbi.2008.04.004
- Lipka, V., Dittgen, J., Bednarek, P., Bhat, R., Wiermer, M., Stein, M., et al. (2005). Pre- and postinvasion defenses both contribute to nonhost resistance in *Arabidopsis*. *Science* 310, 1180–1183. doi: 10.1126/science.1119409
- Liu, Y., Burch-Smith, T., Schiff, M., Feng, S., and Dinesh-Kumar, S. P. (2004a). Molecular chaperone Hsp90 associates with resistance protein N and its signaling proteins SGT1 and Rar1 to modulate an innate immune response in plants. *J. Biol. Chem.* 279, 2101–2108. doi: 10.1074/jbc.m310029200
- Liu, Y., Schiff, M., and Dinesh-Kumar, S. P. (2004b). Involvement of MEK1 MAPKK, NTF6 MAPK, WRKY/MYB transcription factors, COI1 and CTR1 in N-mediated resistance to tobacco mosaic virus. *Plant J.* 38, 800–809. doi: 10.1111/j.1365-313x.2004.02085.x
- Lugtenberg, B., and Kamilova, F. (2009). Plant-growth-promoting rhizobacteria. *Annu. Rev. Microbiol.* 63, 541–556.
- Maayan, Y., Pandaranayaka, E. P., Srivastava, D. A., Lapidot, M., Levin, I., Dombrovsky, A., et al. (2018). Using genomic analysis to identify tomato Tm-2 resistance-breaking mutations and their underlying evolutionary path in a new and emerging tobamovirus. *Arch. Virol.* 163, 1863–1875. doi: 10.1007/s00705-018-3819-5
- Malatrasi, M., Close, T. J., and Marmiroli, N. (2002). Identification and mapping of a putative stress response regulator gene in barley. *Plant Mol. Biol.* 50, 141–150.
- McDowell, J. M., and Dangel, J. L. (2000). Signal transduction in the plant immune response. *Trends Biochem. Sci.* 25, 79–82. doi: 10.1016/s0968-0004(99)01532-7
- Meldau, D. G., Meldau, S., Hoang, L. H., Underberg, S., Wünsche, H., and Baldwin, I. T. (2013). Dimethyl disulfide produced by the naturally associated bacterium *Bacillus* sp. B55 promotes *Nicotiana attenuata* growth by enhancing sulfur nutrition. *Plant Cell* 25, 2731–2747. doi: 10.1105/tpc.113.114744
- Melkina, O. E., Khmel, I. A., Plyuta, V. A., Koksharova, O. A., and Zavilgelsky, G. B. (2017). Ketones 2-heptanone, 2-nonanone, and 2-undecanone inhibit

- DnaK-dependent refolding of heat-inactivated bacterial luciferases in *Escherichia coli* cells lacking small chaperon IbpB. *Appl. Microbiol. Biotechnol.* 101, 5765–5771. doi: 10.1007/s00253-017-8350-1
- Méndez-Bravo, A., Cortazar-Murillo, E. M., Guevara-Avendaño, E., Ceballos-Luna, O., Rodríguez-Haas, B., Kiel-Martínez, A. L., et al. (2018). Plant growth-promoting rhizobacteria associated with avocado display antagonistic activity against *Phytophthora cinnamomi* through volatile emissions. *PLoS One* 13:e0194665. doi: 10.1371/journal.pone.0194665
- Müller, S., Rycak, L., Afonso-Grünz, F., Winter, P., Zawada, A. M., Damrath, E., et al. (2014). APADB: a database for alternative polyadenylation and microRNA regulation events. *Database* 2014:bau076. doi: 10.1093/database/bau076
- Mur, L. A., Kenton, P., Atzorn, R., Miersch, O., and Wasternack, C. (2006). The outcomes of concentration-specific interactions between salicylate and jasmonate signaling include synergy, antagonism, and oxidative stress leading to cell death. *Plant Physiol.* 140, 249–262. doi: 10.1104/pp.105.072348
- Nascimento, F. X., Rossi, M. J., and Glick, B. R. (2018). Ethylene and 1-Aminocyclopropane-1-carboxylate (ACC) in plant–bacterial interactions. *Front. Plant Sci.* 9:114. doi: 10.3389/fpls.2018.00114
- Nielsen, M. E., Feechan, A., Böhlenius, H., Ueda, T., and Thordal-Christensen, H. (2012). *Arabidopsis* ARF-GTP exchange factor, GNOM, mediates transport required for innate immunity and focal accumulation of syntaxin PEN1. *Proc. Natl. Acad. Sci.* 109, 11443–11448. doi: 10.1073/pnas.1117596109
- Park, Y. S., Dutta, S., Ann, M., Raaijmakers, J. M., and Park, K. (2015). Promotion of plant growth by *Pseudomonas fluorescens* strain SS101 via novel volatile organic compounds. *Biochem. Biophys. Res. Commun.* 461, 361–365. doi: 10.1016/j.bbrc.2015.04.039
- Pérez-Flores, P., Valencia-Cantero, E., Altamirano-Hernández, J., Pelagio-Flores, R., López-Bucio, J., García-Juárez, P., et al. (2017). *Bacillus methylotrophicus* M4-96 isolated from maize (*Zea mays*) rhizosphere increases growth and auxin content in *Arabidopsis thaliana* via emission of volatiles. *Protoplasma* 254, 2201–2213. doi: 10.1007/s00709-017-1109-9
- Phukan, U. J., Jeena, G. S., and Shukla, R. K. (2016). WRKY transcription factors: molecular regulation and stress responses in plants. *Front. Plant Sci.* 7:760. doi: 10.3389/fpls.2016.00760
- Piechulla, B., Lemfack, M. C., and Kai, M. (2017). Effects of discrete bioactive microbial volatiles on plants and fungi. *Plant Cell Environ.* 40, 2042–2067. doi: 10.1111/pce.13011
- Pitzschke, A., Schikora, A., and Hirt, H. (2009). MAPK cascade signalling networks in plant defence. *Curr. Opin. Plant Biol.* 12, 421–426. doi: 10.1016/j.pbi.2009.06.008
- Popova, A. A., Koksharova, O. A., Lipasova, V. A., Zaitseva, J. V., Katkova-Zhukotskaya, O. A., Eremina, S. I., et al. (2014). Inhibitory and toxic effects of volatiles emitted by strains of *Pseudomonas* and *Serratia* on growth and survival of selected microorganisms, *Caenorhabditis elegans*, and *Drosophila melanogaster*. *BioMed Res. Int.* 2014:125704.
- Qian, L., Zhao, J., Du, Y., Zhao, X., Han, M., and Liu, Y. (2018). Hsp90 Interacts With Tm-22 and Is Essential for Tm-22-Mediated Resistance to Tobacco mosaic virus. *Front. Plant Sci.* 9:411. doi: 10.3389/fpls.2018.00411
- Qiu, L., Li, J. J., Li, Z., and Wang, J. J. (2019). Production and characterization of biocontrol fertilizer from brewer's spent grain via solid-state fermentation. *Sci. Rep.* 9, 1–9.
- Rajamäki, M. L., Sikorskaite-Gudziuniene, S., Sarmah, N., Varjosalo, M., and Valkonen, J. P. (2020). Nuclear proteome of virus-infected and healthy potato leaves. *BMC Plant Biol.* 20:355. doi: 10.1186/s12870-020-02561-7
- Raut, V., Shaikh, I., Naphade, B., Prashar, K., and Adhupure, N. (2017). Plant growth promotion using microbial IAA producers in conjunction with azolla: a novel approach. *Chem. Biol. Technol. Agricult.* 4, 1–11. doi: 10.1007/bf00024395
- Rees, C. A., Nordick, K. V., Franchina, F. A., Lewis, A. E., Hirsch, E. B., and Hill, J. E. (2017). Volatile metabolic diversity of *Klebsiella pneumoniae* in nutrient-replete conditions. *Metabolomics* 13:18.
- Rehman, S., Aziz, E., Akhtar, W., Ilyas, M., and Mahmood, T. (2017). Structural and functional characteristics of plant proteinase inhibitor-II (PI-II) family. *Biotechnol. Lett.* 39, 647–666. doi: 10.1007/s10529-017-2298-1
- Resjö, S., Zahid, M. A., Burra, D. D., Lenman, M., Levander, F., and Andreasson, E. (2019). Proteomics of PTI and Two ETI Immune Reactions in Potato Leaves. *Int. J. Mol. Sci.* 20:4726. doi: 10.3390/ijms20194726
- Roman, M. L., Izarra, M., Lindqvist-Kreuzer, H., Rivera, C., Gamboa, S., Tovar, J. C., et al. (2017). R/Avr gene expression study of Rpi-vnt1.1 transgenic potato resistant to the *Phytophthora infestans* clonal lineage EC-1. *Plant Cell Tissue Organ Cult.* 131, 259–268. doi: 10.1007/s11240-017-1281-9
- Romera, F. J., García, M. J., Lucena, C., Martínez-Medina, A., Aparicio, M. A., Ramos, J., et al. (2019). Induced systemic resistance (ISR) and Fe deficiency responses in dicot plants. *Front. Plant Sci.* 10:287. doi: 10.3389/fpls.2019.0287
- Rowland, O., Ludwig, A. A., Merrick, C. J., Baillieu, F., Tracy, F. E., Durrant, W. E., et al. (2005). Functional analysis of Avr9/Cf-9 rapidly elicited genes identifies a protein kinase, ACIK1, that is essential for full Cf-9-dependent disease resistance in tomato. *Plant Cell* 17, 295–310. doi: 10.1105/tpc.104.026013
- Ryu, C. M., Farag, M. A., Hu, C. H., Reddy, M. S., Kloepper, J. W., and Paré, P. W. (2004). Bacterial volatiles induce systemic resistance in *Arabidopsis*. *Plant Physiol.* 134, 1017–1026. doi: 10.1104/pp.103.026583
- Ryu, C. M., Farag, M. A., Hu, C. H., Reddy, M. S., Wei, H. X., Paré, P. W., et al. (2003). Bacterial volatiles promote growth in *Arabidopsis*. *Proc. Natl. Acad. Sci.* 100, 4927–4932. doi: 10.1073/pnas.0730845100
- Schornack, S., Ballvora, A., Gölrebeck, D., Peart, J., Ganai, M., Baker, B., et al. (2004). The tomato resistance protein Bs4 is a predicted non-nuclear TIR-NB-LRR protein that mediates defense responses to severely truncated derivatives of AvrBs4 and overexpressed AvrBs3. *Plant J.* 37, 46–60. doi: 10.1046/j.1365-3113.2003.01937.x
- Schulz-Bohm, K., Martín-Sánchez, L., and Garbeva, P. (2017). Microbial volatiles: small molecules with an important role in intra- and inter-kingdom interactions. *Front. Microbiol.* 8:2484. doi: 10.3389/fmicb.2017.02484
- Serrano, M., and Guzmán, P. (2004). Isolation and gene expression analysis of *Arabidopsis thaliana* mutants with constitutive expression of ATL2, an early elicitor-response RING-H2 zinc-finger gene. *Genetics* 167, 919–929. doi: 10.1534/genetics.104.028043
- Sharifi, R., and Ryu, C. M. (2016). Making healthier or killing enemies? Bacterial volatile-elicited plant immunity plays major role upon protection of *Arabidopsis* than the direct pathogen inhibition. *Commun. Integr. Biol.* 9:196.
- Sharifi, R., and Ryu, C. M. (2018). Revisiting bacterial volatile-mediated plant growth promotion: lessons from the past and objectives for the future. *Ann. Bot.* 122, 349–358. doi: 10.1093/aob/mcy108
- Somerville, G. A., and Proctor, R. A. (2013). Cultivation conditions and the diffusion of oxygen into culture media: the rationale for the flask-to-medium ratio in microbiology. *BMC Microbiol.* 13, 1–2. doi: 10.1186/1471-2180-13-9
- Song, G. C., and Ryu, C. M. (2013). Two volatile organic compounds trigger plant self-defense against a bacterial pathogen and a sucking insect in cucumber under open field conditions. *Int. J. Mol. Sci.* 14, 9803–9819. doi: 10.3390/ijms14059803
- Song, G. C., Riu, M., and Ryu, C. M. (2019). Beyond the two compartments Petri-dish: optimising growth promotion and induced resistance in cucumber exposed to gaseous bacterial volatiles in a miniature greenhouse system. *Plant Methods* 15:9.
- Stein, M., Dittgen, J., Sánchez-Rodríguez, C., Hou, B. H., Molina, A., Schulze-Lefert, P., et al. (2006). *Arabidopsis* PEN3/PDR8, an ATP binding cassette transporter, contributes to nonhost resistance to inappropriate pathogens that enter by direct penetration. *Plant Cell* 18, 731–746. doi: 10.1105/tpc.105.038372
- Tahir, H. A. S., Gu, Q., Wu, H., Raza, W., Safdar, A., Huang, Z., et al. (2017). Effect of volatile compounds produced by *Ralstonia solanacearum* on plant growth promoting and systemic resistance inducing potential of *Bacillus* volatiles. *BMC Plant Biol.* 17, 1–16. doi: 10.1186/s12870-017-1083-6
- Tyc, O., Song, C., Dickschat, J. S., Vos, M., and Garbeva, P. (2017). The ecological role of volatile and soluble secondary metabolites produced by soil bacteria. *Trends Microbiol.* 25, 280–292. doi: 10.1016/j.tim.2016.12.002
- Vejan, P., Abdullah, R., Khadiran, T., Ismail, S., and Nasrullah Boyce, A. (2016). Role of plant growth promoting rhizobacteria in agricultural sustainability—a review. *Molecules* 21:573. doi: 10.3390/molecules21050573
- Velázquez-Becerra, C., Macías-Rodríguez, L. I., López-Bucio, J., Altamirano-Hernández, J., Flores-Cortez, I., and Valencia-Cantero, E. (2011). A volatile organic compound analysis from *Arthrobacter agilis* identifies dimethylhexadecylamine, an amino-containing lipid modulating bacterial growth and *Medicago sativa* morphogenesis in vitro. *Plant Soil* 339, 329–340. doi: 10.1007/s11104-010-0583-z

- Velivelli, S. L., Kromann, P., Lojan, P., Rojas, M., Franco, J., Suarez, J. P., et al. (2015). Identification of mVOCs from Andean rhizobacteria and field evaluation of bacterial and mycorrhizal inoculants on growth of potato in its center of origin. *Microb. Ecol.* 69, 652–667. doi: 10.1007/s00248-014-0514-2
- Venkatesh, J., and Park, S. W. (2015). Genome-wide analysis and expression profiling of DNA-binding with one zinc finger (Dof) transcription factor family in potato. *Plant Physiol. Biochem.* 94, 73–85. doi: 10.1016/j.plaphy.2015.05.010
- Venugopal, S. C., Jeong, R. D., Mandal, M. K., Zhu, S., Chandra-Shekara, A. C., Xia, Y., et al. (2009). Enhanced disease susceptibility 1 and salicylic acid act redundantly to regulate resistance gene-mediated signaling. *PLoS Genet.* 5:e1000545. doi: 10.1371/journal.pgen.1000545
- Vespermann, A., Kai, M., and Piechulla, B. (2007). Rhizobacterial volatiles affect the growth of fungi and *Arabidopsis thaliana*. *Appl. Environ. Microbiol.* 73, 5639–5641. doi: 10.1128/aem.01078-07
- Wang, J., Yao, W., Wang, L., Ma, F., Tong, W., Wang, C., et al. (2017). Overexpression of VpEIFP1, a novel F-box/Kelch-repeat protein from wild Chinese *Vitis pseudoreticulata*, confers higher tolerance to powdery mildew by inducing thioredoxin z proteolysis. *Plant Sci.* 263, 142–155. doi: 10.1016/j.plantsci.2017.07.004
- Weise, T., Kai, M., and Piechulla, B. (2013). Bacterial ammonia causes significant plant growth inhibition. *PLoS One* 8:e63538. doi: 10.1371/journal.pone.0063538
- Wenke, K., Kai, M., and Piechulla, B. (2010). Belowground volatiles facilitate interactions between plant roots and soil organisms. *Planta* 231, 499–506. doi: 10.1007/s00425-009-1076-2
- Wenke, K., Kopka, J., Schwachtje, J., van Dongen, J. T., and Piechulla, B. (2019). Volatiles of rhizobacteria *Serratia* and *Stenotrophomonas* alter growth and metabolite composition of *Arabidopsis thaliana*. *Plant Biol.* 21, 109–119. doi: 10.1111/plb.12878
- Wiermer, M., Feys, B. J., and Parker, J. E. (2005). Plant immunity: the EDS1 regulatory node. *Curr. Opin. Plant Biol.* 8, 383–389. doi: 10.1016/j.pbi.2005.05.010
- Wiesel, L., Davis, J. L., Milne, L., Fernandez, V. R., Herold, M. B., Williams, J. M., et al. (2015). A transcriptional reference map of defence hormone responses in potato. *Sci. Rep.* 5:15229.
- Wu, Z., Huang, S., Zhang, X., Wu, D., Xia, S., and Li, X. (2017). Regulation of plant immune receptor accumulation through translational repression by a glycine-tyrosine-phenylalanine (GYF) domain protein. *Elife* 6:e23684.
- Yu, G., Xian, L., Xue, H., Yu, W., Rufian, J., Sang, Y., et al. (2019). A bacterial effector protein prevents MAPK-mediated phosphorylation of SGT1 to suppress plant immunity. *bioRxiv* 641241. [preprint].
- Zamioudis, C., Korteland, J., Van Pelt, J. A., van Hamersveld, M., Dombrowski, N., Bai, Y., et al. (2015). Rhizobacterial volatiles and photosynthesis-related signals coordinate MYB 72 expression in Arabidopsis roots during onset of induced systemic resistance and iron-deficiency responses. *Plant J.* 84, 309–322. doi: 10.1111/tpj.12995
- Zeng, L. R., Qu, S., Bordeos, A., Yang, C., Baraoidan, M., Yan, H., et al. (2004). Spotted leaf11, a negative regulator of plant cell death and defense, encodes a U-box/armadillo repeat protein endowed with E3 ubiquitin ligase activity. *Plant Cell* 16, 2795–2808. doi: 10.1105/tpc.104.025171
- Zhao, P., Wang, D., Wang, R., Kong, N., Zhang, C., Yang, C., et al. (2018). Genome-wide analysis of the potato Hsp20 gene family: identification, genomic organization and expression profiles in response to heat stress. *BMC Genomics* 19:61.
- Zhou, X., Zha, M., Huang, J., Li, L., Imran, M., and Zhang, C. (2017). StMYB44 negatively regulates phosphate transport by suppressing expression of PHOSPHATE1 in potato. *J. Exp. Bot.* 68, 1265–1281. doi: 10.1093/jxb/erx026
- Zhu, T., Li, L., and Feng, L. (2020). StABI5 Involved in the Regulation of Chloroplast Development and Photosynthesis in Potato. *Int. J. Mol. Sci.* 21:1068. doi: 10.3390/ijms21031068
- Zhuang, X., McPhee, K. E., Coram, T. E., Peever, T. L., and Chilvers, M. I. (2012). Rapid transcriptome characterization and parsing of sequences in a non-model host-pathogen interaction; pea-*Sclerotinia sclerotiorum*. *BMC Genomics* 13:668. doi: 10.1186/1471-2164-13-668

Conflict of Interest: The authors declare that the research was conducted in the absence of any commercial or financial relationships that could be construed as a potential conflict of interest.

Copyright © 2021 Heenan-Daly, Coughlan, Dillane and Doyle Prestwich. This is an open-access article distributed under the terms of the Creative Commons Attribution License (CC BY). The use, distribution or reproduction in other forums is permitted, provided the original author(s) and the copyright owner(s) are credited and that the original publication in this journal is cited, in accordance with accepted academic practice. No use, distribution or reproduction is permitted which does not comply with these terms.



Multi-Omic Analysis of Symbiotic Bacteria Associated With *Aedes aegypti* Breeding Sites

Katherine D. Mosquera¹, Luis E. Martinez Villegas^{1,2}, Sacha J. Pidot³, Chinhda Sharif⁴, Sven Klimpel^{4,5,6}, Timothy P. Stinear³, Luciano A. Moreira², Nicholas J. Tobias^{5,6*} and Marcelo G. Lorenzo^{1*}

OPEN ACCESS

Edited by:

Monica T. Pupo,
University of São Paulo, Brazil

Reviewed by:

Loganathan Ponnusamy,
North Carolina State University,
United States
Lily Khadempour,
Rutgers University, Newark,
United States

*Correspondence:

Nicholas J. Tobias
nicholas.tobias@senckenberg.de
Marcelo G. Lorenzo
marcelo.lorenzo@fiocruz.br

[†]These authors share senior
authorship

Specialty section:

This article was submitted to
Microbial Symbioses,
a section of the journal
Frontiers in Microbiology

Received: 30 April 2021

Accepted: 23 July 2021

Published: 12 August 2021

Citation:

Mosquera KD,
Martinez Villegas LE, Pidot SJ,
Sharif C, Klimpel S, Stinear TP,
Moreira LA, Tobias NJ and
Lorenzo MG (2021) Multi-Omic
Analysis of Symbiotic Bacteria
Associated With *Aedes aegypti*
Breeding Sites.
Front. Microbiol. 12:703711.
doi: 10.3389/fmicb.2021.703711

¹ Vector Behavior and Pathogen Interaction Group, Instituto René Rachou (FIOCRUZ), Belo Horizonte, Brazil, ² Mosquito Vectors: Endosymbionts and Pathogen-Vector Interactions Group, Instituto René Rachou (FIOCRUZ), Belo Horizonte, Brazil, ³ Department of Microbiology and Immunology, The Doherty Institute, University of Melbourne, Melbourne, VIC, Australia, ⁴ Institute for Ecology, Evolution and Diversity, Goethe University Frankfurt, Frankfurt, Germany, ⁵ LOEWE Center for Translational Biodiversity Genomics (TBG), Frankfurt, Germany, ⁶ Senckenberg Gesellschaft für Naturforschung, Frankfurt, Germany

Mosquito breeding sites are complex aquatic environments with wide microbial diversity and physicochemical parameters that can change over time during the development of immature insect stages. Changes in biotic and abiotic conditions in water can alter life-history traits of adult mosquitoes but this area remains understudied. Here, using microbial genomic and metabolomics analyses, we explored the metabolites associated with *Aedes aegypti* breeding sites as well as the potential contribution of *Klebsiella* sp., symbiotic bacteria highly associated with mosquitoes. We sought to address whether breeding sites have a signature metabolic profile and understand the metabolite contribution of the bacteria in the aquatic niches where *Ae. aegypti* larvae develop. An analysis of 32 mosquito-associated bacterial genomes, including *Klebsiella*, allowed us to identify gene clusters involved in primary metabolic pathways. From them, we inferred metabolites that could impact larval development (e.g., spermidine), as well as influence the quality assessment of a breeding site by a gravid female (e.g., putrescine), if produced by bacteria in the water. We also detected significant variance in metabolite presence profiles between water samples representing a decoupled oviposition event (oviposition by single females and manually deposited eggs) versus a control where no mosquito interactions occurred (PERMANOVA: $p < 0.05$; $R^2 = 24.64\%$ and $R^2 = 30.07\%$). Five *Klebsiella* metabolites were exclusively linked to water samples where oviposition and development occurred. These data suggest metabolomics can be applied to identify compounds potentially used by female *Ae. aegypti* to evaluate the quality of a breeding site. Elucidating the physiological mechanisms by which the females could integrate these sensory cues while ovipositing constitutes a growing field of interest, which could benefit from a more depurated list of candidate molecules.

Keywords: *Aedes*, *Klebsiella*, breeding sites, genomics, metabolomics

INTRODUCTION

The ability of *Aedes aegypti* to thrive in urban environments and benefit from the available resources (i.e., humans as blood meal sources for reproduction and human-generated breeding sites for progeny), has made this mosquito a permanent threat to human health (Brady and Hay, 2020; Rose et al., 2020). Attempts to understand how this mosquito can effectively exploit nutrient-deficient artificial water-holding containers as breeding sites for its offspring to thrive have opened up new insights into mosquito bionomics (Dada et al., 2021).

The presence of diverse bacteria has been reported in breeding-site water collections, which are considered a fundamental component of larval niches (Wang et al., 2018; Scolari et al., 2019). This is because these immature forms rely on bacteria for their growth and development (Coon et al., 2014). Bacteria can be used as a food source and are often the most abundant microorganisms present in the larval diet (Rozeboom, 1935; Merritt et al., 1992). In general, breeding-site microbiota profiles seem to vary depending on mosquito species, aquatic habitat, and geographical origin (Muturi et al., 2018; Caragata et al., 2021; Juma et al., 2021). However, several bacterial isolates have been consistently detected in breeding sites, mosquito gut, and other mosquito-associated sources (Guégan et al., 2018). This is the case with *Klebsiella*, a genus of bacteria frequently reported in mosquitoes and their breeding sites (Gusmão et al., 2010; Chandel et al., 2013; Dada et al., 2014; Yadav et al., 2015; Wang et al., 2018; Hery et al., 2020; Alvarado et al., 2021; Rocha et al., 2021).

Several authors have identified *Klebsiella* associated with *Aedes*, *Anopheles*, and *Culex* mosquitoes using both culture-dependent and independent methods (Chandel et al., 2013; Yadav et al., 2015; Rocha et al., 2021). Therefore, it seems that these enteric bacteria maintain a stable relationship with the insects. For instance, *Klebsiella* has been isolated from different stages (eggs, larvae, pupae, and adults), tissues (midgut and ovaries), and sugar as well as blood-fed mosquitoes, both in laboratory and field populations (Gusmão et al., 2010; Chandel et al., 2013; Yadav et al., 2015; Wang et al., 2018; Alvarado et al., 2021; Rocha et al., 2021). Furthermore, Petri dishes filled with lyophilized *Klebsiella* resuspended in sterile water have proven to induce oviposition in *Culex pipiens* (Díaz-Nieto, 2014). This is particularly interesting considering that the water samples collected in natural breeding sites and domestic water storage containers have revealed the presence of *Klebsiella* (Dada et al., 2014; Hery et al., 2020; Rocha et al., 2021).

Oviposition-site selection by gravid females depends on water and container properties, with both biotic and abiotic factors shaping the decision on where to lay eggs (Hery et al., 2020). For instance, microbial communities present in water-holding containers have been shown to influence *Ae. aegypti* oviposition. Additionally, volatile compounds emitted by microorganisms act as attractants mediating egg-laying in a given container (Benzon and Apperson, 1988; Ponnusamy et al., 2008, 2015; Melo et al., 2020). Bacteria from breeding sites or water-soluble metabolites secreted by them have also been shown to impact abiotic factors of water, e.g.,

dissolved oxygen, and stimulate egg hatching by *Ae. aegypti* (Ponnusamy et al., 2011).

It has been suggested that gravid females transfer gut symbionts to aquatic niches where they oviposit (Coon et al., 2016). Indeed, this could disturb the pre-existing bacterial community of the water where the progeny will ultimately develop. In fact, midgut bacteria reported for larvae and adults have already been detected on the surface of *Ae. aegypti* eggs (Coon et al., 2014). It has been demonstrated that vertical transmission of microbes occurs mostly by egg-smearing, i.e., females impregnate the egg surface with symbiont-laden feces while ovipositing, allowing hatched larvae to acquire the symbionts (Salem et al., 2015; Sontowski and van Dam, 2020).

Microbial communities interact by producing metabolites that can influence the activity of neighboring microbes. These interactions can determine whether a microbe can subsist in an ecosystem and which features are desired to survive in a given community (Foster et al., 2017). In addition, microbially derived metabolites can also affect the host, helping with nutrition, protecting against pathogens, or causing disease (Fischer et al., 2017; Foster et al., 2017).

In order to investigate potential links between breeding sites and their resident microbes, we set out to address two specific questions: (i) what is the metabolic potential of bacteria commonly isolated in breeding sites? (ii) does the act of oviposition leave a metabolic fingerprint linking breeding sites and these bacteria?

MATERIALS AND METHODS

Mosquito Rearing

Aedes aegypti (BR URCA strain, F5) were reared at $28 \pm 2^\circ\text{C}$, $70 \pm 10\%$ relative humidity, and a 12:12 LL/DD photoperiod. Larvae were fed daily with half a tablet of Tetramin fish food, and pupae were transferred to cages before the adults emerged. Adults were offered 10% sucrose solution *ad libitum*, and one blood meal 7 days post-emergence using human blood. Human blood used to feed adult mosquitoes was obtained from a blood bank (Fundação Hemominas, Belo Horizonte, MG, Brazil), according to the terms of an agreement with Instituto René Rachou, Fiocruz/MG (OF.GPO/CCO agreement-Nr 224/16). Only fully engorged gravid females were used in the experiments 72 h after the blood meal.

Bacteria Isolation, Culture Conditions, and Metabolite Extraction

Bacteria were isolated from fecal samples collected from gravid females. Briefly, individual females were placed inside sterile tubes containing 500 μl PBS for an hour. The feces were homogenized and a 25 μl aliquot of this homogenate was plated on MacConkey agar. Subsequently, the plates were incubated at 25°C for 24 h and sub-cultured on fresh plates to obtain pure single colonies. Colony morphology was inspected for shape, elevation, margin, texture, and pigmentation. DNA samples were extracted using the DNeasy Blood & Tissue Kit (Qiagen), according to the manufacturer's manual. For

taxonomic identification, the 16S rRNA gene was amplified by using the forward primer ENV1 and the reverse primer ENV2 and Sanger sequenced.

For metabolite extractions, bacteria were inoculated in TSB 1%, TSB 0.1%, TSB 0.01%, LB 1%, and LB 0.1%. We opted to switch media from MacConkey to provide a less restricting range of nutrients so that the bacteria could produce as broad a range of metabolites as possible. Furthermore, since breeding sites and their respective nutrients vary greatly in nature, we sought simply to obtain an overview of what *Klebsiella* can produce and whether this correlates with our experimental breeding site setup. The cultures were incubated at 25°C and 200 rpm up to 36 h. For each medium concentration, 500 µl of bacterial culture were mixed with 500 µl of methanol. The mixtures were vortexed and centrifuged for 30 min at 20,000 rcf. 50 µl of the supernatants were recovered and concentrated in a speed vac.

Genome Sequencing, Assembly, and Analysis

Bacterial genomic DNA was extracted as described in section “Bacteria Isolation, Culture Conditions, and Metabolite Extraction.” Isolated DNA was sequenced on the Illumina NextSeq 500 platform. DNA libraries were constructed using the Nextera XT DNA preparation kit (Illumina) and whole-genome sequencing was performed using 2 × 150 bp paired-end chemistry. A sequencing depth of >50× was targeted for each sample.

Raw sequencing reads were trimmed using trimmomatic (v0.38). Sequences were then assembled using SPAdes (v3.12.0) (Bankevich et al., 2012). *Klebsiella* contigs along with several other genomes (**Supplementary Table 1**) were submitted to gutSMASH (v1.0.0) to identify specialized primary metabolite pathways.

Breeding Site Metabolite Extraction and Analysis

To investigate the relationship between bacterial metabolites present in *Ae. aegypti* breeding sites and oviposition, two types of breeding sites, and one control condition were defined for comparison (**Figure 1**). Breeding sites and control containers were set up separately inside mesh cages presenting one plastic cup filled with 80 ml of type I water and 500 µl of sterilized food solution. Five replicate samples containing water plus food served as experimental controls, i.e., no mosquitoes visited them. Additionally, six breeding sites visited by a single gravid female were generated separately. For this, mosquitoes were allowed to lay eggs for 24 h and then removed. Subsequently, the number of eggs laid in each cup was counted using a magnifying glass. This allowed us to calculate the average amount of eggs needed for preparing breeding sites by manually depositing eggs, avoiding the direct action of the female. Another set of five breeding sites was set up with manually deposited eggs. These eggs were derived from groups of gravid females allowed to oviposit on pieces of humid filter paper, which were dried and stored (a standard egg collection method for rearing mosquitoes in insectary conditions; see Imam et al., 2014).

Water samples from controls were collected on day 14. Water samples that had larvae developing were collected when at least one pupa was observed (between 6 and 14 days after the experiment was initiated). Larvae and pupae were removed, and the water samples were frozen and lyophilized.

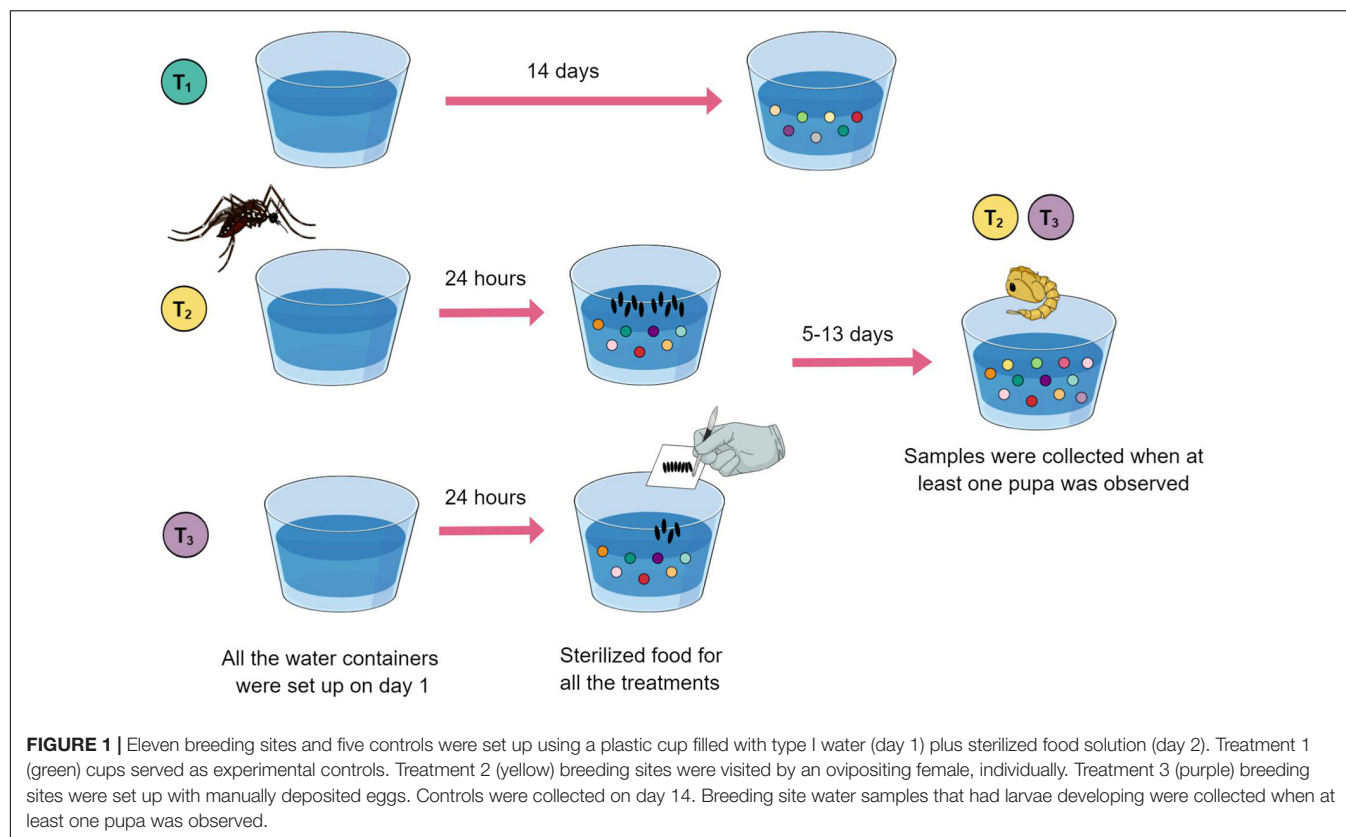
Dried extracts were then resuspended in 1 ml of methanol, centrifuged for 30 min at 13,000 rpm. Liquid chromatography-mass spectrometry (LC-MS) analysis was performed on a Thermo Scientific UltiMate 3000 System using a C18 column (ACQUITY UPLC BEH C18 Column, 1.7 µm, 2.1 mm X 50 mm, Waters) linked to a Bruker Impact II System (Bruker Daltonik GmbH). Runs were performed using a gradient of MeCN/0.1% formic acid in H₂O (5:95% to 95:5% over 16 min). Data acquisition was performed as previously described (Tobias et al., 2017). Acetonitrile was used as a control for blank measurements.

Network Analysis Details

The relevance of isolating extracted metabolites from bacterial cultures and treatment samples was to be able to pinpoint if the metabolites extracted from the water had a bacterial origin (either *Klebsiella* or other bacteria with similar metabolic pathways capable of the same chemical output). A molecular network was created with the Feature-Based Molecular Networking (FBMN) workflow (Nothias et al., 2020) on the GNPS platform (Wang, 2016). The mass spectrometry data were first processed with MZMINE2 (Pluskal et al., 2010) and the results were exported to GNPS for FBMN analysis. The data were filtered by removing all MS/MS fragment ions within ±17 Da of the precursor m/z. MS/MS spectra were window filtered by choosing only the top 6 fragment ions in the ±50 Da window throughout the spectrum. The precursor ion mass tolerance was set to 0.2 Da and the MS/MS fragment ion tolerance to 0.2 Da. A molecular network was then created where edges were filtered to have a cosine score above 0.7 and more than 6 matched peaks. Further, edges between two nodes were kept in the network if and only if each of the nodes appeared in each others respective top 10 most similar nodes. Finally, the maximum size of a molecular family was set to 100, and the lowest scoring edges were removed from molecular families until the molecular family size was below this threshold. The analog search mode was used by searching against MS/MS spectra with a maximum difference of 100.0 in the precursor ion value. The library spectra were filtered in the same manner as the input data. All matches kept between network spectra and library spectra were required to have a score above 0.7 and at least 6 matched peaks. The DEREPLICATOR was used to annotate MS/MS spectra (Mohimani et al., 2018). The molecular networks were visualized using Cytoscape (v3.5.1).

Statistical Analyses

To address if the interactions between gravid females and developing larvae, with the community of microorganisms in the breeding sites were reflected in the chemical composition of the samples at the time of collection, we filtered the detected metabolites table (**Supplementary Table 2**) transforming it into a presence and absence data set. This binary matrix was then utilized to estimate the Jaccard dissimilarities between treatments, visualize the constrained ordination patterns based



on the sample profiles and their group affiliation, and evaluate if the differences between each treatment were significant by means of a pairwise PERMANOVA. All the analyses were performed in the Rstudio environment v1.1.423 (R Core Team, 2020) using the following packages: vegan v2.5-7 (Oksanen et al., 2020), mctoolr v0.1.1.2, and pairwiseAdonis v0.0.1 (Martinez Arbizu, 2020).

RESULTS AND DISCUSSION

Isolation, Identification, and Description of *Klebsiella* sp. MC1F From *Aedes aegypti* Feces

Circular, convex, regular margined, mucoid, and pink colonies were recovered from MacConkey agar plates. After DNA isolation, 16S rRNA amplicon, and genome sequencing, the bacterium was identified as *Klebsiella* sp. Indeed, this bacterial taxon has often been isolated from our mosquito strain (BR URCA, F5). Assembly of *Klebsiella* reads resulted in 175 contigs (N50: 167,915 bp) totaling 5,305,341 bp and a GC content of 57.9%. The genome is available under accession number JAGTYC000000000.

Several authors have reported the association between *Klebsiella* and mosquitoes, including its detection on eggs, larvae, pupae, adults, and their breeding sites (Gusmão et al., 2010; Chandel et al., 2013; Dada et al., 2014; Yadav et al., 2015; Wang et al., 2018; Hery et al., 2020; Rocha et al., 2021).

Culture-dependent approaches have allowed the isolation of *Klebsiella* from the midgut of *Ae. aegypti* adults emerging from larvae and pupae collected from natural breeding sites (Yadav et al., 2015) and from domestic water storage containers (Dada et al., 2014). Using high-throughput 16S rRNA amplicon sequencing, *Klebsiella* has been reported in natural aquatic habitats and in the *Ae. aegypti* larvae developing there (Hery et al., 2020). Díaz-Nieto et al., 2016 have isolated *Klebsiella* from all stages of *Culex pipiens* (for isolation from mosquito gut also Díaz-Nieto, 2014). This bacterial taxon has also been identified in all developmental stages of *Anopheles darlingi* and their breeding environments suggesting a narrow relation between these bacteria and their hosts (Rocha et al., 2021). In addition, our pilot shotgun metagenomic sequencing studies from *Aedes japonicus* larvae and breeding site water (collected from a water basin in a cemetery in Wiesbaden, Germany, coordinates: 50.104510, 8.216475), has identified Gammaproteobacteria, which includes *Klebsiella*, constituting 5 and 9% of all bacterial reads, respectively (**Supplementary Figure 1**). Based on these consistent findings, we suggest that *Klebsiella* is a potential mosquito symbiont that can be found in all stages and transferred to water by females to support early larval development in breeding sites.

Gut bacterial communities can be vertically transferred from adults to eggs as evidenced for tephritid fruit flies and *Ae. aegypti* (Lauzon et al., 2009; Coon et al., 2014). These bacterial taxa detected on insect eggs were also found in the gastrointestinal tracts of adults. The mechanisms by which this transference would occur are not yet elucidated, but one route of interest to

our work involves adults transmitting symbionts by smearing fecal matter on the eggshells during oviposition (Salem et al., 2015; Sontowski and van Dam, 2020). In the case of mosquitoes, this simple process would allow the larvae to acquire the bacteria shortly after hatching or even use them for their initial nurture (Díaz-Nieto et al., 2016). Indeed, throughout the execution of our experiments, we observed that gravid females eventually defecated in breeding sites. As bacterial transference through such a mechanism has been reported in other insect models (Engel and Moran, 2013), we suggest that future studies should test whether this is a stereotypical behavior exhibited by egg-laying females or a stochastic event.

Egg-laying decisions by female *Ae. aegypti* are crucial to grant offspring survival and optimal development. Bacteria belonging to the genus *Klebsiella* have been shown to mediate attraction and induce oviposition in *Cx. pipiens* gravid females (Díaz-Nieto et al., 2016). Moreover, *Klebsiella* nurtures the most vulnerable stage of the mosquito life cycle, L1, to ensure molting to a more resilient stage, L2, and thus increase the larvae's chances of reaching adulthood (Díaz-Nieto et al., 2016). This could be particularly important for *Ae. aegypti* considering its ability to exploit small and temporary rainwater collections as larval breeding sites (Scolari et al., 2019).

Metabolic Pathways Present in *Klebsiella* sp. MC1F

Several studies have shown that microbes are indispensable for mosquito larval development (Coon et al., 2014; Wang et al., 2018). Given the importance of bacteria in breeding sites, we wanted to investigate the metabolic pathways present in organisms that have been isolated from multiple mosquito sources. We concur with the hypothesis that a number of key microbial species present in breeding sites might be deposited by the mosquitoes themselves. We used a recently developed tool, gutSMASH (Andreu et al., 2021), to analyze primary metabolic pathways present in the genomes of facultatively anaerobic as well as aerobic bacteria that have been isolated from mosquitoes (Ganley et al., 2020; **Figure 2** and **Supplementary Table 1**).

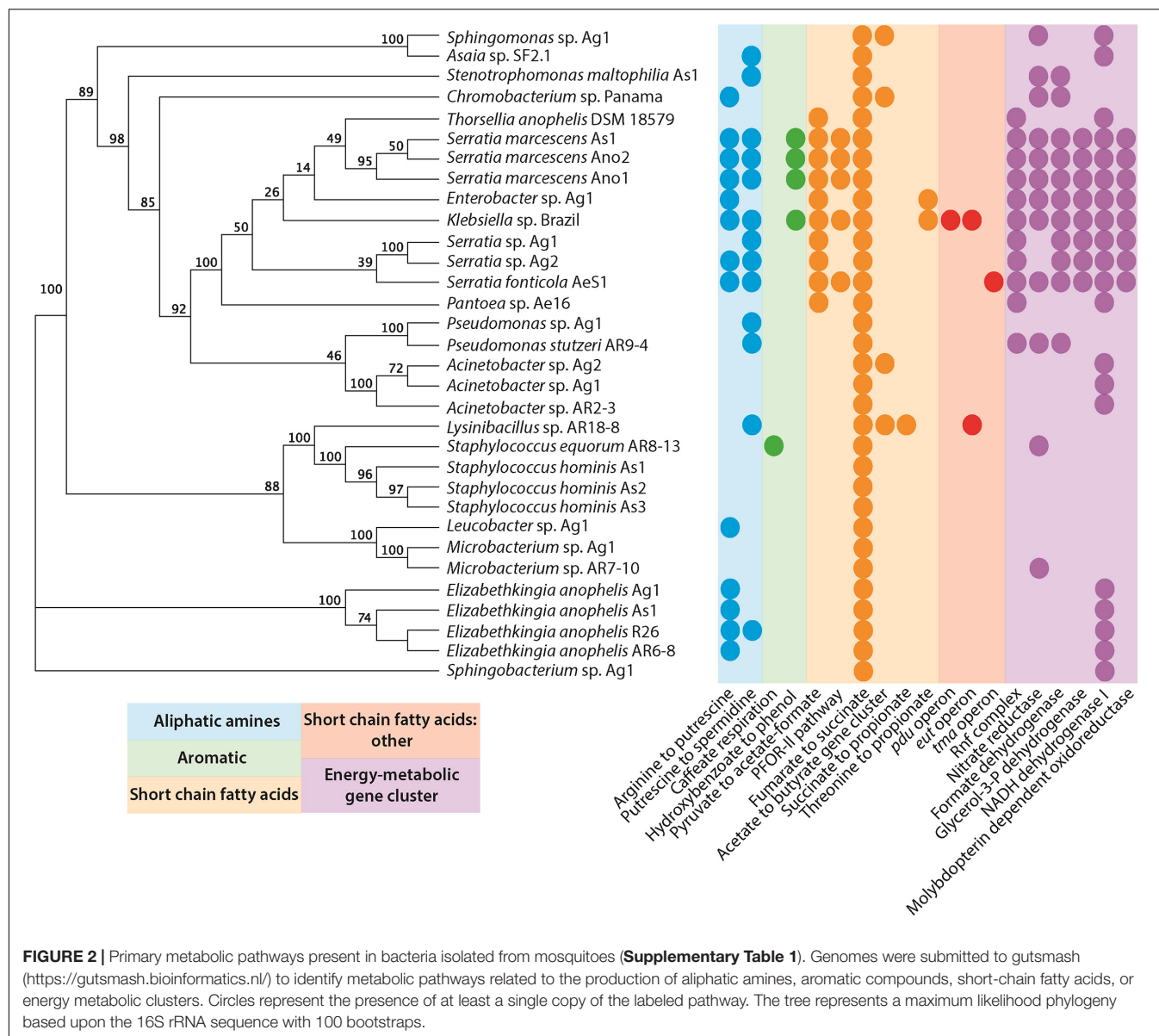
Only a single pathway is present in all of the bacteria examined: the fumarate to succinate pathway. This is perhaps unsurprising since the conversion of fumarate to succinate, mediated by the fumarate reductase enzyme, is an important part of the anaerobic respiration pathway in microbial metabolism (Lu and Imlay, 2017). A number of other short-chain fatty acid pathways are also present, none of which are ubiquitous to all species. However, the pyruvate to acetate/formate pathway was widespread in the Gammaproteobacteria. The pyruvate formate lyase enzyme mediates this reaction, and helps regulate anaerobic glucose metabolism. However, the enzyme is also involved in two other metabolic pathways: butanoate metabolism and propanoate metabolism. Interestingly, butanoate and propanoate esters actually display mosquito repellent effects in *Anopheles stephensi*, perhaps pointing to a role for bacteria in mediating the oviposition site selection by gravid mosquitoes (Sharma et al., 2009). Further to this, the presence of aliphatic amine and aromatic pathways may additionally support this role of

some bacteria. For instance, *Ae. aegypti* mosquitoes are attracted to oviposition sites baited with putrescine (Hussain et al., 2016). Moreover, high levels of putrescine and spermidine have been detected in *Ae. aegypti* ovaries. It has been suggested that these polyamines could be stored in eggs for use during embryogenesis (Kogan and Hagedorn, 2000). This is particularly interesting considering that *Klebsiella* has been isolated from *Ae. aegypti* ovaries (Alvarado et al., 2021). Polyamines have been implicated in growth processes and were highlighted as one of the most important metabolites produced by the intestinal microbiota that affect host health and disease (Matsumoto et al., 2011). A metabolomic study in mice demonstrated that colonic microbiota is primarily responsible for the intestinal luminal concentrations of putrescine and spermidine (Matsumoto et al., 2012). In *Drosophila melanogaster*, a diet high in polyamines was shown to be beneficial and increased its reproductive success (Hussain et al., 2016). Furthermore, the exogenous addition of polyamines, especially spermidine, extended the lifespan in yeast, nematodes, and flies (Eisenberg et al., 2009; Morselli et al., 2009). Therefore, the presence of bacteria producing these metabolites in mosquito breeding sites may play a key role in promoting the successful development of larvae and the fitness of adults.

It is important to highlight that metabolites from other pathways could also influence the female-perceived quality of mosquito breeding sites. Short-chain fatty acids, like isovaleric acid and butyric acid, have been shown to act as deterrents to ovipositing females of *Culex* spp. and *Aedes albopictus* (Hwang et al., 1980; Boullis et al., 2021). Likewise, aromatic compounds like indole mediate oviposition of *Anopheles gambiae* and *Culex* spp. (Millar et al., 1992; Blackwell and Johnson, 2000; Lindh et al., 2008).

Bacterial Metabolites Are Present in Breeding Sites Visited by Female Mosquitoes

One of our main objectives was to describe and measure the effects that oviposition and larval development have on the metabolite composition of breeding sites. To do so we separated the two main interactions mosquitoes have with the water in the breeding site: the direct contact of females with water (and any stereotypical behavior this entails, e.g., grooming, tasting, and defecating, etc.), and the contact of eggs, their eclosion, and larval development. We sought to compare whether water samples exposed to each of these conditions presented qualitatively dissimilar metabolite profiles, i.e., presence/absence. As it can be observed in the RDA plot (**Supplementary Figure 2**), the clustering patterns suggest the biotic and abiotic conditions represented in each treatment generated distinct metabolite profiles at the endpoint of the experiment. Samples from each treatment distributed along the ordination axes in a well-resolved pattern. The constrained variance in the reported plot amounted to 23.89%. Furthermore, the pairwise PERMANOVA revealed that the dissimilarities among treatments were all significant (**Supplementary Table 3**). The effect size (R^2) of the conditions represented by each treatment when compared were as follows: Treatment 1vs Treatment 2 24.64%; Treatment 1vs Treatment 3



30.07%; and Treatment 2vs Treatment 3 21.20%. The remaining variance could be due to relevant interactions between biotic and abiotic explanatory variables that change throughout time and larval development (e.g., bacterial community composition and their metabolic output in response to changes in pH, dissolved oxygen, and conductivity, etc.). Physicochemical parameters were recently described as relevant features of *Ae. aegypti* breeding sites (Hery et al., 2020) and their fluctuations may be drivers (or responses) of bacterial community structures, and thus of their individual and community metabolism. We suggest that the layer of information generated by metabolomic assays may prove relevant as it provides a new source of analytical signal to gain insights into this dimension of the niche where larvae develop and shape key life-history traits (Dickson et al., 2017). For instance, this approach could be enhanced by interrogating

similar sample types using other solvents, as methanol may not extract the entire breadth of metabolites present.

Finally, as we can observe in **Figure 3A**, there were five metabolites that had both a bacterial origin and were present in T₂ which represents the act of oviposition and larval development closer than it occurs in nature (**Figures 3B–F**). These metabolites were absent from both the control (T₁) and manual oviposition conditions (T₃), therefore representing discriminative features among the chemical composition of the samples representing a decoupled oviposition. As these metabolites are unique to the combination of biotic variables, they could potentially act as indicators of successful female oviposition, egg eclosion, and larval development in *Ae. aegypti*. It is relevant to highlight that these metabolites could also originate from bacteria within the breeding site pertaining to taxa with which *Klebsiella* shares

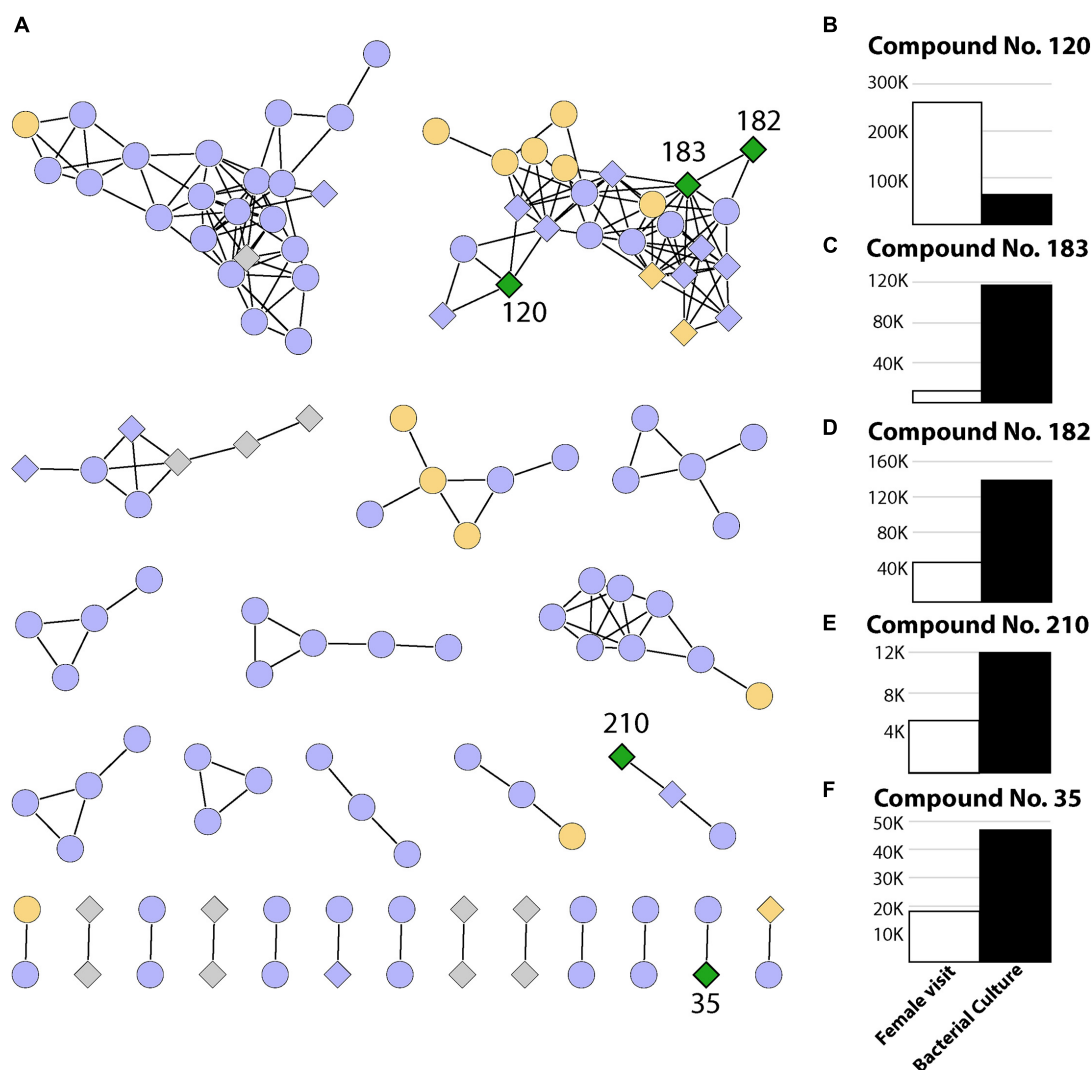


FIGURE 3 | Summary of 239 metabolites identified in this study. **(A)** Networks containing two or more metabolites (nodes) connected by edges when a minimum number of matching fragments is present (see section “Materials and Methods”). The coloring represents metabolites identified in experiments where only the female visited (T_2 , green), where the female visited and/or eggs were manually placed (T_2 and/or T_3 , orange), where metabolites were present in the control sample and/or T_3 and/or T_2 (purple), as well as metabolites detected only in bacterial cultures (gray). Diamonds represent bacterial metabolites, while circles represent metabolites not present in bacterial samples. **(B–F)** Relative abundance (area under the curve from mass spectrometry) for compounds present in breeding site experiments where the female visited (T_2) and also present in bacterial extracts (green diamonds).

metabolic pathways. This is plausible as functional redundancy can be expected in microbial systems (Louca et al., 2018).

FUTURE DIRECTIONS

Metabolites of bacterial origin, particularly from *Klebsiella* (or other related taxa with similar metabolic outputs) could act as guiding and/or decision-making modulating sensory cues (either olfactory or gustatory) for other conspecific females to access the quality of the breeding site (Ponnusamy et al., 2008; Boullis et al., 2021 and references therein). It is known that *Klebsiella* is present in larvae-positive breeding sites (Dada et al., 2014) and that bacteria from this genus produce volatile compounds

(Rees et al., 2017). As thriving larvae alter their niche, potentially modifying the microbial composition (Scolari et al., 2021), these bacteria-derived volatile compounds could accumulate in the headspace of the water. Identifying the nature of these molecules, and using them in chemical ecology and behavioral assays seems to be a promising avenue to explore, as Boullis et al. (2021) recently highlighted, due to the fact that their mechanism of action has not yet been elucidated.

DATA AVAILABILITY STATEMENT

The *Klebsiella* sp. MC1F assembly and annotation can be found in Genbank with accession number JAGTYC000000000.

All metabolomic data are freely available at the MassIVE repository under accession number MSV000087341, <ftp://massive.ucsd.edu/MSV000087341/>.

AUTHOR CONTRIBUTIONS

KM, LEM, CS, SP, SK, TS, LAM, NT, and ML conceived and designed the analysis. KM, LEM, SP, CS, and NT collected the data. KM, LEM, SP, CS, SK, TS, NT, and ML contributed to data or analysis tools. KM, LEM, SP, CS, LAM, NT, and ML performed the analysis. KM, LEM, NT, and ML wrote the initial draft. All authors read and approved the final draft.

FUNDING

This work was funded by the LOEWE-Centre TBG supported by the Hessen State Ministry of Higher Education, Research and the Arts (HMWK), Fundação de Amparo à Pesquisa do Estado de Minas Gerais FAPEMIG – EDITAL 00/2016 –

REFERENCES

- Alvarado, W. A., Agudelo, S. O., Velez, I. D., and Vivero, R. J. (2021). Description of the ovarian microbiota of *Aedes aegypti* (L) Rockefeller strain. *Acta Trop.* 214:105765. doi: 10.1016/j.actatropica.2020.105765
- Andreu, V. P., Augustijn, H. E., Chen, L., Zhernakova, A., Fu, J., Fischbach, M. A., et al. (2021). A systematic analysis of metabolic pathways in the human gut microbiota. *Bioinformatics* [preprint]. doi: 10.1101/2021.02.25.432841
- Bankevich, A., Nurk, S., Antipov, D., Gurevich, A. A., Dvorkin, M., Kulikov, A. S., et al. (2012). SPAdes: a New Genome Assembly Algorithm and Its Applications to Single-Cell Sequencing. *J. Comput. Biol.* 19, 455–477. doi: 10.1089/cmb.2012.0021
- Benzon, G. L., and Apperson, C. S. (1988). Reexamination of Chemically Mediated Oviposition Behavior in *Aedes aegypti* (L.) (Diptera: Culicidae). *J. Med. Entomol.* 25, 158–164. doi: 10.1093/jmedent/25.3.158
- Blackwell, A., and Johnson, S. N. (2000). Electrophysiological investigation of larval water and potential oviposition chemo-attractants for *Anopheles gambiae* s.s. *Ann. Trop. Med. Parasitol.* 94, 389–398. doi: 10.1080/00034983.2000.11813554
- Boullis, A., Mulatier, M., Delannay, C., Héry, L., Verheggen, F., and Vega-Rúa, A. (2021). Behavioural and antennal responses of *Aedes aegypti* (L.) (Diptera: Culicidae) gravid females to chemical cues from conspecific larvae. *PLoS One* 16:e0247657. doi: 10.1371/journal.pone.0247657
- Brady, O. J., and Hay, S. I. (2020). The Global Expansion of Dengue: how *Aedes aegypti* Mosquitoes Enabled the First Pandemic Arbovirus. *Annu. Rev. Entomol.* 65, 191–208. doi: 10.1146/annurev-ento-011019-024918
- Caragata, E. P., Otero, L. M., Tikhe, C. V., Barrera, R., and Dimopoulos, G. (2021). Microbial Diversity of Adult *Aedes aegypti* and Water Collected from Different Mosquito Aquatic Habitats in Puerto Rico. *Microb. Ecol.* [Epub Online ahead of print]. doi: 10.1007/s00248-021-01743-6
- Chandel, K., Mendki, M. J., Parikh, R. Y., Kulkarni, G., Tikar, S. N., Sukumaran, D., et al. (2013). Midgut Microbial Community of *Culex quinquefasciatus* Mosquito Populations from India. *PLoS One* 8:e80453. doi: 10.1371/journal.pone.0080453
- Coon, K. L., Brown, M. R., and Strand, M. R. (2016). Mosquitoes host communities of bacteria that are essential for development but vary greatly between local habitats. *Mol. Ecol.* 25, 5806–5826. doi: 10.1111/mec.13877
- CONFAP – MRC/TEC – APQ-00913-16, CNPq (Project number: 311826/2019-9), INCTEM (Project number: 465678/2014-9), and FIOCRUZ.
- Coon, K. L., Vogel, K. J., Brown, M. R., and Strand, M. R. (2014). Mosquitoes rely on their gut microbiota for development. *Mol. Ecol.* 23, 2727–2739. doi: 10.1111/mec.12771
- Dada, N., Jumas-Bilak, E., Manguin, S., Seidu, R., Stenström, T.-A., and Overgaard, H. J. (2014). Comparative assessment of the bacterial communities associated with *Aedes aegypti* larvae and water from domestic water storage containers. *Parasit. Vectors* 7:391. doi: 10.1186/1756-3305-7-391
- Dada, N., Jupatanakul, N., Minard, G., Short, S. M., Akorli, J., and Villegas, L. M. (2021). Considerations for mosquito microbiome research from the Mosquito Microbiome Consortium. *Microbiome* 9:36. doi: 10.1186/s40168-020-00987-7
- Díaz-Nieto, L. M. (2014). *Diversidad de mosquitos en Mar del Plata y caracterización de microorganismos patógenos y simbioses para el control de culicidos de importancia sanitaria.* Ph.D. thesis, Universidad Nacional de Mar del Plata. 177.
- Díaz-Nieto, L. M., D'Alessio, C., Perotti, M. A., and Berón, C. M. (2016). *Culex pipiens* Development Is Greatly Influenced by Native Bacteria and Exogenous Yeast. *PLoS One* 11:e0153133. doi: 10.1371/journal.pone.0153133
- Dickson, L. B., Jiolle, D., Minard, G., Moltini-Conclois, I., Volant, S., Ghazlane, A., et al. (2017). Carryover effects of larval exposure to different environmental bacteria drive adult trait variation in a mosquito vector. *Sci. Adv.* 3:e1700585.
- Eisenberg, T., Knauer, H., Schauer, A., Büttner, S., Ruckenstein, C., Carmona-Gutierrez, D., et al. (2009). Induction of autophagy by spermidine promotes longevity. *Nat. Cell Biol.* 11, 1305–1314. doi: 10.1038/ncb1975
- Engel, P., and Moran, N. A. (2013). The gut microbiota of insects – diversity in structure and function. *FEMS Microbiol. Rev.* 37, 699–735. doi: 10.1111/1574-6976.12025
- Fischer, C. N., Trautman, E. P., Crawford, J. M., Stabb, E. V., Handelsman, J., and Broderick, N. A. (2017). Metabolite exchange between microbiome members produces compounds that influence *Drosophila* behavior. *Elife* 6:e18855. doi: 10.7554/eLife.18855
- Foster, K. R., Schluter, J., Coyte, K. Z., and Rakoff-Nahoum, S. (2017). The evolution of the host microbiome as an ecosystem on a leash. *Nature* 548, 43–51. doi: 10.1038/nature23292
- Gainley, J. G., Pandey, A., Sylvester, K., Lu, K.-Y., Toro-Moreno, M., Rüttschlin, S., et al. (2020). A Systematic Analysis of Mosquito-Microbiome Biosynthetic Gene Clusters Reveals Antimalarial Siderophores that Reduce Mosquito Reproduction Capacity. *Cell Chem. Biol.* 27, 817–826.e5. doi: 10.1016/j.chembiol.2020.06.004

ACKNOWLEDGMENTS

We would like to thank Helge Bode from Goethe University in Frankfurt for the generous use of his mass spectrometry facilities. We would also like to thank Rickard Ignell from the Swedish University of Agricultural Sciences for managing access to the facilities where the DNA and bacterial metabolite extractions were performed.

SUPPLEMENTARY MATERIAL

The Supplementary Material for this article can be found online at: <https://www.frontiersin.org/articles/10.3389/fmicb.2021.703711/full#supplementary-material>

- Guégan, M., Zouache, K., Démichel, C., Minard, G., Tran Van, V., Potier, P., et al. (2018). The mosquito holobiont: fresh insight into mosquito-microbiota interactions. *Microbiome* 6:49. doi: 10.1186/s40168-018-0435-2
- Gusmão, D. S., Santos, A. V., Marini, D. C., Bacci, M., Berbert-Molina, M. A., and Lemos, F. J. A. (2010). Culture-dependent and culture-independent characterization of microorganisms associated with *Aedes aegypti* (Diptera: culicidae) (L.) and dynamics of bacterial colonization in the midgut. *Acta Trop.* 115, 275–281. doi: 10.1016/j.actatropica.2010.04.011
- Hery, L., Guidez, A., Durand, A.-A., Delannay, C., Normandeux-Guimond, J., Reynaud, Y., et al. (2020). Natural variation in physicochemical profiles and bacterial communities associated with *Aedes aegypti* breeding sites and larvae on Guadeloupe and French Guiana. *In Review* [Preprint]. doi: 10.21203/rs.2.23822/v1
- Hussain, A., Zhang, M., Üçpınar, H. K., Svensson, T., Quillery, E., Gompel, N., et al. (2016). Ionotropic Chemosensory Receptors Mediate the Taste and Smell of Polyamines. *PLoS Biol.* 14:e1002454. doi: 10.1371/journal.pbio.1002454
- Hwang, Y.-S., Kramer, W. L., and Mulla, M. S. (1980). Oviposition attractants and repellents of mosquitoes: isolation and identification of oviposition repellents for *Culex* mosquitoes. *J. Chem. Ecol.* 6, 71–80. doi: 10.1007/BF00987528
- Imam, H., Zarnigar, Sofi, G., and Seikh, A. (2014). The basic rules and methods of mosquito rearing (*Aedes aegypti*). *Trop. Parasitol.* 4, 53–55. doi: 10.4103/2229-5070.129167
- Juma, E. O., Allan, B. F., Chang-Hyun, K., Stone, C., Dunlap, C., and Muturi, E. J. (2021). The larval environment strongly influences the bacterial communities of *Aedes triseriatus* and *Aedes japonicus* (Diptera: culicidae). *Sci. Rep.* 11:7910.
- Kogan, P. H., and Hagedorn, H. H. (2000). Polyamines, and effects from reducing their synthesis during egg development in the yellow fever mosquito, *Aedes aegypti*. *J. Insect Physiol.* 46, 1079–1095. doi: 10.1016/S0022-1910(99)00084-0
- Lauzon, C. R., McCombs, S. D., Potter, S. E., and Peabody, N. C. (2009). Establishment and Vertical Passage of *Enterobacter (Pantoea) agglomerans* and *Klebsiella pneumoniae* through All Life Stages of the Mediterranean Fruit Fly (Diptera: tephritidae). *Ann. Entomol. Soc. Am.* 102, 85–95. doi: 10.1603/008.102.0109
- Lindh, J. M., Borg-Karlson, A.-K., and Faye, I. (2008). Transstadial and horizontal transfer of bacteria within a colony of *Anopheles gambiae* (Diptera: culicidae) and oviposition response to bacteria-containing water. *Acta Trop.* 107, 242–250. doi: 10.1016/j.actatropica.2008.06.008
- Louca, S., Polz, M. F., Mazel, F., Albright, M. B. N., Huber, J. A., O'Connor, M. I., et al. (2018). Function and functional redundancy in microbial systems. *Nat. Ecol. Evol.* 2, 936–943. doi: 10.1038/s41559-018-0519-1
- Lu, Z., and Imlay, J. A. (2017). The Fumarate Reductase of *Bacteroides thetaiotaomicron*, unlike That of *Escherichia coli*, Is Configured so that It Does Not Generate Reactive Oxygen Species. *mBio* 8, e01873–16. doi: 10.1128/mBio.01873-16
- Martinez Arbizu, P. (2020). pairwiseAdonis: pairwise multilevel comparison using adonis. R package version 0.4. Available Online at: <https://github.com/pmartinezarbizu/pairwiseAdonis> (accessed April 26, 2021).
- Matsumoto, M., Kibe, R., Ooga, T., Aiba, Y., Kurihara, S., Sawaki, E., et al. (2012). Impact of Intestinal Microbiota on Intestinal Luminal Metabolome. *Sci. Rep.* 2:233. doi: 10.1038/srep00233
- Matsumoto, M., Kurihara, S., Kibe, R., Ashida, H., and Benno, Y. (2011). Longevity in Mice Is Promoted by Probiotic-Induced Suppression of Colonic Senescence Dependent on Upregulation of Gut Bacterial Polyamine Production. *PLoS One* 6:e23652. doi: 10.1371/journal.pone.0023652
- Melo, N., Wolff, G. H., Costa-da-Silva, A. L., Arribas, R., Triana, M. F., Gugger, M., et al. (2020). Geosmin Attracts *Aedes aegypti* Mosquitoes to Oviposition Sites. *Curr. Biol.* 30, 127–134.e5. doi: 10.1016/j.cub.2019.11.002
- Merritt, R. W., Olds, E. J., and Walker, E. D. (1992). Feeding behavior, natural food, and nutritional relationships of larval mosquitoes. *Annu. Rev. Entomol.* 6, 349–376. doi: 10.1146/annurev.en.37.010192.002025
- Millar, J., Chaney, J., and Mulla, M. (1992). Identification of oviposition attractants for *Culex quinquefasciatus* from fermented Bermuda grass infusions. *J. Am. Mosq. Control Assoc.* 8, 11–17.
- Mohimani, H., Gurevich, A., Shlemov, A., Mikheenko, A., Korobeynikov, A., Cao, L., et al. (2018). Dereplication of microbial metabolites through database search of mass spectra. *Nat. Commun.* 9:4035.
- Morselli, E., Galluzzi, L., Kepp, O., Criollo, A., Maiuri, M. C., Tavernarakis, N., et al. (2009). Autophagy mediates pharmacological lifespan extension by spermidine and resveratrol. *Aging* 1, 961–970. doi: 10.18632/aging.100110
- Muturi, E. J., Lagos-Kutz, D., Dunlap, C., Ramirez, J. L., Rooney, A. P., Hartman, G. L., et al. (2018). Mosquito microbiota cluster by host sampling location. *Parasit. Vectors* 11:468. doi: 10.1186/s13071-018-3036-9
- Nothias, L.-F., Petras, D., Schmid, R., Dührkop, K., Rainer, J., Sarvepalli, A., et al. (2020). Feature-based molecular networking in the GNPS analysis environment. *Nat. Methods* 17, 905–908. doi: 10.1038/s41592-020-0933-6
- Oksanen, J., Guillaume, F., Friendly, M., Kindt, R., Legendre, P., McGlinn, D., et al. (2020). *Vegan: community ecology package. R package. Version 2.5-7*. Available Online at: <https://cran.r-project.org/web/packages/vegan/index.html> (accessed April 26, 2021).
- Pluskal, T., Castillo, S., Villar-Briones, A., and Orešič, M. (2010). MZmine 2: modular framework for processing, visualizing, and analyzing mass spectrometry-based molecular profile data. *BMC Bioinformatics* 11:395. doi: 10.1186/1471-2105-11-395
- Ponnusamy, L., Böröczky, K., Wesson, D. M., Schal, C., and Apperson, C. S. (2011). Bacteria Stimulate Hatching of Yellow Fever Mosquito Eggs. *PLoS One* 6:e24409. doi: 10.1371/journal.pone.0024409
- Ponnusamy, L., Schal, C., Wesson, D. M., Arellano, C., and Apperson, C. S. (2015). Oviposition responses of *Aedes* mosquitoes to bacterial isolates from attractive bamboo infusions. *Parasit. Vectors* 8:486. doi: 10.1186/s13071-015-1068-y
- Ponnusamy, L., Xu, N., Nojima, S., Wesson, D. M., Schal, C., and Apperson, C. S. (2008). Identification of bacteria and bacteria-associated chemical cues that mediate oviposition site preferences by *Aedes aegypti*. *Proc. Natl. Acad. Sci. U. S. A.* 105, 9262–9267. doi: 10.1073/pnas.0802505105
- R Core Team (2020). *R: a language and environment for statistical computing*. Vienna, Austria: R Foundation for Statistical Computing.
- Rees, C. A., Nordick, K. V., Franchina, F. A., Lewis, A. E., Hirsch, E. B., and Hill, J. E. (2017). Volatile metabolic diversity of *Klebsiella pneumoniae* in nutrient-replete conditions. *Metabolomics* 13:18. doi: 10.1007/s11306-016-1161-z
- Rocha, E. M., Marinotti, O., Serrão, D. M., Correa, L. V., Katak, R., de, M., et al. (2021). Culturable bacteria associated with *Anopheles darlingi* and their paratransgenesis potential. *Malar. J.* 20:40. doi: 10.1186/s12936-020-03574-1
- Rose, N. H., Sylla, M., Badolo, A., Lutomiah, J., Ayala, D., Aribodor, O. B., et al. (2020). Climate and Urbanization Drive Mosquito Preference for Humans. *Curr. Biol.* 30, 3570–3579.e6. doi: 10.1016/j.cub.2020.06.092
- Rozeboom, L. E. (1935). The relation of bacteria and bacterial filtrates to the development of mosquito larvae. *Am. J. Hyg.* 21, 167–179. doi: 10.1093/oxfordjournals.aje.a118108
- Salem, H., Florez, L., Gerardo, N., and Kaltenpoth, M. (2015). An out-of-body experience: the extracellular dimension for the transmission of mutualistic bacteria in insects. *Proc. R. Soc. B Biol. Sci.* 282:20142957. doi: 10.1098/rspb.2014.2957
- Scolari, F., Casiraghi, M., and Bonizzoni, M. (2019). *Aedes* spp. and Their Microbiota: a Review. *Front. Microbiol.* 10:2036. doi: 10.3389/fmicb.2019.02036
- Scolari, F., Sandionigi, A., Carlassara, M., Bruno, A., Casiraghi, M., and Bonizzoni, M. (2021). Exploring Changes in the Microbiota of *Aedes albopictus*: comparison Among Breeding Site Water, Larvae, and Adults. *Front. Microbiol.* 12:624170. doi: 10.3389/fmicb.2021.624170
- Sharma, K. R., Seenivasagan, T., Rao, A. N., Ganesan, K., Agrawal, O. P., and Prakash, S. (2009). Mediation of oviposition responses in the malaria mosquito *Anopheles stephensi* Liston by certain fatty acid esters. *Parasitol. Res.* 104, 281–286. doi: 10.1007/s00436-008-1189-8

- Sontowski, R., and van Dam, N. M. (2020). Functional Variation in Dipteran Gut Bacterial Communities in Relation to Their Diet, Life Cycle Stage and Habitat. *Insects* 11:543. doi: 10.3390/insects11080543
- Tobias, N. J., Wolff, H., Djahanschiri, B., Grundmann, F., Kronenwerth, M., Shi, Y.-M., et al. (2017). Natural product diversity associated with the nematode symbionts *Photorhabdus* and *Xenorhabdus*. *Nat. Microbiol.* 2, 1676–1685. doi: 10.1038/s41564-017-0039-9
- Wang, M., (2016). Sharing and community curation of mass spectrometry data with Global Natural Products Social Molecular Networking. *Nat. Biotechnol.* 34, 828–837.
- Wang, X., Liu, T., Wu, Y., Zhong, D., Zhou, G., Su, X., et al. (2018). Bacterial microbiota assemblage in *Aedes albopictus* mosquitoes and its impacts on larval development. *Mol. Ecol.* 27, 2972–2985. doi: 10.1111/mec.14732
- Yadav, K. K., Bora, A., Datta, S., Chandel, K., Gogoi, H. K., Prasad, G. B. K. S., et al. (2015). Molecular characterization of midgut microbiota of *Aedes albopictus* and *Aedes aegypti* from Arunachal Pradesh, India. *Parasit. Vectors* 8:641. doi: 10.1186/s13071-015-1252-0

Conflict of Interest: The authors declare that the research was conducted in the absence of any commercial or financial relationships that could be construed as a potential conflict of interest.

Publisher's Note: All claims expressed in this article are solely those of the authors and do not necessarily represent those of their affiliated organizations, or those of the publisher, the editors and the reviewers. Any product that may be evaluated in this article, or claim that may be made by its manufacturer, is not guaranteed or endorsed by the publisher.

Copyright © 2021 Mosquera, Martinez Villegas, Pidot, Sharif, Klimpel, Stinear, Moreira, Tobias and Lorenzo. This is an open-access article distributed under the terms of the Creative Commons Attribution License (CC BY). The use, distribution or reproduction in other forums is permitted, provided the original author(s) and the copyright owner(s) are credited and that the original publication in this journal is cited, in accordance with accepted academic practice. No use, distribution or reproduction is permitted which does not comply with these terms.



Antimicrobial Compounds in the Volatilome of Social Spider Communities

Alexander Lammers^{1,2*}, Hans Zweers², Tobias Sandfeld³, Trine Bilde⁴, Paolina Garbeva², Andreas Schramm³ and Michael Lalk^{1*}

¹ Department of Cellular Biochemistry and Metabolomics, University of Greifswald, Greifswald, Germany, ² Department of Microbial Ecology, Netherlands Institute of Ecology (NIOO-KNAW), Wageningen, Netherlands, ³ Section for Microbiology, Department of Biology, Aarhus University, Aarhus, Denmark, ⁴ Section for Genetics, Ecology and Evolution, Department of Biology, Aarhus University, Aarhus, Denmark

OPEN ACCESS

Edited by:

Eoin L. Brodie,
Lawrence Berkeley National
Laboratory, United States

Reviewed by:

Hongjie Li,
Ningbo University, China
Martin Kaltenpoth,
Max Planck Institute for Chemical
Ecology, Germany
Michael Poulsen,
University of Copenhagen, Denmark
Nanna Vidkjær,
University of Copenhagen, Denmark,
in collaboration with reviewer MP

*Correspondence:

Alexander Lammers
alexander.lammers@uni-greifswald.de
Michael Lalk
lalk@uni-greifswald.de

Specialty section:

This article was submitted to
Terrestrial Microbiology,
a section of the journal
Frontiers in Microbiology

Received: 26 April 2021

Accepted: 31 July 2021

Published: 24 August 2021

Citation:

Lammers A, Zweers H,
Sandfeld T, Bilde T, Garbeva P,
Schramm A and Lalk M (2021)
Antimicrobial Compounds
in the Volatilome of Social Spider
Communities.
Front. Microbiol. 12:700693.
doi: 10.3389/fmicb.2021.700693

Social arthropods such as termites, ants, and bees are among others the most successful animal groups on earth. However, social arthropods face an elevated risk of infections due to the dense colony structure, which facilitates pathogen transmission. An interesting hypothesis is that social arthropods are protected by chemical compounds produced by the arthropods themselves, microbial symbionts, or plants they associate with. *Stegodyphus dumicola* is an African social spider species, inhabiting communal silk nests. Because of the complex three-dimensional structure of the spider nest antimicrobial volatile organic compounds (VOCs) are a promising protection against pathogens, because of their ability to diffuse through air-filled pores. We analyzed the volatilomes of *S. dumicola*, their nests, and capture webs in three locations in Namibia and assessed their antimicrobial potential. Volatilomes were collected using polydimethylsiloxane (PDMS) tubes and analyzed using GC/Q-TOF. We showed the presence of 199 VOCs and tentatively identified 53 VOCs. More than 40% of the tentatively identified VOCs are known for their antimicrobial activity. Here, six VOCs were confirmed by analyzing pure compounds namely acetophenone, 1,3-benzothiazole, 1-decanal, 2-decanone, 1-tetradecene, and docosane and for five of these compounds the antimicrobial activity were proven. The nest and web volatilomes had many VOCs in common, whereas the spider volatilomes were more differentiated. Clear differences were identified between the volatilomes from the different sampling sites which is likely justified by differences in the microbiomes of the spiders and nests, the plants, and the different climatic conditions. The results indicate the potential relevance of the volatilomes for the ecological success of *S. dumicola*.

Keywords: volatile organic compound, chemical ecology, antimicrobial, *Stegodyphus dumicola*, social arthropods

INTRODUCTION

Organisms use chemicals to exchange information, coordinate their behavior, or protect themselves against pathogens (Chen et al., 1998; Rowan, 2011; Schulz-Bohm et al., 2017). For example, social arthropods depend on chemical compounds, which are vital for communication and other functions mediating a high level of organization. They are able to inhabit extreme environments,

use numerous resources, and finally often outcompete other arthropods (Wilson, 1987; Hölldobler and Wilson, 1990; Fisher et al., 2019). However, a fundamental problem of social arthropods is the elevated risk of acquiring and transmitting pathogens, as their dense colony associations increase the risk of infections and pathogen transmission (Bratburd et al., 2020). The risk of infections has led to a number of adaptations ranging from behaviors that reduce the risk of transmission (Müller and Schmid-Hempel, 1993) to the use of antimicrobial compounds. Antimicrobial compounds can be produced among others by the arthropod hosts themselves (Graystock and Hughes, 2011), symbiotic microorganisms (Musa Bandowe et al., 2009), or surrounding plants (Tariq et al., 2019).

Sociality has also evolved within the class of arachnids (Lubin and Bilde, 2007). *Stegodyphus dumicola* is a social spider species living in large groups in southern and central Africa (Aviles, 1997; Lubin and Bilde, 2007). These spiders build communal nests where reproduction takes place and which protects the spiders against heat/dehydration, UV-radiation, and predators (**Supplementary Figure 1A**; Seibt and Wickler, 1990; Henschel, 1998; Lubin and Bilde, 2007). The nest is surrounded by three-dimensional capture webs used for communal prey capture (Majer et al., 2018). The social lifestyle in spiders comes with elimination of pre-mating dispersal and therefore a strictly inbreeding mating system. Combined with frequent extinction and colonization events, this results in extremely low genetic diversity (Lubin and Bilde, 2007; Settepani et al., 2014, 2016, 2017). Homozygosity in genes within individuals, and low population genetic diversity in for example immune genes is likely to be associated with elevated vulnerability to infections. This substantiates the hypothesis that antimicrobial compounds play an important role in protecting the spider hosts against pathogens.

Due to the complex nest structure, including tightly woven silk structures with multiple narrow tunnels and chambers, volatile organic compounds (VOCs) have a possible importance in pathogen defense. VOCs are carbon-based compounds with molecular masses below 400 Da, high vapor pressures, low boiling points, and lipophilic moiety, properties that imply versatility of these compounds in all terrestrial ecosystems (Rowan, 2011; Schmidt et al., 2015b; Tyc et al., 2015). As opposed to soluble compounds, VOCs can diffuse through air-filled pores in complex ecosystems such as soil and hence do not depend on solvents (Schmidt et al., 2015a). That suggests that VOCs have the potential to reach all the internal surfaces of the spider nest and serve as inhibitors of pathogens from a distance. Antimicrobial VOCs are widely produced by microorganisms, plants, and animals: For example, bacteria isolated from the rhizosphere are known for producing VOCs with antimicrobial properties that can have protective functions for symbiotic plants (Tyc et al., 2015; Ossowicki et al., 2017). Plants use VOCs by themselves in various functions such as preventing microbial infections (Hammerbacher et al., 2019). In termites, volatile pheromones produced by queens, primarily used for communication, were shown to also have antifungal effects, indicating a role in pathogen defense (Matsuura and Matsunaga, 2015). Red fire ants and beetles are also known to use VOCs with antimicrobial

properties (Gross et al., 2008; Wang et al., 2015). Here, we propose that VOCs may have a protective antimicrobial function in the nest system of the social spider *S. dumicola*.

The aim of this study is to describe the volatilomes of the spider *S. dumicola* and its nest and web, respectively, and to assess its potential antimicrobial effects. We hypothesized the presence of antimicrobial VOCs in the volatilomes of *S. dumicola*, its nest, and catching web. Next, we investigated whether the spider, the nest, and the capture web emit different VOC blends. Finally, we investigated volatilomes collected at different geographical locations to assess differences between the VOC blends. For this, we analyzed and compared the volatilomes from spider nests, catching webs, and the spiders themselves at three sampling sites in a north-south gradient in Namibia. Furthermore, we tested a selection of identified VOCs as pure compounds for their antimicrobial activity against microbial pathogens of spiders and humans.

MATERIALS AND METHODS

Sampling Sites

The volatilome samples were taken at three different sampling sites in Namibia between 8th–26th February, 2019 (**Supplementary Figure 2**). The locations were close to the Etosha National Park (“Otavi”; S19.47, E17.19), the capital (“Windhoek”; S22.57, E17.21), and a small town (“Stampriet”; S23.74, E18.19). Otavi and Stampriet are at an altitude of ~1,300 m and Windhoek of ~2,000 m. At each sampling site five nests were analyzed and defined as biological replicates. The maximal distance between the used spider nests were 150 m in Otavi, 300 m in Windhoek, and 1,200 m in Stampriet (**Supplementary Figure 2** inserts). Otavi is a humid sampling site in the North, Windhoek is mountainous, and Stampriet is because of its closeness to the Kalahari Desert on average the warmest region.

In Otavi the nests were located in plants of the species *Combretum imberbe*, *Acacia mellifera*, *Ziziphus mucronata*, and *Grewia flava*; in Windhoek in *Acacia hereroensis*, *Acacia mellifera*, and *Acacia hebeclada*; in Stampriet in *Acacia nebrowii*. We empirically observed the highest density of plants in Otavi and lowest in Stampriet.

The humidity and temperature data during the volatilome trapping were measured using iButton® logger every 300 s (Type DS1923, Maxim Integrated, San Jose, California, United States). The temperature and humidity data inside the nests during the VOC samplings revealed the nests in Otavi as warmest and less humid and the nests in Windhoek as less warm and most humid (**Supplementary Figure 3**).

Volatilome Trapping

Polydimethylsiloxane (PDMS) tubes (internal diameter 1 mm, external diameter 1.8 mm, Carl Roth, Karlsruhe, Germany) were cut into 5 mm pieces and threaded on needles. The tubes were fully covered with acetonitrile/methanol (4/1, v/v) and incubated for 3 h at room temperature. Subsequently they were dried under N₂ flow (5 l/min) and heated up to 210°C for 1.5 h under He flow

(5 l/min). Glass vials for storing the tubes until usage and needles for fixation at the spider nests and webs were cleaned similarly.

The PDMS tubes were used to trap volatile organic compounds (VOCs) from the spider nests, catching webs, and isolated living spiders. For trapping VOCs from the nests, five tubes were fixed with needles at the nest surfaces (**Supplementary Figure 1B**). For trapping VOCs from the catching webs, five PDMS tubes were threaded on needles to increase the surface and stuck to the catching webs in an approximately 30 cm diameter around the nests. PDMS tubes in sterile, open Petri dishes in 1 m distance to the nests were used as controls. The nests and webs were irritated as little as possible before, during, and after VOC trapping to stress the spiders as little as possible. No spiders or material were removed before trapping. VOCs from spiders were trapped by keeping five spiders from each nest together with five PDMS tubes in a sterile Petri dish. The controls for spider VOCs were closed Petri dishes with five PDMS tubes. All PDMS tubes were left for 30 min and immediately stored in closed glass vials at -20°C until VOC analysis. One nest (together with its catching web and spiders) was defined as one replicate. Per sampling site 3–5 replicates were taken.

GC/Q-TOF Analysis

The VOCs were released from the PDMS tubes using an automated thermodesorption unit (Unity TD-100, Markes International, Llantrisant, United Kingdom) at 280°C for 8 min with a He flow of 50 ml/min. The VOCs got cold trapped at -10°C on a Tenax trap (Markes International, Llantrisant, United Kingdom) and released at 300°C within 10 min. A split ratio of 1/4 was used. The VOCs were transferred (195°C transfer line) to the Agilent 7890B GC (Agilent Technologies, Inc., Santa Clara, CA, United States) with an DB-5 ms ultra inert column (30 m length, 0.25 mm internal diameter, 0.25 μm film thickness, 122–5,532, Agilent Technologies, Inc., Santa Clara, CA, United States) and a run time of 35.6 min. The temperature program was set to 39°C for 1 min followed by heating up to 315°C with $10^{\circ}\text{C}/\text{min}$ and holding for 7 min. The MS (280°C transfer line) was performed with Agilent 7200AB Q-TOF at 70 eV in electron ionization mode with a source temperature of 230°C . Mass spectra were recorded in full-scan-mode (m/z 30–400, 4 scans/s, 2 GHz Extended Dynamic Range).

For calibration of the retention index 1 μl alkane standard solution of C_8 – C_{20} (40 mg/l in Hexane; 04070-5ML; Merck, Darmstadt, Germany) was spiked on an empty Tenax trap and measured as described above. The presence of acetophenone, 2-decanone, 1-decanal, 1,3-benzothiazole, 1-tetradecene, and docosane (1 $\mu\text{g}/\text{ml}$ in MeOH; all purchased by Merck, Darmstadt, Germany) in the volatilomes was confirmed by measuring pure standard compounds on the same way.

GC/Q-TOF Data Processing

For GC/Q-TOF data processing the raw data were exported as content definition file (CDF) and imported into MZmine (Version 2.20;[©] Copyright 2015; Pluskal et al., 2010). Mass detection, chromatogram building, deconvolution (local

minimum algorithm), and peak alignment (RANSAC, random sample consensus) were performed using MZmine (for detailed parameters are provided in **Supplementary Table 1**). The peak lists were exported as comma-separated values (CSV) files. The files were uploaded to MetaboAnalyst (Version 4.0, Xia Lab, Montreal, Canada; Xia and Wishart, 2011), filtered (interquartile range), transformed (log transformation), and scaled (auto) before statistical tests were performed. Statistically significant differences between the samples and controls were identified by analysis of variance (ANOVA) followed by Fisher's least significant difference (LSD). Furthermore, a mass feature must be found in at least 4 of 5 or 3 of 4 of the biological replicates to get valued as such.

Compound identification was performed using AMDIS 2.72 (National Institute of Standards and Technology, United States) based on retention index comparison and mass spectrum comparison to three libraries providing more than 1.4 million spectra namely NIST 2014 V2.20 (National Institute of Standards and Technology, Gaithersburg, Maryland, United States), Wiley 7th edition spectral libraries (Wiley, Hoboken, New Jersey, United States), and an internal library of NIOO-KNAW (Netherlands Institute of Ecology, Wageningen, The Netherlands). The retention index tolerance was ± 10 and the minimum mass spectrum match was 600 %. If a mass feature complied both criteria, a visual comparison of the mass spectra was performed, and designated as "tentatively identified." Additionally, the retention indices and mass spectra of the "identified" compounds were compared to pure standard compounds measured in the same GC/Q-TOF system. Unknown mass features were assumed as different ones when the retention indices differed by > 6 .

Antimicrobial Test of Pure VOCs

Five VOCs identified using pure standard compounds, namely acetophenone, 2-decanone, 1-decanal, 1,3-benzothiazole, and 1-tetradecene, were tested as pure compounds for their antimicrobial activity. The compounds were selected based on literature indicating their high antimicrobial activity (**Supplementary Table 2**). We used *Bacillus thuringiensis* (DSM 2046), *Staphylococcus aureus* (DSM 799), *Escherichia coli* (DSM 787), and *Candida albicans* (DSM 10697) as test strains to cover all, a suggested spider pathogen, Gram positive and negative bacteria, as well as a yeast. The latter three strains are common human pathogens and were chosen as model organisms. All strains were bought at the German Collection of Microorganisms and Cell Cultures (DSMZ, Braunschweig, Germany). Before use the strains were pre-cultured overnight at 37°C on Mueller Hinton Agar II (2.0 g/l beef heart infusion, 17.5 g/l acid casein hydrolysate, 1.5 g/l starch, 17.0 g/l agar; Becton Dickinson, Franklin Lakes, New Jersey, United States).

The test strains were diluted to an OD_{600} of 0.1 in Mueller Hinton Broth II (17.5 g/l casein acid hydrolysate, 3 g/l beef extract, 1.5 g/l starch; Sigma-Aldrich, St. Louis, Missouri, United States). 10 ml of the prepared cell solution was transferred into a 100 ml-Erlenmeyer flask and test compounds, were added at a final concentration of 30 mM. The flasks were

sealed immediately with aluminum foil and wrapping film and incubated (37°C, 150 rpm). After 24 h the OD₆₀₀ was measured and compared to the negative control without added compounds (*t*-test, *p* ≤ 0.05). Three biological replicates for each test strain in combination with each test compound were performed.

Additionally, an agar diffusion test was performed based on the protocol of Hudzicki (2009). The test strains were diluted to an OD₆₀₀ of 0.125 in NaCl (0.9%) and spread on Mueller Hinton II agar plates (Becton Dickinson, Franklin Lakes, New Jersey, United States) using cotton swabs. Five microliters of the pure compounds were pipetted on empty cotton disks (6 mm diameter) and placed on the plates before sealing with Parafilm®. Empty cotton disks were used as negative controls. For positive controls cotton disks with gentamicin (Sensi-Disk™, 10 U, Becton Dickinson, Franklin Lakes, New Jersey, United States) were used for bacterial strains and amphotericin B (ROTI® Antibiotic Disks, 100 U, Carl Roth, Karlsruhe, Germany) for the yeast. After incubation (24 h, 37°C) the zones of inhibition (ZOI) were measured.

Identification of Differences Between Volatilomes

To compare the volatilomes between the nests, catching webs, and spiders, and between the sampling sites, partial least squares discriminant analysis (PLS-DA) plots and Euler plots were made. PLS-DA plots were based on all mass features (including relative intensities) and made using MetaboAnalyst (Version 4.0, Xia Lab, Montreal, Canada; Xia and Wishart, 2011). Euler plots were made based on all compounds (Supplementary Table 2) VOCs using RStudio (RStudio, Inc., Version 1.2.5033).

RESULTS

Antimicrobial VOCs in the *Stegodyphus dumicola* Volatilome

The analyses of the volatilomes of all sampling sites resulted in the tentative identification of 53 compounds ranging from C₄ up to C₂₄ (Table 1 and Supplementary Table 2). Most of the identified VOCs were pure hydrocarbons (41%) or contained oxygen (51%). Eight percent of compounds contained nitrogen, sulfur, or halogens. The VOCs belonged to various chemical classes. Most common were alkanes, carboxylic acids, alcohols, benzenes, ketones, alkenes, aldehydes, and terpenoids. One hundred forty-six compounds could not be tentatively identified by mass spectra comparison with databases and are therefore listed as unknown (Supplementary Table 2). Antimicrobial activity was assigned to 21 of the 53 tentatively identified VOCs (Table 1) based on published data for the pure compounds or mixtures such as essential oils containing the compound (references in Supplementary Table 2). Most of those compounds are known for both antibacterial and antifungal activities. By analyzing pure standard compounds, we confirmed the presence of acetophenone, 2-decanone, 1-decanal, 1,3-benzothiazole, 1-tetradecene, and docosane (Supplementary Figure 4).

Effect of Antimicrobial VOCs on Pathogens

A selection of pure compounds found exclusively in the nest volatilome (acetophenone and 2-decanone), the nest and web volatilome (1-decanal and 1,3-benzothiazole) and in the spider volatilome (1-tetradecene) were tested for their antimicrobial activities against a spectrum of microbial pathogens. All five tested compounds displayed antimicrobial activity (Figure 1). Acetophenone, 2-decanone, and 1,3-benzothiazole significantly inhibited all four tested pathogens. 1-Tetradecene and 1-decanal significantly inhibited only three pathogens, namely *B. thuringiensis*, *S. aureus*, and *C. albicans* but not *E. coli*. 1-Decanal even increased the growth of *E. coli* albeit not significantly. The spider pathogen *B. thuringiensis* was significantly inhibited by all five compounds. Additionally, we tested the antimicrobial activity of the compounds using an agar diffusion test resulting in similar inhibitions (Supplementary Figure 5).

Comparison of Nest, Web, and Spider Volatilomes

At all sampling sites, more VOCs were detected in the nest and web samples as compared to the spider samples (Figure 2 and Supplementary Figure 6). The nest and web volatilomes from the site Otavi shared many common VOCs (63 in total, Figure 2A). Only eight unknown VOCs were commonly found in the nest, web, and spider volatilomes. In Windhoek we found nearly twice the number of VOCs in the nest compared to the web and spider volatilomes (Figure 2B). Two unknown VOCs were common and detected in the nest, web, and spider volatilomes. In Stampriet, similar to Otavi, the nest and web shared a high number of VOCs (Figure 2C). Only one compound was found in the combined volatilome of nest, web, and spider and identified as oxymethylenecampher.

Comparison of Volatilomes From Different Climatic Regions

Analyzing the volatilomes of the three sampling sites using PLS-DA indicated that the nest volatilomes from the three sampling sites clearly differed from each other, with the largest differences being observed between Otavi and Windhoek (Figure 3). The confidence regions of Otavi and Stampriet showed only small overlays (Figure 3A). The web volatilomes separated in a similar way with a small overlaid area between Stampriet and Windhoek (Figure 3B). The confidence regions of the spider VOCs of Stampriet overlaid in large parts with those of Windhoek, whereas the Otavi volatilome was clearly separated from the other regions (Figure 3C).

The Euler-plots based on all identified and unknown VOCs indicated that the Otavi volatilomes show the highest number of VOCs in the nest, and web volatilomes, followed by Stampriet, and Windhoek (Figure 4 and Supplementary Figure 6). The spider volatilomes contained the highest number of VOCs in Otavi and the lowest in Stampriet. The nest volatilomes of the three sampling sites shared 12 common VOCs, and the web 11 common VOCs. The spider volatilomes did not contain common

TABLE 1 | List of identified compounds in the nest (N), web (W), and spider (S) volatilomes of the different sampling sites Otavi, Windhoek, and Stampriet with known antimicrobial activity.

Compound	Class	Molecular Formula	Antimicrobial Activity	Compound Origin	Otavi			Windhoek			Stampriet		
					N	W	S	N	W	S	N	W	S
1-Heptanal	Aldehyde	C ₇ H ₁₄ O	b, f	p						x			
2-Ethylhexanol	Alcohol	C ₈ H ₁₈ O	b, f	p, f				x	x		x	x	
Acetophenone	Ketone	C ₈ H ₈ O	b	?	x			x					
1-Non-anal	Aldehyde	C ₉ H ₁₈ O	b, f	p	x						x		
Levomenthol	Alcohol	C ₁₀ H ₂₀ O	b, f	p		x							
2-Decanone	Ketone	C ₁₀ H ₂₀ O	b, f	p, b				x			x		
Dodecane	Alkane	C ₁₂ H ₂₆	b, f	p, b							x		
1-Decanal	Aldehyde	C ₁₀ H ₂₀ O	b, f	p	x	x							
1,3-Benzothiazole	Benzothiazole	C ₇ H ₅ NS	b, f	p	x	x		x					
1-Undecanol	Alcohol	C ₁₁ H ₂₄ O	b	?								x	
1-Dodecene	Alkene	C ₁₂ H ₂₄	b	p							x		
1-Tridecene	Alkene	C ₁₃ H ₂₆	b	p, a	x	x		x	x		x		
2-Ethyl-3-hydroxyhexyl 2-methylpropanoate	Carboxylic Acid	C ₁₂ H ₂₄ O ₃	b, f	p	x								
1-Tetradecene	Alkene	C ₁₄ H ₂₈	b, f	p, f			x						
1-Dodecanal	Aldehyde	C ₁₂ H ₂₄ O	b, f	p							x		
Nerylacetone	Ketone	C ₁₃ H ₂₂ O	b	p	x	x						x	
1-Dodecanol	Alcohol	C ₁₂ H ₂₆ O	b	p		x	x	x			x		
Pentadecane	Alkane	C ₁₅ H ₃₂	b, f	a, i							x	x	
Myristic acid	Carboxylic Acid	C ₁₄ H ₂₈ O ₂	b, f	p	x						x		
Heneicosane	Alkane	C ₂₁ H ₄₄	b	p							x	x	
Docosane	Alkane	C ₂₂ H ₄₆	b, f	p							x	x	

The antimicrobial activity of the VOCs was shown against bacteria (b) and/or fungi (f). The VOCs originated from plants (p), insects (i), algae (a), bacteria (b), and/or fungi (f). Antimicrobial activities and origins are based on literature data (references in **Supplementary Table 2**). Detection of VOCs in the samples is indicated by “x”.

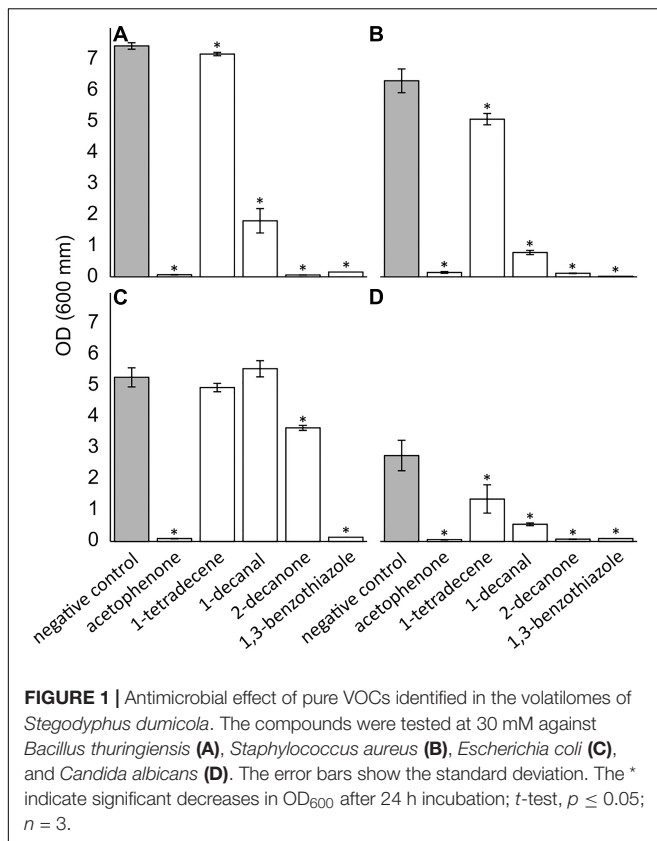
VOCs among sites. 1-Methoxy-2-propanol and 1-tridecene were detected in all nests. 2,6,11-Trimethyldodecane was detected in all web volatilomes. The other shared VOCs remain unknown.

DISCUSSION

The results of our study revealed the presence of numerous VOCs with antimicrobial function in the *S. dumicola* volatilomes. Overall, around 40% of the identified VOCs in the volatilomes of *S. dumicola* exhibit antimicrobial activity based on literature (references in **Supplementary Table 2**). In the present study, several pure VOCs, namely acetophenone, 1-tetradecene, 1-decanal, 2-decanone, and 1,3-benzothiazole, displayed antimicrobial activity against a range of spider and human pathogens. The suggested spider pathogen *B. thuringiensis* (Keiser et al., 2016) and the human pathogens *S. aureus*, *E. coli*, and *C. albicans* (Peterson, 2009; Canet et al., 2018) were significantly inhibited by most of the tested VOCs, indicating a possible protection of *S. dumicola* against bacteria (Gram-positive and -negative) and yeasts. Our results are in line with several other studies that tested the antimicrobial activity of these compounds as pure compounds or extracts with concentrations between 0.55–43.8% (Palic et al., 2002; Shi et al., 2010; Tayung et al., 2011; Li et al., 2012; Liu et al., 2012; Guleria et al., 2013;

Kazemi and Sharifi, 2017). For example, acetophenone and 2-decanone as pure compounds showed both antibacterial and -fungal activity (Rajabi et al., 2005; Sivakumar et al., 2008; Zheng et al., 2013; Jayakumar et al., 2020). The appearance of other antimicrobial VOCs was shown in other arthropod systems, for example in termites (Chen et al., 1998; Matsuura and Matsunaga, 2015), beetles (Gross et al., 2008), and ants (Wang et al., 2015). We found between 7 and 14 antimicrobial VOCs at each sampling site indicating likewise a high potential of the *S. dumicola* volatilomes in pathogen protection.

The origin of the VOCs in *S. dumicola*'s volatilome appears to be diverse—in principle, the spiders themselves, symbiotic microorganisms, prey (and their microbiota), the plants in which the nests are located, and even passing or hostile animals could influence the volatilomes (**Figure 5**). Most of the VOCs with known antimicrobial activity identified in this study were previously reported from essential oils of plants, but some also from fungi, bacteria, algae, or even insects (**Table 1**). The lowest number of VOCs was found in the volatilomes of isolated spiders, whereas relatively more VOCs were detected in the nest and web volatilomes. Furthermore, the spider volatilomes only shared a small number of VOCs with the nest and web volatilomes, whereas the nest and web shared many common VOCs. Particularly the nest may provide a source for a diverse community of microbes as plant material and exoskeletons are

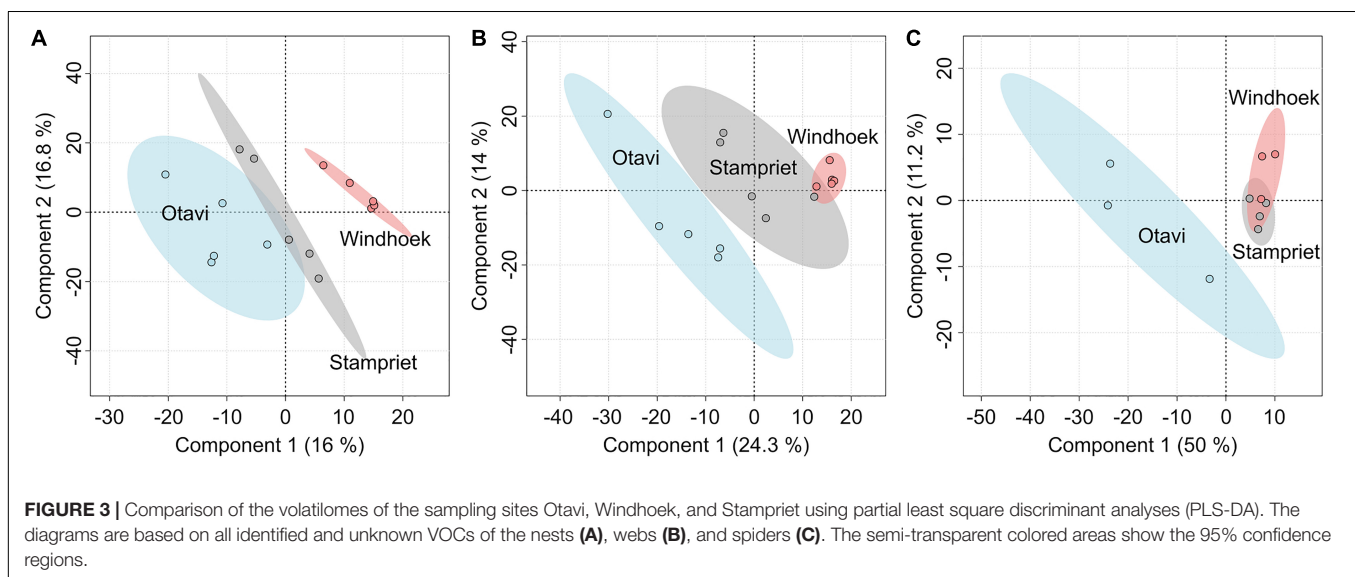
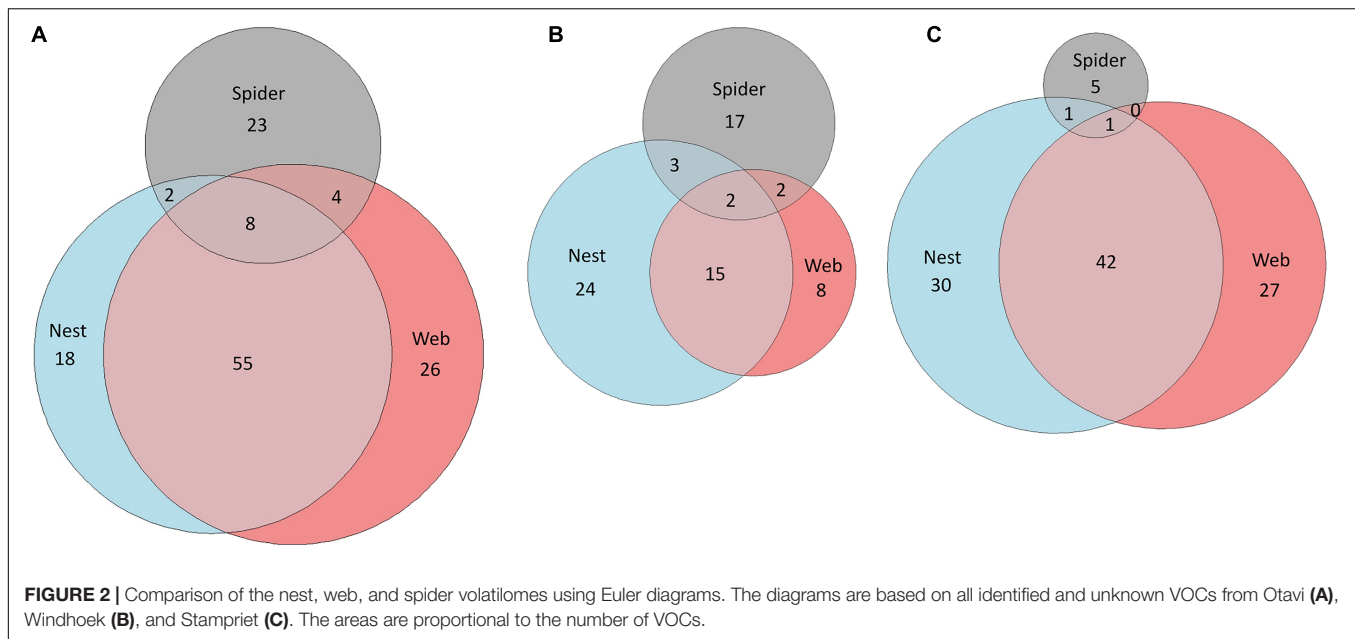


incorporated in the silk structure providing potential substrates for microbes. As the capture web is much more exposed to wind compared with the nest, we expected less VOCs in the web volatilomes than in the nest volatilomes, however, this was only the case in Windhoek.

A likely origin of VOCs is the *S. dumicola* nest microbiome. Although diverse and differing in composition and relative abundance from nest to nest, four bacterial genera (*Curtobacterium*, *Modestobacter*, *Sphingomonas*, and *Massilia*) and four fungal genera (*Aureobasidium*, *Didymella*, *Alternaria*, and *Ascochyta*) were found in all investigated *S. dumicola* nests and thus form a core nest microbiome (Nazipi et al., 2021). Currently, we cannot link specific VOCs to specific genera. However, the microbiome is the source of both soluble (Currie et al., 1999; Chouvenec et al., 2013; Mendes et al., 2013) and volatile (Musa Bandowe et al., 2009) antimicrobial compounds in other social arthropods, and some of the VOCs we identified in the spider nests are produced by microorganisms. For example, 2-decanone was found in the volatilomes of three *Bacillus* species and showed antifungal activity (Yuan et al., 2012; Zheng et al., 2013; Che et al., 2017; Jayakumar et al., 2020). Furthermore, 1-tetradecene was antimicrobial against numerous bacteria and fungi (Tayung et al., 2011). Another probable origin of the VOCs might be the arthropods themselves. A study identified pentadecane, an antimicrobial compound (Ozdemir et al., 2004; Hussain et al., 2017), in extracts of the head and gaster from argentine ants (Cavill and Houghton, 1974), and we identified

the same compound in spider nests and webs in Stampriet. Pentadecane might have originated from dead prey or even hostile ants, even when we didn't observe the latter during field work. The spiders themselves may be a source of the volatilome. For example, it was shown that the cuticular profile of *Stegodyphus lineatus* contains several linear and branched alkanes (Grinsted et al., 2011) and myristic acid plays a role in sexual signaling in *Tegenaria* spp. (Trabalon et al., 1997). Most of the antimicrobial VOCs found in the volatilomes were identified in essential oils of plants, which contain volatile and non-volatile compounds, suggesting that the plants in which the spiders build their nests may influence the nest volatilome. For example, triterpenes extracted from *Combretum imberbe* and *Acacia mellifera* showed antibacterial activity (Angeh et al., 2007; Mutai et al., 2009a). The majority of the plant species in which the spider nests were located in, are known for their antibacterial, antifungal, and/or antiviral activity, even when detailed studies on the chemical compositions are lacking (Masoko et al., 2007, 2010; Peloeuwetse et al., 2008; Mutai et al., 2009b; Arbab et al., 2015; Lamola et al., 2017; Shikwambana and Mahlo, 2020). All in all, we found several VOCs in the nest, web, and spider volatilomes. The highest diversity was found in the nest and web samples even though the spiders are likely exposed to a mixture of all VOCs present in the spider nest ecosystem. It is likely that the volatilomes are produced communally by bacteria, fungi, plants, and the spiders, respectively, even though we have only little hints to concrete origins yet (Figure 5).

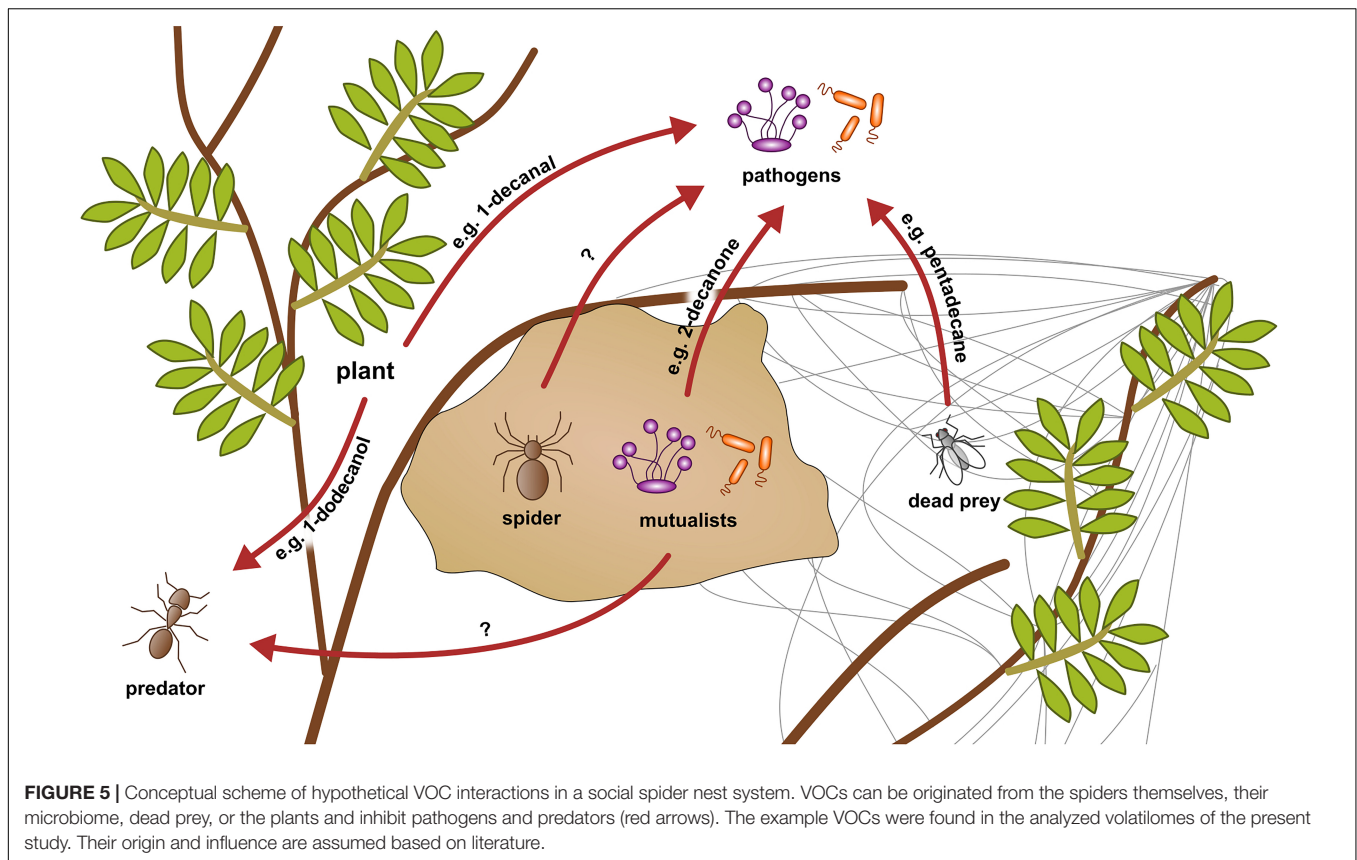
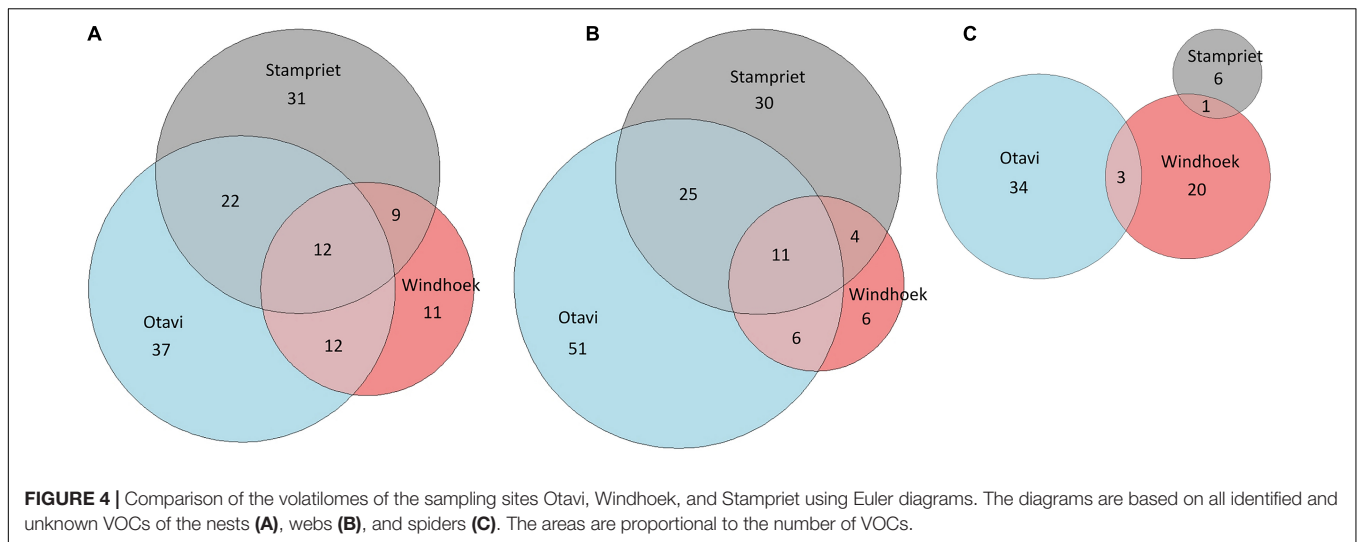
The PLS-DA analyses show clear differences between the three sampling sites for each of the analyzed volatilomes (nest, web, spider). The Euler plots support that finding, as the majority of the VOCs (approx. 94%) were only found at one or two locations. There are various potential factors influencing the volatilomes. The nest microbiomes of *S. dumicola* were shown to differ significantly between different sampling sites, even though there is a core microbiome on genus level (Nazipi et al., 2021). A study investigating the spider microbiome of *S. dumicola* (endo- and exosymbionts) showed significant differences even between spiders from different nests from the same sampling site (Busck et al., 2020). Therefore, differences of the nest and spider microbiomes between the different geographic sites might contribute to the differences between the volatilomes found in the present study. The microbiome itself can be shaped by external factors like temperature, humidity, prey, soil, and plant species (Reese and Dunn, 2018). We found clear differences in temperature, humidity, and plant species between the sampling sites, which also goes in line with the differences between the volatilomes. The quantity and quality of the prey is also likely influenced by the location and climate (Majer et al., 2013, 2018). Furthermore, the plants themselves are a potential VOC source (Hammerbacher et al., 2019) and differed clearly between the sampling sites with a much higher plant density in Otavi compared to Windhoek and Stampriet (own observation). It was also shown that the production of essential oils by plants is decreased with increasing altitude (Haider et al., 2009; El-Jalel et al., 2018) which is in line with our results. Thus, the lowest number of VOCs was found at the highest altitude (Windhoek). In contrast to the spider microbiome, it was shown



that *S. dumicola* shows little genetic differences between sampling sites (Settepani et al., 2017), which makes the spiders themselves very unlikely as an influencing factor for the differences between locations. Even though most of the VOCs were not shared between the sampling sites, some VOCs were present at all sites which suggests a site-independent “core volatilome” of *S. dumicola*. 12 VOCs were found in the nest volatilomes of all sampling sites and 11 VOCs in all web volatilomes. Two tentatively identified VOCs, namely 1-methoxy-2-propanol and 1-tridecene, were found in all nest volatilomes and 2,6,11-trimethyldodecane and 1-tridecene in all web volatilomes. None of these compounds is known from other social insect or spider systems but 1-tridecene showed antibacterial activity (Kumar et al., 2011; Satmi and Hossain, 2016) and 1-dodecanol, a

compound we found at all sampling sites in the nests or webs, is well known for its insecticidal (Tabanca et al., 2014) and antibacterial activity (Togashi et al., 2007; Vairappan et al., 2012). It is conceivable that this compound may protect *S. dumicola* against hostile insects like ants or wasps, but also against bacterial pathogens (Figure 5).

In conclusion, we found distinct differences between the sampling sites that can be explained with differences in the microbiomes, plant quality and quantity, prey quality, and physical parameters like temperature, humidity, and altitude. We lack information about the *in situ* concentrations of the VOCs, because it is technically impossible to combine minimal invasive, untargeted, and *in situ* volatilome analysis with quantitative conclusions. In soil systems it is known, that



aggregates creates micro-“incubators” influencing microbial life (Rillig et al., 2017). Similar phenomena may be possible in the spider nest ecosystem influencing the growth of certain microorganisms and the accumulation of antimicrobial VOCs. Nonetheless, we found hints for a core volatilome that may be important for the ecological success of *S. dumicola*. Overall, our study revealed that the volatilomes of *S. dumicola* contain numerous VOCs with antimicrobial potential that might

play a key role in their pathogen defense. Apart from the tentatively identified VOCs the majority of ~75% remains unknown. Therefore the *S. dumicola* system might contain more antimicrobial VOCs with the potential to protect the spiders and reveal novel classes of antimicrobial compounds. Next to antimicrobial protection VOCs can also play an important role in communication which should be addressed in further studies (Weisskopf et al., 2021).

DATA AVAILABILITY STATEMENT

The original contributions presented in the study are included in the article/**Supplementary Material**, further inquiries can be directed to the corresponding author/s.

AUTHOR CONTRIBUTIONS

AL, AS, HZ, ML, PG, and TS designed the study. AL performed the volatilome trapping, GC/Q-TOF data analysis, and the antimicrobial testing, and wrote the manuscript with support from AS, PG, and TB. TS assisted in planning and realization of the fieldwork. HZ performed the GC/Q-TOF analysis. All authors reviewed the manuscript and approved the submitted version.

FUNDING

The study was supported by the Novo Nordisk Foundation Interdisciplinary Synergy Grant number NNF16OC0021110 and the Leibniz WissenschaftsCampus (ComBioCat) Grant number

W10/2018. We would also like to thank the issued permissions to perform field work, permit no 1362/2017 was granted from the Ministry of Environment and Tourism in Windhoek, Namibia.

ACKNOWLEDGMENTS

We would like to thank Mette Marie Busck for great assistance during field work in Namibia, to Coleen Mannheimer for identifying the Namibian plants, and to John Irish for identifying plants and great support during field work in Namibia. We would also like to thank Sama Shiva for help with antimicrobial testing. This article is NIOO publication number 7244.

SUPPLEMENTARY MATERIAL

The Supplementary Material for this article can be found online at: <https://www.frontiersin.org/articles/10.3389/fmicb.2021.700693/full#supplementary-material>

REFERENCES

- Angeh, J. E., Huang, X., Sattler, I., Swan, G. E., Dahse, H., Haertl, A., et al. (2007). Antimicrobial and anti-inflammatory activity of four known and one new triterpenoid from *Combretum imberbe* (Combretaceae). *J. Ethnopharmacol.* 110, 56–60. doi: 10.1016/j.jep.2006.09.002
- Arbab, A. H., Parvez, M. K., Al-Dosari, M. S., Al-Rehaily, A. J., Al-Sohaibani, M., Zaroug, E. E., et al. (2015). Hepatoprotective and antiviral efficacy of *Acacia mellifera* leaves fractions against Hepatitis B Virus. *Biomed. Res. Int.* 2015:929131. doi: 10.1155/2015/929131
- Aviles, L. (1997). "Causes and consequences of cooperation and permanent-sociality in spiders," in *The Evolution of Social Behavior in Insects and Arachnids*, Vol. 2. eds J. C. Choe and B. J. Crespi (Cambridge: Cambridge University Press), 476–498. doi: 10.1017/CBO9780511721953.024
- Bratburd, J. R., Arango, R. A., and Horn, H. A. (2020). Defensive symbioses in social insects can inform human health and agriculture. *Front. Microbiol.* 11:76. doi: 10.3389/fmicb.2020.00076
- Busck, M. M., Settepani, V., Bechsgaard, J., Lund, M. B., Bilde, T., and Schramm, A. (2020). Microbiomes and specific symbionts of social spiders: compositional patterns in host species, populations, and nests. *Front. Microbiol.* 11:1845. doi: 10.3389/fmicb.2020.01845
- Canet, M., Erdmenger, D., and Perez, W. (2018). ESKAPE pathogens resistance from blood cultures in a social security reference hospital in Guatemala. *Int. J. Infect. Dis.* 73:130. doi: 10.1016/j.ijid.2018.04.3710
- Cavill, G., and Houghton, E. (1974). Volatile constituents of argentine ant, *Iridomyrmex humilis*. *J. Insect Physiol.* 20, 2049–2059. doi: 10.1016/0022-1910(74)90112-7
- Che, J., Liu, B., Liu, G., Chen, Q., and Lan, J. (2017). Volatile organic compounds produced by *Lysinibacillus* sp. FJAT-4748 possess antifungal activity against *Colletotrichum acutatum*. *Biocontrol Sci. Technol.* 27, 1349–1362. doi: 10.1080/09583157.2017.1397600
- Chen, J., Henderson, G., Grimm, C. C., Lloyd, S. W., and Laine, R. A. (1998). Termites fumigate their nests with naphthalene. *Nature* 392, 558–559. doi: 10.1038/33305
- Chouvenc, T., Efstathion, C. A., Elliott, M. L., and Su, N.-Y. (2013). Extended disease resistance emerging from the faecal nest of a subterranean termite. *Proc. R. Soc. B Biol. Sci.* 280:20131885. doi: 10.1098/rspb.2013.1885
- Currie, C. R., Scott, J. A., Summerbell, R. C., and Malloch, D. (1999). Fungus-growing ants use antibiotic-producing bacteria to control garden parasites. *Nature* 398, 701–704. doi: 10.1038/19519
- El-Jalel, L. F. A., Elkady, W. M., Gonaïd, M. H., and El-Gareeb, K. A. (2018). Difference in chemical composition and antimicrobial activity of *Thymus capitatus* L. essential oil at different altitudes. *Future J. Pharm. Sci.* 4, 156–160. doi: 10.1016/j.fjps.2017.12.004
- Fisher, K., West, M., Lomeli, A. M., Woodard, S. H., and Purcell, J. (2019). Are societies resilient? Challenges faced by social insects in a changing world. *Insectes Sociaux* 66, 5–13. doi: 10.1007/s00040-018-0663-2
- Graystock, P., and Hughes, W. O. H. (2011). Disease resistance in a weaver ant, *Polyrhachis dives*, and the role of antibiotic-producing glands. *Behav. Ecol. Sociobiol.* 65, 2319–2327. doi: 10.1007/s00265-011-1242-y
- Grinsted, L., Bilde, T., and d'Ettorre, P. (2011). Cuticular hydrocarbons as potential kin recognition cues in a subsocial spider. *Behav. Ecol.* 22, 1187–1194. doi: 10.1093/beheco/arr105
- Gross, J., Schumacher, K., Schmidtberg, H., and Vilcinskis, A. (2008). Protected by fumigants: beetle perfumes in antimicrobial defense. *J. Chem. Ecol.* 34, 179–188. doi: 10.1007/s10886-007-9416-9
- Guleria, S., Tikku, A. K., Koul, A., Gupta, S., Singh, G., and Razdan, V. K. (2013). Antioxidant and antimicrobial properties of the essential oil and extracts of *Zanthoxylum alatum* grown in North-Western Himalaya. *Sci. World J.* 2013:790580. doi: 10.1155/2013/790580
- Haider, F., Kumar, N., Banerjee, S., Naqvi, A. A., and Bagchi, G. D. (2009). Effect of altitude on the essential oil constituents of *Artemisia roxburghiana* Besser var. *purpurascens* (Jacq.) Hook. *J. Essent. Oil Res.* 21, 303–304. doi: 10.1080/10412905.2009.9700177
- Hammerbacher, A., Coutinho, T. A., and Gershenzon, J. (2019). Roles of plant volatiles in defence against microbial pathogens and microbial exploitation of volatiles. *Plant Cell Environ.* 42, 2827–2843. doi: 10.1111/pce.13602
- Henschel, J. R. (1998). Predation on social and solitary individuals of the spider *Stegodyphus dumicola* (Araneae: Eresidae). *J. Arachnol.* 26, 61–69.
- Hölldobler, B., and Wilson, E. (1990). *The Ants*. Cambridge: Harvard University Press.
- Hudzicki, J. (2009). Kirby-Bauer Disk Diffusion Susceptibility Test Protocol. Available online at: <http://www.asmscience.org/content/education/protocol/protocol.3189> (accessed May 16, 2018)
- Hussain, A., Tian, M.-Y., and Wen, S.-Y. (2017). Exploring the caste-specific multi-layer defense mechanism of formosan subterranean termites, *Coptotermes formosanus* Shiraki. *Int. J. Mol. Sci.* 18:2694. doi: 10.3390/ijms18122694
- Jayakumar, V., Ramesh Sundar, A., and Viswanathan, R. (2020). Biocontrol of *Colletotrichum falcatum* with volatile metabolites produced by endophytic

- bacteria and profiling VOCs by headspace SPME coupled with GC–MS. *Sugar Tech.* 23, 94–107. doi: 10.1007/s12355-020-00891-2
- Kazemi, M., and Sharifi, M. (2017). Composition, Antimicrobial and antioxidant activities of essential oil of *Stachys kermanshahensis*. *Chem. Nat. Compd.* 53, 767–769. doi: 10.1007/s10600-017-2116-y
- Keiser, C. N., Shearer, T. A., DeMarco, A. E., Brittingham, H. A., Knutson, K. A., Kuo, C., et al. (2016). Cuticular bacteria appear detrimental to social spiders in mixed but not monoculture exposure. *Curr. Zool.* 62, 377–384. doi: 10.1093/cz/zow015
- Kumar, V., Bhatnagar, A. K., and Srivastava, J. N. (2011). Antibacterial activity of crude extracts of *Spirulina platensis* and its structural elucidation of bioactive compound. *J. Med. Plants Res.* 5, 7043–7048. doi: 10.5897/JMPRI11.1175
- Lamola, S. M., Dzoyem, J. P., Botha, F., and van Wyk, C. (2017). Antibacterial, free radical scavenging activity and cytotoxicity of acetone extracts of *Grewia flava*. *Afr. Health Sci.* 17, 790–796. doi: 10.4314/ahs.v17i3.22
- Li, M., Han, G., Chen, H., Yu, J., and Zhang, Y. (2012). Chemical compounds and antimicrobial activity of volatile oils from bast and fibers of *Apocynum venetum*. *Fibers Polym.* 13, 322–328. doi: 10.1007/s12221-012-0322-6
- Liu, K., Chen, Q., Liu, Y., Zhou, X., and Wang, X. (2012). Isolation and biological activities of decanal, linalool, valencene, and octanal from sweet orange oil. *J. Food Sci.* 77, C1156–C1161. doi: 10.1111/j.1750-3841.2012.02924.x
- Lubin, Y., and Bilde, T. (2007). The evolution of sociality in spiders. *Adv. Stud. Behav.* 37, 83–145. doi: 10.1016/S0065-3454(07)37003-4
- Majer, M., Holm, C., Lubin, Y., and Bilde, T. (2018). Cooperative foraging expands dietary niche but does not offset intra-group competition for resources in social spiders. *Sci. Rep.* 8:11828. doi: 10.1038/s41598-018-30199-x
- Majer, M., Svenning, J.-C., and Bilde, T. (2013). Habitat productivity constrains the distribution of social spiders across continents – case study of the genus *Stegodyphus*. *Front. Zool.* 10:9. doi: 10.1186/1742-9994-10-9
- Masoko, P., Picard, J., and Eloff, J. N. (2007). The antifungal activity of twenty-four southern African *Combretum* species (Combretaceae). *South Afr. J. Bot.* 73, 173–183. doi: 10.1016/j.sajb.2006.09.010
- Masoko, P., Picard, J., Howard, R. L., Mampuru, L. J., and Eloff, J. N. (2010). In vivo antifungal effect of *Combretum* and *Terminalia* species extracts on cutaneous wound healing in immunosuppressed rats. *Pharm. Biol.* 48, 621–632. doi: 10.3109/13880200903229080
- Matsuura, K., and Matsunaga, T. (2015). Antifungal activity of a termite queen pheromone against egg-mimicking termite ball fungi. *Ecol. Res.* 30, 93–100. doi: 10.1007/s11284-014-1213-7
- Mendes, T. D., Borges, W. S., Rodrigues, A., Solomon, S. E., Vieira, P. C., Duarte, M. C. T., et al. (2013). Anti-Candida properties of uraichimycins from actinobacteria associated with *Trachymyrmex* ants. *Biomed. Res. Int.* 2013:835081. doi: 10.1155/2013/835081
- Montenegro, I., Said, B., Godoy, P., Besoain, X., Parra, C., Diaz, K., et al. (2020). Antifungal activity of essential oil and main components from mentha pulegium growing wild on the Chilean central coast. *Agronomy* 10:254. doi: 10.3390/agronomy10020254
- Müller, C. B., and Schmid-Hempel, P. (1993). Exploitation of cold temperature as defence against parasitoids in bumblebees. *Nature* 363, 65–67. doi: 10.1038/363065a0
- Musa Bando, B. A., Rückamp, D., Bragança, M. A. L., Laabs, V., Amelung, W., Martius, C., et al. (2009). Naphthalene production by microorganisms associated with termites: evidence from a microcosm experiment. *Soil Biol. Biochem.* 41, 630–639. doi: 10.1016/j.soilbio.2008.12.029
- Mutai, C., Bii, C., Rukunga, G., Ondicho, J., Mwitari, P., Abatis, D., et al. (2009a). Antimicrobial activity of pentacyclic triterpenes isolated from *Acacia mellifera*. *Afr. J. Tradit. Complement. Altern. Med.* 6, 42–48.
- Mutai, C., Bii, C., Vagias, C., Abatis, D., and Roussis, V. (2009b). Antimicrobial activity of *Acacia mellifera* extracts and lupane triterpenes. *J. Ethnopharmacol.* 123, 143–148. doi: 10.1016/j.jep.2009.02.007
- Nazipi, S., Lorenzen Elberg, C., Busck, M. M., Lund, M. B., Bilde, T., and Schramm, A. (2021). The bacterial and fungal nest microbiomes in populations of the social spider *Stegodyphus dumicola*. *Syst. Appl. Microbiol.* 44:126222.
- Okla, M. K., Alamri, S. A., Salem, M. Z. M., Ali, H. M., Behiry, S., Nasser, R. A., et al. (2019). Yield, phytochemical constituents, and antibacterial activity of essential oils from the leaves/twigs, branches, branch wood, and branch bark of sour orange (*Citrus aurantium* L.). *Processes* 7:363. doi: 10.3390/pr7060363
- Ossowicki, A., Jafra, S., and Garbeva, P. (2017). The antimicrobial volatile power of the rhizospheric isolate *Pseudomonas donghuensis* P482. *PLoS One* 12:e0174362. doi: 10.1371/journal.pone.0174362
- Ozdemir, G., Karabay, N. U., Dalay, M. C., and Pazarbasi, B. (2004). Antibacterial activity of volatile component and various extracts of *Spirulina platensis*. *Phytother. Res.* 18, 754–757. doi: 10.1002/ptr.1541
- Palic, R., Stojanovic, G., Alagic, S., Nikolic, M., and Lepojevic, Z. (2002). Chemical composition and antimicrobial activity of the essential oil and CO₂ extracts of the oriental tobacco, Prilep. *Flavour Fragr. J.* 17, 323–326. doi: 10.1002/ffj.1084
- Pandey, A., and Banerjee, D. (2014). *Daldinia bambusicola* Ch4/11 an endophytic fungus producing volatile organic compounds having antimicrobial and oil chemical potential. *J. Adv. Microbiol.* 6, 330–337.
- Pavithra, P. S., Sreevidya, N., and Verma, R. S. (2009). Antibacterial activity and chemical composition of essential oil of *Pamburus missionis*. *J. Ethnopharmacol.* 124, 151–153. doi: 10.1016/j.jep.2009.04.016
- Peloewetse, E., Thebe, M. M., Ngila, J. C., and Ekosse, G. E. (2008). Inhibition of growth of some phytopathogenic and mycotoxigenic fungi by aqueous extracts of *Combretum imberbe* (Wawra) wood. *Afr. J. Biotechnol.* 7, 2934–2939. doi: 10.4314/ajb.v7i16.59204
- Peterson, L. R. (2009). Bad bugs, no drugs: no ESCAPE revisited. *Clin. Infect. Dis.* 49, 992–993. doi: 10.1086/605539
- Pluskal, T., Castillo, S., Villar-Briones, A., and Orešič, M. (2010). MZmine 2: modular framework for processing, visualizing, and analyzing mass spectrometry-based molecular profile data. *BMC Bioinformatics* 11:395. doi: 10.1186/1471-2105-11-395
- Rajabi, L., Courreges, C., Montoya, J., Aguilera, R. J., and Primm, T. P. (2005). Acetophenones with selective antimycobacterial activity. *Lett. Appl. Microbiol.* 40, 212–217. doi: 10.1111/j.1472-765X.2005.01657.x
- Reese, A. T., and Dunn, R. R. (2018). Drivers of microbiome biodiversity: a review of general rules, feces, and ignorance. *mBio* 9:e01294-18. doi: 10.1128/mBio.01294-18
- Rillig, M. C., Muller, L. A., and Lehmann, A. (2017). Soil aggregates as massively concurrent evolutionary incubators. *ISME J.* 11, 1943–1948. doi: 10.1038/ismej.2017.56
- Rowan, D. D. (2011). Volatile metabolites. *Metabolites* 1, 41–63. doi: 10.3390/metabo1010041
- Roy, S., Rao, K., Bhuvaneswari, Ch, Giri, A., and Mangamoori, L. N. (2009). Phytochemical analysis of *Andrographis paniculata* extract and its antimicrobial activity. *World J. Microbiol. Biotechnol.* 26, 85–91. doi: 10.1007/s11274-009-0146-8
- Satmi, F. R. S., and Hossain, M. A. (2016). In vitro antimicrobial potential of crude extracts and chemical compositions of essential oils of leaves of *Mentha piperita* L native to the Sultanate of Oman. *Pac. Sci. Rev. Nat. Sci. Eng.* 18, 103–106. doi: 10.1016/j.psra.2016.09.005
- Schmidt, R., Cordovez, V., de Boer, W., Raaijmakers, J., and Garbeva, P. (2015a). Volatile affairs in microbial interactions. *ISME J.* 9, 2329–2335. doi: 10.1038/ismej.2015.42
- Schmidt, R., Etalo, D. W., de Jager, V., Gerards, S., Zweepers, H., de Boer, W., et al. (2015b). Microbial small talk: volatiles in fungal–bacterial interactions. *Front. Microbiol.* 6:1495. doi: 10.3389/fmicb.2015.01495
- Schulz-Bohm, K., Martin-Sanchez, I., and Garbeva, P. (2017). Microbial volatiles: small molecules with an important role in intra- and inter-kingdom interactions. *Front. Microbiol.* 8:2484. doi: 10.3389/fmicb.2017.02484
- Seibt, U., and Wickler, W. (1990). The protective function of the compact silk nest of social *Stegodyphus* spiders (Araneae, Eresidae). *Oecologia* 82, 317–321. doi: 10.1007/BF00317477
- Settepani, V., Bechsgaard, J., and Bilde, T. (2014). Low genetic diversity and strong but shallow population differentiation suggests genetic homogenization by metapopulation dynamics in a social spider. *J. Evol. Biol.* 27, 2850–2855. doi: 10.1111/jeb.12520
- Settepani, V., Bechsgaard, J., and Bilde, T. (2016). Phylogenetic analysis suggests that sociality is associated with reduced effectiveness of selection. *Ecol. Evol.* 6, 469–477. doi: 10.1002/ece3.1886
- Settepani, V., Schou, M. F., Greve, M., Grinsted, L., Bechsgaard, J., and Bilde, T. (2017). Evolution of sociality in spiders leads to depleted genomic diversity at both population and species levels. *Mol. Ecol.* 26, 4197–4210.

- Shi, B., Liu, W., Wei, S., and Wu, W. (2010). Chemical composition, antibacterial and antioxidant activity of the essential oil of *Bupleurum longiradiatum*. *Nat. Prod. Commun.* 5, 1139–1142. doi: 10.1177/1934578X1000500734
- Shikwambana, N., and Mahlo, S. M. (2020). A survey of antifungal activity of selected south African plant species used for the treatment of skin infections. *Nat. Prod. Commun.* 15, 1–10. doi: 10.1177/1934578X20923181
- Sinek, K., Iskender, N. Y., Yayli, B., Karaoglu, S. A., and Yayli, N. (2012). Antimicrobial activity and chemical composition of the essential oil from *Campanula glomerata* L. Subsp. *Hispida* (Witasek) Hayek. *Asian J. Chem.* 24, 1931–1934.
- Sivakumar, P. M., Sheshayan, G., and Doble, M. (2008). Experimental and QSAR of acetophenones as antibacterial agents. *Chem. Biol. Drug Des.* 72, 303–313.
- Tabanca, N., Gao, Z., Demirci, B., Techen, N., Wedge, D. E., Ali, A., et al. (2014). Molecular and phytochemical investigation of *Angelica dahurica* and *Angelica pubescens* essential oils and their biological activity against *Aedes aegypti*, *Stephanitis pyrioides*, and *Colletotrichum* species. *J. Agric. Food Chem.* 62, 8848–8857. doi: 10.1021/jf5024752
- Tariq, S., Wani, S., Rasool, W., Shafi, K., Bhat, M. A., Prabhakar, A., et al. (2019). A comprehensive review of the antibacterial, antifungal and antiviral potential of essential oils and their chemical constituents against drug-resistant microbial pathogens. *Microb. Pathog.* 134:103580. doi: 10.1016/j.micpath.2019.103580
- Tayung, K., Barik, B., Jha, D., and Deka, D. (2011). Identification and characterization of antimicrobial metabolite from an endophytic fungus, *Fusarium solani* isolated from bark of Himalayan yew. *Mycosphere* 2, 203–213.
- Togashi, N., Shiraishi, A., Nishizaka, M., Matsuoka, K., Endo, K., Hamashima, H., et al. (2007). Antibacterial activity of long-chain fatty alcohols against *Staphylococcus aureus*. *Molecules* 12, 139–148. doi: 10.3390/12020139
- Trabalon, M., Bagnères, A. G., and Roland, C. (1997). Contact sex signals in two sympatric spider species, *Tegenaria domestica* and *Tegenaria pagana*. *J. Chem. Ecol.* 23, 747–758. doi: 10.1023/B:JOEC.0000006408.60663.db
- Tyc, O., Zweers, H., de Boer, W., and Garbeva, P. (2015). Volatiles in inter-specific bacterial interactions. *Front. Microbiol.* 6:1412. doi: 10.3389/fmicb.2015.01412
- Vairappan, C. S., Nagappan, T., and Palaniveloo, K. (2012). Essential oil composition, cytotoxic and antibacterial activities of five *Etlingera* species from Borneo. *Nat. Prod. Commun.* 7, 239–249. doi: 10.1177/1934578X1200700233
- Wang, L., Elliott, B., Jin, X., Zeng, L., and Chen, J. (2015). Antimicrobial properties of nest volatiles in red imported fire ants, *Solenopsis invicta* (hymenoptera: formicidae). *Sci. Nat.* 102:66. doi: 10.1007/s00114-015-1316-1
- Weisskopf, L., Schulz, S., and Garbeva, P. (2021). Microbial volatile organic compounds in intra-kingdom and inter-kingdom interactions. *Nat. Rev. Microbiol.* 19, 391–404. doi: 10.1038/s41579-020-00508-1
- Wilson, E. O. (1987). Causes of ecological success: the case of the ants. *J. Anim. Ecol.* 56, 1–9. doi: 10.2307/4795
- Wood, W. F., and Szwczak, J. M. (2007). Volatile antimicrobial compounds in the pelage of the Mexican free-tailed bat, *Tadarida brasiliensis mexicana*. *Biochem. Syst. Ecol.* 35, 566–568. doi: 10.1016/j.bse.2007.04.002
- Xia, J., and Wishart, D. S. (2011). Web-based inference of biological patterns, functions and pathways from metabolomic data using MetaboAnalyst. *Nat. Protoc.* 6, 743–760. doi: 10.1038/nprot.2011.319
- Yuan, J., Raza, W., Shen, Q., and Huang, Q. (2012). Antifungal activity of *Bacillus amyloliquefaciens* NJN-6 volatile compounds against *Fusarium oxysporum* f. sp. *cubense*. *Appl. Environ. Microbiol.* 78, 5942–5944. doi: 10.1128/AEM.01357-12
- Zellagui, A., Gherraf, N., and Rhouati, S. (2012). Chemical composition and antibacterial activity of the essential oils of *Ferula vesceritensis* Coss et Dur. leaves, endemic in Algeria. *Org. Med. Chem. Lett.* 2:31. doi: 10.1186/2191-2858-2-31
- Zheng, M., Shi, J., Shi, J., Wang, Q., and Li, Y. (2013). Antimicrobial effects of volatiles produced by two antagonistic *Bacillus* strains on the anthracnose pathogen in postharvest mangos. *Biol. Control* 65, 200–206. doi: 10.1016/j.biocontrol.2013.02.004
- Zhu, Q., Jiang, M.-L., Shao, F., Ma, G.-Q., Shi, Q., and Liu, R.-H. (2020). Chemical composition and antimicrobial activity of the essential oil from *Euphorbia helioscopia* L. *Nat. Prod. Commun.* 15, 1–6. doi: 10.1177/1934578X20953249

Conflict of Interest: The authors declare that the research was conducted in the absence of any commercial or financial relationships that could be construed as a potential conflict of interest.

Publisher's Note: All claims expressed in this article are solely those of the authors and do not necessarily represent those of their affiliated organizations, or those of the publisher, the editors and the reviewers. Any product that may be evaluated in this article, or claim that may be made by its manufacturer, is not guaranteed or endorsed by the publisher.

Copyright © 2021 Lammers, Zweers, Sandfeld, Bilde, Garbeva, Schramm and Lalk. This is an open-access article distributed under the terms of the Creative Commons Attribution License (CC BY). The use, distribution or reproduction in other forums is permitted, provided the original author(s) and the copyright owner(s) are credited and that the original publication in this journal is cited, in accordance with accepted academic practice. No use, distribution or reproduction is permitted which does not comply with these terms.



A Bacterial Quorum Sensing Molecule Elicits a General Stress Response in *Saccharomyces cerevisiae*

Antonia Delago^{1,2†}, Rachel Gregor^{1,2†}, Luba Dubinsky^{1,2}, Rambabu Dandela^{1,2†}, Adi Hendler^{2,3}, Pnina Krief^{1,2}, Josep Rayo^{1,2}, Amir Aharoni^{2,3} and Michael M. Meijler^{1,2*}

¹ Department of Chemistry, Ben-Gurion University of the Negev, Be'er Sheva, Israel, ² The National Institute for Biotechnology in the Negev, Ben-Gurion University of the Negev, Be'er Sheva, Israel, ³ Department of Life Sciences, Ben-Gurion University of the Negev, Be'er Sheva, Israel

OPEN ACCESS

Edited by:

Elisa Korenblum,
Institute of Plant Sciences, Israel

Reviewed by:

Uelinton Manoel Pinto,
University of São Paulo, Brazil
Randy Ortiz-Castro,
National Council of Science
and Technology (CONACYT), Mexico

*Correspondence:

Michael M. Meijler
meijler@bgu.ac.il

[†] These authors have contributed
equally to this work

*Present address:

Rambabu Dandela,
Department of Industrial and
Engineering Chemistry, Institute of
Chemical Technology, Mumbai Indian
Oil Odisha Campus, Bhubaneswar,
India

Specialty section:

This article was submitted to
Terrestrial Microbiology,
a section of the journal
Frontiers in Microbiology

Received: 23 November 2020

Accepted: 30 June 2021

Published: 16 September 2021

Citation:

Delago A, Gregor R, Dubinsky L,
Dandela R, Hendler A, Krief P, Rayo J,
Aharoni A and Meijler MM (2021) A
Bacterial Quorum Sensing Molecule
Elicits a General Stress Response
in *Saccharomyces cerevisiae*.
Front. Microbiol. 12:632658.
doi: 10.3389/fmicb.2021.632658

Bacteria assess their population density through a chemical communication mechanism termed quorum sensing, in order to coordinate group behavior. Most research on quorum sensing has focused primarily on its role as an intraspecies chemical signaling mechanism that enables the regulation of certain phenotypes through targeted gene expression. However, in recent years several seminal studies have revealed important phenomena in which quorum sensing molecules appear to serve additional roles as interspecies signals that may regulate microbial ecology. In this study, we asked whether the budding yeast *Saccharomyces cerevisiae* can sense chemical signals from prokaryotes. When exposed to a variety of quorum sensing molecules from different bacterial species and from *Candida albicans* we found that *N*-(3-oxododecanoyl)-L-homoserine lactone (C12) from the opportunistic human pathogen *Pseudomonas aeruginosa* induces a remarkable stress response in yeast. Microarray experiments confirmed and aided in interpreting these findings, showing a unique and specific expression pattern that differed significantly from the response to previously described stress factors. We further characterized this response and report preliminary findings on the molecular basis for the recognition of C12 by the yeast.

Keywords: quorum sensing, interkingdom communication, *Saccharomyces cerevisiae*, *Pseudomonas aeruginosa*, stress response, Msn 2/4, *N*-acyl homoserine lactones

INTRODUCTION

Quorum sensing (QS) is a cell-density-dependent communication mechanism used by unicellular organisms to coordinate population-wide gene expression that is of benefit to the group as a whole. It is based on the release and detection of small diffusible signal molecules called autoinducers (AIs). AIs are secreted by individual cells at a given rate during the growth of a population. When the group reaches a threshold cell density and AI concentration, a cascade of gene expression and protein transcription is set in motion, resulting in increased signal and receptor expression that enables a feedback loop to control cell-density-dependent phenotypes and processes (Popat et al., 2015). For example, the sophisticated QS system of *Pseudomonas aeruginosa* has been studied extensively due to the frequent nosocomial infections that this opportunistic pathogen causes,

especially in patients who are immunocompromised or suffer from cystic fibrosis. *P. aeruginosa* has several QS systems which are organized in a hierarchical manner (Lee and Zhang, 2015). On top of this hierarchy is the LasI/LasR system with its AI *N*-(3-oxododecanoyl)-L-homoserine lactone (C12). This system co-regulates the RhlI/RhlR system with its AI *N*-butyryl-homoserine lactone (C4). The third main *P. aeruginosa* QS system is based on the *Pseudomonas* quinolone signal (PQS), a multifaceted QSM (Cugini et al., 2007, 2010) responsible for the expression of several virulence factors (Haussler and Becker, 2008; Maura et al., 2016). The PQS system is intricately connected with the LasI/LasR and the RhlI/RhlR systems and plays an important role in linking these two systems together (Rampioni et al., 2016).

QS exists among eukaryotes as well: It has been demonstrated that the budding yeast *Saccharomyces cerevisiae* uses small aromatic alcohols, such as tryptophol and phenylethanol, to control the formation of pseudohyphae, a trait associated with multicellular processes such as biofilm formation (Reynolds and Fink, 2001). The pathogenic yeast *Candida albicans* utilizes a small acyclic sesquiterpene alcohol, farnesol, as a QSM (Hornby et al., 2001; Lindsay et al., 2012). While *C. albicans* has been shown to also produce tryptophol and phenylethanol (Lingappa et al., 1969; Hazen and Cutler, 1979; Chen and Fink, 2006; Hogan, 2006), these compounds do not promote the *C. albicans* yeast-to-hyphae transition, but rather have been shown to repress hyphal development (Chen and Fink, 2006).

In the past decades QS has mostly been studied as a phenomenon that benefits a particular species in question. However, in recent years it is becoming increasingly evident that other species are able to sense and respond to the secreted signals as well, and that such signals may govern microbial ecology in a given environment (Kravchenko et al., 2008; Jarosz et al., 2011; Teplitski et al., 2011). One such interaction is that between *P. aeruginosa* and *C. albicans*. For example, the *P. aeruginosa* QSM C12 has been shown to inhibit *C. albicans* filamentation (Hogan et al., 2004) via the Ras-cyclic AMP-dependent protein kinase A (cAMP/PKA) pathway, mimicking the effect of *Candida*'s native QSM farnesol (Davis-Hanna et al., 2008; Hall et al., 2011). In *P. aeruginosa*, the *C. albicans* QSM farnesol, in return, inhibits synthesis of the *Pseudomonas* quinolone signal (PQS) (Cugini et al., 2007). *C. albicans* and *P. aeruginosa* are both opportunistic human pathogens able to take advantage of weaknesses in the human immune system, and they coexist in infections such as in the lungs of cystic fibrosis patients (Gibson et al., 2009). In general, recent studies have shown that chemical signaling between bacteria and eukaryotes is a crucial factor in determining the formation of intricate relationships between species in a given environment. Prime examples are the recently revealed interactions between *P. aeruginosa* and *Aspergillus fumigatus* (Moree et al., 2012) and the remarkable effects induced by *Algoriphagus machipongonensis* and *Vibrio fischeri* on the multicellular development and mating behavior of the choanoflagellate *Salpingoeca rosetta*, the closest living relative of animals (Alegado et al., 2012; Woznica et al., 2017).

In this study, we set out to examine potential interactions between *S. cerevisiae* and *P. aeruginosa*, both ubiquitous microbes

that have been isolated from a wide range of plant and soil niches across the globe (Green et al., 1974; Fay and Benavides, 2005). In general, little has been published on interactions between *P. aeruginosa* and fungal species other than *C. albicans*. The molecular basis of such interactions may be similar to what is known regarding *P. aeruginosa* and *C. albicans* or proceed by other mechanisms entirely. We chose to begin with *S. cerevisiae* as it is a well-studied model organism that offers an abundance of genetic tools to study interactions between bacterial and fungal cells.

One field of research for which *S. cerevisiae* is an important model system is the study of cellular stress response. Yeast cells have evolved to survive sudden, often drastic and stressful changes in their environment and a variety of such stressful conditions have already been thoroughly experimentally characterized, including growth temperature, osmotic concentration and ionic strength of the growth medium, exposure to toxins, starvation for a variety of nutrients, irradiation, and desiccation (Attfield et al., 1997). In response to a sudden shift in conditions, yeast cells initiate a multifaceted response that involves an often-transient arrest of normal cellular processes. Cellular response mechanisms include environmental sensing and signal transduction pathways that lead to significant alterations in gene expression programs. Such induction or repression of gene expression under stress conditions enables fast adaptation to diverse conditions, resulting in increased cell fitness and survival (Gasch et al., 2000). To the best of our knowledge, no report has been published on a potential stress response in yeast to QSMs from bacteria or fungi.

In the present study we show that *S. cerevisiae*, like *C. albicans*, responds to the presence of *P. aeruginosa*. We demonstrate a general stress response of *S. cerevisiae* that is specific to the *Pseudomonas* AI C12. We further present data that provide important clues on the role of this signaling molecule for interkingdom communication that could govern the ecology of these microbes in a given environment.

MATERIALS AND METHODS

Strains and Cultivation Conditions

S. cerevisiae strains were grown at 30°C for 48 h on agar plates containing standard YPD or Selective Complete medium (SC, -His). Plated colonies were stored at 4°C. Yeast strains used in this study were: W303 WT, W303 Hsp12-GFP, W303 $\Delta msn2$ Hsp12-GFP, W303 $\Delta msn4$ Hsp12-GFP, W303 $\Delta msn2\Delta msn4$ Hsp12-GFP; MatA WT; BY4741 his3 Δ 1:KanMX. *Pseudomonas aeruginosa* wild-type strain PAO1-UW was grown at 37°C for 18–24 h on LB agar. Overnight liquid cultures were prepared in LB medium without antibiotics; overnight cultures of PAO-JP2 ($\Delta lasI\Delta rhlI$) were prepared in LB medium containing 300 μ g/mL trimethoprim (TMP).

Compounds

A panel of quorum sensing compounds were purchased from Sigma-Aldrich, Acros or synthesized as previously reported: *N*-(3-oxododecanoyl)-L-homoserine lactone (C12)

(Kravchenko et al., 2008), *N*-butyryl-homoserine lactone (C4), *N*-octanoyl-L-homoserine lactone (C8), 4,5-dihydroxy-2,3-pentanedione (DPD) (Mandabi et al., 2015), and farnesol. Control compounds were the unnatural *R* enantiomer of C12, *N*-(3-oxododecanoyl)-D-homoserine lactone (*R*-C12), and the lactam analog of C12 (S)-3-oxo-N-(2-oxopyrrolidin-3-yl)dodecanamide (C12-lactam) (Kravchenko et al., 2006). For receptor labeling experiments, an alkyne-appended diazirine analog of C12 (P6) was synthesized as previously reported by us (Dubinsky et al., 2009).

FACS Analysis of Hsp12-GFP Expression

The above panel of QS molecules was incubated with *S. cerevisiae* cultures labeled with Hsp-12 GFP reporters in order to screen for the induction of a stress response. In brief, *S. cerevisiae* overnight cultures were diluted to OD₆₀₀ ~0.1 and grown at 30°C until reaching the exponential growth phase (OD₆₀₀ ~0.4–0.6). For FACS measurement 500 µL of yeast culture were transferred into 1.5 mL centrifuge tubes and compounds were added at the indicated concentrations. Cells were briefly vortexed and then incubated at room temperature for 40–45 min. Samples were analyzed by flow cytometry (FACS Calibur, BD Biosciences, Franklin Lakes, NJ), and the Hsp12-GFP fluorescence intensity of 10,000 yeast cells was measured. For heat shock controls 500 µL of cell culture was transferred into 1.5 mL centrifuge tubes and incubated at 37°C for 40–45 min. Data acquired from FACS measurements were imported into FlowJo Single Cell Analysis System (FlowJo, LLC, OR, United States), which allowed direct calculation of median, mean and standard error. From FlowJo data were directly exported to Excel for graphical presentation.

Microarray Analysis of Gene Expression

Samples were analyzed by microarray in order to determine the effects of C12 on the yeast transcriptome. First, 1.5 mL of yeast culture *S. cerevisiae* W303 Hsp12-GFP (OD₆₀₀ ~0.4–0.6) was transferred into centrifuge tubes and test compound solutions were added. Treatments used were DMSO (control), 100 µM C12, 100 µM C12-lactam, and 300 µM H₂O₂. Cells were briefly vortexed and incubated at 30°C for 30–35 min, after which 1,000 µL were transferred into fresh tubes and cells were pelleted by centrifugation. The supernatant was discarded and the pellet immediately snap-frozen in liquid nitrogen. The remaining 500 µL were analyzed by FACS for Hsp-12-GFP expression levels in order to validate stress response before performing the microarray experiment. Total RNA was extracted from the frozen pellets using a QuickExtractTM RNA extraction kit (Epicenter, Madison, WI). Extracted total yeast RNA was then checked for integrity using an Affimetrix Bioanalyzer. The microarray experiments were performed using GeneChip Yeast 2.0 Array (Affimetrix, Santa Clara, CA). Sample preparation (50 ng/µL total RNA) was performed according to the protocol provided with the chips.

Microarray Data Analysis

The microarray results were filtered based on threshold intensity, in which probe sets without at least one sample with an intensity value greater or equal to 5 (log2 scale) were discarded,

resulting in a total of 4,612 probe sets. A one-way ANOVA for the treatment effect was applied, with the following groups compared: C12 vs. C12-lactam; H₂O₂ vs. C12-lactam; DMSO (solvent control) vs. C12-lactam; and C12 vs. H₂O₂, with a cutoff of FDR < 0.05 and F_C > 1.3 or < -1.3. The data was visualized by principal coordinates analysis (PCA) and by hierarchical clustering using Pearson dissimilarity, and one of the replicates for the C12 treatments was excluded as an outlier and removed from analysis (Supplementary Figure 1). After data analysis, resulting gene lists were uploaded onto YeastCyc BIOCHEMICAL PATHWAYS¹ and FunSpec² online analysis tools to extract biochemical pathways that are affected by the different stressors.

Co-culture Experiments Between *S. cerevisiae* and *P. aeruginosa*

For liquid co-culture experiments, yeast and *Pseudomonas* overnight starters were diluted to OD₆₀₀ ~ 0.01. Diluted yeast and bacterial cultures were then mixed 1:1 and incubated at 30°C for 10–96 h. Yeast culture diluted 1:1 with LB medium served as control. At various time points (7, 24, and 48 h) co-cultures and controls were diluted in sterile DDW and plated on selective YPD agar containing 150 µg/mL tetracycline (Tet)—allowing the yeast to grow but inhibiting the growth of the bacteria.

Viability Assays

A single colony of *S. cerevisiae* strain BY4741 was inoculated in liquid YPD medium and grown with agitation for 4 h at 30°C. Then, aliquots were incubated with 50 µM C12 or DMSO control for 30 min., followed by 10 min. of extreme oxidative stress with 0.1% H₂O₂. Then, samples were diluted 1:100 and 60 µL each were plated onto YPD agar. After 96 h at 30°C, the number of colony forming units (cfu) on each plate was counted and analyzed.

Receptor Labeling Using Diazirine Alkyne C12 Analog (P6)

Overnight cultures in YPD liquid medium were diluted into YPD to an OD₆₀₀ ~0.1 and incubated at 30°C until they reached OD₆₀₀ ~0.4–0.6. The yeast culture was then divided into aliquots in 50 mL Falcon tubes wrapped in aluminum foil for light protection. To each yeast culture we added test compounds (100 µM probe or 50 µM probe with 100 µM C12) or control solutions (10 µM lysozyme-alkyne; DMSO (0.5%); 100 µM C12). The tubes were vortexed briefly and then incubated for 30–35 min at RT. Following incubation each treatment group was transferred into a separate petri dish and irradiated at 365 nm for 10 min using a UV table. Immediately after, the yeast cultures were pelleted by centrifugation for 2 min at 4,000 rpm at 4°C, the supernatant decanted, and the pellet snap-frozen in liquid nitrogen. Then, 4 µL protein inhibitor (Sigma) and 400 µL CellLyticTM Y Cell Lysis Reagent (Sigma-Aldrich Israel Ltd., Rehovot, Israel) were added and cells were lysed by rigorous

¹<http://pathway.yeastgenome.org/overviewsWeb/celOv.shtml>

²<http://funspec.med.utoronto.ca/>

mixing for 30 min. The lysates were then centrifuged for 25 min at 4,000 rpm at 4°C, and the supernatant was transferred into fresh 1.5 mL centrifuge tubes and kept at 4°C or stored at -20°C until further processing by CuAAC chemistry to rhodamine azide for in-gel visualization.

CuAAC Chemistry Using Rhodamine Azide (RhN₃)

The protein concentration of each sample was measured using a BCA protein assay (Pierce®BCA Protein Assay Kit; THERMO Scientific, Rockford, IL). According to the sample with the lowest protein concentration samples were diluted in PBS. Click chemistry was done with a total volume of 100 µL. To 89 µL sample we added 50 µM RhN₃ (from a 50 mM stock in DMSO), 1 mM tris (2-carboxyethyl)phosphine (TCEP; from a 50 mM solution prepared fresh every time in DDW), 100 µM Tris[(1-benzyl-1H-1,2,3-triazol-4-yl)methyl]amine (TBTA, from a 1.7 mM stock in 1:5 DMSO:t-butanol). Samples were briefly mixed before adding 1 mM CuSO₄ (from a 50 mM stock in DDW). After a final brief mix, samples were incubated overnight at room temperature under constant agitation.

For visualization, samples were then prepared for SDS polyacrylamide gel electrophoretic separation. To each sample we added gel loading buffer and reducing agent. The samples were heated to 70°C for 10 min before loading them onto a NuPAGE® Bis-Tris 12% Precast Gel (Invitrogen Corp., Grand Island, NY). For molecular weight determination a Precision Plus Protein Prestained Dual color Standard (Bio-Rad Laboratories Inc.) was run in parallel to our samples. After electrophoresis, performed under light protection, RhN₃ labeled proteins were visualized with a Fujifilm LAS-3000 Imager.

Initial Chemical Proteomics Experiments

To affinity purify and characterize proteins that covalently bound the C12 probe, we incubated samples as described for the in-gel fluorescence experiments. However, click chemistry was performed using an Azide-PEG3-Biotin Conjugate (Jena Bioscience GmbH, Jena, Germany). The total volume used for the click reaction was 1 mL. To 870 µL sample we added 150 µM Biotin-N₃ (from a 5 mM stock in DDW), 1 mM TCEP, and 100 µM TBTA. Samples were briefly mixed before adding 1 mM CuSO₄. After a final brief vortex, samples were incubated ON at RT under constant agitation. For affinity purification for each sample 200 µL of streptavidin agarose resin (Invitrogen Corp., Grand Island, NY) were transferred into 0.8 mL centrifuge columns (Pierce Biotechnology, Rockford, IL) which were placed into 1.5 mL centrifuge tubes. The resin was washed 5 times with PBS before it was transferred into the click solution. Click solution and beads were incubated for 90–120 min at RT under constant gentle end-over-end rotation. After incubation samples were transferred back into the centrifuge columns and gently spun down. The run through was collected and the agarose beads washed 4 times with 350 µL PBS each—collecting each run through in a separate tube. Then the beads were incubated with 350 µL 0.1% SDS in PBS for 10 min at RT under constant gentle rotation. Thereafter the beads were washed three times

with 350 µL PBS each, followed by three washes with 350 µL DDW each. For Orbitrap analysis, samples were eluted by adding 300 µL 8 M Guanidine HCl, heating them for 10 min at 60°C, then washing them once with 300 µL PBS, before adding another 300 µL 8 M Guanidine HCl and heating them to 90°C for 10 min. All eluted samples were transferred into separate 500 µL Amicon Ultra Centrifugal Filters (10 kDa cut-off; Milipore Corp., Billerica, MA) to concentrate them ~50 times (to about 30–40 µL). Concentrated elutes were collected in low protein binding centrifuge tubes and stored at -20°C. Controls were performed in which either no probe or lysozyme modified with alkyne groups was added to cell lysates before the click reaction and affinity purification. All samples were analyzed (LC-MS/MS—Thermo-Finnigan Orbitrap) by the Smoler Proteomics Center [Israeli Institute of Technology (Technion), Haifa, Israel].

RESULTS

3-Oxo-C12-Homoserine Lactone (C12) Induces a Specific Stress Response in Yeast

S. cerevisiae cells were treated with a diverse panel of QSMs from different bacteria in order to measure the yeast stress response (Figure 1A). The stress response was quantified by the expression of the small heat shock protein Hsp12, labeled with green fluorescent protein (GFP), a system used previously to examine expression and the role of Msn2/4 transcription factors (TF) involved in the general yeast stress response (Sadeh et al., 2011, 2012). Only cells exposed to the *Pseudomonas* QSM C12 showed a significant stress response (Figure 1A, black bars). Other QSMs tested, including C4 HSL (*P. aeruginosa* RhII/RhlR system), *N*-octanoyl-L-homoserine lactone (3-oxo-C8 HSL; *Agrobacterium tumefaciens* TraI/TraR system), 4,5-dihydroxy-2,3-pentanedione (DPD), and the *C. albicans* QSM farnesol did not induce a stress response above control levels (Figure 1A, black bars). Decanoic acid was included as a lipophilic control, and also did not induce a stress response above control levels (Figure 1A, black bars). After initially testing a range of concentrations, we found that the 50–100 µM range elicited the most reproducible Hsp12 signal, and showed no inhibitory effects on growth. While these concentrations are substantially higher than the nanomolar concentrations that activate the cognate receptor in *P. aeruginosa* (Pearson et al., 1994) and other bacteria (Pinto and Winans, 2009; de Almeida et al., 2018), they are comparable to those used in previous interkingdom studies (Chhabra et al., 2003; Kravchenko et al., 2008; Karlsson et al., 2012; Maurer et al., 2015; Rayo et al., 2021). Future studies on the mechanism of this stress response are needed to determine a more precise active concentration range.

To confirm that the increase in Hsp12-GFP expression is an Msn2/4 mediated stress response, we repeated the screen on strains deleted in either one or both of the Hsp12 transcription factors. The stress response was reduced in the Msn4 mutant (Figure 1A, dark gray bars) and completely abolished in the

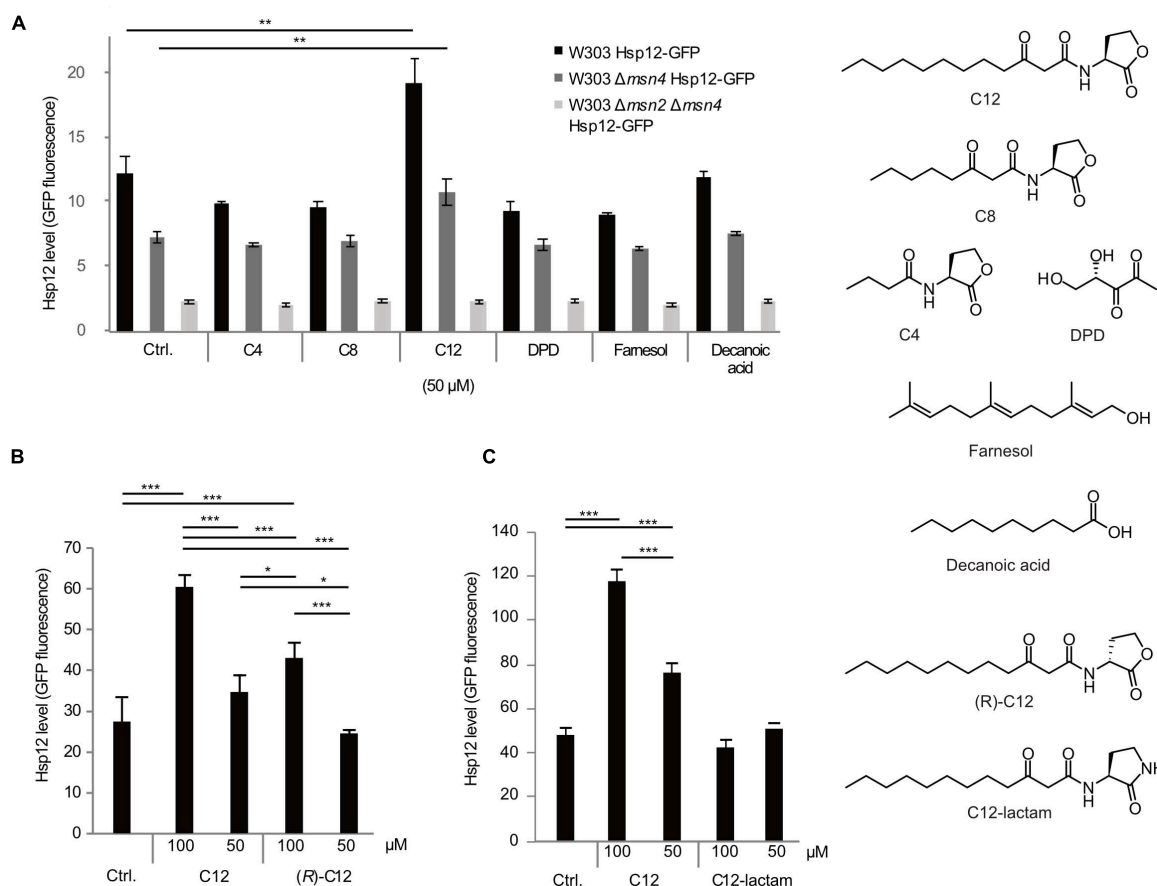


FIGURE 1 | Selective response of *S. cerevisiae* cells to different QSMs. Yeast cells (W303 WT, black bars, $\Delta msn4$ mutant, dark gray bars, and $\Delta msn2 \Delta msn4$ double mutant, light gray bars) were exposed to different QSMs for 45 min and the stress response measured by expression levels of GFP-labeled small heat shock protein Hsp12. **(A)** Initial screening for stress response to different QSMs and controls, tested at 50 μ M concentration: C12: 3-oxo-C12 HSL; C8: 3-oxo-C8 HSL; C4: C4 HSL; DPD: 4,5-dihydroxy-2,3 pentanedione; farnesol; decanoic acid. Ctrl. = solvent control (DMSO). C12 induced a significantly higher stress response than the control. Results are presented as the median of 10,000 cells for duplicate samples (\pm standard deviation) and are representative of other experiments. **(B)** Additional experiments were performed to determine the specificity of the response to C12. The stress response to C12 showed a concentration-dependent effect. The unnatural enantiomer of C12 induced a lower stress response than C12. **(C)** An additional control compound, C12-lactam, did not induce a significant stress response. For all panels, results are presented as the median of 10,000 cells for triplicate samples (\pm standard deviation) and are representative of other experiments. Significance of the variance between groups was calculated using a one-way ANOVA test, followed by pairwise comparisons using Tukey multiple comparison of means. Key: * $p \leq 0.05$, ** $p \leq 0.01$, *** $p \leq 0.001$.

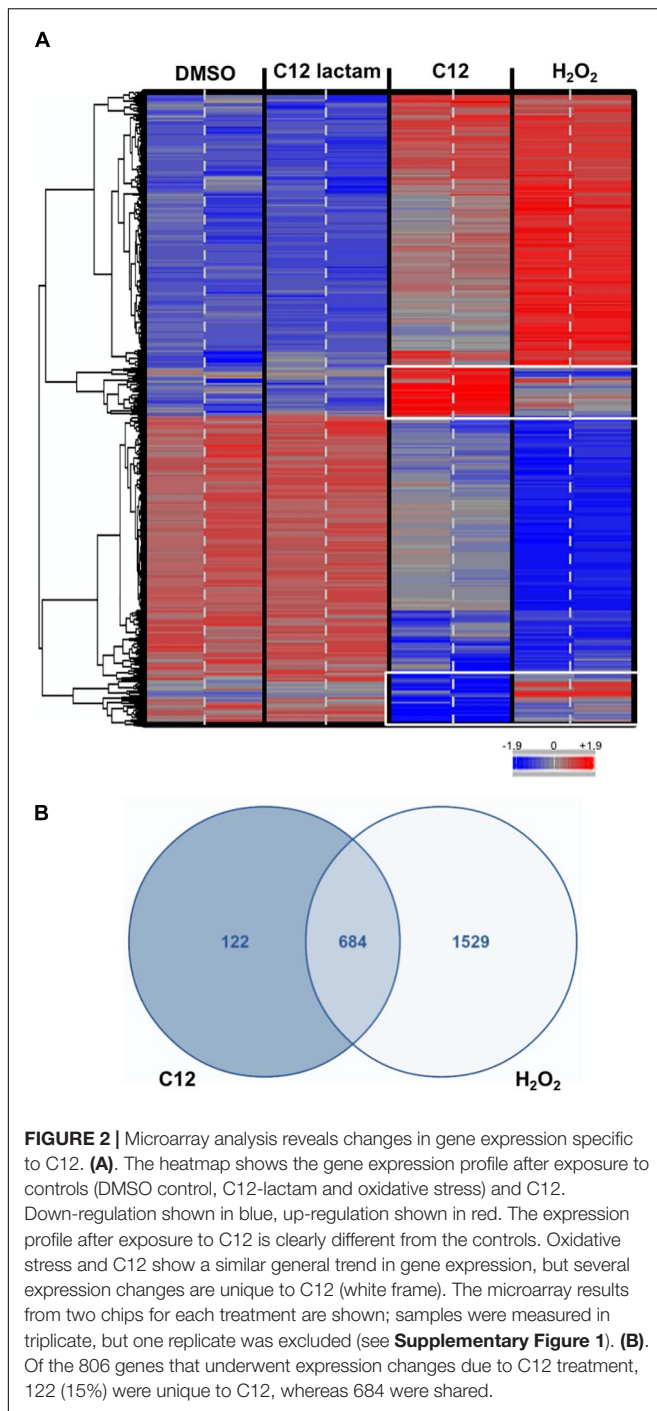
double deletion strain (Figure 1A, light gray bars), indicating that this effect is indeed mediated via the Msn2/4 pathway.

We proceeded with further control experiments to confirm that the yeast response was truly specific to C12. We tested the non-natural (*R*)-enantiomer of C12, (*R*)-C12, which is inactive as a quorum sensing signal in *P. aeruginosa* (Figure 1B). (*R*)-C12 triggered a less strong stress response than that of the natural enantiomer. An additional control compound, C12-lactam, in which the lactone ring is replaced by a lactam ring, did not induce a significant stress response (Figure 1C).

mRNA Microarray Analysis

In order to further explore the C12-induced stress response, microarray assays were performed. Yeast samples treated with 100 μ M of C12 were chosen for microarray analysis, as well as 100 μ M of C12-lactam and a solvent DMSO control (samples

chosen are shown in Figure 1C). Additional samples were treated with 0.3 mM hydrogen peroxide, for comparison to the oxidative stress response, as has been reported previously (Gasch et al., 2000). Microarray analysis revealed that the expression pattern in response to C12 is distinctly different from both the controls (Figure 2A and Supplementary Figure 1). The control C12-lactam shows an expression pattern similar to the solvent control. The expression profile after exposure to 0.3 mM H_2O_2 is similar to what has been reported previously by Gasch et al. (2000) (Supplementary Figure 2). A direct comparison between C12 treatment and oxidative stress reveals similar trends, with some key differences (Figure 2A). Both induced the regulation of a number of antioxidants and proteins involved in carbon metabolism, resulting in metabolic redirection from glycolysis to the pentose phosphate pathway. Other pathways upregulated by both hydrogen peroxide and by C12 include genes involved



in protein degradation, the synthesis of heat shock proteins and chaperones. Pathways involved in DNA replication, on the other hand, were downregulated. However, of the 806 genes up- or down-regulated in response to C12 treatment, 122 (15%) were specific to C12 (**Figure 2B**). Out of the genes found to be uniquely affected by C12, a number are involved in lipid synthesis and transport, including a gene upregulated 20-fold, *RSB1*. Additionally, C12 treatment induced the downregulation of several genes involved in iron transport, assimilation and

homeostasis (*FTR1*, *FET3*, *SIT1*, *FRE1*). In contrast, these same genes are upregulated upon exposure to hydrogen peroxide, indicating that this response pattern is distinct from the oxidative stress response.

S. cerevisiae Shows Reduced Viability in the Presence of *P. aeruginosa*

To examine whether the presence of *P. aeruginosa* affects the growth of *S. cerevisiae*, the two strains were grown together in liquid co-culture. The presence of the bacteria significantly reduced the number of viable yeast cells after 48 h in liquid co-culture (**Figure 3**). We observed a similar result when the yeast was cultured in the presence of *Pseudomonas* supernatant. The latter indicates that the growth inhibitory effect may be caused by the secretion of virulence factors by *P. aeruginosa*. When the yeast was cultured in the presence of PAO-JP2, a mutant deficient in LasI and RhlI, i.e., that cannot synthesize C12 or C4 and produces fewer QS-regulated virulence factors, we also saw a reduction in viable yeast cells. However, in the presence of only bacterial supernatant from JP2, the yeast actually showed a significant increase in growth after 48 h (**Figure 3**).

Rescue Effect of C12 on Yeast Response to Oxidative Stress

Next, we asked if C12 induced a rescue effect based on the environmental stress response (ESR) (Gasch, 2007), in which a mild stressor leads to higher survival rates for a subsequent, severe stress. This effect has been previously shown in *C. albicans* with its native QSM farnesol, via the cAMP/PKA pathway (Westwater et al., 2005; Deveau et al., 2010). Viability assays were performed using CFU counts on agar plates after treatment of the yeast with test or control compounds. Yeast cells in liquid YPD medium were pre-incubated with 50 μ M C12 for 30 min and thereafter exposed to 0.1% H_2O_2 for 10 min. This concentration of hydrogen peroxide results in an approximately 50% reduction in viability (**Supplementary Figure 3**), and is equivalent to 32.6 mM, \sim 100 times higher than the concentration used as a mild stressor in the microarray experiments. The samples were then diluted and plated on YPD agar. After 96 h, the number of colony forming units (CFU) was counted as a measure of viable cells and compared between treatments. In *S. cerevisiae* wild-type strain BY4741, pre-treatment with C12 seems to have slightly increased resistance to oxidative stress on average, although the difference was not significant ($p = 0.07$, one-tailed t -test) (**Figure 4**). However, in another wild-type strain, W303, we did not observe a difference in the number of viable yeast cells dependent on pre-treatment with C12, suggesting that this effect is strain-specific (data not shown).

Labeling Yeast Receptors for C12

In order to investigate the mechanism behind the *S. cerevisiae* response to C12 and activation of the Msn2/4 mediated stress response, we performed experiments to label putative receptors for this compound. Using an activity-based protein profiling (ABPP) approach (Speers and Cravatt, 2009), we synthesized an alkyne-appended diazirine analog of C12 (P6; **Figure 5A**),

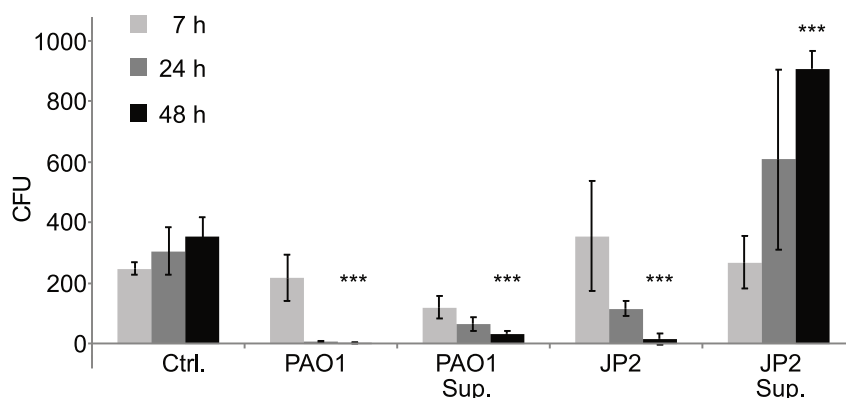


FIGURE 3 | Liquid co-cultures of wild type yeast with *Pseudomonas* reveal growth inhibitory effect of *Pseudomonas* supernatant. Overnight cultures of *S. cerevisiae* wild-type strain W303 and *P. aeruginosa* (wild-type strain PAO1 or the $\Delta rhII\Delta lasI$ mutant PAO-JP2) were both adjusted to $OD_{600} \sim 0.01$ and incubated together at 30°C under constant agitation. Additionally, *S. cerevisiae* was grown under the same conditions in the presence of PAO1 or PAO-JP2 supernatant. After 7, 24 and 48 h samples were taken, diluted in DDW and plated on selective YPD agar containing 50 μ g/mL gentamicin (in order to inhibit bacterial growth and thus monitor only yeast growth/viability). Yeast viability was reduced in the presence of the bacteria for both the wild-type and the mutant, presumably due to competition for resources. However, only the supernatant of PAO1 inhibited yeast growth, indicating inhibition due to bacterial virulence factors or other QS-regulated secondary metabolites. Values are averages of three experiments (\pm standard deviation). The significance of the variance between groups was calculated using a one-way ANOVA test, followed by pairwise comparisons using Tukey multiple comparison of means. Key: *** $p \leq 0.001$.

currently used by us to identify C12-binding proteins in other eukaryotes (Dubinsky et al., 2009). In short, activation of the diazirine moiety through photo-irradiation with UV-light (365 nm) induces covalent binding between the probe and proteins in its vicinity. Then, via a copper-mediated azide-alkyne cycloaddition reaction (CuAAC), the alkyne-appended proteins can be coupled to rhodamine azide, enabling the visualization of labeled proteins using in-gel fluorescence. In fluorescence labeling experiments with wild-type *S. cerevisiae* strain W303, a number of abundant proteins in the molecular weight range of ~ 60 –100 kDa were labeled, as well as some less abundant proteins with lower molecular weights (Figure 5B).

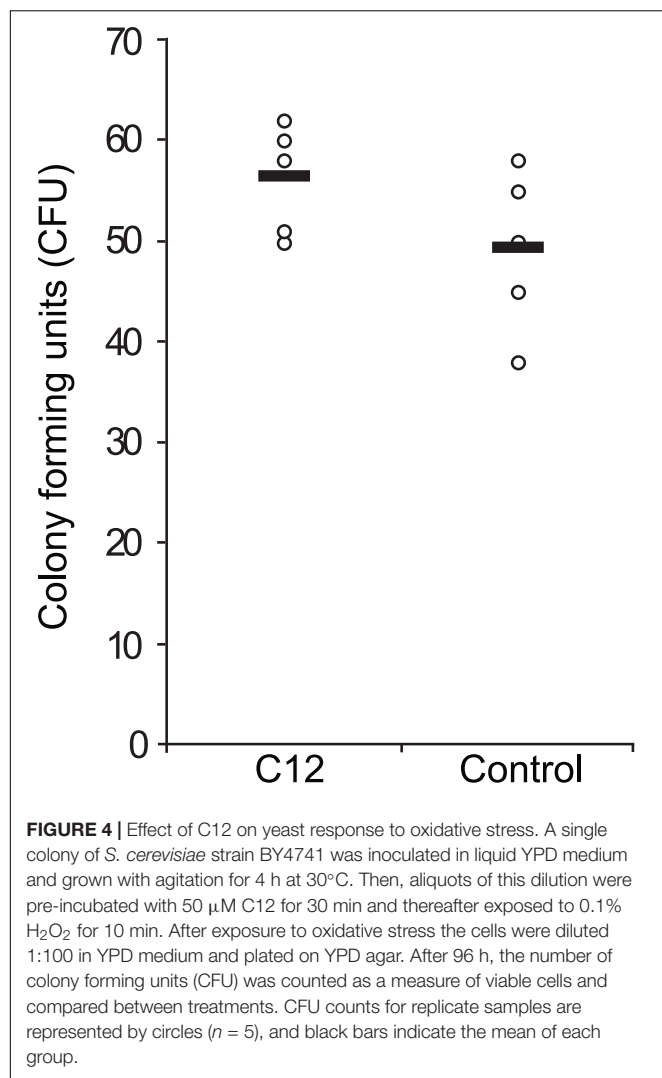
Next, we purified proteins covalently bound to our alkyne probe and performed mass spectrometry analysis, resulting in a number of hits that showed a strong ratio between scores obtained for the probe and for the control labeling experiments (Table 1; full data available in Supplementary Table 2). We selected the HYP2 isoform of the eukaryotic elongation initiation factor 5A (eIF-5A) for further validation. This 17 kDa protein is highly conserved among eukaryotes and has previously been linked to stress responses (Takeuchi et al., 2002; Li et al., 2010). However, initial attempts to purify recombinant eIF-5A to perform direct binding assays proved problematic due to the instability of the protein, and possibly because we only expressed one of the two isoforms, that was additionally lacking a hypusination modification. We are currently engaged in additional approaches to further study the function and role of C12 and eIF-5A in yeast.

DISCUSSION

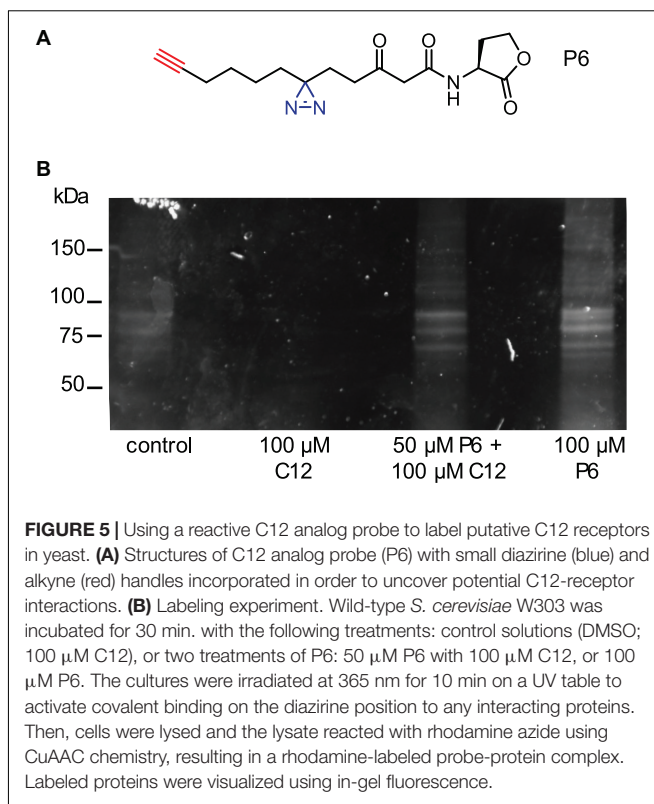
In the present paper we show that the budding yeast *S. cerevisiae* responds to the presence of the Gram-negative bacterium

P. aeruginosa, or more precisely to its primary QSM C12. We provide strong evidence that the observed effect is a general stress response mediated by the transcription factors Msn2/4. Examining changes in the expression of the GFP-labeled small heat shock protein Hsp12, we measured the physiological response of *S. cerevisiae* to different bacterial QSMs. This screen revealed that *S. cerevisiae* specifically responds to the *P. aeruginosa* QSM C12 and to none of the other compounds tested (Figure 1A). It has been shown before in *C. albicans* that the response to bacterial QSMs was limited to compounds with a 12-carbon backbone, similar in size to its native QSM sesquiterpene alcohol, farnesol (Shchepin et al., 2003). Although we did not observe a stress response upon exposure to farnesol, it has been demonstrated that farnesol affects *S. cerevisiae* in other ways, by inhibiting growth and inducing the generation of reactive oxygen species (ROS) (Machida et al., 1998, 1999). We further examined the specificity of the response by testing control compounds similar in structure to C12. The unnatural stereoisomer of C12, (*R*)-C12, induced a decreased response (Figure 1B), while C12-lactam, in which the oxygen of the lactone ring is replaced with a nitrogen, did not induce a stress response above control levels (Figure 1C). This indicates that the response to C12 is specific, and requires an intact lactone ring, a structural element shown to be crucial in the recognition of C12 in its native QS system in *P. aeruginosa*. When we further tested our compounds on a strain deleted in the transcription factors Msn4, the response was diminished, and in a double mutant strain in which both Msn4 and Msn2 were deleted, the response was abolished (Figure 1A). This data provides clear evidence that the response to C12 is Msn2/4 regulated, and to the best of our knowledge, is the first description of an Msn2/4-mediated stress response in yeast induced by a bacterial QSM.

In order to further explore the mechanism behind this stress response to C12, we collected mRNA microarray data. We



compared four treatments: C12, hydrogen peroxide, C12-lactam, and DMSO. Hydrogen peroxide was chosen as a model for oxidative stress, as it is a well-characterized stress response and a common virulence mechanism for *P. aeruginosa*. Exposure to C12 resulted in a unique mRNA expression pattern, while the structurally related control compound, C12-lactam, yielded results similar to incubation with solvent alone (Figure 2). The response to incubation with C12 differs significantly from controls, but also from a previously described stress response to oxidative stress, which we replicated with hydrogen peroxide exposure. Several of the biochemical functions that are affected by up-and/or-down-regulated gene clusters upon C12 treatment overlap with those of the oxidative stress response. A number of genes involved in the Msn2/4 stress response pathways activated by hydrogen peroxide were similarly affected by exposure to C12, as expected for a Msn2/4-regulated response. For example, a number of antioxidants, including catalase T, transketolase, and glutaredoxin, were upregulated upon exposure to C12, with almost identical fold-change as in the response to hydrogen peroxide exposure (Hasan et al., 2002). Carbon metabolism



was also strongly affected, with resources diverted to regenerate NADPH via slowdown of glycolysis and redirection to the pentose phosphate pathway (Estruch, 2000). Other pathways upregulated by both hydrogen peroxide and by C12 include genes involved in protein degradation, the synthesis of heat shock proteins and chaperones, while pathways involved in DNA replication were downregulated. Overall, more than 80% of the total genes affected by exposure to C12 were found to be shared in the response to hydrogen peroxide. However, substantially fewer genes in total were affected by C12 than by hydrogen peroxide treatment (806 vs. 2213), indicating that C12 may induce a more mild or specific stress response than oxidative stress. While the microarray results indicate a number of promising leads as described below, in future work these genes should be further validated by RT-PCR, and their relevance explored by using orthogonal methods such as single-gene knockout mutants.

Out of the remaining genes that were affected specifically by C12 and not by hydrogen peroxide, a number are associated with lipid synthesis and transport. One of the most striking genes found to be unique to the C12 response is *RSB1*, which was the most upregulated gene in this assay, with a 20-fold change compared to the control. *RSB1* encodes for a membranous protein, Rsb1p. The function of this protein has not been fully elucidated, but it has been implicated in the translocation of sphingolipids or similar compounds out of the cell, and may function as a flippase to incorporate sphingolipids into the membrane (Kihara and Igarashi, 2002). We have previously found in our work on bacterial-eukaryotic interactions that a

TABLE 1 | A list of proteins identified using chemical proteomics experiments with probe P6.

SGD	Protein	Description
YEL034W	HYP2	Translation elongation factor eIF-5A
YJL076W	NET1	Core subunit of the RENT complex
YHR193C	EGD2	Alpha subunit of the nascent polypeptide-associated complex (NAC)
YFR033C	QCR6	Subunit 6 of the ubiquinol cytochrome-c reductase complex
YPL022W	RAD1	Single-stranded DNA endonuclease (with Rad10p)
YLR075W	RPL10	Ribosomal 60S subunit protein L10
YLR262C-A	TMA7	Protein of unknown function, associates with ribosomes
YLR363W-A	—	Protein of unknown function, colocalizes with nucleus

Mass spectrometry analysis of proteins covalently bound to our alkyne probe yielded a number of hits that showed a strong ratio between scores obtained for the probe and for the control labeling experiments.

mammalian sphingolipid, ceramide-1-phosphate, is involved in host immune response and pathogen recognition, sharing some of the same pathways shown to be affected by C12 in mammalian cells (Avni et al., 2010). Additionally, it has been suggested that C12 interferes with the integrity of mammalian cell membranes (Davis et al., 2010). The upregulation of *RSB1* in yeast is an intriguing finding adding to what is known about the effect of C12 on eukaryotic membranes, sphingolipids, and the innate immune response, and requires further study.

Another notable cluster we found to be affected in our microarray data is involved in iron homeostasis and transport. Previous work by Trejo-Hernandez et al. (2014) provides a very thorough analysis of differential protein expression in *C. albicans* in a mixed biofilm with *P. aeruginosa*. They conclude that iron deprivation is the driving force in the competition with the bacteria, showing that yeast mutants deficient in iron utilization were unable to compete with *P. aeruginosa* in mixed biofilms. The role of the pyoverdine siderophore produced by *Pseudomonas* sp. in competition between fungus and bacteria has already been demonstrated (Loper and Buyer, 1991; Harrison et al., 2008). It was shown that in mixed biofilms *P. aeruginosa* increases pyoverdine production in response to iron competition with *C. albicans* (Purschke et al., 2012). Our current data show that C12 has a significant effect on iron homeostasis in *S. cerevisiae*, causing downregulation of several genes involved in iron transport, assimilation, and homeostasis. In contrast, these same genes (*FTR1*, *FET3*, *SIT1*, *FRE1*) are upregulated upon exposure to hydrogen peroxide, indicating that this response pattern is distinct to C12.

In order to further investigate the effect of *P. aeruginosa* virulence factors toward *S. cerevisiae*, we performed a series of co-culture viability assays. We grew liquid co-cultures of the yeast with both the wild-type PAO1 and the C4/C12-deficient PAO-JP2, which produces fewer QS-regulated virulence factors. We found that in the liquid co-cultures, the viability of the yeast was significantly decreased by both strains of *P. aeruginosa*

(Figure 3). We hypothesized that the observed effects on growth in liquid media are likely the result of direct competition between the yeast and the bacteria for nutrients and resources. Therefore, in order to isolate the effect of secondary metabolites, we grew *S. cerevisiae* in the presence of PAO1 or PAO-JP2 supernatant and found that exposure to PAO1 supernatant alone significantly inhibited yeast growth, while supernatant from the C4/C12-deficient PAO-JP2 did not, and in fact increased growth (Figure 3). Based on these data, it seems that various bacterial virulence factors or other secreted metabolites indeed play an important role in the inhibition of growth of *S. cerevisiae*, not only competition for resources, or other contact or protein mediated virulence effects. Since the effect was abolished in the PAO-JP2 supernatant, this indicates that these molecules are regulated by the C4 or C12 QS systems. Indeed, treatment with the JP2 supernatant resulted in increased growth, a surprising finding which indicates that perhaps other secreted molecules can also have a beneficial effect on the yeast, a point that requires further study.

Mild stress, such as that induced by C12 in this study, plays a crucial role in what is commonly known as the ESR (Gasch, 2007). It has been shown that if yeast is exposed to mild stress the cells undergo certain physiological changes that lead to overall higher stress tolerance to subsequent, more severe stress (Gasch and Werner-Washburne, 2002; Gasch, 2007). An ESR in response to *P. aeruginosa* C12 may be a good evolutionary adaptation to the intricate *Pseudomonas* QS system, as C12 may be an early indication of the induction of QS and the subsequent presence of QS-regulated virulence factors. One virulence factor in particular, pyocyanin, may be relevant, as it has the ability to oxidize and reduce other molecules and produce reactive oxygen species (ROS). Effects of ROS on cell metabolism are well documented in a variety of species. These include not only roles in apoptosis (programmed cell death) but also positive effects such as the induction of host defense genes (Conner et al., 2002; Rada and Leto, 2008) and mobilization of ion transport systems (Pottosin et al., 2014). In our current model, the ability of the yeast to sense C12 could be the first protective barrier against potential oxidative stress by ROS produced by pyocyanin (Tupe et al., 2015).

Therefore, we performed a rescue effect experiment in order to determine if a C12-induced ESR could indeed protect the yeast from a subsequent, stronger oxidative stress. *S. cerevisiae* cultures were pre-treated with C12 (mild stressor), and thereafter exposed to severe oxidative stress with the addition of H₂O₂ at a concentration which results in 50% cell death. We observed slight indications of an ESR-induced rescue effect, which appears to be strain-specific—a slight rescue effect was seen for wild-type strain BY4741, although the difference was not significant (Figure 4), while no effect was observed for wild-type strain W303.

Based on these data, we concluded that there is a C12-specific effect on *S. cerevisiae*. Therefore, in order to further elucidate the mechanism behind this response, we used our previously developed chemical proteomics approach to identify a eukaryotic receptor for this bacterial signaling molecule (Dubinsky et al., 2009, 2013; Rayo et al., 2021). We synthesized a diazirine-alkyne-tagged C12 analog to capture proteins undergoing interactions

with the probe by activating the diazirine group and inducing covalent binding. The probe-protein complex can then be labeled via CuAAC chemistry to a fluorophore. Using this probe, we labeled several putative receptor proteins in a molecular weight range of ~60–100 kDa, as well as some lower molecular weight proteins (Figure 5). We additionally analyzed samples using mass spectrometry, in order to identify proteins bound to the probe. One promising hit from the proteomics results was eIF-5A, a highly conserved eukaryotic protein previously linked to stress responses (Takeuchi et al., 2002; Li et al., 2010). These results represent preliminary, proof-of-concept experiments, and efforts in the lab to validate these results and explore potential yeast C12 receptors remain on-going.

Our studies indicate that the specific sensing of C12 by *S. cerevisiae* leads to a mild activation of its general stress response, which may enable it to prepare for more severe conditions—such as strong oxidative stress. Future work is needed to elucidate the mechanism by which this stress response is induced, as well as explore whether C12 affects *S. cerevisiae* in additional ways, such as the formation of pseudohyphae or fungal biofilms as has been documented for its native QS signals (Reynolds and Fink, 2001). Whether this directed activation of the stress response benefits the yeast, or *Pseudomonas aeruginosa*, or both, still remains to be resolved. A wealth of knowledge has been gained in recent decades on the importance of QS for bacteria in order to govern the production of various secondary metabolites; however, little is still known about the ability of other organisms to perceive such information on population density and use it to their benefit. This study offers a starting point to study a potential mechanism that may guide the interaction between *P. aeruginosa* and *S. cerevisiae* and may reflect the relationships between bacterial and fungal species that compete and coexist in other environmental niches.

DATA AVAILABILITY STATEMENT

The datasets presented in this study can be found in online repositories. The names of the repository/repositories and accession number(s) can be found below: <https://www.ebi.ac.uk/arrayexpress/>, E-MTAB-4802.

AUTHOR CONTRIBUTIONS

AD, AA, and MM conceived and designed the experiments. AD, RG, LD, RD, JR, and AH performed the experiments. AD,

AH, RG, AA, and MM analyzed the data. LD, RD, PK, and JR contributed reagents, materials, and analysis tools. AD, RG, AA, and MM wrote the manuscript. All authors contributed to the article and approved the submitted version.

FUNDING

This work was funded by the Israel Science Foundation (Personal Grant 749/09, MM and AA), the Germany-Israel Project Grant (DIP ME4476/2, MM) and the European Research Council (Starting Grant 240356, MM).

ACKNOWLEDGMENTS

Microarray analysis was performed with the help of Dr. Micha Volokita at the DNA Microarray and Sequencing Unit of the National Institute for Biotechnology in the Negev (NIBN, Ben Gurion University of the Negev). Bioinformatic data analysis of microarray data was performed with the help of Drs. Vered Caspi and Inbar Plaschke from our on-campus Bioinformatics Core Facility. Mass spectrometry (Orbitrap) analyses were performed with the help of the Smoler Proteomics Center (The Technion, Haifa, Israel). We want to sincerely thank Prof. Pamela Silver at Harvard Medical School (Boston, MA) who provided us with a plasmid for GST-labeled eIF5A, Prof. Maya Schuldiner from the Weizmann Institute of Science (Israel) for helpful discussions and for providing us with *S. cerevisiae* eIF5A mutant strains, and Prof. Jonathan Weissman at the University of California, San Francisco for providing us with *S. cerevisiae* BY4741. We further want to thank our colleagues at Ben Gurion University of the Negev, Ilana Berger-Fridman, Dr. Mehtap Abu-Quarn, and Dror Baran, for their technical assistance, and to thank Prof. Pieter Dorrestein (University of California, San Diego) and his group, and Dr. Aurélie Deveau (INRA and Université de Lorraine, France) for assistance and helpful conversations regarding this work. RG is grateful to the Azrieli Foundation for the award of an Azrieli fellowship.

SUPPLEMENTARY MATERIAL

The Supplementary Material for this article can be found online at: <https://www.frontiersin.org/articles/10.3389/fmicb.2021.632658/full#supplementary-material>

REFERENCES

- Alegado, R. A., Brown, L. W., Cao, S., Dermenjian, R. K., Zuzow, R., Fairclough, S. R., et al. (2012). A bacterial sulfonolipid triggers multicellular development in the closest living relatives of animals. *Elife* 1:e00013.
- Attfield, P., Myers, D., and Hazell, B. (1997). The importance of stress tolerance to baker's yeast. *Australas. Biotechnol.* 7, 149–154.
- Avni, D., Philosoph, A., Meijler, M. M., and Zor, T. (2010). The ceramide-1-phosphate analogue PCERA-1 modulates tumour necrosis factor- α and interleukin-10 production in macrophages via the cAMP-PKA-CREB pathway in a GTP-dependent manner. *Immunology* 129, 375–385. doi: 10.1111/j.1365-2567.2009.03188.x
- Chen, H., and Fink, G. R. (2006). Feedback control of morphogenesis in fungi by aromatic alcohols. *Genes Dev.* 20, 1150–1161. doi: 10.1101/gad.1411806
- Chhabra, S. R., Harty, C., Hooi, D. S. W., Daykin, M., Williams, P., Telford, G., et al. (2003). Synthetic analogues of the bacterial signal (quorum sensing) molecule N-(3-oxododecanoyl)-L-homoserine lactone as immune modulators. *J. Med. Chem.* 46, 97–104. doi: 10.1021/jm020909n
- Conner, G. E., Salathe, M., and Forteza, R. (2002). Lactoperoxidase and hydrogen peroxide metabolism in the airway. *Am. J. Respir. Crit. Care Med.* 166, S57–S61.

- Cugini, C., Calfee, M. W., Farrow, J. M., Morales, D. K., Pesci, E. C., and Hogan, D. A. (2007). Farnesol, a common sesquiterpene, inhibits PQS production in *Pseudomonas aeruginosa*. *Mol. Microbiol.* 65, 896–906. doi: 10.1111/j.1365-2958.2007.05840.x
- Cugini, C., Morales, D. K., and Hogan, D. A. (2010). *Candida albicans*-produced farnesol stimulates *Pseudomonas* quinolone signal production in LasR-defective *Pseudomonas aeruginosa* strains. *Microbiology* 156, 3096–3107. doi: 10.1099/mic.0.037911-0
- Davis, B. M., Jensen, R., Williams, P., and O'Shea, P. (2010). The interaction of N-acylhomoserine lactone quorum sensing signaling molecules with biological membranes: implications for inter-kingdom signaling. *PLoS One* 5:e13522. doi: 10.1371/journal.pone.0013522
- Davis-Hanna, A., Piispanen, A. E., Stateva, L. I., and Hogan, D. A. (2008). Farnesol and dodecanol effects on the *Candida albicans* Ras1-cAMP signalling pathway and the regulation of morphogenesis. *Mol. Microbiol.* 67, 47–62. doi: 10.1111/j.1365-2958.2007.06013.x
- de Almeida, F. A., Carneiro, D. G., de Oliveira Mendes, T. A., Barros, E., Pinto, U. M., de Oliveira, L. L., et al. (2018). N-dodecanoyl-homoserine lactone influences the levels of thiol and proteins related to oxidation-reduction process in *Salmonella*. *PLoS One* 13:e0204673. doi: 10.1371/journal.pone.0204673
- Deveau, A., Piispanen, A. E., Jackson, A. A., and Hogan, D. A. (2010). Farnesol Induces Hydrogen Peroxide Resistance in *Candida albicans* Yeast by Inhibiting the Ras-Cyclic AMP Signaling Pathway. *Eukaryot. Cell* 9, 569–577. doi: 10.1128/ec.00321-09
- Dubinsky, L., Delago, A., Amara, N., Krief, P., Rayo, J., Zor, T., et al. (2013). Species selective diazirine positioning in tag-free photoactive quorum sensing probes. *Chem. Commun.* 49, 5826–5828. doi: 10.1039/c3cc43092h
- Dubinsky, L., Jarosz, L. M., Amara, N., Krief, P., Kravchenko, V. V., Krom, B. P., et al. (2009). Synthesis and validation of a probe to identify quorum sensing receptors. *Chem. Commun.* 47, 7378–7380. doi: 10.1039/b917507e
- Estruch, F. (2000). Stress-controlled transcription factors, stress-induced genes and stress tolerance in budding yeast. *FEMS Microbiol. Rev.* 24, 469–486. doi: 10.1111/j.1574-6976.2000.tb00551.x
- Fay, J. C., and Benavides, J. A. (2005). Evidence for domesticated and wild populations of *Saccharomyces cerevisiae*. *PLoS Genet.* 1:e5. doi: 10.1371/journal.pgen.0010005
- Gasch, A. P. (2007). Comparative genomics of the environmental stress response in ascomycete fungi. *Yeast* 24, 961–976. doi: 10.1002/yea.1512
- Gasch, A. P., Spellman, P. T., Kao, C. M., Carmel-Harel, O., Eisen, M. B., Storz, G., et al. (2000). Genomic expression programs in the response of yeast cells to environmental changes. *Mol. Biol. Cell* 11, 4241–4257. doi: 10.1091/mbc.11.12.4241
- Gasch, A. P., and Werner-Washburne, M. (2002). The genomics of yeast responses to environmental stress and starvation. *Funct. Integr. Genomics* 2, 181–192. doi: 10.1007/s10142-002-0058-2
- Gibson, J., Sood, A., and Hogan, D. A. (2009). *Pseudomonas aeruginosa*-*Candida albicans* interactions: localization and fungal toxicity of a phenazine derivative. *Appl. Environ. Microbiol.* 75, 504–513. doi: 10.1128/aem.01037-08
- Green, S. K., Schroth, M. N., Cho, J. J., Kominos, S. D., and Vitanzajack, V. B. (1974). Agricultural Plants and Soil as a Reservoir for *Pseudomonas-Aeruginosa*. *Appl. Microbiol.* 28, 987–991. doi: 10.1128/aem.28.6.987-991.1974
- Hall, R. A., Turner, K. J., Chaloupka, J., Cottier, F., De Sordi, L., Sanglard, D., et al. (2011). The Quorum-Sensing Molecules Farnesol/Homoserine Lactone and Dodecanol Operate via Distinct Modes of Action in *Candida albicans*. *Eukaryot. Cell* 10, 1034–1042. doi: 10.1128/ec.05060-11
- Harrison, F., Paul, J., Massey, R. C., and Buckling, A. (2008). Interspecific competition and siderophore-mediated cooperation in *Pseudomonas aeruginosa*. *ISME J.* 2, 49–55. doi: 10.1038/ismej.2007.96
- Hasan, R., Leroy, C., Isnard, A. D., Labarre, J., Boy-Marcotte, E., and Toledano, M. B. (2002). The control of the yeast H2O2 response by the Msn2/4 transcription factors. *Mol. Microbiol.* 45, 233–241. doi: 10.1046/j.1365-2958.2002.03011.x
- Haussler, S., and Becker, T. (2008). The *pseudomonas* quinolone signal (PQS) balances life and death in *Pseudomonas aeruginosa* Populations. *PLoS Pathog.* 4:e1000166. doi: 10.1371/journal.ppat.1000166
- Hazen, K. C., and Cutler, J. E. (1979). Auto-regulation of germ tube formation by *Candida albicans*. *Infect. Immun.* 24, 661–666.
- Hogan, D. A. (2006). Quorum sensing: alcohols in a social situation. *Curr. Biol.* 16, R457–R458.
- Hogan, D. A., Vik, A., and Kolter, R. (2004). A *Pseudomonas aeruginosa* quorum-sensing molecule influences *Candida albicans* morphology. *Mol. Microbiol.* 54, 1212–1223. doi: 10.1111/j.1365-2958.2004.04349.x
- Hornby, J. M., Jensen, E. C., Lisec, A. D., Tasto, J. J., Jahnke, B., Shoemaker, R., et al. (2001). Quorum sensing in the dimorphic fungus *Candida albicans* is mediated by farnesol. *Appl. Environ. Microbiol.* 67, 2982–2992. doi: 10.1128/aem.67.7.2982-2992.2001
- Jarosz, L. M., Ovchinnikova, E. S., Meijler, M. M., and Krom, B. P. (2011). Microbial spy games and host response: roles of a *Pseudomonas aeruginosa* small molecule in communication with other species. *PLoS Pathog.* 7:e1002312. doi: 10.1371/journal.ppat.1002312
- Karlssohn, T., Turkina, M. V., Yakymenko, O., Magnusson, K.-E., and Vikström, E. (2012). The *Pseudomonas aeruginosa* N-acylhomoserine lactone quorum sensing molecules target IQGAP1 and modulate epithelial cell migration. *PLoS Pathog.* 8:e1002953. doi: 10.1371/journal.ppat.1002953
- Kihara, A., and Igarashi, Y. (2002). Identification and characterization of a *Saccharomyces cerevisiae* gene, RSB1, involved in sphingoid long-chain base release. *J. Biol. Chem.* 277, 30048–30054. doi: 10.1074/jbc.m203385200
- Kravchenko, V. V., Kaufmann, G. F., Mathison, J. C., Scott, D. A., Katz, A. Z., Grauer, D. C., et al. (2008). Modulation of gene expression via disruption of NF-kappa B signaling by a bacterial small molecule. *Science* 321, 259–263. doi: 10.1126/science.1156499
- Kravchenko, V. V., Kaufmann, G. F., Mathison, J. C., Scott, D. A., Katz, A. Z., Wood, M. R., et al. (2006). N-(3-oxo-acyl) homoserine lactones signal cell activation through a mechanism distinct from the canonical pathogen-associated molecular pattern recognition receptor pathways. *J. Biol. Chem.* 281, 28822–28830. doi: 10.1074/jbc.m606613200
- Lee, J., and Zhang, L. H. (2015). The hierarchy quorum sensing network in *Pseudomonas aeruginosa*. *Protein Cell* 6, 26–41. doi: 10.1007/s13238-014-0100-x
- Li, C. H., Ohn, T., Ivanov, P., Tisdale, S., and Anderson, P. (2010). eIF5A promotes translation elongation, polysome disassembly and stress granule assembly. *PLoS One* 5:e9942. doi: 10.1371/journal.pone.0009942
- Lindsay, A. K., Deveau, A., Piispanen, A. E., and Hogan, D. A. (2012). Farnesol and Cyclic AMP Signaling Effects on the Hypha-to-Yeast Transition in *Candida albicans*. *Eukaryot. Cell* 11, 1219–1225. doi: 10.1128/ec.00144-12
- Lingappa, B. T., Prasad, M., Lingappa, Y., Hunt, D. F., and Biemann, K. (1969). Phenylethyl alcohol and tryptophol - autoantibiotics produced by the fungus *Candida albicans*. *Science* 163, 192–194. doi: 10.1126/science.163.3863.192
- Loper, J. E., and Buyer, J. S. (1991). Siderophores in microbial interactions on plant-surfaces. *Mol. Plant Microbe Interact.* 4, 5–13. doi: 10.1094/mpmi-4-005
- Machida, K., Tanaka, T., Fujita, K. I., and Taniguchi, M. (1998). Farnesol-induced generation of reactive oxygen species via indirect inhibition of the mitochondrial electron transport chain in the yeast *Saccharomyces cerevisiae*. *J. Bacteriol.* 180, 4460–4465.
- Machida, K., Tanaka, T., Yano, Y., Otani, S., and Taniguchi, M. (1999). Farnesol-induced growth inhibition in *Saccharomyces cerevisiae* by a cell cycle mechanism. *Microbiology* 145, 293–299. doi: 10.1099/13500872-145-2-293
- Mandabi, A., Ganin, H., and Meijler, M. M. (2015). Synergistic activation of quorum sensing in *Vibrio harveyi*. *Bioorg. Med. Chem. Lett.* 25, 3966–3969. doi: 10.1016/j.bmcl.2015.07.028
- Maura, D., Hazan, R., Kitao, T., Ballok, A. E., and Rahme, L. G. (2016). Evidence for Direct Control of Virulence and Defense Gene Circuits by the *Pseudomonas aeruginosa* Quorum Sensing Regulator, MvfR. *Sci. Rep.* 6:34083.
- Maurer, S., Wabnitz, G. H., Kahle, N. A., Stegmaier, S., Prior, B., Giese, T., et al. (2015). Tasting *Pseudomonas aeruginosa* Biofilms: human neutrophils express the bitter receptor t2r38 as sensor for the quorum sensing molecule N-(3-Oxododecanoyl)-l-Homoserine Lactone. *Front. Immunol.* 6:369. doi: 10.3389/fimmu.2015.00369
- Moree, W. J., Phelan, V. V., Wu, C. H., Bandeira, N., Cornett, D. S., Duggan, B. M., et al. (2012). Interkingdom metabolic transformations captured by microbial imaging mass spectrometry. *Proc. Natl. Acad. Sci. U. S. A.* 109, 13811–13816. doi: 10.1073/pnas.1206855109
- Pearson, J. P., Gray, K. M., Passador, L., Tucker, K. D., Eberhard, A., Iglewski, B. H., et al. (1994). Structure of the autoinducer required for expression of

- Pseudomonas aeruginosa* virulence genes. *Proc. Natl. Acad. Sci. U. S. A.* 91, 197–201. doi: 10.1073/pnas.91.1.197
- Pinto, U. M., and Winans, S. C. (2009). Dimerization of the quorum-sensing transcription factor TraR enhances resistance to cytoplasmic proteolysis. *Mol. Microbiol.* 73, 32–42. doi: 10.1111/j.1365-2958.2009.06730.x
- Popat, R., Cornforth, D. M., McNally, L., and Brown, S. P. (2015). Collective sensing and collective responses in quorum-sensing bacteria. *J. R. Soc. Interface* 12:20140882. doi: 10.1098/rsif.2014.0882
- Pottosin, I., Velarde-Buendia, A. M., Bose, J., Zepeda-Jazo, I., Shabala, S., and Dobrovinskaya, O. (2014). Cross-talk between reactive oxygen species and polyamines in regulation of ion transport across the plasma membrane: implications for plant adaptive responses. *J. Exp. Botany* 65, 1271–1283. doi: 10.1093/jxb/ert423
- Purschke, F. G., Hiller, E., Trick, I., and Rupp, S. (2012). Flexible Survival Strategies of *Pseudomonas aeruginosa* in Biofilms Result in Increased Fitness Compared with *Candida albicans*. *Mol. Cell. Proteomics* 11, 1652–1669. doi: 10.1074/mcp.m112.017673
- Rada, B., and Leto, T. L. (2008). Oxidative innate immune defenses by Nox/Duox family NADPH oxidases. *Contrib. Microbiol.* 15, 164–187. doi: 10.1159/000136357
- Rampioni, G., Falcone, M., Heeb, S., Frangipani, E., Fletcher, M. P., Dubern, J.-F., et al. (2016). Unravelling the genome-wide contributions of specific 2-alkyl-4-quinolones and PqsE to quorum sensing in *Pseudomonas aeruginosa*. *PLoS Pathog.* 12:e1006029. doi: 10.1371/journal.ppat.1006029
- Rayo, J., Gregor, R., Jacob, N. T., Dandela, R., Dubinsky, L., Yashkin, A., et al. (2021). Immunoeediting role for major vault protein in apoptotic signaling induced by bacterial N-acyl homoserine lactones. *Proc. Natl. Acad. Sci. U. S. A.* 118:e2012529118. doi: 10.1073/pnas.2012529118
- Reynolds, T. B., and Fink, G. R. (2001). *Saccharomyces cerevisiae* as a model for fungal biofilms. *Yeast* 18, S279–S279.
- Sadeh, A., Baran, D., Volokh, M., and Aharoni, A. (2012). Conserved motifs in the Msn2-activating domain are important for Msn2-mediated yeast stress response. *J. Cell Sci.* 125, 3333–3342.
- Sadeh, A., Movshovich, N., Volokh, M., Gheber, L., and Aharoni, A. (2011). Fine-tuning of the Msn2/4-mediated yeast stress responses as revealed by systematic deletion of Msn2/4 partners. *Mol. Biol. Cell* 22, 3127–3138. doi: 10.1091/mbc.e10-12-1007
- Shchepin, R., Hornby, J. M., Burger, E., Niessen, T., Dussault, P., and Nickerson, K. W. (2003). Quorum sensing in *Candida albicans*: probing farnesol's mode of action with 40 natural and synthetic farnesol analogs. *Chem. Biol.* 10, 743–750.
- Speers, A. E., and Cravatt, B. F. (2009). Activity-Based Protein Profiling (ABPP) and Click Chemistry (CC)-ABPP by MudPIT Mass Spectrometry. *Curr. Protoc. Chem. Biol.* 1, 29–41. doi: 10.1002/9780470559277.ch090138
- Takeuchi, K., Nakamura, K., Fujimoto, M., Kaino, S., Kondoh, S., and Okita, K. (2002). Heat stress-induced loss of eukaryotic initiation factor 5A (eIF-5A) in a human pancreatic cancer cell line, MIA PaCa-2, analyzed by two-dimensional gel electrophoresis. *Electrophoresis* 23, 662–669. doi: 10.1002/1522-2683(200202)23:4<662::aid-elps662>3.0.co;2-#
- Teplitski, M., Mathesius, U., and Rumbaugh, K. P. (2011). Perception and Degradation of N-Acyl Homoserine Lactone Quorum Sensing Signals by Mammalian and Plant Cells. *Chem. Rev.* 111, 100–116. doi: 10.1021/cr100045m
- Trejo-Hernandez, A., Andrade-Dominguez, A., Hernandez, M., and Encarnacion, S. (2014). Interspecies competition triggers virulence and mutability in *Candida albicans*-*Pseudomonas aeruginosa* mixed biofilms. *ISME J.* 8, 1974–1988. doi: 10.1038/ismej.2014.53
- Tupe, S. G., Kulkarni, R. R., Shirazi, F., Sant, D. G., Joshi, S. P., and Deshpande, M. V. (2015). Possible mechanism of antifungal phenazine-1-carboxamide from *Pseudomonas* sp against dimorphic fungi *Benjaminiella poitrasii* and human pathogen *Candida albicans*. *J. Appl. Microbiol.* 118, 39–48. doi: 10.1111/jam.12675
- Westwater, C., Balish, E., and Schofield, D. A. (2005). *Candida albicans*-conditioned medium protects yeast cells from oxidative stress: a possible link between quorum sensing and oxidative stress resistance. *Eukaryot. Cell* 4, 1654–1661. doi: 10.1128/ec.4.10.1654-1661.2005
- Woznica, A., Gerdt, J. P., Hulett, R. E., Clardy, J., and King, N. (2017). Mating in the closest living relatives of animals is induced by a bacterial chondroitinase. *Cell* 170, 1175–1183.e11.

Conflict of Interest: The authors declare that the research was conducted in the absence of any commercial or financial relationships that could be construed as a potential conflict of interest.

Publisher's Note: All claims expressed in this article are solely those of the authors and do not necessarily represent those of their affiliated organizations, or those of the publisher, the editors and the reviewers. Any product that may be evaluated in this article, or claim that may be made by its manufacturer, is not guaranteed or endorsed by the publisher.

Copyright © 2021 Delago, Gregor, Dubinsky, Dandela, Hendler, Krief, Rayo, Aharoni and Meijler. This is an open-access article distributed under the terms of the Creative Commons Attribution License (CC BY). The use, distribution or reproduction in other forums is permitted, provided the original author(s) and the copyright owner(s) are credited and that the original publication in this journal is cited, in accordance with accepted academic practice. No use, distribution or reproduction is permitted which does not comply with these terms.



L-Canavanine, a Root Exudate From Hairy Vetch (*Vicia villosa*) Drastically Affecting the Soil Microbial Community and Metabolite Pathways

Hossein Mardani-Korrani¹, Masaru Nakayasu², Shinichi Yamazaki³, Yuichi Aoki³, Rumi Kaida¹, Takashi Motobayashi¹, Masaru Kobayashi⁴, Naoko Ohkama-Ohtsu¹, Yosei Oikawa¹, Akifumi Sugiyama^{2*} and Yoshiharu Fujii^{1*}

¹ Institute of Agriculture, Tokyo University of Agriculture and Technology, Fuchu, Japan, ² Research Institute for Sustainable Humanosphere, Kyoto University, Uji, Japan, ³ Tohoku Medical Megabank Organization, Tohoku University, Sendai, Japan, ⁴ Graduate School of Agriculture, Kyoto University, Kyoto, Japan

OPEN ACCESS

Edited by:

Elisa Korenblum,
Institute of Plant Sciences,
Agricultural Research Organization,
Volcani Center, Israel

Reviewed by:

Joelle Sasse Schlaepfer,
University of Zurich, Switzerland
Rachel Leisso,
Montana State University,
United States

*Correspondence:

Akifumi Sugiyama
sugiyama.akifumi.4m@kyoto-u.ac.jp
Yoshiharu Fujii
yfujii@cc.tuat.ac.jp

Specialty section:

This article was submitted to
Terrestrial Microbiology,
a section of the journal
Frontiers in Microbiology

Received: 28 April 2021

Accepted: 30 August 2021

Published: 27 September 2021

Citation:

Mardani-Korrani H, Nakayasu M,
Yamazaki S, Aoki Y, Kaida R,
Motobayashi T, Kobayashi M,
Ohkama-Ohtsu N, Oikawa Y,
Sugiyama A and Fujii Y (2021)
L-Canavanine, a Root Exudate From
Hairy Vetch (*Vicia villosa*) Drastically
Affecting the Soil Microbial
Community and Metabolite Pathways.
Front. Microbiol. 12:701796.
doi: 10.3389/fmicb.2021.701796

L-Canavanine, a conditionally essential non-proteinogenic amino acid analog to L-arginine, plays important roles in cell division, wound healing, immune function, the release of hormones, and a precursor for the synthesis of nitric oxide (NO). In this report, we found that the L-canavanine is released into the soil from the roots of hairy vetch (*Vicia villosa*) and declines several weeks after growth, while it was absent in bulk proxy. Hairy vetch root was able to exudate L-canavanine in both pots and *in vitro* conditions in an agar-based medium. The content of the L-canavanine in pots and agar conditions was higher than the field condition. It was also observed that the addition of L-canavanine significantly altered the microbial community composition and diversity in soil. Firmicutes and Actinobacteria became more abundant in the soil after the application of L-canavanine. In contrast, Proteobacteria and Acidobacteria populations were decreased by higher L-canavanine concentration (500 nmol/g soil). Prediction of the soil metabolic pathways using PICRUST2 estimated that the L-arginine degradation pathway was enriched 1.3-fold when L-canavanine was added to the soil. Results indicated that carbon metabolism-related pathways were altered and the degradation of nitrogen-rich compounds (i.e., amino acids) enriched. The findings of this research showed that secretion of the allelochemical L-canavanine from the root of hairy vetch may alter the soil microbial community and soil metabolite pathways to increase the survival chance of hairy vetch seedlings. This is the first report that L-canavanine acts as an allelochemical that affects the biodiversity of soil microbial community.

Keywords: allelopathy, hairy vetch (*Vicia villosa* Roth), L-canavanine, soil microbial community (SMC), soil metabolites pathways, cover crop

INTRODUCTION

Amino acids as a significant portion of the root exudates play key roles in shaping the rhizosphere microbial community structure (Hu et al., 2018; Canarini et al., 2019). Rhizosphere amino acids often result from lysis and cellular efflux from plants and soil organisms or proteolysis of existing peptides. They primarily serve as carbon and nitrogen sources in the rhizosphere (Moe, 2013).

Amino acids in the soil are an important microbial pool factor, affecting the physiological function of the soil microbial communities (SMC) and can resonate with global scale nutrient biogeochemistry. Although few studies have focused on the effect of the proteinogenic amino acids on the total SMC, the role of many non-proteinogenic free amino acids (FAAs) produced by plants including L-canavanine from hairy vetch is largely unknown (Aliashkevich et al., 2018).

Few amino acids have been isolated and identified as intermediate compounds of biological phenomena such as allelopathy (Araya et al., 2014). It may be because evaluating FAAs is challenging, since the concentration of FAAs available in plant roots and rhizosphere depends on many factors such as soil type (Cao et al., 2016), soil pH (Rothstein, 2010), temperature, elevation, and analytical methods (Young et al., 1974; Chen et al., 2015). For instance, in many cases FAAs are lost by leaching the soil solution (Raab et al., 1996) or during the analytical procedures.

L-Isomeric amino acids and oligopeptides are the key nitrogen source for plants and have a significant effect on the soil organisms' dynamics, including bacteria and fungi (Jämtgård, 2010; Broughton et al., 2015). So far, there is neither any evidence that the hairy vetch root releases L-canavanine or similar non-proteinogenic amino acids, nor its effect on the soil organism is known. Understanding the hairy vetch root exudates components (i.e., L-canavanine) and their mechanism of action on the soil in organic farming practices is important due to the emerging food security issues caused by climate change.

In plants, seeds often contain a diverse range of compounds during germination that may impact the population and behavior of the soil microorganism in the soil or around the seed environment (Nelson, 2018).

It is well-known that plants often utilize a specific phenomenon called "allelopathy" to combat the competition and/or control their surrounding environment by releasing chemical(s) known as allelochemical (Rice, 2012). Allelochemical can be classified into different groups, including alkaloids, phenols, amino acids, peptides (Fujii and Hiradate, 2007; Rice, 2012), terpenes, ketones, aldehydes (Mardani et al., 2015, 2019), and water-soluble organic acids (Syed et al., 2014).

Also, certain amino acids act as allelochemical or are involved in chemotaxis (Fujii and Hiradate, 2007; Araya et al., 2014). Chemotaxis is a phenomenon by which the chemicals released from seeds stimulate the growth and trivial of the beneficial bacteria toward germinating seeds (Harborne et al., 1971; Peters et al., 1986; Barbour et al., 1991). The current and past trends in chemotaxis research in allelopathy have primarily focused on the major of compounds released from the seeds, including flavonoids, carbohydrates, etc. (Peters et al., 1986; Hartwig et al., 1991). However, the influence of seedling-released amino acids, specifically non-proteinogenic amino acids, on the SMC in organic cultivation practices is largely unexplored. Plants are a great source of proteinogenic or non-proteinogenic amino acids. The presence of non-proteinogenic amino acids is very common in the plant kingdom. In the Leguminosae family alone, over 60 non-proteinogenic amino acids have been isolated and identified (Bell et al., 1977). Plants use these amino acids to interact

with their surrounding environments. Several non-proteinogenic amino acids have been identified to protect plant seeds against insects. For example, L-3,4-dihydroxyphenylalanine (L-dopa) and 5-hydroxy-L-tryptophan are available in high concentrations in *Mucuna pruriens* and *Griffonia simplicifolia* and protect the seeds of these species against insect damage (Harborne et al., 1971; Bell et al., 1977; Fujii et al., 1992), although, L-dopa has long been known for its allelopathic activity against other plants (Fujii et al., 1992). Moreover, some of these amino acids are known to be toxic to other plants and other organisms (Nakajima et al., 2001), or act as nitrogen source for other plants and microbes.

Hairy vetch (*Vicia villosa* Roth subsp. *villosa*) is used as a cover crop or a green manure crop in Japanese orchards and rice fields due to several beneficial characteristics, from weed control to suppression of bacterial and fungal diseases (Fujii, 2003). Hairy vetch can control weeds by releasing cyanamide in the form of a volatile compound (Kamo et al., 2003). Kamo et al. later showed that the cyanamide is biosynthesized from amino acid L-canavanine, a non-proteinogenic amino acid present abundantly in hairy vetch seed and sprouts. L-Canavanine has been reported as one of the main allelochemicals of jack bean with plant inhibitory activity (Nakajima et al., 2001). Nakajima et al. (2001) also found that the suppression of the arginine metabolism in the plant is the main mechanism of the allelopathic activity of L-canavanine. Sasamoto et al. (2019) recently showed that the epicotyl protoplasts of hairy vetch contain high level of canavanine. We have also found that L-canavanine at 10 μ M suppressed the division of lettuce protoplasts, which was more severe than that of cyanamide (Sasamoto et al., 2019).

In this study, we aimed to know if the L-canavanine in the hairy vetch seeds could be released by seedling roots and influence the soil microbial community in the early stages of plant establishment. The findings would provide a better understanding of the reason for the accumulation of non-proteinogenic amino acid in the seeds and their role in plant interaction with microorganisms.

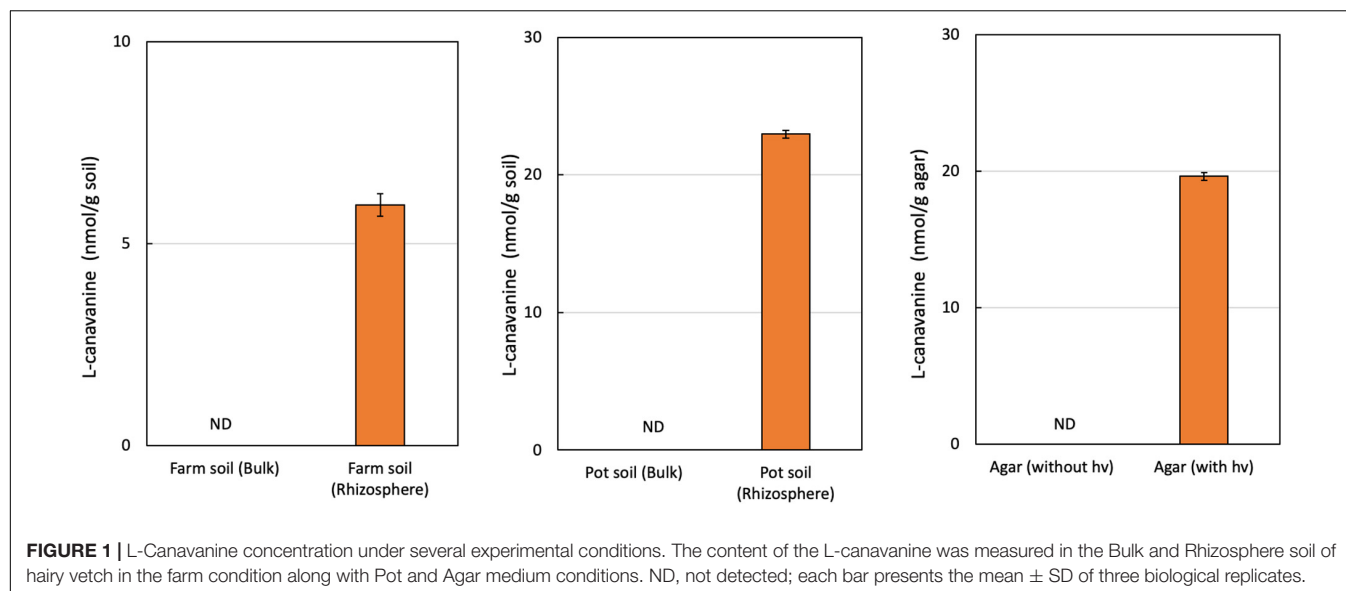
RESULTS

L-Canavanine Exudation From the Hairy Vetch Roots

We extracted FAAs from bulk soil and the rhizosphere of hairy vetch seedlings. Using GC-MS analysis, we detected an L-canavanine derivative only in the rhizosphere soil of both farm soil (8 nmol/g soil) and greenhouse (23 nmol/g soil), but not in the bulk soil. Our results indicated that L-canavanine is secreted from the hairy vetch roots into the rhizosphere soil in considerable amounts (**Figure 1**). We estimated the L-canavanine concentration in the farm and greenhouse condition (pots) to evaluate the exudation in different environments.

In the next step, by growing hairy vetch on agar medium, we validated that L-canavanine can be exuded by the hairy vetch root into the surrounding substrate.

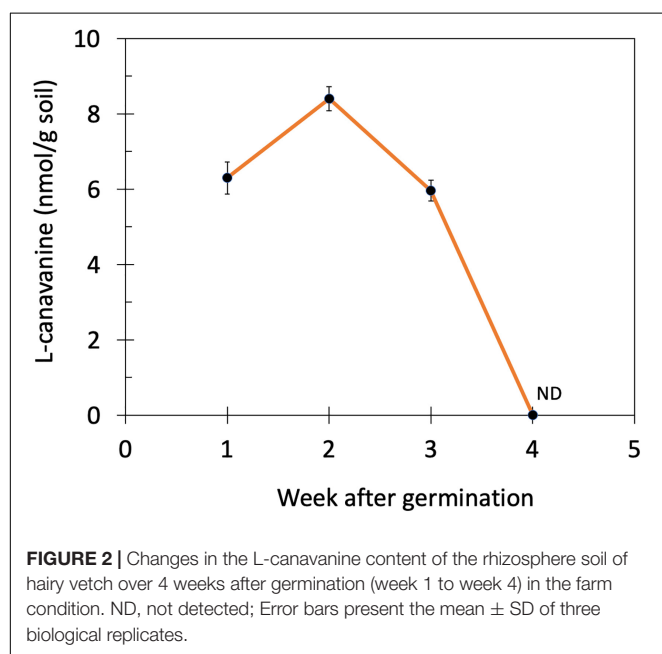
Subsequently, the changes in the L-canavanine content in the rhizosphere soil of hairy vetch were monitored over 4 weeks after germination and during the vegetative stage when plants were



7 cm (week 1), 10 cm (week 2), 15 cm (week 3), and 20 cm (week 4) height (**Figure 2**). The release of L-canavanine continued to increase in the rhizosphere as the seedling grew up to the 2nd week. After that, it started declining to an undetectable level on the 4th week (**Figure 2**).

The Effects of the L-Canavanine on the Soil Microbial Community Dynamics

We then examined the effect of L-canavanine concentrations (low, medium, and high) on SMC and predicted functional potentials of microbes by the 16S rRNA amplicon sequencing analysis. The microbiome analysis in this study showed that



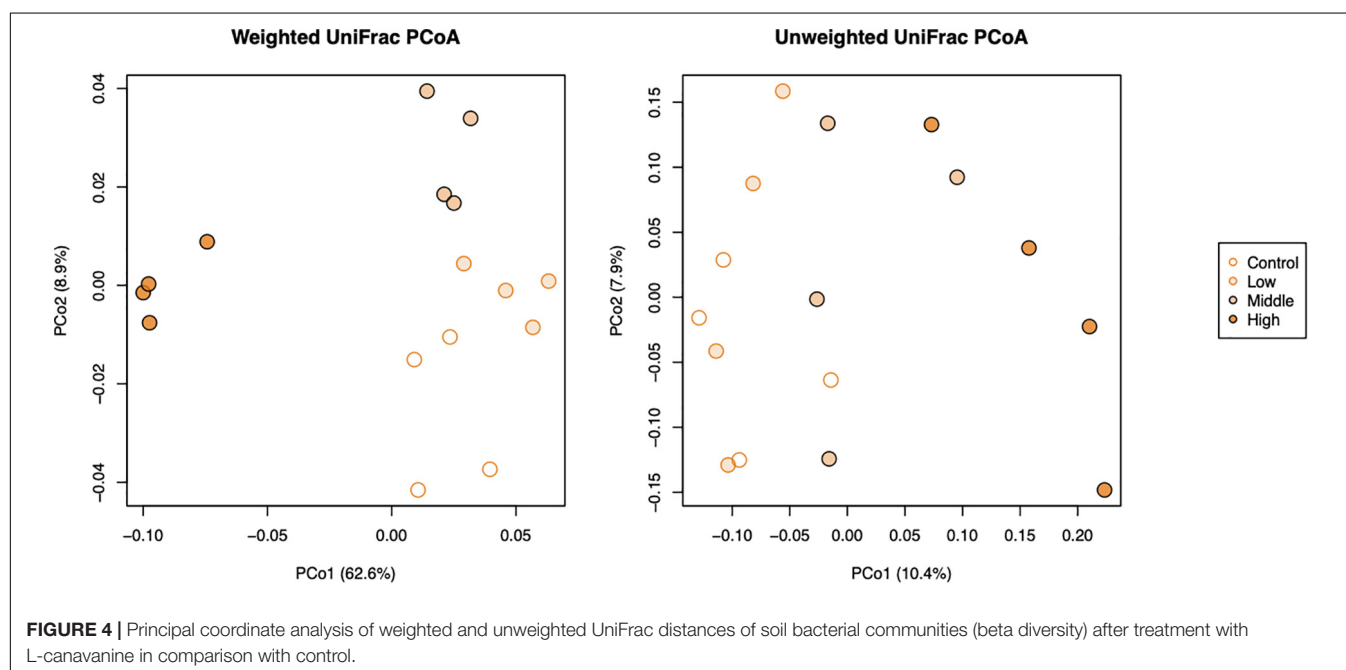
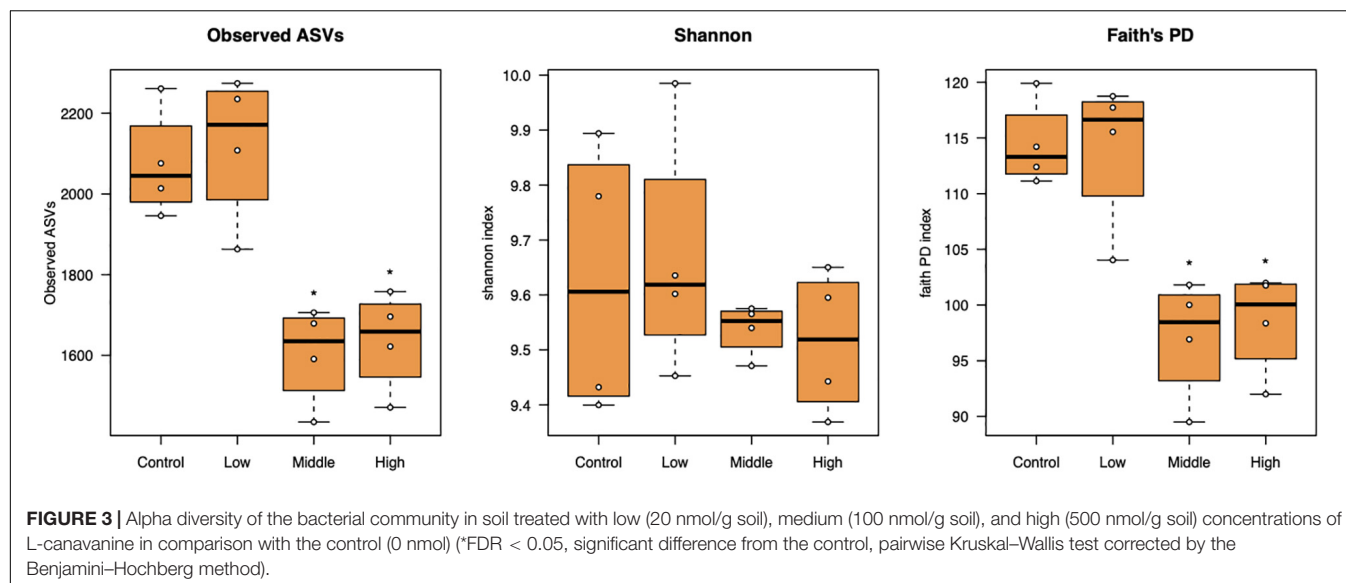
the addition of the L-canavanine in 0 (control), 20 (low), 100 (medium), and 500 (high) nmol/g soil concentrations changed the SMC. In comparison with the control, this effect of L-canavanine was more pronounced at high concentration (500 nmol/g soil). Although this concentration was high in the farm and pot soil, in this study, the microbiome analysis was only done for the incubation test and not for the rhizosphere soil of hairy vetch.

Bacterial alpha diversity as represented by the number of observed ASVs and Faith's phylogenetic diversity significantly decreased at the medium to high L-canavanine concentrations in soil, but the Shannon index did not show any significant changes (**Figure 3**).

The beta diversity of bacterial communities in different applied concentrations as displayed by principal coordinate analysis (PCoA) of weighted and unweighted UniFrac (WUF and UUF) distances revealed that L-canavanine had significant impact on microbiome community structure. Both WUF and UUF PCoA ordination plots showed that the community structure at the high concentration of L-canavanine was distinct from those at none to medium concentration on axis one (**Figure 4**). The permutational multivariate analysis of variance (PERMANOVA) based on WUF and UUF distances confirmed that community structures were significantly different among concentrations (WUF, $R^2 = 0.711$, $p < 0.001$; UUF, $R^2 = 0.229$, $p = 0.002$), and the WUF and UUF distances from the control were increased by L-canavanine addition in a dose-dependent manner (**Supplementary Figure 1**).

We noticed that the abundance of bacteria at the phylum level were notably different between the control (0 nmol/g soil) and high (500 nmol/g soil) concentration of L-canavanine (**Figure 5**). The relative abundance of Acidobacteria and Proteobacteria was low and Firmicutes and Actinobacteria were high at the high L-canavanine level.

After filtering low-abundant taxa (mean $< 0.05\%$), 176 taxa at the family level were used for the differential abundant



test between control and high L-canavanine treatment. The abundance of certain families differed and was more distinct between control and high concentration of L-canavanine. In particular, 12 taxa were enriched, while 10 others were depleted significantly at high L-canavanine treatment compared with the control (Figure 6). Of these, some taxa such as Micrococcaceae and Intrasporangiaceae, showed concentration-dependent enrichment, and some taxa in Acidobacteria and Sphingomonadaceae showed concentration-dependent depletion. In addition, at the family level, Bacillaceae and Micrococcaceae families were most dominant after application of L-canavanine, and their abundance increased significantly (Figure 6).

Prediction of Metagenome Functions From 16S Amplicon Data

We used PICRUSt2 to predict the metagenome functions based on the 16S amplicon sequences (Douglas et al., 2020). Soil treatment with L-canavanine caused extensive changes in the function of the soil metabolic pathways. A total of 439 pathways were predicted, and differential abundant test was performed between control (0 nmol, not affected) and high concentrations of L-canavanine (500 nmol/g soil, most affected) using the ANOVA-like differential expression (ALDEx2) analysis (Fernandes et al., 2013, 2014). ALDEx2 analysis indicated that 65 pathways were significantly enriched while 67 pathways were significantly depleted after soil inoculation with L-canavanine

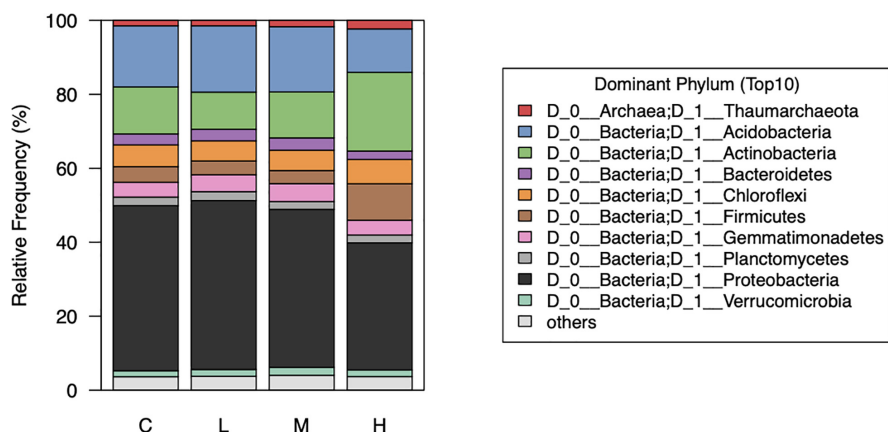


FIGURE 5 | Relative abundance of the top 10 dominant soil bacterial taxa at phylum level after treatment with low, medium, high, and control (0) concentrations of L-canavanine.

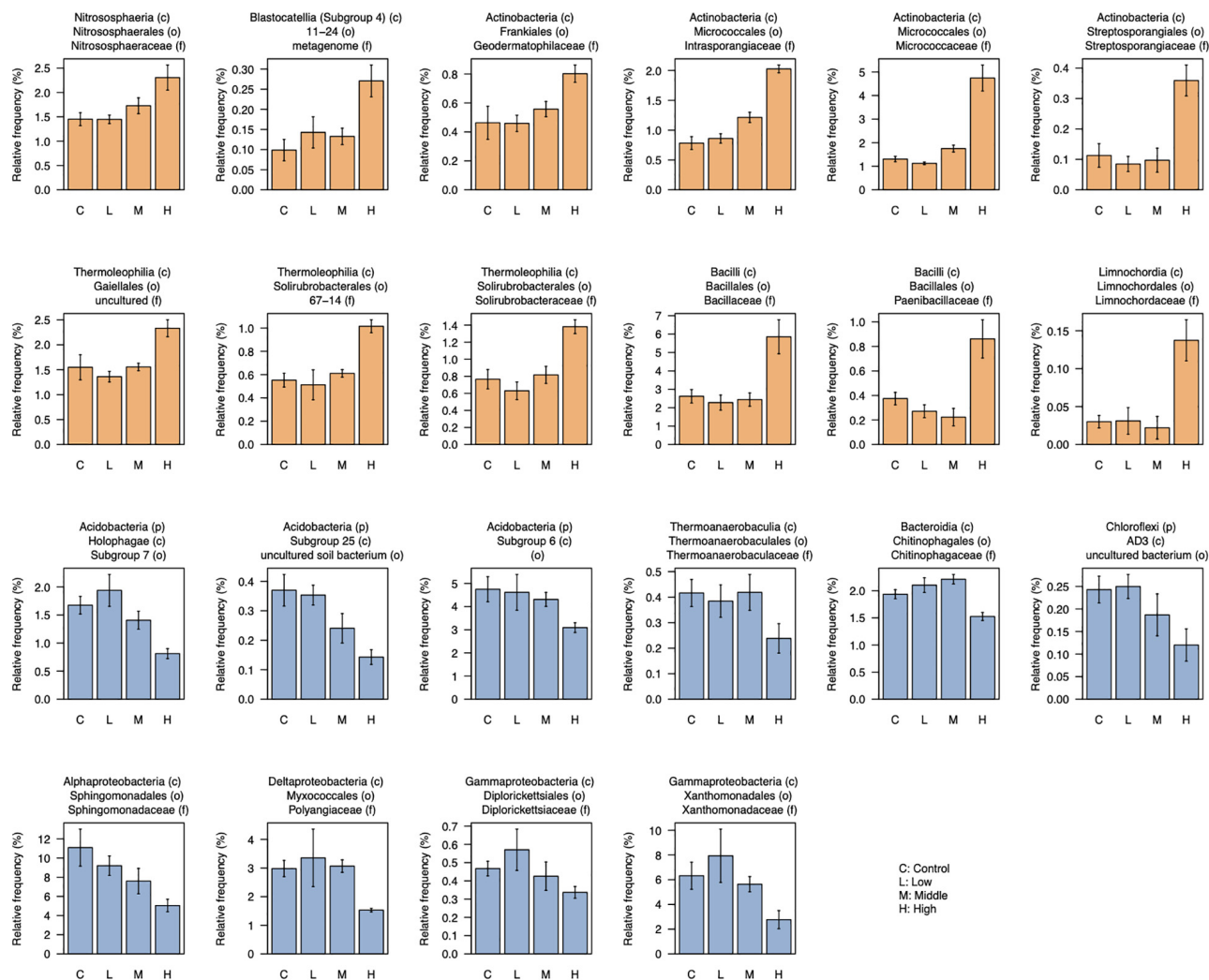


FIGURE 6 | Relative abundance of taxa (family level) that were differentially abundant between control and high concentration of L-canavanine. The 12 taxa were significantly enriched (orange bar), and 10 taxa were significantly depleted (blue bar) after treatment with L-canavanine (FDR < 0.05, Welch's *t*-test corrected by the Benjamini–Hochberg method).

(**Figures 7A,B** and **Supplementary Figure 2**). The heatmap of the fold changes of the pathways affected by L-canavanine indicated that most affected metabolic pathways related to compounds used or produced in the carbon cycle such as “starch degradation III,” “glyoxylate assimilation” (a process that allows bacteria to produce 3-hydroxypropionate utilizing in carbon dioxide) were depleted (**Figure 7B**). Our observation showed that “glucose degradation (oxidative)” pathway along with the major metabolic pathways related to compounds used or produced during the degradation of amino acids including “creatine degradation I,” “L-glutamate degradation VII (to propanoate),” “superpathway of ornithine degradation,” and “L-arginine degradation (Stickland reaction)” was significantly enriched when L-canavanine was added to the soil (**Figure 7A**).

DISCUSSION

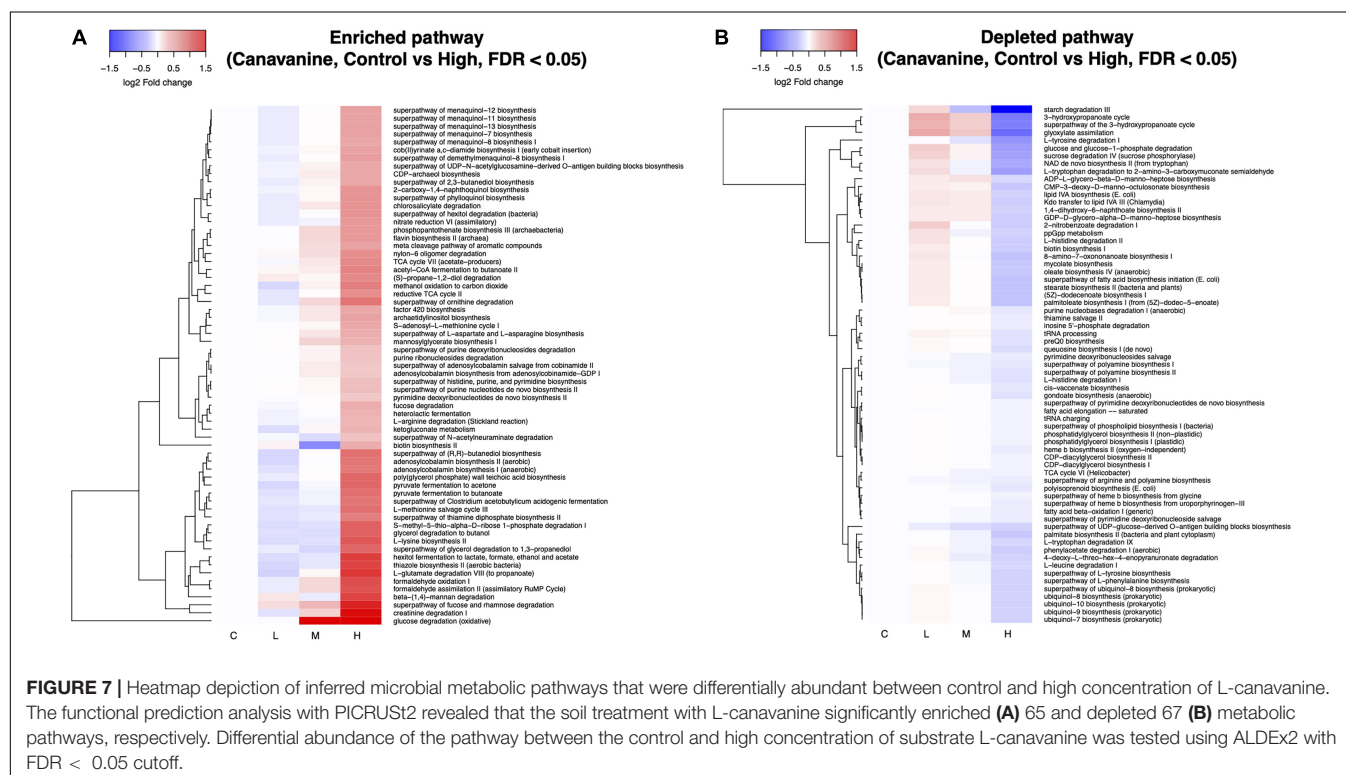
Amino acids are released from the plant roots and serve numerous purposes. The exudation of proteinogenic FAAs from plants affects SMC and characteristics (Moe, 2013). They are released in different types and quantities depending on the plant species and environmental factors (Cao et al., 2016). Studies on the concentration of the FAAs in the soil have been reported (Raab et al., 1996, 1999; Fernández-Aparicio et al., 2017).

To examine the role of root exudated amino acids on soil nitrogen budget and microbiome, the influence of numerous factors such as the availability and ease of uptake by the plant root system needs to be considered (Schulten and Schnitzer, 1997). Thus, in this study we only focused on the exudation of

L-canavanine from hairy vetch root. The observed differences between the pot and field conditions at the same vegetative stages could be due to the difference in the soil parameters, temperature, and environmental condition (Dennis et al., 2019). Also, seasonal precipitation in field soil could be a reason for lower detection of L-canavanine. We sampled the field soil when temperature fluctuates over the months and might affect the biological activity in the soil. Similar to our observation regarding the decline in L-canavanine in the soil, diminution in the concentration of FAAs over the growing season and also during the warmer sessions due to the high underground completion for nitrogen among the plant roots and microorganisms have been reported (Weintraub and Schimel, 2005). Rapid degradation of soil amino acids by SMC has been demonstrated (Jones et al., 2005; Apostel et al., 2013). There is also a possibility for increase in the population SMC capable of utilizing L-canavanine. Although L-canavanine exists in many legume species, its exudation mechanism and its effect on the soil is unknown.

L-Canavanine is known as a natural insecticide. Its analogous structure to L-arginine can interfere with L-arginine metabolism in plants and animals and, therefore, incorporate in *de novo* proteins and result in protein malfunctions (Mitri et al., 2009).

Previously, L-canavanine was found in the young root of the germinating hairy vetch seeds (Kamo et al., 2015). Kamo et al. (2015) also showed that the L-canavanine content in the hairy vetch root declines over several days after seed germination and it converts to “cyanamide,” the major allelochemical of hairy vetch. L-canavanine likely influences the interaction of hairy vetch with surrounding organisms in the soil, including SMC by limiting or stimulating the growth of selected bacteria. Similar to



the 20 canonical proteinogenic amino acids, L-canavanine also contribute to the formation of the soil microbial community that is important in the robustness of the soil.

In our study, hairy vetch grown in *in vitro* agar medium also released L-canavanine through the root system. The seed coats and cotyledons were not in direct contact with the agar medium surface due to the suspended seed culture system, and therefore, the L-canavanine found in the agar medium was directly secreted from the roots and accumulated in the medium.

However, we still do not know if soil bacteria can use L-canavanine as a source of nitrogen. Although there are several reports on the effect of amino acids on SMC, such as disassembly of *Bacillus* species (Aliashkevich et al., 2018), the role of combination and/or single amino acid on the formation of the SMC have not been well studied.

In the agricultural system, any external nutrient sources such as added amino acid from plant roots, or composts have a much shorter lifespan in the soil and therefore may have shorter effect on SMC in comparison with the added agrochemicals (Perez et al., 2015).

Changes in the Soil Bacterial Dynamics Caused by L-Canavanine

To this date, changes in the SMC by a single non-proteinogenic have not been previously observed. It is known that certain proteinogenic amino acid substrate in the soil increases the microbial biomass yield (Vinolas et al., 2001).

It has also been reported that the L-canavanine acts as an inhibitor of bacteria in the seed surroundings of alfalfa (Emmert et al., 1998) to increase the seed chance of survival. Emmert et al. (1998) also observed the selective effect of L-canavanine on different *Bacillus* sp. *in vitro*. L-canavanine has also been found to be incorporated into the antimicrobial protein in insect and reduced their effects (Rosenthal et al., 1989). This malfunction often happens because the arginyltRNA synthetase can discriminate between L-canavanine and L-arginine during the protein synthesis (Bence and Crooks, 2003).

Alpha diversity measures, such as Faith's PD index revealed that SMC diversity was significantly lower in applied 100 and 500 nmol/g soil concentrations than control. Increased soil L-canavanine content may reduce the presence of microbial taxa with low abundance in each sample. This could mean L-canavanine may only be consumed by specific taxa, and it may be an inhibitor for the others. Meanwhile, results showed that dissimilarities of the bacterial community increased with an increase in used concentration of the L-canavanine, indicating that the difference of communities between the control and 500 nmol/g soil L-canavanine in the soil increases with the increase in L-canavanine exudation.

Based on their phylogenetic coverage, it appears that Acidobacteria and Proteobacteria phyla are metabolically diverse. Similarly, it is clear that detailed and functional descriptions of Acidobacteria in the soil are important (Kielak et al., 2016). Proteobacteria are capable of transporting a diverse range of substrates including amino acids, carbohydrate, peptides, siderophores, cation, and anions (Rawat et al., 2012;

Kielak et al., 2016). The α - and β -Proteobacteria are known to be highly capable of the catabolizing D- and L-amino acids as the source of carbon and nitrogen in the soil (Radkov et al., 2016).

Actinobacteria are involved in the important soil ecosystem cycles, such as carbon, nitrogen, phosphorus, and several other nutrients cycling in the soil (Hill et al., 2011; Zhang et al., 2019). It is not clear why L-canavanine increased the population of the Actinobacteria, but it can be speculated that L-canavanine may increase some Actinobacteria and, as a result, regulate the production of secondary metabolites (enzymatic inhibition during the carbon, nitrogen pathways) (Hill et al., 2011) and loss of nutrients in the early stages of hairy vetch growth.

Bacillaceae family is one of the most abundant microorganisms in the soil and plays an important role in many biological phenomena. They confer health benefits to crop plants and therefore are known as plant growth-promoting rhizobacteria (PGPR) (Fan et al., 2018; Saxena et al., 2020). It can be speculated that hairy vetch might also release L-canavanine at the beginning of seedlings' lifecycle in order to increase or control the number of PGPR such as *Bacillus* to the benefit of the seedlings, which also might be related to the selective role of L-canavanine in inhibition or promotion of bacteria. Similarly, several bacteria taxa and families decreased or increased in lower magnitudes by application of L-canavanine, which also might be due to the same phenomenon.

PICRUSt2 and Prediction of Metagenome Functions From 16S Amplicon Data

The reason behind why bacteria uptake and at the same time utilize the nutrient (i.e., amino acids) in complex rich soil ecosystems is still unknown. Yet, it is known that bacteria can change their role in resolving regulatory decisions for uptake and catabolism of alternative carbon sources by inhibition of phosphotransferase system (PTS), and catabolism of alternative carbon sources when they have excess uptake of certain amino acids (Zampieri et al., 2019).

These are a continuous chain pathway related to the superpathway of ornithine that participates in the conversion of the amino acids L-arginine and L-ornithine to the polyamine putrescine in organisms. These will then subsequently be degraded to 4-aminobutanoate, and then convert to 4-aminobutanoate and finally succinate. The succinate is fed into the TCA cycle and energy cycle (Kashiwagi et al., 1991; Kurihara et al., 2005). It might be possible that because L-canavanine is structurally analogous to L-arginine, it might be affected by the similar soil metabolite degradation pathway.

Similarly, the results of this study also showed that L-canavanine changes the catabolism pathways of carbon sources in the soil total metabolite pathway (Figure 7). This might be the case for the hairy vetch strategy by releasing L-canavanine from the root and therefore inhibition of the SMC from consuming the carbon sources (i.e., glucose oxidative degradation pathway). Changes in the glyoxylate cycle in this study due to L-canavanine might help bacteria in energy production and biosynthesis of carbon structure, and therefore, depletion of these pathways

might limit the growth of some competing species (Berg et al., 2002) that may benefit the hairy vetch seedlings.

CONCLUSION

Our results again highlighted the potential allelopathic effect of the hairy vetch, but this time through its root exudates. It is clear from the outcome of the present study that the exudation of non-proteinogenic amino acid L-canavanine from the root of hairy vetch occurs in the natural field condition. The soil microbial diversity was affected by the L-canavanine as well as the specific microbial populations. We also predict that root exudated L-canavanine can influence the kinetics and patterns of depletions of hydrocarbon degradation and amino acid such as arginine and ornithine degradation pathway. Thus, the underlying mechanism of L-canavanine exudation from the root and in which soil microorganism being affected by L-canavanine in rhizosphere soils needs more attention and is of significant interest for predicting the soil robustness, and organic culture practices.

MATERIALS AND METHODS

Plant Materials and Farm Experimental Design

Pot Experiment

Seeds of hairy vetch (*V. villosa*, Roth subsp. *villosa*) were purchased from Takii, Japan, and were grown in a plastic container (20 cm × 20 cm × 60 cm) holding 20 L of commercial soil (Kumiai Nippi Engei Baido No. 1, Zen-Noh Co., Tokyo, Japan) and then were allowed to grow in the greenhouse. After plants reached 20-cm height (3 weeks after germination), 10 plants were gently removed from the pots and placed on a clean plastic sheet. Roots were shaken vigorously to remove any excess soil or organic material. To collect the Rhizosphere soil (Rh), soil adhered to the root were gently brushed off on a clean paper using a clean brush (Daiso Co., Japan). The collected soils were then passed through a 2 mm × 2-mm mesh to remove any excess material and gravels. Bulk soil was collected from plots without cultivation of hairy vetch.

Farm Experiment

For the field experiment, hairy vetch seeds were planted in the field (Tokyo University of Agriculture and Technology, TUAT) from November 2017 to February 2018 and were allowed to grow until the upper part of the plant reach 20 cm (vegetative stage). The soil type in the TUAT field was andosol, and no irrigation system was used during the experiment. Ten healthy plants were dug out using a shovel and placed in a plastic bag in a cool box containing dry ice. The rhizosphere soil was collected as described above after transporting the plants to the laboratory. Bulk soil was collected from the plots with no hairy vetch cultivation. Mineral contents in the farm soil were measured using a set of small-scale protocols for analyzing the nutrient

minerals of small soil samples as described previously (Yamazaki et al., 2019; **Supplementary Table 1**).

Agar Medium Experiment for Validation of Root Exudation of L-Canavanine

To validate that L-canavanine is released from the root of the hairy vetch and not leached from the seed coat or seed itself, we designed a validation step. In this step, some seeds were surface sterilized using sodium hypochlorite (0.1%, 10 min) and washed with distilled autoclaved water (3-times, 5 min). Ten sterilized seeds were then placed on the top of sterile stands made of aluminum foils to keep 0.5 cm distance from the medium surface in 500 ml beakers containing 60 ml agar medium (pH 8.5). This step was to make sure exudation will not occur from the seed coat. After about 3 weeks, all plants were harvested, and the root and shoots were separated and kept in −80°C for the extraction of amino acids. Moreover, the agar medium was extracted using 80% ethanol immediately for the amino acid analysis step.

Amino Acid Extraction

Free amino acids were extracted based on the previously established method (Tsuchiya et al., 2013). The amount of 1 g of soil was extracted three times with 80% (v/v) aqueous ethanol (pH adjusted to 3.0 with HCl) at 60°C. This step was to remove most of the extractable amino acid, which is easily available for plant root and other organisms. Combined fractions were evaporated to dryness using a vacuum centrifugal evaporator (CVE-3100; EYELA, Tokyo, Japan), equipped with a cold glass trap (Uni trap UT-1000; EYELA).

Gas Chromatography-Mass Spectroscopy Analysis of L-Canavanine

For gas chromatography-mass spectrometry (GC-MS), the residues were dissolved in low pH pure water (pH 3.0 adjusted with HCl). To derivatized the amino acids, EZ:Faast GC-MS kit (Phenomenex Inc., Torrance, CA, United States) was used and the standard L-canavanine (M9P5344; Nacalai tesque, Kyoto, Japan) with propyl chloroformate, following the original protocol provided in the kit. The GC-MS system (Shimadzu QP2010) supplied with helium as carrier gas (He, purity 99.999%, Tanaka, Japan) analysis was performed using a gas chromatograph coupled to a mass spectrometer. The oven temperature program was designated as follows: initial temperature 110°C raised to a final temperature of 320°C at 30°C min^{−1}. The injection port temperature was adjusted to 250°C. The temperatures of the ion source were 240°C, quadrupole 180°C, and auxiliary at 310°C. A 1.5 µl sample was injected in split mode (1:15). The flow rate was kept at 1.1 ml min^{−1}. The MS scan range was adjusted from 45 to 450 m/z. The data of two to three separately extracted samples were expressed as averages with SD. The outputs of GC-MS and chromatogram are shown in **Supplementary Figure 3**. Moreover, L-canavanine recovery rate of the pot and farm soil was calculated by adding 500 nmol L-canavanine to 1 g of soil and extracting the mixture. GC-MS analysis results revealed that the recovery rate for pot and farm soil were 42 and 40%, respectively (**Supplementary Table 2**). Studies have shown the recovery of amino acids from hydroponic set ups used in biology

is considered about 70–100% (Persson and Näsholm, 2001; Inoue et al., 2015).

Soil-L-Canavanine Incubation Experiment

To simulate the effect of canavanine on the soil bacteria, different concentrations of L-canavanine [0 (control), 20 (low), 100 (medium), and 500 (high) nmol] was added to 1 g of the filed soil samples in a 5-ml falcon tube. Four replicants for each treatment was made. Samples were then incubated at 25°C for 15 days. L-canavanine treatment was repeated three times during the incubation period. Soil bacterial DNA extraction was performed at the end of the incubation time.

Soil DNA Extraction and Bacteria DNA Sequencing

DNeasy PowerSoil Kit (QIAGEN, Hilden, Germany) was used to extract the soil DNA from 250 mg of the soil samples. To crush soil bacterial cells, a milling machine was used. The quantity of the extracted DNA was evaluated by QuantusTM Fluorometer and QuantiFluor[®] Dyes (Promega Corporation, Madison, CA) and stored at 80°C until use.

Polymerase chain reaction (PCR) amplification of the V4 region of 16S rRNA genes was performed following previously described method (Okutani et al., 2020). The 25- μ l reaction mixture contained 1 ng of template DNA, 0.3 μ l of KOD FX neo (Toyobo, Osaka, Japan), 12.5 μ l of buffer (provided with the polymerase), 5 μ l of dNTPs (2 mM), and 0.75 μ l of 515F (5'-ACACTCTTTCCCTACACGACGCTCTTCCGATCT-GTGCCAGCMGCCGCGGTAA-3') and 806R (5'-GTGACTGGAGTTCAGACGTGTGCTCTTCCGATCT-GGACTACHVGGGTWTCTAAT-3') primers. PCR conditions were as follows: initial denaturation at 94°C for 2 min, 22 cycles at 98°C for 10 s, 50°C for 30 s, and 68°C for 30 s. The PCR products were purified using AMPure XP magnetic beads (Beckman-Coulter, Indianapolis, IN, United States). For the amplification of bacterial endophytic DNA, 2.5 pmol μ l peptide nucleic acid (PNA, Fasmac Co., Ltd., Kanagawa, Japan) were added to the reaction mixture to avoid the amplification of root mitochondrial.

To attach MiSeq adaptors for both bacterial and fungi sequences, the second round of PCR was performed in a 25 μ l reaction mixture containing 2 μ l template DNA (purified 1st PCR product), 0.3 μ l of KOD FX neo (Toyobo, Osaka, Japan), 12.5 μ l of buffer (provided with the polymerase), and 0.75 μ l of primers provided with Fasmac Co., Ltd. The second PCR products were purified using AMPure XP magnetic beads and confirmed by electrophoresis on 1.5% agarose gels. The DNA concentration was measured using the QuantusTM Fluorometer and QuantiFluor Dyes[®] (Promega Corporation, Madison, CA) according to the protocol of the manufacturer. Illumina MiSeq platform (2 \times 250 bp) was used for the amplicon sequencing of V4 region that was outsourced to Fasmac Co., Ltd. (Kanagawa, Japan). Sequence data have been deposited in the DDBJ (DNA Data

Bank of Japan) Sequence Read Archive under the accession number DRA012221.

The sequences were processed and analyzed using the QIIME2 pipeline (version 2019.10) (Bolyen et al., 2019). Raw fastq files were imported into QIIME2, and paired-end sequences were trimmed at first 20 bases, truncated at 200 bases from the start, quality filtered, denoised, and merged using DADA2 (Callahan et al., 2016) with the q2-dada2 plugin in QIIME2. Multiple alignments of the representative sequences were performed using the MAFFT program, and a phylogenetic tree was generated with the FastTree program in the q2-phylogeny plugin (Price et al., 2009; Katoh and Standley, 2013). Taxonomy was assigned to the sequences using the q2-feature-classifier plugin and a Naive Bayes classifier, which was pre-trained on operational taxonomic units (99% identity) from 515F/806R region of sequences on the SILVA rRNA gene database release 132 (Quast et al., 2013; Bokulich et al., 2018). After the DADA2 process, 98,696–198,196 reads per sample were obtained, representing 10,310 ASVs, and they were normalized by rarefaction to 98,000 reads for diversity analysis (Supplementary Figure 4). Alpha and beta diversity analysis was performed using the core-metrics-phylogenetic pipeline in the q2-diversity plugin within QIIME2 to calculate Shannon's diversity index, observed ASVs, Faith's phylogenetic diversity, and Evenness for alpha diversity. It also computes Jaccard, Bray–Curtis, and weighted and unweighted UniFrac distances for beta diversity, and generates PCoA plots for each beta diversity metrics. Association between categorical metadata groups and alpha diversity metrics were tested by Kruskal–Wallis and corrected by the Benjamini–Hochberg method, and that for beta diversity were analyzed by PERMANOVA using the R software packages stats and vegan (Oksanen et al., 2015). Differential abundant test for bacterial taxa at the family level was performed using Welch's *t*-test corrected by the Benjamini–Hochberg method with an FDR cutoff of 0.05. To identify differential abundant metabolic pathways, we used the R software package ALDEx2 (Fernandes et al., 2013, 2014) with an FDR cutoff of 0.05.

Data Visualization

Figures in the current work are drawn using the R packages gplots (Warnes et al., 2020) and beeswarm (Eklund, 2016), and statistical analyses were done using R software.

DATA AVAILABILITY STATEMENT

The original contributions presented in the study are included in the article/Supplementary Material, further inquiries can be directed to the corresponding authors.

AUTHOR CONTRIBUTIONS

HM-K, SY, MN, TM, YF, RK, AS, and NO-O conceived and designed the experiments. HM-K, MK, MN, and YO performed the experiments. SY, HM-K, and YA analyzed the data. HM-K,

SY, MN, YF, RK, AS, NO-O, and YO wrote the manuscript with input from all authors.

FUNDING

This study was supported, in part, by grants from JST-CREST (JPMJCR17O2), from the Research Institute for Sustainable Humanosphere (Mission 5-1) and supported by the Grants-in-Aid for Scientific Research, Fostering Joint International

Research (B) (20KK0136) KAKENHI from the Japan Society for the Promotion of Science.

SUPPLEMENTARY MATERIAL

The Supplementary Material for this article can be found online at: <https://www.frontiersin.org/articles/10.3389/fmicb.2021.701796/full#supplementary-material>

REFERENCES

- Aliashkevich, A., Alvarez, L., and Cava, F. (2018). New insights into the mechanisms and biological roles of D-amino acids in complex eco-systems. *Front. Microbiol.* 9:683. doi: 10.3389/fmicb.2018.00683
- Apostel, C., Dippold, M., Glaser, B., and Kuzyakov, Y. (2013). Biochemical pathways of amino acids in soil: assessment by position-specific labeling and 13C-PLFA analysis. *Soil Biol. Biochem.* 67, 31–40. doi: 10.1016/j.soilbio.2013.08.005
- Araya, H., Nagai, Y., and Otaka, J. (2014). Isolation of (2S,4R)-2-amino-4-methylhex-5-enoic acid, a nonprotein amino acid, as an allelochemical from the fruiting bodies of *Boletus fraternus* Peck. *J. Plant Interact.* 9, 627–631. doi: 10.1080/17429145.2014.880135
- Barbour, W. M., Hattermann, D. R., and Stacey, G. (1991). Chemotaxis of *Bradyrhizobium japonicum* to soybean exudates. *Appl. Environ. Microbiol.* 57, 2635–2639. doi: 10.1128/aem.57.9.2635-2639.1991
- Bell, E. A., Qureshi, M. Y., Charlwood, B. V., Pilbeam, D. J., and Evans, C. S. (1977). "The variability of free amino acids and related compounds in legume seeds," in *Genetic Diversity in Plants*, eds A. Muhammed, R. Aksel, and R. C. von Borstel (Boston, MA: Springer), 397–412.
- Bence, A. K., and Crooks, P. A. (2003). The mechanism of L-canavanine cytotoxicity: arginyl tRNA synthetase as a novel target for anticancer drug discovery. *J. Enzyme Inhib. Med. Chem.* 18, 383–394. doi: 10.1080/1475636031000152277
- Berg, J. M., Tymoczko, J. L., and Stryer, L. (2002). *Biochemistry*. Available online at: <http://catalog.hathitrust.org/api/volumes/oclc/48055706.html>
- Bokulich, N. A., Kaehler, B. D., Rideout, J. R., Dillon, M., Bolyen, E., Knight, R., et al. (2018). Optimizing taxonomic classification of marker-gene amplicon sequences with QIIME 2's q2-feature-classifier plugin. *Microbiome* 6, 1–17. doi: 10.1186/s40168-018-0470-z
- Bolyen, E., Rideout, J. R., Dillon, M. R., Bokulich, N. A., Abnet, C. C., Al-Ghalith, G. A., et al. (2019). Reproducible, interactive, scalable and extensible microbiome data science using QIIME 2. *Nat. Biotechnol.* 37, 852–857. doi: 10.1038/s41587-019-0209-9
- Broughton, R. C. I., Newsham, K. K., Hill, P. W., Stott, A., and Jones, D. L. (2015). Differential acquisition of amino acid and peptide enantiomers within the soil microbial community and its implications for carbon and nitrogen cycling in soil. *Soil Biol. Biochem.* 88, 83–89. doi: 10.1016/j.soilbio.2015.05.003
- Callahan, B. J., McMurdie, P. J., Rosen, M. J., Han, A. W., Johnson, A. J. A., and Holmes, S. P. (2016). DADA2: high-resolution sample inference from Illumina amplicon data. *Nat. Methods* 13, 581–583.
- Canarini, A., Kaiser, C., Merchant, A., Richter, A., and Wanek, W. (2019). Root exudation of primary metabolites: Mechanisms and their roles in plant responses to environmental stimuli. *Front. Plant Sci.* 10:157. doi: 10.3389/fpls.2019.00157
- Cao, X., Ma, Q., Zhong, C., Yang, X., Zhu, L., Zhang, J., et al. (2016). Elevational variation in soil amino acid and inorganic nitrogen concentrations in Taibai Mountain, China. *PLoS One* 11:e0157979.
- Chen, J., Zelikova, T. J., Pendall, E., Morgan, J. A., and Williams, D. G. (2015). Daily and seasonal changes in soil amino acid composition in a semiarid grassland exposed to elevated CO₂ and warming. *Biogeochemistry* 123, 135–146.
- Dennis, P. G., Newsham, K. K., Rushton, S. P., O'Donnell, A. G., and Hopkins, D. W. (2019). Soil bacterial diversity is positively associated with air temperature in the maritime Antarctic. *Sci. Rep.* 9, 1–11. doi: 10.1038/s41598-019-39521-7
- Douglas, G. M., Maffei, V. J., Zaneveld, J. R., Yurgel, S. N., Brown, J. R., Taylor, C. M., et al. (2020). PICRUST2 for prediction of metagenome functions. *Nat. Biotechnol.* 38, 685–688. doi: 10.1038/s41587-020-0548-6
- Eklund, A. (2016). *The Bee Swarm Plot, An Alternative to Stripchart*. Available online at: <https://cran.r-project.org/web/packages/beeswarm/index.html> (accessed September 10, 2021).
- Emmert, E. A. B., Milner, J. L., Lee, J. C., Pulvermacher, K. L., Olivares, H. A., Clardy, J., et al. (1998). Effect of canavanine from alfalfa seeds on the population biology of *Bacillus cereus*. *Appl. Environ. Microbiol.* 64, 4683–4688.
- Fan, B., Wang, C., Song, X., Ding, X., Wu, L., Wu, H., et al. (2018). *Bacillus velezensis* FZB42 in 2018: the gram-positive model strain for plant growth promotion and biocontrol. *Front. Microbiol.* 9:2491.
- Fernandes, A. D., Macklaim, J. M., Linn, T. G., Reid, G., and Gloor, G. B. (2013). ANOVA-like differential expression (ALDEx) analysis for mixed population RNA-Seq. *PLoS One* 8:7019. doi: 10.1371/journal.pone.0067019
- Fernandes, D., Ma, B., Gajer, P., Sengamalai, N., Ott, S., Brotman, R. M., et al. (2014). Unifying the analysis of high-throughput sequencing datasets: characterizing RNA-seq, 16S rRNA gene sequencing and selective growth experiments by compositional data analysis. *Microbiome* 2, 1–13. doi: 10.1186/2049-2618-2-15
- Fernández-Aparicio, M., Bernard, A., Falchetto, L., Marget, P., Chauvel, B., Steinberg, C., et al. (2017). Investigation of amino acids as herbicides for control of orobanche minor parasitism in red clover. *Front. Plant Sci.* 8:842. doi: 10.3389/fpls.2017.00842
- Fujii, Y. (2003). Allelopathy in the natural and agricultural ecosystems and isolation of potent allelochemicals from Velvet bean (*Mucuna pruriens*) and Hairy vetch (*Vicia villosa*). *Biol. Sci. Sp.* 17, 6–13. doi: 10.2187/bss.17.6
- Fujii, Y., and Hiradate, S. (2007). *Allelopathy: New Concepts & Methodology*. Boca Raton, FL: CRC Press.
- Fujii, Y., Shibuya, T., and Yasuda, T. (1992). Allelopathy of velvetbean: its discrimination and identification of L-DOPA as a candidate of allelopathic substances. *JARQ. Japan Agric. Res. Q.* 25, 238–247.
- Harborne, J. B., Boulter, D., and Turner, B. L. (1971). *Chemotaxonomy of the Leguminosae*. New York, NY: Academic Press.
- Hartwig, U. A., Joseph, C. M., and Phillips, D. A. (1991). Flavonoids released naturally from alfalfa seeds enhance growth rate of *Rhizobium meliloti*. *Plant Physiol.* 95, 797–803. doi: 10.1104/pp.95.3.797
- Hill, P., Kristófek, V., Dijkhuizen, L., Boddy, C., Kroetsch, D., and van Elsas, J. D. (2011). Land use intensity controls actinobacterial community structure. *Microb. Ecol.* 61, 286–302. doi: 10.1007/s00248-010-9752-0
- Hu, L., Robert, C. A. M., Cadot, S., Zhang, X., Ye, M., Li, B., et al. (2018). Root exudate metabolites drive plant-soil feedbacks on growth and defense by shaping the rhizosphere microbiota. *Nat. Commun.* 9, 1–13. doi: 10.1038/s41467-018-05122-7
- Inoue, A., Ogita, S., Tsuchiya, S., Minagawa, R., and Sasamoto, H. (2015). A protocol for axenic liquid cell cultures of a woody leguminous mangrove, *Caesalpinia crista*, and their amino acids profiling. *Nat. Prod. Commun.* 10, 755–760. doi: 10.1177/1934578x1501000514
- Jämtgård, S. (2010). *The Occurrence of Amino Acids in Agricultural Soil and their Uptake by Plants*. Doctoral thesis. Umeå: Acta Universitatis Agriculturae Sueciae.
- Jones, D. L., Kemmitt, S. J., Wright, D., Cuttle, S. P., Bol, R., and Edwards, A. C. (2005). Rapid intrinsic rates of amino acid biodegradation in soils are unaffected by agricultural management strategy. *Soil Biol. Biochem.* 37, 1267–1275.
- Kamo, T., Hiradate, S., and Fujii, Y. (2003). First isolation of natural cyanamide as a possible allelochemical from hairy vetch *Vicia villosa*. *J. Chem. Ecol.* 29, 275–283. doi: 10.1023/A:1022621709486

- Kamo, T., Sakurai, S., Yamanashi, T., and Todoroki, Y. (2015). Cyanamide is biosynthesized from L-canavanine in plants. *Sci. Rep.* 5:10527. doi: 10.1038/srep10527
- Kashiwagi, K., Suzuki, T., Suzuki, F., Furuchi, T., Kobayashi, H., and Igarashi, K. (1991). Coexistence of the genes for putrescine transport protein and ornithine decarboxylase at 16 min on *Escherichia coli* chromosome. *J. Biol. Chem.* 266, 20922–20927. doi: 10.1016/s0021-9258(18)54798-0
- Katoh, K., and Standley, D. M. (2013). MAFFT multiple sequence alignment software version 7: improvements in performance and usability. *Mol. Biol. Evol.* 30, 772–780. doi: 10.1093/molbev/mst010
- Kielak, A. M., Barreto, C. C., Kowalchuk, G. A., van Veen, J. A., and Kuramae, E. E. (2016). The ecology of Acidobacteria: Moving beyond genes and genomes. *Front. Microbiol.* 7:1–16. doi: 10.3389/fmicb.2016.00744
- Kurihara, S., Oda, S., Kato, K., Kim, H. G., Koyanagi, T., Kumagai, H., et al. (2005). A novel putrescine utilization pathway involves γ -glutamylated intermediates of *Escherichia coli* K-12. *J. Biol. Chem.* 280, 4602–4608. doi: 10.1074/jbc.M411114200
- Mardani, H., Maninang, J., Appiah, K. S., Oikawa, Y., Azizi, M., and Fujii, Y. (2019). Evaluation of biological response of lettuce (*Lactuca sativa* L.) and weeds to safranal allelochemical of saffron (*Crocus sativus*) by using static exposure method. *Molecules* 24:1788. doi: 10.3390/molecules24091788
- Mardani, H., Sekine, T., Azizi, M., Mishyna, M., and Fujii, Y. (2015). Identification of safranal as the main allelochemical from saffron (*Crocus sativus*). *Nat. Prod. Commun.* 10, 775–777. doi: 10.1177/1934578x1501000519
- Mitri, C., Soustelle, L., Framery, B., Bockaert, J., Parmentier, M. L., and Grau, Y. (2009). Plant insecticide L-canavanine repels *Drosophila* via the insect orphan GPCR DmX. *PLoS Biol.* 7:147. doi: 10.1371/journal.pbio.1000147
- Moe, L. A. (2013). Amino acids in the rhizosphere: from plants to microbes. *Am. J. Bot.* 100, 1692–1705. doi: 10.3732/ajb.1300033
- Nakajima, N., Hiradate, S., and Fujii, Y. (2001). Plant growth inhibitory activity of L-canavanine and its mode of action. *J. Chem. Ecol.* 27, 19–31. doi: 10.1023/A:1005659714947
- Nelson, E. B. (2018). The seed microbiome: origins, interactions, and impacts. *Plant Soil* 422, 7–34. doi: 10.1007/s11104-017-3289-7
- Oksanen, J., Blanchet, F. G., Kindt, R., Legendre, P., Minchin, P. R., O'Hara, R. B., et al. (2015). *Vegan: Community Ecology Package. Ordination Methods, Diversity Analysis and Other Functions for Community and Vegetation Ecologists*. R Package version, 2–3.
- Okutani, F., Hamamoto, S., Aoki, Y., Nakayasu, M., Nihei, N., Nishimura, T., et al. (2020). Rhizosphere modelling reveals spatiotemporal distribution of daidzein shaping soybean rhizosphere bacterial community. *Plant Cell Environ.* 43, 1036–1046. doi: 10.1111/pce.13708
- Perez, P. G., Zhang, R., Wang, X., Ye, J., and Huang, D. (2015). Characterization of the amino acid composition of soils under organic and conventional management after addition of different fertilizers. *J. Soils Sediments* 15, 890–901.
- Persson, J., and Näsholm, T. (2001). A GC-MS method for determination of amino acid uptake by plants. *Physiol. Plant.* 113, 352–358. doi: 10.1034/j.1399-3054.2001.1130308.x
- Peters, N. K., Frost, J. W., and Long, S. R. (1986). A plant flavone, luteolin, induces expression of *Rhizobium meliloti* nodulation genes. *Science* 233, 977–980. doi: 10.1126/science.3738520
- Price, M. N., Dehal, P. S., and Arkin, A. P. (2009). Fasttree: computing large minimum evolution trees with profiles instead of a distance matrix. *Mol. Biol. Evol.* 26, 1641–1650. doi: 10.1093/molbev/msp077
- Quast, C., Pruesse, E., Yilmaz, P., Gerken, J., Schweer, T., Yara, P., et al. (2013). The SILVA ribosomal RNA gene database project: Improved data processing and web-based tools. *Nucleic Acids Res.* 41, 590–596. doi: 10.1093/nar/gks1219
- Raab, T. K., Lipson, D. A., and Monson, R. K. (1996). Non-mycorrhizal uptake of amino acids by roots of the alpine sedge *Kobresia myosuroides*: implications for the alpine nitrogen cycle. *Oecologia* 108, 488–494. doi: 10.1007/BF00333725
- Raab, T. K., Lipson, D. A., and Monson, R. K. (1999). Soil amino acid utilization among species of the Cyperaceae: plant and soil processes. *Ecology* 80, 2408–2419.
- Radkov, A. D., McNeill, K., Uda, K., and Moe, L. A. (2016). D-amino acid catabolism is common among soil-dwelling bacteria. *Microbes Environ.* 31, 165–168. doi: 10.1264/jsme2.ME15126
- Rawat, S. R., Männistö, M. K., Starovoytov, V., Goodwin, L., Nolan, M., Hauser, L., et al. (2012). Complete genome sequence of *Terriglobus saanensis* type strain SP1PR4T, an Acidobacteria from tundra soil. *Stand. Genomic Sci.* 7, 59–69. doi: 10.4056/sigs.3036810
- Rice, E. L. (2012). *Allelopathy*, 2nd Edn. Cambridge, MA: Academic press.
- Rosenthal, G. A., Lambert, J., and Hoffmann, D. (1989). Canavanine incorporation into the antibacterial proteins of the fly, *Phormia terranova* (Diptera), and its effect on biological activity. *J. Biol. Chem.* 264, 9768–9771. doi: 10.1016/s0021-9258(18)81724-0
- Rothstein, D. E. (2010). Effects of amino-acid chemistry and soil properties on the behavior of free amino acids in acidic forest soils. *Soil Biol. Biochem.* 42, 1743–1750.
- Sasamoto, H., Mardani, H., Sasamoto, Y., Wasano, N., Murashige-Baba, T., Sato, T., et al. (2019). Evaluation of canavanine as an allelochemical in etiolated seedlings of *Vicia villosa* Roth: protoplast co-culture method with digital image analysis. *Vitr. Cell. Dev. Biol. Plant* 55, 296–304. doi: 10.1007/s11627-019-09985-3
- Saxena, A. K., Kumar, M., Chakdar, H., Anuroopa, N., and Bagyaraj, D. J. (2020). *Bacillus* species in soil as a natural resource for plant health and nutrition. *J. Appl. Microbiol.* 128, 1583–1594. doi: 10.1111/jam.14506
- Schulten, H. R., and Schnitzer, M. (1997). The chemistry of soil organic nitrogen: a review. *Biol. Fertil. Soils* 26, 1–15. doi: 10.1007/s003740050335
- Syed, S., Ahmed, Z. I., Al-Haq, M. I., Mohammad, A., and Fujii, Y. (2014). The possible role of organic acids as allelochemicals in *Tamarindus indica* L. leaves. *Acta Agric. Scand. Sect. B Soil Plant Sci.* 64, 511–517.
- Tsuchiya, S., Ogita, S., Kawana, Y., Oyanagi, T., Hasegawa, A., and Sasamoto, H. (2013). Relation between amino acids profiles and recalcitrancy of cell growth or salt tolerance in tissue and protoplast cultures of three mangrove species. *Am. J. Plant Sci.* 4, 1366–1374. doi: 10.4236/ajps.2013.47167
- Vinolas, L. C., Healey, J. R., and Jones, D. L. (2001). Kinetics of soil microbial uptake of free amino acids. *Biol. Fertil. Soils* 33, 67–74. doi: 10.1007/s003740000291
- Warnes, G. R., Bolker, B., Bonebakker, L., Gentleman, R., Huber, W., Liaw, A., et al. (2020). *gplots: Various R Programming Tools for Plotting Data*. R Package Version 3.1.1. Available online at: <https://CRAN.R-project.org/package=gplots> (accessed September 10, 2021).
- Weintraub, M. N., and Schimel, J. P. (2005). The seasonal dynamics of amino acids and other nutrients in Alaskan Arctic tundra soils. *Biogeochemistry* 73, 359–380.
- Yamazaki, S., Ochiai, K., Motokawa, J., Hamamoto, S., Sugiyama, A., and Kobayashi, M. (2019). Properties of rhizosphere soil associated with herbaceous plant roots analyzed using small-scale protocols. *bioRxiv* [Preprint]. doi: 10.1101/800664
- Young, C. T., Waller, G. R., Matlock, R. S., Morrison, R. D., and Hammons, R. O. (1974). Some environmental factors affecting free amino acid composition in six varieties of peanuts. *J. Am. Oil Chem. Soc.* 51, 265–268.
- Zampieri, M., Hörl, M., Hotz, F., Müller, N. F., and Sauer, U. (2019). Regulatory mechanisms underlying coordination of amino acid and glucose catabolism in *Escherichia coli*. *Nat. Commun.* 10, 1–13. doi: 10.1038/s41467-019-11331-5
- Zhang, B., Wu, X., Tai, X., Sun, L., Wu, M., Zhang, W., et al. (2019). Variation in actinobacterial community composition and potential function in different soil ecosystems belonging to the arid heihe river basin of Northwest China. *Front. Microbiol.* 10:2209. doi: 10.3389/fmicb.2019.02209

Conflict of Interest: The authors declare that the research was conducted in the absence of any commercial or financial relationships that could be construed as a potential conflict of interest.

Publisher's Note: All claims expressed in this article are solely those of the authors and do not necessarily represent those of their affiliated organizations, or those of the publisher, the editors and the reviewers. Any product that may be evaluated in this article, or claim that may be made by its manufacturer, is not guaranteed or endorsed by the publisher.

Copyright © 2021 Mardani-Korrani, Nakayasu, Yamazaki, Aoki, Kaida, Motobayashi, Kobayashi, Ohkama-Ohtsu, Oikawa, Sugiyama and Fujii. This is an open-access article distributed under the terms of the Creative Commons Attribution License (CC BY). The use, distribution or reproduction in other forums is permitted, provided the original author(s) and the copyright owner(s) are credited and that the original publication in this journal is cited, in accordance with accepted academic practice. No use, distribution or reproduction is permitted which does not comply with these terms.



Genetic Elucidation of Quorum Sensing and Cobamide Biosynthesis in Divergent Bacterial-Fungal Associations Across the Soil-Mangrove Root Interface

Zhengyuan Zhou¹, Ruiwen Hu¹, Yanmei Ni², Wei Zhuang¹, Zhiwen Luo¹, Weiming Huang¹, Qingyun Yan¹, Zhili He¹, Qiuping Zhong¹ and Cheng Wang^{1*}

¹ Environmental Microbiomics Research Center, School of Environmental Science and Engineering, Southern Marine Science and Engineering Guangdong Laboratory (Zhuhai), Sun Yat-sen University, Guangzhou, China, ² Guangdong Agribusiness Tropical Agriculture Institute, Guangzhou, China

OPEN ACCESS

Edited by:

Paolina Garbeva,
Netherlands Institute of Ecology
(NIOO-KNAW), Netherlands

Reviewed by:

Michael Meijer,
Ben-Gurion University of the Negev,
Israel
Jin Zhou,
Tsinghua University, China

*Correspondence:

Cheng Wang
wangcheng5@mail.sysu.edu.cn

Specialty section:

This article was submitted to
Terrestrial Microbiology,
a section of the journal
Frontiers in Microbiology

Received: 21 April 2021

Accepted: 15 September 2021

Published: 05 October 2021

Citation:

Zhou Z, Hu R, Ni Y, Zhuang W,
Luo Z, Huang W, Yan Q, He Z,
Zhong Q and Wang C (2021) Genetic
Elucidation of Quorum Sensing
and Cobamide Biosynthesis
in Divergent Bacterial-Fungal
Associations Across
the Soil-Mangrove Root Interface.
Front. Microbiol. 12:698385.
doi: 10.3389/fmicb.2021.698385

Plant roots in soil host a repertoire of bacteria and fungi, whose ecological interactions could improve their functions and plant performance. However, the potential microbial interactions and underlying mechanisms remain largely unknown across the soil-mangrove root interface. We herein analyzed microbial intra- and inter-domain network topologies, keystone taxa, and interaction-related genes across four compartments (non-rhizosphere, rhizosphere, episphere, and endosphere) from a soil-mangrove root continuum, using amplicon and metagenome sequencing technologies. We found that both intra- and inter-domain networks displayed notable differences in the structure and topology across four compartments. Compared to three peripheral compartments, the endosphere was a distinctive compartment harboring more dense co-occurrences with a higher average connectivity in bacterial-fungal network (2.986) than in bacterial (2.628) or fungal network (2.419), which could be related to three bacterial keystone taxa (*Vibrio*, *Anaerolineae*, and *Desulfarculaceae*) detected in the endosphere as they are known to intensify inter-domain associations with fungi and stimulate biofilm formation. In support of this finding, we also found that the genes involved in cell-cell communications by quorum sensing (*rhlI*, *lasI*, *pqsH*, and *lasR*) and aerobic cobamide biosynthesis (*cobG*, *cobF*, and *cobA*) were highly enriched in the endosphere, whereas anaerobic cobamide biosynthesis (encoded by *cblT* and *cblE*) was dominant in three peripheral compartments. Our results provide genetic evidence for the intensified bacterial-fungal associations of root endophytes, highlighting the critical role of the soil-root interface in structuring the microbial inter-domain associations.

Keywords: network, bacterial-fungal association, endosphere, quorum sensing, cobamide

INTRODUCTION

The roots of soil-grown plants host diverse microbial communities, and microbe-microbe interactions (e.g., inhibition, facilitation, and competition) are highly prevalent and have emerged as an important feature of plant root ecosystems (Gomes et al., 2011; Duran et al., 2018). Recent studies have shown that intra- or inter-domain microbial interactions could sustain the harmony

of biogeochemical processes and keep the nutritional status and ecological balance for plant health (Thatoi et al., 2013; Ma et al., 2016). One typical example is the association between arbuscular mycorrhizal fungi and nitrogen-fixing bacteria, and their synergistical interactions can result in better nutrient uptake and higher plant productivity compared to plants symbiotic with either of them alone (Banerjee et al., 2019). At the community level, inter-domain microbial interactions were specifically enriched with negative correlations between bacteria and filamentous eukaryotes in *Arabidopsis thaliana* roots, where bacterial communities were essential for plant survival and protection against filamentous eukaryotes (Zhang et al., 2019). These studies contribute to the growing body of evidence that the plant growth and health are closely connected to microbial interactions from soil-root system (Duran et al., 2018), which carry out key functions like synergistic effects on plant growth, maintenance of host-microbiota balance, and protection against environmental pathogens (Duran et al., 2018).

Current studies suggested that the soil-root microhabitat could be divided into four continuous compartments: non-rhizosphere (bulk soil), rhizosphere (Saleem et al., 2018), episphere, and endosphere (Duran et al., 2018). Microbial communities in each compartment across the soil-root interface were shown to exhibit unique characteristics (Edwards et al., 2015; Duran et al., 2018). The rhizosphere could selectively gather specific bacterial and fungal populations *via* root exudates, which conversely exerted a marginal influence on microbes in the non-rhizosphere soil (Bais et al., 2006; Sasse et al., 2018). Compared to the rhizosphere, the episphere played a more critical role for the controlled entry of specific soil-borne microbes into the plant root, leading to the selective enrichment of Proteobacteria and the absence of soil-derived fungi in the endosphere (Ofek-Lalzar et al., 2014; Duran et al., 2018). In fact, the significant variations that bacterial and fungal communities underwent across the soil-root interface were irrespective of plant hosts, and microbial diversity inside plant roots was much lower than that in other three exterior root compartments (Edwards et al., 2015). These findings have greatly advanced our understanding of bacterial and fungal community structure and assembly in soil-root system. However, the intra- and inter-domain interactions of microbial communities, and their dynamics across the soil-root interface are poorly understood.

In order to unravel the organization and strength of microbial interactions, network analysis has been widely used as a promising tool to disentangle microbial co-occurrence in various environments, such as groundwater, oceans and soil environments (Shi et al., 2016). Recently, it has been applied to evaluate the microbe-microbe associations in plant roots (Chen et al., 2019; Zhang et al., 2020) and their responses to environmental parameters (Morriën et al., 2017; de Vries et al., 2018). More importantly, the topology-based network analysis provides an opportunity to identify the keystone taxa, which are strongly interconnected and have an important effect on communities (Agler et al., 2016; Ma et al., 2016). In despite of numerically inconspicuous, keystone taxa confer higher biotic connectivity to the microbial community and therefore can be predictors of community shifts and compositional turnover

(Herren and McMahon, 2018). However, the profile of keystone taxa across the soil-root interface and how it relates with the microbial interactions are poorly understood.

Many secondary metabolites are usually bioactive and can perform key functions in microbial interactions. A well-established mechanism of cell-to-cell communications in plant roots is quorum sensing, which is defined to be a stimulus-response system related to cellular density (Miller and Bassler, 2001; Shi et al., 2016; Kareb and Aider, 2020). Early studies have shown that quorum sensing can regulate bioluminescence and biofilm formation by releasing a specific acylated homoserine lactone (HSL) signaling molecule, which is known as an autoinducer produced by *LuxI*-like proteins (Miller and Bassler, 2001), and distinct microbes can produce the same type of signaling molecules, which have a role in both inter- and intra-domain interactions (Banerjee et al., 2018). Similarly, cobamides are recognized as mediators of microbial interactions (Bertrand et al., 2015; Shelton et al., 2019; Olga et al., 2020), making contributions to the nucleotide biosynthesis and catabolism of carbon sources (Olga et al., 2020). It is important to note that, microbes of all domains need cobamides, but many of them rely on the surrounding species to complement. This facilitates the ubiquitous establishment of a network of cobamide-dependent interactions in coastal ecosystems (Olga et al., 2020). Many previous studies have investigated the profile of genes associated with quorum sensing and cobamide biosynthesis in the complex microbial communities; however, little is known about whether and how these genes are connected to the microbe-microbe interaction dynamics at a community level.

As an ecologically important coastal ecosystem, mangrove plays a critical role in carbon storage, climate mitigation, shoreline protection and nutrient filtering (Alongi, 2014). Increasing evidences have revealed a high diversity of bacterial and fungal communities inhabiting across the soil-mangrove root interface (Zhuang et al., 2020), and determined their importance for mangrove growth and function (Reef et al., 2010; Thatoi et al., 2013; Xie et al., 2014). For instance, biological nitrogen fixation performed by diazotrophic bacteria in the vicinity of mangrove roots accounted for 40–60% of the total nitrogen required by mangroves (Holguin et al., 2001; Reef et al., 2010). Rhizosphere fungi not only displayed ligninolytic, cellulolytic, and amylolytic activity (Thatoi et al., 2013), but also could help mangroves adapt to the waterlogged and nutrient-restricted environments (Xie et al., 2014). Despite the improved understanding of functional capabilities of root-associated bacterial and fungal communities, our knowledge of potential interactions and underlying mechanisms within microbial communities from soil-mangrove root system remains largely unknown.

In this study, we profiled bacterial and fungal communities across four compartments (non-rhizosphere, rhizosphere, episphere, and endosphere) of mangrove roots with the aim of inferring the structure of microbial intra- and inter-domain co-occurrence networks and exploring putative keystone taxa across the soil-root interface. Amplicon and metagenome sequencing were performed to examine network topology and profiles of quorum sensing genes, cobamide biosynthesis genes and microbes in microbial communities across the soil-mangrove

root interface. This study uncovers how diverse taxonomic groups of bacteria and fungi can form metacommunity-scale networks of putative microbial intra- and inter-domain interactions, providing a basis for understanding complex spatial processes of soil-microbe-plant systems and engineering complex microbial consortia with predictable behaviors and robust outcomes.

MATERIALS AND METHODS

Site Selection, Sampling, and Environmental Properties

The location of the sampling site is at the Shuidong Bay of Maoming City (21°30'38.82" N, 111°0'37.27"E), Guangdong, China. In April 2019, we collected 12 individual mangrove saplings in a mangrove forest consisting of *Kandelia obovata* and *Sonneratia apetala*, and divided the samples from soil to root into four compartments: non-rhizosphere soil (Non), rhizosphere soil (Rhi), root episphere (Epi), and root endosphere (Endo). These compartments were prepared as described by Edwards et al. (2015) and Duran et al. (2018). The non-rhizosphere soil was shaken off the root, whereas the rhizosphere soil was the part of the soil at ~1 mm thickness around the root and was washed with sterile water. The clean roots were subsequently washed three times to remove the remaining soil and placed into 1 × TE buffer supplemented with 0.1% Triton X-100 in a 50 mL Falcon tube. Next, we collected the episphere samples by washing and extensive shaking in 1 × TE buffer supplemented with 0.1% Triton X-100. The microbial biomass of episphere was obtained *via* filtering the resulting suspension through 0.22 μm pore size membranes (Nuclepore, Whatman, Meterstone, United Kingdom). To capture the endosphere microbial biomass, the roots were surface-sterilized for 1 min in 80% ethanol and then sterilized again for 1 min in 0.25% NaClO. Samples from all four compartments in the soil-root system were stored at −80°C until DNA extraction. For soils in the non-rhizosphere, pH, salinity (permillage), oxidation reduction potential (mV), moisture content (%), total carbon (mg/Kg), total nitrogen (mg/Kg), ammonium-N (mg/Kg), nitrate-N (mg/Kg), and nitrite-N (mg/Kg) were measured (**Supplementary Table 1**) by previously described (Li et al., 2019).

DNA Extraction, PCR Amplification and Sequencing

For each of 12 mangrove saplings, approximately 0.5 g of non-rhizosphere and rhizosphere soil was used for DNA extraction using a Power Soil DNA Isolation Kit following the protocol provided by the manufacturer (MoBio, Carlsbad, CA, United States) with the modified sodium dodecyl sulfate extraction method (Zhou et al., 1996). The episphere compartment DNA was extracted using a Power Water DNA Isolation Kit following the protocol provided by the manufacturer (MoBio, Carlsbad, CA, United States). For the endosphere samples, DNA was extracted from plant samples with the Power Plant DNA Isolation Kit, according to the

manufacturer's protocol (Mo Bio Laboratories, Inc., Carlsbad, CA, United States) after thorough grinding with liquid nitrogen. The DNA quality of four compartments in the soil-root system was assessed by Nano Drop ND-2000 Spectrophotometer (Thermo Fisher Scientific, MA, United States) based on 260/280 and 260/230 nm ratios (Tu et al., 2016). Qualified DNA samples were diluted to 2 ng/μL for subsequent PCR amplification.

The V3-V4 region of 16S rRNA genes was amplified with the primer pair (forward primer, 5'- ACTCCTACGG GAGGCAGCA-3'; reverse primer, 5'- GGACTACHVGGGTW TCTAAT-3') (Peng et al., 2017) and the ITS1 region of fungal ITS genes were amplified with the primer pair (forward primer, 5'-CTTGGTCATTTAGAGGAAGTAA-3'; reverse primer, 5'-G CTGCGTTCCTCATCGATGC-3') (Blaalid et al., 2013). PCR amplification was conducted in a total volume of 50 μL containing 10 μL buffer, 0.2 μL Q5 high-fidelity DNA polymerase, 10 μL high GC enhancer, 1 μL dNTP, 10 μM of each primer and 60 ng microbial community DNA. Thermal cycling conditions were as follows: an initial denaturation at 95°C for 5 min, followed by 15 cycles at 95°C for 1 min, 50°C for 1 min and 72°C for 1 min, with a final extension at 72°C for 7 min. The PCR products from the first step PCR were purified with VAHTSTM DNA Clean Beads, and the second round PCR was performed in a 40 μL reaction containing 20 μL 2 × Phusion HF MM, 8 μL ddH₂O, 10 μM of each primer and 10 μL PCR products from the first step. Thermal cycling conditions were as follows: an initial denaturation at 98°C for 30 s, followed by 10 cycles at 98°C for 10 s, 65°C for 30 s min and 72°C for 30 s, with a final extension at 72°C for 5 min. All PCR products were quantified by Quant-iTTM dsDNA HS Reagent and pooled together. High-throughput sequencing analysis of bacterial rRNA genes and fungal ITS genes was performed on the purified, pooled samples using the Illumina Hiseq 2500 platform (2 × 250 paired ends) at Biomarker Technologies Corporation, Beijing, China.

Sequence Analysis of 16S rRNA and ITS Gene Amplicons

Raw sequences were trimmed using Trimmomatic (Marc et al., 2012) and FLASH (Tanja and Salzberg, 2011), with a moving window of 50-bp and the quality threshold score of 30. After the singleton elimination, paired 16S rRNA amplicon sequences were then clustered into operational taxonomic units (OTUs) by UPARSE (Edgar, 2013) based on a 97% sequence identity using QIIME's (QIIME: Quantitative Insights into Microbial Ecology) (Caporaso et al., 2010) open reference OTU picking strategy with the Greengenes 16S rRNA database (v.13.5) as a reference (DeSantis et al., 2006). Bacterial OTU was represented as OTUB, and fungal OTU was represented as OTUF. We eliminated the sequences matching "Chloroplast" and "Mitochondria" from the datasets. ITS sequences were processed by ITSx (Bengtsson-Palme et al., 2013) and clustered at a 97% sequence identity by UPARSE (Edgar, 2013). Fungal OTUs were checked for chimeric sequences using the Uchime reference against a dedicated chimera detection database (Nilsson et al., 2015), which was based on the UNITE database for

fungi identification. On average, we obtained 70,914 and 77,186 high-quality 16S rRNA and ITS gene amplicon sequences per sample, respectively. For all samples, the 16S rRNA and ITS sequences were clustered into 1,290 and 1,240 OTUs ($>0.01\%$ of total abundance), respectively. The nucleotide sequences were deposited in SRA database under accession numbers PRJNA685020 and PRJNA685297.

Network Construction and Analysis

Microbial intra- and inter-domain networks were constructed based on bacterial and fungal OTU relative abundances across each root compartment. Covariations were measured across 12 biological replicates to create each network. Only OTUs detected in 8 out of 12 replicate samples were used for network construction. Random matrix theory (RMT) was used to automatically identify the appropriate similarity threshold (St) before network construction, since RMT could minimize the uncertainty in network construction by using mathematically defined non-arbitrary correlation cut-off (Yuan et al., 2021). St defined the minimal strength of the connections between each pair of nodes (Zhou et al., 2010). Global network properties were characterized as described in Deng et al. (2012). All analyses were performed with the Molecular Ecological Network Analyses (MENA) Pipeline¹ (Deng et al., 2012) and the network structures were visualized using Cytoscape 3.6.1 (Shannon et al., 2003) and Gephi 0.9.2-beta (Bastian et al., 2009).

Module Detection and Node Role Identification

We examined network modularity for each network constructed in this study. A module is a set of nodes (OTUs) that are highly connected inside the group but few connected outside the group (Newman, 2006). Modules were identified using the greedy modularity optimization method in this study. Modularity (M) is an indicator that measures the extent of network module division, and $M > 0.4$ is used as the threshold to define module structure (Newman, 2006). Additionally, the connectivity of each node was determined according to its within-module connectivity (Z_i) and among-module connectivity (P_i) (Roger, 2005). Based on the topological roles in the network, we organized node topology into four categories: network hubs (nodes with high connectivity in the entire network, $Z_i > 2.5$ and $P_i > 0.62$), module hubs (nodes with high connectivity inside modules, $Z_i > 2.5$), connectors (nodes that connect modules, $P_i > 0.62$) and peripherals (nodes with few outside connections, $Z_i < 2.5$ and $P_i < 0.62$) (Olesen et al., 2007; Deng et al., 2012).

Shotgun Metagenome Sequencing and Data Analysis

Metagenomic sequencing library preparation was performed as previously described (Zhuang et al., 2020). Briefly, using 1 microgram DNA with Illumina (NEB, United States) NEBNext[®] Ultra[™] DNA Library Prep Kit as recommended by the manufacturer. The index codes were added to attribute sequence

of each compartment sample, and these samples then were purified (AMPure XP system). Agilent 2100 bioanalyzer (Agilent Technologies, CA, United States) was used to check the libraries. Paired-end reads with poor quality (quality score ≤ 38 ; base N > 10 bp, and the overlap length between adapter and reads was greater than 15 bp) are filtered. The filtered clean reads (about 11.8–12.5 Gb per sample) were used for metagenomic analyses. The metagenomic assembly was performed using Megahit (Li et al., 2015) in default mode. MetaGeneMark (v 2.10) were employed to predict genes from the assembled contigs, and redundancy was removed using CD-HIT Software (Fu et al., 2012).

For the assembled metagenomes, MetaGeneMark v. 2.10 was used to predict open reading frames, CD-HIT v. 4.5.8 was used to construct Unigenes (Fu et al., 2012), and SoapAligner v. 2.21 was used for quality control. We used DIAMOND combined with the KEGG database (blastp, e -value $\leq 1e-5$) (Moriya et al., 2007) to perform functional annotation on genes related to quorum sensing and cobamide biosynthesis. In detail, we first determined the processes of quorum sensing and cobamide biosynthesis by referring to relevant studies (Warren et al., 2002; Ng and Bassler, 2009; Mukherjee and Bassler, 2019; Shelton et al., 2019), and the quorum sensing and cobamide biosynthesis pathways in KEGG database. Key genes that were involved in the quorum sensing and cobamide biosynthesis pathways were subsequently identified. The keywords of each gene were determined by its gene code and corresponding protein name, and were further refined by manually checking the description (Supplementary Table 2). The gene reading counts were normalized to transcripts per-million (TPM) counts. Statistical enrichment of a given gene between compartments was determined by pairwise comparisons using two-tailed Fisher's exact test, with confidence intervals at 99% significance and Benjamini–Hochberg correction ($P < 0.05$). The Mantel tests between microbial communities and environmental factors were performed in R with the mantel function in the package {ggcor}. To get the taxonomical profile of cobamide biosynthesis microbiomes, the sequences were extracted by the *seqtk* program (Shen et al., 2016), and subsequently annotated with the Kraken2 program (Wood et al., 2019). The metagenome sequencing data were deposited in SRA database with accession numbers of PRJNA613873.

Root Exudate Analysis and Biofilm Microscopic Analysis

To identify potential substances related to biofilm formation, we used liquid chromatography–mass spectrometry (LC/MS) analysis (1290 infinity series UHPLC system, Agilent Technologies) to detect the root exudates. In detail, mangrove saplings were transferred to 1-L hydroponic tubes with sterile Milli-Q water, and hydroponic tubes were incubated at 24°C for 24 h for root exudates collection. Ethyl acetate and dichloromethane were used to extract the resulting solution in a rotary evaporator, and we subsequently frozen it. Next, the sample was dissolved in 100 μ L methanol, and we added 400 μ L extract solution (acetonitrile:methanol = 1:1) containing

¹<http://ieg2.ou.edu/MENA/>

the internal standard (L-2-Chlorophenylalanine, 2 $\mu\text{g/mL}$). After vortexing for 30 s, the sample was sonicated with an ice-water bath and then incubated at -40°C . After the sample was centrifuged at 4°C , the supernatant was dried in a vacuum concentrator at 37°C and reconstituted in 200 μL acetonitrile (50%) via sonication on ice. The resulting solution was then centrifuged at 4°C , and 75 μL supernatant was finally transferred into a sterile glass vial for LC/MS analysis. We used positive and negative modes with ion spray voltage floating (ISVF) at 5,000 or $-4,000$ V, respectively. MS raw data files were transformed into the mzXML format by ProteoWizard, and subsequently processed via the R package XCMS (v3.2), including peak deconvolution, alignment, and integration.

To visualize mangrove root structure and biofilm formation, we used a hybrid microscope (REVOLVE 3, Echo Laboratories) to investigate slices of fresh roots in both brightfield and fluorescence field (488 nm, Mercury Free LED). Before microscopic examination, fresh mangrove roots stored in -80°C were washed by 80% ethanol for surface sterilization, and cut into slices using sterile blades. Afterward, the root slices were fixed with glutaraldehyde (2.5%) and rinsed by phosphate buffered saline (PBS) powder (pH 7.4). We applied Alexa Fluor[®] 488 conjugate of concanavalin A (Thermo Fisher Scientific, China), which could be excited with a 488 nm laser line and detected with a BP (band-pass) 500–530 nm filter, to label α -mannopyranosyl and α -glucopyranosyl residues in extracellular polysaccharides constituting the basic structure of root biofilm.

RESULTS

Distinctive Molecular Ecological Network Structure and Connectivity Within Four Compartments Across the Soil-Mangrove Root Interface

To explore putative microbe-microbe interactions across the soil-mangrove root interface, we analyzed microbial intra-domain and inter-domain co-occurrences based on sequencing datasets of bacterial and fungal communities (Figure 1A and Supplementary Table 3), which were represented as single bacterial and fungal network, and bacterial-fungal association (BFA) networks. Across four compartments in the soil-root system, we obtained a total of 12 microbial co-occurrence networks and their R^2 of power-law ranged from 0.860 to 0.929 (Supplementary Table 4), suggesting that those network connectivity distributions were fitted well with the scale-free property (Deng et al., 2012).

Multiple network topological metrics consistently revealed that microbial co-occurrence patterns differed profoundly across four compartments (Figure 1). The assemblages of three peripheral compartments (non-rhizosphere, rhizosphere and episphere) formed larger and more complex networks with more nodes and edges than that of the endosphere, especially for BFA (Figures 1B,C). More interestingly, network complexity also differed between microbial intra-domain and inter-domain co-occurrence networks. The BFA networks exhibited a lower

average connectivity than their corresponding bacterial and fungal networks in three peripheral compartments (Figure 1D). However, in the endosphere, a significantly ($P < 0.05$, two-tailed Fisher's exact test) higher average connectivity was detected in the BFA network (2.986) than in the fungal (2.419) network (Figure 1D and Supplementary Table 4), and more nodes and edges were also observed in the BFA network (426 and 636) than in the single bacterial or fungal networks (210 and 276 for bacteria; 186 and 225 for fungi) (Figures 1B,C). The results revealed that the endosphere was the only compartment in which the BFA network harbored a denser co-occurrence pattern than the single bacterial or fungal networks, creating a distinctive niche inside root with the enhanced microbial inter-domain associations.

We next identified inter-domain microbial assemblages that potentially interacted or shared niches across four compartments in the soil-root system. Four representative BFA networks contained modules with modularity >0.5 (Supplementary Table 4), and we concentrated on modules with more than 15 nodes. Similar to the overall BFA network structure (Figure 1A), the number of modules became smaller in transition from the non-rhizosphere, rhizosphere to episphere, but became larger again in the endosphere (Supplementary Figure 1). Notably, we found that module composition did not show clear differences across four compartments, in which the proportions of bacteria and fungi were nearly identical (Supplementary Figure 1). The results indicated that the bacteria and fungi contributed similar proportion to the microbial inter-domain associations in the soil-mangrove root continuum.

The Profile of Keystone Taxa Varied Across the Soil-Mangrove Root Interface

On the basis of within-module connectivity (Z_i) and among-module connectivity (P_i) values, we classified all network nodes into four parts: module hubs, network hubs, peripherals and connectors (Shi et al., 2016). Due to the roles in network topology, the taxa detected as module hubs, network hubs and connectors were proposed to be keystone taxa in the complex microbial communities. The results showed that most nodes from each network were peripherals, and no network hubs were identified (Figure 2). Intriguingly, in the episphere, more module hubs and connectors were detected in the single bacterial (14) and fungal (13) networks than in the BFA (0) networks (Supplementary Figure 2); however, in the endosphere compartment, the corresponding BFA network harbored more keystone taxa (Supplementary Figure 2), which is consistent with its more complicated networks (Figure 1A).

To investigate the role of keystone taxa in microbial inter-domain associations, we focused on BFA networks and their associated keystone taxa across four compartments in the soil-root system. We found that 15, 23, and 13 keystone taxa were observed in the BFA networks of the non-rhizosphere, rhizosphere, and endosphere, respectively, but no keystone taxa were detected in the episphere (Figure 2). Consistently, most of these putative keystone taxa had low relative abundances (Supplementary Figure 2 and Supplementary Table 3),

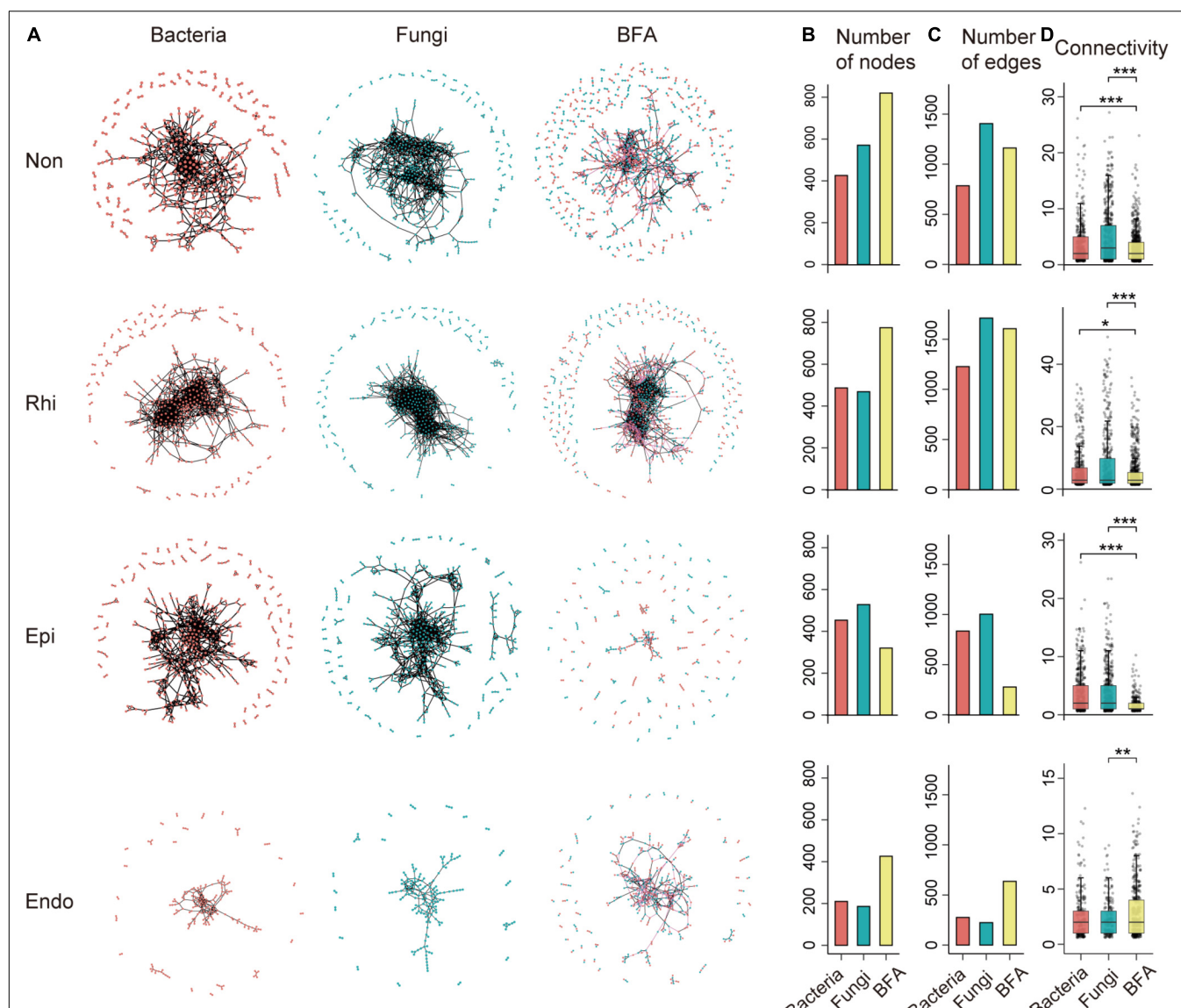


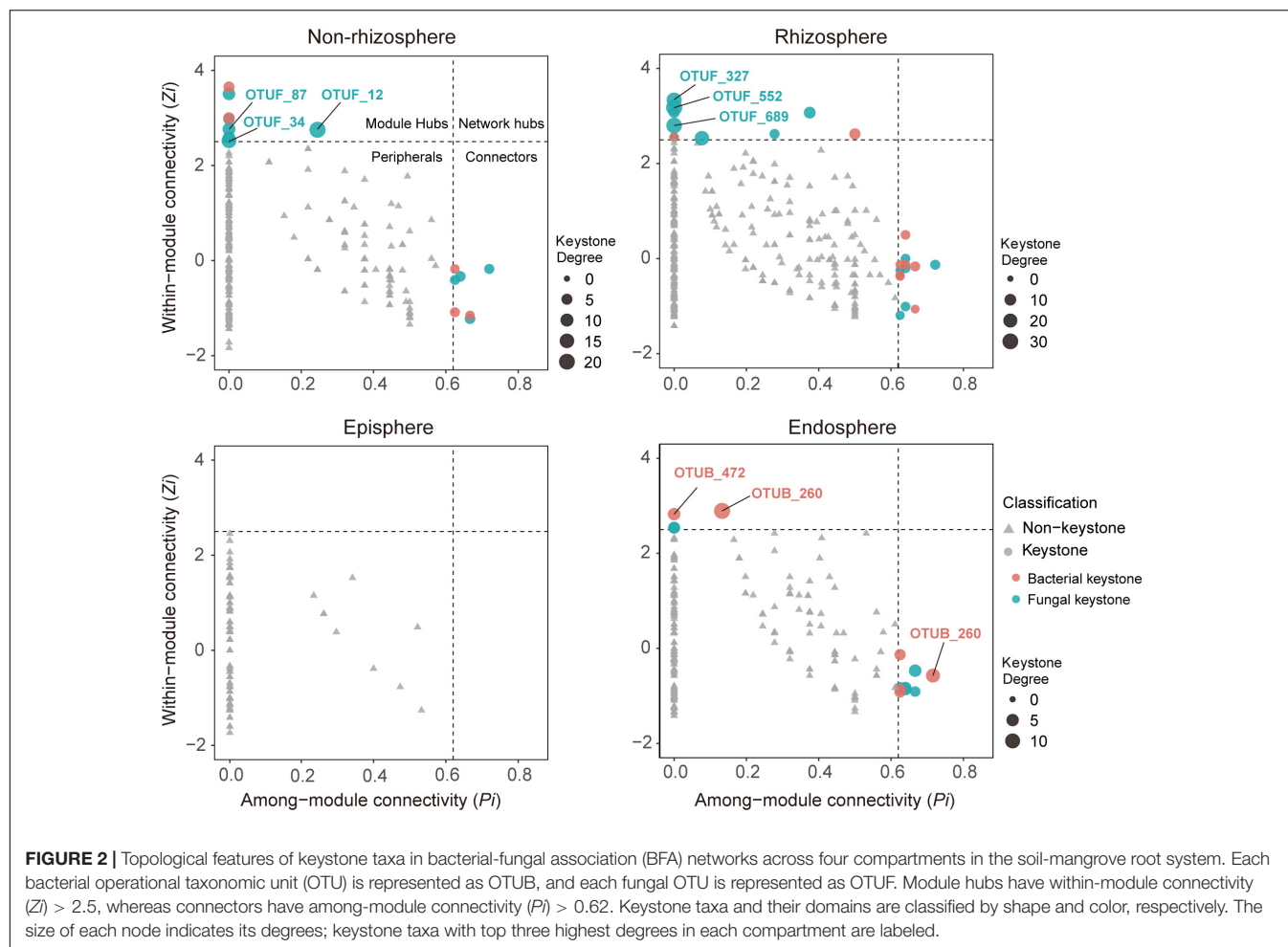
FIGURE 1 | The profile of intra-domain and inter-domain networks across the non-rhizosphere (Non), rhizosphere (Rhi), episphere (Epi), and endosphere (Endo) compartments. **(A)** A representation of bacterial, fungal and bacterial-fungal association (BFA) networks across four compartments in the soil-mangrove root system. Each node represents an operational taxonomic unit (OTU), and each edge represents a correlation between two OTUs. Red and blue nodes represent bacteria and fungi, respectively, whereas black and pink edges represent intra-domain and inter-domain interactions, respectively. **(B,C)** Show the total number of nodes and edges for each network. **(D)** The distribution of connectivity harbored by each node in bacterial, fungal and BFA networks. Connectivity is measured by degrees, which refers to the number of edges one node links with. Significance is tested with a two-sided Fisher's exact test: * $P < 0.05$; ** $P < 0.01$; *** $P < 0.001$.

suggesting that low-abundant taxa may significantly contribute to mangrove root functions. Further analysis of keystone taxa indicated that fungi accounted for a larger proportion (60.5%) in module hubs and connectors of BFA networks than bacteria (39.5%). Nonetheless, they displayed distinct importance across those four compartments. In the non-rhizosphere and rhizosphere, keystone taxa with top three highest degrees (the number of links for a particular node) were all monopolized by fungi (**Supplementary Figure 3**). However, in the endosphere, keystone taxa with top three highest degrees belonged to bacteria, and they were affiliated with *Vibrio* (OTUB_1491), *Anaerolineae*

(OTUB_472) and *Desulfarculaceae* (OTUB_260) (**Figure 2** and **Supplementary Table 3**).

Genetic Divergence of Quorum Sensing and Cobamide Biosynthesis Across the Soil-Mangrove Root Interface

In order to understand possible mechanisms of microbial interactions across soil-root interface, we investigated the functional profile of microbial communities by shotgun metagenome sequencing. We focused on functional genes



and pathways involved in quorum sensing and cobamide biosynthesis as they have been considered as typical strategies of microbial interactions possessed by various communities (Milton et al., 1997; Olga et al., 2020).

Quorum sensing served as a cell-cell communication device, which was exploited by many microflora (Milton et al., 1997). Here, we detected quorum sensing circuits with two modules represented by Gram-negative bacteria, and found that genes involved in quorum sensing were unevenly distributed across four continuous compartments (Figure 3). In module 1, the genes individually related to the production of autoinducer (S)-3-hydroxytridecan-4-one (CAI-1) and the mediation of group behaviors, *cqsA*, and *luxR*, were highly abundant in the episphere and endosphere, respectively. As the most abundant gene in module 1, *tdh* relates to the production of autoinducer 3,5-dimethyl-pyrazin-2-ol (DPO) and its abundance continuously decreased from the non-rhizosphere to the endosphere. In module 2, *lasI* and *pqsH*, related to production of autoinducer N-(3-oxododecanoyl)-L-homoserine lactone (3OC12-HSL) and 2-heptyl-3-hydroxy-4-quinolone (PQS), were detected across four compartments, but showed a relatively higher abundance in the endosphere. More strikingly, the endosphere was the only compartment that simultaneously contained *rhlI* and *lasR*, which

were involved into the syntheses of autoinducers N-butyryl-L-homoserine lactone (C4-HSL) and the mediation of group behaviors, respectively. The divergent pattern of genes involved in quorum sensing indicated that three peripheral compartments held a greater potential in conducting module 1, whereas module 2 was more likely to be conducted in the endosphere (Figure 3).

Cobamide, as one of the sharing valuable nutrients, was widely used by microbes to interact with each other (Olga et al., 2020). Our metagenome sequencing analysis revealed that among 15 cobamide biosynthesis genes, six genes (*cysG*, *cobF*, *cbiB*, *cobC*, *cobA*, and *cobD*) were significantly ($P < 0.05$, two-tailed Fisher's exact test) higher in the endosphere than in other three compartments, and they were involved in each of key steps for cobamide biosynthesis, including the tetrapyrrole precursor biosynthesis, corrin ring adenosylation, nucleotide loop assembly and aminopropanol phosphate production (Figure 4A). Intriguingly, a compartment specificity was detected for anaerobic or aerobic corrin ring adenosylation. Compared to three peripheral compartments, the endosphere harbored a higher abundance of genes associated with aerobic adenosylation (*cobG*, *cobE* and *cobA*) and a lower abundance of genes associated with anaerobic adenosylation (*cbiT* and *cbiE*) (Figure 4A). Furthermore, the taxonomic composition of all

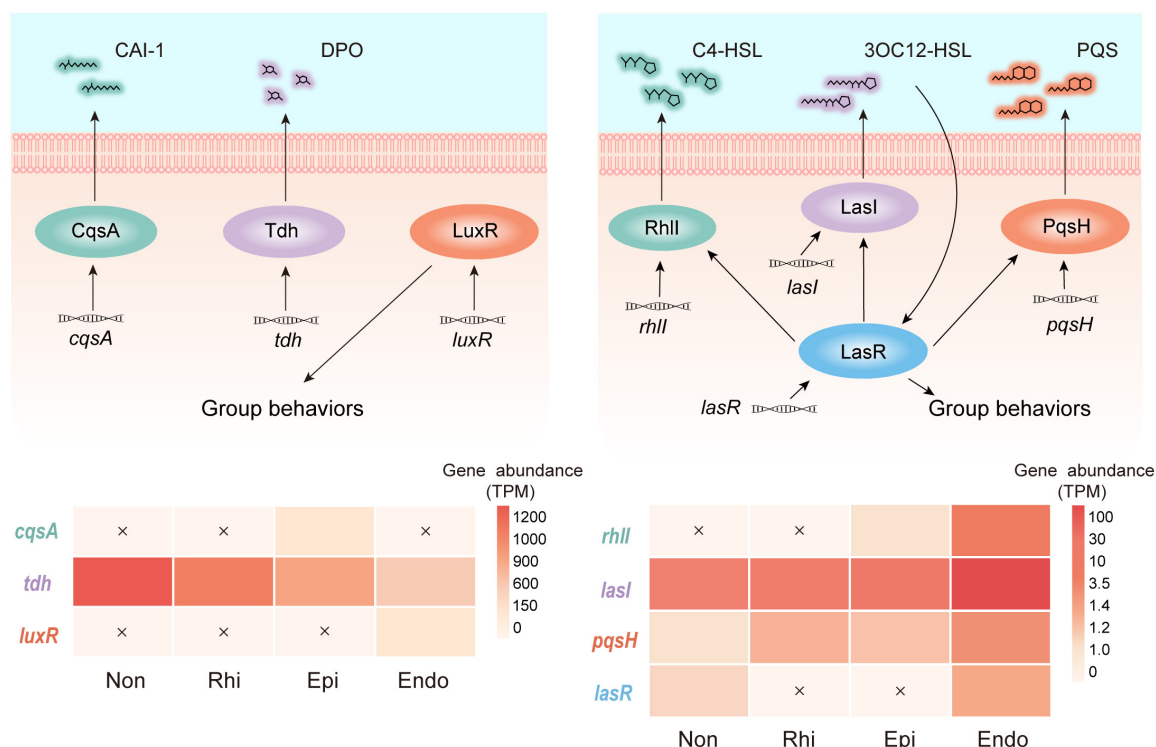


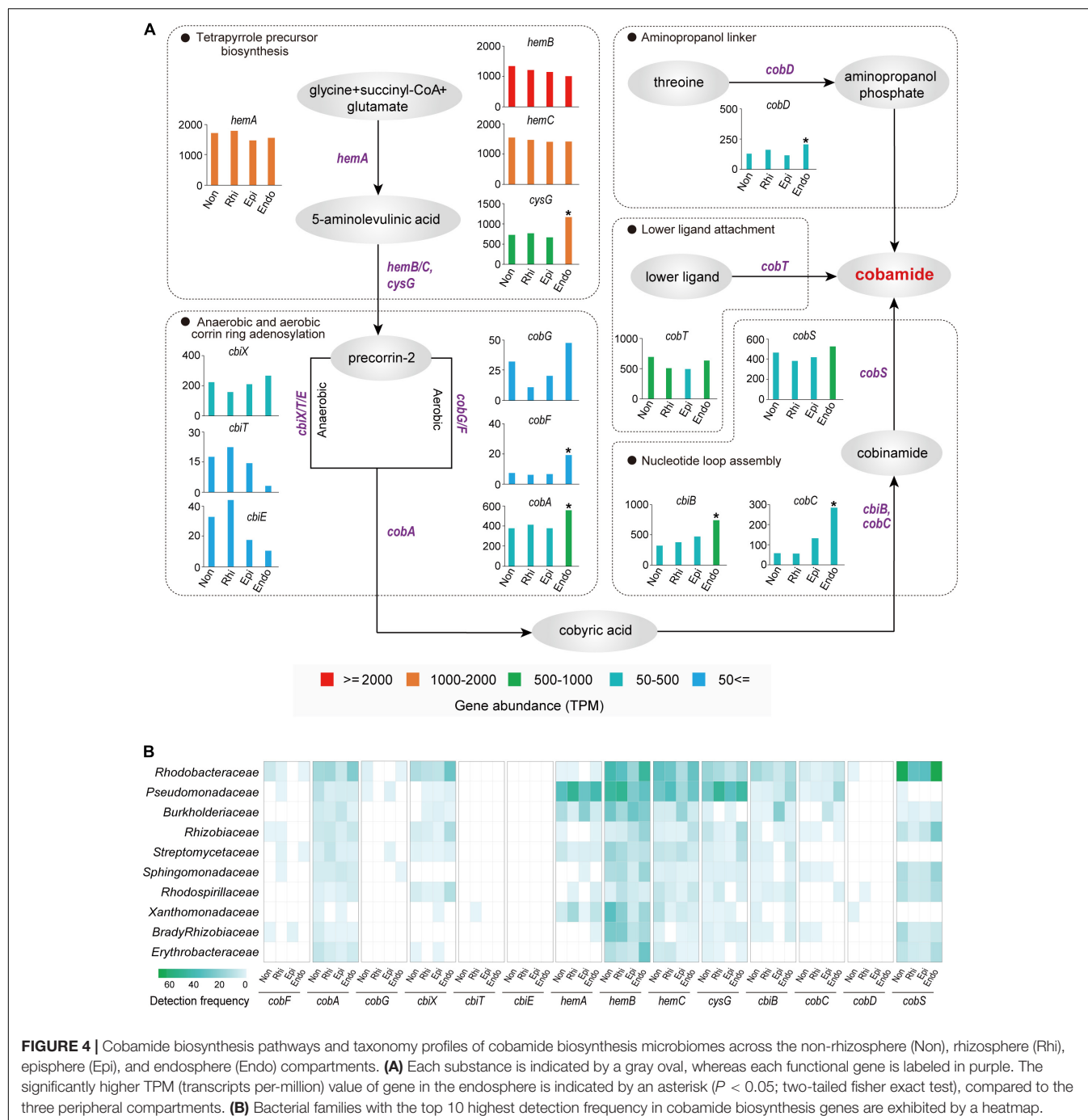
FIGURE 3 | Profiles of two quorum sensing modules across the non-rhizosphere (Non), rhizosphere (Rhi), episphere (Epi) and endosphere (Endo) compartments. In module 1, *cqsA* and *tdh* encode the autoinducers (S)-3-hydroxytridecan-4-one (CAI-1) and 3,5-dimethyl-pyrazin-2-ol (DPO), respectively, and *luxR* mediates group behaviors. In module 2, *lasI*, *rhII*, and *pqsH* encode the autoinducers N-(3-oxododecanoyl)-L-homoserine lactone (3OC12-HSL), N-butyl-L-homoserine lactone (C4-HSL), and 2-heptyl-3-hydroxy-4-quinolone (PQS), respectively. *lasR* encodes the receptor of 3OC12-HSL which mediates group behaviors. The relative abundance (TPM, transcripts per-million) of genes belonging to each module across four compartments in the soil-mangrove root system is represented by heatmaps, and each undetected gene is marked with a cross.

cobamide-related genes across four compartments (**Figure 4B**) revealed a high detection frequency of *Rhodobacteraceae* and *Pseudomonadaceae*, highlighting their key roles in mediating microbial interactions by producing cobamides. It is important to note that these two families were characterized by a nearly equal detection frequency across four compartments in the soil-root system (**Figure 4B**), with a low abundance (2.98–6.81%) in the whole bacterial community (**Supplementary Figure 4**). Therefore, these results indicated the intensified microbial associations in the endosphere were linked to aerobic cobamide biosynthesis performed by specialists (*Rhodobacteraceae* and *Pseudomonadaceae*). Apart from these two families, other cobamide-producing members (e.g., *Rhizobiaceae*, *Sphingomonadaceae*, and *Rhodospirillaceae*; **Figure 4B**) also played non-negligible roles in mediating microbial associations since we detected them as the keystone taxa in microbial networks (**Supplementary Table 3**).

Metagenomic, Microscopic, and Root Exudate Analyses Provide Evidences for Biofilm Formation in the Endosphere

To further consolidate the existence of biofilm in the endosphere compartment of mangrove roots, we provided multiple lines

of evidence based on metagenomic, microscopic and root exudate analyses. First, our metagenomic data determined that the endosphere contained high abundance of KOs related to the biosynthesis of extracellular polymeric substances (EPS) (**Supplementary Figure 5**), which were well known as structural and functional elements crucial to the formation of biofilms (Karygianni et al., 2020). Second, microscopic analysis confirmed the occurrence of biofilm inside mangrove roots, since we detected α -mannopyranosyl and α -glucopyranosyl residues that constituted the basic structure of EPS in root biofilm (**Figure 5**). Third, through root exudate analysis with LC/MS, we detected two EPS compounds yielding from the mangrove root interior, and they were trehalose with median retention time at 147.22 s (negative mode) and 149.87 (positive mode), and glucans with median retention time at 48.13 s (negative mode) and 345.06 s (positive mode) (**Supplementary Table 5**). In addition, we also detected adenine with median retention time at 107.68 s (negative mode) and 149.88 s (positive mode) as the component of root exudates, and this substance was reported to participate in the biosynthesis of lower ligand structure of cobamide (Shelton et al., 2019). Collectively, these results from multiple assays demonstrated the occurrence of biofilm and cobamide inside root, which built foundations for the intensified microbial associations in the endosphere of mangrove roots.



DISCUSSION

Understanding the network structure of microbial communities is essential to decipher their putative interactions and ecological roles (Zhou et al., 2010; Yuan et al., 2021). Through network topology and analysis of genes related to quorum sensing and cobamide biosynthesis, we found niche differentiation of microbial associations and keystone taxa across the soil-mangrove root interface. Compared to three peripheral compartments, the endosphere exhibited an intensified

association between bacterial and fungal communities, which was largely attributable to the specific keystone taxa and distinctive interaction strategies.

Given the essential topological role of keystone taxa in microbial networks (Ma et al., 2018; Fan et al., 2020), previous studies have determined the importance of keystone taxa in regulating microbial interactions. In this study, keystone taxa showed a clear divergence across the soil-mangrove root interface. In the endosphere, the bacterial keystone taxa with top three highest degrees were likely to have a role in

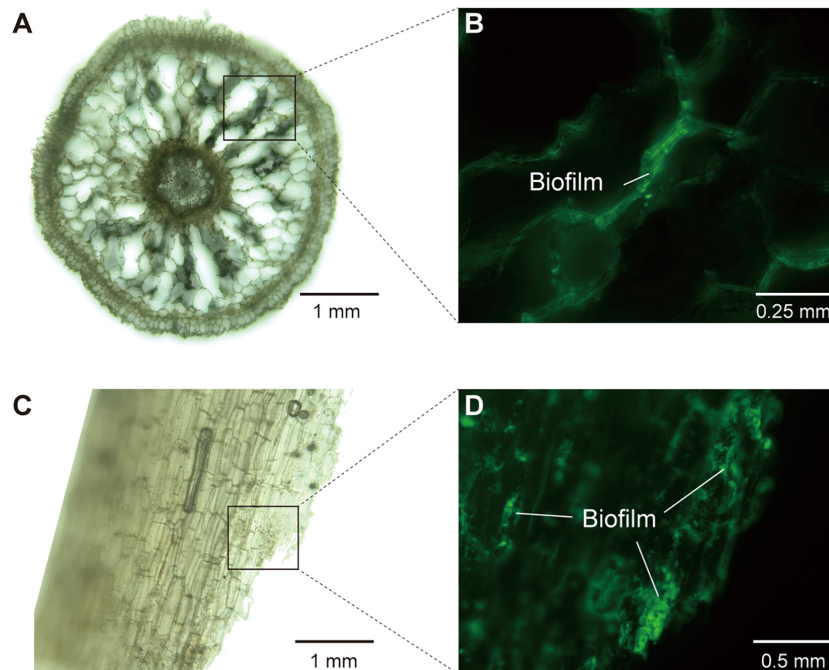


FIGURE 5 | The structure of mangrove roots and the detection of biofilm in root interior under hybrid microscope. **(A,B)** The images of longitudinal section of mangrove roots ($\times 10$ and $\times 20$ magnification, respectively). **(C,D)** The images of transverse section of mangrove roots ($\times 10$ and $\times 40$ magnification, respectively). **(A,C)** Were in brightfield, whereas **(B,D)** were in fluorescence field (488 nm, Mercury Free LED) with extracellular polysaccharides in biofilm being stained and glowing green light.

enhancing inter-domain microbial associations, validating their important status in bacterial-fungal co-occurrence networks. OTUB_260 was affiliated with the *Vibrio* genus, and its members were capable of inhibiting fungal phytopathogens by releasing antimicrobial compounds, thereby conducting negative bacterial-fungal associations (Rameshkumar and Nair, 2009). OTUB_472, was affiliated to *Anaerolineae*, and the members of this class were known to accelerate organic matter degradation when they were stimulated by hyphae exudates of arbuscular mycorrhizal fungi (Cao et al., 2018; Toju and Sato, 2018). Additionally, OTUB_1491 was a member in *Desulfarculaceae* family, and these typical sulfate-reducing bacteria were reported to act as nutrient providers for fungi and trigger fungal colonization (Drake et al., 2017; He et al., 2019). Apart from the natural feature of keystones, biofilm also played an important role in regulating microbial interactions. Early evidence showed that biofilm could form in mangrove roots (Mallick et al., 2018; Glasenapp et al., 2019). Combined with the fact that endophytes were capable of forming mixed-community biofilms inside roots (van Overbeek and Saikonen, 2016), we supposed a high potential of the mixed-community biofilm formation in the endosphere of the mangrove root, thereby providing a niche for intensive microbial inter-domain associations (Cai et al., 2019). In support of this view, we found that the endosphere contained a high abundance of KOs related to the biosynthesis of EPS, and was capable of producing two EPS compounds (trehalose and glucans) and forming biofilms. More importantly, we identified one keystone taxa

(OTUB_260) belong to *Vibrio* sp., which was reported to promote microbial biofilm formation when it communicated with fungi and utilized volatile organic compounds produced by fungi (Cosetta et al., 2020). Correspondingly, these results indicated that the intensified inter-domain microbial associations in the endosphere were related to the specific keystone composition and biofilm formation.

Quorum sensing controls biofilm formation and has been established as a widespread strategy of cell-cell communications in microbial communities (Kim et al., 2017; Padder et al., 2018). In the module 1 we detected in this study (Figure 3), the simultaneous occurrence of *tdh* and *cqsA* may be attributable to the weak microbial inter-domain associations in the episphere. This is because the autoinducers encoded by these two genes were considered to inhibit biofilm formation (Zhu and Mekalanos, 2003; Papenfort et al., 2017) and hence have the potential to hamper microbial cell-cell communications. On the contrary, the module 2 of quorum sensing tended to play a major role in the endosphere, where its involved genes (*rhII* and *lasI*) were highly abundant. The autoinducers C4-HSL and 3OC12-HSL that were regulated by *rhII* and *lasI*, respectively, were reported to facilitate the establishment of biofilms in the endosphere (Ozer et al., 2005), potentially leading to the divergent microbial associations across the soil-mangrove root interface. Besides, the level of quorum sensing autoinducers was related to the variations in environmental factors. Through our mantel test, we found that salinity, temperature and oxidation reduction potential significantly affected ($P < 0.01$) the composition of bacteria and

fungi communities in mangrove soils (**Supplementary Figure 6**). Among these influencing factors, salinity was previously known to play an essential role in affecting the root-associated microbial communities of mangrove (Yin et al., 2018) and the stability of quorum sensing molecules (Huang et al., 2018). Hence, we indicated that environmental factors, especially salinity, could influence quorum sensing autoinducers via shifting mangrove root-associated microbial communities.

Similar to quorum sensing, cobamide has been also widely used as model nutrients for studying microbial interactions (Olga et al., 2020). It was established that cobamide mediated microbial interactions through cobamide-dependent metabolism in a metabolic network elicited by cobamide-dependent reactions (Olga et al., 2020). As the most well-known cobamide, vitamin B12 produced by bacteria was reported to have stimulatory effect on mycorrhizal growth in the rhizosphere soil (Singh et al., 1991), highlighting mutualistic interactions between bacteria and their eukaryotic partners (van Overbeek and Saikkonen, 2016). In this study, we detected adenines within root exudates and the functional genes involving into each step of cobamide biosynthesis, proposing the functional genes involving into each step of cobamide biosynthesis, and proposed *Rhodobacteraceae* and *Pseudomonadaceae* as the key taxa for cobamide synthesis across soil-mangrove root interface. Their crucial roles in synthesizing cobamide for mediating microbial interactions have been documented in artificial seawater (Wienhausen, 2018). Through metagenome

sequencing analysis across four compartments in the soil-root system, we surprisingly found that the endosphere contained a high abundance of cobamide biosynthesis related genes, and there are two reasons for such enrichment inside plant roots. First, abiotic factors (e.g., oxygen) might contribute to the discrepancy of cobamide biosynthesis between outside and inside roots. Due to the tidal process in mangrove ecosystems (Wang et al., 2014), a relatively anoxic circumstance probably existed in peripheral compartments (Wang et al., 2014). This could explain why we detected a high abundance of *cbiT* and *cbiE* encoding for anaerobic corrin ring adenosylation in three peripheral compartments. On the contrary, mangroves were thought to contain large lacunae in the cortex to efficiently transfer internal oxygen, thereby preventing oxygen loss and maintaining aerobic inside the root environment (Pi et al., 2009). As a function of such aerobic condition, we observed that the endosphere harbored a high abundance of *cobG*, *cobF* and *cobA* encoding for aerobic corrin ring adenosylation. Second, cobamide utilization can be mediated by quorum sensing molecules. Previous studies have indicated that certain quorum sensing autoinducers, such as 3OC12-HSL from the module 2, would stimulate microbial communities to accumulate cobamides and subsequently promote microbial growth (Johnson et al., 2016; Das and Ghangrekar, 2019). In support of this hypothesis, we detected the concurrently enriched genes encoding both the module 2 of quorum sensing and cobamide biosynthesis in the endosphere, which

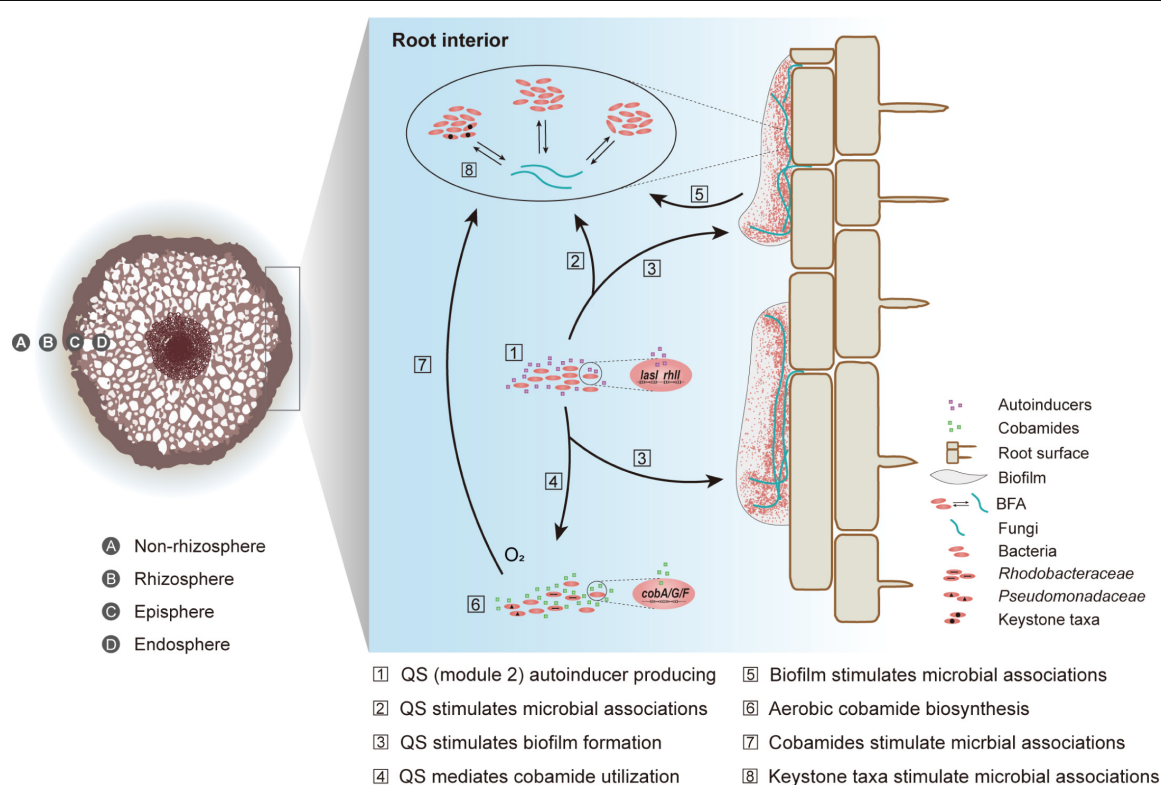


FIGURE 6 | A conceptual model of the intensified bacterial-fungal association (BFA) in root interior. Quorum sensing is abbreviated to QS.

coincided well with intensified associations between bacterial and fungal communities.

Based on our findings and relevant studies (Bertrand et al., 2015; Banerjee et al., 2018; Huang et al., 2018; Shelton et al., 2019; Olga et al., 2020), we built a conception model to illustrate how microbial inter-domain interactions were enhanced in the endosphere of mangrove roots (**Figure 6**). First, through network topological analysis and metagenomic function survey, we found that BFA was divergent across four mangrove root compartments. The intensified BFA in the endosphere could be attributed to the three bacterial keystones (*Vibrio*, *Anaerolineae*, and *Desulfarculaceae*). This was because these bacterial taxa have been thought to closely react with fungal members (Drake et al., 2017; Cao et al., 2018; Toju and Sato, 2018; He et al., 2019; Cosetta et al., 2020). Second, compared to three peripheral compartments, the endosphere contained a higher abundance of genes related to module 2 of quorum sensing and aerobic cobamide biosynthesis, which was consolidated by root exudate analysis. Such enrichment could contribute to the intensified BFA in the endosphere (Bertrand et al., 2015; Banerjee et al., 2018; Huang et al., 2018; Shelton et al., 2019; Olga et al., 2020). Third, quorum sensing could indirectly regulate microbial interactions via mediating cobamide utilization (Johnson et al., 2016; Das and Ghangrekar, 2019) and stimulating biofilm formation (Miller and Bassler, 2001; Kim et al., 2017). Last, the high abundance of EPS-related genes, the production of two EPS compounds within root exudates and the detection of extracellular polysaccharides in the endosphere collectively suggested the existence of biofilm inside mangrove root, which provided a niche for endophytes to develop intensive microbial inter-domain associations. While this study is the first to molecularly characterize the roles of quorum sensing and cobamide biosynthesis across the soil-mangrove root interface, the underlying mechanism at biochemical and phenotypical scales needs further investigation.

CONCLUSION

Through topological and metagenomic analyses of microbial communities across four compartments in the soil-root system, we profiled the varied bacterial-fungal associations across the soil-mangrove root interface. Particularly, we found that the bacterial keystone taxa, the mediation of quorum sensing (module 2), biofilm formation as well as the aerobic cobamide biosynthesis by *Rhodobacteraceae* and *Pseudomonadaceae* might jointly contribute to the intensified bacterial-fungal associations in the endosphere. On the whole, our study provides the genetic elucidation of quorum sensing and cobamide biosynthesis in divergent bacterial-fungal associations across the soil-root interface.

DATA AVAILABILITY STATEMENT

The datasets presented in this study including nucleotide sequences and metagenome sequencing data can be found in online SRA repositories with accession numbers as PRJNA685020, PRJNA685297 and PRJNA613873, respectively.

AUTHOR CONTRIBUTIONS

ZZ: investigation, data curation, formal analysis, and writing-original draft. RH, YN, WH, and QZ: methodology, writing-review, and editing. WZ and ZL: investigation, writing-review, and editing. QY: methodology and funding acquisition. ZH: methodology, supervision, and funding acquisition. CW: conceptualization, supervision, funding acquisition, writing-review, and editing. All authors contributed to the article and approved the submitted version.

FUNDING

This study was supported by the Innovation Group Project of Southern Marine Science and Engineering Guangdong Laboratory (Zhuhai) (No. 311021006), the Innovation Group Project of Southern Marine Science and Engineering Guangdong Laboratory (Zhuhai) (No. 311020005), the National Natural Science Foundation of China (Nos. 91951207, 52070196, 32000070, and 41771095), the Guangdong Basic and Applied Basic Research Foundation (No. 2019A1515011406), the Fundamental Research Funds for the Central Universities (Nos. 19lgpy165, 19lgzd28, and 19lgpy162), and the Hundred Talents Program through Sun Yat-sen University (Nos. 38000-18841205, 99318-18841205, and 38000-18821107).

SUPPLEMENTARY MATERIAL

The Supplementary Material for this article can be found online at: <https://www.frontiersin.org/articles/10.3389/fmicb.2021.698385/full#supplementary-material>

Supplementary Figure 1 | Highly connected modules within bacterial-fungal association (BFA) networks across the non-rhizosphere (Non), rhizosphere (Rhi), episphere (Epi), and endosphere (Endo) compartments.

Supplementary Figure 2 | Topological features of keystone taxa in (A) bacterial, (B) fungal and (C) bacterial-fungal association (BFA) networks across the non-rhizosphere (Non), rhizosphere (Rhi), episphere (Epi), and endosphere (Endo) compartments.

Supplementary Figure 3 | Degrees of keystone taxa from bacterial and fungal phyla in bacterial-fungal association (BFA) networks.

Supplementary Figure 4 | Bacterial community compositions across the non-rhizosphere (Non), rhizosphere (Rhi), episphere (Epi), and endosphere (Endo) compartments.

Supplementary Figure 5 | The relative abundance (TPM, transcripts per-million) of KOs (KEGG Orthology) that related to the biosynthesis of extracellular polymeric substances (EPS) across the non-rhizosphere (Non), rhizosphere (Rhi), episphere (Epi), and endosphere (Endo) compartments.

Supplementary Figure 6 | Correlations of the microbial communities (Bray-Curtis distance) with environmental factors (Euclidean distance) in the non-rhizosphere soil. Edge width corresponded to the Mantel's r -value, and the edge color denoted the statistical significance. Pairwise correlations of the variables were shown with a color gradient denoting Pearson's correlation coefficient.

Supplementary Table 1 | Environmental factors in the non-rhizosphere soil of mangrove.

Supplementary Table 2 | KO (KEGG Orthology) numbers of quorum sensing and cobamide biosynthesis related genes.

Supplementary Table 3 | Taxonomy information and relative abundance of keystone taxa in bacterial-fungal association (BFA), bacterial and fungal networks across the non-rhizosphere (Non), rhizosphere (Rhi), episphere (Epi), and endosphere (Endo) compartments.

Supplementary Table 4 | Key network topological characteristics for bacterial, fungal and bacterial-fungal association (BFA) networks across the non-rhizosphere (Non), rhizosphere (Rhi), episphere (Epi), and endosphere (Endo) compartments.

Supplementary Table 5 | Root exudates that related to biofilm formation and cobamide biosynthesis.

REFERENCES

- Agler, M. T., Ruhe, J., Kroll, S., Morhenn, C., Kim, S. T., and Weigel, D. (2016). Microbial hub taxa link host and abiotic factors to plant microbiome variation. *PLoS Biol.* 14:e1002352. doi: 10.1371/journal.pbio.1002352
- Alongi, D. M. (2014). Carbon cycling and storage in mangrove forests. *Annu. Rev. Mar. Sci.* 6, 195–219. doi: 10.1146/annurev-marine-010213-135020
- Bais, H. P., Weir, T. L., Perry, L. G., Gilroy, S., and Vivanco, J. M. (2006). The role of root exudates in rhizosphere interactions with plants and other organisms. *Annu. Rev. Plant Biol.* 57, 233–266. doi: 10.1016/B978-0-12-818469-1.0009-2
- Banerjee, S., Schlaeppi, K., and van der Heijden, M. G. (2018). Keystone taxa as drivers of microbiome structure and functioning. *Nat. Rev. Microbiol.* 16, 567–576. doi: 10.1038/s41579-018-0024-1
- Banerjee, S., Walder, F., Buchi, L., Meyer, M., Held, A. Y., and Gatterer, A. (2019). Agricultural intensification reduces microbial network complexity and the abundance of keystone taxa in roots. *ISME J.* 13, 1722–1736. doi: 10.1038/s41396-019-0383-2
- Bastian, M., Heymann, S., and Jacomy, M. (2009). Gephi, an open source software for exploring and manipulating networks. *Third Int. Ernational AAAI Confer. Weblogs Soc. Med.* 2009:1520. doi: 10.13140/2.1.1341.1520
- Bengtsson-Palme, J., Ryberg, M., Hartmann, M., Branco, S., Wang, Z., and Godhe, A. (2013). Improved software detection and extraction of ITS1 and ITS2 from ribosomal ITS sequences of fungi and other eukaryotes for analysis of environmental sequencing data. *Methods Ecol. Evol.* 4, 914–919. doi: 10.1111/2041-210X.12073
- Bertrand, E. M., McCrow, J. P., Moustafa, A., Zheng, H., McQuaid, J. B., and Delmont, T. O. (2015). Phytoplankton-bacterial interactions mediate micronutrient colimitation at the coastal Antarctic sea ice edge. *Proc. Natl. Acad. Sci. U. S. A.* 112, 9938–9943. doi: 10.1073/pnas.1501615112
- Blaalid, R., Kumar, S., Nilsson, R. H., Abarenkov, K., and Kausserud, H. (2013). ITS1 versus ITS2 as DNA metabarcodes for fungi. *Mol. Ecol. Resour.* 13, 218–224. doi: 10.1111/1755-0998.12065
- Cai, P., Sun, X., Wu, Y., Gao, C., Mortimer, M., and Holden, P. A. (2019). Soil biofilms, microbial interactions, challenges, and advanced techniques for ex-situ characterization. *Soil Ecol. Lett.* 1, 85–93. doi: 10.1007/s42832-019-0017-7
- Cao, J., Wang, C., Dou, Z., Liu, M., and Ji, D. (2018). Hyphospheric impacts of earthworms and arbuscular mycorrhizal fungus on soil bacterial community to promote oxytetracycline degradation. *J. Hazard. Mater.* 341, 346–354. doi: 10.1016/j.jhazmat.2017.07.038
- Caporaso, J. G., Kuczynski, J., Stombaugh, J., Bittinger, K., Bushman, F. D., and Costello, E. K. (2010). QIIME allows analysis of high-throughput community sequencing data. *Nat. Methods* 7, 335–336. doi: 10.1038/nmeth.f.303
- Chen, L., Xin, X., Zhang, J., Redmile-Gordon, M., Nie, G., and Wang, Q. (2019). Soil Characteristics Overwhelm Cultivar Effects on the Structure and Assembly of Root-Associated Microbiomes of Modern Maize. *Pedosphere* 29, 360–373. doi: 10.1016/S1002-0160(17)60370-9
- Cosetta, C. M., Kfoury, N., Robbat, A., and Wolfe, B. E. (2020). Fungal volatiles mediate cheese rind microbiome assembly. *Environ. Microbiol.* 22, 4745–4760. doi: 10.1111/1462-2920.15223
- Das, S., and Ghangrekar, M. M. (2019). Quorum-sensing mediated signals, A promising multi-functional modulators for separately enhancing algal yield and power generation in microbial fuel cell. *Bioresour. Technol.* 294, 122–138. doi: 10.1016/j.biortech.2019.122138
- de Vries, F. T., Griffiths, R. I., Bailey, M., Craig, H., Girlanda, M., and Gweon, H. S. (2018). Soil bacterial networks are less stable under drought than fungal networks. *Nat. Commun.* 9:3033. doi: 10.1038/s41467-018-05516-7
- Deng, Y., Jiang, Y. H., Yang, Y., He, Z., Luo, F., and Zhou, J. (2012). Molecular ecological network analyses. *BMC Bioinform.* 13:113. doi: 10.1186/1471-2105-13-113
- DeSantis, T. Z., Hugenholtz, P., Larsen, N., Rojas, M., Brodie, E. L., and Keller, K. (2006). Greengenes, a chimera-checked 16S rRNA gene database and workbench compatible with ARB. *Appl. Environ. Microb.* 72, 5069–5072. doi: 10.1128/AEM.03006-05
- Drake, H., Ivarsson, M., Bengtson, S., Heim, C., Siljestrom, S., and Whitehouse, M. J. (2017). Anaerobic consortia of fungi and sulfate reducing bacteria in deep granite fractures. *Nat. Commun.* 8:55. doi: 10.1038/s41467-017-00094-6
- Duran, P., Thiergart, T., Garrido-Oter, R., Agler, M., Kemen, E., and Schulze-Lefert, P. (2018). Microbial Interkingdom Interactions in Roots Promote Arabidopsis Survival. *Cell* 175, 973–983e14. doi: 10.1016/j.cell.2018.10.020
- Edgar, R. C. (2013). UPARSE, highly accurate OTU sequences from microbial amplicon reads. *Nat. Methods* 10, 996–998. doi: 10.1038/nmeth.2604
- Edwards, J., Johnson, C., Santos-Medellín, C., Lurie, E., Podishetty, N. K., and Bhatnagar, S. (2015). Structure, variation, and assembly of the root-associated microbiomes of rice. *Proc. Natl. Acad. Sci. U. S. A.* 112, E911–E920. doi: 10.1073/pnas.1414592112
- Fan, K., Delgado-Baquerizo, M., Guo, X., Wang, D., Zhu, Y. G., and Chu, H. (2020). Biodiversity of key-stone phylotypes determines crop production in a 4-decade fertilization experiment. *ISME J.* 15, 550–561. doi: 10.1038/s41396-020-00796-8
- Fu, L., Niu, B., Zhu, Z., Wu, S., and Li, W. (2012). CD-HIT, accelerated for clustering the next-generation sequencing data. *Bioinformatics* 28, 3150–3152. doi: 10.1093/bioinformatics/bts565
- Glaserapp, Y., Catto, C., Villa, F., Saracchi, M., Cappitelli, F., and Papenbrock, J. (2019). Promoting Beneficial and Inhibiting Undesirable Biofilm Formation with Mangrove Extracts. *Int. J. Mol. Sci.* 20, 35–49. doi: 10.3390/ijms20143549
- Gomes, N. C., Cleary, D. F., Calado, R., and Costa, R. (2011). Mangrove bacterial richness. *Commun. Integr. Biol.* 4, 419–423. doi: 10.4161/cib.15253
- He, H., Fu, L., Liu, Q., Fu, L., Bi, N., and Yang, Z. (2019). Community Structure, Abundance and Potential Functions of Bacteria and Archaea in the Sansha Yongle Blue Hole, Xisha, South China Sea. *Front. Microbiol.* 10:2404. doi: 10.3389/fmicb.2019.02404
- Herren, C. M., and McMahon, K. D. (2018). Keystone taxa predict compositional change in microbial communities. *Environ. microbiol.* 20, 2207–2217. doi: 10.1111/1462-2920.14257
- Holguin, G., Vazquez, P., and Bashan, Y. (2001). The role of sediment microorganisms in the productivity, conservation, and rehabilitation of mangrove ecosystems, an overview. *Biol. Fert. Soils* 33, 265–278. doi: 10.1007/s003740000319
- Huang, X., Zhu, J., Cai, Z., Lao, Y., Jin, H., Yu, K., et al. (2018). Profiles of quorum sensing (QS)-related sequences in phycospheric microorganisms during a marine dinoflagellate bloom, as determined by a metagenomic approach. *Microbiol. Res.* 217, 1–13. doi: 10.1016/j.micres.2018.08.015
- Johnson, W. M., Kido Soule, M. C., and Kujawinski, E. B. (2016). Evidence for quorum sensing and differential metabolite production by a marine bacterium in response to DMSP. *ISME J.* 10, 2304–2316. doi: 10.1038/ismej.2016.6
- Kareb, O., and Aider, M. (2020). Quorum Sensing Circuits in the Communicating Mechanisms of Bacteria and Its Implication in the Biosynthesis of Bacteriocins by Lactic Acid Bacteria, a Review. *Probiot. Antimicro.* 12, 5–17. doi: 10.1007/s12602-019-09555-4
- Karygianni, L., Ren, Z., Koo, H., and Thurnheer, T. (2020). Biofilm Matrixome, Extracellular Components in Structured Microbial Communities. *Trends Microbiol.* 28, 668–681. doi: 10.1016/j.tim.2020.03.016
- Kim, M. K., Zhao, A., Wang, A., Brown, Z. Z., Muir, T. W., and Stone, H. A. (2017). Surface-attached molecules control *Staphylococcus aureus* quorum sensing and

- biofilm development. *Nat. Microbiol.* 2, 170–180. doi: 10.1038/nmicrobiol.2017.80
- Li, D., Liu, C. M., Luo, R., Kunihiko, S., and Tak-Wah, L. (2015). MEGAHIT, an ultra-fast single-node solution for large and complex metagenomics assembly via succinct de Bruijn graph. *Bioinformatics* 31, 1674–1676. doi: 10.1093/bioinformatics/btv033
- Li, M., Ren, L., Zhang, J., Luo, L., Qin, P., Zhou, Y., et al. (2019). Population characteristics and influential factors of nitrogen cycling functional genes in heavy metal contaminated soil remediated by biochar and compost. *Sci. Total Environ.* 651(Pt 2), 2166–2174. doi: 10.1016/j.scitotenv.2018.10.152
- Ma, B., Wang, H., Dsouza, M., Lou, J., He, Y., and Dai, Z. (2016). Geographic patterns of co-occurrence network topological features for soil microbiota at continental scale in eastern China. *ISME J.* 10, 1891–1901. doi: 10.1038/ismej.2015.261
- Ma, B., Zhao, K., Lv, X., Su, W., Dai, Z., and Gilbert, J. A. (2018). Genetic correlation network prediction of forest soil microbial functional organization. *ISME J.* 12, 2492–2505. doi: 10.1038/s41396-018-0232-8
- Mallick, I., Bhattacharyya, C., Mukherji, S., Dey, D., Sarkar, S. C., Mukhopadhyay, U. K., et al. (2018). Effective rhizoinoculation and biofilm formation by arsenic immobilizing halophilic plant growth promoting bacteria (PGPB) isolated from mangrove rhizosphere: A step towards arsenic rhizoremediation. *Sci. Total Environ.* 610–611, 1239–1250. doi: 10.1016/j.scitotenv.2017.07.234
- Marc, L., Bolger, A. M., Axel, N., Fernie, A. R., Lunn, J. E., and Mark, S. (2012). RobiNA, a user-friendly, integrated software solution for RNA-Seq-based transcriptomics. *Nucleic Acids Res. W* 1, W622–W627. doi: 10.1093/nar/gks540
- Miller, M. B., and Bassler, B. L. (2001). Quorum sensing in bacteria. *Annu. Rev. Microbiol.* 55, 165–199. doi: 10.1146/annurev.micro.55.1.165
- Milton, D. L., Hardman, A., Camara, M., Chhabra, S. R., Bycroft, B. W., and Stewart, G. (1997). Quorum sensing in *Vibrio anguillarum*, characterization of the *vanI/vanR* locus and identification of the autoinducer N-(3-oxodecanoyl)-L-homoserine lactone. *J. Bacteriol.* 179, 3004–3012. doi: 10.1128/jb.179.9.3004-3012
- Moriya, Y., Itoh, M., Okuda, S., Yoshizawa, A. C., and Kanehisa, M. (2007). KAAS, an automatic genome annotation and pathway reconstruction server. *Nucleic Acids Res.* 35, W182–W185. doi: 10.1093/nar/gkm321
- Morriën, E., Hannula, S. E., Snoek, L. B., Helmsing, N. R., Zweers, H., and De Hollander, M. (2017). Soil networks become more connected and take up more carbon as nature restoration progresses. *Nat. Commun.* 8, 1–10. doi: 10.1038/ncomms14349
- Mukherjee, S., and Bassler, B. L. (2019). Bacterial quorum sensing in complex and dynamically changing environments. *Nat. Rev. Microbiol.* 17, 371–382. doi: 10.1038/s41579-019-0186-5
- Newman, M. E. (2006). Modularity and community structure in networks. *Proc. Natl. Acad. Sci. U. S. A.* 103, 8577–8582. doi: 10.1073/pnas.0601602103
- Ng, W. L., and Bassler, B. L. (2009). Bacterial quorum-sensing network architectures. *Annu. Rev. Genet.* 43, 197–222. doi: 10.1146/annurev-genet-102108-134304
- Nilsson, R. H., Tedersoo, L., Ryberg, M., Kristiansson, E., Hartmann, M., and Unterseher, M. (2015). A Comprehensive, Automatically Updated Fungal ITS Sequence Dataset for Reference-Based Chimera Control in Environmental Sequencing Efforts. *Microbes Environ.* 30, 145–150. doi: 10.1264/jsme2.ME14121
- Ofek-Lalzar, M., Sela, N., Goldman-Voronov, M., Green, S. J., Hadar, Y., and Minz, D. (2014). Niche and host-associated functional signatures of the root surface microbiome. *Nat. Commun.* 5, 49–50. doi: 10.1038/ncomms5950
- Olesen, J. M., Bascompte, J., Dupont, Y. L., and Jordano, P. (2007). The modularity of pollination networks. *Proc. Natl. Acad. Sci. U. S. A.* 104, 19891–19896. doi: 10.1073/pnas.0706375104
- Olga, S., Shelton, A., and Taga, M. (2020). Sharing vitamins, Cobamides unveil microbial interactions. *Science* 3:369. doi: 10.1126/science.aba0165
- Ozer, E. A., Pezzulo, A., Shih, D. M., Chun, C., Furlong, C., and Lusi, A. J. (2005). Human and murine paraoxonase 1 are host modulators of *Pseudomonas aeruginosa* quorum-sensing. *FEMS Microbiol. Lett.* 253, 29–37. doi: 10.1016/j.femsle.2005.09.023
- Padder, S. A., Prasad, R., and Shah, A. H. (2018). Quorum sensing, A less known mode of communication among fungi. *Microbiol. Res.* 210, 51–58. doi: 10.1016/j.micres.2018.03.007
- Papenfort, K., Silpe, J. E., Schramma, K. R., Cong, J. P., Seyedsayamdost, M. R., and Bassler, B. L. (2017). A *Vibrio cholerae* autoinducer-receptor pair that controls biofilm formation. *Nat. Chem. Biol.* 13, 551–557. doi: 10.1038/nchembio.2336
- Peng, W., Bo, C., and Hua, Z. (2017). High throughput sequencing analysis of bacterial communities in soils of a typical Poyang Lake wetland. *Acta Ecol. Sin.* 37, 2026–2027. doi: 10.1186/s40064-016-2026-7
- Pi, N., Tam, N. F. Y., Wu, Y., and Wong, M. H. (2009). Root anatomy and spatial pattern of radial oxygen loss of eight true mangrove species. *Aquat. Bot.* 90, 222–230. doi: 10.1016/j.aquabot.2008.10.002
- Rameshkumar, N., and Nair, S. (2009). Isolation and molecular characterization of genetically diverse antagonistic, diazotrophic red-pigmented vibrios from different mangrove rhizospheres. *FEMS Microbiol. Ecol.* 67, 455–467. doi: 10.1111/j.1574-6941.2008.00638.x
- Reef, R., Feller, I. C., and Lovelock, C. E. (2010). Nutrition of mangroves. *Tree Physiol.* 30, 1148–1160. doi: 10.1093/treephys/tpq048
- Roger, G. (2005). Functional cartography of complex metabolic networks. *Nature* 433, 895–900. doi: 10.1038/nature03288
- Saleem, M., Law, A. D., Sahib, M. R., Pervaiz, Z. H., and Zhang, Q. (2018). Impact of root system architecture on rhizosphere and root microbiome. *Rhizosphere* 6, 47–51. doi: 10.1016/j.rhisph.2018.02.003
- Sasse, J., Martinoia, E., and Northen, T. (2018). Feed Your Friends, Do Plant Exudates Shape the Root Microbiome? *Trends Plant Sci.* 23, 25–41. doi: 10.1016/j.tplants.2017.09.003
- Shannon, P., Markiel, A., Ozier, O., Baliga, N. S., Wang, J. T., and Ramage, D. (2003). Cytoscape, a software environment for integrated models of biomolecular interaction networks. *Genome Res.* 13, 2498–2504. doi: 10.1101/gr.1239303
- Shelton, A. N., Seth, E. C., Mok, K. C., Han, A. W., Jackson, S. N., and Haft, D. R. (2019). Uneven distribution of cobamide biosynthesis and dependence in bacteria predicted by comparative genomics. *ISME J.* 13, 789–804. doi: 10.1038/s41396-018-0304-9
- Shen, W., Le, S., Li, Y., and Hu, F. (2016). SeqKit, A cross-platform and ultrafast toolkit for FASTA/Q file manipulation. *PLoS One* 11:e0163962. doi: 10.1371/journal.pone.0163962
- Shi, S., Nuccio, E. E., Shi, Z. J., He, Z., Zhou, J., and Firestone, M. K. (2016). The interconnected rhizosphere, High network complexity dominates rhizosphere assemblages. *Ecol. Lett.* 19, 926–936. doi: 10.1111/ele.12630
- Singh, C. S., Kapoor, A., and Wange, S. S. (1991). The enhancement of root colonisation of legumes by vesicular-arbuscular mycorrhizal (VAM) fungi through the inoculation of the legume seed with commercial yeast (*Saccharomyces cerevisiae*). *Plant Soil* 131:129. doi: 10.1007/BF00010427
- Tanja, M., and Salzberg, S. L. (2011). FLASH, fast length adjustment of short reads to improve genome assemblies. *Bioinformatics* 27, 2957–2963. doi: 10.1093/bioinformatics/btr507
- Thatoi, H., Behera, B. C., Mishra, R. R., and Dutta, S. K. (2013). Biodiversity and biotechnological potential of microorganisms from mangrove ecosystems, a review. *Ann. Microbiol.* 63, 1–19. doi: 10.1007/s13213-012-0442-7
- Toju, H., and Sato, H. (2018). Root-Associated Fungi Shared Between Arbuscular Mycorrhizal and Ectomycorrhizal Conifers in a Temperate Forest. *Front. Microbiol.* 9:433. doi: 10.3389/fmicb.2018.00433
- Tu, Q., Deng, Y., Yan, Q., Shen, L., Lin, L., and He, Z. (2016). Biogeographic patterns of soil diazotrophic communities across six forests in North America. *Mol. Ecol.* 25, 2937–2948. doi: 10.1111/mec.13651
- van Overbeek, L. S., and Saikkonen, K. (2016). Impact of Bacterial-Fungal Interactions on the Colonization of the Endosphere. *Trends Plant Sci.* 21, 230–242. doi: 10.1016/j.tplants.2016.01.003
- Wang, H. T., Su, J. Q., Zheng, T. L., and Yang, X. R. (2014). Impacts of vegetation, tidal process, and depth on the activities, abundances, and community compositions of denitrifiers in mangrove sediment. *Appl. Microbiol. Biotechnol.* 98, 9375–9387. doi: 10.1007/s00253-014-6017-8
- Warren, M. J., Raux, E., Schubert, H. L., and Escalante-Semerena, J. C. (2002). The biosynthesis of adenosylcobalamin (vitamin B12). *Nat. Prod. Rep.* 19, 390–412. doi: 10.1039/B108967F
- Wienhausen, G. M. (2018). *Linking the Exometabolome of Selected Organisms of the Roseobacter Group to Marine Dissolved Organic Matter, a Microbiological Perspective*. Oldenburg: Carl-von-Ossietzky Universität Oldenburg.

- Wood, D. E., Lu, J., and Langmead, B. (2019). Improved metagenomic analysis with Kraken 2. *Genome Biol.* 20:257. doi: 10.1186/s13059-019-1891-0
- Xie, X., Weng, B., Cai, B., Dong, Y., and Yan, C. (2014). Effects of arbuscular mycorrhizal inoculation and phosphorus supply on the growth and nutrient uptake of *Kandelia obovata* (Sheue, Liu & Yong) seedlings in autoclaved soil. *Appl. Soil. Ecol.* 75, 162–171. doi: 10.1016/j.apsoil.2013.11.009
- Yin, P., Yin, M., Cai, Z., Wu, G., Lin, G., and Zhou, J. (2018). Structural inflexibility of the rhizosphere microbiome in mangrove plant *Kandelia obovata* under elevated CO₂. *Mar. Environ. Res.* 140, 422–432. doi: 10.1016/j.marenvres.2018.07.013
- Yuan, M. M., Guo, X., Wu, L., Zhang, Y., Xiao, N., and Ning, D. (2021). Climate warming enhances microbial network complexity and stability. *Nat. Clim. Change* 11, 343–348. doi: 10.1038/s41558-021-00989-9
- Zhang, C., Zhang, Y., Ding, Z., and Bai, Y. (2019). Contribution of Microbial Inter-kingdom Balance to Plant Health. *Mol. Plant* 12, 148–149. doi: 10.1016/j.molp.2019.01.016
- Zhang, Y., Zheng, L., Zheng, Y., Xue, S., Zhang, J., and Huang, P. (2020). Insight into the assembly of root-associated microbiome in the medicinal plant *Polygonum cuspidatum*. *Ind. Crop Prod.* 145:112163. doi: 10.1016/j.indcrop.2020.112163
- Zhou, J., Bruns, M. A., and Tiedje, J. M. (1996). DNA recovery from soils of diverse composition. *Appl. Environ. Microb.* 62, 316–322. doi: 10.1128/AEM.62.2.316-322.1996
- Zhou, J., Deng, Y., Luo, F., He, Z., Tu, Q., and Zhi, X. (2010). Functional molecular ecological networks. *MBio* 1, e169–e110. doi: 10.1128/mBio.00169-10
- Zhu, J., and Mekalanos, J. J. (2003). Quorum sensing-dependent biofilms enhance colonization in *Vibrio cholerae*. *Dev. Cell.* 5, 647–656. doi: 10.1016/s1534-5807(03)00295-8
- Zhuang, W., Yu, X., Hu, R., Luo, Z., Liu, X., and Zheng, X. (2020). Diversity, function and assembly of mangrove root-associated microbial communities at a continuous fine-scale. *NPJ Biofilms Microbi.* 6:52. doi: 10.1038/s41522-020-00164-6

Conflict of Interest: The authors declare that the research was conducted in the absence of any commercial or financial relationships that could be construed as a potential conflict of interest.

Publisher's Note: All claims expressed in this article are solely those of the authors and do not necessarily represent those of their affiliated organizations, or those of the publisher, the editors and the reviewers. Any product that may be evaluated in this article, or claim that may be made by its manufacturer, is not guaranteed or endorsed by the publisher.

Copyright © 2021 Zhou, Hu, Ni, Zhuang, Luo, Huang, Yan, He, Zhong and Wang. This is an open-access article distributed under the terms of the Creative Commons Attribution License (CC BY). The use, distribution or reproduction in other forums is permitted, provided the original author(s) and the copyright owner(s) are credited and that the original publication in this journal is cited, in accordance with accepted academic practice. No use, distribution or reproduction is permitted which does not comply with these terms.



Predominant Biphenyl Dioxygenase From Legacy Polychlorinated Biphenyl (PCB)-Contaminated Soil Is a Part of Unusual Gene Cluster and Transforms Flavone and Flavanone

Jachym Suman^{1*}, Michal Strejcek¹, Andrea Zubrova¹, Jan Capek¹, Jiri Wald¹, Klara Michalikova², Miluse Hradilova³, Kamila Sredlova², Jaroslav Semerad^{2,4}, Tomas Cajthaml^{2,4} and Ondrej Uhlik^{1*}

OPEN ACCESS

Edited by:

Monica T. Pupo,
University of São Paulo, Brazil

Reviewed by:

Stephen Seah,
University of Guelph, Canada
Cintia Duarte de Freitas Milagre,
São Paulo State University, Brazil
Norberto Peoporine Lopes,
University of São Paulo, Brazil

*Correspondence:

Jachym Suman
jachym.suman@vscht.cz
Ondrej Uhlik
ondrej.uhlik@vscht.cz

Specialty section:

This article was submitted to
Terrestrial Microbiology,
a section of the journal
Frontiers in Microbiology

Received: 21 December 2020

Accepted: 20 September 2021

Published: 14 October 2021

Citation:

Suman J, Strejcek M, Zubrova A, Capek J, Wald J, Michalikova K, Hradilova M, Sredlova K, Semerad J, Cajthaml T and Uhlik O (2021) Predominant Biphenyl Dioxygenase From Legacy Polychlorinated Biphenyl (PCB)-Contaminated Soil Is a Part of Unusual Gene Cluster and Transforms Flavone and Flavanone. *Front. Microbiol.* 12:644708. doi: 10.3389/fmicb.2021.644708

¹ Department of Biochemistry and Microbiology, Faculty of Food and Biochemical Technology, University of Chemistry and Technology, Prague, Czechia, ² Institute of Microbiology, Academy of Sciences of the Czech Republic, Prague, Czechia, ³ Institute of Molecular Genetics of the Czech Academy of Sciences, Prague, Czechia, ⁴ Faculty of Science, Institute for Environmental Studies, Charles University, Prague, Czechia

In this study, the diversity of *bphA* genes was assessed in a ¹³C-enriched metagenome upon stable isotope probing (SIP) of microbial populations in legacy PCB-contaminated soil with ¹³C-biphenyl (BP). In total, 13 *bphA* sequence variants (SVs) were identified in the final amplicon dataset. Of these, one SV comprised 59% of all sequences, and when it was translated into a protein sequence, it exhibited 87, 77.4, and 76.7% identity to its homologs from *Pseudomonas furukawii* KF707, *Cupriavidus* sp. WS, and *Pseudomonas alcaliphila* B-367, respectively. This same BphA sequence also contained unusual amino acid residues, Alanine, Valine, and Serine in region III, which had been reported to be crucial for the substrate specificity of the corresponding biphenyl dioxygenase (BPDO), and was accordingly designated BphA_AVS. The DNA locus of 18 kbp containing the BphA_AVS-coding sequence retrieved from the metagenome was comprised of 16 ORFs and was most likely borne by *Paraburkholderia* sp. The BPDO corresponding to *bphAE_AVS* was cloned and heterologously expressed in *E. coli*, and its substrate specificity toward PCBs and a spectrum of flavonoids was assessed. Although depleting a rather narrow spectrum of PCB congeners, the efficient transformation of flavone and flavanone was demonstrated through dihydroxylation of the B-ring of the molecules. The homology-based functional assignment of the putative proteins encoded by the rest of ORFs in the AVS region suggests their potential involvement in the transformation of aromatic compounds, such as flavonoids. In conclusion, this study contributes to the body of information on the involvement of soil-borne BPDOs in the metabolism of flavonoid compounds, and our paper provides a more advanced context for understanding the interactions between plants, microbes and anthropogenic compounds in the soil.

Keywords: aromatic ring-hydroxylating dioxygenases, biphenyl dioxygenase, secondary plant metabolites, flavonoids, polychlorinated biphenyls, functional metagenomics

INTRODUCTION

Biphenyl dioxygenases (BPDOs) are type IV multicomponent aromatic ring-hydroxylating dioxygenases (ARHDs) (Kweon et al., 2008). They consist of a large and small subunit of a terminal dioxygenase (in the case of BPDO, designated BphA and BphE, also referred to as BphA1 and BphA2, respectively) and an electron transfer chain (Furukawa et al., 1989; Furukawa et al., 2004; Kweon et al., 2008). ARHDs play a crucial role in nature, being used by many aerobic bacteria for the activation of a thermodynamically stable benzene ring for its further fission and catabolism (Mason and Cammack, 1992). BPDOs, similarly to other ring hydroxylating dioxygenases, exhibit broad substrate specificity. For instance, not only do BPDOs oxidize biphenyl (BP) but also molecules with a similar structure, such as anthropogenic halogenated BPs, including polychlorinated biphenyls (PCBs) and diphenyl ethers (Furukawa et al., 1989; Sylvestre et al., 1996; Furukawa, 2000; Pieper, 2005; Robrock et al., 2011).

Although PCBs are not commonly present in soils, PCB-degrading bacteria are ubiquitous in soils and sediments (Focht, 1995). Additionally, efficient PCB degraders have been isolated from termite guts where their lignin-rich diet is decomposed (Chung et al., 1994). Consequently, lignin-derived phenolics have been proposed as evolutionary original substrates of PCB-degrading enzymes (Focht, 1995; Furukawa et al., 2004). More recently, Sylvestre and colleagues postulated that the BP degradation pathway in soil bacteria may have evolved to serve different ecological functions (Pham and Sylvestre, 2013), including the metabolism of secondary plant metabolites (SPMs) (Toussaint et al., 2012; Pham et al., 2015). It is hypothesized that SPMs, being a wide array of compounds, including flavonoids (Singer et al., 2003), evolved to assist the plant in tolerating frost, storing nutrients, reinforcing structurally, signaling to mutualists, as well as acting as allelopathic chemicals and chemicals protecting the plant from herbivory (Rausher, 2001). Because insects and other herbivores are continually developing mechanisms of resistance to SPMs, plants are driven to modify and develop new mechanisms of protection, including the modification of SPMs. These changes in plant SPM content and composition in turn affect soil microbial communities, which has resulted in the establishment of enzymes with broad substrate specificity in soil bacteria (Singer et al., 2003); this then leads to the hypothesis that enzymes originally evolved for the degradation, transformation and/or detoxification of SPMs are also fortuitously involved in the degradation of anthropogenic pollutants. However, there is still a severe lack of data on how SPMs are linked with biodegradative broad-substrate-specificity enzymes, including BPDOs.

The affinity between the substrate and the BPDO enzyme is determined by amino acid (AA) residues in key positions

of the large subunit of the terminal dioxygenase. Mondello et al. (1997) identified four sequence regions of the C-terminal portion of BphA from *Paraburkholderia xenovorans* LB400 (BphA_{LB400}) which have a direct impact on the catabolic properties of the enzyme. Region III, a consecutive span of seven amino acids (Tyr335-Phe-Asn-Asn-Ile-Arg-Ile341 in the wild-type BphA_{LB400}), was found to have the largest influence on substrate specificity and regioselectivity (Vézina et al., 2008), with residues Tyr335 and Phe336 impacting on substrate binding and orientation (Barriault et al., 2004) and residues Asn338 or Ile341 on catalytic activity (Mohammadi and Sylvestre, 2005). More recently, the sequence of BPDO BphA_{II9}, a BphA_{LB400}-derivative whose region III was engineered toward more efficient PCB transformation (Dhindwal et al., 2016), was analyzed by Zhu et al. (2020) in order to reveal the contribution of the AA residues of this region and others in the sequence to its catalytic efficiency. The authors concluded that the residues Gly335, Asn337, Thr338, and Ile339 within region III together with Asp230 facilitate the catalysis of both BP and 4, 4'-diCB.

The majority of data on BPDOs accumulated to date have described BPDOs in bacterial isolates. However, more recent studies (Iwai et al., 2010; Strejcek et al., 2015) on BPDOs in environmental matrices have shown an extensive diversity of environmental BphA, sometimes differing in the AA patterns common for region III in the isolates (Sul et al., 2009; Strejcek et al., 2015). Nevertheless, there is an immense lack of knowledge about the function of such diverse BPDOs, and especially about their substrate specificity, which would enable predictions of the role of these BPDOs in the transformation of various aromatic substances present in the environment. With this in mind, the objective of this study was to characterize a *bphA*-coding sequence which was isolated from ¹³C-labeled DNA fractions after stable isotope probing (SIP) with ¹³C-BP performed in legacy PCB-contaminated soil (Uhlík et al., 2012). Due to an unusual AA pattern in region III of its predicted protein sequence, namely, Ala333, Val335, and Ser340, we designated the sequence BphA_{AVS} and aimed to reveal its presumably unusual substrate specificity and thus predict its function in the soil environment. For this purpose, we elucidated the genomic context of the *bphA*_{AVS} sequence and experimentally revealed the substrate specificity of the corresponding BPDO through heterologous expression in *E. coli*. The transformation of a Delor 103-contained spectrum of PCB congeners was investigated along with a series of flavonoids as compounds of plant origin widely found in soils and exhibiting structural homology with BP/PCBs (Singer, 2006).

MATERIALS AND METHODS

Amplicon Sequencing and Processing of *bphA* Genes

The *bphA* genes were amplified from the ¹³C-enriched metagenome isolated from legacy PCB-contaminated soil after SIP with ¹³C-BP (14-day incubation time), as was described

Abbreviations: AA, amino acid; ARHD, aromatic ring-hydroxylating dioxygenase; HOPDA, 2-hydroxy-6-oxo-6-phenyl-2,4-hexadienoic acid; BP, biphenyl; BPDO, biphenyl 2,3-dioxygenase; CB, monochlorobiphenyl; diCB, dichlorobiphenyl; triCB, trichlorobiphenyl; IPTG, isopropyl-β-D-1-thiogalactopyranoside; PCB, polychlorinated biphenyl; SIP, stable isotope probing; SV, sequence variant.

earlier (Uhlík et al., 2012). The amplicons were generated by PCR with primers adapted from Iwai et al. (2010), which were fused with barcode sequences (only forward primer) and sequencing adapters (454 Sequencing Application Brief No. 001-2009, Roche). PCR was performed in 20- μ l reactions containing 0.2 mM dNTPs (Finnzymes, Finland), 0.2 μ M primers (Generi Biotech, Czechia), 0.1 mg.ml⁻¹ bovine serum albumin (New England BioLabs, Great Britain), 0.4 U of Phusion Hot Start II DNA Polymerase (Finnzymes, Finland) in the corresponding buffer, and template DNA (10–50 ng). The cycling conditions were as follows: 98°C for 3 min, 35 cycles of 98°C for 10 s, 56°C for 30 s, and 72°C for 30 s with final extension at 72°C for 10 min. The resulting PCR products were re-amplified in the 8-cycle reconditioning step (Thompson et al., 2002) using 0.5 μ l of the first PCR product, 0.2 mM dNTPs, 0.2 μ M primers, 0.1 mg.ml⁻¹ bovine serum albumin and 1 U of Phusion Hot Start II DNA Polymerase in the corresponding buffer. Reconditioning PCR products were purified using AMPure XP Beads (Agencourt, Beckman Coulter, Brea, CA, United States) following the manufacturer's instructions and pooled together for sequencing. Pyrosequencing was performed unidirectionally from the forward primer using a GS FLX + system with Titanium reagents (Roche, Germany) as described elsewhere (Polivkova et al., 2018). An analogous procedure was applied to total community DNA, which was isolated prior to the construction of SIP microcosms (Uhlík et al., 2012).

Sequence data were translated from the SFF to FASTQ format using the `sff2fastq` (v0.9.2¹) utility. The sample barcode-forward primer and reverse primer sequences were trimmed off from the reads using `Cutadapt` (v2.10) (Martin, 2011) in linked adaptor mode (-g). The reads with untrimmed barcode-forward primer sequences and those shorter than 400 bp were discarded. The read error correction was performed using the package `DADA2` (v1.12.1) (Callahan et al., 2016) in the R environment (R Core Team, 2017) with default settings except that the reads were truncated to 400 bp. Chimeric sequences were detected with the “pooled” method. To correct potential frameshifts remaining in the data, the nucleotide sequences were subjected to a frameshift-aware DIAMOND `blastx` search (v0.9.30) (Buchfink et al., 2015) against RefSeq bacterial proteins (downloaded 02/19/2020) (O'Leary et al., 2016) with subsequent frameshift-corrected sequence export as described by Arumugam et al. (2019). Using the DIAMOND `blastx` results, sequences with a top hit not relevant to the terms “Rieske domain” or “dioxygenase” were removed from the dataset as non-specific targets. Finally, as the frameshift correction approach left “n” or “nn” in the sequences that represented deletion or insertion, respectively, and since all the frameshifts were localized in homopolymer regions, the inserted “n/nn” were corrected accordingly, i.e., changing “n” to a nucleotide from the homopolymer or removing “nn” together with one extra nucleotide from the homopolymer. This final set of corrected amplicon sequences will be further referred to as sequence variants (SVs).

Sequencing of the ¹³C-Metagenome and Recovery of *bphA_AVS* and the Surrounding Region

Prior to shotgun sequencing, the ¹³C-metagenome was amplified using a REPLI-g Mini Kit (Qiagen) according to the manufacturer's recommendations, in a 50 μ l reaction with a DNA input amount of 0.3 ng and a reaction time of 8 h. Upon amplification, DNA was precipitated with 70% ethanol and 0.3 M sodium acetate at -20°C for 16 h. DNA was harvested by centrifugation (20,000 \times g, 4°C, 20 min), washed twice with 70% ethanol, and finally resuspended in 50 μ l of molecular biology-grade water. The amplified DNA was fragmented with a Bioruptor NextGen Sonication System (Diagenode) for 30 cycles with high performance set up to achieve 300–400 bp-long inserts. Fragment length distribution was controlled with an Agilent Bioanalyzer 2100 (High Sensitivity DNA chip). The sequencing library was prepared from an input amount of 82 ng of fragmented DNA using a NEBNext Ultra DNA Library Prep Kit for Illumina (New England BioLabs) with size selection conditions adjusted to the final library size in the range of 400–500 bp. Illumina Index Primer 11 was used for barcoding the sample. Final library PCR amplification included 9 cycles, and the resultant product was cleaned up with AMPure XP Beads (Agencourt). Library length profile and concentration were controlled with Agilent Bioanalyzer (High Sensitivity DNA chip) and Qubit 2.0 Fluorimeter (Life Technologies, Carlsbad, CA, United States), respectively. The library was sequenced in a NextSeq 500 Illumina platform (NextSeq Control Software 4.0), 2 \times 150 bp paired-end mode using a High-Output v2.1 (300 cycles) Kit with loading molarity 1.8 pM, including 1% PhiX control.

Raw FASTQ files were processed with BBtools (v38.70² as follows: (1) optical duplicates were removed with `clumpify.sh dedupe optical`; (2) low-quality regions were removed with `filterbytile.sh`; (3) reads with low average quality as well as adapters were removed with `bbduk.sh ktrim = r k = 23 mink = 11 hdist = 1 tbo tpe minlen = 100 ref = adapters ftm = 5 ordered maq = 18 maxns = 0`; (4) synthetic artifacts were removed using `bbduk.sh k = 31 ref = artifacts,phix ordered cardinality`; (5) read coverage was normalized using `bbnorm.sh target = 1000`; (6) paired-end reads were merged with the use of `bbmerge-auto.sh strict k = 93 extend2 = 80 rem ordered`; and (7) unmerged reads were once more filtered using `bbduk.sh qtrim = r trimq = 10 minlen = 100 ordered`. Contigs were assembled and scaffolded with metaSPAdes (v3.13.1) (Nurk et al., 2017) using both merged and unmerged reads.

The scaffold bearing *bphA_AVS* was identified by searching against the *bphA_AVS* amplicon SV in the assembly output using `blastn` (BLAST + v2.9.0) (Camacho et al., 2009). Genomic features were predicted and annotated using Prokka (v1.14.6) (Seemann, 2014). The putative functions of deduced proteins encoded by ORFs within the genomic proximity of *bphA_AVS*, herein referred to as the AVS region, were assessed manually by

¹<https://github.com/indranil/sff2fastq>

²<https://sourceforge.net/projects/bbmap/>

a blastp search against the UniProtKB/Swiss-Prot (The UniProt Consortium, 2018) and RefSeq database (O'Leary et al., 2016), combined with the literature review.

Taxonomic Classification of the Putative *bphA_AVS*-Bearing Organism

To determine the putative organism of origin of the *bphA_AVS* sequence, ORFs localized on the scaffold were searched against the NCBI RefSeq protein database (downloaded 02/19/2020) (O'Leary et al., 2016) using DIAMOND (v0.9.30) (Buchfink et al., 2015). For each query, the top hit subject's taxonomy was extracted. In addition to NCBI taxonomy, the Genome Taxonomy Database's (GTDB) (Parks et al., 2020) rank normalized classification was derived as well. The number of top hits and their average protein identity were used to assign the putative taxonomy of the *bphA_AVS*-host organism.

Phylogeny Reconstruction of ARHD Large Subunits

In order to assess the phylogenetic relationship of BphA proteins corresponding to the *bphA* amplicon SVs, their deduced AA sequences were used for a homology search through the BLASTp (BLAST + v2.9.0) algorithm against the RefSeq database (O'Leary et al., 2016). The top hits, together with the set of exemplary BphA large subunit sequences whose functional characterization has been reported to date, were cropped to the length of *bphA* SVs (corresponding to the positions Gln226-Val358 in BphA_{LB400}). The cropped sequences were aligned using T-Coffee (mode Expresso) (Di Tommaso et al., 2011), and their phylogeny was reconstructed using the Maximum Likelihood method and JTT matrix-based model (Jones et al., 1992) within the MEGA X environment (5 categories for the discrete gamma distribution of rates among sites, some sites allowed to be evolutionarily invariable, all sites were used for the reconstruction) (Kumar et al., 2018). To reveal the phylogeny of the complete BphA_{AVS} mined from the metagenome in the context of Rieske-type ARHDs functionally characterized to date, the set of full-length sequences of ARHD large subunits was created based on a manual literature research. The AA sequences were aligned, and their phylogeny was reconstructed in the same way as for amplicon SVs. The alignment of BphA sequences was visualized using BOXSHADE version 3.21.

Growth Media, Plasmids, Strains, and Growth Conditions

Lysogeny Broth (LB, 10 g/l Tryptone, 5 g/l yeast extract, 10 g/l NaCl) was used for all cultivations in this study. *Escherichia coli* DH11S (Lin et al., 1992) was used for both vector construction and gene expression. When needed, the antibiotics ampicillin, kanamycin, or their combination were added to the media to final concentrations of 150 and 50 µg·ml⁻¹, respectively. The following plasmids were used: (i) for the expression of BPDO mined from the metagenome, pQE-31 plasmid was employed (ampicillin selection; Qiagen), (ii) for the complementation of BphF and BphG activities necessary for the BPDO function, pYH31-bphFGBC_{LB400} plasmid was used,

bearing the bphFGBC gene cluster from *Par. xenovorans* LB400 [kanamycin selection; original name pYH31[LB400-*bphFGBC*], kindly provided by prof. Michel Sylvestre (Chebrou et al., 1999)].

BPDO_AVS Expression Vector Construction

The expression plasmid using the pQE-31 (Qiagen) backbone was constructed employing an In-Fusion® HD Cloning Kit (Clontech Laboratories). The target cluster bphAE_AVS was amplified from the ¹³C-enriched DNA using HotStart ReadyMix (KAPA Biosystems) employing the primers AVS_F (5'-GAGGAGAAATTAAGTATGAGTACGACGATGAAGGAA) and AVS_R (5'-AACAGGAGTCCAAGCTTAGAAGAACATGCTGAGGTTGTTTCG; the 15 bp overlap sequences on the 5'-ends enabling cloning by the In-Fusion® HD Cloning Kit are underlined). The backbone of pQE31 was inverse PCR-amplified using the primers pQE_F (5'-GCTTGGACTCCTGTTGATAGATCC) and pQE_R (5'-AGTTAATTTCTCCTCTTTAATGAATTCTGTGTG) (Supplementary Figure 1). Both fragments were then fused using the In-Fusion® HD Cloning Kit, yielding the plasmid pQE31-bphAE_AVS, in which the genes bphAE_AVS are located 8 bp downstream from the pQE-31 *E. coli*-consensual ribosome binding site; the DNA span encoding for the His-tag was omitted from the original plasmid sequence. The nucleotide sequence of the insert was verified by Sanger sequencing. The resulting plasmid, pQE31-bphAE_AVS, was used for the transformation of *E. coli* DH11S competent cells already hosting pYH31-bphFGBC_{LB400}. Upon their selection in the presence of a combination of ampicillin and kanamycin, grown colonies were PCR-screened for the presence of both plasmids and used for BPDO-heterologous expression assays.

Heterologous Expression of BPDO_AVS and PCB/flavonoid Depletion Assay

In order to assess the PCB/flavonoid transformation capability of the BPDO_AVS, the cells of *E. coli* DH11S were employed, bearing pYH31-bphFGBC_{LB400} either in combination with the plasmid pQE31-bphAE_AVS or empty pQE-31 (control cells in terms of the presence of BPDO_AVS), following a modified procedure of San-Miguel et al. (2013). A single colony picked from a plate was grown overnight in LB medium supplemented with ampicillin and kanamycin. This culture was then used for the inoculation of fresh LB medium with antibiotics. The cells were cultivated at 37°C on a rotary shaker (220 rpm) until OD₆₀₀ reached a value of ca 0.5 (ca 5 h). The culture was then cooled down on ice and IPTG was added to a final concentration of 0.3 mM. The culture was then cultivated for ca 20 h at 16°C/130 rpm. Upon cultivation, the cells were harvested (5,000 × g/5 min), washed twice with cold mineral salt solution (MSS) (Uhlík et al., 2009; Wald et al., 2015) and eventually resuspended in MSS to achieve a final OD₆₀₀ = 5. Prior to further assays, the activity of BPDO in *E. coli* cells was verified by adding 10 µl of 50 mM ethanolic BP solution to a 1 ml-aliquot of the washed cells suspension – in the presence of the active BPDO holoenzyme as well as BphB and BphC

proteins, this amendment resulted in the quick evolution of the bright yellow BP-transformation intermediate 2-hydroxy-6-oxo-6-phenyl-2,4-hexadienoic acid (HOPDA). The cells were then subjected to a modified resting cell assay as described in Vergani et al. (2019) and Garrido-Sanz et al. (2020). Briefly, 5 ml aliquots of the cell suspension were distributed to 119 ml glass microcosms, then the substrate was added, and the microcosms were hermetically sealed and cultivated for 24 h at 28°C/130 rpm. For PCB depletion assessment, 3 μ l of 10 mg/ml of Delor 103 solution in acetone was added. SPMs (flavone, flavanone, daidzein, quercetin, chrysin, naringenin, apigenin, morin, and coumarin, **Figure 1**) or BP (all purchased from MilliporeSigma, DE, except daidzein that was provided by Cayman Chemical, United States) were added in the form of an ethanolic solution so that the final concentration was 25 μ M. Upon incubation with the substrates, the microcosms were stored at -80°C until further analyses. All microcosms were set up in quadruplicates. For the SPMs, non-biotic control, i.e., microcosms containing only MSS with added substrate with no cells, were also prepared and analyzed in order to assess non-specific transformation/depletion during the experiment.

Depletion of Biphenyl, Flavone, and Flavanone Using Crude Whole-Cell Extract

In order to compare the depletion rates of biphenyl, flavone and flavanone, the BPDO_AVS was expressed in *E. coli* cells as described above. The resulting *E. coli* cell suspension with active BPDO_AVS was concentrated in MSS by centrifugation to the theoretical $\text{OD}_{600} = 20$ and disrupted using a One Shot cell disruptor (pressure 1.95 k Bar; Constant Systems Ltd.). Upon disruption, cell debris was removed by centrifugation ($20,000 \times g$, 10 min) and microfiltration (0.45 μm). The crude whole-cell extract was then distributed by 50 μ l into 1.2 ml glass vials, followed by the addition of 2 μ l of 0.5 mM substrate solution in DMSO corresponding to a final concentration of 20 μ M. The reactions were terminated by the addition of an equal volume of methanol and the samples were stored at -80°C until further analyses. The crude cell extract from *E. coli* cells bearing empty

pQE-31 plus pYH31-bphFGBC_LB400 was used as a control of non-enzymatic substrate depletion.

Analysis of PCB and SPM Depletion and Resultant Transformation Products

PCB depletion in microcosms was analyzed using gas chromatography-mass spectrometry (GC-MS) as described in Vergani et al. (2019). The individual PCB congeners were quantified using external calibration. The calibration curves were constructed in the concentration range of 0.001 to 0.750 $\mu\text{g/ml}$ using the IADN PCB Congener Set (AccuStandard, United States) and several other pure congeners obtained from AccuStandard, Merck (Germany) and Dr. Ehrenstorfer (Germany). The regression coefficients of the calibration curves were >0.998 . The depletion rates of individual congeners or SPMs were expressed as $R = (\text{SPM content in the presence of a respective strain})/(\text{SPM content in the abiotic control sample})$. The calculation of standard deviations (SD) of the resulting R values was based on the propagation of errors according to Tellinghuisen (2001).

The depletion of SPMs was assessed by liquid chromatography-mass spectrometry (LC-MS). The cell suspension after the resting cell assay was sonicated for 15 min (Ecoson, Slovakia) and centrifuged at $2,000 \times g$ for 10 min (Hettich EBA200, Germany). The supernatant was diluted appropriately with 50% methanol and analyzed with LC-MS. Analysis of SPMs in the extract was performed using an Agilent 1260 Infinity II liquid chromatograph coupled to an Agilent 6470 LC/TQ mass spectrometer (target analysis) or a high-resolution Agilent QTOF 6546 mass spectrometer – QTOF MS (non-target analysis), both equipped with an Agilent Jet Stream electrospray ion source (Agilent Technologies, Santa Clara, CA, United States). The separation of analyses was performed in a 2.7 μm Poroshell 120 EC-C18 chromatographic column (3.0×100 mm, Agilent, Santa Clara, CA, United States). The mobile phase was composed of 0.5 mM ammonium fluoride in water and methanol. The gradient elution started with 5% methanol for 0.5 min and increased to 100% in 5 min. After 10 min at 100% methanol, the starting conditions were established and the column was equilibrated for 3 min prior

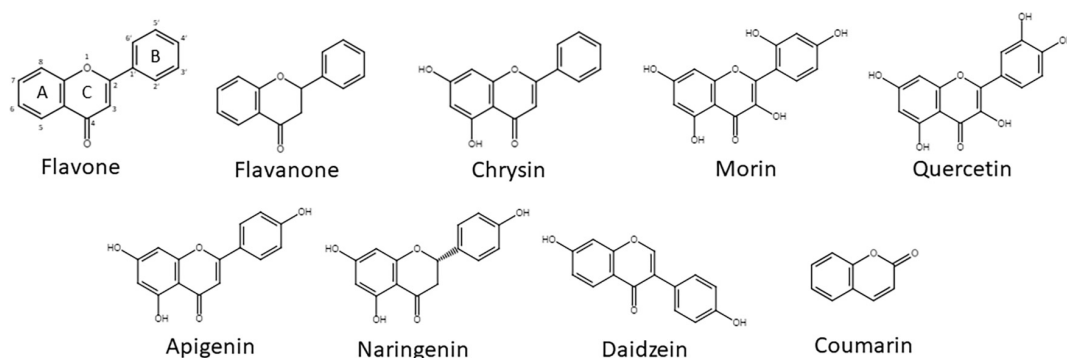


FIGURE 1 | SPMs used in this study. The numbering of atoms is shown, as well as the designation of the A-, B-, and C-rings in the flavone structure.

to injection of the next sample. The flow rate was 0.6 ml/min and the column temperature was maintained at 40°C. 20 µl of sample extract was injected. For the target analysis, electrospray ionization (ESI) was operated in both positive and negative modes. Two specific ion transitions were monitored for each analyte in multiple-reaction monitoring mode (MRM): negative (Q1/Q3): apigenin 269/117; 205, chrysin 253/209; 135, daidzein 253/209; 135, naringenin 271/151; 119, morin 301/151; 125, quercetin 301/151; 179, positive: coumarin 147/103; 65, flavanone 225/121; 210, flavone 223/121; 178). The conditions for the electrospray were as follows: drying gas temperature 250°C, drying gas flow 8 l min⁻¹, nebulizer pressure 35 psi, sheath gas temperature 400°C, sheath gas flow 12 l.min⁻¹, capillary voltage ± 3500 V, nozzle voltage +0 V and -900 V. MassHunter Workstation software version 10.1 was used for data acquisition and post-run processing (Agilent, Santa Clara, CA, United States). For the non-target analysis, QTOF MS, operating in positive mode, was tuned using Swarm Autotune for the mass range *m/z* 50–750. Purine (*m/z* = 121.050873) was used as the reference molecule during the analysis to achieve the best mass accuracy. A single MS mode (ESI +, 5 spectra/s) in the range 50–600 *m/z* was chosen to perform metabolite profiling on the cell extracts. Agilent MassHunter Profinder version B.08.00 was used for recursive molecular feature extraction. The resulting features were evaluated with Agilent MassHunter Profiler Professional 15.1 (MPP) using the filter on the volcano plot algorithm with a cutoff of *p* < 0.05 and fold change > 1.5. Unique features revealed in the BPDO_AVS samples were exported to the inclusion list of an autoMS/MS method and acquired using two different collision energies (CE = 20 and 40 eV) and fragmentor voltage 140 V. The mass range was 50–600 *m/z* and MS/MS acquisition rate was 5 spectra/s.

Sequence Deposition

Raw sequencing data were deposited in SRA under the BioProject no. PRJNA641877. Processed sequences were deposited in GenBank; these include 13 *bphA* SV: SV3 (GenBank accession no. MT671559), SV23 (MT671560), SV27 (MT671561), SV39 (MT671562), SV40 (MT671563), SV63 (MT671564), SV75 (MT671565), SV79 (MT671566), SV115 (MT671567), SV116 (MT671568), SV117 (MT671569), SV122 (MT671570), SV167 (MT671571), and the AVS region scaffold (MT680029).

RESULTS

Diversity of *bphA* Genes in ¹³C-Enriched Metagenome After ¹³C-BP-SIP

In total, 358 sequences spanning 13 unique *bphA* SVs were obtained by amplicon sequencing from the ¹³C-enriched metagenome after SIP with ¹³C-BP (further referred to as heavy DNA) (Supplementary Figure 2). SV3, the most abundant SV in the heavy DNA, accounted for 59% of all sequences and was also the most abundant in the total community DNA, where it accounted for 23% of sequences. The corresponding protein sequence was the only one in the data set with sequence identity <90% to hitherto described BphA sequences; in fact,

it was only 77.4% identical to the closest detected sequence from *Cupriavidus* sp. WS and 76.7% to that of *Pseudomonas alcaliphila* B-367 (Vézina et al., 2008). Furthermore, in the phylogeny reconstruction based on the portion of ARHD large subunits corresponding to the amplicons sequenced, SV3 formed a separate branch outside the cluster formed by BPDOs from the strain *Par. xenovorans* LB400, *Ps. furukawaii* KF707, *Ps. alcaliphila* B-367, and the ARHD from *Cupriavidus* sp. WS (Figure 2). The other most abundant sequences in the heavy DNA were similar to the sequences of *Pseudomonas alcaliphila* JAB1 and *Ps. furukawaii* KF707 (designated SV27; 95.5% identity; accounted for 18% of all sequences) and *Panacagrimonas perspica* Gsoil 142 (designated SV23; 98.5% identity; accounted for 9% of all sequences). Other sequences accounted for <5% of all sequences and are depicted in Figure 2 and Supplementary Figure 2 in Supplementary Material.

SV3 was chosen for further investigation due to its low similarity to known BphA sequences and especially due to the unusual AA pattern of its region III, namely, Ala333, Val335, and Ser340 (Supplementary Figure 2). With this in mind, we designated the sequence *bphA_AVS*, and aimed to reveal the substrate specificity of the corresponding BPDO and thus predict its ecological function.

Sequence Analysis of *bphA_AVS* and the Surrounding Region

Shotgun sequencing of the multiple-displacement-amplified ¹³C-metagenome yielded a 48.5 kbp scaffold which bore the *bphA_AVS* sequence. The DNA span of 18 kbp containing *bphA_AVS*, referred to hereinafter as the AVS region, is flanked on both ends by the remnants of IS3 family transposases, and contains 16 ORFs in total; its architecture is shown in Figure 3. The putative functions of the corresponding proteins inferred by homolog search analysis suggest their involvement in the metabolism of aromatic compounds as shown in Table 1. This region includes the *bphAE* genes encoding for a putative two-component Rieske-type BPDO, with the *bphA* gene corresponding to SV3. Putative ferredoxin and ferredoxin reductase genes (*bphF* and *bphG*, respectively) are located downstream of *bphAE*, followed by genes encoding for a *cis*-2,3-dihydrobiphenyl-2,3-diol dehydrogenase (*bphB*), biphenyl-2,3-diol 1,2-dioxygenase (*bphC*), and HOPDA-hydrolase (*bphD*). Putative products of ORFs *nahJ* (encoding for a putative 4-oxalocrotonate tautomerase), *bphH* (2-keto-4-pentenoate hydratase), *bphI* (4-hydroxy-2-oxovalerate aldolase), and *bphJ* [acetaldehyde dehydrogenase (acetylating)] are enzymes for the utilization of the catechol *meta*-cleavage intermediate, 2-hydroxymuconate (Sala-Trepat and Evans, 1971). Moreover, ORF1-ORF6 were identified within the AVS region, whose corresponding protein sequences show only a limited similarity to proteins characterized to date (in the range of 45–56%, Table 1). Except for the divergently oriented ORF1, which encodes a putative transcriptional regulatory protein, the deduced products of ORF2-ORF6 exhibit homology to enzymes involved in the metabolism of aromatic compounds, including cholesterol and 4-hydroxyphenyl acetate (Table 1).

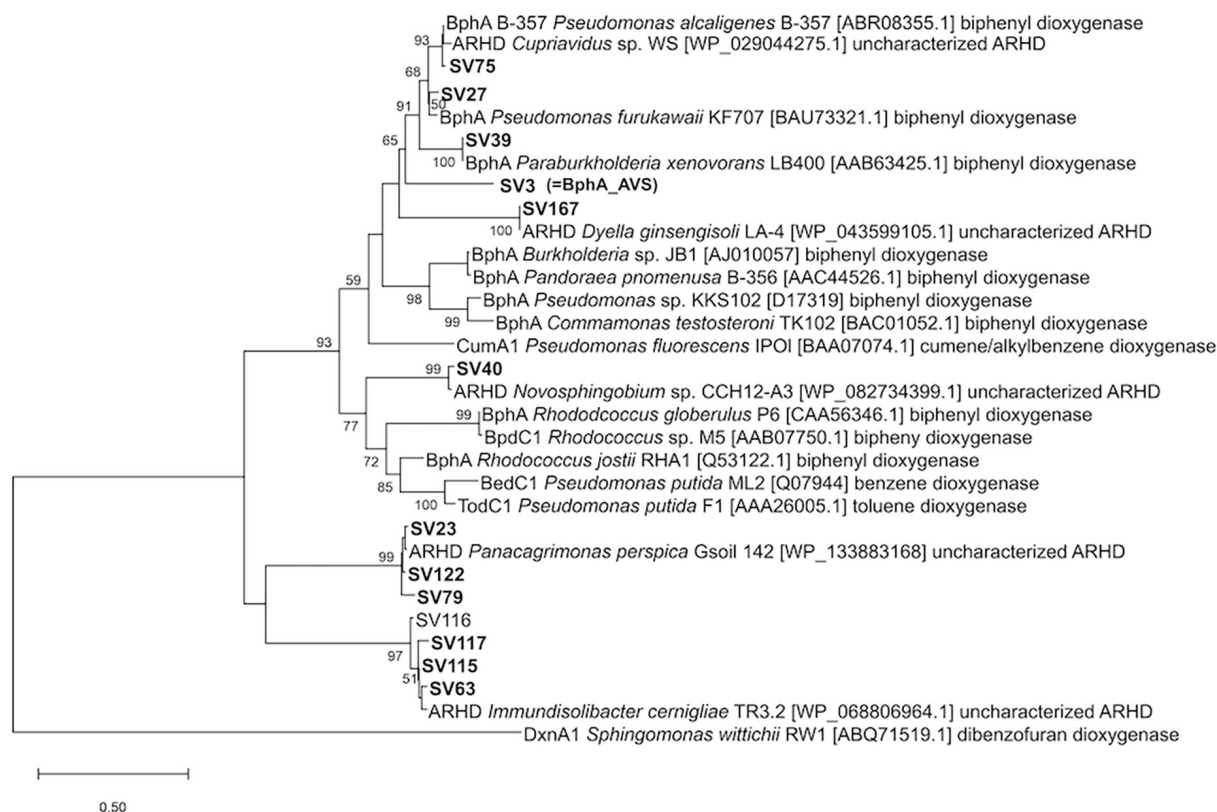


FIGURE 2 | Phylogeny reconstruction of SVs of *bphA* amplicons in the context of typical ARHD large subunits. Accession numbers shown in brackets. The tree is drawn to scale, branch lengths represent the number of substitutions per site. Bootstrapping was used to test the tree topology (500 bootstraps), only bootstrap values > 50 are shown. The final dataset was comprised of 140 positions.

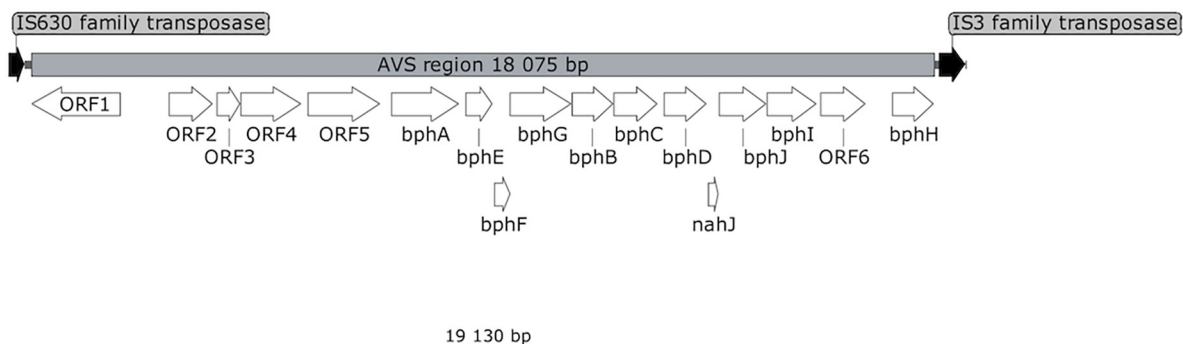


FIGURE 3 | Map of AVS region. White arrows represent ORFs discussed in the text. ORFs encoding for putative transposases are shown in black.

Taxonomic Assignment of *bphA*_AVS-Host Organism

Based on a sequence search against the protein RefSeq database of all 59 detected ORFs localized in the *bphA*_AVS-bearing scaffold, the most likely genus assignment of the *bphA*_AVS-bearing organism is *Paraburkholderia*. Eighteen ORFs were found to have a protein identity higher than 90% to the reference proteins, of which 11 were assigned to the genus *Burkholderia*, 6 to *Paraburkholderia* and 1 to *Cupriavidus*

according to the NCBI taxonomy system. All 11 hits for *Burkholderia* originated in the same genome of *Burkholderia* sp. OLG172. Upon translating the NCBI taxonomy to GTDB taxonomy, which uses only genome information to classify prokaryotes, *Burkholderia* sp. OLG172 was found to be reclassified into the *Paraburkholderia* genus, which made us conclude that the majority of proteins with high similarity to the references were of *Paraburkholderia* origin (Supplementary Table 1).

TABLE 1 | Functional assignment of deduced proteins encoded by ORFs within the AVS region.

Gene designation	Product length [AA]	Closest UniProtKB/Swiss-Prot database hit (% of aa sequence similarity)	Presumed activity/function	Note
ORF1	588	Transcriptional regulatory protein XylR (<i>Pseudomonas putida</i> TOL plasmid pWWO), P06519.1 (56%)	Transcriptional regulatory protein	Divergently oriented
ORF2	293	4,5:9,10-diseco-3-hydroxy-5,9,17-trioxoandrosta-1(10),2-diene-4-oate hydrolase HsaD (<i>Rhodococcus jostii</i> RHA1), Q9KWQ6.1 (45%)	meta-cleavage product hydrolase analogous to BphD in <i>bph</i> -encoded pathway	Unknown function – presumably degradation of an aromatic moiety
ORF3	157	NADH:flavin oxidoreductase 2, RutF (<i>Agrobacterium radiobacter</i> K84), B9JLT5.1 (55%)	NADH:flavin oxidoreductase	
ORF4	404	3-hydroxy-9,10-secoandrosta-1,3,5(10)-triene-9,17-dione 4-hydroxylase, oxygenase subunit HsaA (<i>Rhodococcus jostii</i> RHA1), Q0S811.1 (50%)	Hydroxylase of aromatic ring	
ORF5	486	4-hydroxyphenylacetate 3-monooxygenase oxygenase component HpaH (<i>Geobacillus</i> sp. PA-9), Q4L1M7.1 (53%)	Hydroxylase of aromatic ring	
<i>bphA</i>	458	Biphenyl 2,3-dioxygenase (<i>Pseudomonas furukawaii</i> KF707), Q52028.1 (87%)	Biphenyl 2,3-dioxygenase subunit α	Biphenyl upper degradation pathway: from biphenyl to benzoate
<i>bphE</i>	182	Biphenyl 2,3-dioxygenase subunit β (<i>Paraburkholderia xenovorans</i> LB400), P37334.3 (87%)	Biphenyl 2,3-dioxygenase subunit β	
<i>bphF</i>	109	Biphenyl 2,3-dioxygenase ferredoxin subunit (<i>Pseudomonas</i> sp. KKS102), Q52440.1 (79%)	Biphenyl 2,3-dioxygenase ferredoxin subunit	
<i>bphG</i>	413	Biphenyl 2,3-dioxygenase system ferredoxin-NAD(+) reductase component (<i>Paraburkholderia xenovorans</i> LB400), P37337.2 (79%)	Biphenyl 2,3-dioxygenase system ferredoxin-NAD(+) reductase	
<i>bphB</i>	279	cis-2,3-dihydrobiphenyl-2,3-diol dehydrogenase (<i>Comamonas testosteroni</i> B-356), 46381.1 (88%)	cis-2,3-dihydrobiphenyl-2,3-diol dehydrogenase	
<i>bphC</i>	293	Biphenyl-2,3-diol 1,2-dioxygenase (<i>Pseudomonas furukawaii</i> KF707), P08695.2 (81%)	Biphenyl-2,3-diol 1,2-dioxygenase	
<i>bphD</i>	286	2,6-dioxo-6-phenylhexa-3-enoate hydrolase (<i>Polaromonas naphthalenivorans</i> CJ2), A1VUV0.1 (79%)	2,6-dioxo-6-phenylhexa-3-enoate hydrolase	
<i>nahJ</i>	74	4-oxalocrotonate tautomerase (<i>Comamonas testosteroni</i> TA441), Q9RHM8.3 (72%)	4-oxalocrotonate tautomerase	Degradation of catechol meta-cleavage intermediate 2-hydroxymuconate yielding pyruvate and acetyl-CoA; missing 4-oxalocrotonate decarboxylase (e.g., NahK and its homologs DmpH, XylI, etc.)
<i>bphJ</i>	319	Acetaldehyde dehydrogenase (acetylating) 1 (<i>Azotobacter vinelandii</i> DJ, C1DMT1.1 (90%)	Acetaldehyde dehydrogenase (acetylating)	
<i>bphI</i>	335	4-hydroxy-2-oxovalerate aldolase 3 (<i>Dechloromonas aromatica</i> RCB), Q47B13.1 (92%)	4-hydroxy-2-oxovalerate aldolase	
ORF6	300	No significant hit in UniProtKB/Swiss-Prot database; in RefSeq database: non-characterized phenol degradation protein (<i>Paraburkholderia rhynchosiae</i>), WP_102636641.1 (80%); FdeA protein involved in flavonoid degradation (<i>Herbaspirillum seropedicae</i> SmR1), WP_041310253.1 (43%)	Unknown function	
<i>bphH</i>	278	2-keto-4-pentenoate hydratase 1 (<i>Dechloromonas aromatica</i> RCB), Q47HM0.1 (74%)	2-keto-4-pentenoate hydratase	

The putative functions were assessed by blastp search against UniProtKB/Swiss-Prot (The UniProt Consortium, 2018) and RefSeq database (O'Leary et al., 2016), combined with the literature review.

BPDO_AVS-Mediated PCB Depletion

The PCB congeners contained in the Delor 103 mixture that were significantly (Student *t*-test, $\alpha = 0.05$) depleted by BPDO_AVS-expressing *E. coli* cells compared to control cells lacking BPDO_AVS are displayed in **Figure 4** and **Supplementary Figure 4** in **Supplementary Material**. Among the congeners analyzed, the activity of BPDO_AVS led to the depletion of 2-CB, 4-CB, of the sum of 2,3-diCB + 2,4'-diCB, sum of 2,5-diCB + 2,4-diCB, 2,2',5-triCB, 2,3',4'-triCB, and the sum of 2,4,4'-triCB + 2,4',5-triCB. The congeners whose depletion was not significant are listed in **Supplementary Table 2**.

BPDO_AVS-Mediated SPM Transformation

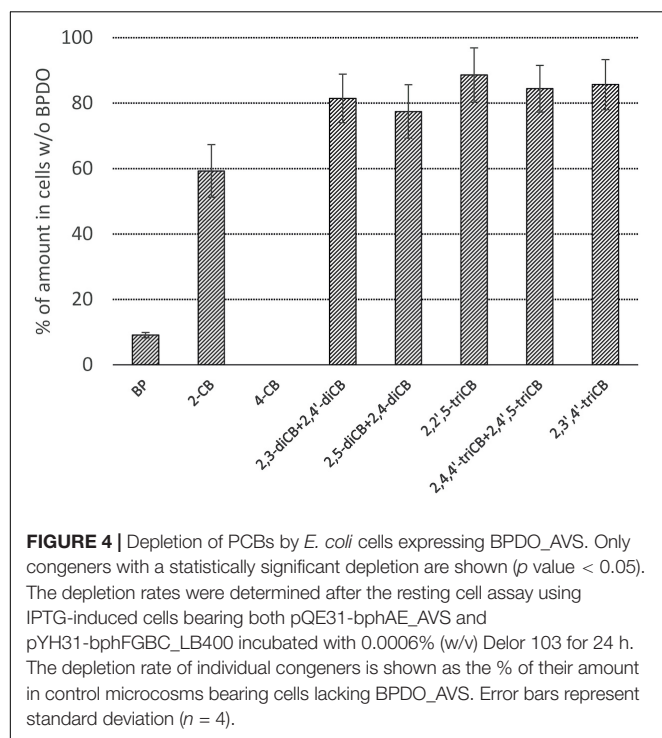
BPDO_AVS-bearing cells exhibited statistically significant depletions (% \pm SD of SPM amount in control cell cultures lacking BPDO_AVS) of flavone (32 ± 9) and flavanone (30 ± 4), with percentage values being similar to those of BP (32 ± 6), as shown in **Figure 5**. Interestingly, when the substrate amounts of control cell cultures lacking BPDO_AVS were compared to the corresponding abiotic controls (no cells added), chrysin, apigenin, quercetin, and morin were found to be significantly depleted (by 17, 36, 53, and 43%, respectively), indicating substrate transformation mediated through enzymes other than BPDO_AVS.

The depletion rates of biphenyl, flavone, and flavanone by BPDO_AVS were determined in crude whole cell extract of *E. coli* cells with active BPDO_AVS to avoid bias in the substrate availability for the BPDO holoenzyme in production cells caused by potential differences in the permeability of the bacterial cell

wall for the substrates. As shown in **Figure 6**, 20 μ M biphenyl was almost fully depleted (to 1% of the initial amount) after 0.5 h of incubation, with the calculated reaction rate of 33 pmol/min. Flavone and flavanone were fully depleted after 1.5 and 4.5 h of incubation with reaction rates for the initial 0.5 h of incubation of 13 and 14 pmol/min, respectively.

Analysis of Transformation Products of Flavone and Flavanone

The high-resolution QTOF LC-MS differential analysis workflow was used to identify the products of the BPDO_AVS-mediated transformation of flavone and flavanone (**Figure 7**). The LC-MS analysis of flavone transformation products revealed a molecular feature with the $m/z = 255.0652$ found solely in the supernatant of the BPDO-bearing cells and not in either cells without BPDO or abiotic control. Based on the m/z and the isotopic pattern, the molecular formula of the corresponding compound was deduced as $C_{15}H_{16}O_5$. Subsequent MS/MS fragmentation analyses suggest that the structure is m,n-dihydroxyflavone, which has the two hydroxyls on the B-ring (**Figure 7**). For flavanone, a molecular feature unique for BPDO-bearing cells with $m/z = 257.0809$ was found. The measured m/z and the isotopic pattern suggested the corresponding molecular formula as $C_{15}H_{12}O_4$. Based on subsequent MS/MS fragmentation analysis, the compound was proposed as x,y-dihydroxyflavanone (**Figure 7**). Fragmentation spectra of the deduced compounds m,n-dihydroxyflavone and x,y-dihydroxyflavanone showed the same pattern as it was reported previously for B-ring-hydroxylated flavones/flavanones (Shimada et al., 2021). Therefore, we assume that BPDO_AVS mediated the hydroxylation of the B-ring of flavone and flavanone; nevertheless, the precise position of the two hydroxyls could not be determined due to the inaccessibility of commercial analytical standards, hence labeling m,n and x,y is used herein.



DISCUSSION

Recalcitrant organic compounds are not a negligible portion of organic carbon in soils, be it plant-derived organic compounds in vegetated soils (Cortes-Tolalpa et al., 2018; Hu et al., 2018), or persistent organic pollutants in contaminated soils (Mackova et al., 2006). Our understanding of the biodegradation of recalcitrant compounds requires a complex insight into the indigenous soil microbial populations, their enzymatic equipment, and specific functions that the enzymes perform. Molecular techniques such as SIP in tandem with metagenomics not only permit microbial ecologists to assign a specific function to individual, metabolically active microbial taxa, but also to explore the function of specific genes (Uhlík et al., 2013; Hernández et al., 2017). In this research, we have followed up on our previous study, in which we used SIP to identify metabolically active BP-utilizing bacteria in the legacy PCB-contaminated soil (Uhlík et al., 2012), and analyzed the prevailing *bphA* sequence in the heavy DNA. Unlike the other SVs in the data set, whose protein sequences were similar to previously studied BphAs from pure cultures, the prevailing SV3 sequence was uncommon in its deduced primary structure. In addition to the relatively low

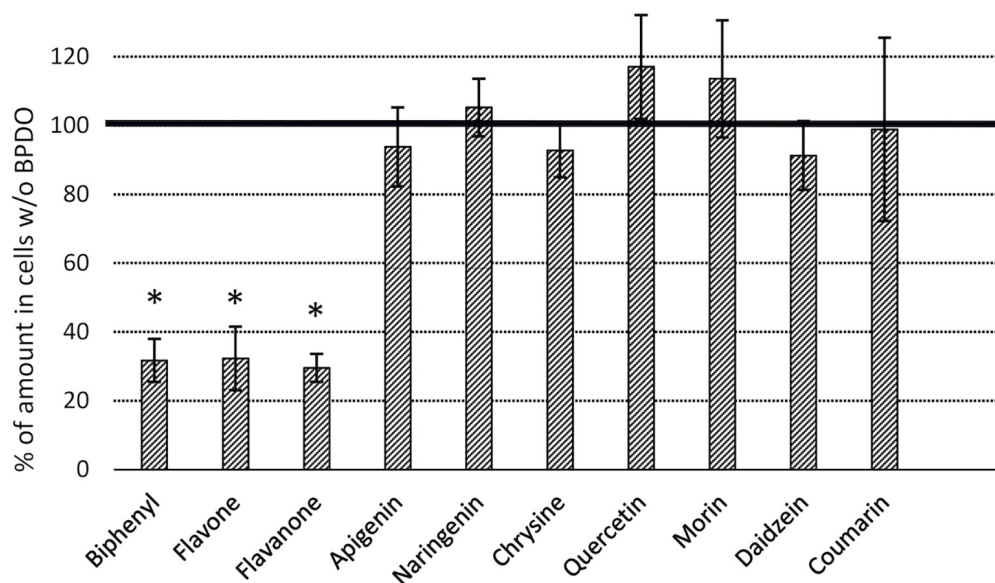


FIGURE 5 | Depletion of flavonoids by *E. coli* cells expressing BPDO_AVS. The depletion rates were determined after the resting cell assay using IPTG-induced cells bearing both pQE31-bphAE_AVS and pYH31-bphFGBC_LB400 incubated with a 25 μ M substrate for 24 h. The BPDO activity is shown as % of a SPM amount in control microcosms bearing cells lacking BPDO_AVS. (*) statistically significant difference from the corresponding control (p value < 0.05). Error bars represent standard deviation ($n = 4$).

sequence similarity of the translated SV3 sequence to known BphAs (Table 1), the AA pattern in region III differed as well (Supplementary Figure 2). Based on multiple previous reports of Sylvestre et al. (Mondello et al., 1997; Barriault et al., 2002; Barriault and Sylvestre, 2004; Vézina et al., 2008; Mohammadi et al., 2011), this region is crucial for the substrate specificity of

the BPDO. More recent reports also showed that diverse BPDOs play different ecological roles associated with the transformation of various types of recalcitrant compounds, such as flavonoids, in addition to PCBs (Pham and Sylvestre, 2013). With this in mind, the complete *bphA* coding sequence corresponding to SV3 and the surrounding region were retrieved from the metagenome and the substrate specificity of the corresponding BPDO_AVS toward PCBs and flavonoids was determined.

The AVS region (Figure 3) is flanked on both ends by the remnants of IS3 family transposases, therefore it presumably arose from horizontal gene transfer. ORF4 and ORF2 exhibit a certain level of sequence homology with the enzymes involved in steroid degradation found in *R. jostii* RHA1 and other actinobacteria, specifically the oxygenase subunit HsaA, which hydroxylates aromatic ring A in the cholesterol-degradation intermediate (50% similarity to ORF4), and the meta-cleavage product hydrolase HsaD (45% similarity to ORF2) (Van der Geize et al., 2007). Nevertheless, no ORF potentially encoding for a functional homolog of HsaC, enabling the meta-cleavage of the product of the HsaA-mediated reaction, has been found in the AVS region. The following ORF5 encodes for another putative monooxygenase hydroxylating an aromatic ring.

The predicted protein sequences of the seven subsequent ORFs *bphAEFGBCD* resemble the enzymes of the BP upper-degradation pathway of known BP/PCB degraders such as *Paraburkholderia xenovorans* LB400 (Erickson and Mondello, 1992), *Pseudomonas furukawii* KF707 (Taira et al., 1992), *Ps. alcaliphila* JAB1 (Ridl et al., 2018), *Acidovorax* sp. KKS102 (Fukuda et al., 1994), *Rhodococcus jostii* RHA1 (Masai et al., 1995), *Rhodococcus* sp. strain R04 (Yang et al., 2007), etc. In bacteria, this pathway enables the activation and further

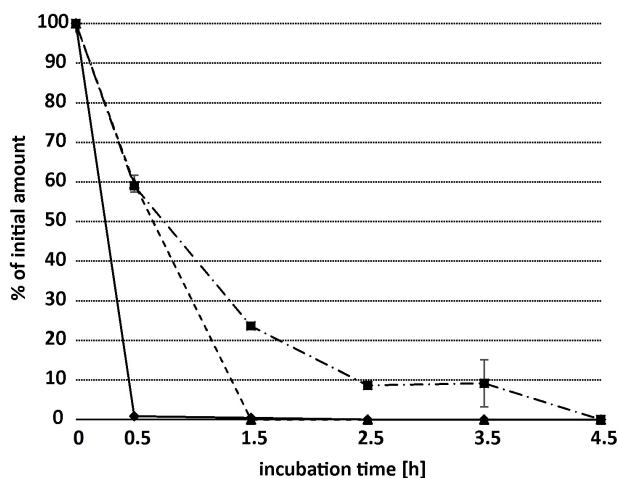
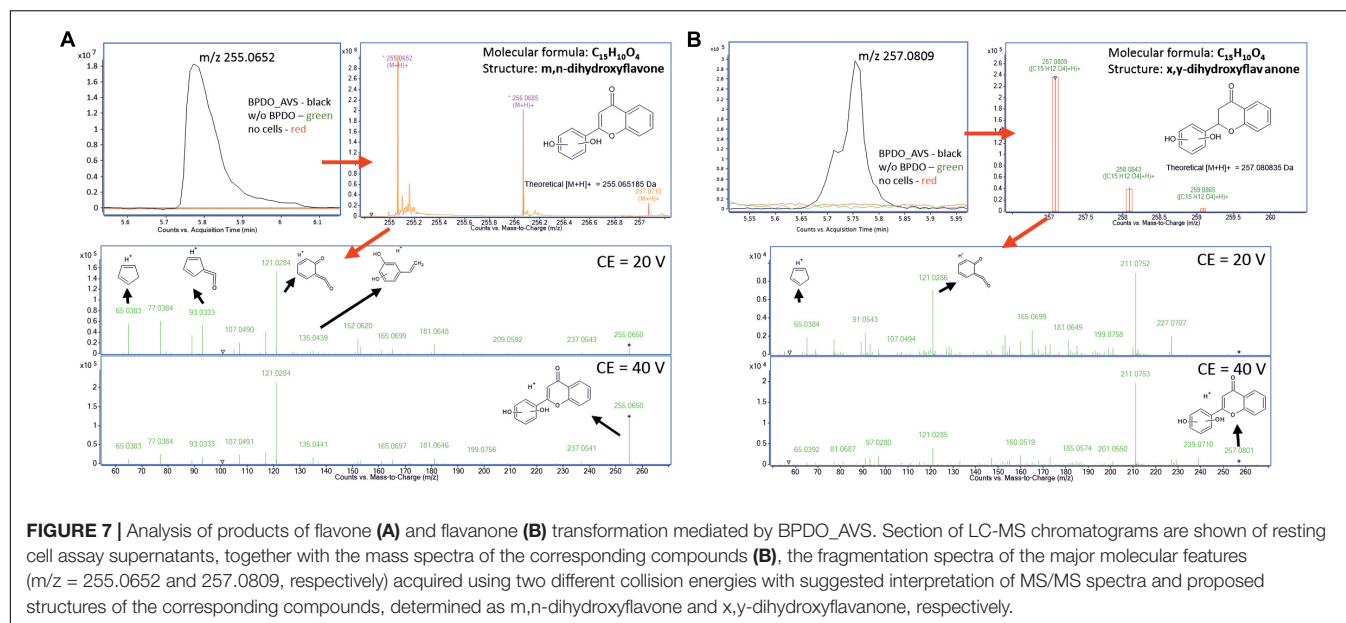


FIGURE 6 | Time-dependent depletion of biphenyl (diamonds, solid line), flavone (triangles, dashed line), and flavanone (squares, dash-and-dot line) by the whole-cell extract of *E. coli* expressing BPDO_AVS. The depletion of substrates was determined using the crude extract of *E. coli* IPTG-induced cells bearing pQE31-bphAE_AVS and pYH31-bphFGBC_LB400, incubated with a 20 μ M substrate. Error bars represent standard deviation ($n = 3$).



degradation of the otherwise recalcitrant BP aromatic structure by dihydroxylation, extradiol cleavage, and hydrolysis of the corresponding intermediate, while yielding benzoic acid and 2-hydroxy-penta-2,4-dienoic acid. In the phylogeny reconstruction, the full-length BP 2,3-dioxygenase large subunit encoded by the *bphA_AVS* gene shared a common ancestor with a discrete cluster formed by BphA sequences from the strains *Ps. furukawii* KF707, *Acinetobacter* sp. KKS102, *Ps. alcaliphila* JAB1, *Pandoraea pnomenusa* B-356, *Par. xenovorans* LB400, and *Cupriavidus oxalaticus* A5 (**Supplementary Figure 3**). These were separated from a cluster formed by BphA of *R. jostii* RHA1 (Masai et al., 1995) and *Rhodococcus* sp. M5 (Wang et al., 1995), as well as by BphAs from both *Rhodococcus erythropolis* TA431 (Chung et al., 1994) and *Rhodococcus* sp. R04 (Yang et al., 2007). Subsequent ORFs *nahJ*, *bphH*, *bphI*, and *bphJ* encode enzymes enabling utilization of the catechol *meta*-cleavage pathway intermediate 2-hydroxymuconate (Austen and Dunn, 1977). Nevertheless, due to the absence of a 2-oxo-3-hexenedioate decarboxylase homolog in the AVS region, the corresponding pathway would not be complete *per se* and would require complementation *in trans*. The protein product of ORF6 might be the missing step to potentially complement the missing function, however, such an assumption is highly hypothetical with no experimental evidence.

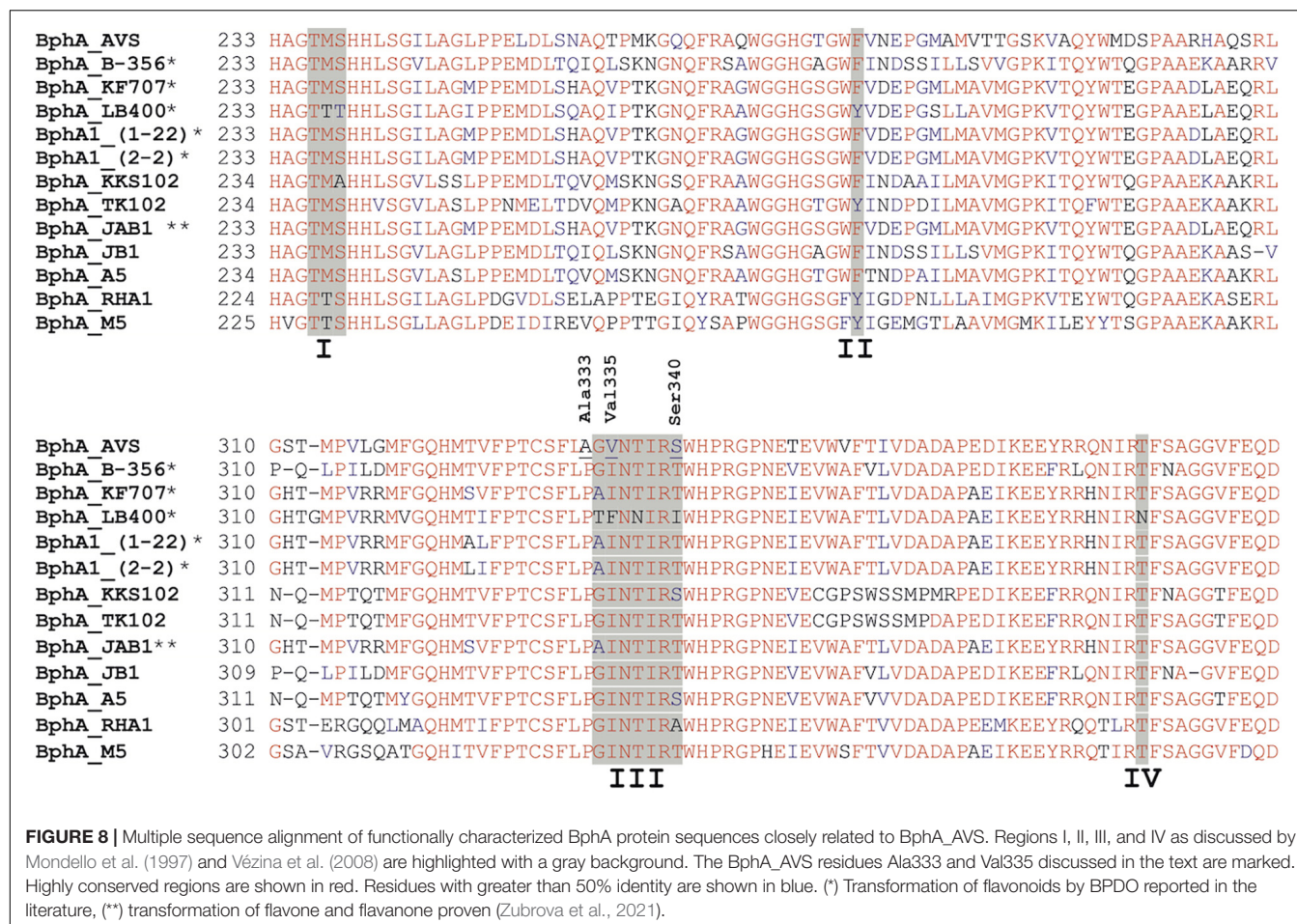
Taking into account the entire *bphA_AVS*-bearing scaffold, the *bphA_AVS*-bearing organism is very likely a bacterium of the genus *Paraburkholderia*, based on the high protein identity of ORFs to those of *Paraburkholderia* (**Supplementary Table 1**). *Paraburkholderia* identity is further supported by a high prevalence of *Paraburkholderia* (formerly *Burkholderia*) 16S rRNA gene sequences in this heavy DNA, as was reported previously (Uhlík et al., 2012).

To investigate the substrate preferences of the metagenome-extracted BPDO_AVS, the gene cluster *bphAE_AVS* was heterologously co-expressed with the gene cluster *bphFGBC*

from *Par. xenovorans* LB400 (Chebrou et al., 1999; Vézina et al., 2007). Such a whole-cell-based approach to infer the catalytic activity of various BPDOs has been already successfully applied (Chebrou et al., 1999; Shindo et al., 2003; Barriault et al., 2004; Kagami et al., 2008; Pham et al., 2012; Toussaint et al., 2012). The advantage of BPDO co-expression with the genes BphB and BphC is the possibility to easily verify the presence of the active BPDO enzyme pathway through the evolution of the yellow BP transformation product HOPDA (Kumamaru et al., 1998; Barriault and Sylvestre, 2004).

As is evident from the depletion assay performed with the PCB mixture Delor 103, BPDO_AVS was able to catalyze transformation of only several lower chlorinated congeners (**Figure 4**). Predictably, BPDO_AVS exhibited a strong preference for 4-CB, resulting in its complete depletion under the tested conditions; 4-CB is a PCB congener considered to be normally transformed at rates similar to or higher than BP by most BPDOs (Kumamaru et al., 1998). All other depleted congeners had a chlorine substitution in the *ortho* and/or *para* positions. Such a finding of relatively narrow regioselectivity is in strong contrast with the phylogenetically close relatives BPDO_B-356 (Gómez-Gil et al., 2007), BPDO_LB400 (Mondello, 1989) and BPDO_JAB1 (Vergani et al., 2019; Garrido-Sanz et al., 2020).

However, BphA_AVS bears an unusual AA motif in region III, as shown in **Figure 8**, which was the rationale for choosing *bphA_AVS* as the target of this study for determining its substrate specificity. To the best of our knowledge, the BphA_AVS Ala333 preceding region III is a residue totally unique in BphA sequences, in which proline is most commonly present (Vézina et al., 2008; **Figure 8**). Another uncommon AA residue in BphA_AVS is Val335, which has only been found in a few ARHD sequences other than BPDO, e.g., benzene 1,2-dioxygenase large subunit BedC1 (Tan et al., 1993) and in a couple of environmental sequences (Vézina et al., 2008). The Ser340 in the BphA_AVS sequence is found commonly in BPDO sequences nevertheless,



its combination with Ala333 and Val335 is unique. Pham et al. (2012) linked the presence of Gly333 and Ile334 in region III of BphA_B-356, corresponding to Thr335 and Phe336 in BphA_LB400 (Figure 8), to the superior ability of the BPDO_B-356 to transform larger substrates, such as DDT, 2,6-di-*tert*-butylphenol, and flavonoids. The Phe336 found in BphA_LB400 hinders the productive binding of bulkier substrates due to the larger side chain compared to Ile334 of BphA_B-356, and, simultaneously, the substitution of Thr335 of BphA_LB400 for Gly333 in BphA_B-356 results in higher protein structural flexibility during substrate binding (Pham et al., 2012). Gly334 and Val335 at the corresponding positions of BphA_AVS, the latter being even less bulky than Ile334 in BphA_B-356 and also totally unique in BphA sequences, led us to hypothesize that BphA_AVS could accommodate more bulky substrates into the binding pocket, including the chromone/chromanone moiety of flavonoids. To test this hypothesis, we proceeded to investigate the substrate preference of the BPDO_AVS toward flavonoids.

Our data demonstrate that the BPDO_AVS was capable of efficiently transforming flavone and flavanone (Figure 5). The initial reaction rates of both flavone and flavanone were approx. 40% of that determined for BP (Figure 6). No transformation was observed for daidzein (a representative of isoflavonoids), naringenin (a flavanone), chrysin and apigenin

(hydroxylated flavones), quercetin and morin (flavonols), and coumarin (structure analogous to the chromene moiety of flavones). The transformation of flavonoids in control *E. coli* cells cultures lacking BphA_AVS, which could not be attributed to the activity of BPDO_AVS, could be explained by the action of the enzymes encoded by pYH31-bphFGB_C_LB400. For instance, extradiol dioxygenases BphC from *Rhodococcus* sp. R04, *Dyella ginsengisoli* LA-4, and *Comamonas* sp. SMN4 were found to transform substituted catechols in addition to 2,3-dihydroxybiphenyl (Yang et al., 2008; Li et al., 2009; Lee and Kwon, 2016). Therefore, BphC_LB400 could possibly also act on the catechol moieties present in quercetin. Alternatively, the non-BPDO-mediated depletion of flavonoids could also be caused by other non-specific enzymes indigenous to the *E. coli* genetic background. For instance, the extradiol dioxygenases MhpB and HcaB were reported to possess relatively broad substrate specificities (Spence et al., 1996; Díaz et al., 1998), and could act on the hydroxylated aromatic moieties within the structure of the flavonoids discussed here.

The products of both flavone and flavanone transformation revealed here suggest that BPDO_AVS mediated the formation of dihydrodiol on the B-ring. In general, the *ortho-meta* dihydroxylation of an aromatic ring by BPDOs results in the production of *cis*-dihydrodiols that are further converted to

the respective aromatic diols *via* the action of BphB (Barriault et al., 1999; Li et al., 2009). Analogously, we assume that BphB encoded on the plasmid pYH31-bphFGBC_LB400 mediated such transformation of flavone- and flavanone-dihydroxylated intermediates produced by BPDO_AVS, resulting in the re-aromatization of the dihydrodiol B-ring, similarly as in the studies of Seeger et al. (2003) and Kagami et al. (2008). Flavone and flavanone, unlike the rest of the flavonoids tested, lack hydroxyl groups on the B-ring. Therefore, the absence of substituents at the B-ring seems to be determinative for the activity of BPDO_AVS. On the other hand, saturation of the C2 and C3 bond, which differentiates flavanone from flavone, does not seem to influence the selectivity of the BPDO_AVS enzyme. Attack of the B-ring in the flavonoid structure by Rieske-type ARHD has also been reported for other BPDOs closely related to BPDO_AVS (**Supplementary Figure 3**). For instance, the BPDO from *Ps. furukawaii* KF707 was demonstrated to catalyze the dihydroxylation of the flavone B-ring at positions C2' and C3' (Kim et al., 2003). Interestingly, the study of Han et al. (2005) reported that with flavanone, 6-hydroxyflavanone and 7-hydroxyflavanone, BPDO_KF707 acted as a monooxygenase introducing an epoxide functional group between C2' and C3' of the B-ring. The attack on the B-ring of flavone and flavanone, followed by its subsequent transformation yielding 4-oxo-4H-chromene-2-carboxylic acid, was also reported in our recent study with the PCB-degrader *Ps. alcaliphila* JAB1 which has a KF707-type BPDO (Zubrova et al., 2021). Similarly, the formation of *cis*-diols on the B-ring of flavone, flavanone, and isoflavone, was reported for the BPDO from *Pan. pnomensua* B-356, with k_{cat} and k_{cat}/K_m values comparable to those of BP (flavone and isoflavone) or even higher (flavanone). In contrast, BPDO_LB400 was only poorly active toward all of these simple flavonoids (Pham et al., 2012). Apart from wild-type enzymes, several artificially engineered BPDOs have been reported with improved substrate preferences toward flavonoids. Of those, a BphA_LB400 mutant BphA_p4 is worth mentioning, which was prepared by the substitution of Thr335 and Phe336 in region III for less bulky Ala and Met, respectively, that efficiently transformed isoflavone through the dihydroxylation of the B-ring, and flavone and flavanone through the dihydroxylation of both B- and C-rings (Pham et al., 2012). Similarly, BphA_KF707-derivatives BphA1 (1-22) and BphA1 (2-2) mediated dihydroxylation at positions C1' and C2' of the B-ring of both 7-hydroxyflavone and chrysin (Kagami et al., 2008). Another BphA_KF707-derivative BphA1 (2072) was shown to transform flavone, flavanone, 6-hydroxyflavone, 6-hydroxyflavanone, 7-hydroxyflavone, and chalcone also through dihydroxylation of the B-ring (Misawa et al., 2002; Shindo et al., 2003).

In contrast, naphthalene dioxygenase NdoB from *Pseudomonas* sp. strain NCIB 9816-4 was demonstrated to hydroxylate the A-ring of flavone and isoflavone (Seo et al., 2010). As shown in the phylogeny reconstruction of full-length ARHD large subunits in **Supplementary Figure 3** in **Supplementary Material**, NdoB is distant from the cluster formed by model BPDO large subunits, including BphA_AVS.

Several studies also aimed to link BPDOs with the bacterial transformation of SPMs at the level of regulating gene/protein expression. For instance, in the survey performed with a diverse spectrum of aromatic substances including the flavonoids myricetin and naringenin, none of the tested flavonoids were able to significantly increase the induction of the *bphA* gene in either *Pseudomonas* sp. Cam-1 or *Par. xenovorans* LB400 (Master and Mohn, 2001), and of other SPMs tested, only salicylic acid induced *bphA* in the Cam-1 strain. In contrast, Pham et al. (2015) found a wide spectrum of flavonoids to be efficient promoters of the BPDO activity of the rhizosphere bacterium *Rhodococcus erythropolis* U23A. Flavone, isoflavone, and flavanone were even better inducers of the BP catabolic enzymes than BP itself. Moreover, the PCB-degrading activity in *R. erythropolis* U23A was significantly induced by *Arabidopsis thaliana* root exudates in hydroponics-based experiments, which was attributed to flavanone present in the exudates (Toussaint et al., 2012). In our aforementioned study with *Ps. alcaliphila* JAB1, the BPDO borne by this strain was induced by multiple SPMs including flavonoids, umbelliferone (a coumarin), monoterpenes, and phenolic acids (Zubrova et al., 2021).

The poor catalytic efficiency of BPDO_AVS toward PCBs congeners on the one hand and the ability to efficiently transform flavonoids on the other are further evidence of the role of BPDOs in the transformation of specific SPMs. The demonstrated ability of BPDO_AVS to mediate dihydroxylation of flavonoids supports the hypothesis primed by Focht (1995) and further discussed by Pham et al. (2012) of the divergent evolution of individual BPDOs to serve different functions in the environment. These functions can include, apart from the degradation of recalcitrant pollutants such as PCBs, an involvement of soil BPDOs in environmental processes that are mediated by flavonoids (Shaw et al., 2006; Cesco et al., 2012). Presumably, these could be (i) the ability to utilize a pool of soil flavonoids as growth substrates, (ii) the transformation of those flavonoids which are potentially inhibitory for the host microorganisms, (iii) the modulation of flavonoid-mediated signaling processes in soil during the formation of nodules with nitrogen-fixing rhizobacteria, mycorrhiza, interactions with phytopathogens, and others (Shaw et al., 2006; Subramanian et al., 2007; Cesco et al., 2012; Liu and Murray, 2016). Given rather limited capacity of the BPDO_AVS to transform PCBs and the genetic context of the whole AVS region, especially the presence of ORF2-6 with the putative function in degradation of an aromatic moiety, we hypothesize that the utilization of biphenyl by BPDO_AVS is a result of exaptation of the enzyme. As for the utilization of flavonoids as a sole carbon source, there is a lack of direct experimental evidence that BPDOs are a determinative factor for such an environmental function. To the best of our knowledge, the only genetic determinant of flavonoid utilization reported to date is the *fde* locus from the diazotrophic endophyte *Herbaspirillum seropedicae* SmR1 (Marin et al., 2013). This bacterium is capable of utilizing the flavanone naringenin through monohydroxylation on the C8 of the A-ring followed by A-ring fission and further transformation (Marin et al., 2016). The initial hydroxylation was shown to be catalyzed by the complex FdeED comprising putative

FAD-binding monooxygenase (FdeE) and the non-heme Rieske-protein electron carrier FdeD. Hypothetically, in the AVS-bearing organism, the putative products of ORF2-ORF6 could complement such activation of the A-ring *via* hydroxylation and subsequent fission, thus enabling the degradation of the rest of the flavonoid backbone. Such a hypothetical functional analogy between the *fde* pathway in *H. seropediacae* and the AVS region raises the need for further investigation. In particular, potential involvement of the putative proteins ORF2-ORF6 borne by the AVS region in the degradation of flavonoids should be studied, together with the regulation of the expression of these genes in response to SPMs.

CONCLUSION

Based on the genetic context and the enzymatic activity of BPDO_AVS toward flavonoids demonstrated here, we assume that BPDO_AVS primarily evolved for the transformation of flavonoids present in the soil/rhizosphere of various characters, either released, for instance, as part of the root exudates (Cesco et al., 2010) or originating from the plant necromass (Kraus et al., 2003; Iwashina, 2015). The putative protein products of ORF2-ORF5 in tandem with those encoded downstream of *bphAEFG* could be involved in the further transformation of the resulting flavonoid moiety, which remains to be confirmed.

DATA AVAILABILITY STATEMENT

The datasets presented in this study can be found in online repositories. The names of the repository/repositories and accession number(s) can be found in the article/**Supplementary Material**.

REFERENCES

- Arumugam, K., Bağcı, C., Bessarab, I., Beier, S., Buchfink, B., Górska, A., et al. (2019). Annotated bacterial chromosomes from frame-shift-corrected long-read metagenomic data. *Microbiome* 7:61. doi: 10.1186/s40168-019-0665-y
- Austen, R., and Dunn, N. (1977). A comparative study of the NAH and TOL catabolic plasmids in *Pseudomonas putida*. *Aust. J. Biol. Sci.* 30, 357–366. doi: 10.1071/BI9770357
- Barriault, D., Lepine, F., Mohammadi, M., Milot, S., Leberre, N., and Sylvestre, M. (2004). Revisiting the regiospecificity of *Burkholderia xenovorans* LB400 biphenyl dioxygenase toward 2,2'-dichlorobiphenyl and 2,3,2',3'-tetrachlorobiphenyl. *J. Biol. Chem.* 279, 47489–47496. doi: 10.1074/jbc.M406808200
- Barriault, D., Plante, M. M., and Sylvestre, M. (2002). Family shuffling of a targeted bphA region to engineer biphenyl dioxygenase. *J. Bacteriol.* 184, 3794–3800.
- Barriault, D., and Sylvestre, M. (2004). Evolution of the biphenyl dioxygenase BphA from *Burkholderia xenovorans* LB400 by random mutagenesis of multiple sites in region III. *J. Biol. Chem.* 279, 47480–47488.
- Barriault, D., Vedadi, M., Powlowski, J., and Sylvestre, M. (1999). Cis-2,3-dihydro-2,3-dihydroxybiphenyl dehydrogenase and cis-1,2-dihydro-1,2-dihydroxynaphthalene dehydrogenase catalyze dehydrogenation of the same range of substrates. *Biochem. Biophys. Res. Commun.* 260, 181–187. doi: 10.1006/bbrc.1999.0706
- Buchfink, B., Xie, C., and Huson, D. H. (2015). Fast and sensitive protein alignment using DIAMOND. *Nat. Methods* 12, 59–60. doi: 10.1038/nmeth.3176

AUTHOR CONTRIBUTIONS

JSu and OU designed the experiments and wrote the manuscript. JSu, AZ, JC, JW, KM, MH, JSe, and KS conducted the experiments and generated the data. JSu and MS analyzed the data. TC and OU provided the equipment and supplies. All authors contributed to the article and approved the submitted version.

FUNDING

This research was supported by the Czech Science Foundation under grant no. 20-00291S, and the INTER-EXCELLENCE program of the Ministry of Education, Youth and Sports of the Czech Republic under grant no. LTAUSA19013. Further support was acknowledged of the ELIXIR CZ research infrastructure project (Ministry of Education, Youth and Sports of the Czech Republic grant no. LM2018131), specifically for access to computing and storage facilities.

ACKNOWLEDGMENTS

We would like to thank prof. Michel Sylvestre for providing *E. coli* strain DH11S and the plasmid pYH31[LB400-*bphFGBC*].

SUPPLEMENTARY MATERIAL

The Supplementary Material for this article can be found online at: <https://www.frontiersin.org/articles/10.3389/fmicb.2021.644708/full#supplementary-material>

- Callahan, B. J., McMurdie, P. J., Rosen, M. J., Han, A. W., Johnson, A. J. A., and Holmes, S. P. (2016). DADA2: high-resolution sample inference from Illumina amplicon data. *Nat. Methods* 13, 581–583. doi: 10.1038/nmeth.3869
- Camacho, C., Coulouris, G., Avagyan, V., Ma, N., Papadopoulos, J., Bealer, K., et al. (2009). BLAST+: architecture and applications. *BMC Bioinformatics* 10:421. doi: 10.1186/1471-2105-10-421
- Cesco, S., Mimmo, T., Tonon, G., Tomasi, N., Pinton, R., Terzano, R., et al. (2012). Plant-borne flavonoids released into the rhizosphere: impact on soil bio-activities related to plant nutrition. A review. *Biol. Fertil. Soils* 48, 123–149. doi: 10.1007/s00374-011-0653-2
- Cesco, S., Neumann, G., Tomasi, N., Pinton, R., and Weisskopf, L. (2010). Release of plant-borne flavonoids into the rhizosphere and their role in plant nutrition. *Plant Soil* 329, 1–25. doi: 10.1007/s11104-009-0266-9
- Chebrou, H., Hurtubise, Y., Barriault, D., and Sylvestre, M. (1999). Heterologous expression and characterization of the purified oxygenase component of *Rhodococcus globulus* P6 biphenyl dioxygenase and of chimeras derived from it. *J. Bacteriol.* 181, 4805–4811.
- Chung, S.-Y., Maeda, M., Song, E., Horikoshij, K., and Kudo, T. (1994). A Gram-positive Polychlorinated Biphenyl-degrading Bacterium, *Rhodococcus erythropolis* Strain TA421, Isolated from a Termite Ecosystem. *Biosci. Biotechnol. Biochem.* 58, 2111–2113. doi: 10.1271/bbb.58.2111
- Cortes-Tolalpa, L., Norder, J., Van Elsas, J. D., and Falcao Salles, J. (2018). Halotolerant microbial consortia able to degrade highly recalcitrant plant biomass substrate. *Appl. Microbiol. Biotechnol.* 102, 2913–2927. doi: 10.1007/s00253-017-8714-6

- Dhindwal, S., Gomez-Gil, L., Neau, D. B., Pham, T. T. M., Sylvestre, M., Eltis, L. D., et al. (2016). Structural basis of the enhanced pollutant-degrading capabilities of an engineered biphenyl dioxygenase. *J. Bacteriol.* 198, 1499–1512. doi: 10.1128/JB.00952-15
- Di Tommaso, P., Moretti, S., Xenarios, I., Orobitt, M., Montanyola, A., Chang, J. M., et al. (2011). T-Coffee: a web server for the multiple sequence alignment of protein and RNA sequences using structural information and homology extension. *Nucleic Acids Res.* 39, W13–W17. doi: 10.1093/nar/gkr245
- Díaz, E., Ferrández, A., and García, J. L. (1998). Characterization of the hca cluster encoding the dioxygenolytic pathway for initial catabolism of 3-phenylpropionic acid in *Escherichia coli* K-12. *J. Bacteriol.* 180, 2915–2923. doi: 10.1128/jb.180.11.2915-2923.1998
- Erickson, B. D., and Mondello, F. J. (1992). Nucleotide sequencing and transcriptional mapping of the genes encoding biphenyl dioxygenase, a multicomponent polychlorinated biphenyl-degrading enzyme in *Pseudomonas* strain LB400. *J. Bacteriol.* 174, 2903–2912. doi: 10.1128/jb.174.9.2903-2912.1992
- Focht, D. D. (1995). Strategies for the improvement of aerobic metabolism of polychlorinated biphenyls. *Curr. Opin. Biotechnol.* 6, 341–346. doi: 10.1016/0958-1669(95)80057-3
- Fukuda, M., Yasukochi, Y., Kikuchi, Y., Nagata, Y., Kimbara, K., Horiuchi, H., et al. (1994). Identification of the bphA and bphB genes of *Pseudomonas* sp. strains KKS102 involved in degradation of biphenyl and polychlorinated biphenyls. *Biochem. Biophys. Res. Commun.* 202, 850–856. doi: 10.1006/bbrc.1994.2008
- Furukawa, K. (2000). Biochemical and genetic bases of microbial degradation of polychlorinated biphenyls (PCBs). *J. Gen. Appl. Microbiol.* 46, 283–296.
- Furukawa, K., Hayase, N., Taira, K., and Tomizuka, N. (1989). Molecular relationship of chromosomal genes encoding biphenyl/polychlorinated biphenyl catabolism: some soil bacteria possess a highly conserved bph operon. *J. Bacteriol.* 171, 5467–5472.
- Furukawa, K., Suenaga, H., and Goto, M. (2004). Biphenyl dioxygenases: functional versatility and directed evolution. *J. Bacteriol.* 186, 5189–5196.
- Garrido-Sanz, D., Sansegundo-Lobato, P., Redondo-Nieto, M., Šuman, J., Cajthaml, T., Blanco-Romero, E., et al. (2020). Analysis of the biodegradative and adaptive potential of the novel polychlorinated biphenyl degrader *Rhodococcus* sp. WAY2 revealed by its complete genome sequence. *Microb. Genomics* 6:000363. doi: 10.1099/mgen.0.000363
- Gómez-Gil, L., Kumar, P., Barriault, D., Bolin, J. T., Sylvestre, M., and Eltis, L. D. (2007). Characterization of biphenyl dioxygenase of *Pandora pnumenusa* B-356 as a potent polychlorinated biphenyl-degrading enzyme. *J. Bacteriol.* 189, 5705–5715. doi: 10.1128/jb.01476-06
- Han, J., Kim, S.-Y., Jung, J., Lim, Y., Ahn, J.-H., Kim, S.-I., et al. (2005). Epoxide formation on the aromatic B Ring of Flavanone by Biphenyl Dioxygenase of *Pseudomonas pseudoalcaligenes* KF707. *Appl. Environ. Microbiol.* 71, 5354–5361. doi: 10.1128/aem.71.9.5354-5361.2005
- Hernández, M., Neufeld, J. D., and Dumont, M. G. (2017). “Enhancing functional metagenomics of complex microbial communities using stable isotopes,” in *Functional Metagenomics: Tools and Applications*, eds T. C. Charles, M. R. Liles, and A. Sessitsch (Cham: Springer), 139–150.
- Hu, J., Wu, J., and Qu, X. (2018). Decomposition characteristics of organic materials and their effects on labile and recalcitrant organic carbon fractions in a semi-arid soil under plastic mulch and drip irrigation. *J. Arid Land* 10, 115–128. doi: 10.1007/s40333-017-0035-1
- Iwai, S., Chai, B., Sul, W. J., Cole, J. R., Hashsham, S. A., and Tiedje, J. M. (2010). Gene-targeted-metagenomics reveals extensive diversity of aromatic dioxygenase genes in the environment. *ISME J.* 4, 279–285.
- Iwashina, T. (2015). Contribution to flower colors of flavonoids including anthocyanins: a review. *Nat. Prod. Commun.* 10, 529–544.
- Jones, D. T., Taylor, W. R., and Thornton, J. M. (1992). The rapid generation of mutation data matrices from protein sequences. *Bioinformatics* 8, 275–282. doi: 10.1093/bioinformatics/8.3.275
- Kagami, O., Shindo, K., Kyojima, A., Takeda, K., Ikenaga, H., Furukawa, K., et al. (2008). Protein engineering on biphenyl dioxygenase for conferring activity to convert 7-hydroxyflavone and 5,7-dihydroxyflavone (chrysin). *J. Biosci. Bioeng.* 106, 121–127. doi: 10.1263/jbb.106.121
- Kim, S. Y., Jung, J., Lim, Y., Ahn, J. H., Kim, S. I., and Hur, H. G. (2003). Cis-2', 3'-dihydrodiol production on flavone B-ring by biphenyl dioxygenase from *Pseudomonas pseudoalcaligenes* KF707 expressed in *Escherichia coli*. *Antonie Van Leeuwenhoek* 84, 261–268. doi: 10.1023/a:1026081824334
- Kraus, T. E. C., Dahlgren, R. A., and Zasoski, R. J. (2003). Tannins in nutrient dynamics of forest ecosystems - a review. *Plant Soil* 256, 41–66.
- Kumar, S., Stecher, G., Li, M., Knyaz, C., and Tamura, K. (2018). MEGA X: molecular evolutionary genetics analysis across computing platforms. *Mol. Biol. Evol.* 35, 1547–1549. doi: 10.1093/molbev/msy096
- Kumamaru, T., Suenaga, H., Mitsuoka, M., Watanabe, T., and Furukawa, K. (1998). Enhanced degradation of polychlorinated biphenyls by directed evolution of biphenyl dioxygenase. *Nat. Biotechnol.* 16, 663–666. doi: 10.1038/nbt0798-663
- Kweon, O., Kim, S. J., Baek, S., Chae, J. C., Adjei, M. D., Baek, D. H., et al. (2008). A new classification system for bacterial Rieske non-heme iron aromatic ring-hydroxylating oxygenases. *BMC Biochem.* 9:11. doi: 10.1186/1471-2091-9-11
- Lee, N., and Kwon, D. Y. (2016). Characteristics of a recombinant 2,3-dihydroxybiphenyl 1,2-dioxygenase from *Comamonas* sp. Expressed in *Escherichia coli*. *Indian J. Microbiol.* 56, 467–475. doi: 10.1007/s12088-016-0599-z
- Li, A., Qu, Y., Zhou, J., and Ma, F. (2009). Enzyme-substrate interaction and characterization of a 2,3-dihydroxybiphenyl 1,2-dioxygenase from *Dyella ginsengisoli* LA-4. *FEMS Microbiol. Lett.* 292, 231–239. doi: 10.1111/j.1574-6968.2009.01487.x
- Lin, J. J., Smith, M., Jessee, J., and Bloom, F. (1992). DH11S: an *Escherichia coli* strain for preparation of single-stranded DNA from phagemid vectors. *Biotechniques* 12, 718–721.
- Liu, C.-W., and Murray, J. D. (2016). The role of flavonoids in nodulation host-range specificity: an update. *Plants* 5:33.
- Mackova, M., Dowling, D., and Macek, T. (eds) (2006). *Phytoremediation and Rhizoremediation*. Dordrecht: Springer.
- Marin, A. M., De La Torre, J., Ricardo Marques, Oliveira, A., Barison, A., Satie Chubatsu, L., et al. (2016). Genetic and functional characterization of a novel meta-pathway for degradation of naringenin in *Herbaspirillum seropedicae* SmR1. *Environ. Microbiol.* 18, 4653–4661. doi: 10.1111/1462-2920.13313
- Marin, A. M., Souza, E. M., Pedrosa, F. O., Souza, L. M., Sassaki, G. L., Baura, V. A., et al. (2013). Naringenin degradation by the endophytic diazotroph *Herbaspirillum seropedicae* SmR1. *Microbiology* 159, 167–175. doi: 10.1099/mic.0.061135-0
- Martin, M. (2011). Cutadapt removes adapter sequences from high-throughput sequencing reads. *EMBnet J.* 17, 10–12. doi: 10.14806/ej.17.1.200
- Masai, E., Yamada, A., Healy, J. M., Hatta, T., Kimbara, K., Fukuda, M., et al. (1995). Characterization of biphenyl catabolic genes of gram-positive polychlorinated biphenyl degrader *Rhodococcus* sp. strain RHA1. *Appl. Environ. Microbiol.* 61, 2079–2085.
- Mason, J. R., and Cammack, R. (1992). The electron-transport proteins of hydroxylating bacterial dioxygenases. *Annu. Rev. Microbiol.* 46, 277–305. doi: 10.1146/annurev.mi.46.100192.001425
- Master, E. R., and Mohn, W. W. (2001). Induction of bphA, encoding biphenyl dioxygenase, in two polychlorinated biphenyl-degrading bacteria, psychrotolerant *Pseudomonas* strain Cam-1 and mesophilic *Burkholderia* strain LB400. *Appl. Environ. Microbiol.* 67, 2669–2676. doi: 10.1128/AEM.67.6.2669-2676.2001
- Misawa, N., Shindo, K., Takahashi, H., Suenaga, H., Iguchi, K., Okazaki, H., et al. (2002). Hydroxylation of various molecules including heterocyclic aromatics using recombinant *Escherichia coli* cells expressing modified biphenyl dioxygenase genes. *Tetrahedron* 58, 9605–9612. doi: 10.1016/S0040-4020(02)01253-X
- Mohammadi, M., and Sylvestre, M. (2005). Resolving the profile of metabolites generated during oxidation of Dibenzofuran and Chlorodibenzofurans by the Biphenyl Catabolic Pathway Enzymes. *Chem. Biol.* 12, 835–846. doi: 10.1016/j.chembiol.2005.05.017
- Mohammadi, M., Viger, J.-F., Kumar, P., Barriault, D., Bolin, J. T., and Sylvestre, M. (2011). Retuning Rieske-type Oxygenases to expand substrate range. *J. Biol. Chem.* 286, 27612–27621. doi: 10.1074/jbc.M111.255174
- Mondello, F. J. (1989). Cloning and expression in *Escherichia coli* of *Pseudomonas* strain LB400 genes encoding polychlorinated biphenyl degradation. *J. Bacteriol.* 171, 1725–1732. doi: 10.1128/jb.171.3.1725-1732.1989
- Mondello, F. J., Turcich, M. P., Lobos, J. H., and Erickson, B. D. (1997). Identification and modification of biphenyl dioxygenase sequences that

- determine the specificity of polychlorinated biphenyl degradation. *Appl. Environ. Microbiol.* 63, 3096–3103.
- Nurk, S., Meleshko, D., Korobeynikov, A., and Pevzner, P. A. (2017). metaSPAdes: a new versatile metagenomic assembler. *Genome Res.* 27, 824–834. doi: 10.1101/gr.213959.116
- O'Leary, N. A., Wright, M. W., Brister, J. R., Ciufo, S., Haddad, D., McVeigh, R., et al. (2016). Reference sequence (RefSeq) database at NCBI: current status, taxonomic expansion, and functional annotation. *Nucleic Acids Res.* 44, 733–745. doi: 10.1093/nar/gkv1189
- Parks, D. H., Chuvochina, M., Chaumeil, P. A., Rinke, C., Mussig, A. J., and Hugenholtz, P. (2020). A complete domain-to-species taxonomy for Bacteria and Archaea. *Nat. Biotechnol.* 38, 1079–1086. doi: 10.1038/s41587-020-0501-8
- Pham, T. T., Pino Rodriguez, N. J., Hijri, M., and Sylvestre, M. (2015). Optimizing Polychlorinated Biphenyl Degradation by Flavonoid-Induced Cells of the Rhizobacterium *Rhodococcus erythropolis* U23A. *PLoS One* 10:e0126033. doi: 10.1371/journal.pone.0126033
- Pham, T. T., and Sylvestre, M. (2013). Has the bacterial biphenyl catabolic pathway evolved primarily to degrade biphenyl? The diphenylmethane case. *J. Bacteriol.* 195, 3563–3574. doi: 10.1128/JB.00161-13
- Pham, T. T. M., Tu, Y., and Sylvestre, M. (2012). Remarkable ability of *Pandoraea pnomenusa* B356 biphenyl dioxygenase to metabolize simple flavonoids. *Appl. Environ. Microbiol.* 78, 3560–3570. doi: 10.1128/aem.00225-12
- Pieper, D. H. (2005). Aerobic degradation of polychlorinated biphenyls. *Appl. Microbiol. Biotechnol.* 67, 170–191.
- Polivkova, M., Suman, J., Strejcek, M., Krcmarova, M., Hradilova, M., Filipova, A., et al. (2018). Diversity of root-associated microbial populations of *Tamarix parviflora* cultivated under various conditions. *Appl. Soil Ecol.* 125, 264–272. doi: 10.1016/j.apsoil.2018.02.002
- R Core Team (2017). *R: A Language and Environment for Statistical Computing*. Vienna: R Foundation for Statistical Computing.
- Rauscher, M. D. (2001). Co-evolution and plant resistance to natural enemies. *Nature* 411, 857–864.
- Ridl, J., Suman, J., Fraraccio, S., Hradilova, M., Strejcek, M., Cajthaml, T., et al. (2018). Complete genome sequence of *Pseudomonas alcaliphila* JAB1 (=DSM 26533), a versatile degrader of organic pollutants. *Stand. Genomic Sci.* 13:3. doi: 10.1186/s40793-017-0306-7
- Robrock, K. R., Mohn, W. W., Eltis, L. D., and Alvarez-Cohen, L. (2011). Biphenyl and ethylbenzene dioxygenases of *Rhodococcus jostii* RHA1 transform PBDEs. *Biotechnol. Bioeng.* 108, 313–321. doi: 10.1002/bit.22952
- Sala-Trepat, J. M., and Evans, W. C. (1971). The meta cleavage of catechol by *Azotobacter* species. *Eur. J. Biochem.* 20, 400–413. doi: 10.1111/j.1432-1033.1971.tb01406.x
- San-Miguel, T., Perez-Bermudez, P., and Gavidia, I. (2013). Production of soluble eukaryotic recombinant proteins in *E. coli* is favoured in early log-phase cultures induced at low temperature. *Springerplus* 2:89. doi: 10.1186/2193-1801-2-89
- Seeger, M., González, M., Cámara, B., Muñoz, L., Ponce, E., Mejías, L., et al. (2003). Biotransformation of natural and synthetic isoflavonoids by two recombinant microbial enzymes. *Appl. Environ. Microbiol.* 69, 5045–5050. doi: 10.1128/aem.69.9.5045-5050.2003
- Seemann, T. (2014). Prokka: rapid prokaryotic genome annotation. *Bioinformatics* 30, 2068–2069. doi: 10.1093/bioinformatics/btu153
- Seo, J., Kang, S. I., Ryu, J. Y., Lee, Y. J., Park, K. D., Kim, M., et al. (2010). Location of flavone B-ring controls regioselectivity and stereoselectivity of naphthalene dioxygenase from *Pseudomonas* sp. strain NCIB 9816-4. *Appl. Microbiol. Biotechnol.* 86, 1451–1462. doi: 10.1007/s00253-009-2389-6
- Shaw, L. J., Morris, P., and Hooker, J. E. (2006). Perception and modification of plant flavonoid signals by rhizosphere microorganisms. *Environ. Microbiol.* 8, 1867–1880. doi: 10.1111/j.1462-2920.2006.01141.x
- Shimada, T., Nagayoshi, H., Murayama, N., Takenaka, S., Katahira, J., Kim, V., et al. (2021). Liquid chromatography-tandem mass spectrometry analysis of oxidation of 2', 3', 4'- and 6-hydroxyflavonones by human cytochrome P450 enzymes. *Xenobiotica* 51, 139–154. doi: 10.1080/00498254.2020.1836433
- Shindo, K., Kagiya, Y., Nakamura, R., Hara, A., Ikenaga, H., Furukawa, K., et al. (2003). Enzymatic synthesis of novel antioxidant flavonoids by *Escherichia coli* cells expressing modified metabolic genes involved in biphenyl catabolism. *J. Mol. Catal. B Enzym.* 23, 9–16. doi: 10.1016/S1381-1177(03)00038-9
- Singer, A. C. (2006). “The chemical ecology of pollutant biodegradation: bioremediation and Phytoremediation from mechanistic and ecological perspectives,” in *Phytoremediation and Rhizoremediation*, 9th Edn, eds M. Macková, D. Dowling, and T. Macek (Dordrecht: Springer), 5–21.
- Singer, A. C., Crowley, D. E., and Thompson, I. P. (2003). Secondary plant metabolites in phytoremediation and biotransformation. *Trends Biotechnol.* 21, 123–130. doi: 10.1016/S0167-7799(02)00041-0
- Spence, E. L., Kawamukai, M., Sanvoisin, J., Braven, H., and Bugg, T. D. (1996). Catechol dioxygenases from *Escherichia coli* (MhpB) and *Alcaligenes eutrophus* (MpcI): sequence analysis and biochemical properties of a third family of extradiol dioxygenases. *J. Bacteriol.* 178, 5249–5256. doi: 10.1128/jb.178.17.5249-5256.1996
- Strejcek, M., Wang, Q., Ridl, J., and Uhlik, O. (2015). Hunting down frame shifts: ecological analysis of diverse functional gene sequences. *Front. Microbiol.* 6:1267. doi: 10.3389/fmicb.2015.01267
- Subramanian, S., Stacey, G., and Yu, O. (2007). Distinct, crucial roles of flavonoids during legume nodulation. *Trends Plant Sci.* 12, 282–285. doi: 10.1016/j.tplants.2007.06.006
- Sul, W. J., Park, J., Quensen, J. F., Iii, Rodrigues, J. L., Seliger, L., et al. (2009). DNA-stable isotope probing integrated with metagenomics for retrieval of biphenyl dioxygenase genes from polychlorinated biphenyl-contaminated river sediment. *Appl. Environ. Microbiol.* 75, 5501–5506.
- Sylvestre, M., Sirois, M., Hurtubise, Y., Bergeron, J., Ahmad, D., Shareck, F., et al. (1996). Sequencing of *Comamonas testosteroni* strain B-356-biphenyl/chlorobiphenyl dioxygenase genes: evolutionary relationships among Gram-negative bacterial biphenyl dioxygenases. *Gene* 174, 195–202.
- Taira, K., Hirose, J., Hayashida, S., and Furukawa, K. (1992). Analysis of bph operon from the polychlorinated biphenyl-degrading strain of *Pseudomonas pseudoalcaligenes* KF707. *J. Biol. Chem.* 267, 4844–4853.
- Tan, H.-M., Tang, H.-Y., Joannou, C., Abdel-Wahab, N., and Mason, J. (1993). The *Pseudomonas putida* ML2 plasmid-encoded genes for benzene dioxygenase are unusual in codon usage and low in G + C content. *Gene* 130, 33–39. doi: 10.1016/0378-1119(93)90343-2
- Tellinghuisen, J. (2001). Statistical error propagation. *J. Phys. Chem. A* 105, 3917–3921. doi: 10.1021/jp003484u
- The UniProt Consortium (2018). UniProt: a worldwide hub of protein knowledge. *Nucleic Acids Res.* 47, D506–D515. doi: 10.1093/nar/gky1049
- Thompson, J. R., Marcelino, L. A., and Polz, M. F. (2002). Heteroduplexes in mixed-template amplifications: formation, consequence and elimination by 'reconditioning PCR'. *Nucleic Acids Res.* 30, 2083–2088.
- Toussaint, J.-P., Pham, T., Barriault, D., and Sylvestre, M. (2012). Plant exudates promote PCB degradation by a rhodococcal rhizobacteria. *Appl. Microbiol. Biotechnol.* 95, 1589–1603. doi: 10.1007/s00253-011-3824-z
- Uhlik, O., Jecna, K., Mackova, M., Vlcek, C., Hroudova, M., Demnerova, K., et al. (2009). Biphenyl-metabolizing bacteria in the rhizosphere of horseradish and bulk soil contaminated by polychlorinated biphenyls as revealed by stable isotope probing. *Appl. Environ. Microbiol.* 75, 6471–6477.
- Uhlik, O., Leewis, M. C., Strejcek, M., Musilova, L., Mackova, M., Leigh, M. B., et al. (2013). Stable isotope probing in the metagenomics era: a bridge towards improved bioremediation. *Biotechnol. Adv.* 31, 154–165. doi: 10.1016/j.biotechadv.2012.09.003
- Uhlik, O., Wald, J., Strejcek, M., Musilova, L., Ridl, J., Hroudova, M., et al. (2012). Identification of bacteria utilizing biphenyl, benzoate, and naphthalene in long-term contaminated soil. *PLoS One* 7:e40653. doi: 10.1371/journal.pone.0040653
- Van der Geize, R., Yam, K., Heuser, T., Wilbrink, M. H., Hara, H., Anderton, M. C., et al. (2007). A gene cluster encoding cholesterol catabolism in a soil actinomycete provides insight into Mycobacterium tuberculosis survival in macrophages. *Proc. Natl. Acad. Sci. U.S.A.* 104, 1947–1952.
- Vergani, L., Mapelli, F., Suman, J., Cajthaml, T., Uhlik, O., and Borin, S. (2019). Novel PCB-degrading *Rhodococcus* strains able to promote plant growth for assisted rhizoremediation of historically polluted soils. *PLoS One* 14:e0221253. doi: 10.1371/journal.pone.0221253
- Vézina, J., Barriault, D., and Sylvestre, M. (2007). Family shuffling of soil DNA to change the regiospecificity of *Burkholderia xenovorans* LB400 biphenyl dioxygenase. *J. Bacteriol.* 189, 779–788.

- Vézina, J., Barriault, D., and Sylvestre, M. (2008). Diversity of the C-terminal portion of the biphenyl dioxygenase large subunit. *J. Mol. Microbiol. Biotechnol.* 15, 139–151.
- Wald, J., Hroudova, M., Jansa, J., Vrchotova, B., Macek, T., and Uhlik, O. (2015). Pseudomonads rule degradation of polyaromatic hydrocarbons in aerated sediment. *Front. Microbiol.* 6:1268. doi: 10.3389/fmicb.2015.01268
- Wang, Y., Garnon, J., Labbe, D., Bergeron, H., and Lau, P. C. (1995). Sequence and expression of the bpdC1C2BADE genes involved in the initial steps of biphenyl/chlorobiphenyl degradation by *Rhodococcus* sp. M5. *Gene* 164, 117–122. doi: 10.1016/0378-1119(95)00448-f
- Yang, X., Liu, X., Song, L., Xie, F., Zhang, G., and Qian, S. (2007). Characterization and functional analysis of a novel gene cluster involved in biphenyl degradation in *Rhodococcus* sp. strain R04. *J. Appl. Microbiol.* 103, 2214–2224. doi: 10.1111/j.1365-2672.2007.03461.x
- Yang, X., Xie, F., Zhang, G., Shi, Y., and Qian, S. (2008). Purification, characterization, and substrate specificity of two 2,3-dihydroxybiphenyl 1,2-dioxygenase from *Rhodococcus* sp. R04, showing their distinct stability at various temperature. *Biochimie* 90, 1530–1538. doi: 10.1016/j.biochi.2008.05.020
- Zhu, L., Zhou, J., Zhang, R., Tang, X., Wang, J., Li, Y., et al. (2020). Degradation mechanism of biphenyl and 4-4'-dichlorobiphenyl cis-dihydroxylation by non-heme 2,3 dioxygenases BphA: a QM/MM approach. *Chemosphere* 247, 125844. doi: 10.1016/j.chemosphere.2020.125844
- Zubrova, A., Michalikova, K., Semerad, J., Strejcek, M., Cajthaml, T., Suman, J., et al. (2021). Biphenyl 2,3-dioxygenase in *Pseudomonas alcaliphila* JAB1 is both induced by phenolics and monoterpenes and involved in their transformation. *Front. Microbiol.* 12:657311. doi: 10.3389/fmicb.2021.657311

Conflict of Interest: The authors declare that the research was conducted in the absence of any commercial or financial relationships that could be construed as a potential conflict of interest.

Publisher's Note: All claims expressed in this article are solely those of the authors and do not necessarily represent those of their affiliated organizations, or those of the publisher, the editors and the reviewers. Any product that may be evaluated in this article, or claim that may be made by its manufacturer, is not guaranteed or endorsed by the publisher.

Copyright © 2021 Suman, Strejcek, Zubrova, Capek, Wald, Michalikova, Hradilova, Sredlova, Semerad, Cajthaml and Uhlik. This is an open-access article distributed under the terms of the Creative Commons Attribution License (CC BY). The use, distribution or reproduction in other forums is permitted, provided the original author(s) and the copyright owner(s) are credited and that the original publication in this journal is cited, in accordance with accepted academic practice. No use, distribution or reproduction is permitted which does not comply with these terms.



Soil Microbial Resource Limitations and Community Assembly Along a *Camellia oleifera* Plantation Chronosequence

Hang Qiao^{1,2†}, Longsheng Chen^{3†}, Yajun Hu^{1,4*}, Chenghua Deng¹, Qi Sun^{1,2}, Shaohong Deng^{1,2}, Xiangbi Chen¹, Li Mei⁵, Jinshui Wu¹ and Yirong Su¹

¹Key Laboratory of Agro-ecological Processes in Subtropical Region, Institute of Subtropical Agriculture, Chinese Academy of Sciences, Changsha, China, ²College of Resource and Environment, University of Chinese Academy of Sciences, Beijing, China, ³Research Institute of Economic Forest and Fruit (Research Institute of Oil Tea Camellia), Hunan Academy of Forestry, Changsha, China, ⁴College of Agronomy, Hunan Agricultural University, Changsha, China, ⁵College of Horticulture and Forestry Sciences/Hubei Engineering Technology Research Center for Forestry Information, Huazhong Agricultural University, Wuhan, China

OPEN ACCESS

Edited by:

Paolina Garbeva,
Netherlands Institute of Ecology
(NIOO-KNAW), Netherlands

Reviewed by:

Wenli Chen,
Huazhong Agricultural University,
China
Dhiraj Kumar Chaudhary,
Korea University,
South Korea

*Correspondence:

Yajun Hu
yjh@isa.ac.cn

[†]These authors have contributed
equally to this work

Specialty section:

This article was submitted to
Terrestrial Microbiology,
a section of the journal
Frontiers in Microbiology

Received: 04 July 2021

Accepted: 09 November 2021

Published: 02 December 2021

Citation:

Qiao H, Chen L, Hu Y, Deng C,
Sun Q, Deng S, Chen X, Mei L,
Wu J and Su Y (2021) Soil Microbial
Resource Limitations and Community
Assembly Along a *Camellia oleifera*
Plantation Chronosequence.
Front. Microbiol. 12:736165.
doi: 10.3389/fmicb.2021.736165

Understanding soil microbial element limitation and its relation with the microbial community can help in elucidating the soil fertility status and improving nutrient management of planted forest ecosystems. The stand age of a planted forest determines the aboveground forest biomass and structure and underground microbial function and diversity. In this study, we investigated 30 plantations of *Camellia oleifera* distributed across the subtropical region of China that we classified into four stand ages (planted <9 years, 9–20 years, 21–60 years, and >60 years age). Enzymatic stoichiometry analysis showed that microbial metabolism in the forests was mainly limited by C and P. P limitation significantly decreased and C limitation slightly increased along the stand age gradient. The alpha diversity of the soil microbiota remained steady along stand age, while microbial communities gradually converged from scattered to clustered, which was accompanied by a decrease in network complexity. The soil bacterial community assembly shifted from stochastic to deterministic processes, which probably contributed to a decrease in soil pH along stand age. Our findings emphasize that the stand age regulated the soil microbial metabolism limitation and community assembly, which provides new insight into the improvement of C and P management in subtropical planted forest.

Keywords: soil microbial limitation, community assembly, stand age, planted forest, *Camellia oleifera*

INTRODUCTION

Planted forests, established by planting and/or deliberate seeding, provide critical ecosystem services, such as carbon storage, soil conservation, and wood production (FAO, 2015). Planted forests have been estimated to have increased globally from 277.9 million ha to 320 million ha between 2015 and 2020 (Nepal et al., 2019). Compared to natural forests, planted forests, which are generally established with the aim to restore plant cover on agricultural and mined lands, are characterized by a lower plant diversity (Martínez-Jauregui et al., 2016). According to the widely accepted resource diversity hypothesis, plant communities with a high diversity

support higher soil microbial activity and diversity owing to a diverse and complex organic substrate input from the various species planted. For example, the soil microbial activity in a mixed hornbeam and ironwood forest was found to be higher than in an ash planted forest (Kooch et al., 2018). The microbial diversity in a natural hygrophilic deciduous mixed forest was higher than that in the poplar planted forest (Vitali et al., 2016). The investigation of soil microbial processes in planted forests is expected to deepen our understanding of why the microbes show a low activity and diversity in such forests.

Soil microbial metabolic limitation, which reflects the nutrient demands of soil microorganisms for microbial metabolic processes, can be analyzed based on microbial enzyme activity as indicated by eco-enzymatic stoichiometry (Sinsabaugh et al., 2015). Previous studies have reported that soil microbial carbon (C) limitation is common in terrestrial ecosystems (Schimel and Weintraub, 2003), whereas microbial nitrogen (N) and phosphorus (P) limitations are more generally found in grassland and wetland ecosystems (Hill et al., 2018; Yang et al., 2020). Soil microbial metabolic limitation is influenced by multiple environmental factors, including climatic and plant-related factors. Microbial C limitation reportedly decreases with increasing precipitation in the Loess Plateau region (Cui et al., 2019). Soil microbial P limitation increases during forest succession from coniferous to broad-leaf forest due to substantial competition for P in the later stages of forest succession (Huang et al., 2013). Thus, the identification of the variation in soil microbial metabolic limitation in a specific forest ecosystem will improve our knowledge of the soil biogeochemical constraints in the system.

Stand age is a primary driver of forest structure and function, including plant net primary productivity, carbon storage (Pregitzer and Euskirchen, 2004), and the soil microbial community (Kang et al., 2018). A previous study showed that soil bacterial alpha diversity increased linearly with increasing stand age in *Caragana liouana* plantations (Na et al., 2018), whereas it exhibited a nonlinear pattern along stand age in *Hevea brasiliensis* plantations (Zhou et al., 2017). The inconsistency of microbial diversity patterns is usually attributed to the plant species involved and the soil physicochemical properties. For example, *Alnus cremastogyne*, as a pioneer species, gradually decreases the soil pH through the secretion of organic acids during tree growth, thus increasing soil bacterial diversity (Sun et al., 2018). The progressive accumulation of lignin-rich litter from oak trees on the soil surface along stand age provides a moist soil microclimate that supports the growth of anaerobic bacterial species (Canessa et al., 2020). Additionally, forest stand age also affects microbial metabolic limitation *via* influencing soil nutrients. A study in a Douglas-fir forest revealed that microbial N limitation increased with stand age (Vittori Antisari et al., 2018). In Eucalyptus plantations, microbial metabolism was mainly limited by P and increased with stand age (Fan et al., 2015). Thus, the effect of stand age on the soil microbial diversity depends on the forest species.

Shifts in a microbial community along ecological successions are controlled by microbial assembly processes (Stegen et al., 2012). Deterministic processes result from environmental abiotic and biotic filtering that shapes species abundances, whereas

stochastic processes reflect changes in species abundances by random processes, such as ecological drift and dispersal (Dini-Andreote et al., 2015). The relative importance of these two processes is determined by various factors, including spatial variation (Gao et al., 2019), ecosystem succession (Måren et al., 2018), and environmental disturbances (Ferrenberg et al., 2013). For example, the soil bacterial community assembly generally shifts with the spatial scale, with stochastic processes dominating at small spatial scales and deterministic processes dominating at larger scales (Feng et al., 2019). In a subtropical forest succession, deterministic processes have been found to govern the soil fungal assembly in the early succession stage, whereas both deterministic and stochastic processes were predominant in later succession stages (Chai et al., 2016). However, the factors influencing soil microbial assembly on a short time scale, such as stand age, remain largely unknown.

Camellia oleifera, one of the four major woody oil plants in the world, is widely planted in the subtropical zone of South China (Jin and Ning, 2012). The planting area of *C. oleifera* increases at the rate of 0.1 million ha annually and covers about 4.5 million ha as of 2019 (State Forestry Bureau, 2009). Besides the economic purpose of oil production, *C. oleifera* is planted as a pioneer species to colonize acid, infertile soils for ecological restoration (Yang et al., 2016). However, continuous product harvesting has been shown to decrease soil fertility in *C. oleifera* forests. Under infertile conditions, soil microbes compete with plants for nutrients, such as N and P, resulting in low tea quality and oil yield (Liu et al., 2017). Understanding soil microbial metabolism and community dynamics is expected to provide useful information for soil fertility management. In this study, field investigation experiments were conducted to examine the effects of stand age on soil microbial metabolic limitation and community assembly in *C. oleifera* plantations. We hypothesized that (i) microbial C limitation would increase with stand age due to a decrease in soil fertility along stand age, and (ii) deterministic processes rather than random processes determine the soil bacterial community assembly along stand age because *C. oleifera* plants secrete organic acids from their roots and thus decrease soil pH.

MATERIALS AND METHODS

Field Experimental Design and Sample Collection

We collected soil samples in plantations of four stand ages, classified as young (planted <9 years ago), near-mature (planted 9–20 years ago), mature (planted 21–60 years ago), or over-mature (planted >60 years ago), based on the space-for-time substitution method, during from December 2017 and January 2018. In total, 30 *C. oleifera* plantations across South China [from a latitude of 25°21' to 29°42' (N) and a longitude of 110°28' to 115°34' (E)] were investigated (Figure 1). Three independent 100 m² (10 m × 10 m) plots within each plantation were randomly designated for soil sampling. Twelve soil cores taken to a depth of 15 cm were randomly collected within the drip line of a tree in each plot as composite soil samples. The samples were transported to the laboratory in ice boxes.

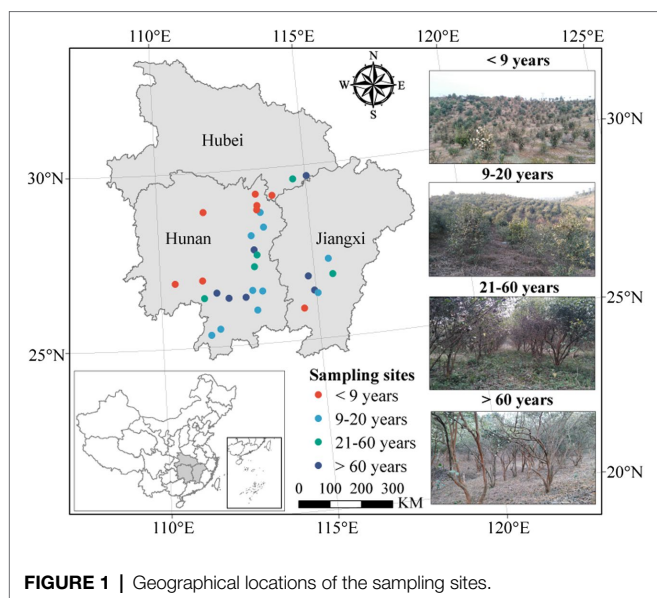


FIGURE 1 | Geographical locations of the sampling sites.

After homogenization, the soil samples were passed through a 2 mm sieve to remove plant residues and stones and were then divided into three subsamples. One subsample was stored at -80°C for microbial DNA analysis, one was air-dried for physicochemical analysis, and one was stored at 4°C until determination of the soil microbial biomass and enzyme activities.

Determination of Soil Enzyme Activities and Quantification of Microbial Metabolic Limitation

The activities of five extracellular enzymes, including two C acquisition enzymes [β -1,4-glucosidase (BG) and β -D-cellobiosidase (CBH)], two N acquisition enzymes [L-leucine aminopeptidase (LAP) and β -N-acetylglucosaminidase (NAG)], and P acquisition enzyme [acid phosphatase (AP)], were determined using published standard fluorometric techniques (**Supplementary Table S1**; Saiya-Cork et al., 2002). Briefly, 1 g of fresh soil was homogeneously suspended in 125 ml of 50 mM sodium acetate trihydrate (CAS). Then, 250 μl of CAS, 200 μl of the soil suspensions, 50 μl of 10 M methylumbelliferyl solution, and 50 μl of substrate were added into each well of 96-well microplates and incubated at 25°C in the dark for 4 h. Then, 10 μl of 1 M NaOH was added to stop the reaction. Fluorescence was determined using a Synergy H4 multimode microplate reader (Infinite 200 Pro, Tecan, Switzerland).

Soil microbial metabolic limitation was evaluated by two different methods. The first method uses a scatter plot of soil enzymatic activities, represented by the N:P versus C:N enzymatic activity ratios (Sinsabaugh et al., 2009). This quadrantal diagram provides information regarding four types of microbial metabolic limitation, that is, P limitation, N limitation, C&P limitation, and N&P limitation (Schmidt et al., 2016). The second method uses vector analysis of the enzymatic stoichiometry and considers the lowest kurtosis for vector angle, as suggested by Moorhead et al. (2016). Vector length (L) was used to describe the microbial C limitation (i.e., increased vector L suggests increased

microbial C limitation), whereas the vector angle (A°) was used to indicate microbial N and P limitation, with vector $A > 45^{\circ}$ and $< 45^{\circ}$ representing P limitation and N limitation, respectively. Vector L and vector A were calculated using the following formulae (Moorhead et al., 2016):

$$\text{Vector } L = \sqrt{\left(\frac{\ln[\text{BG} + \text{CBH}]}{\ln[\text{NAG} + \text{LAP}]}\right)^2 + \left(\frac{\ln[\text{BG} + \text{CBH}]}{\ln \text{AP}}\right)^2}$$

$$\text{Vector } A = \text{Degrees} \left(\text{ATAN2} \left(\frac{\ln[\text{BG} + \text{CBH}]}{\ln \text{AP}}, \frac{\ln[\text{BG} + \text{CBH}]}{\ln[\text{NAG} + \text{LAP}]} \right) \right)$$

DNA Extraction, PCR, and High-Throughput Sequencing

Soil DNA was extracted using the PowerSoil DNA Isolation Kit (MoBio Laboratories, Carlsbad, CA, United States), according to the manufacturer's manual. DNA quality was evaluated using a NanoDrop ND-2000 spectrophotometer (Thermo Scientific, United States). The 16S rRNA gene V3-V4 region was amplified using the primer set 343F (5'-TACGGR AGGCAGCAG-3')/798R (5'-AGGGTATCTAATCCT-3'; Nossa et al., 2010). A unique 8-mer tag was designed and linked to the 5' end of each primer to allow sample identification in multiplex samples. PCRs were run using 25 μl reaction mixtures containing 12.5 μl of $2\times$ KAPA HiFi HotStart ReadyMix, 5 μl of each primer (1 μM), and 2.5 μl of diluted DNA (5 ng/ μl) and the following thermal cycling program: 95°C for 3 min, 30 cycles of 95°C for 30 s, 60°C for 30 s, and 72°C for 30 s, and 72°C for 10 min. PCR products were purified using AMPure XP Beads (Beckman Coulter, United Kingdom). Purified PCR amplicons were combined at equimolar concentrations after quantification using the Qubit dsDNA HS Assay Kit (Invitrogen, United States) for sequencing library construction. The library was sequenced on an Illumina MiSeq platform (2×300 bp) at Shanghai Hanyu Biotech (Shanghai, China).

Pair-end raw reads were assembled, screened, and trimmed using the mothur software (v.1.36.1; Schloss et al., 2009). Briefly, stringent quality-based trimming was first used to minimize sequencing error effects (Kunin et al., 2010). Sequences were removed based on the following criteria: average quality score of 50-bp windows < 25 , homopolymers of more than eight bases, primer sequence, ambiguous base call, and read length < 200 bp. The remaining sequences were sorted by tag sequence and then checked for chimeras using the "screen.seqs" command. The USEARCH algorithm with a 97% identity threshold was adopted for operational taxonomic units (OTUs) clustering (Edgar, 2010). Representative sequences of OTUs were used for BLAST searches against the Greengenes Database (release 13.5) for taxonomic annotation (DeSantis et al., 2006). Each soil bacterial 16S gene sequence was rarified to the same sequencing depth (6,996 sequences per sample) for community analysis. The raw reads were deposited in the NCBI Sequence Read Archive under accession number PRJNA577346.

Soil Bacterial Community Assembly Processes and Co-occurrence Network Analysis

Soil bacterial community assembly was inferred based on deterministic and stochastic processes. The β -nearest taxon index (β NTI) was calculated to discriminate these processes using the “picante” package in R. Soil bacterial community assembly was inferred based on deterministic and stochastic processes. The β NTI was calculated to discriminate these processes using the “picante” package in R. Values of $|\beta$ NTI| > 2 indicated that deterministic processes are dominant, and β NTI > +2 and β NTI < -2 reflected variable selection and homogeneous selection, respectively. However, $|\beta$ NTI| values < 2 indicated stochastic processes are dominant, the Raup-Crick metric (RCbray) based on Bray-Curtis distance were calculated to distinguish these stochastic scenarios, including homogenizing dispersal, dispersal limitation, and undominated. The relative influence of homogenizing dispersal and dispersal limitation denoted by $|\beta$ NTI| < 2 but RCbray < -0.95 and $|\beta$ NTI| < 2 but RCbray > +0.95, respectively. The scenario of $|\beta$ NTI| < 2 but |RCbray| < 0.95 indicated the undominated fraction (Stegen et al., 2015). Relationships between β NTI values and soil properties based on Euclidean distance matrices were evaluated using a Mantel test with 999 permutations using the “vegan” package in R.

Soil bacterial co-occurrence networks were constructed based on the sparse correlations for compositional data (sparCC) correction, using bacterial OTU profiles. The random matrix theory-based method was first used to assess the threshold value for the correlation coefficients between the OTUs, using the “RMThreshold” package in R. Correlation coefficients with an absolute value of ≥ 0.5924 and $p < 0.05$ were considered for co-occurrence networks analysis (Supplementary Figure S1). Then, we constructed a global co-occurrence network using all selected significant species-species (OTU-OTU) associations using the “igraph” package (Csardi and Nepusz, 2006). Sub-networks were extracted from the global network to identify topological network features for each soil sample using the “induced_subgraph” function. Topological features, including transitivity, average degree, betweenness centrality, average path length, and density, were calculated. Additionally, the topological characteristic of each node in the network was assessed based on within-module connectivity (Z_i) and among-module connectivity (P_i). All species were divided into four groups, that is, module hubs ($Z_i > 2.5$), network hubs ($Z_i > 2.5$ and $P_i > 0.62$), peripherals ($Z_i < 2.5$ and $P_i < 0.62$), and connectors ($P_i > 0.62$; Olesen et al., 2007). The species identified as module hubs, network hubs, or connectors were suggested as keystone species. Network visualization and modular analysis were achieved using the interactive Gephi 0.9.2 platform (Bastian et al., 2009).

Measurements of Soil Physicochemical Properties

Soil pH was measured in a 1:2.5 (v:v) soil:water suspension with a digital pH meter (Mettler-Toledo 320, China; Bao, 2000). Soil organic carbon (SOC) was determined using the

Walkley-Black method (Walkley and Black, 1934). Soil total N (TN) was measured by flow injection analysis based on the Kjeldahl method (Bremner, 1960). Soil total P (TP) and Olsen-P were determined using the ammonium molybdate method on an UV spectrophotometer (UV-2550, Shimadzu, Japan) at 700 nm (Olsen and Sommers, 1982). TP was extracted by NaOH digestion, and Olsen-P was extracted using 0.5 M NaHCO_3 .

Statistical Analysis

Significant differences in soil physicochemical properties, vector characteristics, enzyme activities, enzymatic stoichiometry, bacterial diversity indices, and β NTI values across stand ages were determined by ANOVA using the “aov” function. Linear regressions were used to examine relationships between vector L, vector A, and soil physicochemical properties. A simple clustering heatmap of dominant soil bacterial species was produced using the “heatmap” package. Principal co-ordinates analysis (PCoA) was carried out to detect bacterial community dissimilarity based on the Bray-Curtis distance. The multivariate dispersion index analysis (MVDISP) and permutational analysis of multivariate dispersions (PERMDISP) were adopted to examine the significant differences in bacterial communities among stand ages using the “vegan” package in R. Redundancy analysis (RDA) was performed to investigate the effect of soil physicochemical properties on soil bacterial community structure using the “vegan” package. Data visualization was achieved using the “ggplot2” package. Phylogenetic tree was annotated and visualized in iTOL website¹ (Letunic and Bork, 2019). Statistical analysis was conducted in R 3.6.1.²

RESULTS

Soil Enzymatic Activities and Soil Microbial Metabolic Limitations Along a Stand Age Gradient

C-acquiring (CBH and BG), N-acquiring (LAP and NAG), and P-acquiring (AP) enzyme activities tended to increase along stand age (Supplementary Figure S2). The enzymatic stoichiometry of N:P, represented by (LAP + NAG):AP, showed a gradually increasing trend along stand age, whereas stand age had no effect on the enzymatic ratios of C:N and C:P, indicated by (BG + CBH):(LAP + NAG) and (BG + CBH):AP, respectively (Supplementary Figure S3). The scatter plot of enzymatic stoichiometry showed that all soil samples tested were P-limited or co-C- and P-limited (Figure 2). Vector L, as an indicator of microbial C limitation, tended to slightly increase along stand age (Figure 3A). In contrast, vector A, indicating microbial N and P limitations, significantly decreased with increasing stand age (Figure 3B). Soil parameters, including SOC, TN, and TP, were negatively related to vector A, whereas TN was positively related to vector L (Supplementary Figure S4).

¹<https://itol.embl.de/>

²<https://cran.r-project.org/>

Soil Bacterial Diversity and Community Structure

Soil bacterial alpha diversity, including richness and the Shannon index, showed a decreasing trend in near-mature plantations (planted 9–20 years ago) when compared to plantations of the other three stand ages (Supplementary Figure S5). To better characterize bacterial community, we established phylogenetic tree using the top 100 OTUs with high relative abundance. The results showed these dominant OTUs were mainly affiliated within phyla Proteobacteria, Acidobacteria, and Actinobacteria, with a relative abundance of 38–42%, 31–34% and 18–23% among four stand ages (Supplementary Figure S6). The Alphaproteobacteria contain the largest number of OTUs which

was classified to seven families. The dominant bacterial species (i.e., the 30 most abundant OTUs) comprised Proteobacteria (31.9–46.5%), Acidobacteria (12.0–46.6%), and Actinobacteria (10.7–42.6%; Figures 4A,B, Supplementary Figure S7). There were no significant differences in bacterial phyla with a relative abundance >10% across all stand ages. Gemmatimonadetes, Chloroflexi, and Cyanobacteria, whose relative abundances were <10%, tended to decrease, whereas TM6 and OD1 showed an opposite trend along stand age. The relative abundance of TM7 was higher in mature plantations (planted 21–60 years ago) than in plantations of other stand ages.

We found significant difference in bacterial community among stand ages based on PERMDISP (Table 1). The soil bacterial communities under both young and near-mature plantations had significant difference with mature plantation, as well as over-mature plantation (Supplementary Table S2). Moreover, the PCoA plot showed that soil samples clustered tighter with increasing stand age (Figure 4C). Soil pH ($F=1.51$, $p=0.016$) and SOC content ($F=1.56$, $p=0.012$) were identified as drivers of the bacterial community structure based on RDA (Figure 4D).

Assembly Processes of Bacterial Communities Along Stand Age

β -nearest taxon index values provide insights into the potential roles of deterministic and stochastic forces in bacterial community dynamics. The β NTI distribution gradually shifted along stand age, from stochastic community assembly ($|\beta\text{NTI}| < 2$) to homogeneous selection ($\beta\text{NTI} < -2$; Figure 5A). Specifically, stochastic processes contributed to the community assembly in young plantations (53.6%), whereas deterministic process mostly contributed to assembly in near-mature (60.0%), mature (50.0%), and over-mature plantations (81.0%). The community assembly in young plantations was primarily governed by homogenizing dispersal (21.4%) and dispersal limitation (32.1%),

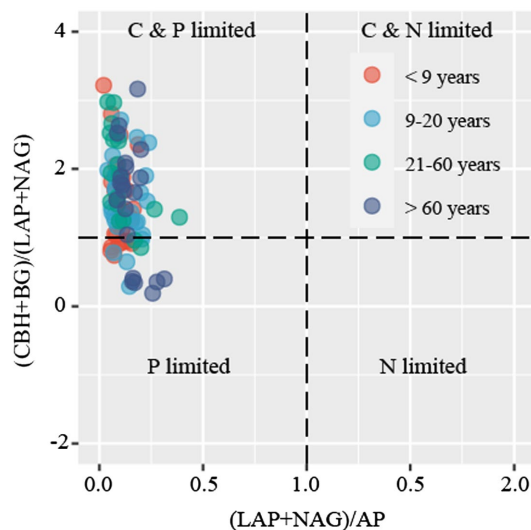


FIGURE 2 | Scatter plots of soil enzymatic stoichiometry for the studied sites. Dots with different colors represent different stand ages.

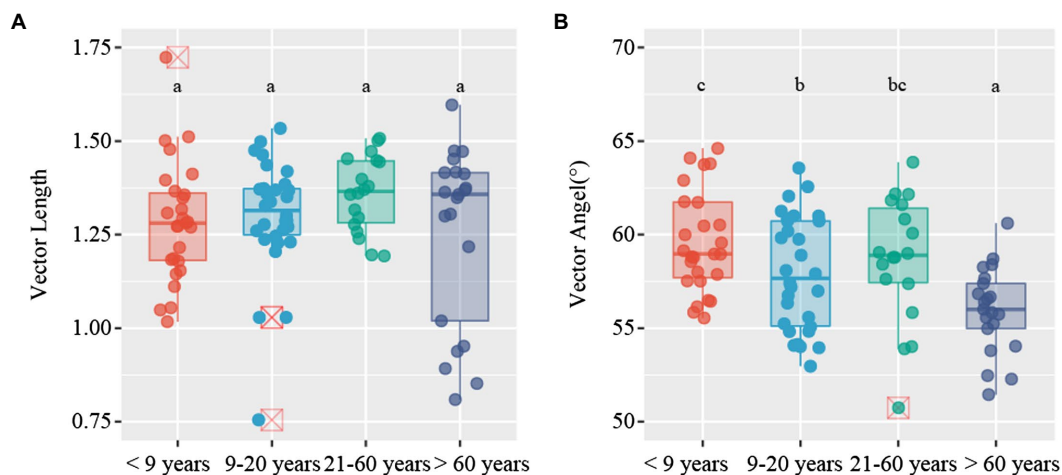


FIGURE 3 | Variations in vector characteristics for *Camellia oleifera* plantations of different stand ages. (A) vector length; (B) vector angle. Different letters denote significant differences among stand ages ($p < 0.05$).

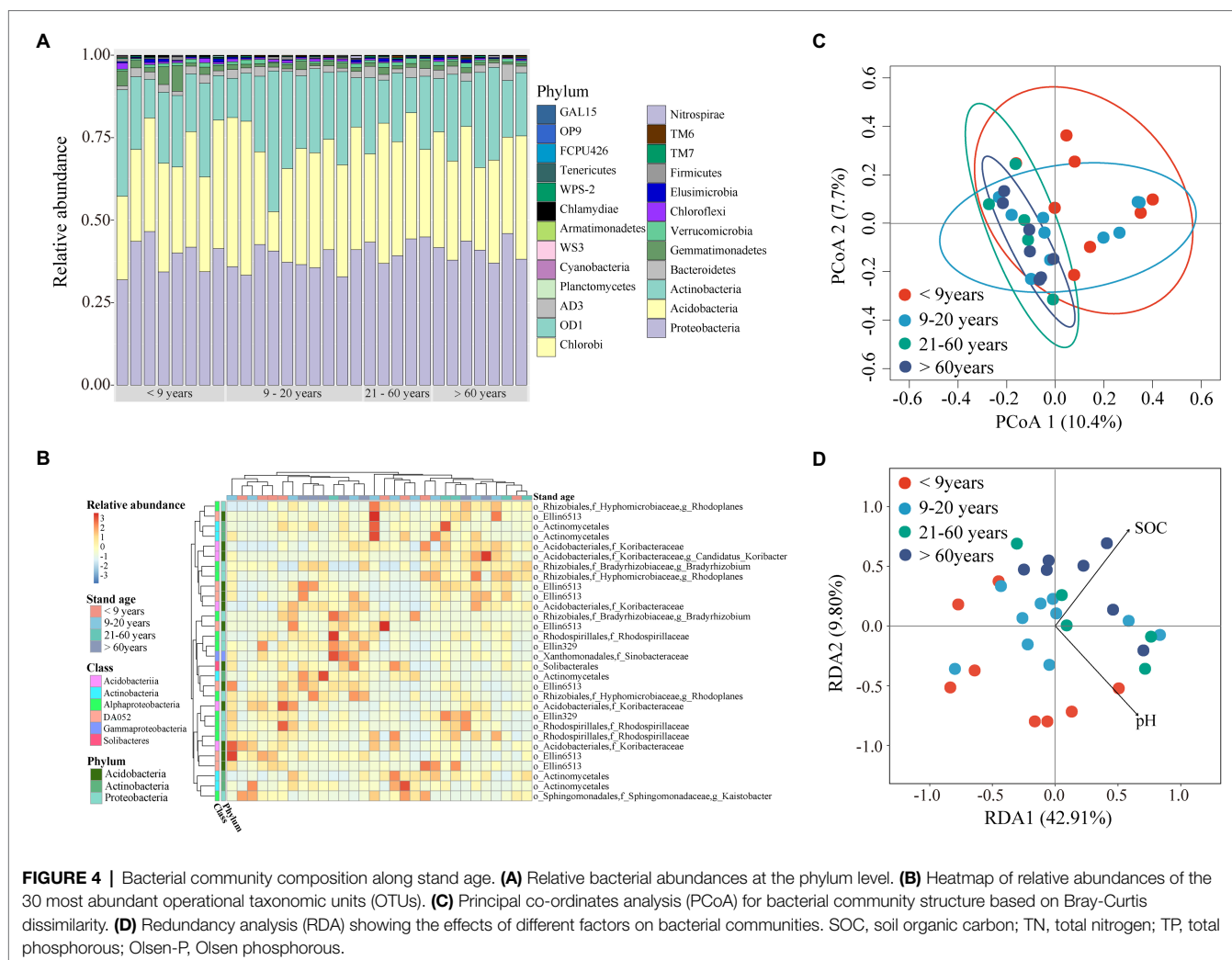


TABLE 1 | Significance test of the differences of centroids with the succession age.^a

Centroid of <9 years communities	Centroid of 9–20 years communities	Centroid of 21–60 years communities	Centroid of >60 years communities	F	p
0.5008	0.4870	0.4262	0.4218	8.1067	0.001

^aPermutational analysis of multivariate dispersions (PERMDISP) was performed to test the significance of the difference.

respectively. Conversely, strong homogeneous selection of deterministic processes dominated the near-mature (51.1%), mature (50.0%), and over-mature plantations (71.4%; **Table 2**). The Mantel test results suggested that β NTI values were significantly affected by soil pH ($\rho=0.130$, $p<0.05$; **Figure 5B**, **Supplementary Table S3**).

Global Co-occurrence Patterns of Bacterial Communities

The global co-occurrence network generated based on soil bacterial OTU profiles comprised 218 nodes and 478 links. The global network contained six modules, and two main

modules accounted for 48.62 and 38.99% of the total number of nodes (**Figure 6A**). Alphaproteobacteria, Acidobacteria, Actinobacteria, and DA052 mainly occupied the nodes (**Figure 6B**). Sixty-eight percent of the links in the global co-occurrence network were positive. According to the Zi-Pi plot, most OTUs were identified as peripherals. Only OTU0113, assigned to Acidobacteria, served as a connector, and four OTUs, including OTU0046 (Proteobacteria), OTU0134 (Proteobacteria), OTU0003 (Acidobacteria), and OTU0378 (Acidobacteria), were module hubs (**Figure 7**). The topological properties of transitivity, average degree, and density tended to slightly decrease, whereas the average path length increased along stand age (**Supplementary Table S4**).

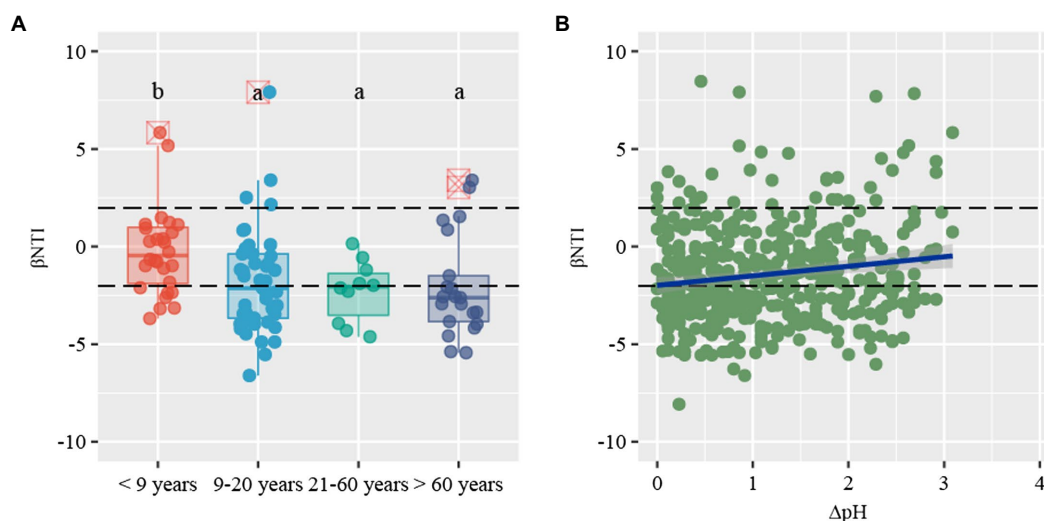


FIGURE 5 | (A) Distribution patterns of β -nearest taxon index (β NTI) values along stand age. **(B)** The relationship between β NTI values and changes of soil pH. Horizontal dashed lines indicate lower and upper significance thresholds at -2 and $+2$, respectively.

TABLE 2 | The relative contributions of ecological assembly processes across successional age.

Years	Variable selection	Homogeneous selection	Deterministic ^a	Homogenizing dispersal	Dispersal limitation	Stochastic ^b	Undominated
<9	0.107	0.250	0.357	0.214	0.321	0.536	0.107
9–20	0.089	0.511	0.600	0.200	0.111	0.311	0.089
21–60	0	0.500	0.500	0.300	0	0.300	0.200
>60	0.095	0.714	0.810	0.190	0	0.190	0

^aDeterministic = Variable selection + Homogeneous selection.

^bStochastic = Dispersal limitation + Homogenizing dispersal.

DISCUSSION

Soil Microbial Resource Limitations Along Stand Age

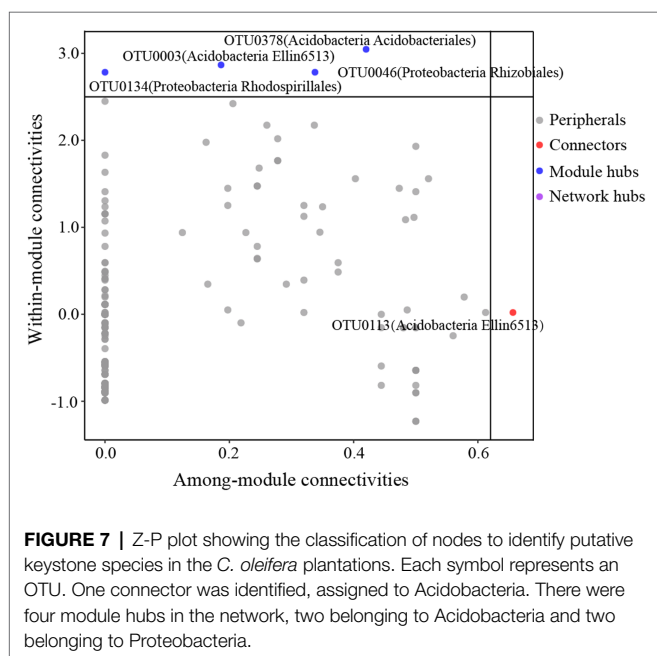
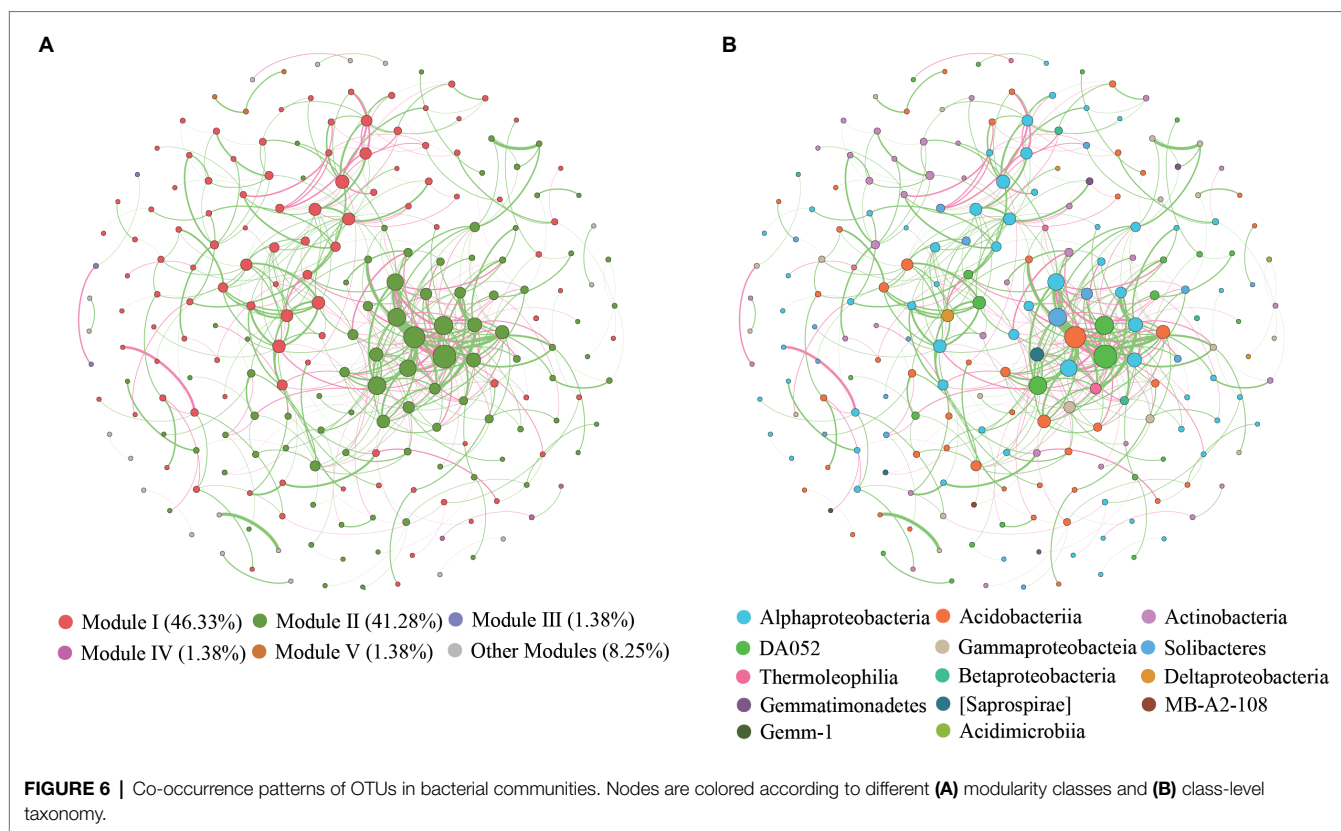
Microbial C limitation is widespread in forest ecosystems (Soong et al., 2020). Although the SOC was gradually accumulated (Supplementary Table S5), we found that microbial C limitation progressively increased with increasing stand age. This is inconsistent with a previous finding that microbial C limitation decreased with increasing stand age in *Robinia pseudoacacia* planted forest (Zhong et al., 2020). One possible reason for this discrepancy is that microbial C limitation is, at least in part, determined by plant litter quality. Refractory organic materials from *C. oleifera* are more abundant in lignin than in cellulose (Hu et al., 2015), which result in a lower efficient C resource for soil microbe.

Our results indicated that microbial P limitation rather than microbial N limitation is common in the subtropical region, which was supported by the eco-enzymatic stoichiometry plot and vector analyses. Dissolved N reportedly is three times higher in subtropical areas than in temperate regions

(Wu et al., 2019; Xiao et al., 2019), leading to the alleviation of microbial N limitation in those areas. Artificial N input in the initial stage of *C. oleifera* cultivation may also explain this result. Considering that P deficiency due to the strong adsorption of orthophosphates to soil aluminum (Al) and iron (Fe) oxides is common in subtropical regions, the widespread microbial P limitation observed in the soils evaluated in our study was not surprising. Notably, microbial P limitation tended to decrease along stand age, which is inconsistent with a previous finding that forest succession aggravated microbial P limitation (Huang et al., 2013). One possible explanation is that the continuous release of organic acids from *C. oleifera* roots can mobilize soil fixed P and alleviate microbial P limitation in more mature stands (Yuan et al., 2013).

Soil Bacterial Community Changes Along Stand Age

Our results indicated that soil bacterial alpha diversity did not significantly change with stand age, which is inconsistent with a previous finding that the soil bacterial alpha diversity increased



with succession age in a reforestation context (Jiao et al., 2018). This may be explained by plant diversity; as mentioned above, the resource diversity hypothesis states that diversified plant species provide various organic substrates and thus, diverse C

resources, to the soil microorganisms (Liu et al., 2018). In contrast, in the *C. oleifera* plantations in our study, due to management practices such as weeding, only one species was present, providing only a simple carbon substrate for the soil microbes. Additionally, soil bacterial community was irrelevant to microbial C and P limitation when we analysis the effect of enzymatic stoichiometric parameters on soil bacterial community using the RDA selection, the possible reason could be that microbial metabolic limitation calculated by both soil bacterial and fungal enzyme activity.

Soil bacterial communities are strongly influenced by the plant communities in forest ecosystems (Dang et al., 2017). Our study indicated that the soil bacterial communities have significant change among stand ages, and the soil bacterial communities become more clustered in the later stage, suggesting that the special plant could shape soil bacterial community, because of the special plant has distinctive root characteristics including morphology, quantity, and exudates components (Wang et al., 2018). Previous studies revealed that root exudates in certain plant can modify soil bacterial community. For example, the root exudates of barrel clover and wheat enriched Proteobacteria and Actinobacteria in the rhizosphere (Haichar et al., 2008).

Besides Acidobacteria, Proteobacteria was reported to be the most abundant bacterial phyla in terrestrial soil (Wei et al., 2018), which is consistent with our study that Proteobacteria always was a major abundant phylum in the soil samples among stand ages. Interestingly, although the soil fundamental physic-chemistry parameters varied with stand age, such as SOC, the relative abundance of phylum

Proteobacteria had no significant change along the stand age, suggesting that the Proteobacteria has strong sophisticated adaptations. Proteobacteria are also predominant in glacial ice and deep undersurface soils, suggesting that species within this phylum are highly resistant to various harsh environments (Shtarkman et al., 2013). Notably, Chloroflexi were more abundant in young stands than in older stands. Chloroflexi are reported to prefer nutrient-poor soils (Wang et al., 2019). Before the plantation of the *C. oleifera* stands evaluated in our study, the topsoil was widely destroyed by land leveling, which had caused runoff loss of soil nutrients and resulted in high microbial nutrient limitation in the young stands. High Gemmatimonadetes abundance was more often found in younger than in older stands. Gemmatimonadetes reportedly better prevail in dry soils than in moisture soils (Fawaz, 2013). The young *C. oleifera* plantations had lower vegetation coverage, and therefore, a lower ability to maintain soil moisture. Interestingly, we found that the relative abundances of some soil rare bacteria, such as TM7, TM6, and OD1, increased along stand age. Previous studies have shown that these species are widely detected in anaerobic environments (Winsley et al., 2014). Indeed, in the old *C. oleifera* plantations, the soil surface was covered with litter, which would have provided a more anaerobic soil condition.

Assembly Processes and Co-occurrence Network of the Soil Bacterial Community

Stochastic and deterministic processes control the assembly of microbial communities along ecological succession (Fargione et al., 2003). We found that the soil bacterial community assembly of the *C. oleifera* plantations initially was governed by stochasticity. A possible reason may be that the strong soil disturbance before the establishment of the *C. oleifera* plantations destroyed the microbial community structure, resulting in a weak environmental filter. A previous study showed that stochastic processes dominated plant community assembly after fire disturbance (Måren et al., 2018). Therefore, plant-associated and soil microbes may undergo the same assemblage processes after intense disturbance. Interestingly, we found that the contribution of homogeneous selection was far more than the variable selection in all stand ages, which indicated that the bacterial community driven by consistent selective pressure of local environmental condition. A previous study demonstrated that deterministic processes are more likely to be driven by environmental gradients, for example, in soil pH and soil temperature (Jiao and Lu, 2020). In line herewith, we observed a decreasing trend in soil pH with stand age, and β NTI values were highly correlated with soil pH. Interestingly, a previous study showed that stochasticity drove soil bacterial community assemblage also under neutral pH (Tripathi et al., 2018). Therefore, the soil pH range may control soil bacterial community assembly. Considering that the fairly low soil pH in our studied ecosystem, a small decrease of pH in acid soil may provide a strong selection pressure on certain bacterial species.

Furthermore, according to the established conceptual model, the stochastic processes governed the bacterial community initially. With the microbial succession, consistent microbial interaction progressively altered shelter environment through products of microbial metabolism and the change of nutrients, which provided a selective pressure from stochastic processes to deterministic processes.

An ecological soil bacterial network can reflect the complex interactions of soil bacteria (Chow et al., 2014). We found more positive than negative links in our global co-occurrence network, suggesting a high level of cooperation between the soil bacterial species in the *C. oleifera* plantations. The main modules, including modules I and II, mainly comprised Proteobacteria and Acidobacteria. Modules I and II represented two ecological types (Ishimoto et al., 2021), suggesting that those species belong to Proteobacterial and Acidobacterial phyla could be located in different functional niche. Intriguingly, rare species were found to occupy several modules with a few nodes, which implied that these species exist in distinct ecological niches. Keystone species in our study belonged to Koribacteraceae, Hyphomicrobiaceae, and Rhodospirillaceae. Previous studies have demonstrated that Koribacteraceae, which can decompose complex carbon polymers, are widely distributed in woodlands (Ward et al., 2009). Additionally, Koribacteraceae are involved in iron redox reactions in iron-rich environments, which may have benefited their survival in the *C. oleifera* plantations in this study (Su et al., 2020). The *C. oleifera* plantations were located in subtropical regions, where the soil is rich in iron and low in C due to strong weathering and nutrient leaching. Hyphomicrobiaceae and Rhodospirillales reportedly commonly occur in hypoxic environments, and species of these classes can photosynthesize and are involved in oxidative metabolism (Anderson et al., 2011). The possible reasons for the occurrence of these species may be that the compact soil structure led to a low soil oxygen content, and the occasional heavy rains diminished soil aeration.

Stand age contributes to the topological features of bacterial co-occurrence networks in *Cunninghamia lanceolata* planted forests (Cao et al., 2020). We observed a loss of network complexity with stand age, suggesting a progressively weaker interaction between bacteria. The soil disturbance before the establishment of the *C. oleifera* plantations may have contributed to a more diverse array of ecologically functional groups, which would imply more potential interactions. Subsequent the progressive acidification of soil in the *C. oleifera* ecosystem would have decreased the microbial growth condition along the stand age, which may have inhibited the activity of soil bacteria, resulting in weaker cooperation among the bacterial species.

CONCLUSION

This study investigated soil microbial limitation and soil microbial community dynamics along stand age in a planted *C. oleifera* forest in a subtropical region in China. Our study

provided solid evidence that P and co-C and P limitations were dominant soil microbial resource limitations in this ecosystem. Soil microbial P limitation tended to decrease with stand age. Microbial community assembly tended to shift from stochastic to deterministic processes along stand age, and soil pH was identified as filtering factor for soil bacterial community assembly. Additionally, we found that soil bacteria likely experienced more extensive nutrient depletion in young stands, suggesting that low soil fertility promotes microbial cooperation to obtain essential nutrients. Our findings shed light on microbial limitations and assemblage patterns in planted forest ecosystems and improve our knowledge regarding the drivers of community assembly along stand age. In addition, our finding suggested the importance of proper nutriment management, especially for P, in *C. oleifera* plantations in subtropical area.

DATA AVAILABILITY STATEMENT

The data sets presented in this study can be found in online repositories. The names of the repository/repositories and accession number(s) can be found in the article/**Supplementary Material**.

REFERENCES

- Anderson, C. R., Condon, L. M., Clough, T. J., Fiers, M., Stewart, A., Hill, R. A., et al. (2011). Biochar induced soil microbial community change: implications for biogeochemical cycling of carbon, nitrogen and phosphorus. *Pedobiologia* 54, 309–320. doi: 10.1016/j.pedobi.2011.07.005
- Bao, S. (2000). *Soil and Agricultural Chemistry Analysis*. 3rd Edn. Beijing: China Agriculture Press.
- Bastian, M., Heymann, S., and Jacomy, M. (2009). “Gephi: an open source software for exploring and manipulating networks.” in *Proceedings of the International AAAI Conference on Web and Social Media*; May 17–20, 2009; San Jose, California, USA, 361–362.
- Bremner, J. M. (1960). Determination of nitrogen in soil by the Kjeldahl method. *J. Agric. Sci.* 55, 11–33. doi: 10.1017/S0021859600021572
- Canessa, R., van den Brink, L., Saldana, A., Rios, R. S., Hättenschwiler, S., Mueller, C. W., et al. (2020). Relative effects of climate and litter traits on decomposition change with time, climate and trait variability. *J. Ecol.* 109, 447–458. doi: 10.1111/1365-2745.13516
- Cao, J., Zheng, Y., and Yang, Y. (2020). Phylogenetic structure of soil bacterial communities along age sequence of subtropical *Cunninghamia lanceolata* plantations. *Sustainability* 12:1864. doi: 10.3390/su12051864
- Chai, Y., Yue, M., Liu, X., Guo, Y., Wang, M., Xu, J., et al. (2016). Patterns of taxonomic, phylogenetic diversity during a long-term succession of forest on the Loess Plateau, China: insights into assembly process. *Sci. Rep.* 6:27087. doi: 10.1038/srep27087
- Chow, C. E. T., Kim, D. Y., Sachdeva, R., Caron, D. A., and Fuhrman, J. A. (2014). Top-down controls on bacterial community structure: microbial network analysis of bacteria, T4-like viruses and protists. *ISME J.* 8, 816–829. doi: 10.1038/ismej.2013.199
- Csardi, G., and Nepusz, T. (2006). The igraph software package for complex network research. *Int. J. Complex Syst.* 1695, 1–9. doi: 10.3724/SPJ.1087.2009.02191
- Cui, Y., Fang, L., Deng, L., Guo, X., Han, F., Ju, W., et al. (2019). Patterns of soil microbial nutrient limitations and their roles in the variation of soil organic carbon across a precipitation gradient in an arid and semi-arid region. *Sci. Total Environ.* 658, 1440–1451. doi: 10.1016/j.scitotenv.2018.12.289
- Dang, P., Yu, X., Le, H., Liu, J., Shen, Z., and Zhao, Z. (2017). Effects of stand age and soil properties on soil bacterial and fungal community composition

AUTHOR CONTRIBUTIONS

YH and YS designed the study. YH and CD collected the soil samples. HQ, CD, QS, and SD performed physicochemical, enzymatic, and bacterial analysis of all soil samples. HQ and LC analyzed the data with help from YR, YH, XC, JW, LM, HQ, and LC wrote the paper with inputs from all co-authors.

FUNDING

This research was supported by grants from the National Key Research Program (2017YFC0505503); Science and Technology Innovation Program of Hunan (2020NK2005); National Science Foundation (41601260); and Natural Science Foundation of Guangxi (2018GXNSFAA138020).

SUPPLEMENTARY MATERIAL

The Supplementary Material for this article can be found online at: <https://www.frontiersin.org/articles/10.3389/fmicb.2021.736165/full#supplementary-material>

- in Chinese pine plantations on the Loess Plateau. *PLoS One* 12:e0186501. doi: 10.1371/journal.pone.0186501
- DeSantis, T. Z., Hugenholtz, P., Larsen, N., Rojas, M., Brodie, E. L., Keller, K., et al. (2006). Greengenes, a chimera-checked 16S rRNA gene database and workbench compatible with ARB. *Appl. Environ. Microbiol.* 72, 5069–5072. doi: 10.1128/AEM.03006-05
- Dini-Andreote, F., Stegen, J. C., Van Elsas, J. D., and Salles, J. F. (2015). Disentangling mechanisms that mediate the balance between stochastic and deterministic processes in microbial succession. *Proc. Natl. Acad. Sci. U. S. A.* 112, E1326–E1332. doi: 10.1073/pnas.1414261112
- Edgar, R. C. (2010). Search and clustering orders of magnitude faster than BLAST. *Bioinformatics* 26, 2460–2461. doi: 10.1093/bioinformatics/btq461
- Fan, H., Wu, J., Liu, W., Yuan, Y., Hu, L., and Cai, Q. (2015). Linkages of plant and soil C:N:P stoichiometry and their relationships to forest growth in subtropical plantations. *Plant Soil* 392, 127–138. doi: 10.1007/s11104-015-2444-2
- FAO (2015). FRA 2015 terms and definition. Forest Resource Assessment Working Paper 180. Rome, Italy: Food and Agriculture Organization of the United Nations. Available at: <http://www.fao.org/docrep/017/ap862e/ap862e00.pdf> (Accessed April 6, 2018).
- Fargione, J., Brown, C. S., and Tilman, D. (2003). Community assembly and invasion: an experimental test of neutral versus niche processes. *Proc. Natl. Acad. Sci. U. S. A.* 100, 8916–8920. doi: 10.1073/pnas.1033107100
- Fawaz, M. N. (2013). Revealing the ecological role of gemmatimonadetes through cultivation and molecular analysis of agricultural soils. masters theses. Knoxville: University of Tennessee, 64–65.
- Feng, M., Tripathi, B. M., Shi, Y., Adams, J. M., Zhu, Y. G., and Chu, H. (2019). Interpreting distance-decay pattern of soil bacteria via quantifying the assembly processes at multiple spatial scales. *MicrobiologyOpen* 8:e00851. doi: 10.1002/mbo3.851
- Ferrenberg, S., O'Neill, S. P., Knelman, J. E., Todd, B., Duggan, S., Bradley, D., et al. (2013). Changes in assembly processes in soil bacterial communities following a wildfire disturbance. *ISME J.* 7, 1102–1111. doi: 10.1038/ismej.2013.11
- Gao, Q., Yang, Y., Feng, J., Tian, R., Guo, X., Ning, D., et al. (2019). The spatial scale dependence of diazotrophic and bacterial community assembly in paddy soil. *Glob. Ecol. Biogeogr.* 28, 1093–1105. doi: 10.1111/geb.12917
- Haichar, F., Marol, C., Berge, O., Rangel-Castro, J. I., Prosser, J. I., Balesdent, J., et al. (2008). Plant host habitat and root exudates shape soil bacterial community structure. *ISME J.* 2, 1221–1230. doi: 10.1038/ismej.2008.80

- Hill, B. H., Elonen, C. M., Herlihy, A. T., Jicha, T. M., and Serenbetz, G. (2018). Microbial coenzyme stoichiometry, nutrient limitation, and organic matter decomposition in wetlands of the conterminous United States. *Wetl. Ecol. Manag.* 26, 425–439. doi: 10.1007/s11273-017-9584-5
- Hu, J., Chang, S., Peng, K., Hu, K., and Thévenon, M. F. (2015). Bio-susceptibility of shells of *Camellia oleifera* Abel. fruits to fungi and termites. *Int. Biodeterior. Biodegrad.* 104, 219–223. doi: 10.1016/j.ibiod.2015.06.011
- Huang, W., Liu, J., Wang, Y. P., Zhou, G., Han, T., and Li, Y. (2013). Increasing phosphorus limitation along three successional forests in southern China. *Plant Soil* 364, 181–191. doi: 10.1007/s11104-012-1355-8
- Ishimoto, C. K., Aono, A. H., Nagai, J. S., Sousa, H., Miranda, A. R. L., Melo, V. M. M., et al. (2021). Microbial co-occurrence network and its key microorganisms in soil with permanent application of composted tannery sludge. *Sci. Total Environ.* 789:147945. doi: 10.1016/j.scitotenv.2021.147945
- Jiao, S., Chen, W., Wang, J., Du, N., Li, Q., and Wei, G. (2018). Soil microbiomes with distinct assemblies through vertical soil profiles drive the cycling of multiple nutrients in reforested ecosystems. *Microbiome* 6:146. doi: 10.1186/s40168-018-0526-0
- Jiao, S., and Lu, Y. (2020). Soil pH and temperature regulate assembly processes of abundant and rare bacterial communities in agricultural ecosystems. *Environ. Microbiol.* 22, 1052–1065. doi: 10.1111/1462-2920.14815
- Jin, X., and Ning, Y. (2012). Antioxidant and antitumor activities of the polysaccharide from seed cake of *Camellia oleifera* Abel. *Int. J. Biol. Macromol.* 51, 364–368. doi: 10.1016/j.ijbiomac.2012.05.033
- Kang, H., Gao, H., Yu, W., Yi, Y., Wang, Y., and Ning, M. (2018). Changes in soil microbial community structure and function after afforestation depend on species and age: case study in a subtropical alluvial island. *Sci. Total Environ.* 625, 1423–1432. doi: 10.1016/j.scitotenv.2017.12.180
- Kooch, Y., Sanji, R., and Tabari, M. (2018). Increasing tree diversity enhances microbial and enzyme activities in temperate Iranian forests. *Trees* 32, 809–822. doi: 10.1007/s00468-018-1674-3
- Kunin, V., Engelbrektson, A., Ochman, H., and Hugenholtz, P. (2010). Wrinkles in the rare biosphere: pyrosequencing errors can lead to artificial inflation of diversity estimates. *Environ. Microbiol.* 12, 118–123. doi: 10.1111/j.1462-2920.2009.02051.x
- Letunic, I., and Bork, P. (2019). Interactive Tree of Life (iTOL) v4: recent updates and new developments. *Nucleic Acids Res.* 47, W256–W259. doi: 10.1093/nar/gkz239
- Liu, J., Dang, P., Gao, Y., Zhu, H., Zhu, H., Zhao, F., et al. (2018). Effects of tree species and soil properties on the composition and diversity of the soil bacterial community following afforestation. *For. Ecol. Manag.* 427, 342–349. doi: 10.1016/j.foreco.2018.06.017
- Liu, J., Wu, L., Chen, D., Li, M., and Wei, C. (2017). Soil quality assessment of different *Camellia oleifera* stands in mid-subtropical China. *Appl. Soil Ecol.* 113, 29–35. doi: 10.1016/j.apsoil.2017.01.010
- Måren, I. E., Kapfer, J., Aarrestad, P. A., Grytnes, J. A., and Vandvik, V. (2018). Changing contributions of stochastic and deterministic processes in community assembly over a successional gradient. *Ecology* 99, 148–157. doi: 10.1002/ecy.2052
- Martínez-Jauregui, M., Díaz, M., de Ron, D. S., and Soliño, M. (2016). Plantation or natural recovery? Relative contribution of planted and natural pine forests to the maintenance of regional bird diversity along ecological gradients in Southern Europe. *For. Ecol. Manag.* 376, 183–192. doi: 10.1016/j.foreco.2016.06.021
- Moorhead, D. L., Sinsabaugh, R. L., Hill, B. H., and Weintraub, M. N. (2016). Vector analysis of coenzyme activities reveal constraints on coupled C, N and P dynamics. *Soil Biol. Biochem.* 93, 1–7. doi: 10.1016/j.soilbio.2015.10.019
- Na, X., Li, X., Zhang, Z., Li, M., Kardol, P., Xu, T. T., et al. (2018). Bacterial community dynamics in the rhizosphere of a long-lived, leguminous shrub across a 40-year age sequence. *J. Soils Sediments* 18, 76–84. doi: 10.1007/s11368-017-1745-x
- Nepal, P., Korhonen, J., Prestemon, J. P., and Cubbage, F. W. (2019). Projecting global planted forest area developments and the associated impacts on global forest product markets. *J. Environ. Manag.* 240, 421–430. doi: 10.1016/j.jenvman.2019.03.126
- Nossa, C. W., Oberdorf, W. E., Yang, L., Aas, J. A., Paster, B. J., DeSantis, T. Z., et al. (2010). Design of 16S rRNA gene primers for 454 pyrosequencing of the human foregut microbiome. *World J. Gastroenterol.* 16:4135. doi: 10.3748/wjg.v16.i33.4135
- Olesen, J. M., Bascompte, J., Dupont, Y. L., and Jordano, P. (2007). The modularity of pollination networks. *Proc. Natl. Acad. Sci. U. S. A.* 104, 19891–19896. doi: 10.1073/pnas.0706375104
- Olsen, S. R., and Sommers, L. E. (1982). “Phosphorous” in *Methods of Soil Analysis, Part 2, Chemical and Microbial Properties. Agronomy Monograph, Vol. 9*. eds. A. L. Page, R. H. Miller and D. R. Keeney (Madison, Wisconsin: Agronomy Society of America), 403–430.
- Pregitzer, K. S., and Euskirchen, E. S. (2004). Carbon cycling and storage in world forests: biome patterns related to forest age. *Glob. Change Biol.* 10, 2052–2077. doi: 10.1111/j.1365-2486.2004.00866.x
- Saiya-Cork, K. R., Sinsabaugh, R. L., and Zak, D. R. (2002). The effects of long term nitrogen deposition on extracellular enzyme activity in an *Acer saccharum* forest soil. *Soil Biol. Biochem.* 34, 1309–1315. doi: 10.1016/S0038-0717(02)00074-3
- Schimel, J. P., and Weintraub, M. N. (2003). The implications of exoenzyme activity on microbial carbon and nitrogen limitation in soil: a theoretical model. *Soil Biol. Biochem.* 35, 549–563. doi: 10.1016/S0038-0717(03)00015-4
- Schloss, P. D., Westcott, S. L., Ryabin, T., Hall, J. R., Hartmann, M., Hollister, E. B., et al. (2009). Introducing mothur: open-source, platform-independent, community-supported software for describing and comparing microbial communities. *Appl. Environ. Microbiol.* 75, 7537–7541. doi: 10.1128/AEM.01541-09
- Schmidt, S. K., Porazinska, D., Concienne, B. L., Darcy, J. L., King, A. J., and Nemergut, D. R. (2016). Biogeochemical stoichiometry reveals P and N limitation across the post-glacial landscape of Denali National Park, Alaska. *Ecosystems* 19, 1164–1177. doi: 10.1007/s10021-016-9992-z
- Shtarkman, Y. M., Koçer, Z. A., Edgar, R., Veerapaneni, R. S., D’Elia, T., Morris, P. F., et al. (2013). Subglacial Lake Vostok (Antarctica) accretion ice contains a diverse set of sequences from aquatic, marine and sediment-inhabiting bacteria and eukarya. *PLoS One* 8:e67221. doi: 10.1371/journal.pone.0067221
- Sinsabaugh, R. L., Hill, B. H., and Shah, J. J. F. (2009). Ecoenzymatic stoichiometry of microbial organic nutrient acquisition in soil and sediment. *Nature* 462, 795–798. doi: 10.1038/nature08632
- Sinsabaugh, R. L., Shah, J. J. F., Findlay, S. G., Kuehn, K. A., and Moorhead, D. L. (2015). Scaling microbial biomass, metabolism and resource supply. *Biogeochemistry* 122, 175–190. doi: 10.1007/s10533-014-0058-z
- Soong, J. L., Fuchslueger, L., Maraño-Jimenez, S., Torn, M. S., Janssens, I. A., Penuelas, J., et al. (2020). Microbial carbon limitation: the need for integrating microorganisms into our understanding of ecosystem carbon cycling. *Glob. Change Biol.* 26, 1953–1961. doi: 10.1111/gcb.14962
- State Forestry Bureau (2009). The planning of national *Camellia oleifera* industry development. Available at: <http://wenku.baidu.com/view/a386ccc10c22590102029d8d.html>.
- Stegen, J. C., Lin, X., Fredrickson, J. K., and Konopka, A. E. (2015). Estimating and mapping ecological processes influencing microbial community assembly. *Front. Microbiol.* 6:370. doi: 10.3389/fmicb.2015.00370
- Stegen, J. C., Lin, X., Konopka, A. E., and Fredrickson, J. K. (2012). Stochastic and deterministic assembly processes in subsurface microbial communities. *ISME J.* 6, 1653–1664. doi: 10.1038/ismej.2012.22
- Su, C., Zhang, M., Lin, L., Yu, G., Zhong, H., and Chong, Y. (2020). Reduction of iron oxides and microbial community composition in iron-rich soils with different organic carbon as electron donors. *Int. Biodeterior. Biodegrad.* 148:104881. doi: 10.1016/j.ibiod.2019.104881
- Sun, X., Zhou, Y., Tan, Y., Wu, Z., Lu, P., Zhang, G., et al. (2018). Restoration with pioneer plants changes soil properties and remodels the diversity and structure of bacterial communities in rhizosphere and bulk soil of copper mine tailings in Jiangxi Province, China. *Environ. Sci. Pollut. Res.* 25, 22106–22119. doi: 10.1007/s11356-018-2244-3
- Tripathi, B. M., Stegen, J. C., Kim, M., Dong, K., Adams, J. M., and Lee, Y. K. (2018). Soil pH mediates the balance between stochastic and deterministic assembly of bacteria. *ISME J.* 12, 1072–1083. doi: 10.1038/s41396-018-0082-4
- Vitali, F., Mastromei, G., Senatore, G., Caroppo, C., and Casalone, E. (2016). Long lasting effects of the conversion from natural forest to poplar plantation on soil microbial communities. *Microbiol. Res.* 182, 89–98. doi: 10.1016/j.micres.2015.10.002

- Vittori Antisari, L., Papp, R., Vianello, G., and Marinari, S. (2018). Effects of Douglas fir stand age on soil chemical properties, nutrient dynamics, and enzyme activity: a case study in Northern Apennines, Italy. *Forests* 9:641. doi: 10.3390/f9100641
- Walkley, A., and Black, I. A. (1934). An examination of the Degtjareff method for determining soil organic matter, and a proposed modification of the chromic acid titration method. *Soil Sci.* 37, 29–38. doi: 10.1097/00010694-193401000-00003
- Wang, J., Liu, G., Zhang, C., Wang, G., Fang, L., and Cui, Y. (2019). Higher temporal turnover of soil fungi than bacteria during long-term secondary succession in a semiarid abandoned farmland. *Soil Till. Res.* 194:104305. doi: 10.1016/j.still.2019.104305
- Wang, S., Zuo, X., Zhao, X., Awada, T., Luo, Y., Li, Y., et al. (2018). Dominant plant species shape soil bacterial community in semiarid sandy land of northern China. *Ecol. Evol.* 8, 1693–1704. doi: 10.1002/ece3.3746
- Ward, N. L., Challacombe, J. F., Janssen, P. H., Henrissat, B., Coutinho, P. M., Wu, M., et al. (2009). Three genomes from the phylum Acidobacteria provide insight into their lifestyles in soils. *Appl. Environ. Microbiol.* 75, 2046–2056. doi: 10.1128/AEM.02294-08
- Wei, H., Peng, C., Yang, B., Song, H., Li, Q., Jiang, L., et al. (2018). Contrasting soil bacterial community, diversity, and function in two forests in China. *Front. Microbiol.* 9:1693. doi: 10.3389/fmicb.2018.01693
- Winsley, T. J., Snape, I., McKinlay, J., Stark, J., van Dorst, J. M., Ji, M., et al. (2014). The ecological controls on the prevalence of candidate division TM7 in polar regions. *Front. Microbiol.* 5:345. doi: 10.3389/fmicb.2014.00345
- Wu, H., Song, X., Zhao, X., Peng, X., Zhou, H., Hallett, P. D., et al. (2019). Accumulation of nitrate and dissolved organic nitrogen at depth in a red soil critical zone. *Geoderma* 337, 1175–1185. doi: 10.1016/j.geoderma.2018.11.019
- Xiao, S. S., Ye, Y. Y., Xiao, D., Chen, W. R., Zhang, W., and Wang, K. L. (2019). Effects of tillage on soil N availability, aggregate size, and microbial biomass in a subtropical karst region. *Soil Till. Res.* 192, 187–195. doi: 10.1016/j.still.2019.05.006
- Yang, Y., Liang, C., Wang, Y., Cheng, H., An, S., and Chang, S. X. (2020). Soil extracellular enzyme stoichiometry reflects the shift from P-to N-limitation of microorganisms with grassland restoration. *Soil Biol. Biochem.* 149:107928. doi: 10.1016/j.soilbio.2020.107928
- Yang, C., Liu, X., Chen, Z., Lin, Y., and Wang, S. (2016). Comparison of oil content and fatty acid profile of ten new *Camellia oleifera* cultivars. *J. Lipids* 2016:3982486. doi: 10.1155/2016/3982486
- Yuan, J., Tan, X., Yuan, D., Zhang, X., Ye, S., and Zhou, J. (2013). Effect of phosphates on the growth, photosynthesis, and P content of oil tea in acidic red soils. *J. Sustain. Forest.* 32, 594–604. doi: 10.1080/10549811.2013.798827
- Zhong, Z., Li, W., Lu, X., Gu, Y., Wu, S., Shen, Z., et al. (2020). Adaptive pathways of soil microorganisms to stoichiometric imbalances regulate microbial respiration following afforestation in the Loess Plateau, China. *Soil Biol. Biochem.* 151:108048. doi: 10.1016/j.soilbio.2020.108048
- Zhou, Y. J., Li, J. H., Ross Friedman, C., and Wang, H. F. (2017). Variation of soil bacterial communities in a chronosequence of rubber tree (*Hevea brasiliensis*) plantations. *Front. Plant Sci.* 8:849. doi: 10.3389/fpls.2017.00849

Conflict of Interest: The authors declare that the research was conducted in the absence of any commercial or financial relationships that could be construed as a potential conflict of interest.

The reviewer WC declared a shared affiliation with one of the authors, LM, to the handling editor at time of review.

Publisher's Note: All claims expressed in this article are solely those of the authors and do not necessarily represent those of their affiliated organizations, or those of the publisher, the editors and the reviewers. Any product that may be evaluated in this article, or claim that may be made by its manufacturer, is not guaranteed or endorsed by the publisher.

Copyright © 2021 Qiao, Chen, Hu, Deng, Sun, Deng, Chen, Mei, Wu and Su. This is an open-access article distributed under the terms of the Creative Commons Attribution License (CC BY). The use, distribution or reproduction in other forums is permitted, provided the original author(s) and the copyright owner(s) are credited and that the original publication in this journal is cited, in accordance with accepted academic practice. No use, distribution or reproduction is permitted which does not comply with these terms.

Advantages of publishing in Frontiers



OPEN ACCESS

Articles are free to read
for greatest visibility
and readership



FAST PUBLICATION

Around 90 days
from submission
to decision



HIGH QUALITY PEER-REVIEW

Rigorous, collaborative,
and constructive
peer-review



TRANSPARENT PEER-REVIEW

Editors and reviewers
acknowledged by name
on published articles

Frontiers

Avenue du Tribunal-Fédéral 34
1005 Lausanne | Switzerland

Visit us: www.frontiersin.org

Contact us: frontiersin.org/about/contact



REPRODUCIBILITY OF RESEARCH

Support open data
and methods to enhance
research reproducibility



DIGITAL PUBLISHING

Articles designed
for optimal readership
across devices



FOLLOW US

@frontiersin



IMPACT METRICS

Advanced article metrics
track visibility across
digital media



EXTENSIVE PROMOTION

Marketing
and promotion
of impactful research



LOOP RESEARCH NETWORK

Our network
increases your
article's readership